

Realising lead-oriented synthesis

Daniel Jason Foley

Submitted in accordance with the requirements for the degree of
Doctor of Philosophy

The University of Leeds

School of Chemistry

May 2015

Declaration

The candidate confirms that the work submitted is his own, except where work which has formed part of jointly authored publications has been included. The contribution of the candidate and the other authors to this work has been explicitly indicated below. The candidate confirms that appropriate credit has been given within the thesis where reference has been made to the work of others.

The work in Chapter 1, Section 1.5.3.3; and Chapter 4 of the thesis has appeared in publication as follows:

“A unified lead-oriented synthesis of over fifty molecular scaffolds” Doveston, R. G.; Tosatti, P.; Dow, M.; Foley, D. J.; Li, H. Y.; Campbell, A. J.; House, D.; Churcher, I.; Marsden, S. P.; Nelson, A. *Org. Biomol. Chem.* **2015**, *13*, 859–865.

In order of contribution, the experimental work was performed by RD, PT, MD, the candidate (five scaffolds and three building blocks prepared) and HYL. The supporting information was written by RD. Computational studies were performed by RD. The manuscript was written by RD, SPM and AN. AN, SPM, IC, DH and AJC supervised the research programme.

The work in the above publication is summarised in Chapter 1 (introduction), Section 1.5.3.3. Chapter 4 compares the virtual library of compounds from the above publication with virtual libraries of compounds enumerated from scaffolds prepared by the candidate in this thesis.

The work in Chapter 2 of the thesis has appeared in publication as follows:

“A systematic approach to diverse, lead-like scaffolds from α,α -disubstituted amino acids” Foley, D. J.; Doveston, R. G.; Churcher, I.; Nelson, A.; Marsden, S. P. *Chem. Commun.* **2015**, manuscript accepted.

All experimental work was completed by the candidate. Computational studies were performed by the candidate using computational tools developed by RD. The supporting information was prepared by the candidate. The initial draft of the manuscript was written by the candidate and AN. SPM wrote the final version of

the manuscript for submission. SPM, AN and IC supervised the research programme.

Other contributions:

George Burslem generated the lowest energy conformers for the virtual compounds described in this thesis, which were used by the candidate to prepare the principal moments of inertia (PMI) plots found in Sections 2.5.3.2, 3.3.3.2 and 4.2. The PMI binning calculation described in Section 2.5.3.2 and Appendix 1, Section 6.3.1, was derived by the candidate and Stuart Warriner. Richard Doveston prepared compounds **215**, **227**, **228**, **237**, which are detailed in Chapter 3. The contributions of GB, RD, and SW are given appropriate credit within.

This copy has been supplied on the understanding that it is copyright material and that no quotation from the thesis may be published without proper acknowledgement.

© 2015 The University of Leeds and Daniel Jason Foley

The right of Daniel Jason Foley to be identified as Author of this work has been asserted by him in accordance with the Copyright, Designs and Patents Act 1988.

Acknowledgements

First of all, I thank Steve and Adam for their support and advice during my studies. I am grateful to Steve for his excellent training, for his advice about scientific writing and presentations, and for all the meals and nights out. I'd like to thank Adam for always finding time to discuss ideas and for making me write monthly-meeting forms – they turned out to be extremely useful for writing-up! I am grateful to the EPSRC and the University of Leeds for funding. I am also indebted to Ian Churcher at GSK for valuable discussions about the LOS project.

I would like to express my gratitude to the other LOS-ers: Richard, for his approachable manner, excellent ideas, and drive to get things done; Phil, for his enthusiasm and help with planning my work; and Steven.

I am extremely grateful to the past and present members of the Marsden group, thanks for all the tea-break chats and for making the lab a fun place to be! I thank Nic ('N-Webb'), for being "a ray of sunlight on a rainy day"; Tony ('Big Tone'), for his 'appy disposition and for his fantastic proof-reading; Mark ('MD'), for all of his excellent ideas (and sarcasm); Chris ('Chone'), for being a "nice guy with a lot to offer people"; Seb(o), for all the antics; David; John; Mary ('Meg'); Crossley; Roberta; Gayle ('G-Dog'); Tarn ('Turn'); Andrea; and James. In the Nelson group I thank: George B ('GB'), for all the PLP advice; Alun ('A-bomb'); George K ('GK'); and James F. I also thank Stuart for the GCSE-level maths lesson.

Outside of the Department, I am grateful to Steve Wailes for the advice that set me on this path, and for suggesting that I apply to join the Marsden group. I thank my family and friends for their reassurance: mum; dad; my brothers, Kieran and Alex; my sister, Anna; and Steve and Sarah Hulbert. Finally, I cannot thank Alison enough for her unerring love and support during my studies: thank you for your encouragement, compassion and patience, all of which have greatly helped to make this achievement possible (not to mention all of the proof-reading, sitting through presentations, and putting up with the occasional bit of 'science-chat!').

This thesis dedicated to the memory of my grandad, Daniel (Donal) Foley, 1933–2013.

Abstract

The concept of lead-oriented synthesis (LOS) seeks to address to the paucity of diverse compounds with appropriate properties for biological screening. This thesis focuses on the preparation of diverse scaffolds, which, following decoration, may provide access to lead-like compounds. Key polyfunctionalised building blocks were prepared to enable the synthesis of such scaffolds by applying small tool-kits of robust synthetic methodologies. Computational tools were used to guide the development of key methodologies and to target the preparation of specific scaffolds. In addition, computational tools were used to retrospectively analyse the ability of the scaffolds prepared to provide access to lead-like space.

Chapter 1 discusses ideal molecular properties for drugs and leads, modern synthetic approaches to the preparation of diverse screening compounds, and the emergence of LOS as a concept to resolve the challenge of sourcing large numbers of ideal screening compounds.

Chapter 2 details the preparation of small polyfunctionalised building blocks through the allylation of amino acid-derivatives. A building-up ('bottom-up') approach was used to prepare scaffolds, exploiting the intramolecular capture of pendant nucleophiles at alkene or ester functionalities, and the use of transition metal-catalysed cyclisations. Four building blocks were used to prepare 22 scaffolds. A virtual library of 1110 compounds was enumerated from the scaffolds, of which 66% were found to be lead-like.

Chapter 3 describes the preparation of larger polycycles using an intramolecular [5+2] oxidopyrylium cycloaddition. The two polycyclic assemblies prepared were deconstructed using a 'top-down' approach to give six scaffolds. A virtual library of 798 compounds was enumerated from the scaffolds, of which 72% would be lead-like.

Chapter 4 compares the value of the different LOS approaches developed, this considers the ability of the scaffolds to provide access to lead-like space, their three-dimensionality, and the synthetic economy of their preparation.

Contents

Declaration	ii
Acknowledgements	iv
Abstract	v
Contents	vi
Symbols and abbreviations	x
1.0 Introduction	1
1.1 Challenges facing the pharmaceutical industry	1
1.2 An overview of the drug discovery process	1
1.2.1 The role of synthesis in drug discovery	3
1.3 Characteristics of drug-like molecules	4
1.4 Characteristics of lead-like molecules	5
1.4.1 Diversity considerations	7
1.5 Approaches to the synthesis of diverse screening libraries	8
1.5.1 Diversity-oriented Synthesis (DOS)	8
1.5.1.1 Substrate-based DOS: Folding pathways	9
1.5.1.2 Reagent-based DOS: Branching pathways	10
1.5.1.3 Oligomer-based approaches	11
1.5.1.4 DOS: A summary	12
1.5.2 Fragment-based drug discovery (FBDD)	13
1.5.3 Lead-oriented synthesis (LOS)	14
1.5.3.1 Combinatorial considerations	15
1.5.3.2 Lead-like arrays based on specific scaffolds	15
1.5.3.3 Unified approaches to diverse lead-like compounds	16
1.6 Project aims and thesis outline	20
2.0 Results and discussion 1: A bottom-up approach to LOS	21
2.1 The selection of a connective reaction for LOS	21
2.2 Selection of a suitable methodology for the allylic alkylation of amino acid derivatives	26
2.2.1 The asymmetric allylic alkylation (AAA) reaction	26
2.2.1.1 Asymmetric allylic alkylation (AAA) of amino acid derivatives: The Tsuji–Trost reaction	26
2.2.2 Benchmarking the asymmetric allylic alkylation (AAA) of azlactones	28
2.2.2.1 Optimisation of the Pd-catalysed AAA of azlactones	29
2.2.3 Substitution at the azlactone carbonyl	30

2.2.3.1 Addition of <i>N</i> -centred nucleophiles	30
2.2.3.2 Addition of <i>C</i> -centred nucleophiles	31
2.2.4 Deprotection of <i>N</i> -amido protected amines.....	32
2.2.4.1 Attempted deprotection of an <i>N</i> -benzamido protected amine ..	33
2.2.4.2 AAA of azlactones bearing a CF ₃ -substituent at C-2.....	33
2.2.4.3 AAA and deprotection of azlactones bearing a 4-chlorobutyryl substituent at C-2.....	35
2.2.4.4 Attempted deprotection of an <i>N</i> -4-chlorobutyryl protected amine with butylamine	35
2.2.4.5 Deprotection of an <i>N</i> -4-chlorobutyryl protected amino ester with AgBF ₄	36
2.2.5 Critical analysis of the suitability of the AAA of azlactones for LOS	37
2.2.6 Preparation of quaternary amino esters by simple allylation	38
2.3 Establishing a chemical tool-kit: Synthetic strategy.....	39
2.3.1 Cyclisations exploiting the electrophile-induced capture of tethered nucleophiles	40
2.3.1.1 Oxyiodinations.....	40
2.3.1.2 Aminoiodinations	43
2.3.2 Cyclisations between tethered <i>N</i> -centred nucleophiles and the adjacent ester.....	46
2.3.2.1 Hydantoin formations.....	46
2.3.2.2 Lactamisations	47
2.3.3 Transition metal-catalysed cyclisations between the capping group and the allyl functionality	49
2.3.3.1 Intramolecular Heck reactions	50
2.3.3.2 Ring-closing metathesis (RCM).....	52
2.3.4 Cyclisation toolkit: A summary.....	54
2.4 Generation of sites for further diversification	55
2.4.1 Oxidation of cyclic alkenes in the presence of tertiary amines	56
2.4.2 Oxidation of terminal alkenes in the presence of tertiary amines	59
2.4.3 Oxidation chemistry: Summary and outlook.....	61
2.5 Computational assessment of the scaffolds prepared.....	62
2.5.1 Novelty assessment	62
2.5.2 Diversity assessment.....	63
2.5.3 Virtual decoration of the scaffolds.....	65
2.5.3.1 Molecular properties analysis	67
2.5.3.1.1 Lead-likeness assessment	67
2.5.3.2 Principal moments of inertia study	74

2.5.4 Computational assessment: A summary.....	77
2.6 Exemplar decorations of scaffolds	77
2.6.1 Computational assessment of exemplar scaffolds	78
2.7 Conclusions and future work.....	81
3.0 Results and discussion 2: A top-down approach to LOS.....	82
3.1 The selection of a connective reaction for LOS.....	82
3.1.1 Intramolecular oxidopyrylium [5+2] cycloadditions	84
3.1.1.1 Benchmarking of an intramolecular [5+2] cycloaddition of an oxidopyrylium generated by group elimination.....	84
3.1.2 Intramolecular [5+2] cycloadditions of oxidopyryliums generated by group transfer.....	87
3.1.2.1 Preparation of β -alkoxy- γ -pyrone starting materials	91
3.1.2.2 [5+2] cycloaddition of oxidopyryliums generated from β -alkoxy- γ -pyrones	93
3.2 Establishing a chemical toolkit	94
3.2.1 Previous work.....	94
3.2.1.1 Ring-constructing reactions	94
3.2.1.1.1 Tandem cycloadditions.....	94
3.2.1.1.2 Ring closing metathesis to form medium-sized rings	95
3.2.1.2 Ring-cleaving reactions	96
3.2.1.2.1 Semi-permanent tethers	96
3.2.1.2.2 Cleavage of the ether bridge	97
3.2.1.3 Previous work: A summary.....	98
3.2.2 Functional group interconversions (FGI) of α -silyloxyenones.....	99
3.2.2.1 Reductions	99
3.2.2.2 Silyl deprotection	103
3.2.2.3 FGI summary.....	103
3.2.3 Synthesis of new scaffolds from polycyclic assemblies.....	104
3.2.3.1 Ring-constructing reactions	105
3.2.3.2 Ring-cleaving reactions	105
3.2.3.2.1 Cleavage of the ether bridge	105
3.2.3.2.2 Oxidative cleavages and subsequent reductive aminations	107
3.2.3.3 Scaffold synthesis: A summary.....	110
3.3 Computational assessment of the scaffolds prepared.....	111
3.3.1 Novelty assessment	112
3.3.2 Diversity assessment.....	112
3.3.3 Virtual decoration of the scaffolds.....	113

3.3.3.1 Molecular properties analysis	115
3.3.3.1.1 Lead-likeness assessment	115
3.3.3.2 Principal moments of inertia study	118
3.3.4 Conclusions and future work	119
4.0 Comparison of approaches to LOS	124
4.1 Lead-likeness assessment.....	124
4.2 PMI assessment	124
4.3 Synthetic efficiency	126
4.4 Summary and outlook	129
5.0 Experimental	130
5.1 General experimental	130
5.2 Experimental for 'bottom-up' approach to LOS	131
5.2.1 General procedures	131
5.2.2 Compound data for 'bottom-up' approach to LOS.....	138
5.2.3 Synthesis of scaffold derivatives.....	186
5.3 Experimental for 'top-down' approach to LOS.....	190
5.3.1 A note on NMR assignments	190
5.3.2 General procedures	190
5.3.3 Compound data for 'top-down' approach to LOS	191
6.0 Appendix 1: Computational tools and related data	216
6.1 Capping groups for virtual library enumeration.....	216
6.2 Lead-likeness analysis.....	216
6.3 Shape analysis: Principal moments of inertia.....	217
6.3.1 PMI plot binning.....	217
6.4 Data for the 'bottom-up' compound library	221
6.4.1 Lead-likeness assessment: Per scaffold basis.....	221
6.4.2 Lead-likeness assessment: Per building block basis	227
6.4.3 PMI assessment: Per scaffold basis	229
6.4.4 PMI assessment: Per building block basis	231
6.5 Data for the 'top-down' compound library.....	233
6.5.1 Lead-likeness assessment: Per scaffold basis.....	233
6.5.2 PMI assessment: Per scaffold basis	237
7.0 Appendix 2: NOESY and HMBC Spectra	240
8.0 References	257

Symbols and abbreviations

9-BBN	9-borabicyclo[3.3.1]nonane
δ	chemical shift
μ	mean
σ	standard deviation from the mean
λ	wavelength
AAA	asymmetric allylic alkylation
Ac	acetyl
acac	acetylacetonate
ACD	Available Chemicals Directory
AlogP	logarithm of the partition coefficient (atom-based prediction)
Ar	aryl
Bn	benzyl
Boc	<i>tert</i> -butyloxycarbonyl
br.	broad
Bu	butyl
Bz	benzoyl
CAS	Chemical Abstracts Service
Cbz	carboxybenzyl
cf.	<i>confer</i>
clogP	logarithm of the partition coefficient (fragment-based prediction)
COSY	correlation spectroscopy
CPBA	chloroperbenzoic acid
CSA	camphor sulfonic acid
Cy	cyclohexyl
d	doublet
Da	Daltons
DACH	diaminocyclohexyl
DEPT	distortionless enhancement through polarisation transfer
DIBAL	diisobutylaluminium hydride
DIPEA	<i>N,N</i> -diisopropylethylamine
dr	diastereomeric ratio
DMAP	4-dimethylaminopyridine
DMF	<i>N,N</i> -dimethylformamide
DMSO	dimethylsulfoxide
DOS	diversity-oriented synthesis
<i>E</i>	<i>entgegen</i>
EDCI	1-ethyl-3-(3-dimethylaminopropyl)carbodiimide
ee	enantiomeric excess
e.g.	<i>exempli gratia</i>
EI	electron impact
ESI	electrospray ionisation
eq.	equivalents
er	enantiomeric ratio
Et	ethyl
FBDD	fragment-based drug discovery
FDA	US Food and Drug Administration
Fsp ³	fraction of sp ³ hybridised carbons
GII	Grubbs' first generation catalyst
GII	Grubbs' second generation catalyst

GNB	graph-node-bond
GSK	GlaxoSmithKline
h	hours
HA	heavy atom count
HMBC	heteronuclear multiple bond connectivity
HMDS	hexamethyldisilazane
HMQC	heteronuclear multiple quantum coherence
HPLC	high performance liquid chromatography
HRMS	high resolution mass spectroscopy
HTS	high-throughput screening
Hz	Hertz
<i>i</i>	iso-
imid	imidazole
IR	infrared
<i>J</i>	coupling constant
L	laevrorotatory
L*	chiral ligand
LCMS	liquid chromatography mass spectrometry
LOS	lead-oriented synthesis
LRMS	low resolution mass spectroscopy
<i>m</i>	<i>meta</i>
m	milli
M	molar
mol%	mole percent
m.p.	melting point
Me	methyl
Mes	mesityl (2,4,6-trimethylphenyl)
min	minutes
MOM	methoxymethyl
MS	molecular sieves
mw	molecular weight
<i>n</i>	normal-
N	normal
n.d.	not determined
NBS	<i>N</i> -bromosuccinimide
NCS	<i>N</i> -chlorosuccinimide
NIS	<i>N</i> -iodosuccinimide
NME	new molecular entity
NMR	nuclear magnetic resonance
No.	number
nOe	nuclear Overhauser effect
NOESY	nuclear Overhauser effect spectroscopy
Ns	nitrophenylsulfonyl
<i>o</i>	<i>ortho</i>
[o]	oxidation
nr	no reaction
Nu	nucleophile
<i>p</i>	<i>para</i>
Ph	phenyl
PG	protecting group
PMI	principal moments of inertia
ppm	parts per million

Pr	propyl
py	pyridine, pyridyl
q	quartet
<i>R</i>	<i>rectus</i>
RCM	ring-closing metathesis
<i>R_f</i>	retention factor
RNA	ribonucleic acid
RO5	rule of five
rt	room temperature
s	singlet
<i>s</i>	secondary-
<i>S</i>	<i>sinister</i>
SCX	strong cation exchange
SPE	solid phase extraction
S _N	nucleophilic substitution
t	time
t	triplet
<i>t</i>	<i>tert</i> (tertiary-)
T	temperature
TBAF	tetrabutylammonium fluoride
TBS	<i>tert</i> -butyldimethylsilyl
TBHP	<i>tert</i> -butyl hydroperoxide
Tf	trifluoromethanesulfonyl
TFA	trifluoroacetic acid
THF	tetrahydrofuran
THP	tetrahydropyran
TLC	thin layer chromatography
TMP	2,2,6,6-tetramethylpiperidine
TMS	trimethylsilyl
Ts	<i>p</i> -toluenesulfonyl
TSA	toluenesulfonic acid
US	United States of America
vs	versus
<i>Z</i>	<i>zusammen</i>

1.0 Introduction

1.1 Challenges facing the pharmaceutical industry

In 2010, the pharmaceutical industry was the largest investor (~£4.5bn) in research and development in the UK, and furthermore, contributed £17bn to exports.¹ The challenges facing the sector are numerous² and, amongst others, include long and costly campaigns to prepare new drug candidates,³ income losses from expiring patents,⁴ diminishing drug pipelines,² healthcare systems that are increasingly cost-constrained,⁵ and tightened regulations.⁶⁻⁸ It is no surprise then that improving productivity in drug discovery has been framed as the sector's "grand challenge".³ However, perhaps most importantly, the high attrition rate of drug candidates in clinical trials has been marked as the biggest roadblock to the delivery of new treatments.³ The overall attrition rate (~96%) in early-stage drug discovery is crippling, and has ultimately been associated with poorly defined physical property constraints for the lead compounds from which drug candidates are derived.^{3,9-12}

1.2 An overview of the drug discovery process

Bioactive small molecules continue to dominate Man's ability to treat disease;¹³ of the 41 new molecular entities (NMEs) approved by the US Food and Drug Administration (FDA) in 2014, 29 were small molecules.¹⁴ Furthermore, this figure may underestimate the overall benefit of small drugs to patients.¹⁵

The purpose of drug discovery is to identify safe and effective new candidates for medical treatments. Drug discovery is currently a risky, lengthy (on average 13.5 years) and expensive (on average £1.8bn) process (Figure 1).³

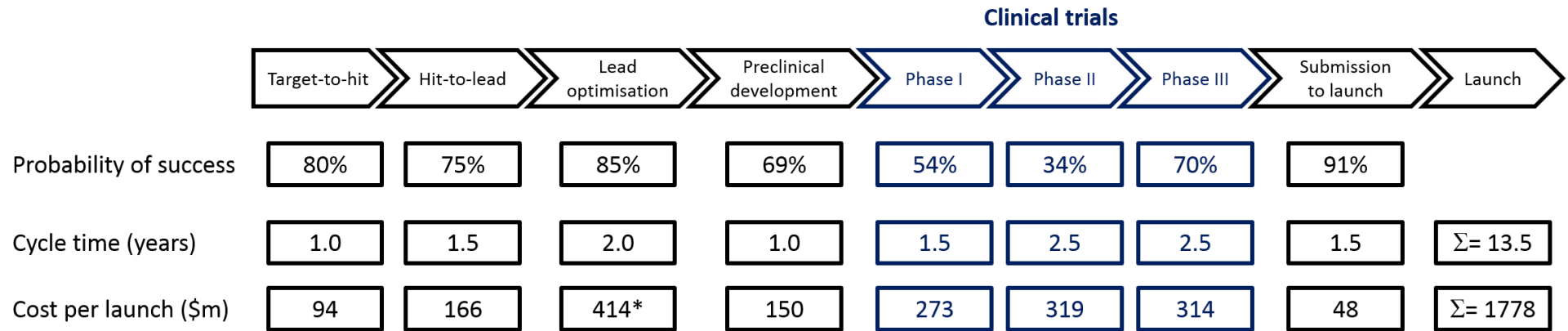


Figure 1 A summary of the key stages in drug discovery and their associated success rates, cycle times and costs. Does not include costs for target identification and validation, or for salaries for employees not involved in R&D but who are essential to support the organisation (accounts for an additional 20-30% in cost). *The cost for lead optimisation takes attrition into account. Image adapted from work by Paul.³

The drug discovery process starts with the identification of a druggable target (protein, gene, RNA *etc.*), which is validated using a range of chemical, biological and biophysical techniques.¹⁶ Typically, high-throughput screening (HTS) of large (>10⁵) libraries of diverse molecules is used to identify compounds which interact with the target.¹⁷ A compound which binds and inhibits (or activates) the target is called a “hit”. High-quality hits may be developed into “leads”. These leads are optimised (through the synthesis of analogues) to improve their affinity, selectivity and safety. The resulting final compound is termed a “drug candidate”, which must then successfully navigate clinical trials to become a marketable medication.¹⁶ An alternative method for small molecule drug discovery is to screen fragments (‘fragment-based drug discovery’, FBDD) and is discussed in Section 1.5.2.

Drug candidates are often prone to failure in clinical trials due to unforeseen complications, such as poor bioavailability, poor pharmacokinetic properties or unwanted toxicological effects. Attrition in phase II (66% of compounds) and phase III (30% of compounds) are the most important contributing factors for efficiency in R&D.³ Advances in cheminformatics in recent years have exposed an intrinsic link between the success of drug candidates in clinical trials and the molecular properties of the leads from which these candidates are derived.^{3,9,10} By preparing leads with more appropriate screening properties, it may be possible to reduce the failure rate,¹⁰ leading to substantial increases in productivity, a reduction in costs, and an increase in the likelihood of more new molecular entities (NMEs) reaching the market.

1.2.1 The role of synthesis in drug discovery

The early stages of drug discovery (hit-to-lead; lead optimisation) are heavily reliant on the availability of appropriate synthetic methods to deliver compounds for high-throughput screening. In recent years, synthetic efforts in the lead generation process have particularly focused on the preparation of small libraries (10-100 compounds) of drug-like molecules called “arrays”.¹⁸ However, a recent study by Macdonald found that of ~5000 reactions used to prepare arrays at GlaxoSmithKline (GSK), 63% of these reactions fell into just four reaction classes (alkylations, condensations, palladium-catalysed couplings, and protecting-group manipulations).¹⁸ A lack of methodologies that introduce new stereocentres was

also reported, despite evidence that lower attrition rates may be associated with clinical candidates containing more stereocentres.¹⁹ In addition, many reactions have limited success rates with building blocks containing polar medicinal chemistry motifs, prompting the need to re-tool methodologies for use in array synthesis.^{20,21}

As a result of the routine use of a limited number of reactions in medicinal chemistry,^{22,23} compounds prepared by medicinal chemists have typically only explored a limited area of chemical space. The lack of diversity in screening collections^{24,25} reflects the wider uneven and unsystematic exploration of chemical space: ~50% of all known compounds are based on just 0.25% of all the known small molecular scaffolds.²⁶ The introduction of multiple new methodologies that are broad in scope, robust,²⁷ and functional group tolerant will play a key role in allowing chemists to access more diverse screening collections in years to come.¹³

1.3 Characteristics of drug-like molecules

In recent decades chemists have developed criteria to assess the drug-likeness of small molecules;^{28–40} these analyses consider a range of physicochemical properties (molecular weight, partition coefficient (logP), number of hydrogen-bond donors and acceptors, polar surface area *etc.*). Most famously, in 1997 Lipinski's seminal 'rule of five' (RO5) paper introduced ideal physicochemical parameters to increase the bioavailability of orally available drugs (Table 1).²⁸ Such parameters can help guide medicinal chemists towards drug-relevant chemical space.

Entry	Physicochemical property	Ideal value
1	Molecular weight	≤500
2	logP	≤5
3	H-bond donors	≤5
4	H-bond acceptors	≤10

Table 1 Summary of Lipinski's 'rule of five' parameters.^{28,31}

It should be noted that any molecular property criteria for drug discovery are intended only as guidelines, but aim to represent chemical space that is known to give rise to safe and effective drugs. There are outliers to any defined drug space, and indeed preferred parameters for drug-like space differ between organisations as well as against different biological targets (for instance, to

modulate protein-protein interactions;⁴¹ and to penetrate the blood-brain barrier⁴²).

Molecular properties have a significant effect on the likelihood of success in drug discovery.^{3,9,10} Recent studies have shown that logP is generally the most important parameter to control.^{43–46} Parameters such as molecular weight, polarity, and the potential to hydrogen bond to a target are also extremely important,⁴⁷ but are ultimately entangled to some degree within the composite nature of logP. Molecules with high lipophilicities (clogp >3) generally experience increased binding to the biological target but also exhibit promiscuous and uncontrollable off-target binding. This off-target activity can amplify toxicological effects and markedly reduce the safety of the drug.⁹

Recently, the importance of shape in drug discovery has come to the fore.^{19,48} Compounds with higher fractions of sp³-hybridised carbons (Fsp³) have been found to have higher success rates in clinical testing and often have more favourable solubility properties than flatter molecules of similar size and logP.¹⁹ Furthermore, as drug candidates pass through development, those containing a large number of aromatic rings (≥3) are more likely to fail.⁴⁸

1.4 Characteristics of lead-like molecules

If chemists want to systematically target drug candidates that fall within typical drug-like space (e.g. Lipinski RO5 space, or similar), they must first be able to prepare leads which have appropriate properties to allow for the tendency for increases in lipophilicity, molecular weight and molecular complexity as the lead is optimised towards a drug candidate.^{49–53} A recent study of 62 lead/drug pairs showed that compared to leads, drugs have higher complexity, molecular weight and cLogP, and have more rotatable bonds, hydrogen-bond donors and acceptors.⁴⁹

A group of chemists at GlaxoSmithKline, led by Churcher, recently defined an ideal lead-like chemical space to facilitate the preparation of leads which allow greater flexibility in the optimisation stage of drug discovery (Figure 2, Table 2).¹⁰ In addition to constraints on lipophilicity, molecular weight and number of aromatic rings, the highlighted parameters also include filters to remove

undesirable substructures (chemically-reactive, electrophilic, or redox-active groups).

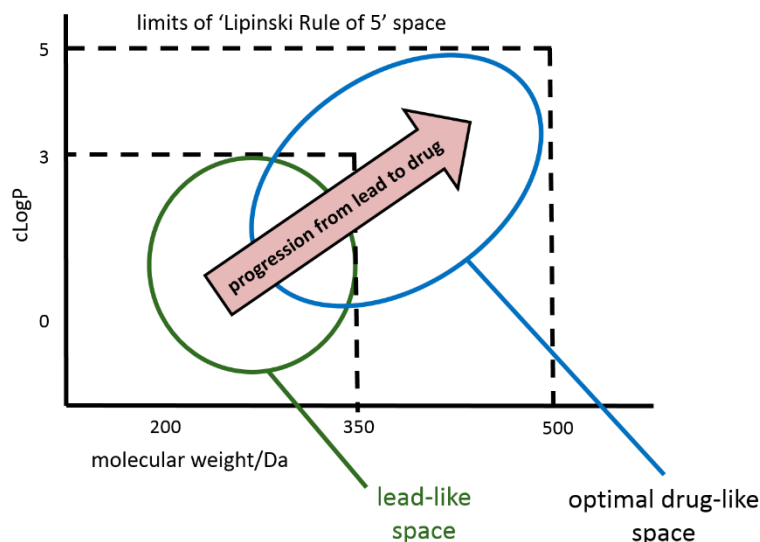


Figure 2 A Venn diagram showing lead-like space in relation to drug-like space. The pink arrow shows the typical drift in clogP and molecular weight as a hit is optimised towards a drug. Image adapted from work by Churcher.¹⁰

Entry	Physicochemical property	Ideal value
1	Molecular size	$14 \leq \text{Heavy atoms} \leq 26$ $\sim 200 \leq \text{mw} \leq 350 \text{ Da}$
2	Lipophilicity	$-1 < \text{clogP} < +3$
3	No. aromatic rings	1-2 ^a
4	Shape	High F_{sp}^{3a}
5	Substructures	Absence of chemically-reactive, electrophilic or redox-active groups

Table 2 Summary of Churcher's lead-likeness rules.¹⁰ ^aInterpreted from discussion in the text.

The above study also assessed the lead-likeness of 4.9×10^6 commercially available compounds and found that just 2.6% fell within the desired parameters. In addition, all of the reaction products formed in *The Journal of Organic Chemistry* in 2009 were assessed. Just 2.0% of the 32,700 compounds assessed were found to be lead-like. Consequently, it was inferred that sourcing large numbers of diverse compounds with the desired lead-like properties for screening would be a major challenge.

A logP drift in array chemistry was also noted, whereby final compound libraries were often found to be more lipophilic than intended. This was attributed to the poor tolerance of many methodologies towards polar functionalities, with the less polar array compounds having a better chance of being prepared and isolated. The concept of lead-oriented synthesis (LOS) was introduced to develop

synthetic methodologies that are robust towards polar functionalities and that systematically allow for the preparation of diverse new leads using array approaches (discussed further in Section 1.5.3). It remains a significant and largely unmet challenge.¹⁰

1.4.1 Diversity considerations

The diversity of a library of compounds can be considered from many points of view.⁵⁴ Here particular value is placed on skeletal diversity between compounds, as this is the most important factor when it comes to delivering molecules with diverse biological functions.^{24,55,56} Natural products arguably represent the most diverse collection of molecules currently available. Nature has produced vast numbers of stereochemically-complex secondary metabolites which have evolved through natural selection to modulate specific biological functions. Screening of natural products has historically generated several starting points for drug discovery.⁵⁷ However, there are several drawbacks associated with preparing screening collections based solely on natural products. As well as challenges in sourcing and isolating large numbers of natural products, they are not always susceptible to chemical modification and often their structures are not initially known. Furthermore many features of modern drugs (for instance polyfluorination) are typically not observed in natural products. A recent study by Ertl assigned 'natural product-likeness' scores to drugs, natural products and synthetic molecules.⁵⁸ Interestingly, while a lack of similarity between synthetic molecules and natural products was apparent, the largest proportion of drugs were found at the node between synthetic molecule space and natural product space (Figure 3).

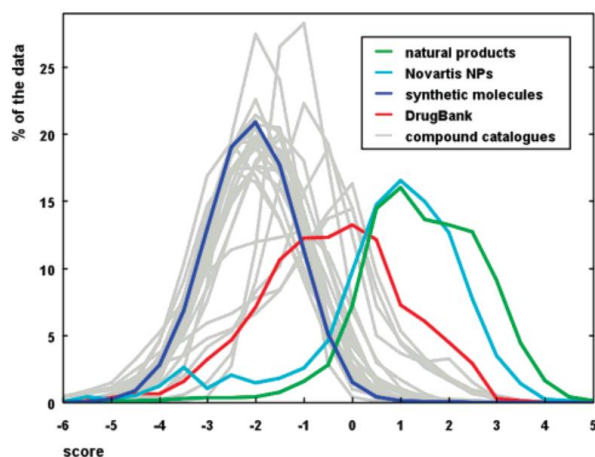


Figure 3 Ertl's natural product-likeness scores for drugs (red), natural products (green) and synthetic molecules (blue). The compound catalogues used for analysis of the synthetic molecules are shown in light grey. Image: Ertl *et al.*, *J. Chem. Inf. Model.* Copyright © 2008 American Chemical Society.⁵⁸

The above study suggests that the preparation of synthetic molecules which exhibit some features associated with natural products (such as the number of stereocentres, aromatic rings, nitrogen and oxygen atoms) may be of particular value to maintaining high-quality screening collections.

1.5 Approaches to the synthesis of diverse screening libraries

As discussed earlier, the exploration of chemical space has been uneven and unsystematic.²⁶ Recent decades have seen chemists begin to address the problem of diversity in screening libraries.^{11,59,60} This section will discuss a range of modern synthetic techniques which have been developed to address the lack of diversity in screening collections, with the overall aim of systematically targeting new leads, drugs, and/or tool compounds.

1.5.1 Diversity-oriented Synthesis (DOS)

Diversity-oriented synthesis, first introduced by Schreiber,⁶¹ aims to prepare a large number of structurally diverse compounds for use in HTS against untried targets with a view to identifying new leads, drugs, or chemical probes.⁶⁰ A range of synthetic strategies have been developed to prepare diverse libraries of compounds,^{54,62,63} and the most successful of these approaches is the 'build-couple-pair' strategy (Figure 4).⁶⁴ In this approach building blocks are prepared ('built'), linked together ('coupled') and subsequently cyclised ('paired').

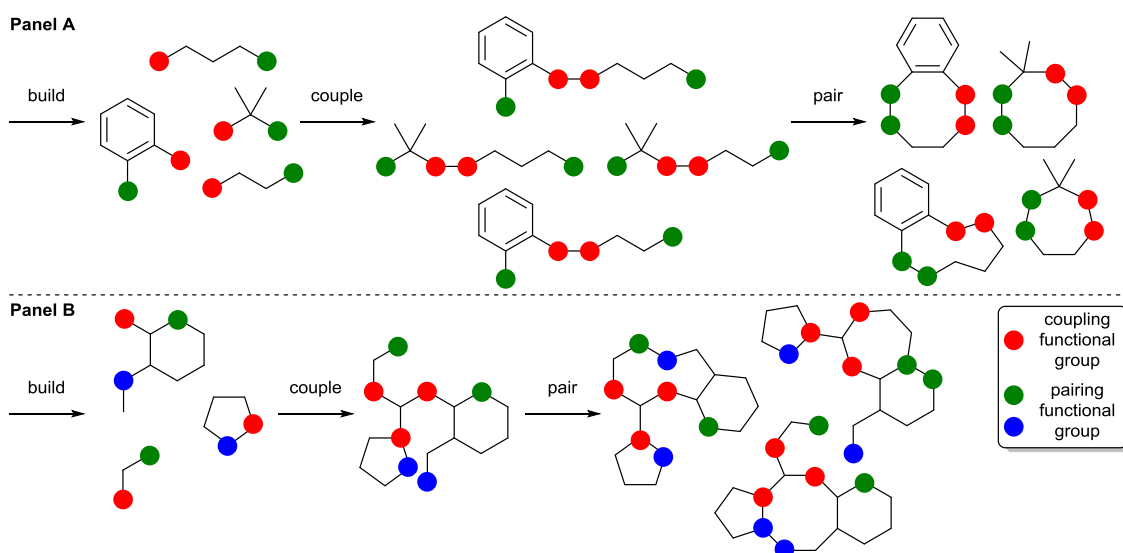
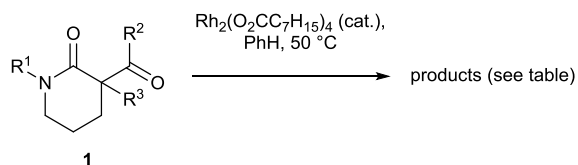


Figure 4 Build-couple-pair strategies in which coupling functional groups (red dots) are used to link together building blocks, the resulting assemblies are then cyclised through pairing functional groups (green and blue dots). **Panel A:** folding (substrate-based) diversification. **Panel B:** branching (reagent-based) diversification. Image reproduced from work by Spring.⁵⁴

Key examples of the ‘build-couple-pair’ strategy will be discussed herein.

1.5.1.1 Substrate-based DOS: Folding pathways

In ‘folding’ pathways, the application of a key common reaction to alternative building blocks provides access to different scaffolds.^{65,66} For instance, through the use of a unifying Rh(II)-catalysed tandem cyclisation-cycloaddition, Schreiber demonstrated that the careful choice of substrates **1** enabled the preparation of three distinct molecular architectures (Table 3).⁶⁶



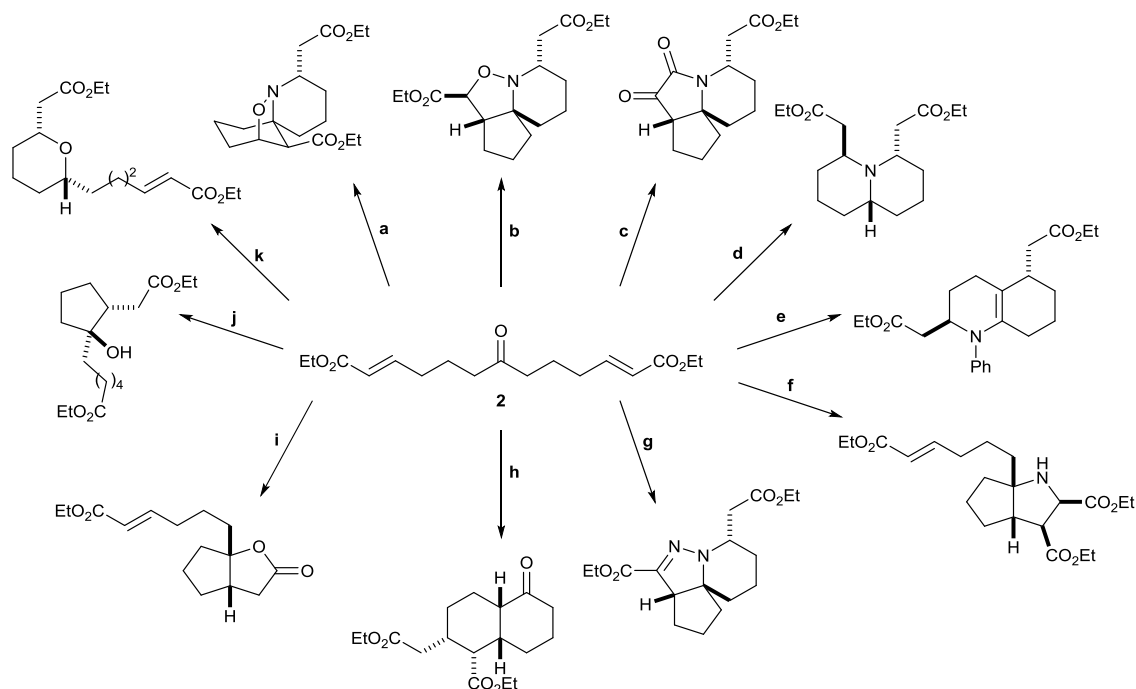
Entry	Starting material 1	Product
1		<p style="text-align: center;">74%</p>
2		<p style="text-align: center;">73%</p>
3		<p style="text-align: center;">57%</p>

Table 3 Schreiber's folding approach to DOS.⁶⁶

Some other approaches which exploit the folding pathway are based on the Achmatowicz reaction,^{65,67} three-component coupling reactions,⁶⁸ and, ring-closing metathesis cascades.⁶⁹

1.5.1.2 Reagent-based DOS: Branching pathways

In 'branching' pathways, the design of key polyfunctionalised intermediates enables downstream conversion to a range of molecular scaffolds through the use of different methodologies.^{70–72} For example, Stockman showed that the key intermediate **2** could undergo a range of cyclisation reactions to give access to diverse ring systems (Scheme 1).⁷² This strategy is especially efficient because in each case, a new molecular scaffold is prepared in ≤ 2 steps.

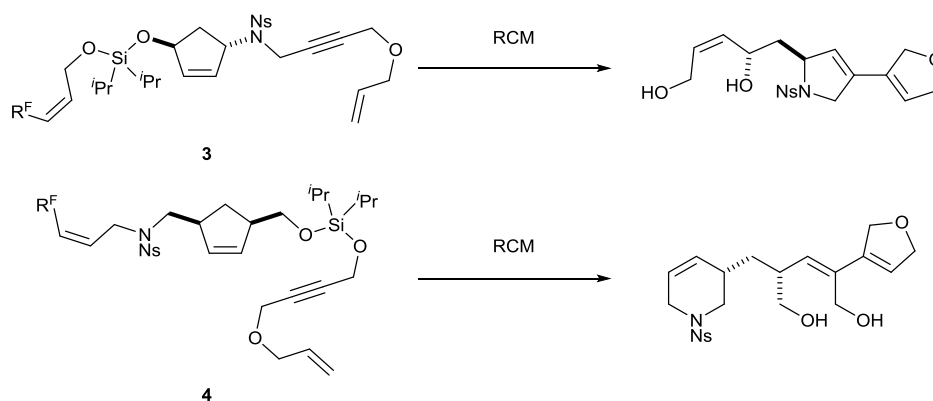


Scheme 1 Stockman's branching pathway.⁷² **Reagents and conditions:** (a) (i) $\text{NH}_2\text{OH}\cdot\text{HCl}$, NaOAc , MeCN . (ii) PhMe , μW 140°C , 36%; (b) $\text{NH}_2\text{OH}\cdot\text{HCl}$, NaOAc , MeCN , 60°C , 68%; (c) $\text{NH}_2\text{OH}\cdot\text{HCl}$, NaOEt , EtOH , 12%; (d) (i) NaBH_4 , NH_3 , EtOH , $\text{Ti}(\text{OEt})_4$, 74%. (ii) AcOH ; (e) PhNH_2 , TiCl_4 , CH_2Cl_2 , rt, 65%; (f) DIPEA , $\text{H}_2\text{NCH}_2\text{CO}_2\text{Et}$, 71%; (g) NH_2NHTs , PhMe , reflux, 41%; (h) NaH , THF , 70%; (i) Sml_2 (2 eq.), THF , MeOH , -78°C , 70%; (j) Sml_2 (5 eq.), THF , MeOH , -78°C , 70%; (k) superhydride, THF , 50%.

Other branching pathways exploit cyclisations of enynes,⁷³ *N*-allyl amino propargylic alcohols,⁷⁴ building blocks derived from the Petasis reaction,⁷¹ polymer-supported building blocks,^{75,76} and a fluororous-tagged diazoacetate.⁷⁰

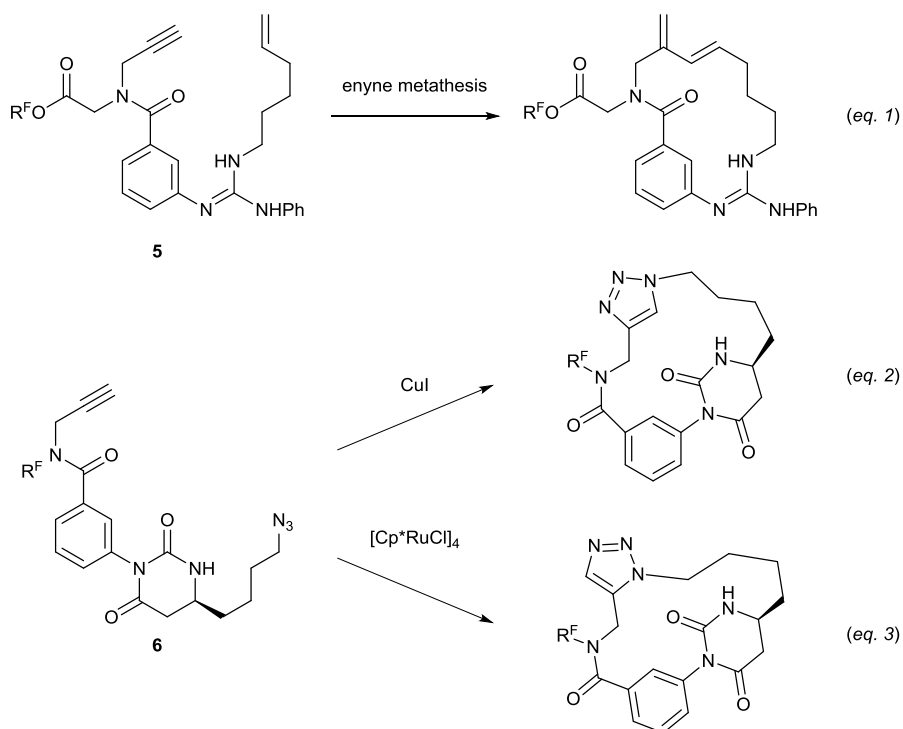
1.5.1.3 Oligomer-based approaches

In an oligomer-based folding approach by Nelson, carefully designed fluororous-tagged unsaturated building blocks (e.g. **3**, **4**) were subjected to ring-closing metathesis (RCM) cascade reactions (Scheme 2).⁷⁷ The use of fluororous tags allowed rapid purification of intermediates and final compounds *via* fluororous solid phase extraction (SPE). Through variation of different unsaturated linkers in the building blocks, a library of over 80 distinct molecular scaffolds was prepared.



Scheme 2 Nelson's oligomer based approach to DOS.⁷⁷ R_F= fluoruous tag. Illustrative examples from a review by Nelson and Marsden.¹²

Spring pioneered the use of oligomer-based approaches to prepare libraries of diverse macrocycles (Scheme 3).^{78–80} The iterative preparation of oligomers (e.g. **5**, **6**) terminating in alkenes, alkynes and azides enabled macrocyclisation through the use of enyne metathesis (equation 1), and both Cu- and Ru-catalysed 1,3-dipolar cycloadditions (equations 2 and 3).⁷⁹ In this way over 200 peptidomimetic compounds were prepared, which showed great diversity in molecular shape.⁷⁸



Scheme 3 Spring's oligomer based approach to the synthesis of diverse macrocycles.⁷⁹ R_F= fluoruous tag.

1.5.1.4 DOS: A summary

Diversity-oriented synthesis has played a crucial role in the development of effective strategies to prepare diverse compound libraries. However, there has

not been deliberate consideration of molecular property constraints in DOS approaches to focus synthetic efforts towards drug-like or lead-like compounds. In addition, because the number of possible molecules rises exponentially as molecular weight increases,⁸¹ the efficiency of the exploration of molecular shape is often poor for typical DOS compounds, which are frequently large.

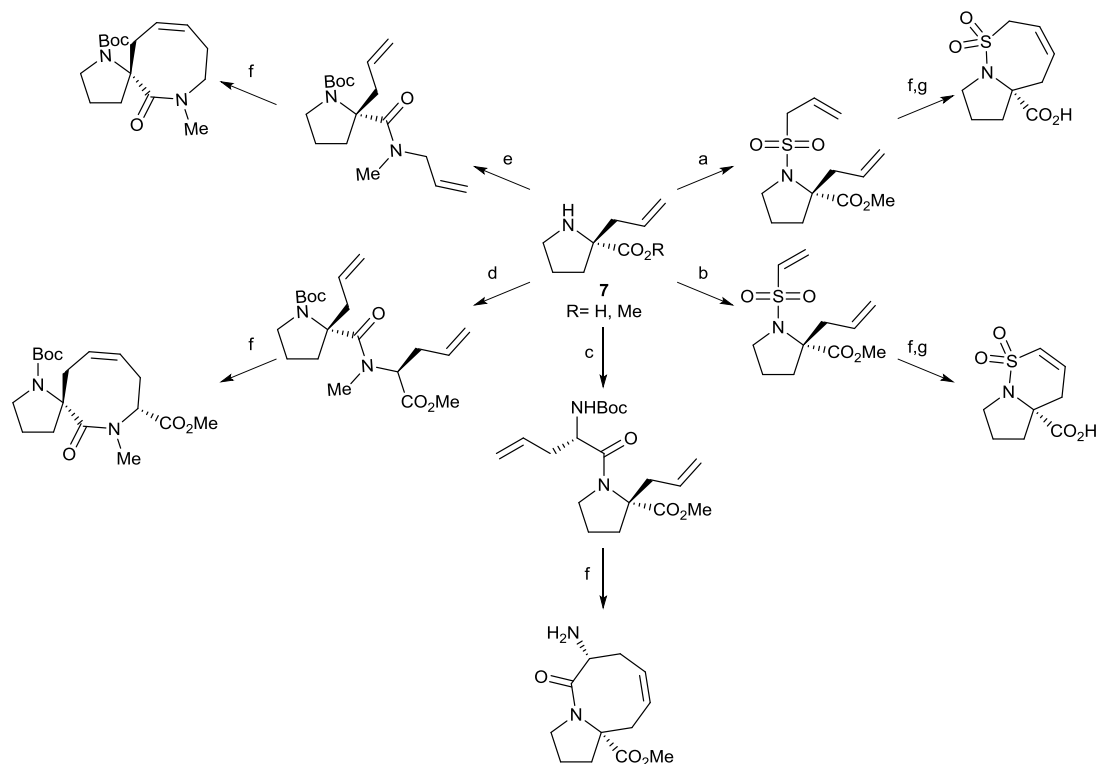
Fortunately, DOS is reaching maturity and the key strategies developed in the last two decades are now being shown to be readily refitted for use towards lead generation. Lead-oriented synthesis (LOS) incorporates elements of DOS to target the generation of new leads that efficiently sample chemical space and allow room for combinatorial variation of scaffolds (see Section 1.5.3 for further discussion).^{11,12,82}

1.5.2 Fragment-based drug discovery (FBDD)

Fragment-based drug discovery relies on the screening of smaller libraries ($\sim 10^3$) of small molecules (“fragments”). In contrast to DOS, a relatively small number of fragments are needed to efficiently cover a large area of chemical space.⁸³ The viability of this approach has been proven and has already resulted in a marketed drug (Vermurafenib). ‘Rule of three’ molecular property constraints (mw <300; clogP <3) are often used to guide the preparation of high-quality fragments.⁸⁰ However, a drawback of FBDD is that high-quality structural data is generally required to determine binding of a fragment to a target. X-ray diffraction of co-crystals of the fragment bound to the target, and/or NMR spectroscopy, is typically used to confirm binding. Due to their modest affinities (~ 1 mM) fragments are unlikely to be of use in phenotypic screens.⁸⁴ However, when measurable, affinities of the order of just ~ 1 mM can indicate high-quality interactions between a fragment and a target, since smaller molecules have fewer atoms with which to form favourable interactions with a target.⁸⁵ Fragment hits can be ‘grown’ into high affinity drugs through linkage to fragments which bind to other sites on the target, and through combinatorial modification.⁸⁶

FBDD and DOS can be combined in a complementary way. A folding DOS approach was recently used by Young to prepare three-dimensional fragments (Scheme 4).⁸⁷ Proline-derived building block **7** was armed with a variety of alkene-containing handles to facilitate cyclisation by ring-closing metathesis,

giving rise to a wide variety of bicyclic scaffolds. Although the authors prepared the scaffolds with a view towards fragment-based screening, there are several sites on the scaffolds which could be used for combinatorial derivatisation, which may give access to lead-like compounds.



Scheme 4 Young's DOS approach to 3-D fragments.⁸⁷ **Reagents and conditions:** (a) prop-2-ene-1-sulfonyl chloride, Et₃N, CH₂Cl₂, 44%; (b) vinylsulfonyl chloride, Et₃N, CH₂Cl₂, 62%; (c) (S)-N-Boc-allylglycine, EDCI, Oxyma, Et₃N, CH₂Cl₂, 48%; (d) (S)-allylglycine methyl ester, EDCI, Oxyma, Et₃N, CH₂Cl₂, 89%; (e) (i) allylamine, EDCI, Oxyma, Et₃N, CH₂Cl₂, 91%; (ii) NaH, MeI, dimethylformamide (DMF), 72%; (f) Gil, various conditions, 34-96%. (g) LiOH, THF, 53-71%.

1.5.3 Lead-oriented synthesis (LOS)

The concept of lead-oriented synthesis (LOS) was introduced to promote the development of synthetic methodologies that systematically allow for the preparation of diverse compounds within lead-like space. Particular value was placed on efficiency, appropriateness for array synthesis, compatibility with polar functional groups and avoidance of logP drift in the compounds prepared.¹⁰ The utility of LOS approaches may be evaluated in terms of the diversity of the scaffolds prepared and the molecular properties of accessible derivative compounds. The strategies herein focus on the preparation of specific and/or diverse scaffolds which lend themselves to further diversification with medicinal chemistry capping groups to give lead-like compounds.

1.5.3.1 Combinatorial considerations

In order to prepare large numbers of screening compounds based on specific scaffolds it is important to maintain the availability of high-quality medicinal chemistry capping groups for use in the combinatorial decoration of leads. For instance, against protein targets, capping groups can dictate which amino acid moieties a compound interacts with.⁸⁸

A recent study by Goldberg underlined the importance of capping groups to medicinal chemistry programmes. Data mining and the opinions of expert medicinal chemists were used to design a library of ~3000 custom capping reagents that were not found in the Available Chemicals Directory (ACD).⁸⁹ Particular focus was given to the preparation reagents (~20 g scale) that would provide broad utility against a range of target classes. Reagents were designed so that they would not add more than 200 Da in molecular weight, or alter the overall logP by more than 2 units, and had ≤ 2 hydrogen-bond donors and ≤ 4 hydrogen-bond acceptors (examples shown in Figure 5). Analysis of uptake of these reagents by medicinal chemists at AstraZeneca found that amine (especially secondary amine), carboxylic acid and boronic acid capping groups were most commonly used by medicinal chemists. Ultimately, since 2009 at AstraZeneca this initiative has resulted in incorporation of the reagents in three drug candidates, along with numerous short-listed candidates.

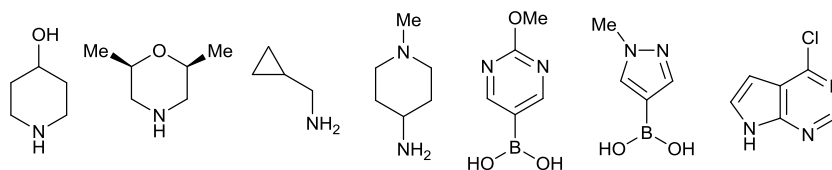
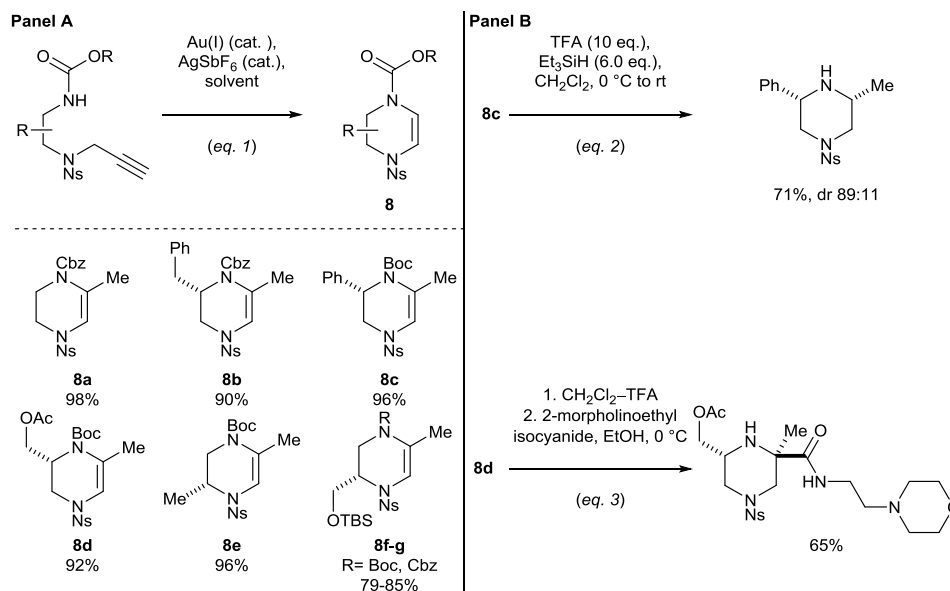


Figure 5 Examples of novel capping groups that were found to have 'unusually popular' uptake (used in >200 reactions) by medicinal chemists at AstraZeneca.⁸⁸

1.5.3.2 Lead-like arrays based on specific scaffolds

Making lead-like compound libraries is not necessarily difficult *per se*, but without careful planning comes at the expense of diversity. A number of methodologies are already in existence that would be appropriate to allow the preparation of specific classes of scaffolds.^{11,12} Combinatorial decoration of such scaffolds gives expedient access to arrays of lead-like compounds.^{90–93}

For instance, Nelson recently described the synthesis of piperazines **8** using a modular Au-catalysed approach (Scheme 5, Panel A, equation 1).^{90,92} The potential to prepare lead-like compounds from the scaffolds **8** was shown through (i) reduction using TFA/triethylsilane (Panel B, equation 2); and (ii) a multicomponent reaction with an isocyanide (Panel B, equation 3).⁹⁰

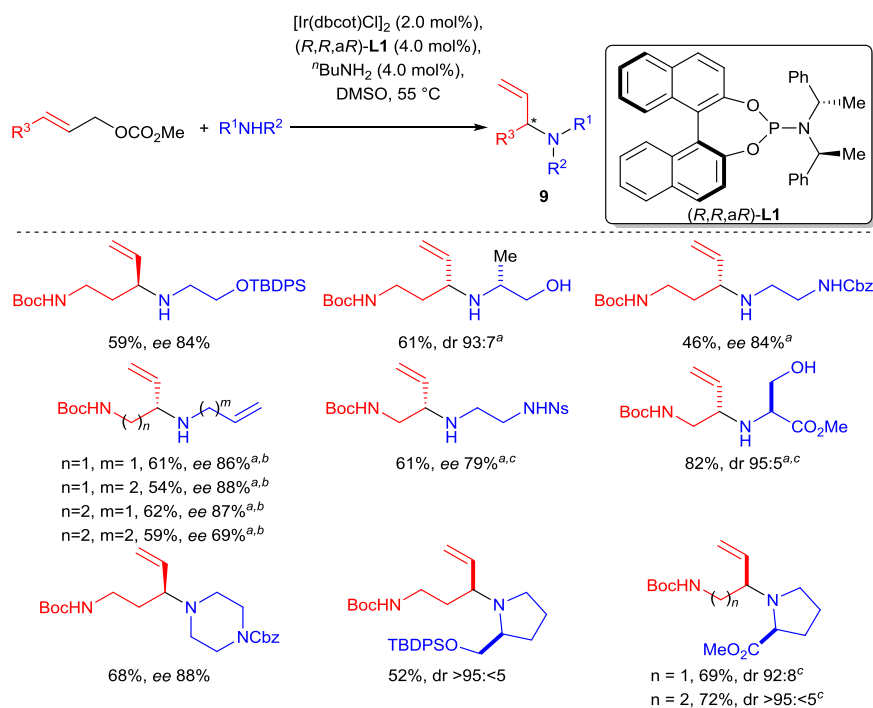


Scheme 5 Nelson's Au-catalysed piperazine synthesis (Panel A) and exemplar decorations to give compounds which may find value as leads (Panel B).⁹⁰

1.5.3.3 Unified approaches to diverse lead-like compounds

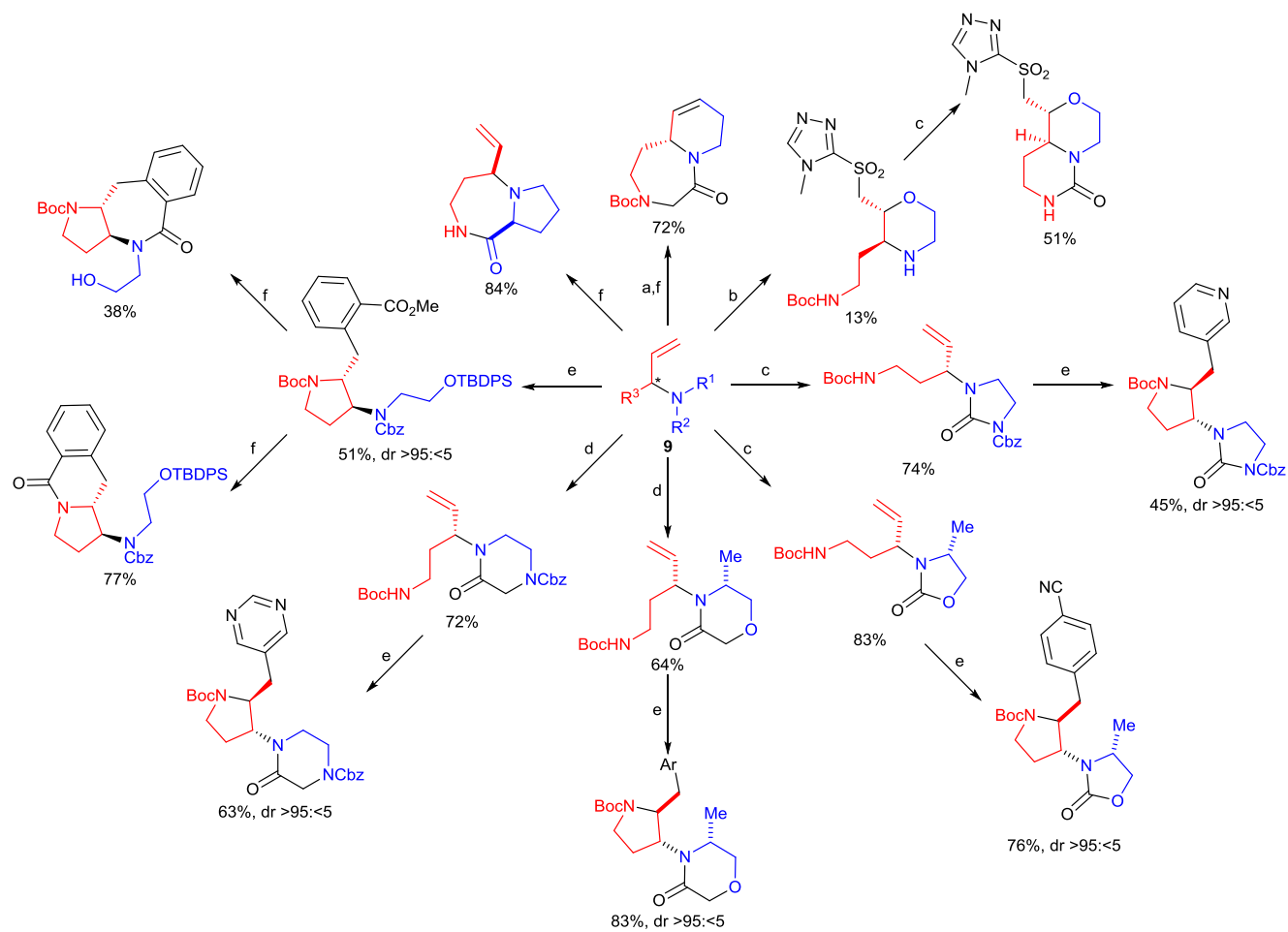
In order to fully realise the potential of LOS, the targeted preparation of compounds with lead-like properties must be incorporated into strategies (e.g from DOS) that enable access to diverse scaffolds. Sites for further decoration on the scaffolds would potentially give access to diverse screening compounds.

The candidate was recently involved in a LOS study led by Richard Doveston, Stephen Marsden and Adam Nelson which ran concurrently with the work described in this thesis.⁸² The preparation of a library of over 50 molecular scaffolds was realised by using a unified LOS approach. Ir-catalysed allylic amination, which was recently re-tooled for use with highly polar functionalities by Paolo Tosatti, Nelson and Marsden^{20,21} was used as a connective reaction to prepare 13 building blocks **9** as pre-cursors for cyclisation (Scheme 6).



Scheme 6 Ir-catalysed allylic amination of polar substrates to prepare building blocks **9** for later cyclisation.⁸²
^a(*S,S,aS*)-L1 used. ^bPrNH₂ and THF used. ^cThe amine HCl salt and K₃PO₄ (1.3 eq) were used.

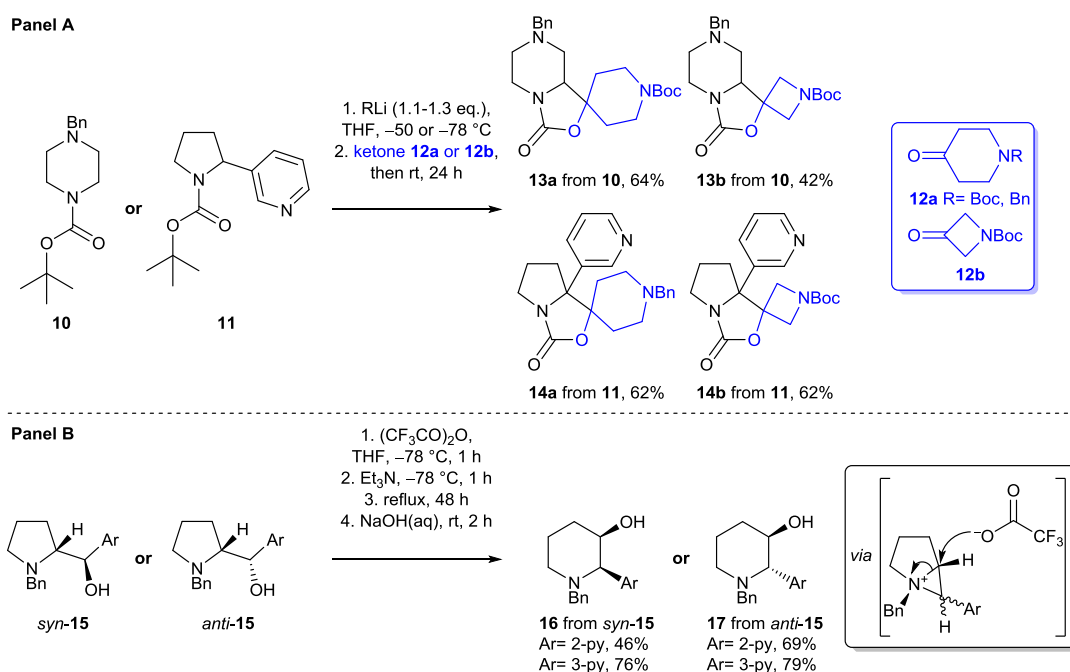
The building blocks **9** were exposed to a toolkit of just six distinct cyclisation strategies (ring-closing metathesis, iodocyclisations, urea/oxazolidinone formation, ketopiperazine/morpholine formation, aminoarylations, lactamisations) to form scaffolds (Scheme 7). In several instances the initial cyclisation products could be cyclised again, using the same toolkit of reactions, to give additional scaffolds. In total 52 diverse scaffolds were prepared in an average of two steps per scaffold.



Scheme 7 Exemplar scaffolds prepared from the building blocks **9** using a focused toolkit of cyclisation methodologies: (a) ring-closing metathesis; (b) iodocyclisations; (c) urea/oxazolidinone formation; (d) ketopiperazine/morpholine formation; (e) aminoarylations; (f) lactamisations.⁸² Ar = 3-pyrimidyl.

Virtual decoration of the compounds with 59 medicinal chemistry capping groups suggested that significant lead-like space may be accessed through combinatorial decoration of the compounds. Each compound was decorated twice with the 59 medicinal chemistry capping groups (except where a decoration step was used as part of the scaffold forming reaction [i.e. where the aminoarylation reaction was used]). In all, 59% (11,468) of the 19,530 derivatives enumerated would be lead-like, underscoring the value of our approach.

A recent study by O'Brien described the use of *N*-Boc-directed α -lithiation of amines to prepare six novel lead-like scaffolds that would be appropriate for combinatorial decoration to give screening compounds.⁹⁴ Reaction of the lithium carbanions generated from compounds **10-11**, with heterocyclic ketones **12a-b**, gave carbamates **13-14** (Scheme 8, Panel A). Alternatively, aminoalcohols **15** underwent a ring-expansion reaction, mediated by trifluoroacetic anhydride, to give scaffolds **16-17** (Panel B). Orthogonal deprotection of the scaffolds was demonstrated, then virtual decoration of the compounds with chosen capping groups enumerated a library of 190 potential screening compounds, of which 48% would be lead-like according to Churcher's criteria. In addition, 24% of the 190 derivatives were found to access underrepresented three-dimensional shape space compared to traditional pharmaceutically-relevant space.



Scheme 8 Synthesis of lead-like scaffolds using O'Brien's lithiation strategy.⁹⁴

In summary, robust methods for the preparation of large numbers of diverse lead-like compounds are beginning to emerge, but such studies still remain under-represented in the literature. As such there is still a substantial demand to increase the arsenal of complementary methodologies for LOS.

1.6 Project aims and thesis outline

The research described in this thesis is targeted towards the synthesis of large numbers of cyclic molecular scaffolds which, upon decoration, would provide access to broad regions of lead-like chemical space. In order to achieve this, strategies were devised relying upon the careful selection and synthetic preparation of specific classes of polyfunctional substrates. The modular application of small toolkits of broadly applicable cyclisation methodologies to these substrates allowed the generation of novel and diverse molecular scaffolds.

Chapter two describes the preparation of small polyfunctionalised precursors and their use in a building-up ('bottom-up') approach to synthesise scaffolds. Strategically this is analogous to the allylic amination strategy described in Section 1.5.3.3. In contrast, chapter three describes the preparation of larger polycycles which were deconstructed in a 'top-down' approach to give scaffolds. Chapter four goes on to compare the value of the different LOS approaches developed.

2.0 Results and discussion 1: A bottom-up approach to LOS

Our 'bottom-up' strategy for lead-oriented synthesis depended upon the synthetic accessibility of specific classes of small polyfunctionalised substrates which could be cyclised to afford scaffolds. We proposed to prepare quaternary amino acid derivatives as a representative class of such building blocks to meet this end. These substrates would bear four branch points which may be exploited to form scaffolds, or may later serve as points for further derivatisation to enable the preparation of subsequent compound libraries.

2.1 The selection of a connective reaction for LOS

The allylic alkylation of amino acid derivatives **18** was put forward as an established transformation which could deliver α -allyl, α -amino acid building blocks **19** (Figure 6). Inherent in these building blocks is an assortment of different functionalities which may be exploited in order to form scaffolds: alkenes can undergo a variety of cyclisation reactions and redox chemistry, esters are prone to nucleophilic substitution, amines can potentially be capped with a variety of different functionalised tethers, and there was also the possibility of introducing variable functionality through the amino acid side-chain.

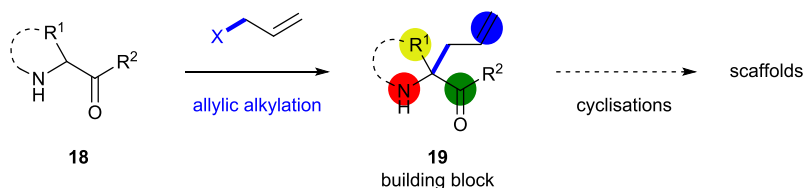


Figure 6 The proposed synthetic transformation to prepare polyfunctionalised building blocks. The coloured dots represent functionalities that may potentially be exploited to form scaffolds.

We envisioned a synergistic approach to LOS where computational tools could be used to direct synthetic chemistry. In order to systematically target lead-like compounds, we needed to assess the ability of known and speculative synthetic transformations to provide access to lead-like chemical space. A computational protocol was developed by Richard Doveston using Accelrys Pipeline Pilot to identify valuable methodologies for LOS which would then be exemplified synthetically (Figure 7).⁹⁵ Such tools were used throughout the course of the project to aid the decision making process, including: (i) the selection of appropriate connective reactions to prepare building blocks for LOS, and (ii) the

selection of appropriate methodologies to cyclise the building blocks to form scaffolds.

An illustrative example to show how Pipeline Pilot was used to identify methodologies for LOS is shown below (Figure 7): (i) the connective reaction of interest (in this case allylic alkylation) was performed; (ii) the cyclisation precursor was armed with a variety of different functionalised handles; (iii) chosen cyclisation methodologies were performed (these were typically based on good literature precedence, but more speculative transformations were also programmed); (iv) any latent functionality was cleaved using well-established functional group interconversions, especially with a view to removing any undesired substructures (the 'GSK B' filter described by Churcher was used¹⁰), and to generate points for further diversification; (v) the novelty of the scaffold was assessed against the ZINC database⁹⁶ of commercially available compounds (Murcko-assemblies⁹⁷ with and without substitution were mapped); (vi) each point for further diversification was decorated with medicinal chemistry capping groups (from a list provided by GSK) to generate a structurally diverse compound library; (vii) the properties of the compound library were assessed and a penalty point scoring system (Table 4) was assigned to the scaffold to give an indication of its ability to provide access to lead-like molecules.

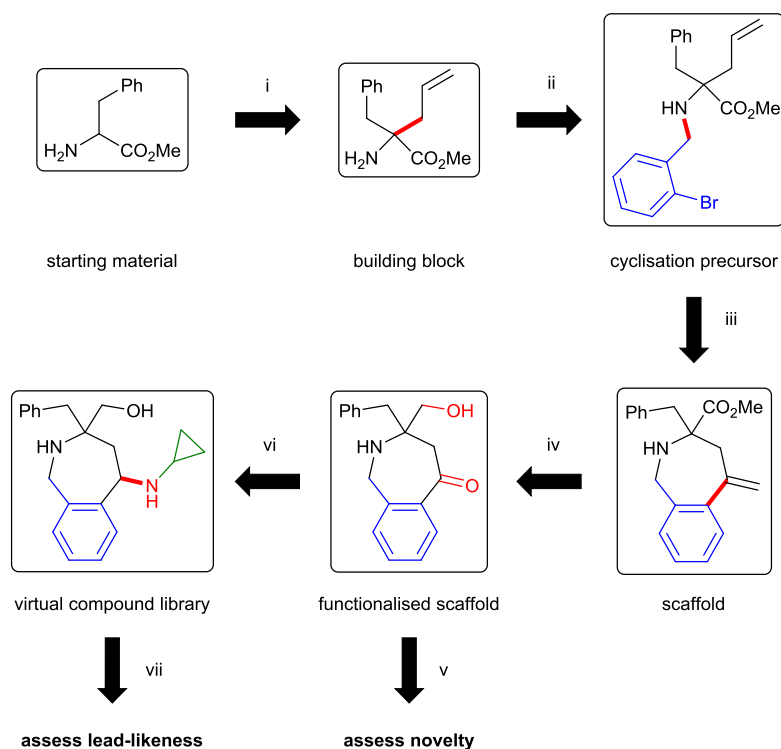


Figure 7 An illustrative example to show how Pipeline Pilot was used to identify methodologies for LOS: i) the connective reaction was performed; ii) the cyclisation precursor was armed with different functionalised handles; iii) chosen cyclisation methodologies were performed; iv) any latent functionality was cleaved using FGIs; v) the novelty of the scaffold was assessed; vi) each point for further diversification was decorated with medicinal chemistry capping groups; vii) the properties of the compound library were assessed (Table 4) and an average score was assigned to the scaffold to indicate its ability to provide access to lead-like molecules.

Property	Value	Penalty Score
Heavy Atom Count	17-24	0
	25 and 16	1
	26 and 15	2
	27 and 14	3
Lipophilicity (AlogP)	-1.0 - +3.0	0
	>3.0 and <-1.0	1
	>3.5 and <-1.5	2
	>4.0 and <-2.0	3
No. aromatic rings	1, 2	0
	0, 3	1
	4	2
	5	3
Biological interaction (sum of N and O atoms)	<4	2
Undesirable functionality	n/a	5

Table 4 A penalty point system was applied to determine how well the final decorated compounds map onto the lead-like parameters outlined by Churcher.¹⁰ This score was averaged over all of the decorated compounds that can be prepared from each scaffold, providing a mean score per scaffold. This score gives a good indication about whether a scaffold can readily access lead-like space (the lower the score, the more lead-like the scaffold is).⁹⁵

Using highly interactive data visualisation software (Dotmatics Vortex) we were able to determine which methodologies and building blocks may potentially prepare the most lead-like scaffolds (Figure 8), and we could then investigate the most promising methodologies synthetically. For instance, the bicyclic carbamate **20** is an example of an attractive scaffold to target synthetically, as it is novel (no substructure hits) and has the potential to access ca. 200 lead-like derivative

compounds (the average lead-likeness penalty for the decorated scaffolds ≈ 2). In contrast, the piperazine **21** is an example of a scaffold that is extremely well represented in commercially available compound libraries (17K substructure hits!) and was therefore not of interest as a synthetic target. Compounds derived from the scaffold **22** would have extremely poor lead-like properties due to high molecular weights and low ALogP, hence this scaffold may not be useful in a LOS programme.

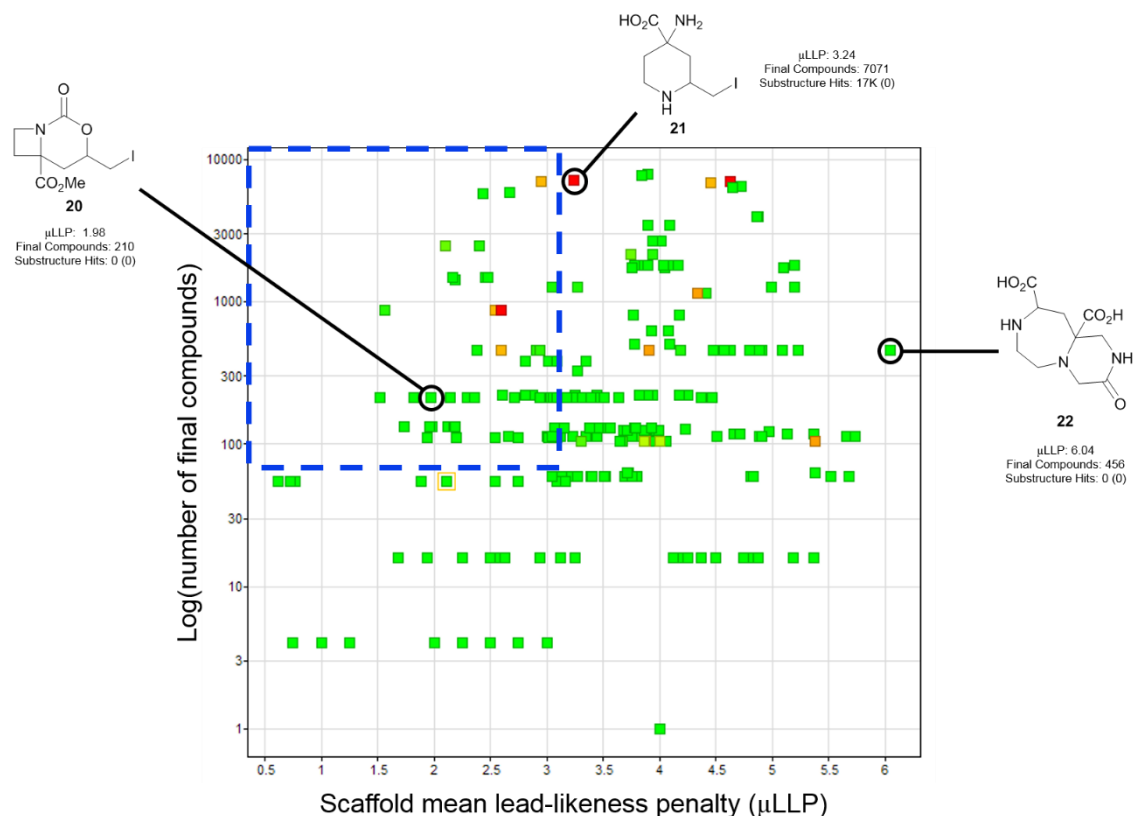


Figure 8 A useful plot to generate in Dotmatics Vortex was the log of the number of final decorated compounds that can be derived from each scaffold (y-axis) versus the average scaffold lead-likeness penalty (x-axis, see also Table 4). The data were coloured depending on the novelty of the scaffold (following a sub-structure search against the ZINC database [green= novel; red= known substructure]). The most interesting compounds fall at the top-left corner of the graph (marked by the blue box) where a scaffold can deliver large numbers of highly lead-like scaffolds. This highly interactive software enabled the candidate to identify which methodologies were associated with preparing the scaffolds found in this area of the graph. Substructure hits are for the Murcko fragment. The substructure hits for the Murcko fragment with alpha-attachments are shown in parentheses.

The significance of this computational protocol lies in the ability of the user to relate a potentially valuable scaffold to synthetically plausible routes. We inevitably programmed more hypothetical reactions than were ever successfully developed synthetically, but the tools helped us semi-quantitatively rank methodologies for development based on (i) their general ability to provide access to lead-like molecules and (ii) literature precedence. For instance, the tool indicated that both the oxyiodination reaction to form carbamates **23** (equation 1) and the aminoiodination to form diazepanes **24** (equation 2) would form scaffolds

that would be valuable in a LOS programme (Figure 9). However, when deciding which chemistry to apply synthetically, the oxyiodination was found to have good literature precedence,^{98–103} whereas the aminoiodination had no literature precedence. The development of the oxyiodination chemistry was therefore prioritised (see Section 2.3.1.1).

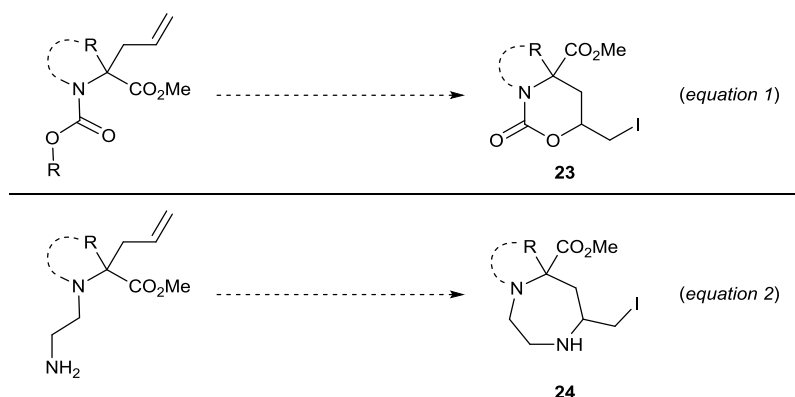


Figure 9 Proposed synthetic transformations for LOS.

Another important aspect of the computational tool is that it allows the user to identify unknown transformations that would broadly allow access to lead-like compounds (such as formation of diazepanes **24**, equation 2). Valuable new methodologies may then be developed based on their ability to target novel areas of chemical space.

In summary, we were able to semi-quantitatively determine that our proposed strategy involving the cyclisation of allylated amino acid derivatives had the potential to access many useful scaffolds for LOS, if some of the transformations that were shown to be valuable by the synthetic tools could be synthetically validated. Ultimately the computational tools are only as useful as the sum of the successfully developed chemistries that they directed. As a result of this, to provide clear evidence of success from an academic standpoint, it is perhaps more useful to retrospectively analyse the scaffolds that we found to be synthetically accessible and interrogate their potential ability to access lead-like space. Indeed such an analysis is included towards the end of the chapter (Section 2.5), following the discussion of the development of the suite of synthetic chemistry.

2.2 Selection of a suitable methodology for the allylic alkylation of amino acid derivatives

In order to demonstrate that the allylic alkylation of amino acid derivatives was indeed a suitable reaction for delivering exemplar polyfunctionalised cyclisation precursors, we needed to establish an appropriate synthetic strategy for their preparation. Ideally this approach would be high yielding, synthetically tractable and scalable. An enantioselective synthesis would be attractive, but not essential, since it can be advantageous to initially screen drug leads as racemates.¹⁰⁴

2.2.1 The asymmetric allylic alkylation (AAA) reaction

Transition metal-catalysed allylic substitutions are an extremely important and extensively studied class of transformations in organic synthesis (Figure 10).^{105,106} Allyl-metal complexes **25** undergo S_N2 or S_N2' substitutions with a range of nucleophiles to form new $C-H$, $C-C$, $C-F$, $C-O$, $C-N$ and $C-S$ bonds. These processes are catalysed by a range of transition metals including Cu, Ir, Ni, Mo, Pd, Pt, Rh, Ru and W. The nature of the metal has a profound effect on the regioselectivity of the reaction, whilst the use of chiral ligands can enable high levels of asymmetric induction.

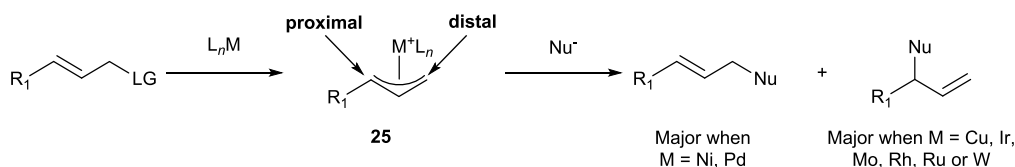


Figure 10 Regioselectivity in metal-catalysed allylic substitution reactions of terminal allylic electrophiles.¹⁰⁵

2.2.1.1 Asymmetric allylic alkylation (AAA) of amino acid derivatives: The Tsuji–Trost reaction

The Pd-catalysed allylation of nucleophiles (e.g. enolates [and equivalents], amines, phenols) by allylic acetates, bromides and carbonates to give linear products **26** was extensively developed by Trost from earlier work described by Tsuji (Figure 11).¹⁰⁵

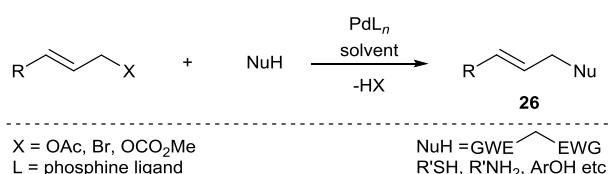
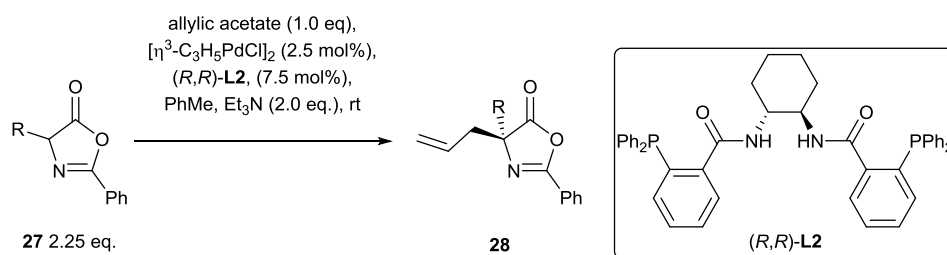


Figure 11 General conditions for the Tsuji–Trost reaction.¹⁰⁵

In one variant of the reaction, Trost developed the Pd-catalysed asymmetric allylic alkylation (AAA) of azlactones **27**, which are derivatives of amino acids.^{107,108} In the presence of the chiral ligand (*R,R*)-DACH-phenyl **L2** the reaction affords the linearly allylated quaternary azlactones **28** with a high degree of enantioselectivity (Table 5). Prenylation with either linear (entry 1) or branched (entry 2) prenyl acetate gave the linearly alkylated azlactones in good yields and with excellent enantioselectivity. Curiously, while linear cinnamyl acetate (entry 3) gave linearly alkylated azlactones, branched cinnamyl acetate (entry 4) gave a mixture of linear and branched products. The reaction also tolerated cyclic acetates (entry 5) and diacetylated starting materials (entry 6), proceeding to give the respective products in high dr. However, substitution at the central carbon of the allylating agent substantially decreased the enantioselectivity of the reaction (entry 7).



Entry	Allylic acetate	Product 28	R	Yield linear /% (Yield branched /%) [dr linear]	er linear (er branched)
1			Bn Me <i>i</i> Pr	72 (23) 55 (13) 57 (-)	99:1 (60:40) 98:2 (57:43) 97:3 (-)
2			Bn Me <i>i</i> Pr	78 (12) 67 (17) 47 (-)	99:1 (63:37) 99:1 (60:40) 95:5 (-)
3			Bn Me	91 (-) 74 (-)	95:5 (-) 93:7 (-)
4			Bn	45 (47 ^a)	95:5
5 ^b			Bn Me <i>i</i> Pr	74 [92:8] 90 [90:10] 77 [>95:5]	99:1 99:1 97:3
6			Bn Me <i>i</i> Pr ^b	75 [90:10] (6) 60 [87:13] (9) 88 [>95:5] (4)	99:1 (98:2) 99:1 (98:2) 99:1 (-)

Entry	Allylic acetate	Product 28	R	Yield linear /% (Yield branched /%) [dr linear]	er linear (er branched)
7			Bn	79°	55:45

Table 5 Selected examples of Trost's asymmetric allylic alkylations of azlactones.^{107,108}
^a68:32 mixture of diastereomers. ^bReaction performed at 0-5 °C. ^cReaction performed in MeCN.

2.2.2 Benchmarking the asymmetric allylic alkylation (AAA) of azlactones

We sought to establish the suitability of the Tsuji-Trost reaction for meeting the requirements of our lead-oriented synthesis programme. In particular we envisioned an overall three-component coupling strategy to prepare building blocks for LOS (Figure 12), whereby following the AAA of azlactones, a range of different nucleophiles could be utilised to introduce additional functionality into the building blocks. Deprotection and cyclisation reactions would then furnish scaffolds.

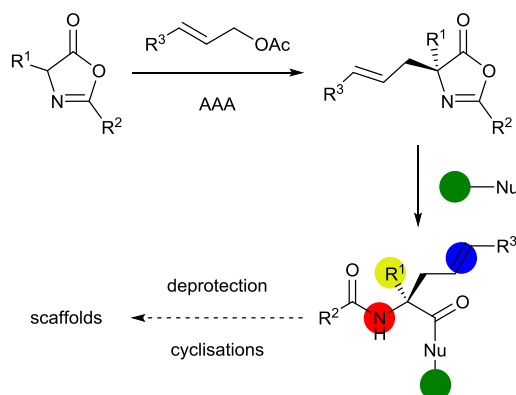
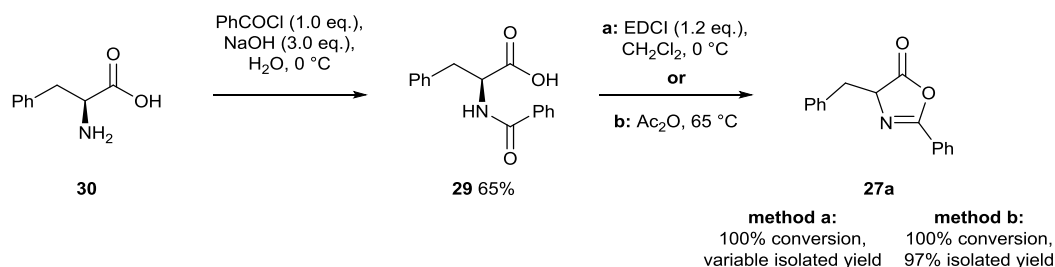


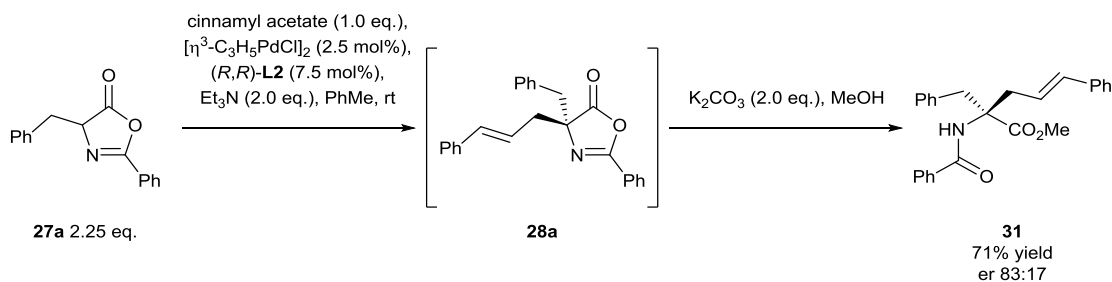
Figure 12 Proposed strategy for LOS by using the AAA of azlactones as a connective reaction. The coloured dots highlight functionalities that may potentially be exploited to form scaffolds.

To commence this study, we attempted the known cinnamylation (Table 5, entry 3) of azlactone **27a**.¹⁰⁸ Firstly, azlactone **27a** was prepared from the *N*-benzoylated amino acid **29**, which in turn was derived from *L*-phenylalanine **30** (Scheme 9). Preparation of azlactone **27a** by using EDCI as the dehydrating agent (route a) consistently gave 100% conversion to the desired product (as judged by analysis of the crude product by ¹H NMR spectroscopy).¹⁰⁹ However, the requirement for an aqueous work-up following the reaction invariably led to a significant amount of hydrolysis of azlactone **27a** to reform *N*-benzoylated amino acid **29**. In contrast, the use of acetic anhydride as the dehydrating agent (route b) gave a robust route to the desired azlactone **27a**, because exposure to an aqueous work-up could be avoided following the reaction.¹¹⁰



Scheme 9 Synthesis of azlactone **27a**.

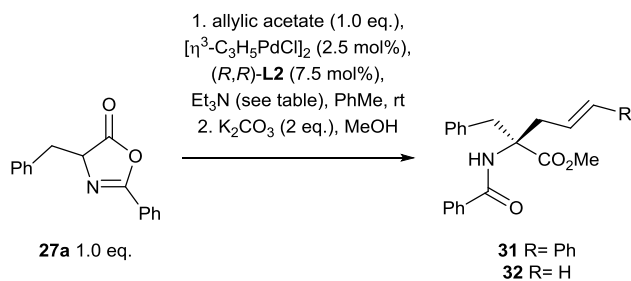
With azlactone **27a** in hand, known Pd-catalysed cinnamylation was carried out (Scheme 10).¹⁰⁸ Attempted isolation of quaternary azlactone **28a** by silica gel flash chromatography led to low yields of impure product due to hydrolysis on SiO₂. However, following alkylation, methanolysis of quaternary azlactone **28a** furnished protected amino ester **31** in 71% yield and in 83:17 er (as determined by chiral HPLC). The transformation was not optimised further at this stage.



Scheme 10 Pd-catalysed cinnamylation of azlactone **27a**, followed by subsequent methanolysis.

2.2.2.1 Optimisation of the Pd-catalysed AAA of azlactones

Given that the conditions described above required 2.25 equivalents of azlactone **27a**, optimisation for use of 1 equivalent of azlactone **27a** was sought in order to prevent the waste of any bespoke azlactone starting materials. One equivalent of cinnamyl acetate was reacted with the azlactone **27a** in the presence of different quantities of triethylamine as base, which enolised the azlactone and enabled reaction with the allyl electrophile (Table 6). This study found that one equivalent of base (entry 2) gave the highest yield whilst maintaining high levels of enantioselectivity. Interestingly, while the reaction worked without any base, it was sluggish (reaction incomplete after 6 h, entry 4). The optimal conditions (entry 2) were extended to allyl acetate to afford compound **32** in 72% yield (entry 5).



Entry	Allylic acetate	Et ₃ N /eq.	Yield /%	er*
1	Cinnamyl acetate	2	76	95:5
2	Cinnamyl acetate	1	78	95:5
3	Cinnamyl acetate	0.2	75	95:5
4 ^a	Cinnamyl acetate	0	68	94:6
5	Allyl acetate	1	73	n.d.

Table 6 Optimisation of the Pd-catalysed AAA of azlactones.
 *determined by chiral HPLC. ^a15 h reaction time.

2.2.3 Substitution at the azlactone carbonyl

Once conditions had been established for the Pd-catalysed AAA of azlactones, variation of the nucleophilic opening of the quaternary azlactone **28a** was considered (Figure 13). This step affects which functionalities can be installed at the carbonyl of the building block, and hence any downstream possibilities for cyclisation to form scaffolds.

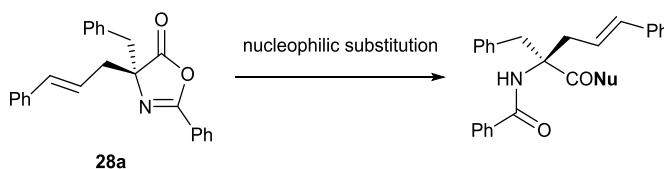
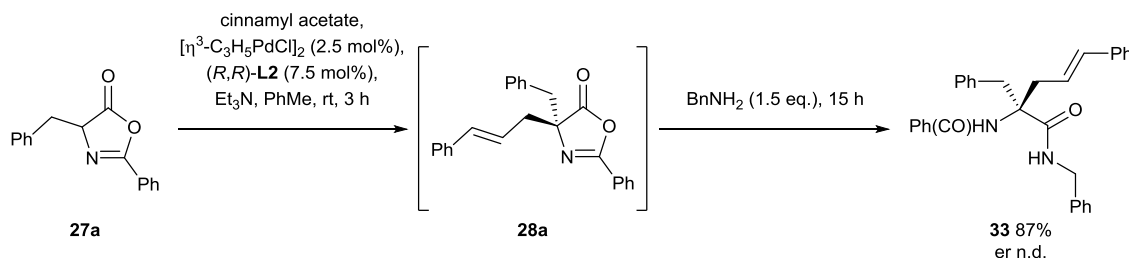


Figure 13 Proposed nucleophilic addition to azlactones.

2.2.3.1 Addition of *N*-centred nucleophiles

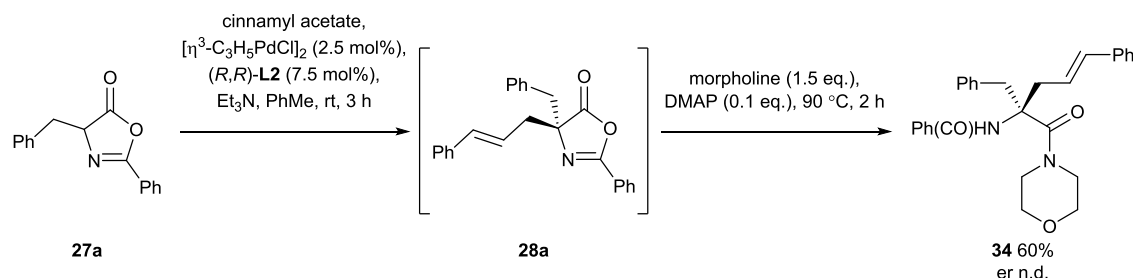
Quaternary azlactone **28a** was opened with benzylamine to give amide **33** in 87% yield (Scheme 11).^{111–113}



Scheme 11 Ring-opening of the quaternary azlactone **28a** with benzylamine.

Opening quaternary azlactone **28a** with a cyclic secondary amine, morpholine, was also possible (Scheme 12). This reaction did not take place at room temperature, as judged by analysis of the crude reaction mixture by ¹H NMR

spectroscopy, even following the addition of DMAP (0.1 eq.) as a nucleophilic catalyst. Fortunately, heating the resulting mixture to 90 °C gave access to the targeted secondary amide **34**, which was isolated in 60% yield (Scheme 12). The opening of quaternary azlactones with secondary cyclic amines has not been widely exploited in the literature.^{114,115}

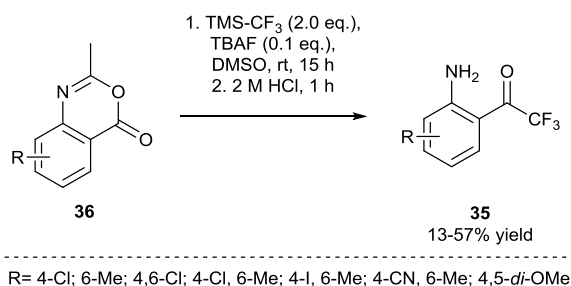


Scheme 12 Ring-opening of quaternary azlactone **28a** with morpholine.

2.2.3.2 Addition of C-centred nucleophiles

Recent years have seen large increases in the number of methodologies available for trifluoromethylation.¹¹⁶ In medicinal chemistry, ready access to fluorinated compounds is desired as they can display better membrane permeability, increased bioavailability and increased metabolic stability, when compared to their non-fluorinated analogues. In 2012, two of the top thirty best-selling drugs in the US contained trifluoromethyl groups, whilst five more were fluorinated in some manner.^{117,118}

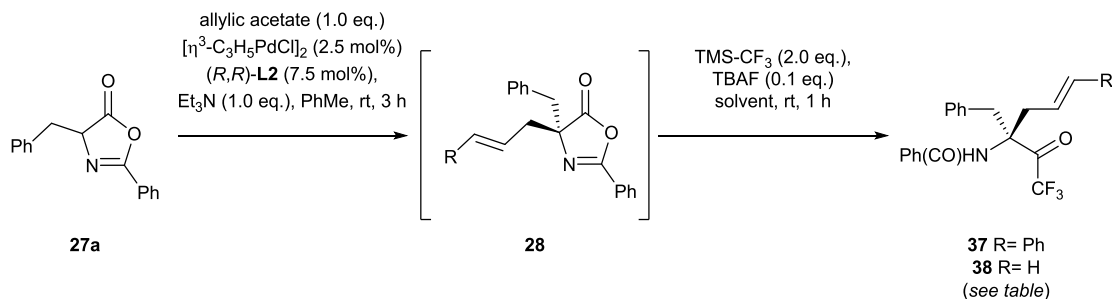
Bräse recently described the synthesis of trifluoromethylketones **35** through the fluoride-mediated addition of the Ruppert–Prakash reagent (TMS-CF₃) to benzoxazinones **36** (Scheme 13).¹¹⁹



Scheme 13 Bräse's synthesis of trifluoromethylketones **35** from benzoxazinones **36**.¹¹⁹

Under rigorously anhydrous conditions it was found that quaternary azlactones **28** could be opened by applying an adaption of Bräse's protocol, giving rise to trifluoromethyl ketones **37-38** (Table 7). Changing the solvent from DMSO to toluene (Table 7, entry 2) led to an increase in the yield of trifluoromethyl

ketone **37**, however these are preliminary studies and further investigations may improve this procedure in the future.



Entry	Allylic acetate	Product	Solvent	Yield /%*
1	Cinnamyl acetate	37	DMSO	52
2	Cinnamyl acetate	37	PhMe	63
3	Allyl acetate	38	PhMe	43

Table 7 Formation of trifluoromethyl ketones **37-38** from quaternary azlactones **28**. *er n.d.

2.2.4 Deprotection of *N*-amido protected amines

One of the major limitations of the AAA of azlactones was the presence of the phenyl ring at the C-2 position of azlactone **27**. Following the addition of a nucleophile to quaternary azlactone, the C-2 substituent goes on to form a benzamide **39** which can be regarded as an amine protecting group (Figure 14). Removal of this protecting group to release the free amine **40**, under mild conditions, would be essential to fully realise the full potential of the AAA of azlactones in a LOS programme.

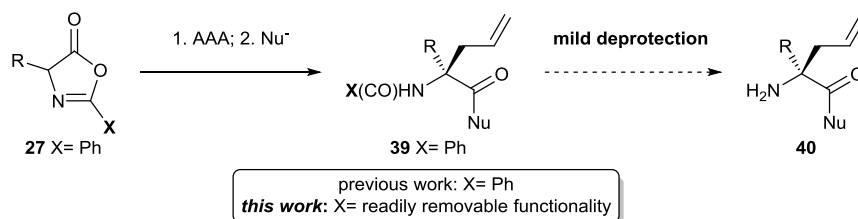


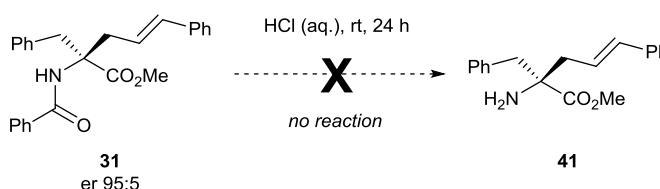
Figure 14 The required route to free amines **40**. The C-2 substituent (X) of azlactone **27** goes on to form an amine protecting group in compound **39**, which must then be deprotected to reveal free amine **40**.

The C-2 substituent must be derived from an amide. While there are a limited number of accounts detailing the preparation of azlactones bearing atoms other than carbon at the C-2 position, for instance, *O*-benzyl and *O-tert*-butyl substituents (which form the corresponding carbamate derivatives following the opening of the azlactone), the routes to prepare them are low yielding and alkylation of these substrates remains unknown.^{120–123}

2.2.4.1 Attempted deprotection of an *N*-benzamido protected amine

Typical literature conditions for deprotection of the *N*-benzoyl protecting group are harsh, requiring the use of concentrated aqueous acid at reflux with extended reaction times.^{108,124,125} Since we were interested in preparing azlactones bearing potentially sensitive functionalities (for instance Boc-protected alkylamino chains, silyl protected alkylether chains etc.), application of such conditions would not be synthetically useful as they would potentially result in the simultaneous deprotection of the side-chain.

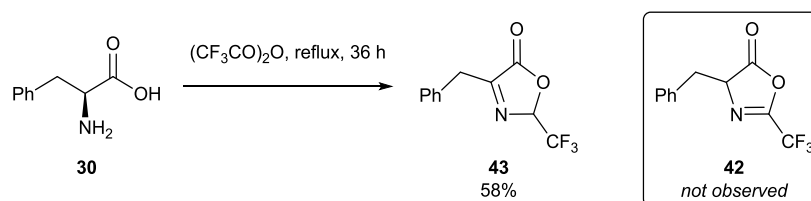
In an attempt to hydrolyse the *N*-benzoyl protected amino ester **31** under mild conditions, it was stirred with dilute acid at room temperature (Scheme 14). However, only starting material was observed after 24 h (as judged by analysis of the crude reaction mixture by ¹H NMR spectroscopy) when using 1 N, 2 N or 6 N hydrochloric acid.



Scheme 14 Attempted hydrolysis of benzamide **31** with hydrochloric acid at rt.

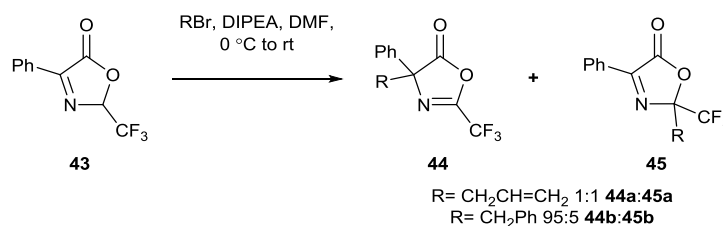
2.2.4.2 AAA of azlactones bearing a CF₃-substituent at C-2

The *N*-trifluoroacetyl group can be readily cleaved by alkanolysis under basic conditions and we sought to harness this protecting group in our strategy.¹²⁵ Preparation of the azlactone **42** was attempted by heating L-phenylalanine **30** in refluxing trifluoroacetic anhydride, following a procedure by Ries (Scheme 15).¹²⁶ However, careful analysis of the reaction product contradicted Ries' findings; the tautomeric pseudoazlactone **43** was identified as the only product. We subsequently found that this was consistent with the findings of several other research groups.^{127–129}



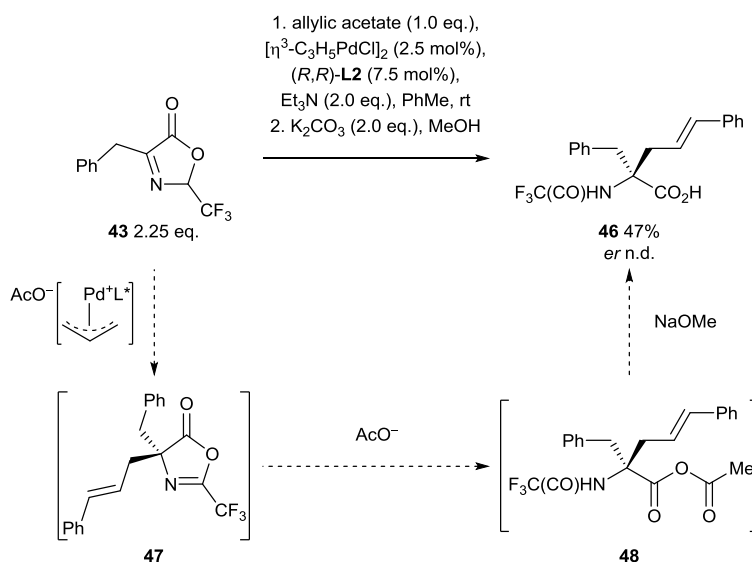
Scheme 15 Preparation of pseudoazlactone **43**.

With pseudoazlactone **43** in hand we decided to attempt the asymmetric allylic alkylation reaction. Heimgartner previously reported that simple alkylation of pseudoazlactone **43** was possible. Benzylation proceeded with high selectivity for the C-4 alkylated product **44b**. However, allylation gave a 1:1 mixture of the C-2 alkylated product **44a** and the C-4 alkylated product **45a** (Scheme 16).¹³⁰



Scheme 16 Alkylation of pseudoazlactone **43** by Heimgartner.¹³⁰

Exposure of pseudoazlactone **43** to Trost's AAA protocol resulted in successful alkylation (as judged by analysis of the crude product by ¹H NMR spectroscopy, Scheme 17). However, to our surprise only protected amino acid **46** was isolated. Attempts to prevent the formation of acid **46** by using a freshly-distilled batch of pseudoazlactone **43**, and by performing the reaction under rigorously anhydrous conditions, failed. We therefore postulated that, following allylic alkylation, the resulting trifluoromethylated quaternary azlactone **47** was highly electrophilic towards nucleophilic attack by acetate. Treatment of the resulting anhydride **48** with sodium methoxide then liberated the acid **46**. It was clear that a significant amount of study and optimisation would be required to improve the suitability of this reaction for LOS, which was beyond the scope of the project.

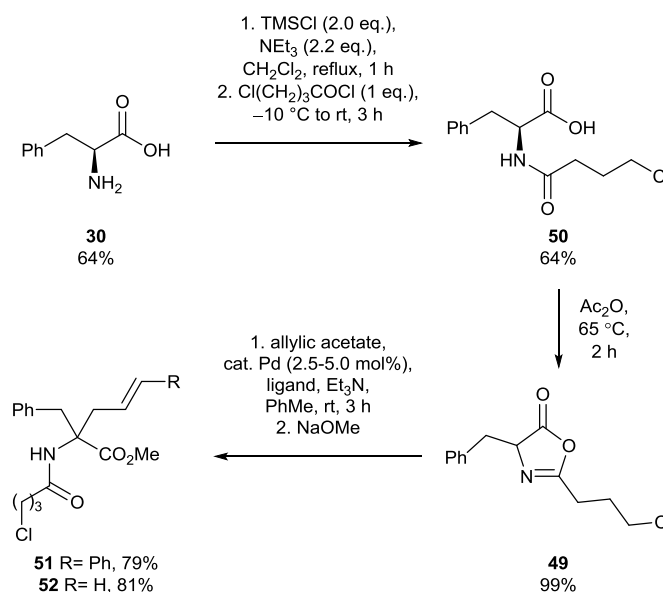


Scheme 17 Allylic alkylation of pseudoazlactone **43**.

2.2.4.3 AAA and deprotection of azlactones bearing a 4-chlorobutyryl substituent at C-2

We turned our attention to the possibility of using a protecting group which could be removed through a highly selective ‘triggered-release’ strategy. *N*-4-Chlorobutyryl protected amines can be deprotected through triggered-release reactions to give the corresponding free amine, and therefore we chose to investigate the use of this protecting group in our synthesis.^{131,132}

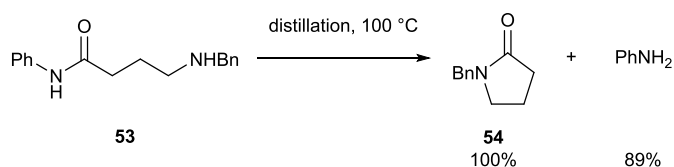
Azlactone **49** bearing a 4-chlorobutyryl substituent at C-2 was synthesised by following a procedure developed by Mandić to prepare the analogous phenylglycine-derived azlactone (Scheme 18).¹³³ Protection of phenylalanine **30** gave amide **50**, which was cyclised to give azlactone **49** using acetic anhydride. Pd-catalysed allylic alkylation, followed by methanolysis, gave the protected amino esters **51-52**. The cinnamylated product **51** was prepared using the aforementioned AAA protocol, whereas the allylated product **52** was prepared using Pd(PPh₃)₄ (see experimental for details).



Scheme 18 Synthesis of protected amino esters **51-52**.

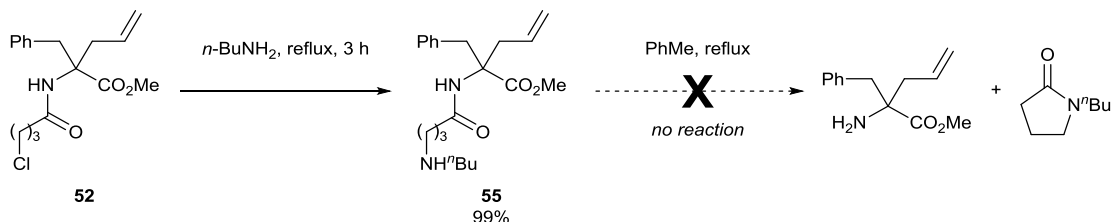
2.2.4.4 Attempted deprotection of an *N*-4-chlorobutyryl protected amine with butylamine

Stirling reported the deprotection of amide **53** using distillation to drive off the aniline released during the formation of lactam **54** (Scheme 19).¹³¹



Scheme 19 Stirling's amide deprotection *via* lactamisation.¹³¹

In an attempt to see if lactamisation would take place thermally, without the need for distillation, chloride **52** was substituted with *n*-butylamine. The resulting amine **55** was heated to reflux in toluene but no reaction took place (Scheme 20).

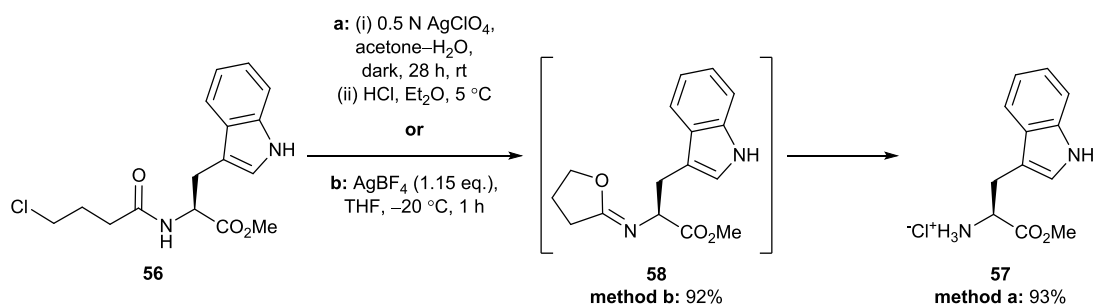


Scheme 20 Attempted deprotection of *N*-protected amino ester **55**.

As a result of the failure of this reaction we turned our attention towards an Ag-mediated deprotection.

2.2.4.5 Deprotection of an *N*-4-chlorobutryl protected amino ester with AgBF₄

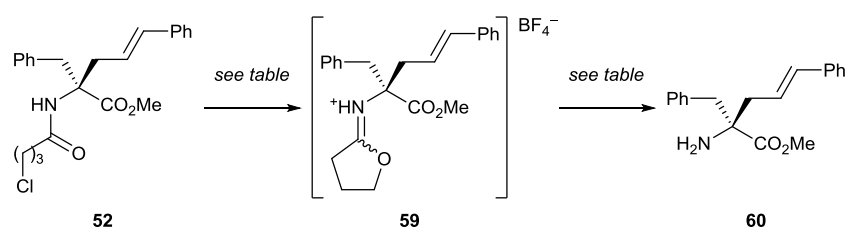
In 1963, Peter described the Ag-mediated deprotection of *N*-4-chlorobutrylated tyrosine methyl ester **56** (Scheme 21).¹³² Treatment of protected amino ester **56** with AgClO₄, followed by the addition of dilute hydrochloric acid, gave the ammonium salt **57** in 93% yield *via* the formation of iminolactone **58**. Alternatively, the use of AgBF₄ allowed the isolation of iminolactone **58**, providing a safer alternative to the use of potentially explosive AgClO₄.



Scheme 21 Deprotection of protected amino ester **56** *via* formation of iminolactone **58** by Peter.¹³²

Using Peter's protocol, protected amino ester **52** was treated with AgBF₄ in THF (Table 8). Analysis of the crude reaction mixture by ¹H NMR spectroscopy after 2 h showed complete conversion to the iminolactone tetrafluoroborate salt **59**. In

an attempt to isolate the iminolactone, Et₃N•HCl was added in the work-up (as described by Peter), however only re-formed starting material **52** was isolated (entry 1). It was subsequently found that the iminolactone tetrafluoroborate salt **59** could be isolated by simply filtering away the insoluble AgCl following the reaction (entry 2). Using Peter's one-pot deprotection conditions (condition a, Scheme 21), using AgBF₄ in place of AgClO₄, gave only partial conversion to the deprotected amine (entry 3). However, the use of a telescoped procedure where the iminolactone was first formed in anhydrous THF and then subsequently hydrolysed in acetone–water successfully furnished amine **60**, which was isolated in 95% yield.



Entry	Reaction conditions	Conversion*	Isolated Product (Yield)
1	(i) AgBF ₄ (1.1 eq.), THF, -20 °C to rt, 3.5 h. (ii) Et ₃ N•HCl (0.5 eq.)	100% 59	52 *
2	AgBF ₄ (1.1 eq.), THF, -20 °C to rt, 2 h.	100% 59	59 (80%)
3	AgBF ₄ (1.1 eq.), 1:1 acetone–H ₂ O, 4 days.	50% 60 25% 59 25% 52	–
4	(i) AgBF ₄ (1.1 eq.), THF, 0 °C to rt, 2 h. (ii) 1:1 acetone–H ₂ O, 15 h.	100% 60	60 (95%)

Table 8 Optimisation of the AgBF₄ mediated deprotection of compound **52**.
*As judged by analysis of the crude reaction product by ¹H NMR spectroscopy.

Whilst the optimised conditions for this deprotection worked nearly quantitatively, the use of stoichiometric silver salts was undesirable as they are expensive (AgBF₄ retails at £1411 mol⁻¹!).*

2.2.5 Critical analysis of the suitability of the AAA of azlactones for LOS

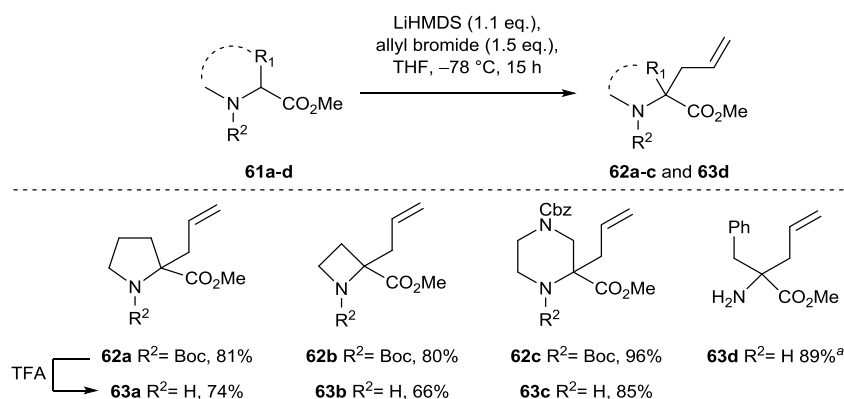
The AAA of the model azlactone **27a** with cinnamyl acetate was robust and gave good yields and high enantioselectivity. The resulting quaternary azlactone **28a** could be opened with *O*-, *N*- and *C*-centred nucleophiles. However, ultimately all

* Based on 50 g material, Sigma Aldrich, <http://www.sigmaaldrich.com/catalog/product/aldrich/208361?lang=en®ion=GB>, accessed 01/26/2015.

of the methodologies investigated to introduce a readily removable protecting group into the AAA strategy either failed, needed considerable optimisation, or were not scalable. As a result of this, alternative methodologies for the construction of quaternary amino acid derivatives were sought.

2.2.6 Preparation of quaternary amino esters by simple allylation

Due to the limited applicability of the AAA of azlactones to LOS, the allylation of cheap and readily accessible Boc-protected cyclic secondary amines **61a-c** and α -iminoester **61d** using LiHMDS and allyl bromide was investigated (Scheme 22).¹³⁴ This methodology was found to be broadly applicable and scalable, giving compounds **62a-c** in 80-96% yield. The Boc-groups of compounds **62a-c** were readily removed using TFA to furnish amino esters **63a-c** in 66-85% yield. Phenylalanine-derived amino ester **63d** was furnished in 89% yield by using an aqueous acidic work-up following allylation of α -iminoester **61d**.



Scheme 22 Allylation of protected amino esters **61a-c** (R²= Boc) and α -iminoester **61d** (R²= benzamine).
^aAqueous acidic work-up used.¹³⁵

The above reaction is more limited in terms of introducing functional handles into the building blocks **64** for cyclisation (this two component coupling lacks the final substitution step that the three-component AAA strategy offers, Figure 15). Nevertheless, the starting materials are readily available and this process also offers the advantage of being applicable to secondary cyclic amino esters (building in such rings using the AAA strategy may have taken several steps).

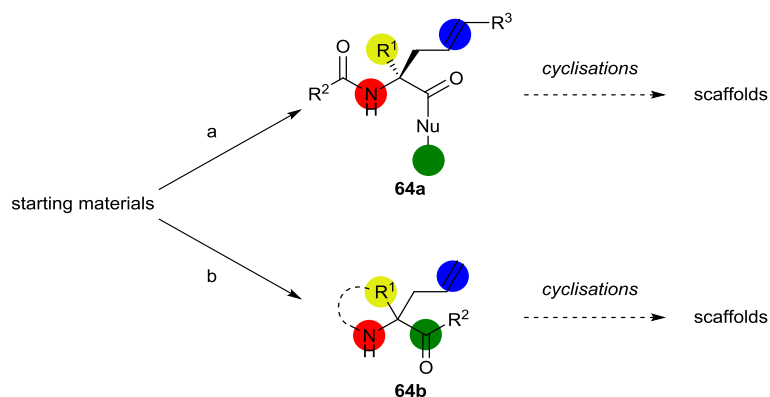


Figure 15 Differences between the points of potential connectivity available to form scaffolds when using the simple allylation methodology (method **b**) compared to the products of the AAA of azlactones (method **a**). The coloured dots highlight functionalities that may potentially be exploited to form scaffolds.

2.3 Establishing a chemical tool-kit: Synthetic strategy

Having established conditions for the connective reaction to synthesise quaternary amino esters **63a-d**, a tool-kit of reliable cyclisation methodologies was sought for the construction of lead-like molecules. It was proposed that the amine could be armed with a functional group (red) which would tune the precursor for cyclisation with either the adjacent alkene (cyan, equation 1) or the adjacent ester (green, equation 2) to form diverse cyclic molecules (Figure 16). Widely applicable and robust reaction methodologies were sought. Variation of the derivative scaffolds would be achieved by exploiting acyclic or cyclic amino acid starting materials **63a-d**; by varying the appended functionality (red); and by varying the cyclisation reaction. Methodologies were developed based on their potential ability to provide access to scaffolds that could generate expansive libraries of highly lead-like products as judged by using our computational protocol (as described in Section 2.1). In particular we sought to exploit the addition of nucleophilic tethers to alkenes and esters, and transition metal-catalysed reactions between the functional tether and the alkene.

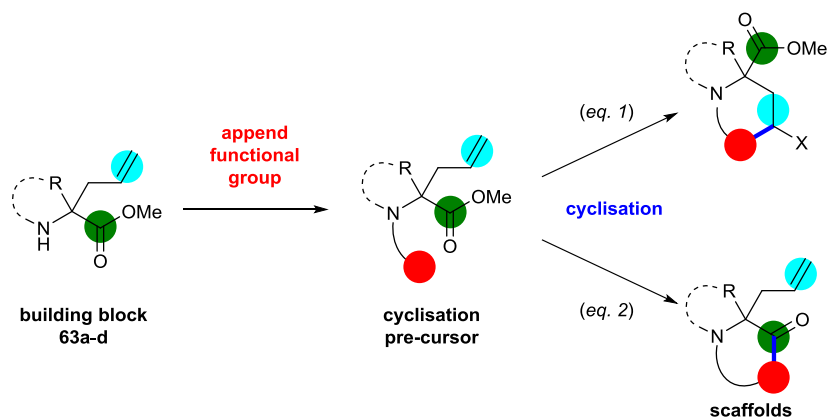


Figure 16 Proposed strategies for the cyclisation of quaternary amino esters.

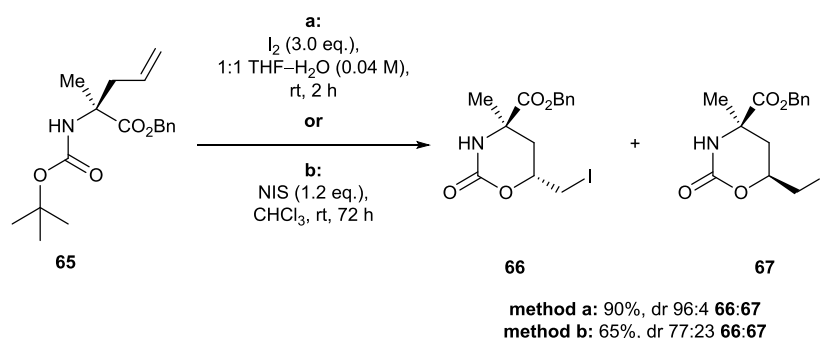
For the synthetic transformations that were successfully developed, a detailed interrogation of their ability to provide access to lead-like space is provided towards the end of the chapter (Section 2.5).

2.3.1 Cyclisations exploiting the electrophile-induced capture of tethered nucleophiles

1,2-Amino alcohols and diamines and their functionalised derivatives are prevalent in many bioactive compounds.^{136,137} We therefore explored oxy- and aminoamination through the reaction of alkene-iodine π -complexes with tethered nucleophiles, followed by substitution of the resulting alkyl iodides.^{98–102,138}

2.3.1.1 Oxyiodinations

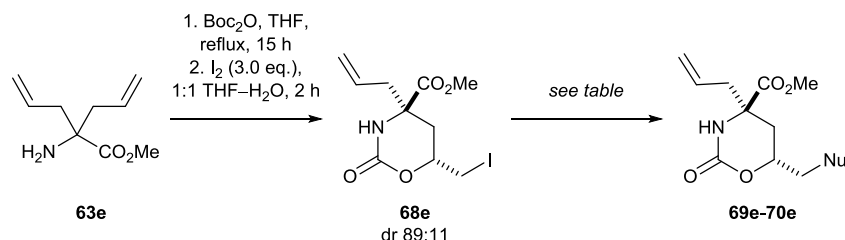
Licini described the cyclisation of the Boc-protected amino ester **65** with both molecular iodine and *N*-iodosuccinimide to give cyclic carbamates **66-67** with high diastereoselectivity (Scheme 23).¹⁰²



Scheme 23 Iodine-mediated cyclic carbamate synthesis by Licini.¹⁰²

Pipeline pilot confirmed that it would be valuable to apply this methodology to building blocks **62a-d**. In initial studies, the iodine-mediated cyclisation of the diallylated amino ester **63e** was investigated (prepared by dialylation of glycine – see experimental for full details). Boc-protection of compound **63e**, followed by treatment with iodine in 1:1 THF–H₂O, gave 100% conversion to alkyl iodide **68e**. Purification of compound **68e** proved challenging as it was unstable on SiO₂. However we saw this as an opportunity to displace the iodide with a range of nucleophiles which would either generate a point for further diversity, or introduce a decorative capping group which may be useful in the generation of derivative compound libraries (Table 9). Potassium phthalimide, a poor nucleophile, did not displace the iodide even when the reaction was heated (entries 1-2). Surprisingly,

the iodide decomposed in the presence of sodium and potassium phenolates (entries 3 and 5). Good nucleophiles such as sodium thiophenolate (entry 6) and sodium azide (entry 7) were found to readily displace the iodide to give compounds **69e** and **70e** respectively. We considered the azide functional handle to be particularly valuable as it had the potential to undergo reduction to the amine, or click reactions to introduce triazoles.

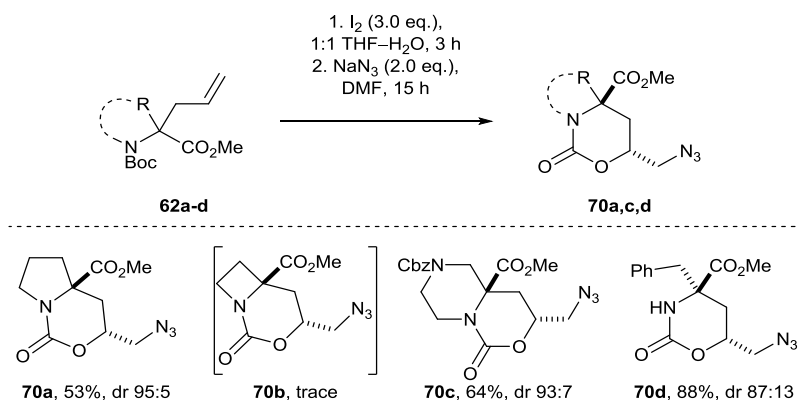


Entry	Nucleophile	Base	Solvent	T / °C	t / h	Yield / % (Conversion)*	No.
1	potassium phthalimide (2.0 eq.)	–	DMF	rt	15	nr	–
2	potassium phthalimide (2.0 eq.)	–	DMF	90	3	nr	–
3	PhOH (2.0 eq.)	NaH (2.0 eq.)	DMF	rt	15	decomposition*	–
4	PhOH (2.0 eq.)	K ₂ CO ₃ (4.0 eq.)	MeCN	rt	15	nr	–
5	PhOH (2.0 eq.)	K ₂ CO ₃ (4.0 eq.)	MeCN	82	15	decomposition*	–
6	PhSH (1.3 eq.)	DBU (1.4 eq.)	DMF	rt	15	80 (100)	69e
7	NaN ₃ (2.0 eq.)	–	DMF	rt	15	78 (100)	70e

Table 9 Displacement of alkyl iodide **68e** with nucleophiles.

*As judged by analysis of the crude reaction product by ¹H NMR spectroscopy.

Applying Licini's protocol to building blocks **62a-d**, followed by treatment of the resulting alkyl iodide with NaN₃, provided an overall oxyamination reaction to provide the cyclic carbamates **70a,c-d** (Scheme 24).



Scheme 24 Oxyamination of the Boc-protected amino esters **62a-d**.

The relative configuration of the minor diastereomer of the phenylalanine-derived carbamate **70d** was determined by an nOe enhancement between the benzylic protons and the proton alpha to the azidomethyl group (Figure 17).

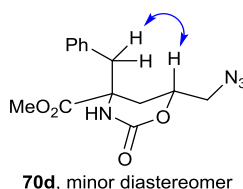


Figure 17 Key nOe enhancement for compound **70d**.

Crystallographic studies confirmed the relative configuration of the major diastereomer of proline-derived carbamate **70a** (Figure 18).

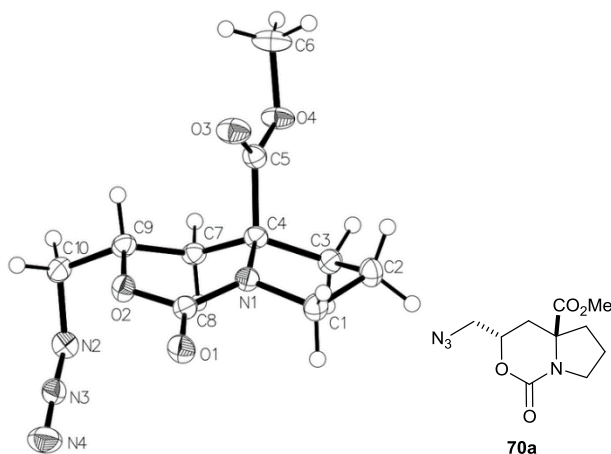


Figure 18 X-ray crystal structure of the proline derived carbamate **70a**.

Whilst the reaction was successful for phenylalanine, proline and piperazine-derived starting materials **62a,c-d**, the azetidine-derived starting material **62b** only gave a trace of product (Figure 19). This is because azetidine **62b** was undergoing a competing intermolecular hydroiodination process under the aqueous reaction conditions, giving rise to iodoalcohols **71-72** (as judged by analysis of the crude residue by ^1H NMR spectroscopy and LCMS). Since a trace of the targeted product **70b** was observed by analysis of the crude product by both ^1H NMR spectroscopy and LCMS (mass observed at 348.1, which corresponds to the $[\text{M}+\text{Na}]^+$ ion of the targeted cyclic carbamate **70b**) we can postulate that the required six-membered transition state **73b** can form under these conditions. The hydroiodination products **71-72** may therefore arise through the intermolecular addition of H_2O to the transition states **73a-b**, although we cannot rule out neighbouring group participation of the ester functionality (as in transition state **74**) and subsequent addition of H_2O . The favourability of the intermolecular pathway may arise from increased strain in the transition state caused by the presence of the azetidine ring.

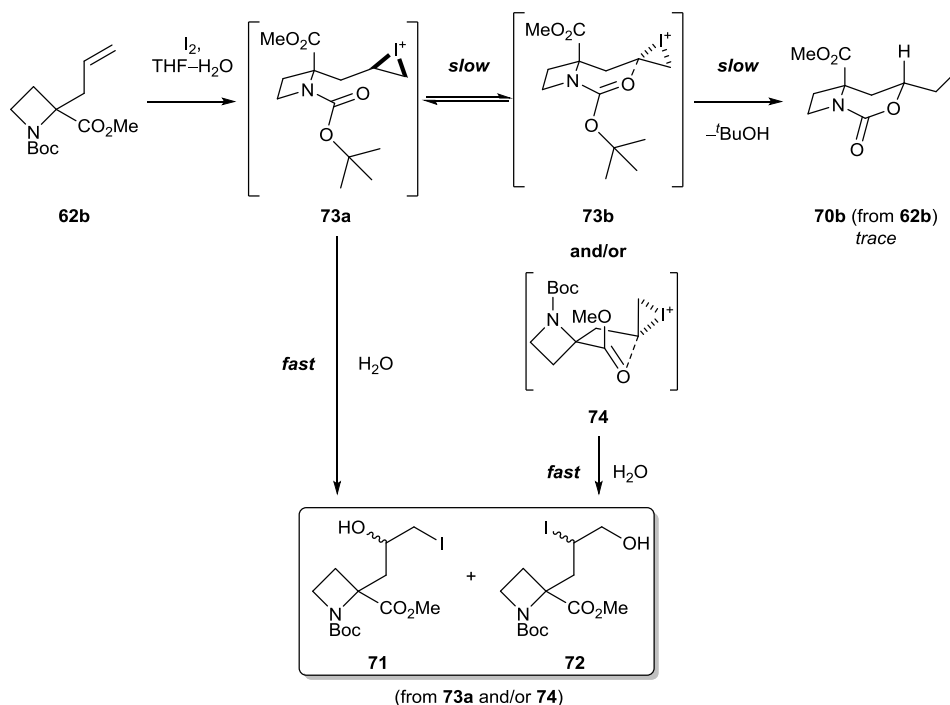
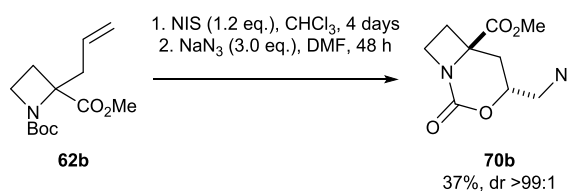


Figure 19 Attempted cyclisation of the Boc-protected azetidine **62b**.

The work of Licini also describes the use of anhydrous conditions of *N*-iodosuccinimide in $CHCl_3$ to give alkyl iodides **66-67**, albeit with poorer diastereoselectivity (Scheme 23). Applying these conditions to the Boc-protected azetidine **62b** gave the desired alkyl iodide, which was subsequently displaced with sodium azide to give compound **70b** (Scheme 25). Both steps of the reaction were extremely sluggish when compared with the analogous steps to prepare **70a,c,d** in $THF-H_2O$.



Scheme 25 Oxyamination of the Boc-protected azetidine **62b**.

2.3.1.2 Aminoiodinations

Following on from the success of the oxyiodination-displacement protocol, we chose to investigate analogous aminoiodination reactions to give access to biologically relevant cyclic ureas.¹³⁹ Unprotected cyclic ureas have the advantage of having an additional site to diversify when compared with the analogous carbamates. However, one difficulty with the halocyclisation of ureas **75** with alkenes lies in the ambident nature of the urea nucleophile, where *O*-cyclised products **76** are typically favoured over *N*-cyclised products **77** (Figure 20).^{140,141}

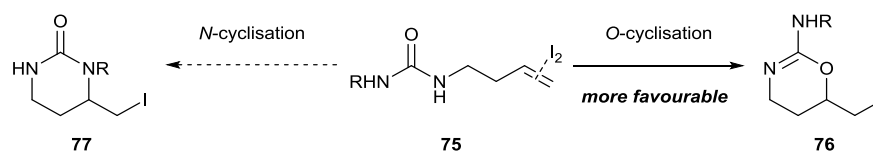
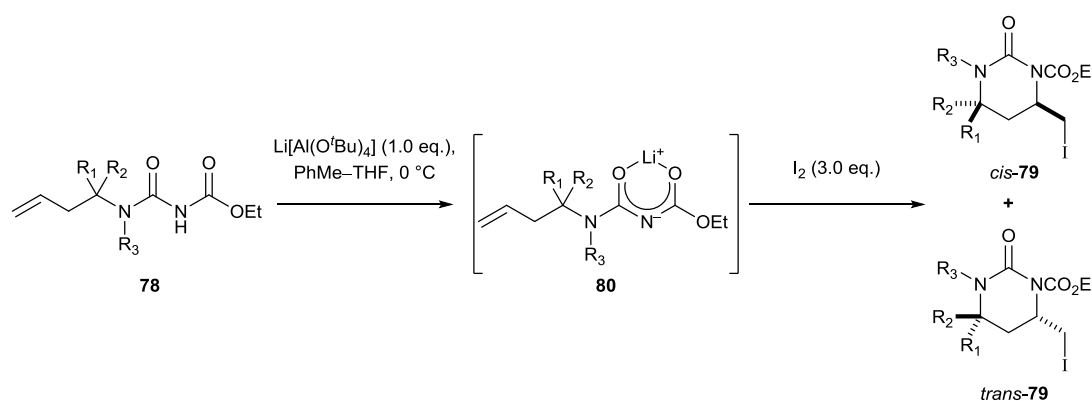


Figure 20 Typical regioselectivity in the iodocyclisation of ureas **75**. R= H, alkyl, aryl.

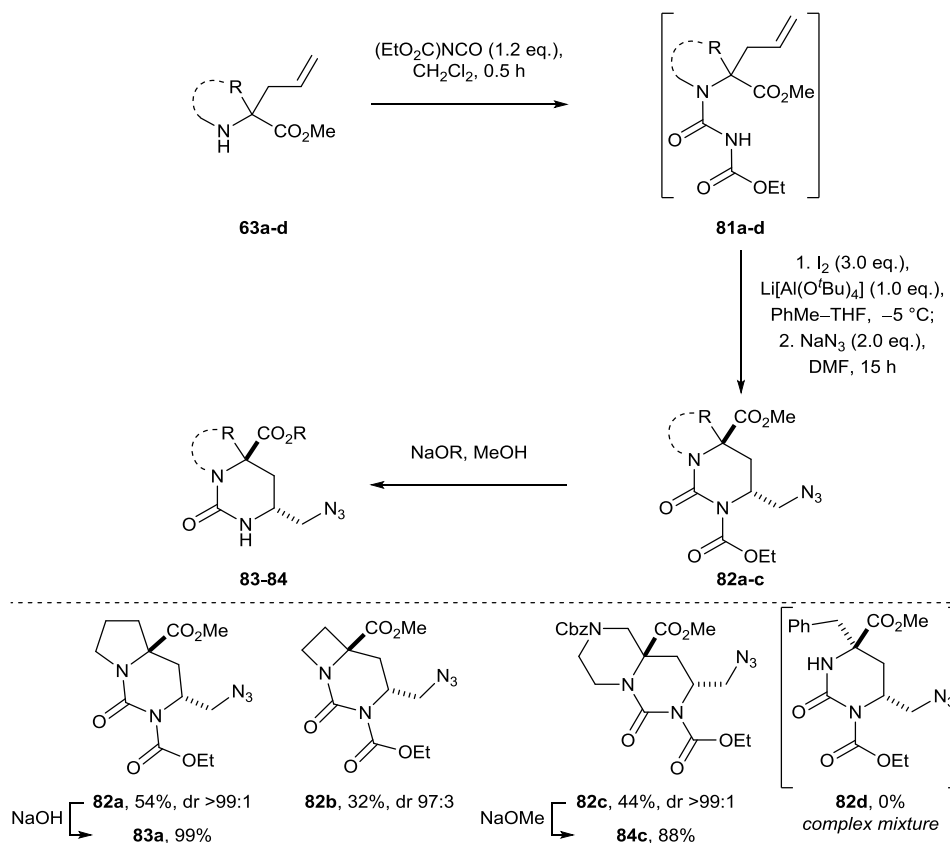
Taguchi reported the iodine-mediated cyclisation of carbamoyl ureas **78**, using $\text{Li}[\text{Al}(\text{O}^t\text{Bu})_4]$ as a base, which cyclised through nitrogen to give six-membered cyclic ureas **79** in 64-86% yields and with reasonable to high diastereoselectivities (Table 10).¹³⁸ Taguchi postulates that the role of $\text{Li}[\text{Al}(\text{O}^t\text{Bu})_4]$ is to act as a chelating agent between the two carbonyls of carbamoyl urea **78**, locking these into a six-membered ring **80** to promote *N*-cyclisation of the otherwise ambident nucleophile.



Entry	R ¹	R ²	R ³	Yield /%	<i>cis/trans</i>
1	Ph(CH ₂) ₂	H	H	80	2:1
2	Ph(CH ₂) ₂	H	PhCH ₂	64	1:30
3	Ph(CH ₂) ₂	H	Ph ₂ CH	70	>1:100
4	Me	H	Ph ₂ CH	64	1:64
5	CO ₂ Et	CO ₂ Et	H	86	N/A

Table 10 Iodine-mediated *N*-cyclisation of ureas by Taguchi.¹³⁸

Taguchi's conditions were applied to building blocks **63a-d**. Carbamoyl ureas **81a-d** were generated by reaction of amines **63a-d** with ethyl isocyanatoformate. Ureas **81a-d** were then treated with iodine and $\text{Li}[\text{Al}(\text{O}^t\text{Bu})_4]$, giving rise to the bicyclic scaffolds **82a-c** (Scheme 26). Phenylalanine-derived urea **81d** gave a complex mixture of inseparable products under these reaction conditions. Analysis of the crude reaction mixture by ¹H NMR spectroscopy suggests that this may be due to the formation of a mixture of *N*- and *O*-cyclised products and their de-carbamoylated derivatives.



Scheme 26 Aminoamination to form the cyclic ureas **82a-c**.

Crystallographic studies confirmed the relative configuration of the decarbomoylated derivatives **83** and **84**, prepared by treating scaffolds **82a,c** with sodium hydroxide (Figure 21) and sodium methoxide respectively (Figure 22).

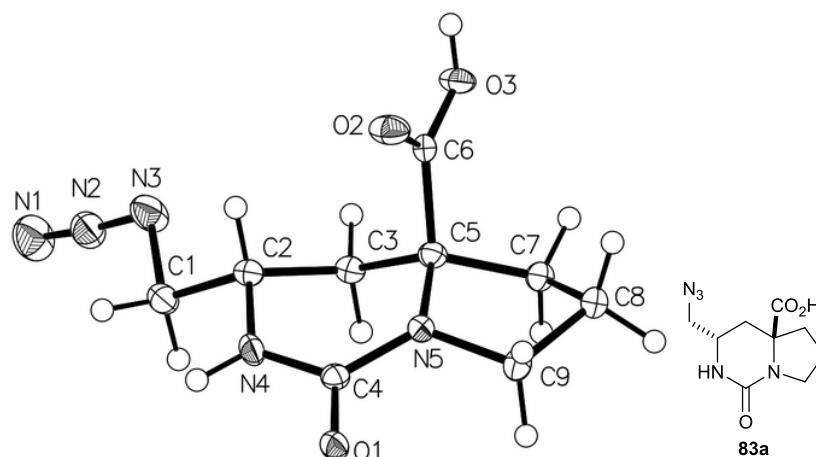


Figure 21 X-ray crystal structure of urea **83a**.

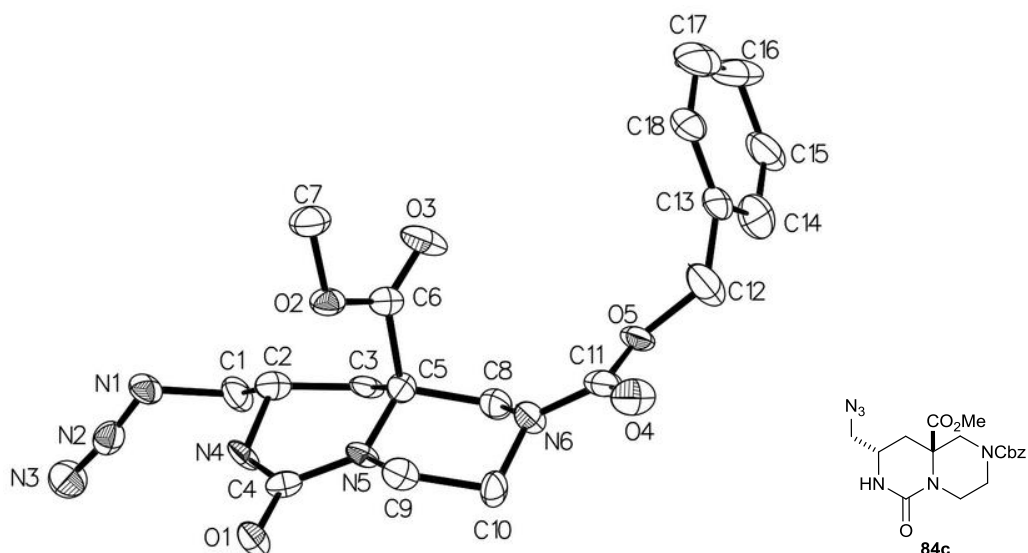


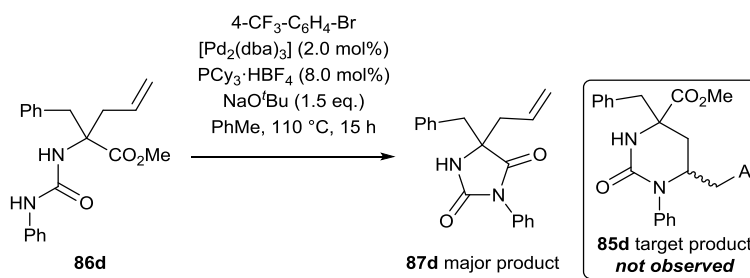
Figure 22 X-ray crystal structure of urea **84c**. Both molecules in the asymmetric unit exhibited disorder around the benzyl ester groups. For both molecules, this was modelled as two parts in a 60:40 ratio. Only one of the benzyl ester conformations is shown for clarity.

2.3.2 Cyclisations between tethered *N*-centred nucleophiles and the adjacent ester

In this section, the inherent susceptibility of the ester to cyclisations through nucleophilic attack is exploited.

2.3.2.1 Hydantoin formations

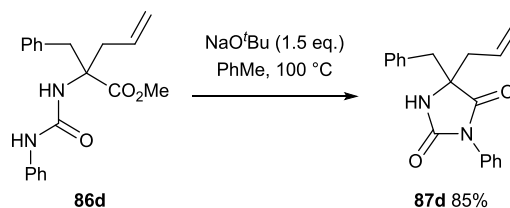
During our investigations to form cyclic ureas **82a-c**, we also investigated the possibility of forming scaffold **85d** by using an aminoarylation reaction, which would allow scaffold formation and decoration in one step.^{82,142} However, on exposure of urea **86d** to typical basic conditions for aminoarylation, hydantoin **87d** was observed as the major product (as judged by analysis of the crude product using ¹H NMR spectroscopy, Scheme 27).



Scheme 27 Attempted aminoarylation.¹⁴²

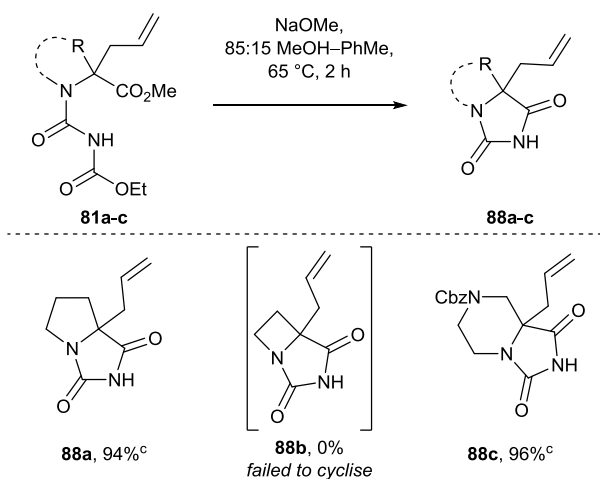
Hydantoins are known for their anticonvulsant biological activity (e.g. phenytoin, mephentoin, nirvanol), and we saw an opportunity to harness this transformation

to give access to new classes of hydantoin scaffolds. Heating urea **86d** with sodium *tert*-butoxide gave hydantoin **87d** in 85% yield (Scheme 28).



Scheme 28 Base-mediated hydantoin formation.

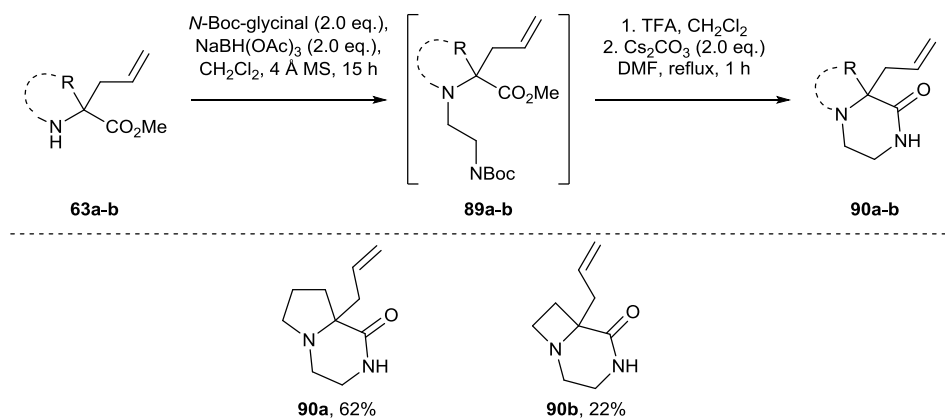
For carbamoyl ureas **81a,c**, it was possible to achieve a one-pot hydantoin formation and carbamoyl deprotection. Treatment of **81a,c** with sodium methoxide gave hydantoins **88a,c**. Urea **81b** failed to cyclise (only decarbamoylation was observed by analysis of the crude reaction mixture using ^1H NMR spectroscopy), presumably due to the strained nature of the azetidine ring (Scheme 29).



Scheme 29 One-pot hydantoin formation-deprotection.

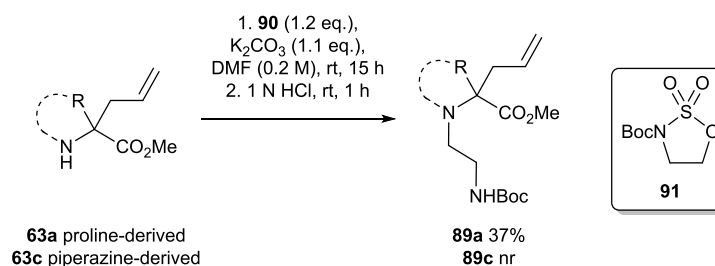
2.3.2.2 Lactamisations

Arming the building blocks **63a-b** with an alkylamino functional handle opened up the possibility of preparing scaffolds by lactamisation. Reductive amination with *N*-Boc glycinal gave the Boc-protected diamines **89a-b**, which were carried forward crude, as they could not be separated from trace impurities during attempted purification using flash chromatography. Treatment of the protected diamines **89a-b** with TFA, followed by base-mediated cyclisation afforded lactams **90a-b** (Scheme 30).



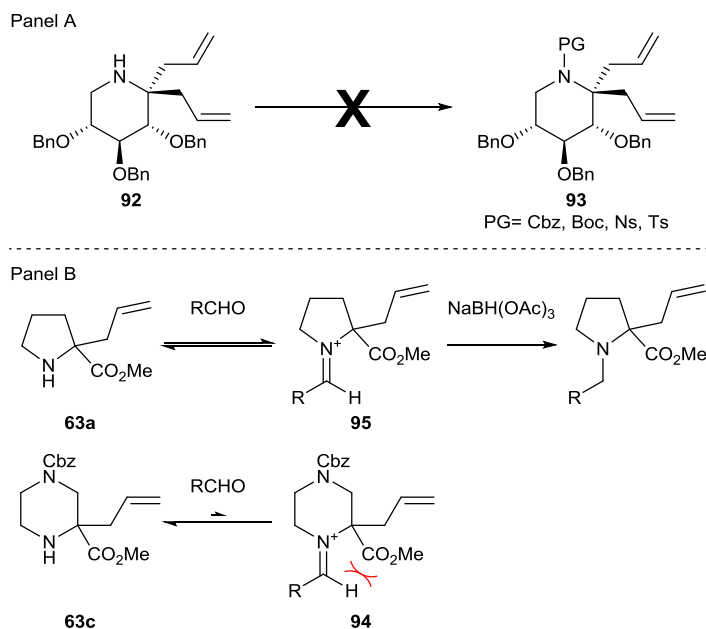
Scheme 30 *N*-alkylation and lactamisation.

Piperazine **63c** failed to undergo reductive amination to generate the required precursor for lactamisation. The Nelson group has previously had success using cyclic sulfamidates as electrophilic coupling partners to alkylate amine nucleophiles.^{90,92} In a preliminary study, alkylation of proline-derived starting material **63a** with commercially available cyclic sulfamidate **91** proceeded with complete conversion to give Boc-protected diamine **89a**, following an acidic work-up (Scheme 31). However, extension of these conditions to piperazine **63c** resulted in no reaction.



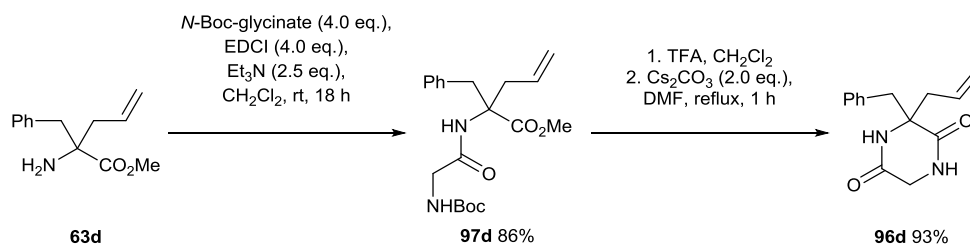
Scheme 31 Alkylation with cyclic sulfamidate **91**.

Jarosz noted difficulties when trying to react α,α -disubstituted piperidine **92** with common electrophiles to give protected piperidine **93** (Panel A, Scheme 32).¹⁴³ The origin of the lack of reactivity of piperazine **63c** may lie in the decreased bond angle between the iminium double bond and the α -substituents in intermediate **94**, compared with the analogous pyrrolidine-derived iminium intermediate **95**, this results in steric hindrance and forces the equilibrium towards the starting amine **63c** (Panel B).



Scheme 32 Panel A: attempted protection of amine **93** by Jarosz.¹⁴³
 Panel B: rationale for the failure of the attempted reductive amination of piperazine **63c**.

It was also possible to prepare a diketopiperazine **96d** through an analogous cyclisation strategy (Scheme 33). The precursor **97d** to this reaction was first prepared through reaction of compound **63d** with *N*-Boc glycine, mediated by EDCI. Amide **97d** was treated with Cs₂CO₃ in refluxing DMF to furnish diketopiperazine **96d** in 93% yield.



Scheme 33 Synthesis of diketopiperazine **96d**.

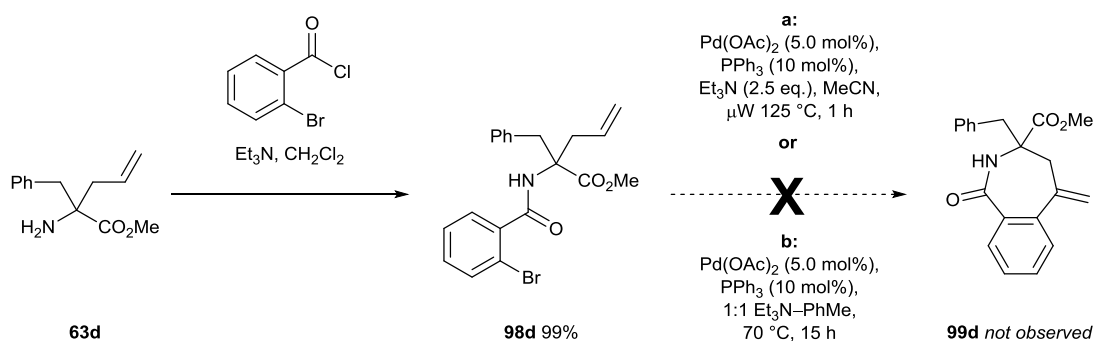
2.3.3 Transition metal-catalysed cyclisations between the capping group and the allyl functionality

There is a wealth of literature describing the synthesis of scaffolds (natural products or otherwise) through the transition metal-catalysed formation of C-C bonds. The value of these types of transformation cannot be understated; two Nobel prizes in the last decade have been awarded for the development of such transformations: metathesis and Pd-catalysed cross coupling reactions.^{144,145} Due to the wealth of literature on these processes, we chose to investigate the use of selected amine capping groups that would enable scaffold formations through C-C bond formations.

2.3.3.1 Intramolecular Heck reactions

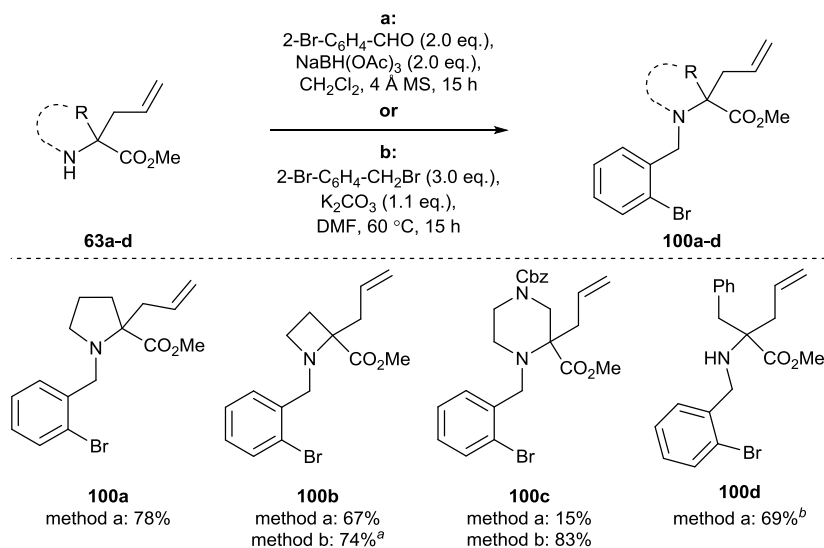
The intramolecular Heck reaction has been extensively developed¹⁴⁶ and has been shown to be of particular value in the preparation of natural product skeletons.¹⁴⁷ Consequently, we endeavoured to harness this approach to prepare scaffolds.

In preliminary studies, *N*-benzoylation of **63d** using 2-bromobenzoyl chloride, followed by treatment of the resulting benzamide **98d** with Pd(OAc)₂ gave none of the targeted seven-membered Heck product **99d** under either thermal or microwave conditions (Scheme 34). We postulated that this lack of reactivity was caused by the thermodynamically favoured, but unreactive, *s-trans* geometry of the amide bond (this would be akin to trying to form a seven-membered ring containing a *trans* C=C bond, which is geometrically unfavourable).¹⁴⁸



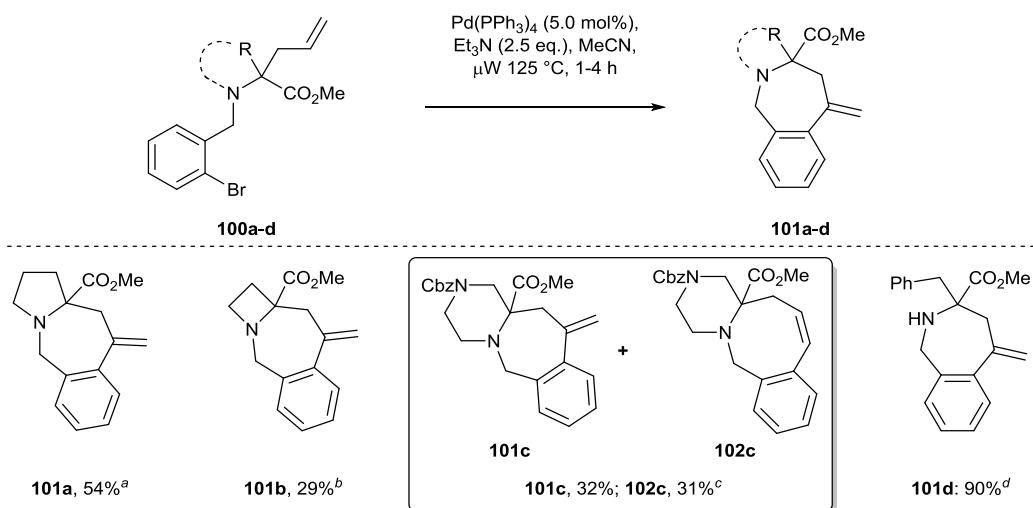
Scheme 34 Attempted Heck cyclisation of benzamide **98**.

We postulated that the increased flexibility of the analogous amines **100a-d** would allow the required Heck cyclisations to take place. Firstly, 2-bromobenzylated amines **100a-d** were prepared by reductive amination. Once again, the piperazine **100c** was reluctant to undergo reductive amination (33% conversion in 24 h, 15% isolated yield). However, alkylation with 2-bromobenzyl bromide provided **100c** in 83% yield (Scheme 35).



Scheme 35 Alkylation of the amines **63a-d** to give precursors for the intramolecular Heck reaction.
^aThe TFA salt of **63b** and 2.2 eq. K₂CO₃ were used (see experimental). ^bAlternative reaction conditions used:
 2-Br-C₆H₄-CHO (2.0 eq.), NaBH(OAc)₃ (4.0 eq.), THF, 45 °C, 3 days.

Treatment of precursors **100a-d** under standard Heck conditions¹⁴⁶ with 5-10 mol% Pd(PPh₃)₄ at 125 °C in the microwave gave azepanes **101a-d**, which bear an exocyclic alkene (Scheme 36). However the reaction of piperazine **100c** was poorly regioselective under the reaction conditions; analysis of the crude product by ¹H NMR spectroscopy showed that azocane **102c** was favoured in a 6:4 ratio to azepane **101c**, which were isolated in 31% and 32% yields respectively. It is also worth noting that while **100c-d** formed only the products isolated (**101c/102c** and **101d**), **100a-b** formed other unknown products (as judged by analysis of the crude reaction product using ¹H NMR spectroscopy) which could not be recovered following purification using flash chromatography or SPE-SCX. We postulate that these side products may have arisen through the alkene 'walking' around the ring following the Heck reaction to give unstable intermediates which later decomposed during purification.



Scheme 36 Intramolecular Heck cyclisations. ^a92:8 mixture with the regioisomeric azocane (see experimental). ^b10 mol% $\text{Pd}(\text{PPh}_3)_4$ used. ^cAnalysis of the crude reaction product by ^1H NMR showed 100% conversion to a 42:58 mixture of **101c**:**102c**. ^d $\text{Pd}(\text{OAc})_2$ (10 mol%) and PPh_3 (20 mol%) used.

2.3.3.2 Ring-closing metathesis (RCM)

In recent years, ring-closing metathesis has been an extremely valuable synthetic method for preparing ring systems in many bioactive natural products¹⁴⁹ and it was thought that this methodology could potentially be applied to our building blocks to prepare scaffolds.

Gracias reported that the ring-closing metathesis of unprotected amines **103** could be achieved by treating the derived ammonium tosylate salts with Grubbs second generation catalyst (**GII**) to generate spirocyclic scaffolds **104** (Table 11).¹⁵⁰ The prior preparation of the ammonium salt ostensibly prevents the unwanted coordination of the nitrogen lone pair to the catalyst.

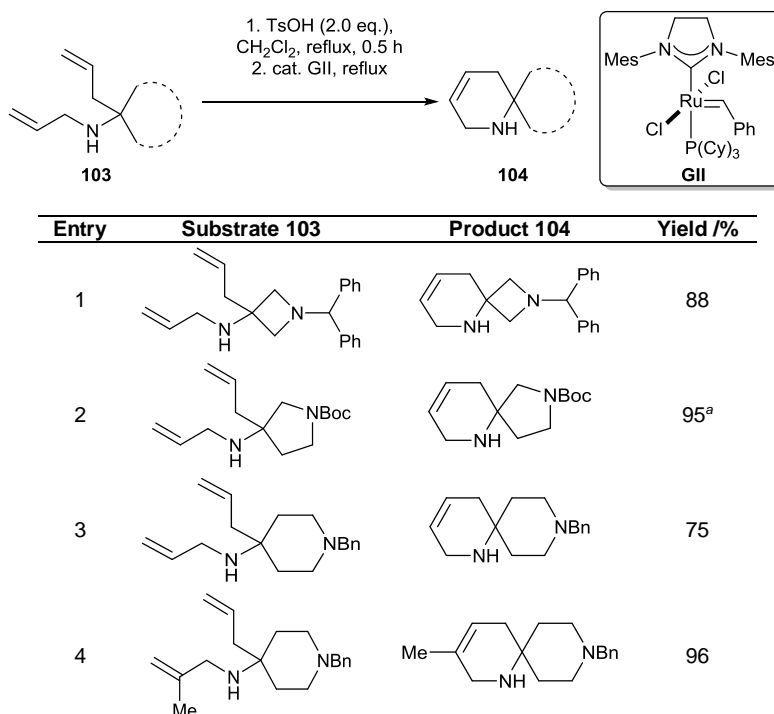
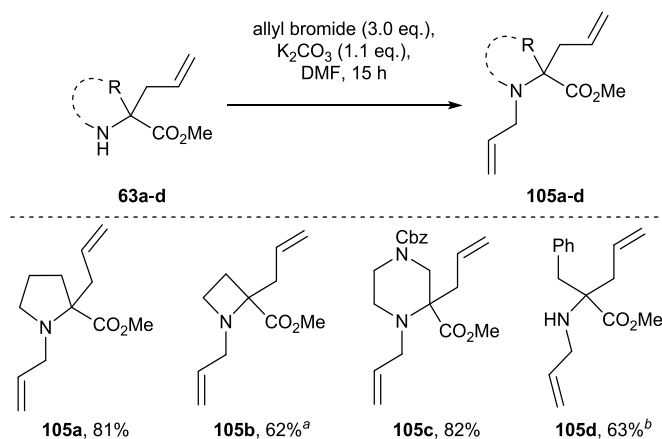


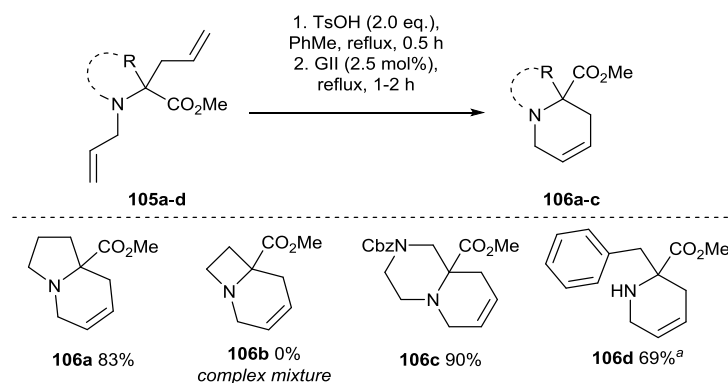
Table 11 RCM of ammonium tosylate salts to give spirocyclic scaffolds **104** by Gracias. ^a1.0 eq. TsOH used.¹⁵⁰

N-Allylation of the amine building blocks **63a-d** with allyl bromide in DMF furnished precursors **105a-d** for ring-closing metathesis (Scheme 37).



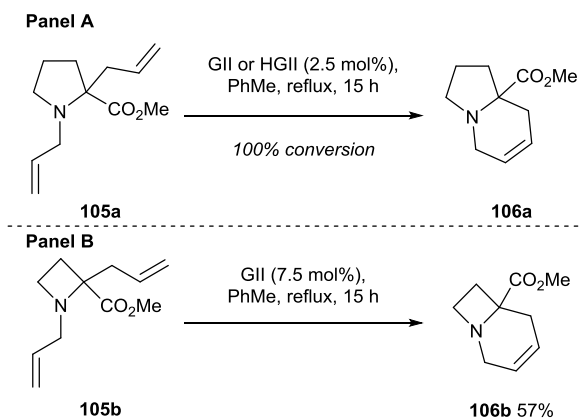
Scheme 37 Allylation of amines **63a-d** to give precursors for ring-closing metathesis. ^aThe TFA salt of **63b** and 2.2 eq. K_2CO_3 used (see experimental). ^b5.0 eq. allyl bromide used.

Gracias' reaction conditions were applied to substrates **105a-d** to give bicyclic scaffolds **106a,c-d** (Scheme 38). While these conditions worked well for phenylalanine-derived **105d** it was found that reactions of cyclic substrates **105a,c** were more efficient when conducted in toluene at reflux. Azetidine **105b** gave a complex mixture of products under these reaction conditions.



Scheme 38 Ring-closing metathesis. ^a5 mol% GII used in CH₂Cl₂.

To test whether the reaction worked in the absence of *p*-toluenesulfonic acid, two reactions were conducted using proline-derived **105a**. Heating substrate **105a** overnight with either Grubbs second generation (**GII**) or Hoveyda–Grubbs second generation (**HGII**) gave, in both instances, complete conversion to the target product **106a** (Scheme 39, Panel A). Following the success of these reactions, the azetidine **105b** was treated with Grubbs second generation catalyst. Using 2.5 mol% catalyst loading resulted in no reaction, but increasing the catalyst loading to 7.5 mol% led to the formation of the target product **106b**, which was isolated in 57% yield (Scheme 39, Panel B).



Scheme 39 Ring-closing metathesis in the absence of *p*-toluenesulfonic acid.

2.3.4 Cyclisation toolkit: A summary

A focused toolkit of chemical transformations was developed to allow the parallel synthesis of scaffolds for LOS (Figure 23). Overall, 22 novel scaffolds were prepared from four building blocks **63a-d** in a total of 49 synthetic operations.*

* Defined as a process conducted in a single reaction vessel.

The toolkit consisted of just six reaction methodologies following an *N*-capping event.

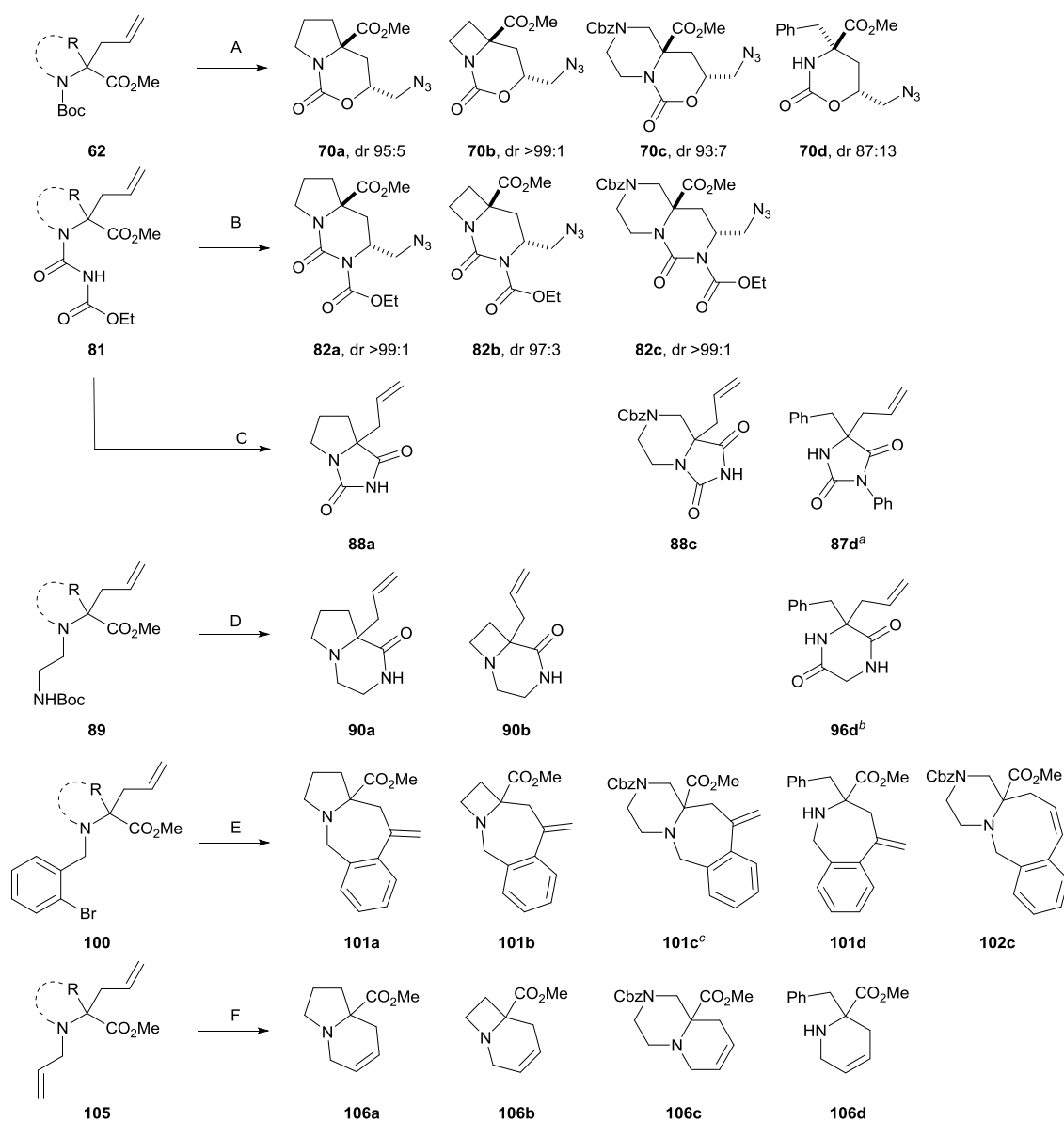


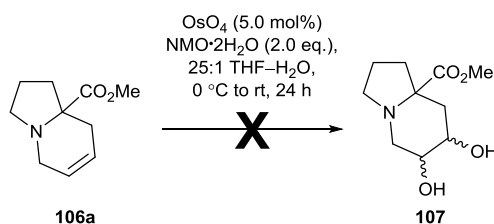
Figure 23 A summary of the methods used to prepare 22 scaffolds. A: iodine-mediated cyclic carbamate synthesis; B: iodine mediated cyclic urea synthesis; C: hydantoin formation; D: lactamisation; E: intramolecular Heck reaction; F: RCM. ^aPhenylisocyanate derived urea **86d** used as the starting material (see experimental, Section 5.2.2). ^bStarting material **97d** derived from *N*-Boc-glycine. ^cFormed as part of a separable mixture with the azocane **102c**.

2.4 Generation of sites for further diversification

With the 22 scaffolds in hand we wanted to show that the scaffolds could be further functionalised to generate points that could be diversified to form derivative compound libraries. In particular, we wanted to show that oxidation of the alkene functional handles was possible in the presence of tertiary amines.

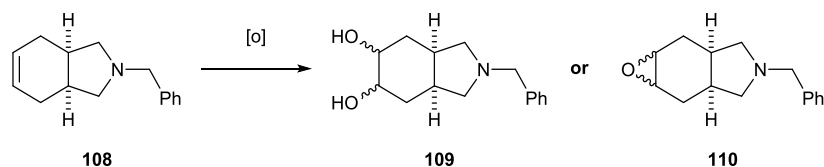
2.4.1 Oxidation of cyclic alkenes in the presence of tertiary amines

In an initial attempt to oxidise cyclic alkene **106a** to form the natural product-like diol **107**, it was exposed to Upjohn dihydroxylation conditions using OsO₄ and NMO (Scheme 40).^{143,151} Unexpectedly, no reaction was observed (by analysis of the crude reaction mixture using TLC and ¹H NMR spectroscopy).



Scheme 40 Attempted dihydroxylation of alkene **106a**.

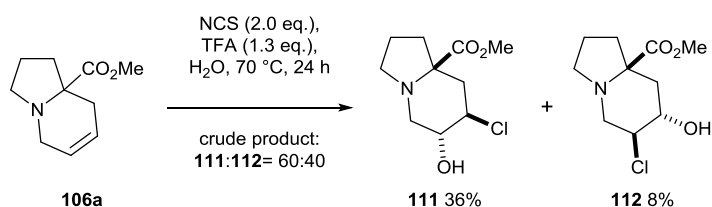
We opted to prepare compound **108** (prepared in two steps – see experimental), bearing a tertiary amine and an alkene, to act as a model substrate to enable the development of suitable oxidation conditions. In addition to preventing the waste of bespoke scaffolds, the presence of the benzyl group added a chromophore which aided TLC analysis of the oxidation reactions. Curiously, the previously described Upjohn dihydroxylation conditions were successful when applied to model substrate **108** (Table 12, entry 1), diol **109** was isolated in 69% yield. Attempted dihydroxylations using modified Prevost–Woodward conditions¹⁵² (entry 2) and attempted transition metal-free diboration¹⁵³ (entry 3) gave only traces of the targeted products. Attempted epoxidation of alkene **108** using peracids (entries 4-7) gave mixtures of products including the *N*-oxide of starting material **108** and/or over-oxidation to the *N*-oxide of epoxide **110** (as judged by analysis of the crude reaction products by ¹H NMR spectroscopy and LCMS). However, epoxidation could be achieved by a two-step sequence involving chlorohydrin formation, using *N*-chlorosuccinamide and TFA in water, followed by closure of the resulting chloroalcohol with sodium methoxide (entry 8). While this procedure gave a low isolated yield, complete conversion was observed in both steps of the reaction.



Entry	Conditions	Target product	Products (isolated yield)
1	OsO ₄ (5.0 mol%), NMO (2.0 eq.), 25:1 THF–H ₂ O, 0 °C, 8 h ¹⁴³	109	109 (69%)
2	NaIO ₄ (30 mol%), LiBr (20 mol%), AcOH, 95 °C, 18 h ¹⁵²	109	Mainly 108 [*] , trace of monoacetylated 109 [†]
3	B ₂ pin ₂ (1.1 eq.), NaOt-Bu (0.15 eq.), THF–MeOH, 70 °C, 16 h ¹⁵³	109	Mainly 108 [*] , trace of diborylated alkene [†]
4	<i>m</i> -CPBA (1.50 eq.), CH ₂ Cl ₂ , 2 h	110	Mainly the <i>N</i> -oxide of 108 and the <i>N</i> -oxide of 110 ^{*†}
5	<i>m</i> -CPBA (1.50 eq.), TFA (1.25 eq.), CH ₂ Cl ₂ , 15 h	110	Mixture of 108 ; 110 ; the <i>N</i> -oxide of 110 ^{*†}
6	F ₃ CCO ₂ H, F ₃ CCO ₃ H, CH ₂ Cl ₂ , 0 °C to rt, 16 h ¹⁵⁴	110	complex mixture [*]
7	H ₂ O ₂ , trichloroacetonitrile, TFA, CH ₂ Cl ₂ , 48 h ¹⁵⁵	110	complex mixture [*]
8	(i) NCS (1.2 eq.), TFA (1.3 eq.), H ₂ O, 70 °C, 4 h ¹⁵⁶ (ii) K ₂ CO ₃ (2.0 eq.), MeOH, 24 h	110	110 (42%) [‡]

Table 12 Oxidation studies on model substrate **108**. ^{*}By analysis of the crude reaction mixture using ¹H NMR spectroscopy. [†]By analysis of the crude reaction mixture using LCMS. [‡]100% conversion for each step as judged by analysis of the crude reaction products by ¹H NMR spectroscopy.

The hydroxychlorination conditions (Table 12, entry 8) were applied to the cyclic alkene **106a** (Scheme 41). Two equivalents of NCS were required in order for the reaction to go to completion. A 60:40 mixture of the separable regioisomers **111-112** was formed (as judged by analysis of the crude reaction product using ¹H NMR spectroscopy), which were isolated in 36% and 8% yields respectively.



Scheme 41 Preparation of the chloroalcohols **111** and **112**.

Isolation of the products allowed assignment of their regio- and relative stereochemical configurations by NOESY and HMQC (Figure 24).

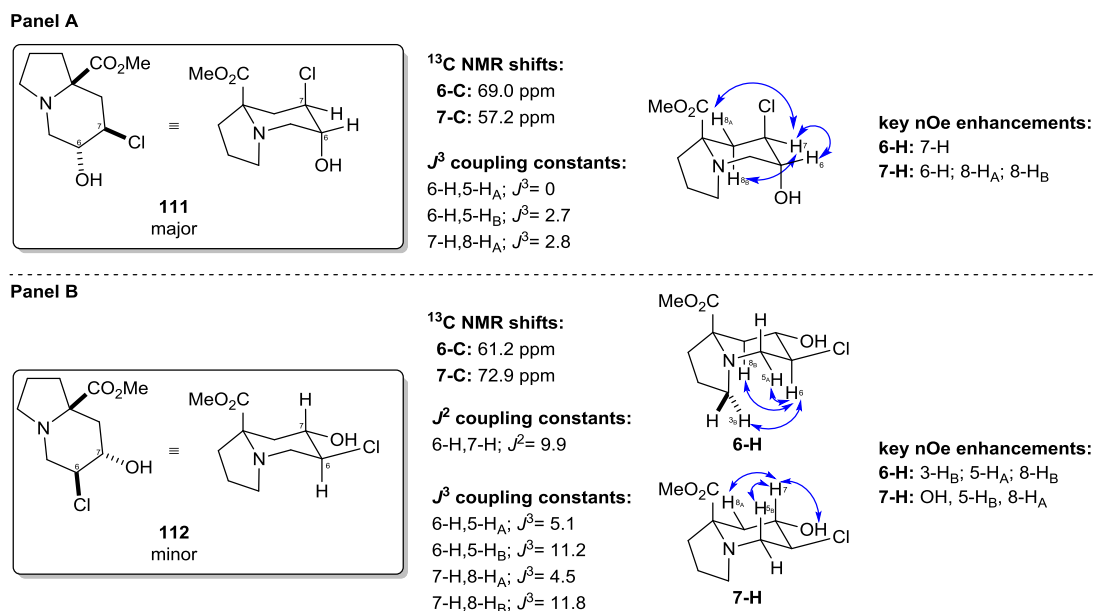


Figure 24 Assignment of regioisomers **111** (Panel A) and **112** (Panel B).

Products **111-112** arise from the *trans*-diaxial ring opening of the interconverting chloronium-ion conformers **113-114** (Figure 25).¹⁵⁷

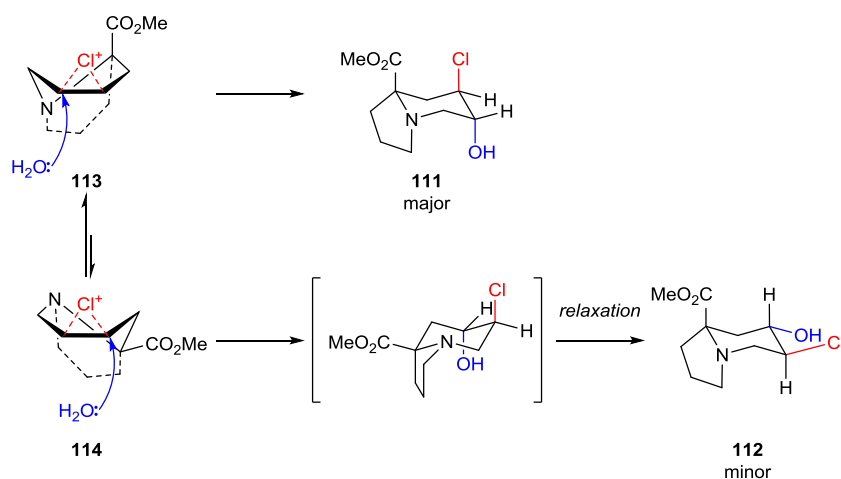
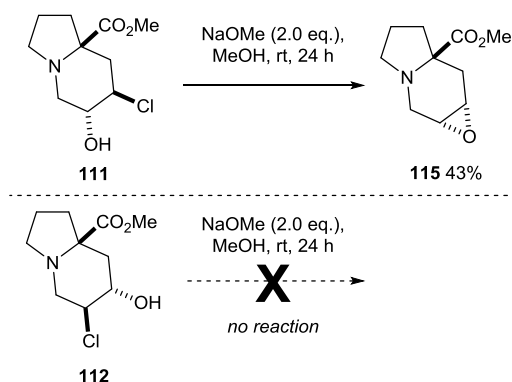


Figure 25 Rationale for the regiochemical outcome of the hydrochlorination reaction.

Treatment of major chlorohydrin **111** with sodium methoxide gave access to epoxide **115**, which was isolated in 43% yield (Scheme 42). Surprisingly, minor chlorohydrin **112** did not react under the same conditions (as judged by analysis of the crude reaction mixture using LCMS).



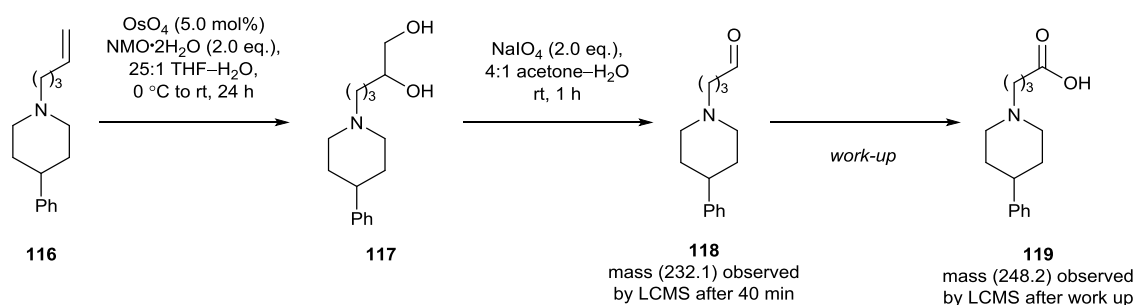
Scheme 42 Base-mediated epoxide formation.

The hydrochlorination-epoxidation sequence provides a potential starting point for the oxidation of the cyclic alkene systems in the presence of the tertiary amine. Further optimisation is required to improve this process in the future.

2.4.2 Oxidation of terminal alkenes in the presence of tertiary amines

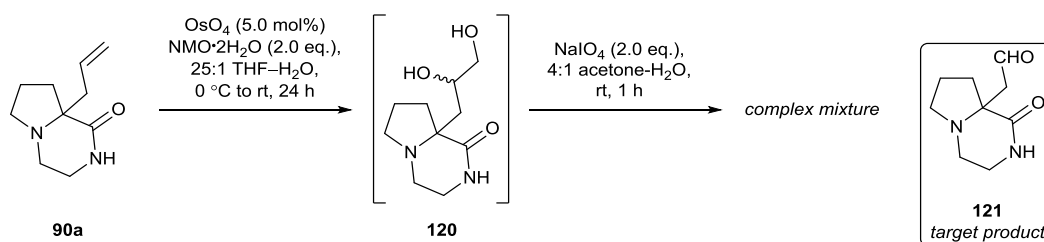
Due to the difficulties met when trying to oxidise the cyclic alkenes in the presence of the tertiary amine, we decided to start our investigations into the oxidation of terminal alkenes by using a suitable model system. Terminal alkene **116** was prepared by reductive amination (route not shown, see experimental). Oxidation systems were investigated to try to convert the alkene to a more readily functionalised group.

Firstly, the aforementioned dihydroxylation conditions were attempted, resulting in successful formation of diol **117** (Scheme 43). Oxidative cleavage of diol **117** with sodium periodate initially gave aldehyde **118** in <40 min (as judged by LCMS analysis of the crude reaction mixture). However, following the work-up the observed mass by LCMS agreed with the corresponding acid **119**. In addition, analysis of the crude product using ^{13}C NMR spectroscopy showed a peak at 177.2 ppm which indicated that the carboxylic acid had formed.



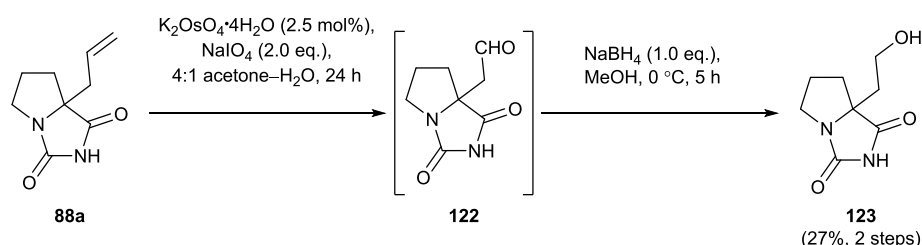
Scheme 43 Dihydroxylation of alkene **116** and attempted oxidative cleavage of the resulting diol **117**.

Application of the above conditions to lactam **90a** gave diol **120**, however, subsequent cleavage with sodium periodate gave a complex mixture (as judged by analysis of the crude reaction mixture by ^1H NMR spectroscopy after each step) and none of the targeted aldehyde **121** was isolated following purification (Scheme 44).



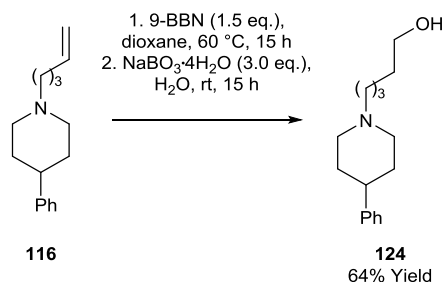
Scheme 44 Dihydroxylation of compound **90a** and attempted oxidative cleavage of the resulting diol **120**.

In contrast to the above result, one-pot dihydroxylation and oxidative cleavage of alkene **88a**, which does not contain a free amine, delivered aldehyde **122** (Scheme 45). Aldehyde **122** was reduced with NaBH_4 to furnish alcohol **123**, which was isolated in 27% yield, although this procedure needs to be optimised.



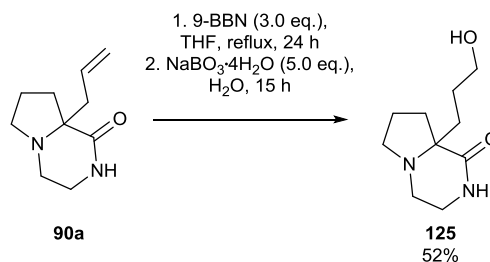
Scheme 45 One-pot oxidative cleavage of alkene **88a** and subsequent reduction of aldehyde **122**.

Returning to the model system **116**, a hydroboration-oxidation sequence was attempted to investigate the possibility of preparing terminal alcohols in the presence of the amine (Scheme 46). Hydroboration using 9-BBN in dioxane gave complete conversion to the hydroborated intermediate, this was then oxidised under mild conditions with $\text{NaBO}_3 \cdot 4\text{H}_2\text{O}$ to give alcohol **124**, which was isolated in 64% yield.¹⁵⁸



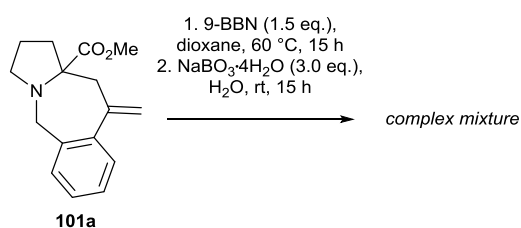
Scheme 46 Hydroboration-oxidation of terminal alkene **116**.

A variant of the above oxidation conditions was successfully applied to lactam **90a** to give alcohol **125** in 52% yield (Scheme 47).



Scheme 47 Hydroboration-oxidation of alkene **90a**.

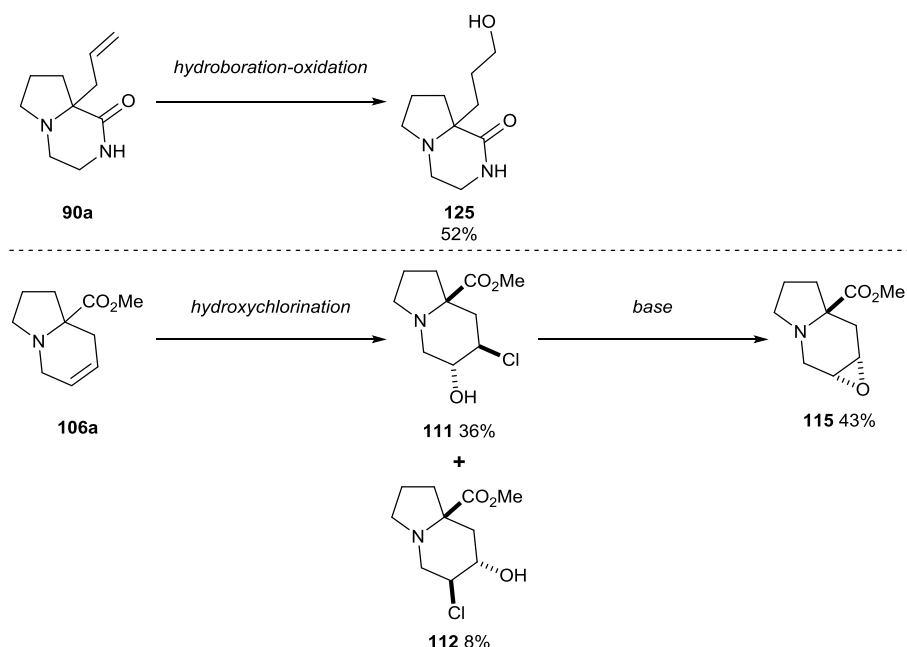
Application of the hydroboration-oxidation conditions to exocyclic alkene **101a** gave a complex mixture of products that could not be separated by flash chromatography (Scheme 48).



Scheme 48 Attempted hydroboration-oxidation of exocyclic alkene **101a**.

2.4.3 Oxidation chemistry: Summary and outlook

The identification of suitable conditions for the oxidation of the alkenes in the presence of tertiary amines was challenging and it is clear that we need to study this area further. However, we were able to gain some initial insights about which methods are best to achieve such transformations. A hydroboration-oxidation protocol was used to prepare terminal alcohol **125**, whilst hydroxychlorination followed by base-mediated epoxidation furnished chlorohydrins **111-112** (Scheme 49).



Scheme 49 Successful oxidations in the presence of tertiary amines.

Since amines have such high prevalence in drug molecules,¹¹⁸ it is extremely important to develop more compatible oxidation methodologies in the future.

2.5 Computational assessment of the scaffolds prepared

Now that preliminary studies had demonstrated the generation of points for further decoration, we wanted to assess the novelty and diversity of the 22 scaffolds and show that they could be virtually decorated to provide access to a computer-generated library of lead-like molecules. To achieve this we used several new computational protocols.⁹⁵

2.5.1 Novelty assessment

To assess the novelty of these scaffolds, a structure search was performed for the 22 compounds prepared (carboxybenzyl and ethoxycarbonyl urea protecting groups were removed, Figure 26). None of the deprotected compounds were found in the ZINC database of commercially available compounds (9×10^6 compounds). In addition, none of the deprotected compounds were found within the CAS registry, apart from **106a** which has been previously reported. However, no yield for scaffold **106a** or experimental procedure for its formation (including supporting analytical data) were given.¹⁵⁹

The Murcko assemblies⁹⁷ (with alpha attachments) were also generated and compared against the Murcko assemblies (with alpha attachments) of a random 5% sample of the ZINC database (4.5×10^5 compounds). Only the assemblies derived from scaffold **90a** (2 hits) and **106a** (1 hit) were found as substructure matches.

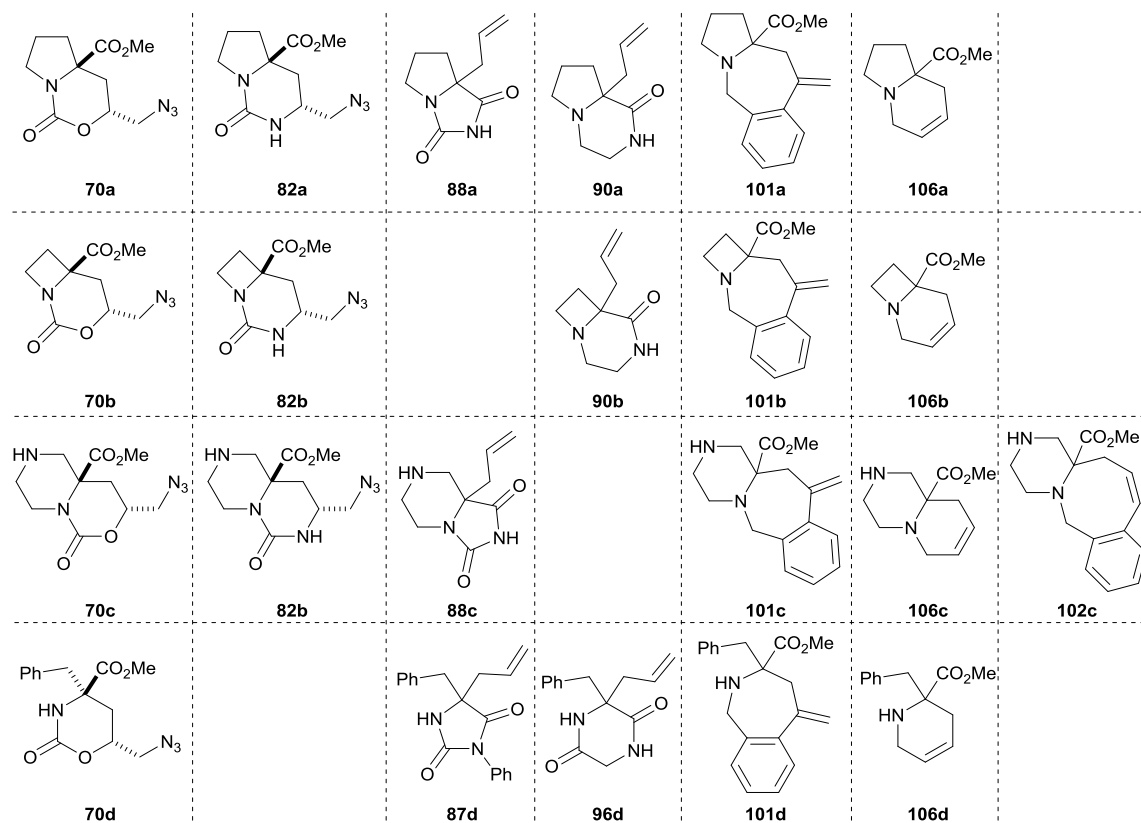


Figure 26 A summary of the deprotected scaffolds used in the computational analysis to generate a virtual library of compounds.

2.5.2 Diversity assessment

The skeletal diversity and relationship between the scaffolds were assessed using the ‘scaffold tree’ hierarchical analysis developed by Waldmann.¹⁶⁰ This is based on deconstruction of the scaffolds by iterative removal of rings, until a final ‘root’ ring is obtained. At each iteration step, prioritisation rules dictate which ring to remove next, typically retaining central and complex rings and removing peripheral rings.

By applying Waldmann’s prioritisation rules to the 22 scaffolds, it was found that each scaffold comprised a unique (with respect to this work) molecular framework at the graph-node-bond (GNB) level. Thus, the scaffolds are not simple derivatives of each other, but represent a skeletally diverse collection. The results

are summarized in Figure 27 and the frameworks illustrated in Figure 28. The 22 frameworks were represented at the graph-node-bond level, and were ultimately related to 7 parental frameworks. One of the particular advantages of our parallel approach to scaffold preparation is that, if any potential leads were identified in a screening campaign, one would be able to ‘scaffold hop’ to related structures, retaining the decorative groups from the lead, yet modifying the core scaffold.¹⁶¹

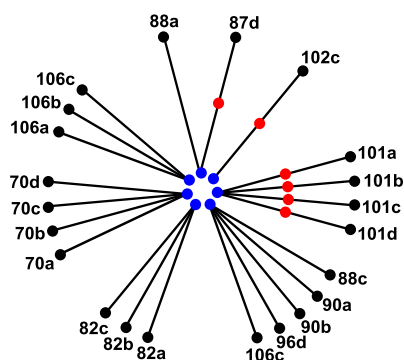


Figure 27 The hierarchical relationship between the 22 distinct molecular frameworks at the graph-node-bond level (black) and the 7 parental frameworks (blue). Daughter frameworks are shown in red.

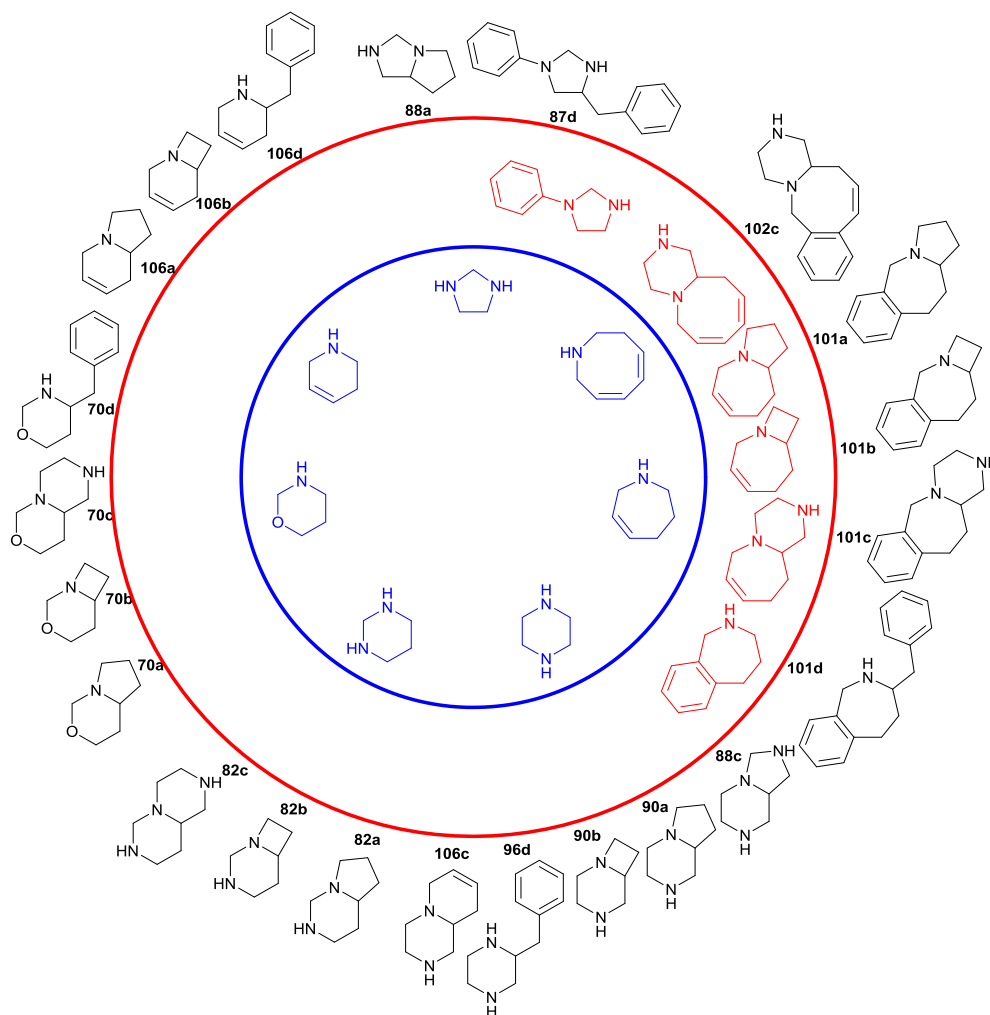


Figure 28 The 22 distinct molecular frameworks at the graph-node-bond level (black), and the seven parental frameworks (blue). Daughter frameworks are shown in red. The scaffolds that represent each framework are indicated. See Figure 27 for the relationship between scaffolds at each level of hierarchy.

2.5.3 Virtual decoration of the scaffolds

To determine the potential ability of the scaffolds to provide access to lead-like screening compounds, a virtual library of compounds was enumerated using Accelrys Pipeline Pilot.

The enumeration process illustrated in Figure 29 was applied to the 22 scaffolds. Firstly, removal of the carboxybenzyl and ethoxycarbonyl urea protecting groups was performed to give the deprotected scaffolds as shown in Figure 26. Certain functional groups were then manipulated to generate sites for further decoration (Table 13): (i) azides were both retained and reduced (entry 1); (ii) terminal alkenes were converted to aldehydes and carboxylic acids (entry 2) and; (iii) esters were saponified (entry 3). Decoration reactions (Table 14) were performed using 80 typical medicinal chemistry capping groups from a list provided by our industrial collaborators GlaxoSmithKline (see Appendix 1). Subsequent manipulation (Table 13, entries 4-5) reduced any aldehydes and acids to alcohols (entry 4) and converted any remaining azides and primary amines to dimethylamines (entry 5). The deprotected but underivatised scaffolds (i.e. the scaffolds as shown in Figure 26) were also retained in the final virtual library. Overall this process generated a library of 1110 virtual screening compounds.

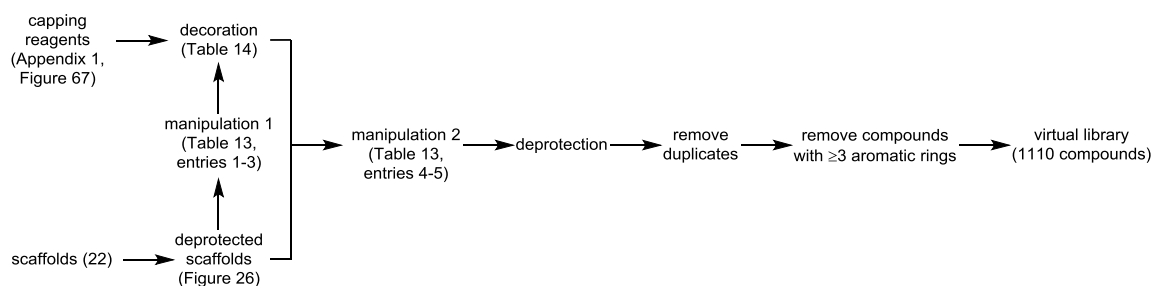


Figure 29 An overview of the process for the enumeration of the virtual library.

Entry	Manipulation 1 or 2	Synthetic transformation	Description
1	1	$\text{R-N}_3 \begin{cases} \longrightarrow \text{R-NH}_2 \\ \longrightarrow \text{R-N}_3 \end{cases}$	Azides reduced and retained
2	1	$\begin{array}{c} \text{H} & \text{H} \\ & \backslash / \\ & \text{C} \\ & / \backslash \\ \text{H} & \text{R} \end{array} \begin{cases} \longrightarrow \text{H-C(=O)-R} \\ \longrightarrow \text{HO-C(=O)-R} \end{cases}$	Terminal alkenes oxidised to aldehyde and acid
3	1	$\text{R-C(=O)-O-CH}_3 \longrightarrow \text{R-C(=O)-OH}$	Esters saponified
4	2	$\begin{array}{c} \text{H} \\ \backslash \\ \text{C=O} \\ / \\ \text{R} \end{array} \text{ and } \begin{array}{c} \text{HO} \\ \backslash \\ \text{C=O} \\ / \\ \text{R} \end{array} \longrightarrow \begin{array}{c} \text{OH} \\ \\ \text{R-CH}_2 \end{array}$	Aldehydes and acids reduced to alcohols
5	2	$\begin{array}{c} \text{R-NH}_2 \\ \text{and} \\ \text{R-N}_3 \end{array} \longrightarrow \begin{array}{c} \text{Me} \\ \\ \text{R-N} \\ \\ \text{Me} \end{array}$	Azides and primary amines converted to dimethylamines

Table 13 Functional group manipulations of scaffolds (Manipulation 1) and final compounds (Manipulation 2).

Entry	Functional group decoration	Synthetic transformation	Description
1	Acid	$\text{R-C(=O)-OH} \xrightarrow{\text{R}_2\text{-NH-R}^1} \begin{array}{c} \text{O} \\ \\ \text{R-C-N-R}^2 \\ \\ \text{R}^1 \end{array}$	Amide coupling (R ¹ = H, alkyl, aryl)
2	Aldehyde	$\text{R-C(=O)-H} \xrightarrow{\text{R}_2\text{-NH-R}^1} \begin{array}{c} \text{R}^1 \\ \\ \text{R-CH}_2\text{-N-R}^2 \\ \\ \text{R}^1 \end{array}$	Reductive amination (R ¹ = H, alkyl, aryl)
3	Amide	$\text{R-C(=O)-NH-R}^1 \xrightarrow{\text{R}^2\text{Br}} \begin{array}{c} \text{O} \\ \\ \text{R-C-N-R}^2 \\ \\ \text{R}^2 \end{array}$	Alkylation
4	Amide	$\text{R-C(=O)-NH-R}^1 \xrightarrow{\text{ArBr}} \begin{array}{c} \text{O} \\ \\ \text{R-C-N-R}^2 \\ \\ \text{Ar} \end{array}$	Arylation
5	Amine (R ¹ = H, alkyl)	$\text{R-NH-R}^1 \xrightarrow{\text{R}^2\text{Br}} \begin{array}{c} \text{R}^2 \\ \\ \text{R-N-R}^1 \end{array}$	Alkylation
6	Amine (R ¹ = H, alkyl)	$\text{R-NH-R}^1 \xrightarrow{\text{R}^2\text{COOH}} \begin{array}{c} \text{R}^1 \\ \\ \text{R-N-C(=O)-R}^2 \\ \\ \text{O} \end{array}$	Amide coupling
7	Amine (R ¹ = H, alkyl)	$\text{R-NH-R}^1 \xrightarrow{\text{ArBr}} \begin{array}{c} \text{Ar} \\ \\ \text{R-N-R}^1 \end{array}$	Arylation
8	Amine (R ¹ = H, alkyl)	$\text{R-NH-R}^1 \xrightarrow{\text{R}^2\text{COR}^3} \begin{array}{c} \text{R}^1 \\ \\ \text{R-N-CH(R}^2\text{)-R}^3 \end{array}$	Reductive amination (R ² = H, alkyl, aryl)
9	Amine (R ¹ = H, alkyl)	$\text{R-NH-R}^1 \xrightarrow{\text{R}^2\text{SO}_2\text{Cl}} \begin{array}{c} \text{R}^1 \\ \\ \text{R-N-S(=O)}_2\text{-R}^2 \end{array}$	Sulfonamide formation

Entry	Functional group decoration	Synthetic transformation	Description
10	Amine (R ¹ = H, alkyl)		Urea formation
11	Azide		Click
12	Carbamate		Alkylation
13	Carbamate		Arylation
14	Urea		Alkylation
15	Urea		Arylation

Table 14 Decoration reactions exploited in the enumeration of the virtual library.

2.5.3.1 Molecular properties analysis

The molecular properties (AlogP, heavy atom count [HA], Fsp³) of the compounds in the virtual library were calculated using the built-in tools in Pipeline Pilot and Dotmatics Vortex. The data which follow were visualised and analysed using Dotmatics Vortex.

2.5.3.1.1 Lead-likeness assessment

The highly interactive Dotmatics Vortex software allows analysis of the library from many standpoints. For instance, it is useful to consider the virtual compound library as a whole (for example to compare it to the rest of chemical space), on a scaffold basis (to determine which scaffold could prepare the most valuable screening libraries), and in addition it is useful to determine if there is any intrinsic bias towards more lead-like compounds depending upon which initial building block is used.

The lead-likeness of the virtual compound library was assessed in accordance with the criteria designated by Churcher (Figure 30, boxed area):¹⁰ 66% of compounds survived filtering by molecular size ($14 \leq \text{heavy atom count} \leq 26$), lipophilicity ($-1 < \text{AlogP} < 3$) and structural filters (see Appendix 1) – heavy atoms: $\mu = 22.8$, $\sigma = 3.57$; AlogP: $\mu = 0.38$, $\sigma = 1.38$. By comparison, just 23% of 9×10^6 compounds from the ZINC database of commercially-available compounds⁹⁶

survived this filtering process (Figure 31), with most compounds lying well outside lead-like chemical space (heavy atoms: $\mu= 25.9$, $\sigma= 5.4$; AlogP: $\mu= 1.7$, $\sigma= 2.9$).

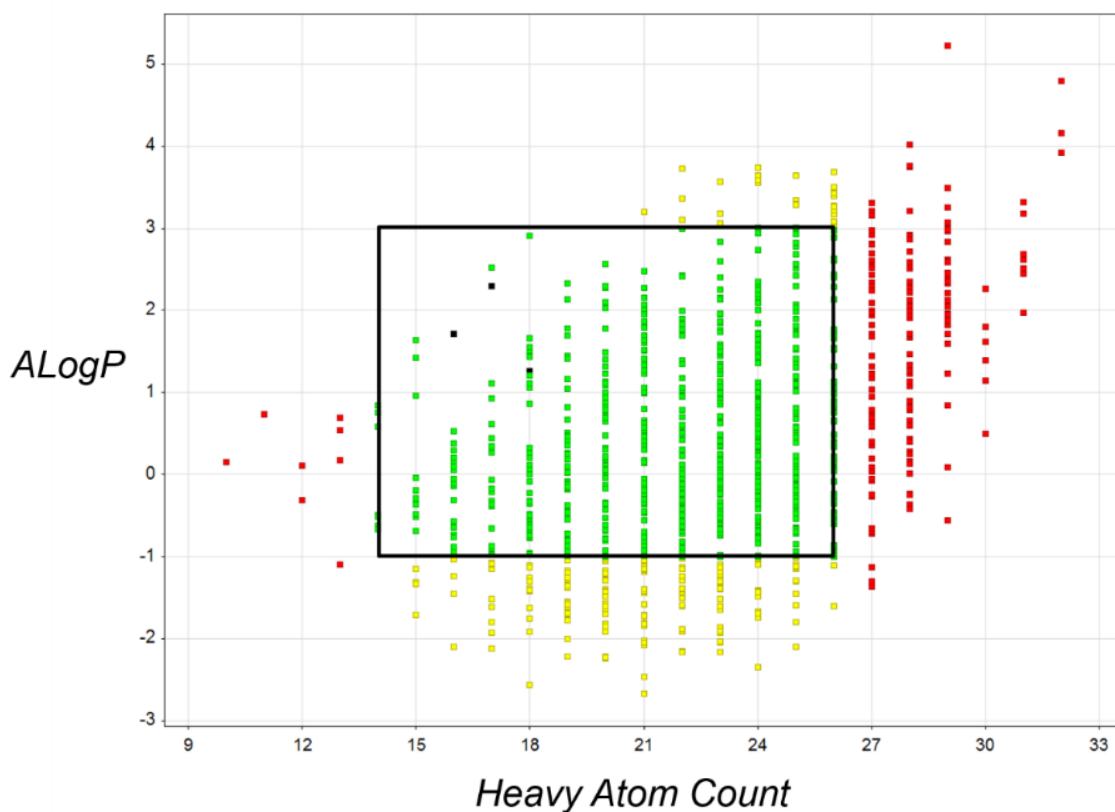


Figure 30 Distribution of the number of heavy atoms and AlogP for the 1110 decorated final compounds derived from the 22 scaffolds using the virtual library enumeration process. Compounds that survive successive filtering are shown in green (734 compounds, 66%). Compounds that fail successive filtering by number of heavy atoms (red, 173 compounds, 16%), AlogP (yellow, 200 compounds, 18%) and structural liabilities (black, 3 compounds, 0.3%) are shown. The black box shows the limit of lead-like space as outlined by Churcher.¹⁰ A larger annotated version of this plot is included in Appendix 1.

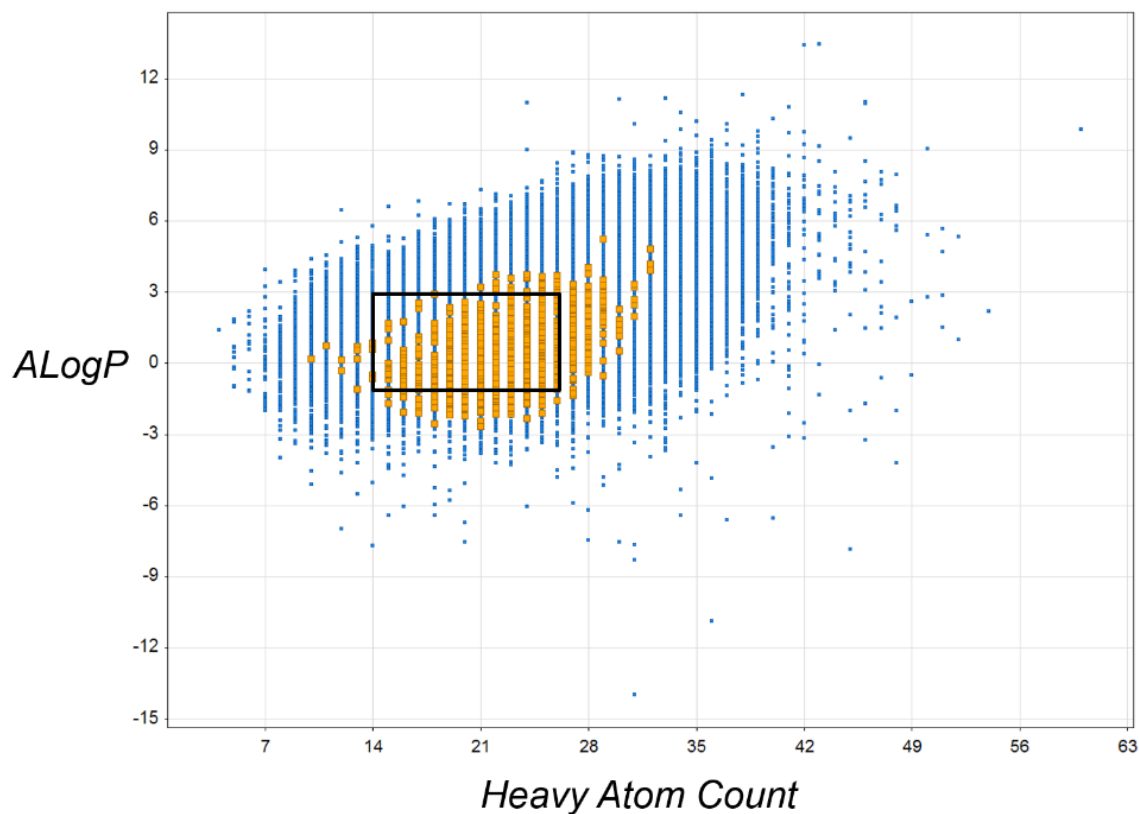


Figure 31 The distribution of molecular properties of the virtual library of 1110 compounds, derived from the 22 scaffolds (orange, enlarged for clarity), compared with 90911 randomly selected compounds from the ZINC database (blue). Our virtual library is considerably more focused on lead-like space compared to the rest of commercially-available compound space.

Remarkably, when decorated with the same set of 80 capping groups, each of the 22 scaffolds allow significant lead-like chemical space to be targeted. Each scaffold was ranked on its ability to provide access to lead-like compounds (see Appendix 1, Section 6.4.1 for individual AlogP vs heavy atom count plots). When deciding which scaffolds were the most valuable, both the percentage of lead-like compounds accessible from each scaffold (top histogram, Figure 32) and the absolute number of potentially accessible compounds are valuable to consider (middle histogram, Figure 32). Both of these were taken into consideration by calculating the weighted average (calculated as shown in equation below) to give an idea of which scaffolds can deliver the highest quantity of lead-like compounds (bottom histogram, Figure 32).

$$\text{weighted average} = 100 \times \left(\frac{n \times p}{\sum_{\text{all scaffolds}} (n \times p)} \right)$$

where n = no. lead-like compounds and p = percentage of lead-like compounds

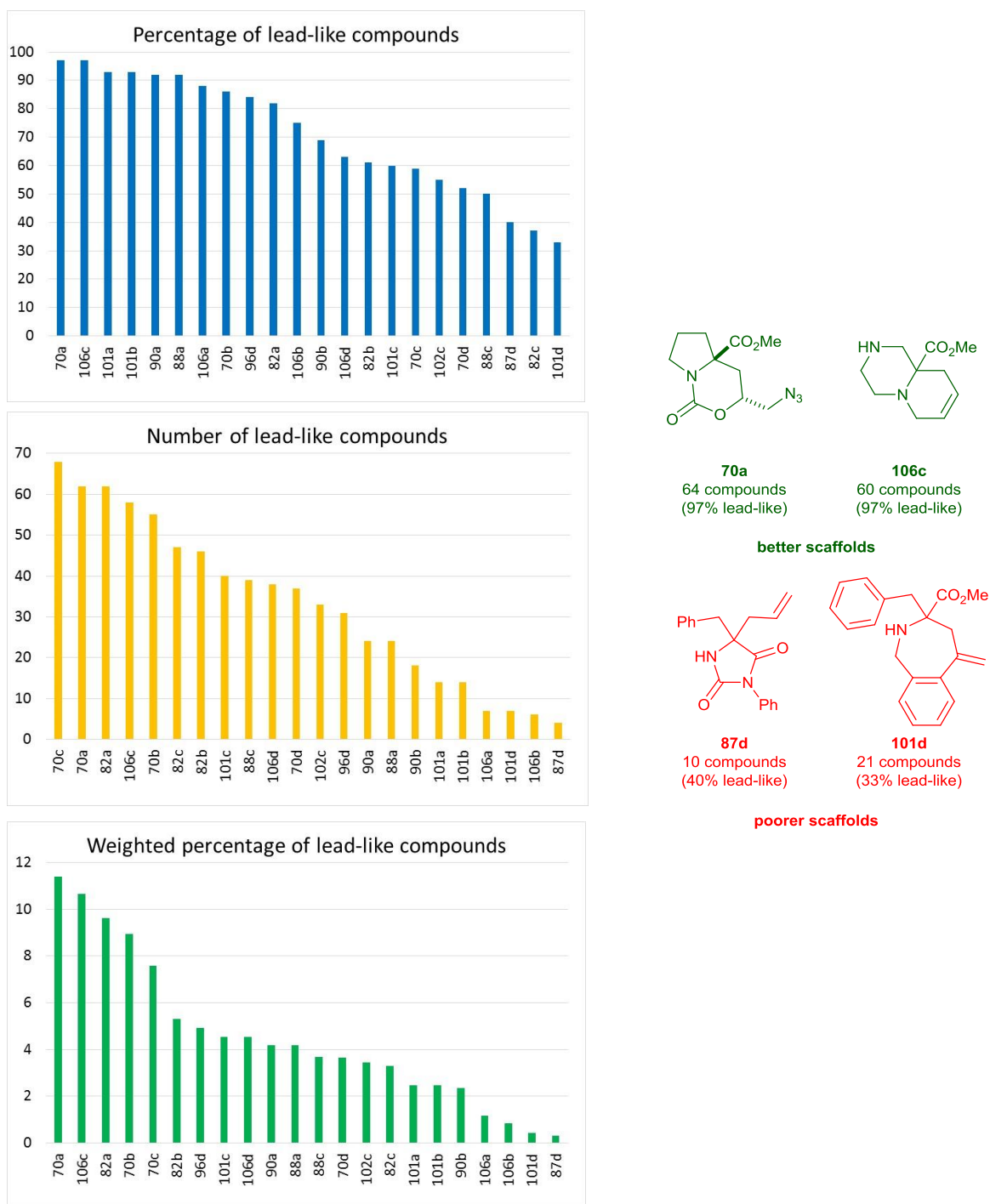


Figure 32 Histograms to show: the percentage of lead-like compounds derived from each scaffold (top); the absolute number of lead-like compounds that may be derived from each scaffold (middle); and the weighted average of the number of lead-like compounds and the percentage of lead-like compounds (bottom).

Decoration of scaffolds **70a** and **106c** would generally give large numbers of high-quality lead-like compounds and would be ideal starting points for compound library synthesis (Figure 32). The poorest scaffolds for generating lead-like compounds were **87d** and **101d**, where respectively only 4 out of 10, and, 7 out of 21 compounds were lead-like. Virtual compounds derived from scaffold **101d** generally suffered from high molecular weight (10 out of 21 fail the heavy atom filter), while compounds derived from **87d** had high molecular weights and AlogP.

By contrast the other hydantoins **88a,c** performed better (Panel A, Figure 33): for pyrrolidine-derived **88a**, 24 out of 26 compounds would be lead-like; for piperazine-derived **88c** 39 out of 78 derivatives would be lead-like.

In the urea series, pyrrolidine-derived **82a** and azetidine-derived **82b** perform well (Panel B, Figure 33). While piperazine-derived **82c** may be used to prepare many scaffolds (127), less than half of them would be lead-like (47%); most of these derivatives fail the AlogP filter (55 failures, which were generally too polar) with the remainder (25) failing the heavy atoms filter.

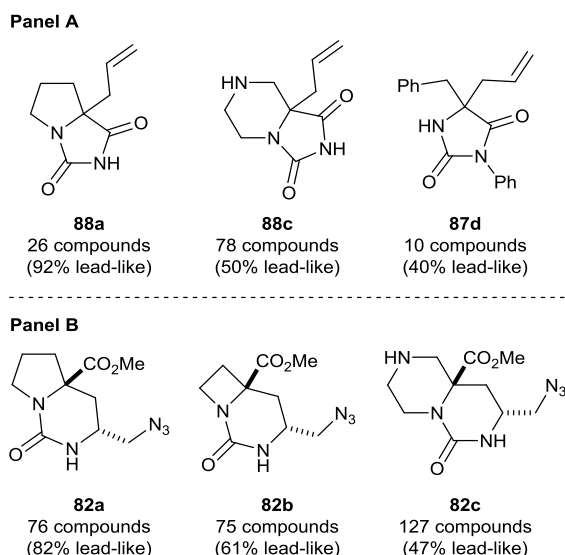


Figure 33 Panel A: comparison of the ability of the urea scaffolds **82a-c** to prepare lead-like compounds. Panel B: comparison of the ability of the hydantoin scaffolds **87d** and **88a-c** to prepare lead-like compounds.

It is also possible to rank potential for each building block to provide access to lead-like compounds. This approach would be particularly useful when deciding which bespoke starting materials would be most valuable to synthesise and use for the generation of compound libraries (Figure 34, for full details see Appendix 1, Table 24). In terms of absolute numbers (top histogram, Figure 34), the piperazine-derived building block **63c** would deliver the largest number of lead-like compounds (285). This result is not unexpected as the additional amine in the scaffold increases the number of sites available for decoration, allowing the generation of a large compound library. This compares with 193, 139 and 117 lead-like compounds for the pyrrolidine-, azetidine- and phenylalanine-derived libraries respectively. However, in terms of the percentage of lead-like compounds that may be derived per scaffold (middle histogram, Figure 34), the pyrrolidine-derived scaffolds would return 90% lead-like compounds, whilst the

piperazine-derived scaffold scores lowest at 56%. Once again, it is useful to consider the weighted average of the two aforementioned parameters (calculated as shown below). This analysis suggests that it would be most synthetically valuable to pursue the synthesis of the pyrrolidine-derived compounds (bottom histogram, Figure 34).

$$\textit{weighted average} = 100 \times \left(\frac{n \times p}{\sum_{\textit{all scaffolds}} (n \times p)} \right)$$

where n = no. lead-like compounds per building block and p = percentage of lead-like compounds per building block.

Whilst the pyrrolidine- and azetidine-derived scaffolds only differ by one methylene group, there is still value in preparing both sets of compound libraries, not least because analogous scaffolds in each series would explore different vectors in chemical space. In terms of physicochemical properties, the virtual compounds have similar average heavy atom counts (21.1 and 20.4 for the pyrrolidine-derived and azetidine-derived compounds respectively), but notably have different AlogP (0.24 and -0.30 respectively).

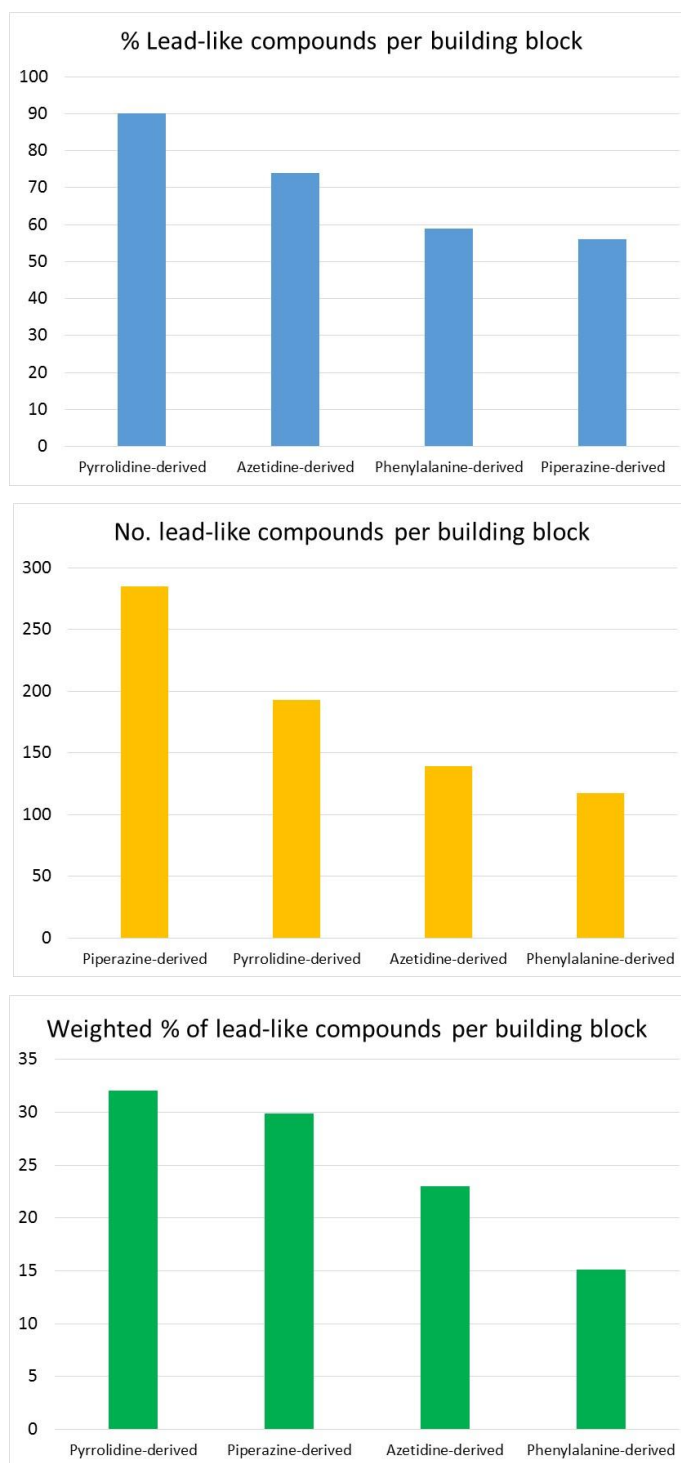


Figure 34 Histograms to show: the average number of lead-like compounds per scaffold for each building block (top); the percentage of lead-like compounds per building block (middle); and the weighted average of the number of lead-like compounds per scaffold and the percentage of lead-like compounds per building block (bottom).

The virtual library has significantly higher sp^3 content (F_{sp^3} : $\mu= 0.57$) than the commercially available compounds in the ZINC database (F_{sp^3} : $\mu= 0.33$). The phenylalanine-derived final compounds gave the lowest average F_{sp^3} (0.37), whilst the final compounds derived from the remaining building blocks had $F_{sp^3} \approx 0.6$ (see Appendix 1, Table 24 for more details). This is not unexpected due to the inclusion of an aromatic ring in the phenylalanine-derived building

block **63a**. However, the phenylalanine-derived scaffolds still performed very well in the PMI analysis (see next section).

2.5.3.2 Principal moments of inertia study

More three-dimensional compounds typically have lower attrition rates in drug discovery,¹⁹ and may serve as better leads. The shape diversity of the virtual library was compared with that of 90911 randomly selected compounds from the ZINC database (Figure 35). For each compound, the two normalised principal moments of inertia values were determined for a low energy conformation (for individual PMI plots for each scaffold see Appendix 1, Section 6.4.3).¹⁶²

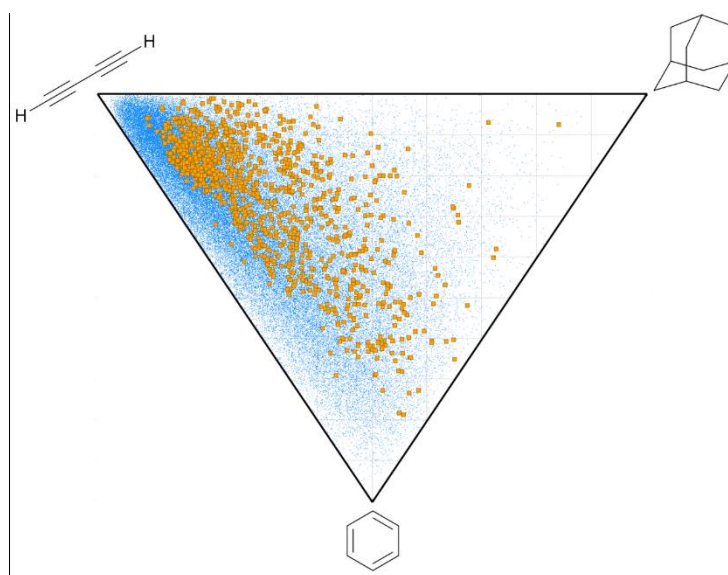


Figure 35 A normalised principal moment of inertia plot to show the shapes of the 1110 virtual compounds in relation to three idealised molecular shapes: a rod, a disk and a sphere. A systematic shift away from the flat-linear edge of the graph towards more three-dimensional molecular space can be observed for the 1110 virtual library compounds derived from the 22 scaffolds (orange, enlarged for clarity) when compared with 90911 randomly selected compounds from the ZINC database (blue). A larger annotated version of this plot is included in Appendix 1, Section 6.4.

By dividing the PMI plot into 20 bins (Figure 36, see Appendix 1, Section 6.3 for details of the associated calculation) and counting the number of compounds in each bin (Figure 37), we were able to semi-quantitatively determine the relative three-dimensionality of the virtual library compared with the rest of commercially available compounds. Notably, while 44% of ZINC compounds fall within the first bin (which lies along the flat-linear edge of the PMI plot), 0% of the virtual library compounds fall within the same space. In addition, a higher proportion of the virtual library compounds fall within the bins 3-11 which represent more three-dimensional space.

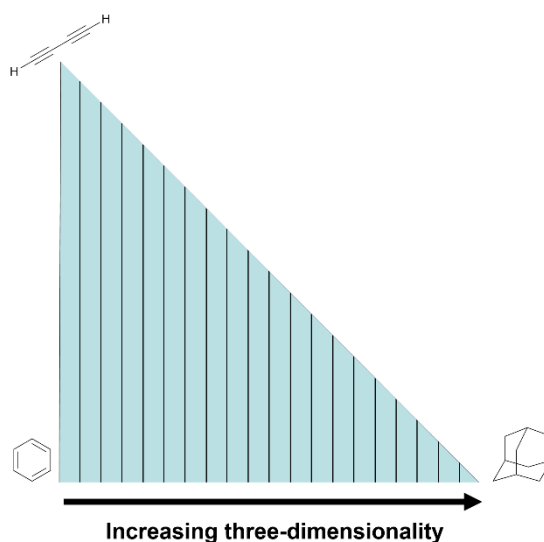


Figure 36 An axis rotation was performed, then the PMI plot was binned into 20 sections. The relative count of compounds in each bin was assessed for the virtual library compounds against 1% of the ZINC database (Figure 37).

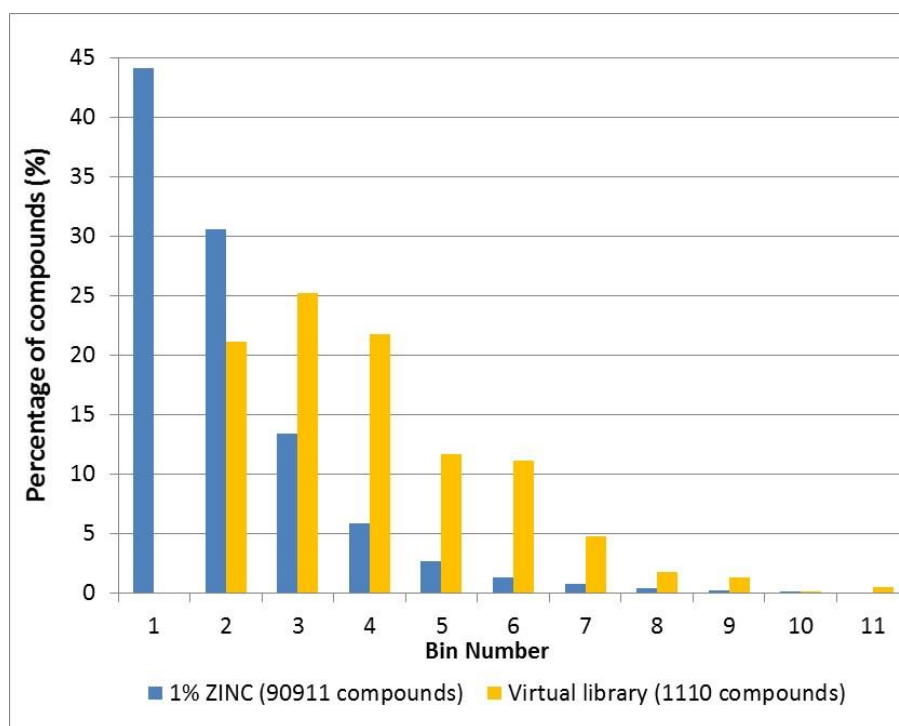


Figure 37 The relative proportions of the compounds found when the PMI was divided into twenty bins for the virtual library compounds versus 1% of the ZINC database (11 of 20 bins shown).

It was also possible to bin the PMI plot with respect to which amino ester building block was used (Figure 38). Notably, the cyclic amino esters had reasonably similar distributions. However, for the phenylalanine-derived compounds, in addition to the absence of scaffolds in bin 1, these compounds also barely occupy the next bin (3% occupancy in bin 2). In contrast, the cyclic building blocks all have >23% occupancy in bin 2. This verifies the value of including a non-cyclic amino ester in our LOS strategy.

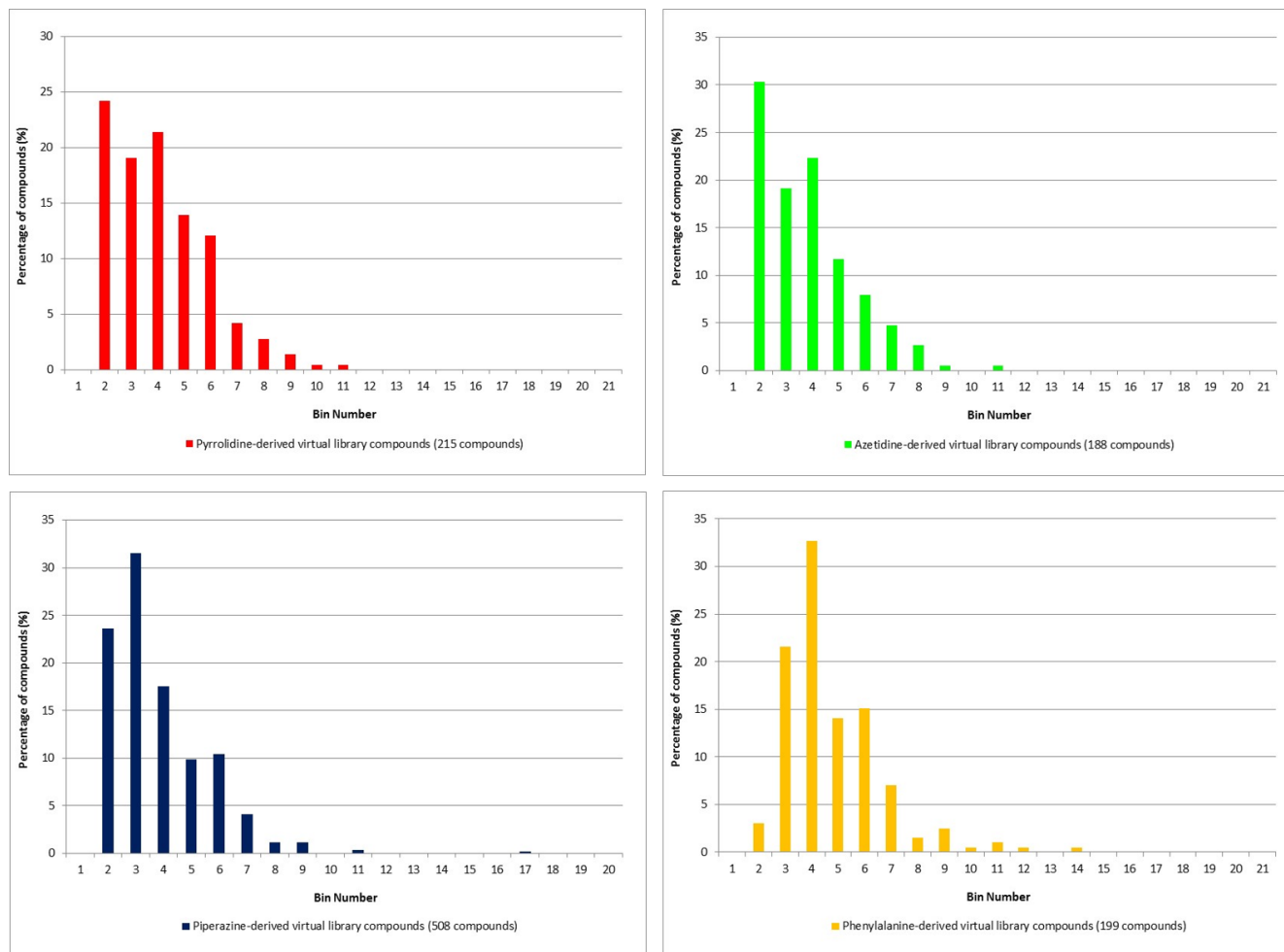


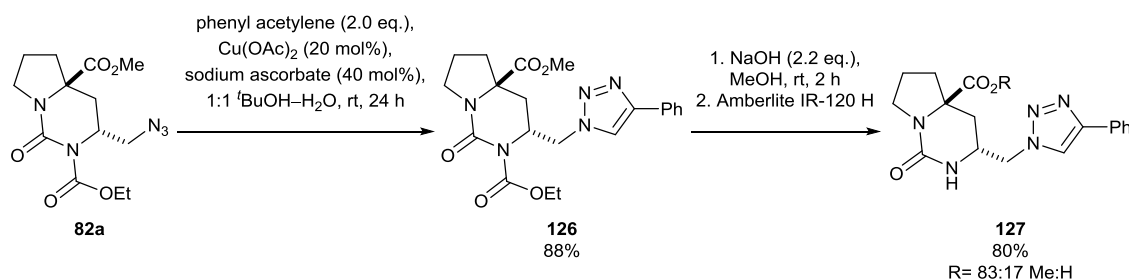
Figure 38 Relative distributions of the virtual library compounds in the PMI plot with respect to the amino ester building block **63a-d** used. The associated PMI plots are shown in Appendix 1.

2.5.4 Computational assessment: A summary

Our studies have shown that the scaffolds prepared are novel and diverse. In addition, the computational protocol has shown that decoration of the scaffolds with typical medicinal chemistry capping groups would give access to large numbers of lead-like molecules. We therefore endeavoured to put theory into practice by preparing some exemplary lead-like molecules.

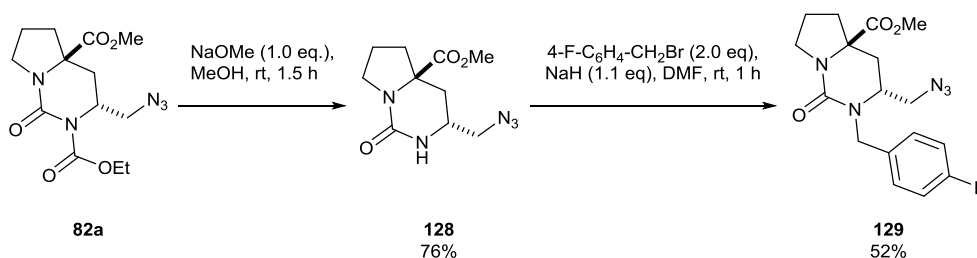
2.6 Exemplar decorations of scaffolds

The cyclic urea scaffold **82a** could undergo a Cu-mediated 1,3-dipolar cycloaddition (click reaction) with phenyl acetylene to give compound **126** in 88% yield. Removal of the ethoxycarbonyl protecting group, by treatment with sodium hydroxide, led to precipitation of a white solid after two hours. Addition of Amberlite IR-120 H (hydrogen form), followed by filtration, gave compound **127** as an 8:2 mixture of the ester:acid (Scheme 50). A longer reaction time is required in future to ensure that the starting material undergoes complete conversion to the targeted acid.



Scheme 50 Click reaction of azide **82a** and subsequent deprotection to give urea **127**.

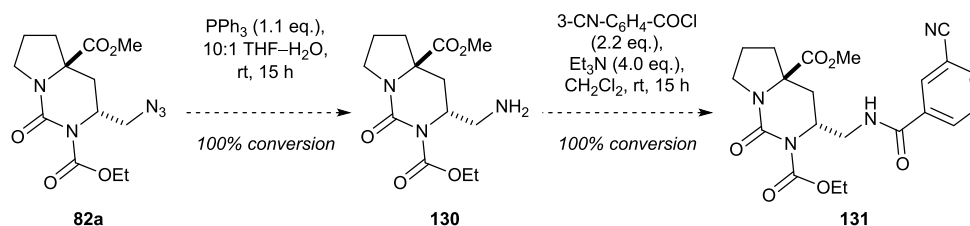
Decarbamylation of compound **82a** with sodium methoxide, to give compound **128**, followed by *N*-alkylation with 4-fluorobenzyl bromide gave **129** (Scheme 51).



Scheme 51 *N*-alkylation of urea **128**.

Reduction of the azide functionality was also investigated. Under Staudinger conditions the reaction gave complete conversion to amine **130** (as judged by

analysis of the crude with LCMS and ^1H NMR spectroscopy, Scheme 52). However, purification to remove the triphenylphosphine oxide following the reaction proved difficult, even when the reaction was telescoped with subsequent benzoylation. The characteristic ^1H NMR spectroscopy data for amine **130** and its benzoylated derivative **131** are reported in the experimental.



Scheme 52 Staudinger reduction of azide **82a** and subsequent benzoylation.

Other conditions were investigated in an attempt to simplify purification of amine **130** including: (i) the use of polymer-supported triphenylphosphine, which gave a complex mixture of inseparable products; and (ii) the use of SnCl_2 in methanol, which gave unwanted side products along with amine **130** (conditions not shown). Future experimentation may determine a more suitable purification method for products **130-131**.

2.6.1 Computational assessment of exemplar scaffolds

The plot below shows where these compounds fall in the lead-likeness assessment compared to the computationally generated library (Figure 39). These molecules fall within the bounds of lead-like space (26 heavy atoms; $\text{AlogP} \approx 0.5\text{-}2.5$) and therefore may be considered lead-like. The decorated scaffolds are also shown on a PMI plot (Figure 40). While *N*-alkylated urea **129** was more spherical, the triazole **127** and amide **131** were more rod-like.

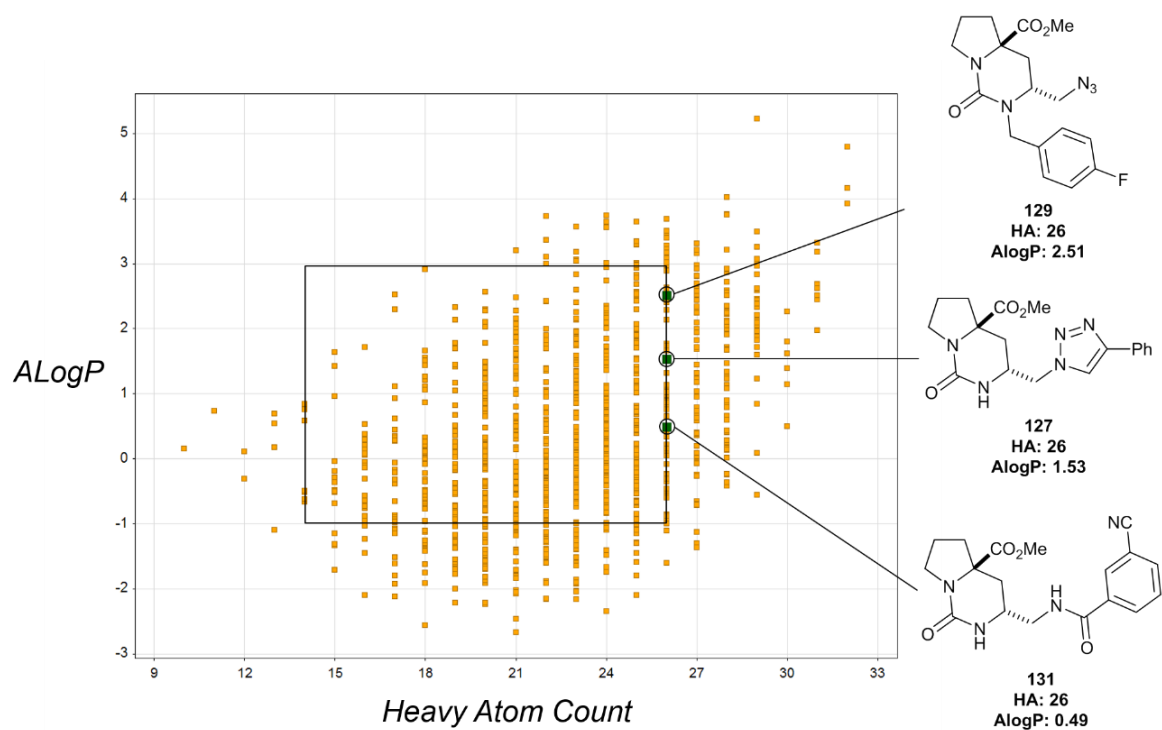


Figure 39 The distribution of molecular properties of compounds **127**, **129** and **131** (green, enlarged for clarity), derived from scaffold **82a**, compared with the virtual library of 1110 molecules derived from the 22 scaffolds (orange).

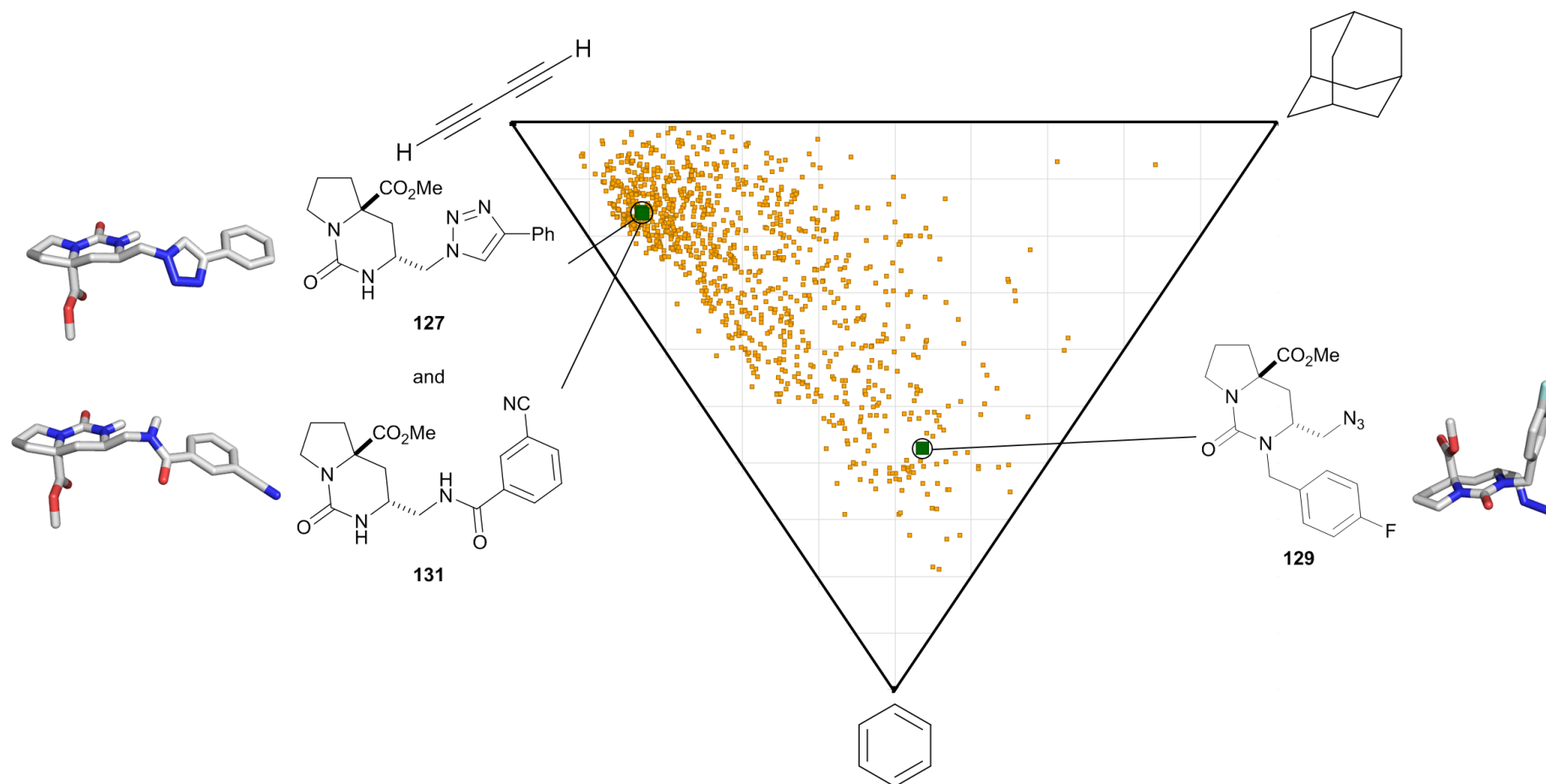


Figure 40 A PMI plot to show the relative shapes of compounds **127**, **129** and **131** compared to the rest of the virtual library. The lowest energy three-dimensional representations were generated using OpenEye Omega by George Burslem.

2.7 Conclusions and future work

In summary, the careful selection of small, polyfunctional substrates in the form of quaternary allylated amino acid esters has facilitated a modular approach to the efficient synthesis of molecular scaffolds that are novel, diverse, and can specifically target lead-like chemical space.

Two methods were investigated to prepare the quaternary allylated amino acid esters. Asymmetric allylic alkylation of azlactones was found to be robust and the resulting quaternary azlactones could be opened with *O*-, *N*- and *C*-centred nucleophiles. However, the compatibility of this method with a readily removable amide protecting group was elusive. Consequently, building blocks were prepared by allylation of Boc-protected amino esters.

A strategy to prepare scaffolds was realised, relying upon the variation of amine capping groups to tune the amino ester building blocks for cyclisation. Six cyclisation methodologies were exploited, four of which enabled the intramolecular capture of pendant nucleophiles by the alkene or ester functionalities, and two of which used transition metal-catalysed reactions between the capping group and the alkene. The use of four building blocks allowed a library of 22 scaffolds to be prepared in only 49 synthetic operations.

We attempted to generate sites on the scaffolds for further decoration. Oxidations in the presence of tertiary amines were found to be challenging. Some successes were met in the form of chlorohydrin formation and a hydroboration-oxidation protocol, but it is clear that more work is required to develop oxidations that work consistently in the presence of unprotected amines.

Virtual decoration of the scaffolds with 80 medicinal chemistry capping groups showed that the library has the potential to access large numbers of lead-like molecules. Three exemplar decorative steps were applied to a bicyclic urea.

This general approach should be applicable to many classes of polyfunctional substrate in the future, enabling the more efficient exploration of lead-like chemical space.

3.0 Results and discussion 2: A top-down approach to LOS

In contrast to the bottom-up approaches to lead-oriented synthesis developed previously in the Marsden and Nelson groups, we proposed to investigate a ‘top-down’ strategy (Figure 41). This strategy would depend on the synthetic accessibility of complex polycyclic assemblies **132**, which would be pre-engineered to bear selectively cleavable and modifiable chemical bonds. A key requirement of this strategy is for any complexity-generating steps to take place in a single operation, avoiding laborious synthetic routes to bespoke starting materials. A toolkit of chemical methodologies would then be used to break apart the assemblies to generate multiple diverse lead-like molecules.

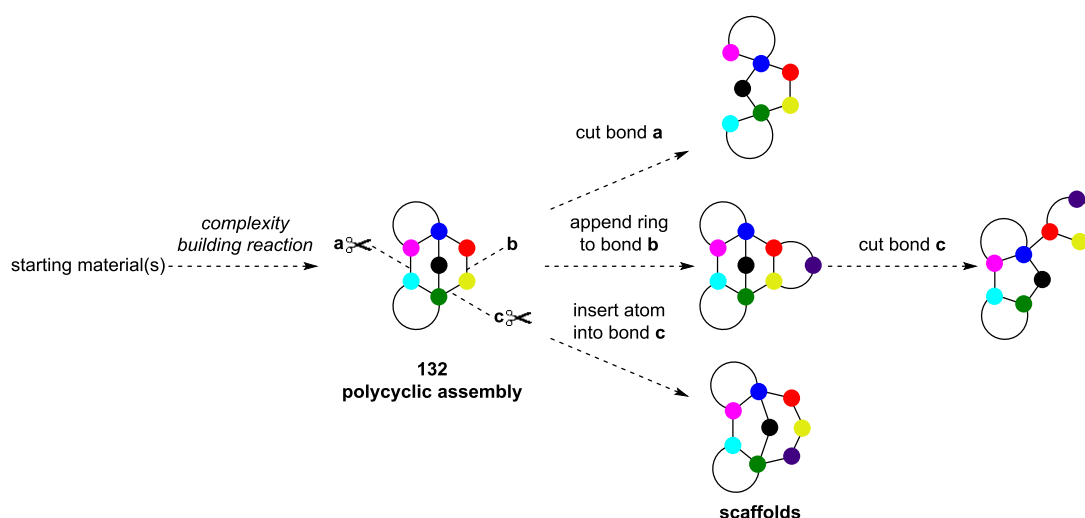


Figure 41 The proposed strategy to prepare a polycyclic assembly and illustrations of key strategies that may be used to generate scaffolds.

Ring-distortion strategies have previously been used to prepare specific classes of natural products¹⁶³ and have also been used to modify natural product scaffolds in diversity-oriented synthesis approaches.^{164–169} However, this strategy remains unexplored within the framework of LOS.

3.1 The selection of a connective reaction for LOS

Intramolecular [5+2] cycloadditions were proposed as a class of connective reactions which may efficiently deliver complex polycyclic assemblies **133** (Figure 42).¹⁶³ While intramolecular [5+2] cycloadditions are known for both oxidopyridiniums **134a** (X= N) and oxidopyryliums **134b** (X= O), there is a wealth of literature on the latter whilst there are considerably fewer accounts detailing

use of the former.^{163,170} This may be due to difficulties in preparing the appropriate starting materials for oxidopyridinium cycloadditions.¹⁷⁰ As a result of this we chose to begin our studies by investigating intramolecular [5+2] cycloadditions of oxidopyryliums. We were particularly interested in preparing cycloadducts **133b**, derived from oxidopyryliums **134b**, which bear amine-containing tethers (Y= N), as this would provide a potential point for diversification in any derived scaffolds.

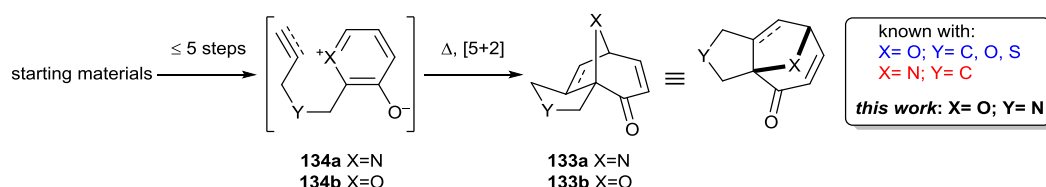


Figure 42 The proposed intramolecular [5+2] strategy to prepare polycyclic assemblies **133**.^{163,170}

Inherent in the framework **135** are a variety of different functionalities which may potentially be cleaved in order to form scaffolds (Figure 43), for instance: alkenes can undergo oxidative cleavage (equation 1), while α -oxy-ketones may be cleaved with SmI_2 (equation 2).¹⁷¹ There would also be the possibility of using 'break-and-make' strategies, for instance, oxidative cleavage of the alkene, followed by double reductive amination of intermediate **136** (equation 3). Finally, the addition of further rings may provide access to new scaffolds, for instance through the use of a condensation reaction (equation 4).¹⁷² In this way, increasing or reducing the complexity of the initial cycloadduct **135** would provide access to a variety of novel scaffolds for use in a LOS programme.

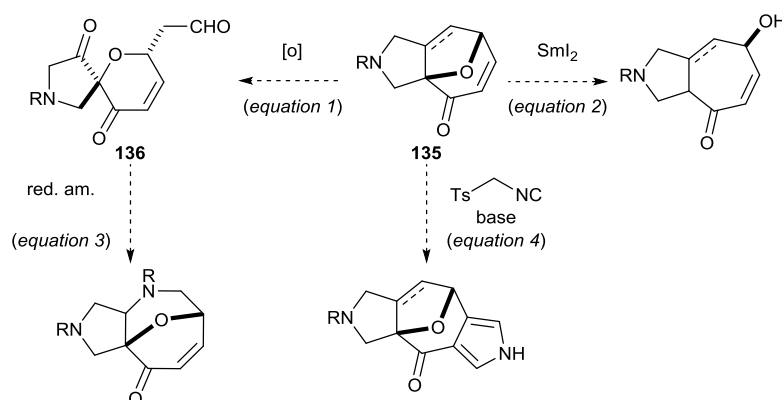


Figure 43 Potential strategies to realise the synthesis of scaffolds from polycyclic assembly **135**. The examples shown here are used to illustrate the concept and do not necessarily represent feasible transformations.

In order for the top-down strategy to be effective, preparation of any polycyclic frameworks would need to be short (≤ 5 steps), scalable and synthetically tractable. Following the establishment of a suitable methodology for the

cycloaddition, an appropriate toolkit for the cleavage of the framework would be investigated (see Section 3.2).

3.1.1 Intramolecular oxidopyrylium [5+2] cycloadditions

Intramolecular [5+2] oxidopyrylium cycloadditions have been used in the total synthesis of several natural products.¹⁶³ While oxidopyryliums **137** bearing allylic and propargylic tethers that contain carbon, oxygen and sulfur atoms are known to work in this reaction (Figure 44, Panel A, see later for specific modes of activation),^{163,170} there is only one account detailing the use of an amine-containing tether. Jacobsen reported the preparation of four cycloadducts **138a-d**, which contain protected amines (Panel B).¹⁷³ However, no supporting analytical data was given for cycloadducts **138a-d** or for the corresponding starting materials to prepare them.

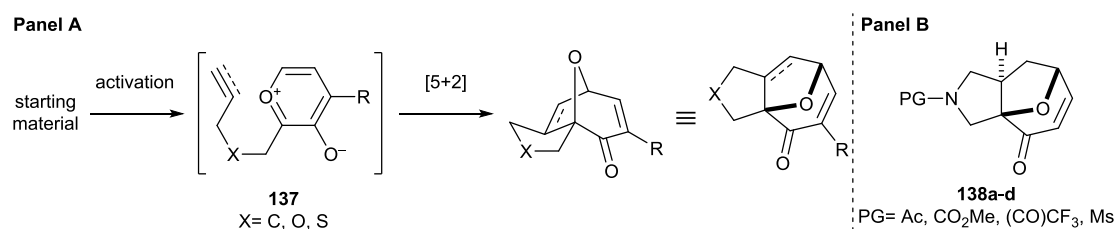


Figure 44 Panel A: intramolecular [5+2] cycloadditions of oxidopyryliums. Panel B: amine-containing cycloadducts **138a-d** reported by Jacobsen.¹⁷³

3.1.1.1 Benchmarking of an intramolecular [5+2] cycloaddition of an oxidopyrylium generated by group elimination

One of the main strategies to generate oxidopyryliums for [5+2] cycloadditions is through the thermally initiated elimination of an O-acyl group from α -hydroxypyranone derivatives **139**, followed by subsequent enolisation (Figure 45).¹⁶³

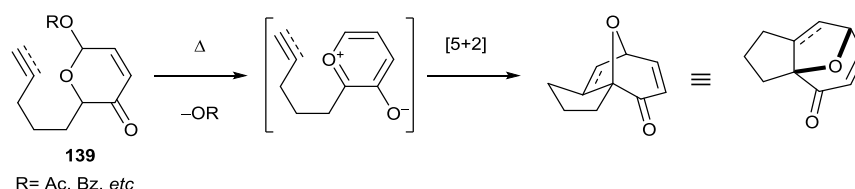


Figure 45 Intramolecular [5+2] cycloadditions of oxidopyryliums generated by group elimination.

We proposed to prepare polycyclic assemblies **140a-b** through the [5+2] cycloaddition of oxidopyryliums generated from α -acetoxyranones **141a-b**, which would bear *N*-allyl- and *N*-propargyl tethers respectively (Figure 46). Ideally for our purposes, alkylation of sulfonamide **142** with allyl and propargyl bromides

would provide late-stage divergence in the route, enabling different cycloaddition products **140a-b** to be accessed. α -Acetoxypyranone **142** could be delivered by oxidative-rearrangement (Achmatowicz reaction)¹⁷⁴ of furan **143**, followed by acetylation. Furan **143** would be prepared *via* a known¹⁷⁵ Henry reaction between furfural and nitromethane, to give adduct **144**, followed by reduction and nosylation.

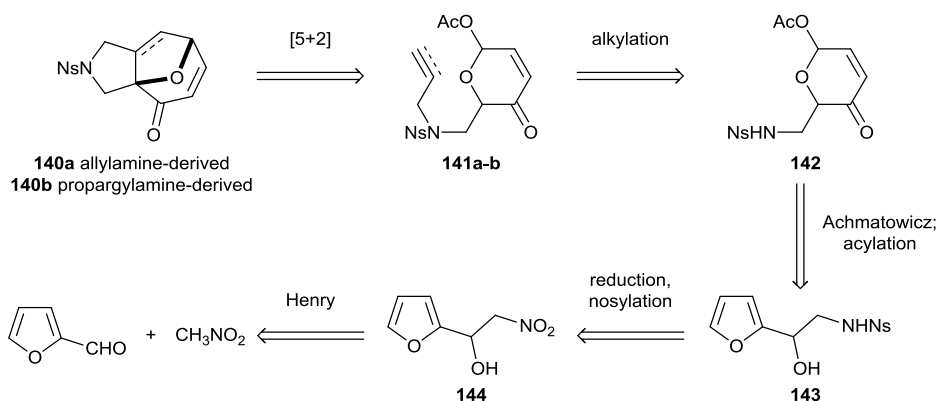
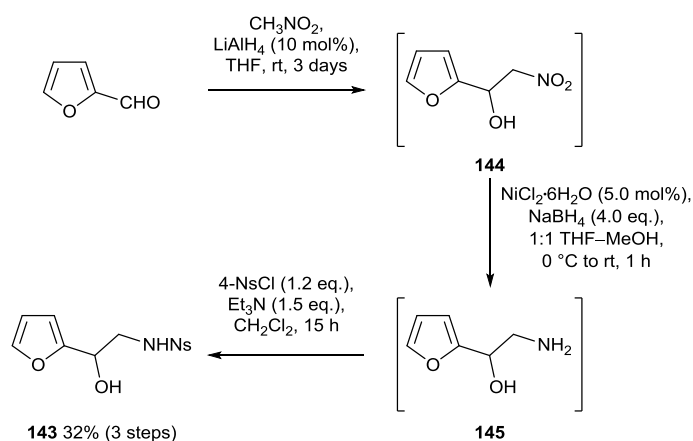


Figure 46 Proposed retrosynthetic route to polycyclic assemblies **140a-b**.

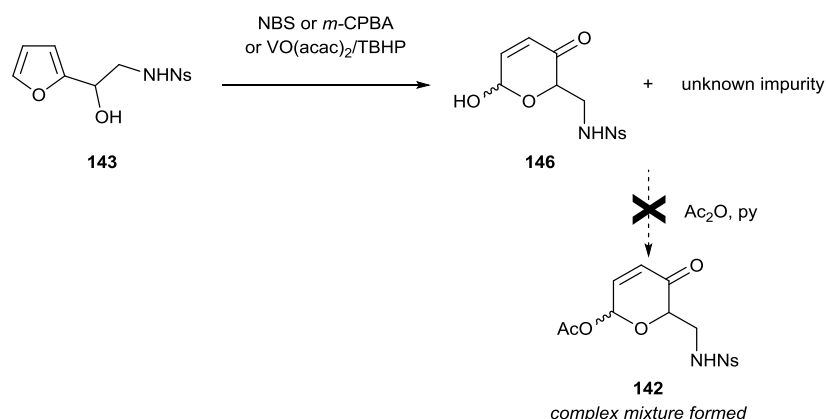
Reaction of furfural with nitromethane in the presence of 10 mol% lithium aluminium hydride provided access to adduct **144** which was used without further purification in the following steps (Scheme 53).¹⁷⁵ A catalytic nickel boride reduction¹⁷⁶ gave amino alcohol **145**. Subsequent protection with 4-nitrobenzenesulfonyl chloride gave the protected amino alcohol **143**, which was isolated in 32% yield over three steps.



Scheme 53 Preparation of protected amino alcohol **143**.

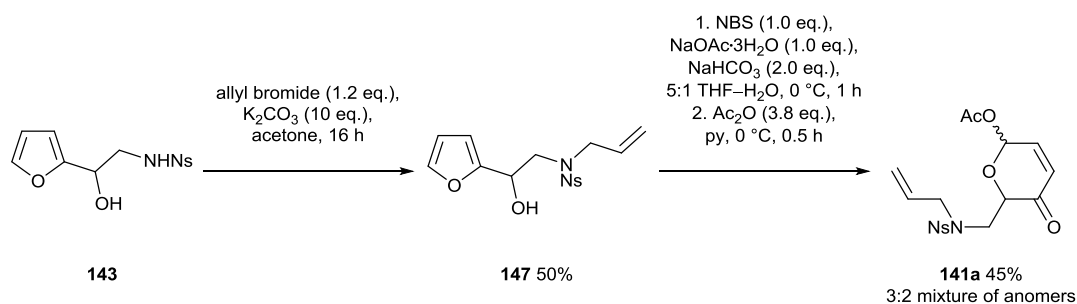
Attempted Achmatowicz reaction of furan **143** using a range of oxidative conditions (NBS;¹⁷⁷ *m*-CPBA;¹⁷⁸ and VO(acac)₂/TBHP¹⁷³) gave the desired rearranged product **146** (the characteristic enone peaks were observed in the crude reaction mixture by ¹H NMR spectroscopy) along with an unknown

aromatic side product (Scheme 54). However, the targeted product **146** could not be separated from the impurity using flash chromatography. Acetylation was also attempted, however this gave a complex mixture.



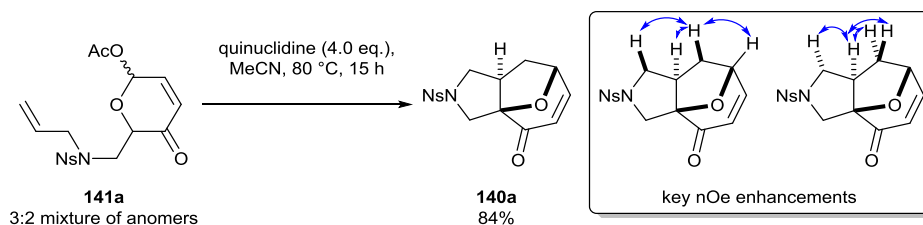
Scheme 54 Attempted preparation of α -acetoxypyranone **142**.

We chose to investigate whether prior allylation of furan **143** followed by Achmatowicz reaction would prevent the formation of the unwanted side product (Scheme 55). This strategy was less attractive than our originally proposed route as the opportunity for a late-stage alkylation with allyl and propargyl bromides was lost, resulting in earlier divergence in our routes to cycloadducts **140a-b**. Nonetheless, allylation using allyl bromide and potassium carbonate in acetone gave compound **147** in 50% yield. Compound **147** cleanly underwent the Achmatowicz rearrangement, mediated by *N*-bromosuccinimide. Acetylation of the intermediate hemiacetal gave the required cycloaddition precursors **141a** as a 3:2 mixture of anomers.



Scheme 55 Preparation of α -acetoxypyranone **141a**.

Heating α -acetoxypyranone **141a** with quinuclidine in acetonitrile¹⁷⁹ gave 100% conversion to cycloadduct **140a**, which was isolated in 84% yield (Scheme 56). The relative configuration of cycloadduct **140a** was determined by the key nOe enhancements shown.



Scheme 56 [5+2] cycloaddition of α -acetoxypyranone **141a**.

While the [5+2] oxidopyrylium cycloaddition was successful, the synthetic route to prepare starting material **141a** was laborious (seven steps) and the opportunity for late stage divergence was removed by the need to introduce the allyl group early in the synthesis to ensure a clean Achmatowicz rearrangement. As a result of this we chose to investigate whether the generation of oxidopyryliums through a different mode of activation would enable a more rapid synthesis of a polycyclic assembly.

3.1.2 Intramolecular [5+2] cycloadditions of oxidopyryliums generated by group transfer

Oxidopyryliums **148-149** can be generated from β -alkoxy- γ -pyrones **150-151** derivatives of the inexpensive commercially available natural products kojic acid **152** and maltol **153**. On heating β -alkoxy- γ -pyrones **150-151**, 1,2-migration of a labile group (R= H, SiR₃, Ac, Bz) from O-3 to O-4 generates oxidopyryliums **148-149**, which then undergoes [5+2] cycloaddition (Figure 47).¹⁶³ Early investigations by Garst relied upon a prototropic shift to generate oxidopyryliums **148-149** (R= H),¹⁸⁰ whilst Wender and Mascareñas pioneered the use of silyl group transfer.^{170,181} Oxidopyryliums **148** generated by group migration are known to undergo intramolecular [5+2] cycloadditions when X= C, O and S.^{163,170} However, the corresponding amine-containing series (X= N) is not known (although two examples are known with tethers containing amides¹⁸⁰).

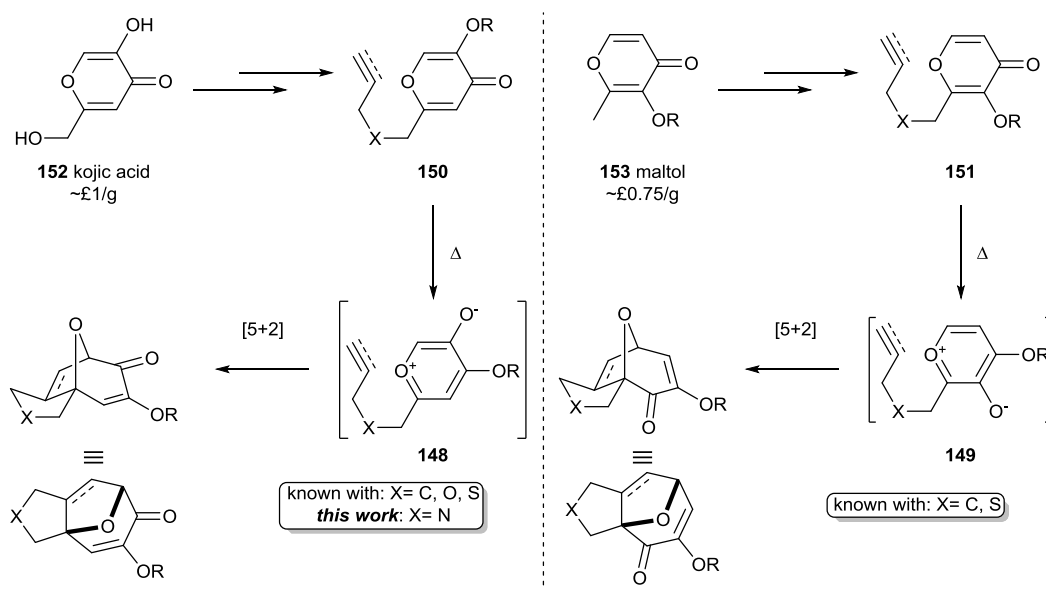
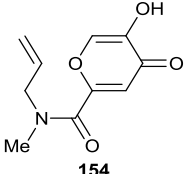
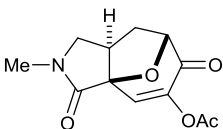
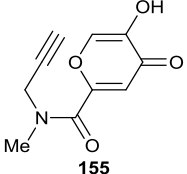
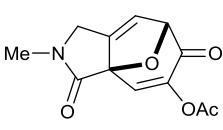
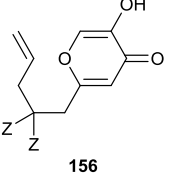
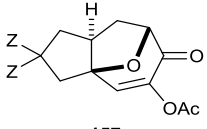
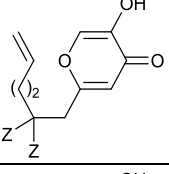
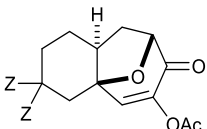
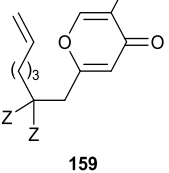
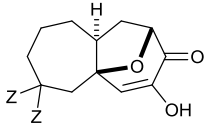
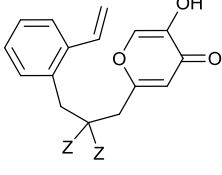
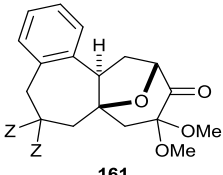
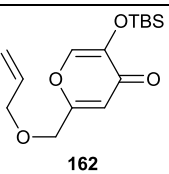
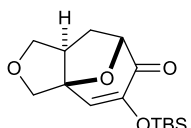
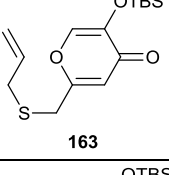
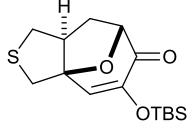
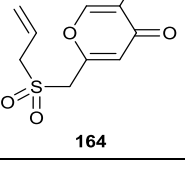
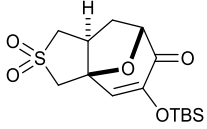


Figure 47 Intramolecular [5+2] cycloadditions of kojic acid and maltol derivatives. R= H, SiR₃, Ac, Bz etc.

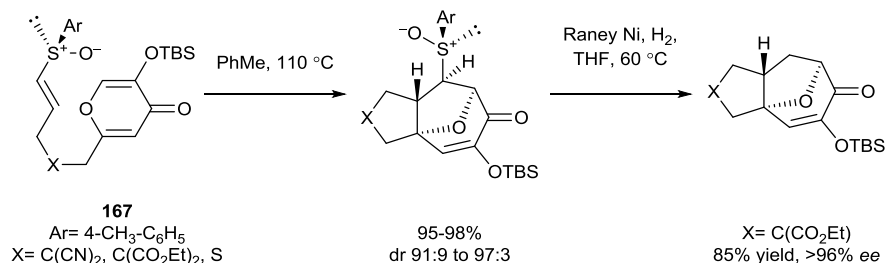
A summary of the known intramolecular [5+2] cycloadditions, using β -alkoxy- γ -pyrones as the starting materials, is detailed in Table 15. In initial studies, Garst showed that amide-containing **154-155** could undergo a prototropic shift followed by an intramolecular [5+2] cycloaddition (Table 15, entries 1-2).¹⁸⁰ Under similar conditions, substrate **156**, which bears a three-carbon tether between the alkene and the β -alkoxy- γ -pyrone, gave access to a fully carbocyclic cycloadduct **157** (entry 3). Increasing the carbon chain by one methylene gave cycloadduct **158**, albeit at a slower rate (entry 4). The analogous two-carbon homologue **159** did not react (entry 5). However, heating compound **160**, which bears a five-membered carbon tether, with methyl sulfonic acid in methanol furnished dimethylacetal **161** (entry 6). Aside from all-carbon tethers, Mascareñas showed that ethers **162** (entry 7),^{182,183} thioethers **163** (entry 8)¹⁸⁴ and sulfones **164** (entry 9)¹⁸⁵ underwent [5+2] cycloaddition when *tert*-butyldimethylsilyl ethers were used as the migrating group at O-3. Conjugated diene **165** could undergo [5+2] cycloaddition, but required prior activation with methyl triflate to form the salt **166** (entry 10). Salt **166** was then heated with cesium fluoride, which removed the silyl group and generated the zwitterion required to effect the cycloaddition.¹⁸⁶

Entry	Substrate	Conditions	Product	Yield /%
1	 154	1. PhH, 80 °C, 12 h 2. Ac ₂ O, py ¹⁸⁰	 157	55
2	 155	1. MeCN, 82 °C, 60 h 2. Ac ₂ O, py ¹⁸⁰	 158	42
3	 156	1. PhH, 80 °C, 12 h 2. Ac ₂ O, py ¹⁸⁰	 157	70
4	 158	1. PhH, 110 °C, 48 h 2. Ac ₂ O, py ¹⁸⁰	 158	65
5	 159	A variety of thermal conditions ¹⁸⁰	 159	nr
6	 160	(a) a variety of thermal conditions (b) MeSO ₃ H (1.7 eq.), MeOH, 65 °C, 12 h ¹⁸⁰	 161	(a) nr (b) 87
7	 162	PhMe, 180 °C, 12 h ^{182,183}	 162	79
8	 163	PhMe, 145 °C, 40 h ¹⁸⁴	 163	71
9	 164	PhMe, 90 °C, 18 h ¹⁸⁵	 164	91

Entry	Substrate	Conditions	Product	Yield /%
10		(i) MeOTf, CH ₂ Cl ₂ (gives 166) (ii) CsF (xs), CH ₂ Cl ₂ -DMF, 10 h ¹⁸⁶ <i>via</i>		84 dr 79:21

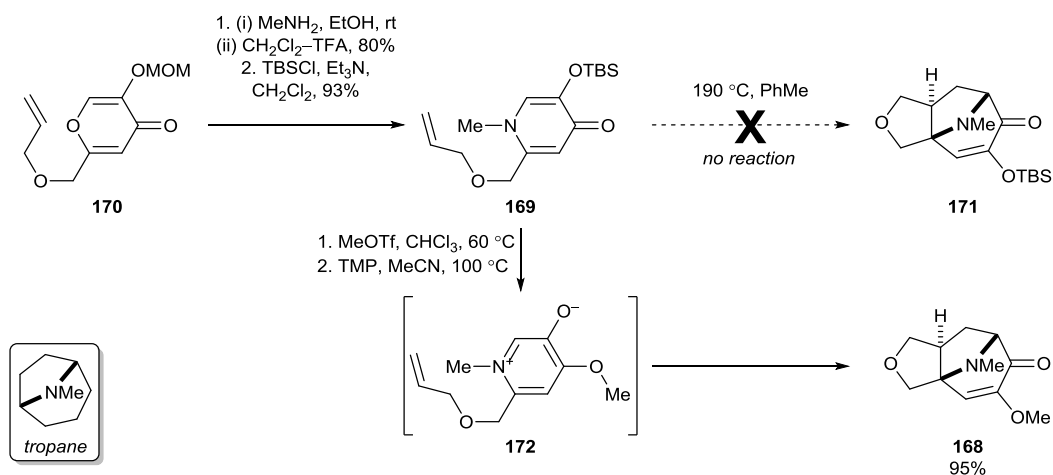
Table 15 Examples of known intramolecular [5+2] cycloadditions *via* oxidopyryliums generated from β -alkoxy- γ -pyrones. Z = CO₂Me.

An asymmetric variant of the intramolecular [5+2] cycloaddition of β -alkoxy- γ -pyrones has also been developed (Scheme 57). The use of enantiopure starting materials **167** bearing sulfinyl chiral auxiliaries allowed the cycloaddition to proceed with excellent diastereoselectivity.^{185,187–189} The auxiliary could subsequently be removed using Raney nickel. The use of sulfoximine auxiliaries in place of sulfinyl groups switches the diastereoselectivity of the reaction (not shown).¹⁹⁰



Scheme 57 Mascaréñas' diastereoselective intramolecular [5+2] cycloaddition.¹⁸⁷

It was also possible to generate cycloadduct **168** which has a nitrogen-containing bridge; embedded in this structure is the core scaffold of the tropane alkaloids (Scheme 58).¹⁸² The starting material **169** for the cycloaddition was generated through reaction of MOM-protected **170** with methylamine followed by a deprotection-reprotection sequence. The starting material **169** did not undergo [5+2] cycloaddition to give compound **171**, even when heated at 190 °C for several hours. This lack of reactivity may be due to the greater aromatic character of the pyridine and pyridinium systems when compared with their O-containing analogues.¹⁷⁰ However, methylation of compound **169**, followed by treatment with 2,2,6,6-tetramethylpiperidine (TMP), gave access to the cycloadduct **168** *via* zwitterion **172**. The cycloadduct **168** was isolated as a single diastereomer in 95% yield.



Scheme 58 Mascareñas' synthesis of cycloadduct **168**.¹⁸²

In summary, given the large reaction scope of the [5+2] cycloaddition of oxidopyryliums generated from β -alkoxy- γ -pyrones, we endeavoured to harness this methodology to prepare the targeted amine-containing polycyclic assemblies.

3.1.2.1 Preparation of β -alkoxy- γ -pyrone starting materials

In order to realise our top-down lead-oriented synthesis approach, our initial studies focused on assessing the synthetic accessibility cycloadducts **173** (Figure 48). For our purposes, ideally the R-group would be H or a readily removable protecting group (Boc, Cbz etc.).

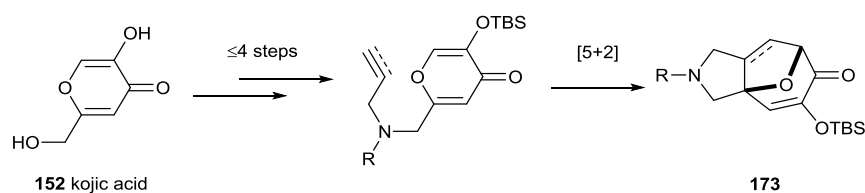
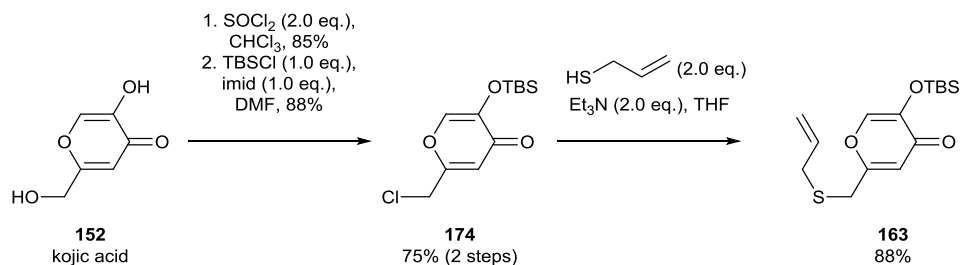


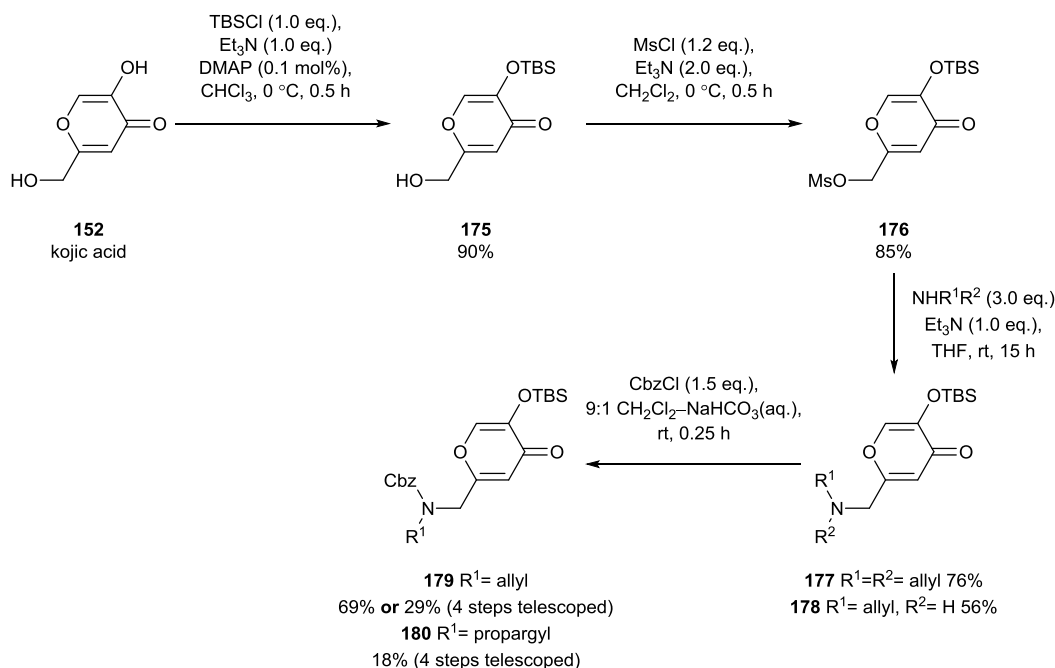
Figure 48 Proposed route to cycloadducts **173**.

Mascareñas reported the preparation of the aforementioned thioether **163** through chlorination of kojic acid to give compound **174**. Silylation, and subsequent displacement of the chloride with allyl mercaptan gave compound **163** (Scheme 59).¹⁸⁴

Scheme 59 Mascareñas' route to thioether **163**.¹⁸⁴

We found that the chlorination step of the procedure (Scheme 59) gave an unsatisfactory yield (57%) and consequently we chose to investigate an alternative route (Scheme 60). The known silylation delivered protected kojic acid **175**.¹⁹¹ Mesylation gave compound **176**, and subsequent displacement furnished amines **177-178**. Carboxybenzyl-protection of compound **178** gave carbamate **179**.

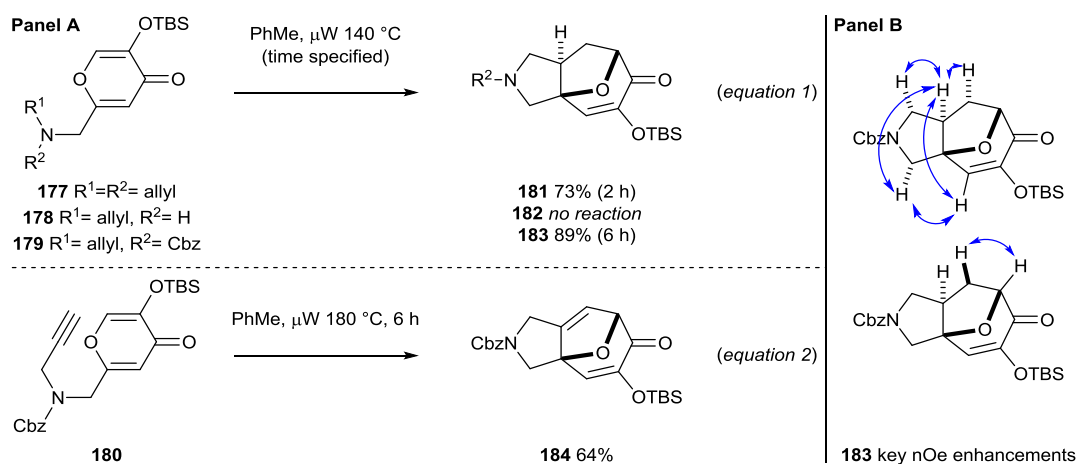
We later routinely used compounds **179-180** as substrates for our cycloaddition. Conveniently, it was found that the procedure to prepare compounds **179-180** could be telescoped. No significant change in overall yield was found for the telescoped procedure to prepare compound **179**.



Scheme 60 Preparation of starting materials for the proposed cycloaddition.

3.1.2.2 [5+2] cycloaddition of oxidopyryliums generated from β -alkoxy- γ -pyrones

With starting materials **177-180** in hand, we investigated the [5+2] cycloaddition (Scheme 61, Panel A). The diallylated starting material **177** was heated at 140 °C under microwave irradiation for two hours. Complete conversion to cycloadduct **181** was observed, which was isolated in 73% yield (equation 1). Foreseeing that the basic amine in cycloadduct **181** would be incompatible with some of the proposed scaffold-cleaving reactions (e.g. ozonolysis), we endeavoured to prepare a cycloadduct containing either a free amine **182** (which could subsequently be protected as required) or a readily removable protecting group (e.g. Cbz). However, amine **178** did not undergo cycloaddition at 140 °C or 180 °C under microwave irradiation (as judged by analysis of the crude reaction mixture by ^1H NMR spectroscopy). Heating amine **178** in DMF under microwave irradiation at 250 °C for five minutes led to complete decomposition of the starting material. Consequently we chose to attempt the cycloaddition using the Cbz-protected starting material **179**. The reaction was slower than for the analogous diallylated starting material **177**, taking 6 h to go to completion at 140 °C under microwave irradiation, but gave access to cycloadduct **183** in 89% yield (key nOe enhancements are shown in Panel B). Cycloaddition of the analogous propargyl starting material **180** (equation 2) required a higher reaction temperature of 180 °C (no reaction took place at 140 °C), furnishing cycloadduct **184** in 64% yield.



Scheme 61 Panel A: [5+2] cycloadditions of precursors **177-180**. Panel B: key nOe enhancements for compound **183**.

3.2 Establishing a chemical toolkit

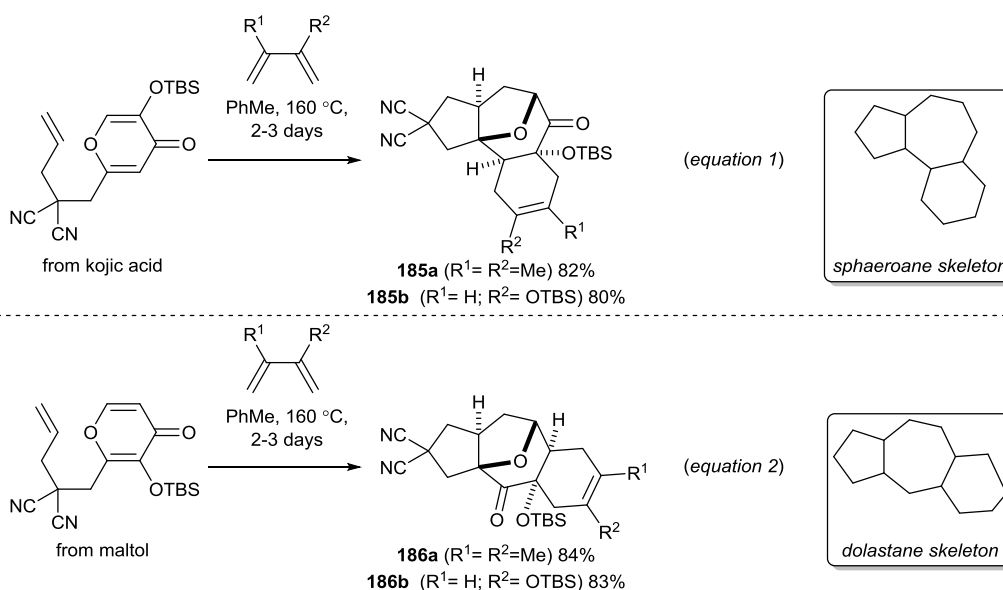
3.2.1 Previous work

With scalable and synthetically tractable routes to cycloadducts **183-184** in hand, we wanted to explore the development of a toolkit of chemical methodologies that would transform these polycyclic intermediates into new scaffolds that would be able to systematically target the synthesis of derivative lead-like compound libraries. Once again, Mascareñas has carried out substantial research into the chemistry of the cycloadducts, converting them into other scaffolds (natural products or otherwise). This work will herein be discussed.

3.2.1.1 Ring-constructing reactions

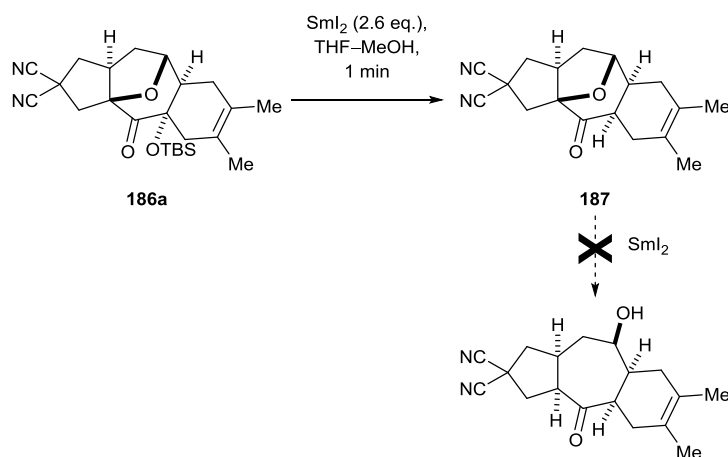
3.2.1.1.1 Tandem cycloadditions

A one-pot [5+2]/[4+2] tandem cycloaddition was developed by Mascareñas, providing rapid access to tricyclic systems **185-186** with complete diastereoselectivity (Scheme 62). Both kojic acid-derived (equation 1) and maltol-derived precursors (equation 2) were effective coupling partners in this reaction providing access to skeletons resembling dolastane and sphaeroane diterpenes.¹⁹² An analogous process has been developed for the analogous alkynyl systems (not shown).¹⁹³



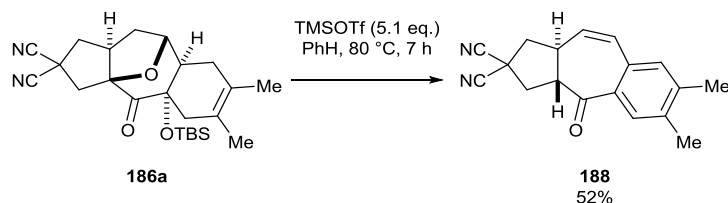
Scheme 62 Mascareñas' tandem [5+2]/[4+2] cycloaddition.¹⁹²

Attempts to open the ether bridge of compound **186a** using Sml₂ failed, instead giving rapid deoxygenation of the silyl ether (Scheme 63).¹⁹² Further treatment of compound **187** with Sml₂ did not open the bridge, even when heated.¹⁷⁰



Scheme 63 Mascareñas' attempt to open the ether bridge using Sml_2 .¹⁹²

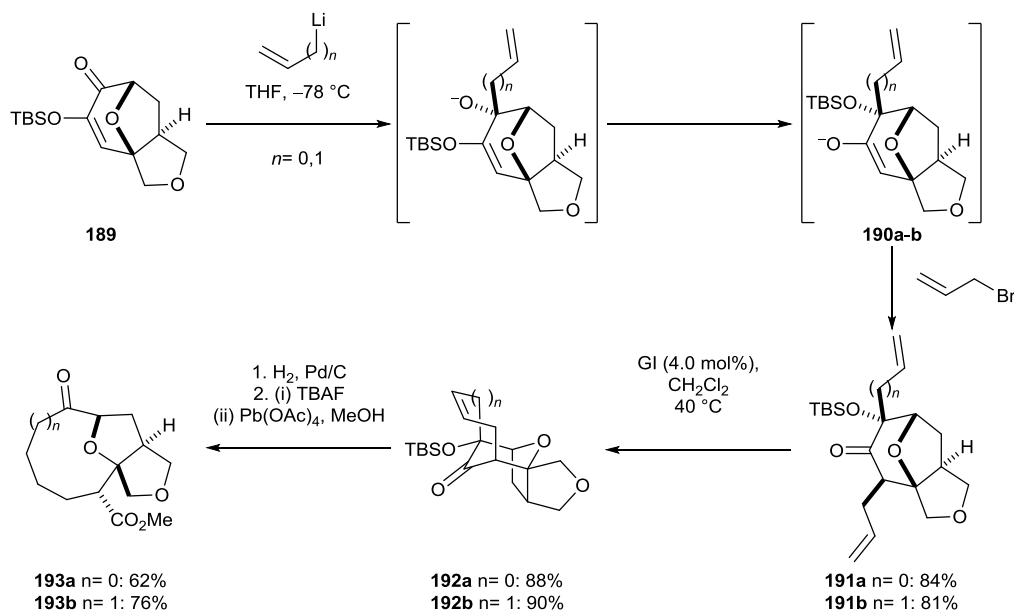
Treatment of compound **186a** with trimethylsilyl triflate in refluxing benzene gave ring-opening of the ether bridge along with aromatisation of the cyclohexene ring, furnishing compound **188** which contains a *trans*-cyclopentane ring (Scheme 64).¹⁹²



Scheme 64 Mascareñas' procedure to open the ether bridge using TMSOTf. The configuration of compound **188** was confirmed by x-ray crystallography studies.¹⁹²

3.2.1.1.2 Ring closing metathesis to form medium-sized rings

Mascareñas exploited the electrophilic reactivity of the α -silyloxyenone in the rigid polycyclic framework **189** to append *exo*-alkenyl groups to the structure (Scheme 65).¹⁸³ Double alkylations were achieved in one-pot. First, axial nucleophilic addition of organolithiums, followed by silyl migration, generated the intermediate enolates **190a-b**. Subsequent alkylation of the resulting enolates with allyl bromide gave dialkenes **191a-b**. Treatment of dialkenes **191a-b** with Grubbs' first generation catalyst (**GI**) furnished medium-sized rings **192a-b**. Following hydrogenation of the products, an oxidative ring-cleavage was employed to give nine-membered carbocycles **193a-b**, a structural motif found in terpenoids.¹⁷⁰

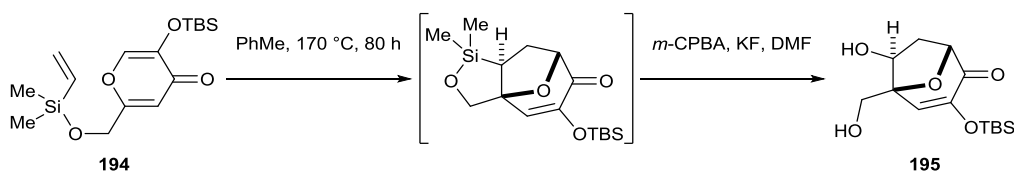


Scheme 65 Ring-closing metathesis to form medium and large rings by Mascareñas.¹⁸³

3.2.1.2 Ring-cleaving reactions

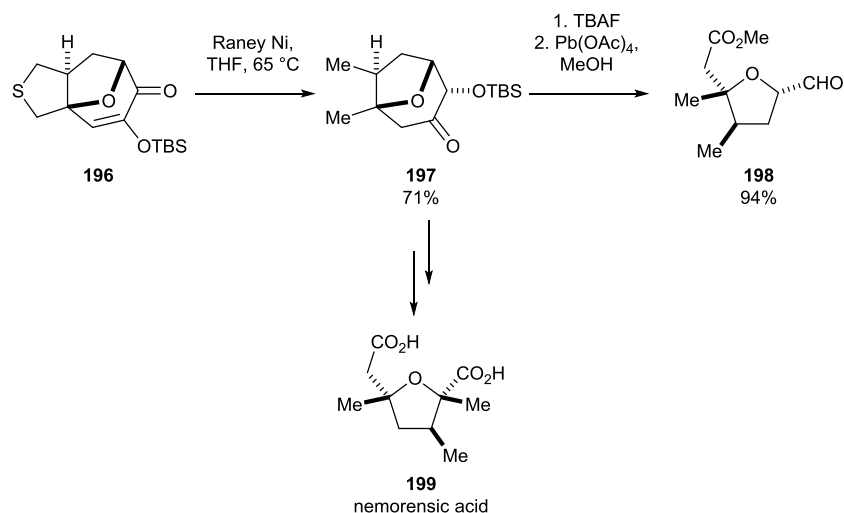
3.2.1.2.1 Semi-permanent tethers

The sluggish and poor yielding nature of the intermolecular variant of the [5+2] cycloadditions of β -alkoxy- γ -pyrones¹⁷⁰ led Mascareñas to design new substrates bearing selectively cleavable tethers for use in the more efficient intramolecular cycloaddition. For instance, following the [5+2] cycloaddition of dimethylvinylsilane-protected alcohol **194**, an oxidative work-up liberated diol **195** in 78% yield (Scheme 66).¹⁸⁴



Scheme 66 Mascareñas' temporary tethering strategy using a silyloxy tether.¹⁸⁴

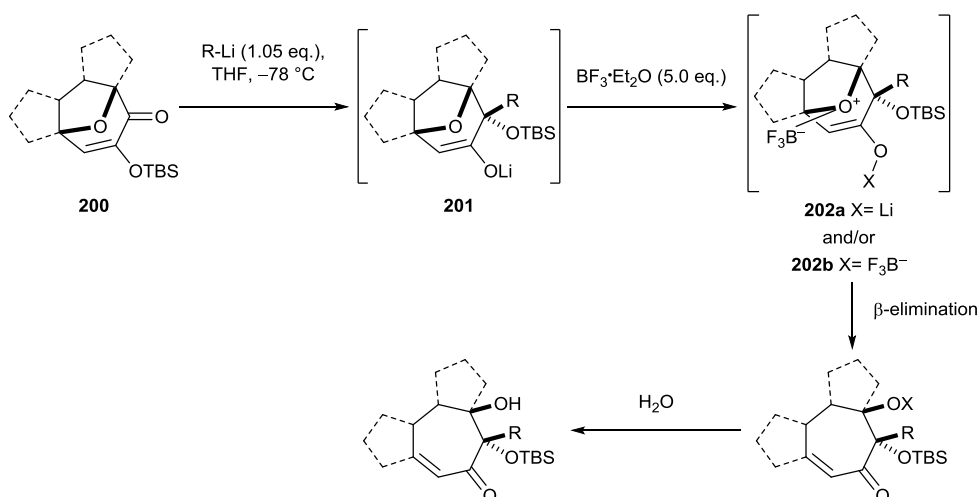
The thioether-containing cycloadduct **196** could be cleaved using Raney nickel.^{183,194} Surprisingly, this procedure also reduces the ketone to furnish the silylated α -hydroxyketone **197** following rearrangement (Scheme 67). Mascareñas cleaved α -silyloxyketone **197** by using a deprotection-oxidation sequence to provide access to highly substituted tetrahydrofuran **198**. A similar protocol was applied in the synthesis of (\pm)-nemorensic acid **199**.^{183,194}



Scheme 67 Mascareñas' reductive cleavage of thioether **196** and subsequent oxidative cleavage of compound **197**.^{183,194}

3.2.1.2.2 Cleavage of the ether bridge

It was possible to open the ether bridge of polycyclic assemblies **200** through the nucleophilic addition of organolithiums, which, following silyl migration, generated lithium enolate **201** (Scheme 68). The enolate **201** undergoes fragmentation when treated with excess boron trifluoride diethyl etherate. Mascareñas postulated that this reaction proceeds through coordination of boron trifluoride to the ether bridge, which is subsequently ejected through beta-elimination initiated by the lithium enolate **202a**. However, given that five equivalents of boron trifluoride are used in this reaction, the beta-elimination step may take place *via* the boron enolate **202b**. Notably, Mascareñas stated that the same transformation could not be achieved by heating the lithium enolate alone in THF.¹⁹⁵



Scheme 68 Opening of the ether bridge of cycloadducts **200** by Mascareñas.^{188,195} Specific examples are given in Table 16.

Alkyl, alkenyl and alkynyl organolithiums were all tolerated in the bridge-opening procedure when applied to the thioether substrate **196** (Table 16, entry 1). Ethers **203**, carbocycles **204** and esters **205** were all tolerated under the reaction conditions using methyl lithium (entries 2-4). The corresponding maltol-derived cycloadducts **206-207** could also be opened to give regioisomeric tertiary alcohols (entries 6 and 7).^{170,188} However, maltol-derived diester **210** did not open (entry 5), whilst in contrast the related kojic acid-derived cycloadduct **205** successfully underwent ring-opening (entry 4).

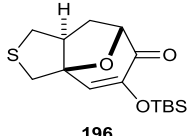
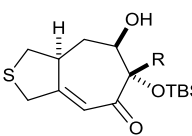
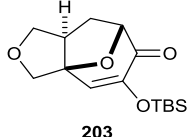
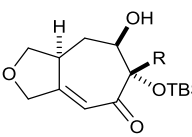
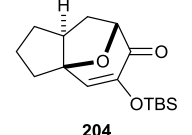
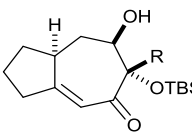
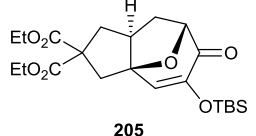
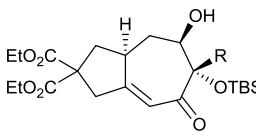
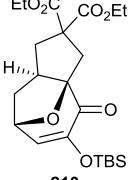
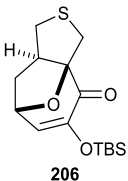
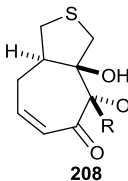
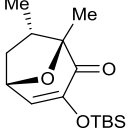
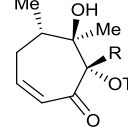
Entry	Starting material	Product	R	Yield /%
1	 196		Me Bu -CH=CH ₂ -C≡C-TMS	88 78 75 67
2	 203		Me	77
3	 204		Me	71
4	 205		Me	79
5	 210	-	Me	0
6	 206	 208	Me	80
7	 207	 209	Me	72

Table 16 Opening of the ether bridge of cycloadducts derived from kojic acid and maltol by Mascareñas.^{188,195}

3.2.1.3 Previous work: A summary

Mascareñas has developed many synthetic strategies that enable efficient access to new scaffolds from cycloadducts **208-209** (Figure 49). Mascareñas has

focused on modifications that allow access to specific classes of natural products (or natural product-like scaffolds), and consequently there remain multiple scaffold-altering reactions that could be developed and used in a LOS programme.

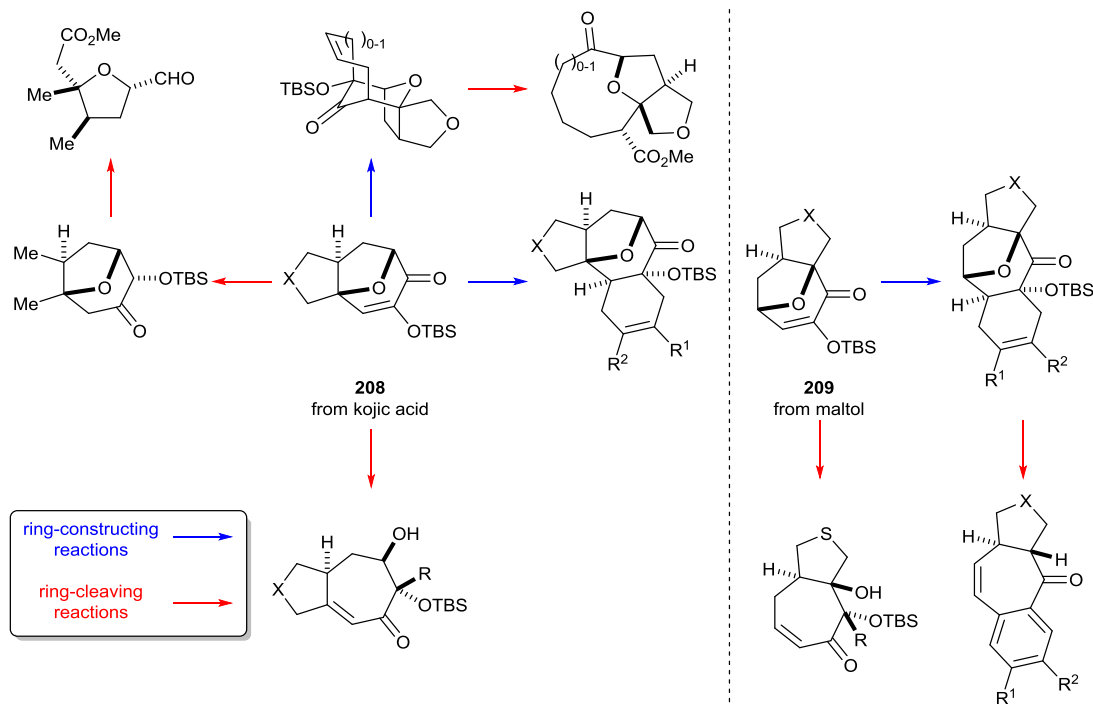


Figure 49 A summary of the scaffolds prepared by Mascareñas.¹⁷⁰

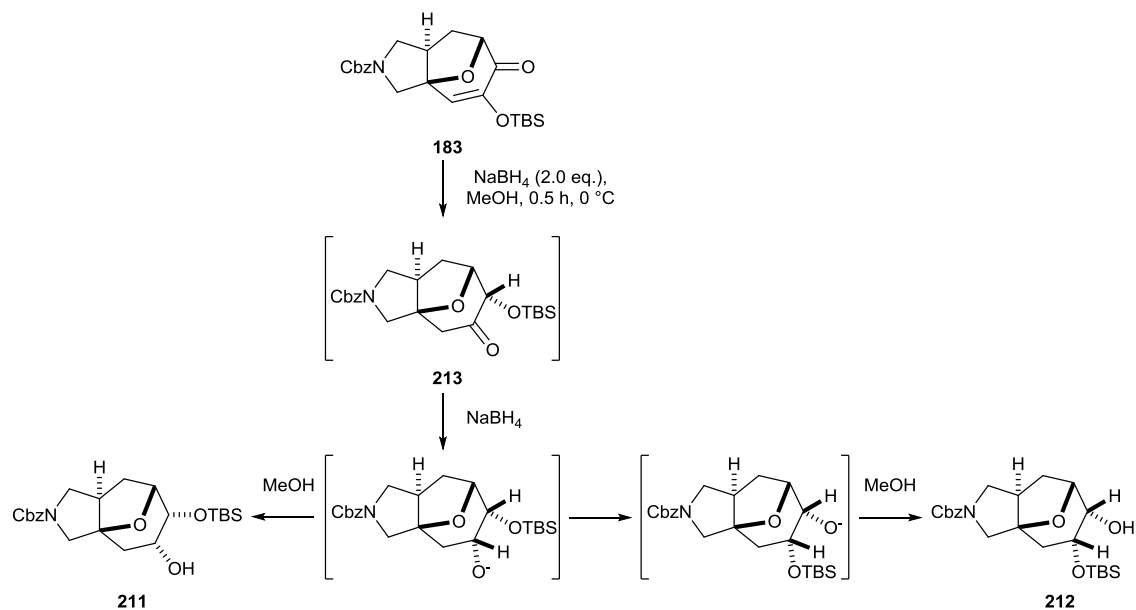
3.2.2 Functional group interconversions (FGI) of α -silyloxyenones

To identify suitable methodologies for a top-down approach to LOS from cycloadducts **183-184**, the reactivity of the α -silyloxyenone functionality was probed to investigate whether useful functionalities could be accessed that may enable scaffold preparation. Reactions of the allylamine-derived cycloadduct **183** were investigated by the candidate, whilst reactions of the propargylamine-derived cycloadduct **184** were herein investigated by Richard Doveston.

3.2.2.1 Reductions

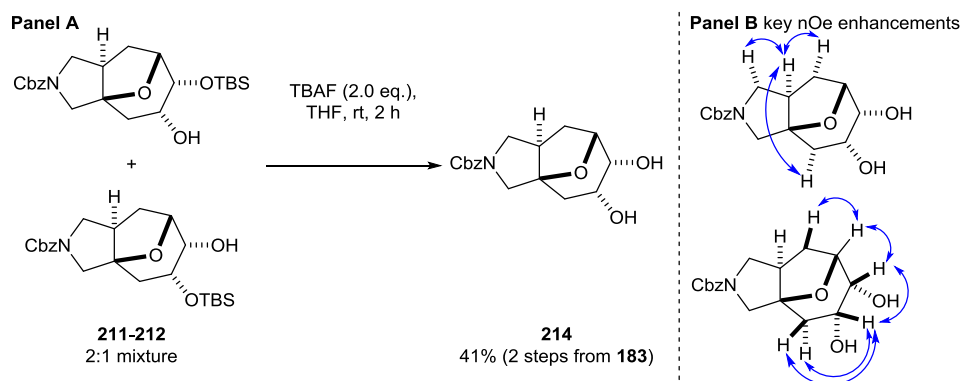
Studies commenced with the investigation of conditions for chemo- and stereoselective reductions of the α -silyloxyenone. Treatment of cycloadduct **183** with sodium borohydride in methanol gave a mixture of regioisomeric monosilylated diols **211-212** (Scheme 69), which were carried on to the next step without further purification. These products presumably arose through silyl migration following reduction of cycloadduct **183** to generate the silylated

α -hydroxyketone **213**. Compound **213** is then reduced further, leading either to remigration of the silyl group to form compound **212**, or protonation from the solvent to form compound **211**.



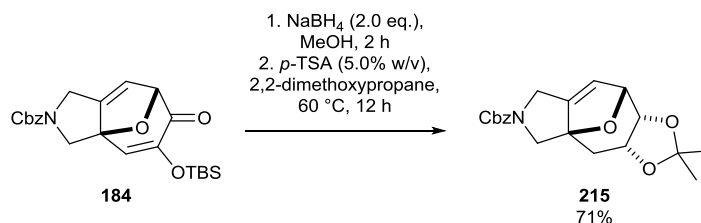
Scheme 69 NaBH₄ reduction of cycloadduct **183** to give a 2:3 mixture of the regioisomeric monosilylated diols (as judged by analysis of the crude reaction product by ¹H NMR spectroscopy).

Deprotection of the silyl protected diols **211-212** with TBAF proceeded with complete conversion (as judged by analysis of the crude product using ¹H NMR spectroscopy, Scheme 70). However, it was difficult to separate diol **214** from the tetrabutylammonium-containing side product using column chromatography, leading to a poor isolated yield (41%). The procedure needs further optimisation in future. NOESY analysis of compound **214** showed that the diol was in the *cis* configuration and located on the bottom face of the molecule.



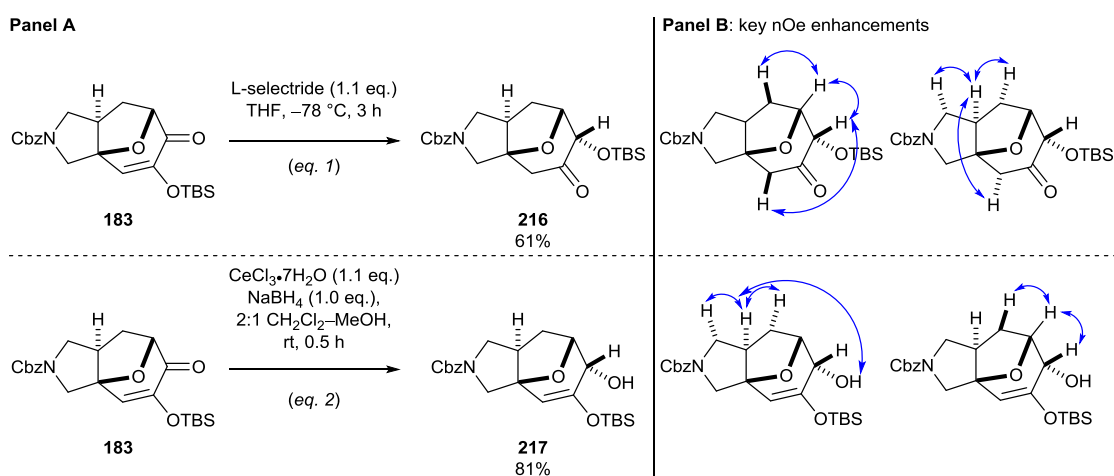
Scheme 70 Panel A: preparation of diol **214**. Panel B: key nOe assignments of diol **214**.

Richard Doveston showed that application of the aforementioned reduction conditions to cycloadduct **184**, followed by a one-pot deprotection-reprotection sequence, gave acetonide **215** (Scheme 71).



Scheme 71 Preparation of acetonide **215**.⁹⁵

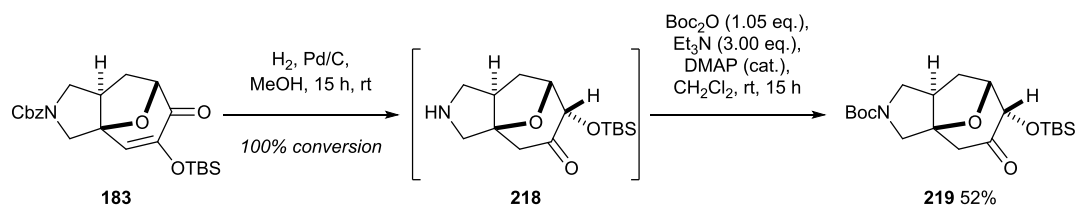
Reduction of cycloadduct **183** using L-selectride in THF resulted in silyl migration to form silylated α -hydroxyketone **216** (Scheme 72, Panel A, equation 1). However, under Luche conditions the reduction proceeded without silyl migration to give α -silyloxyenol ether **217** (equation 2). Both of the products **216-217** formed through the axial addition of the hydride reagent. NOESY analysis confirmed the relative configuration of products **216-217** (Panel B). Presumably the hardness of the oxyanion generated following the addition of the hydride reagent affects whether the silyl migration takes place. Mascareñas has previously noted that the nucleophilic addition of organolithium reagents to analogous cycloadducts results in silyl migration, whilst the addition of Grignard reagents does not lead to silyl migration.¹⁷⁰



Scheme 72 Panel A: selective reductions. Panel B: key nOe enhancements.

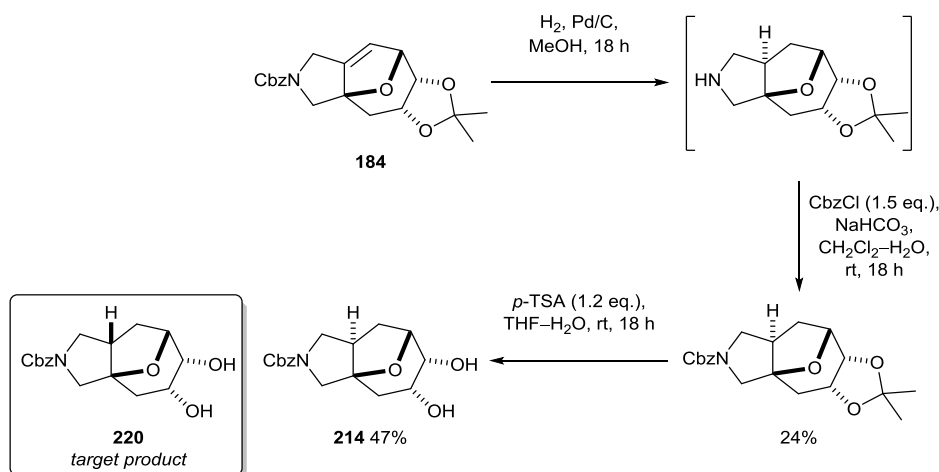
Exposure of the cycloadduct **183** to hydrogenation conditions using Pd/C as the catalyst led to reductive rearrangement of the ketone (along with reductive removal of the Cbz protecting group) to give amine **218** (Scheme 73). Attempted

Boc-protection to give compound **219** was sluggish and did not go to completion after 15 h, this requires further optimisation in the future.



Scheme 73 Hydrogenation of cycloadduct **183**.

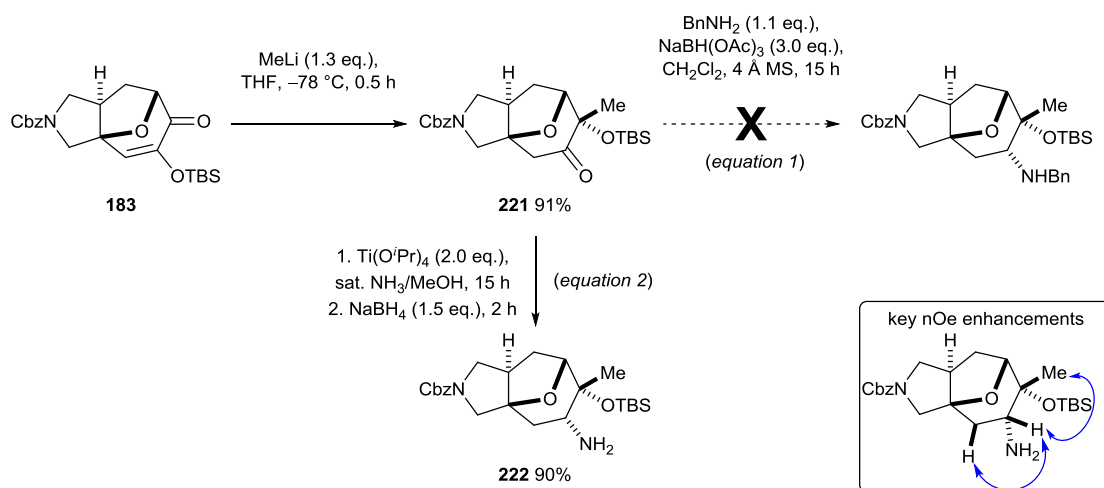
Richard Doveston investigated whether hydrogenation of cycloadduct **184** would provide access to the diastereomeric scaffold **220**, bearing a *trans*-fused five-membered ring, which would in turn offer downstream access to a diastereomeric scaffold series (Scheme 74). However, following a re-protection-deprotection sequence the resulting product was found to be identical to the previously prepared diol **214**. Presumably the added ring-strain associated with the potential formation of a *trans*-fused five membered ring renders reduction from the top face unfavourable.



Scheme 74 Hydrogenation of cycloadduct **184** and subsequent formation of diol **214**.⁹⁵

Reductive amination of α -silyloxyketone **221**, derived from cycloadduct **183**, was also investigated. First, addition of methyl lithium to the cycloadduct **183** resulted in silyl migration to form the lithium enolate, this then tautomerised upon aqueous work-up to form the silyl protected α -silyloxyketone **221** as a single diastereomer. Attempted reductive amination of ketone **221** with benzylamine and sodium triacetoxyborohydride resulted in no reaction (Scheme 75, equation 1). However, an alternative sequence was realised (equation 2). Treatment of ketone **221** with methanolic ammonia in the presence of titanium isopropoxide, followed by the

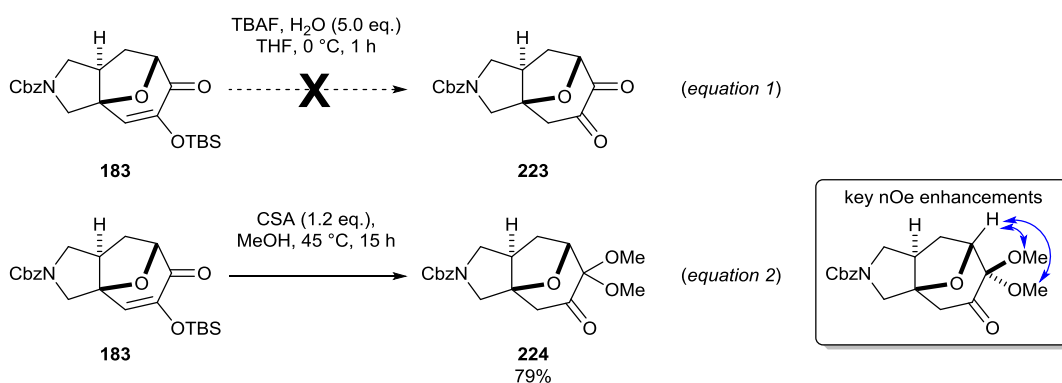
addition of sodium borohydride,¹⁹⁶ gave protected aminoalcohol **222** in 90% yield. The configuration of product **222** was confirmed by analysing the NOESY correlations.



Scheme 75 Preparation and reductive amination of ketone **221**.

3.2.2.2 Silyl deprotection

In an attempt to reveal 1,2-diketone **223**, cycloadduct **183** was treated with TBAF, however, this led to a complex mixture (Scheme 76, equation 1). Treating cycloadduct **183** with (\pm)-camphorsulfonic acid (CSA) in methanol gave access to dimethyl acetal **224** which was isolated in 79% yield (Scheme 76, equation 2). NOESY studies confirmed the regiochemistry of dimethylacetal **224**.



Scheme 76 Equation 1: attempted formation of 1,2-diketone **223**.
Equation 2: formation of 1,2-dimethylacetal **224**.

3.2.2.3 FGI summary

A range of reduction conditions have been explored which allow access to diols (both protected **211-212** and unprotected **214**), protected α -hydroxyketones **216**, **218**, **219** and **221**, a protected α -silyloxyenol ether **217**, a protected aminoalcohol **222** and a dimethylacetal **224**. This toolkit of functional group

interconversions enabled us to understand the reactivity of the α -silyloxyenone functionality and provided access to a range of useful motifs which may be exploited in the synthesis of new scaffolds (Figure 50). Unfortunately, hydrogenation of acetonide **215** did not provide access to the targeted diastereomeric series of compounds. Nonetheless, acetonide **215** later proved useful in the formation of novel scaffolds (see Sections 3.2.3.2.1 and 3.2.3.2.2).

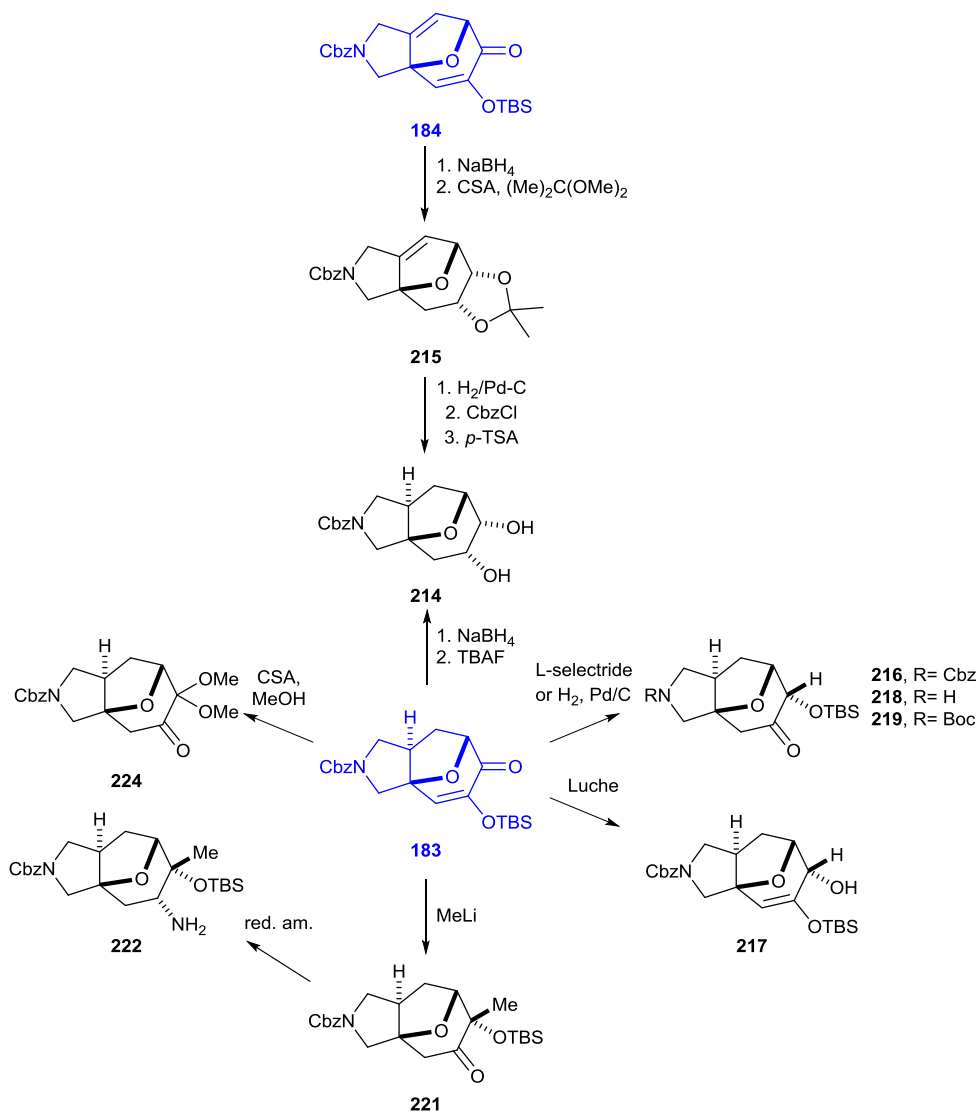


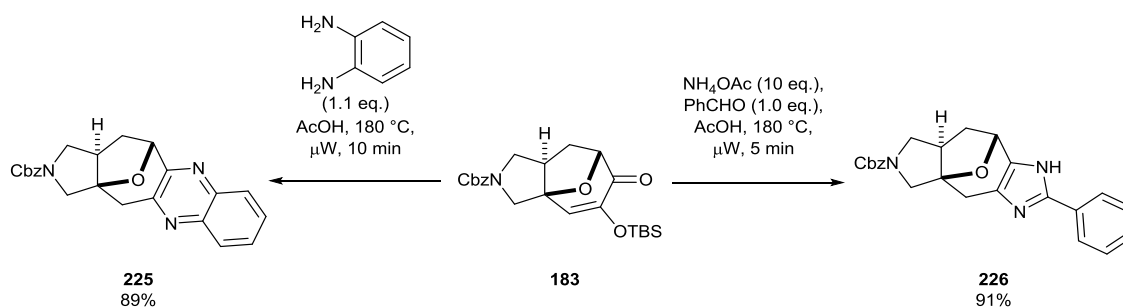
Figure 50 A summary of the FGIs investigated using cycloadducts **183-184**.

3.2.3 Synthesis of new scaffolds from polycyclic assemblies

With a clear understanding of the reactivity of the α -silyloxyenone functionality, we sought to exploit this knowledge in the preparation of scaffolds.

3.2.3.1 Ring-constructing reactions

We commenced our studies to prepare new scaffolds by exploring ring-constructing reactions. We exploited the latent 1,2-diketone functionality of cycloadduct **183** for use in modified versions of known condensation-aromatisation reactions (Scheme 77). Heating cycloadduct **183** in acetic acid with 1,2-diaminobenzene at 180 °C in the microwave for ten minutes gave rapid access to the quinoxaline **225**, which was isolated in 89% yield.^{197,198} Quinoxalines are known to have biological activity against multiple targets.^{198,199} Alternatively, cycloadduct **183** underwent condensation with ammonium acetate and benzaldehyde (Debus-Radziszewski reaction) to form imidazole **226**, which was isolated in 91% yield.²⁰⁰



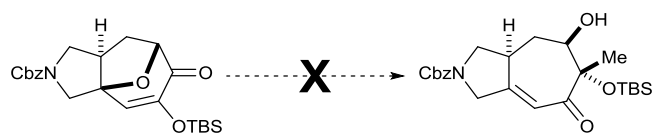
Scheme 77 Condensation-aromatisation reactions.

3.2.3.2 Ring-cleaving reactions

This section explores the preparation of new scaffolds through ring-cleaving reactions.

3.2.3.2.1 Cleavage of the ether bridge

Our initial attempts to open the ether bridge of cycloadduct **183** focused on the application of Mascareñas' previously developed conditions (see Section 3.2.1.2.2). However, these conditions failed to open the ether bridge; the only product formed was the previously prepared protected α -hydroxyketone **221** (Table 17, entry 1). A range of modifications to the procedure were applied to compound **221** including heating the presumed boron enolate (entry 2); heating the lithium enolate (entry 3); the use of TMSOTf as the Lewis acid in place of $\text{BF}_3 \cdot \text{Et}_2\text{O}$ (entry 4); and heating the substrate in sodium hydroxide, all to no avail.



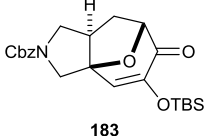
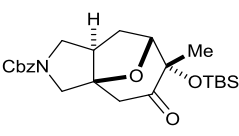
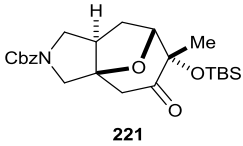
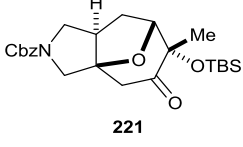
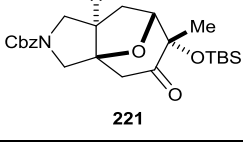
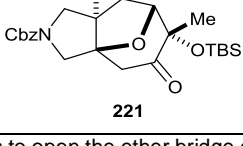
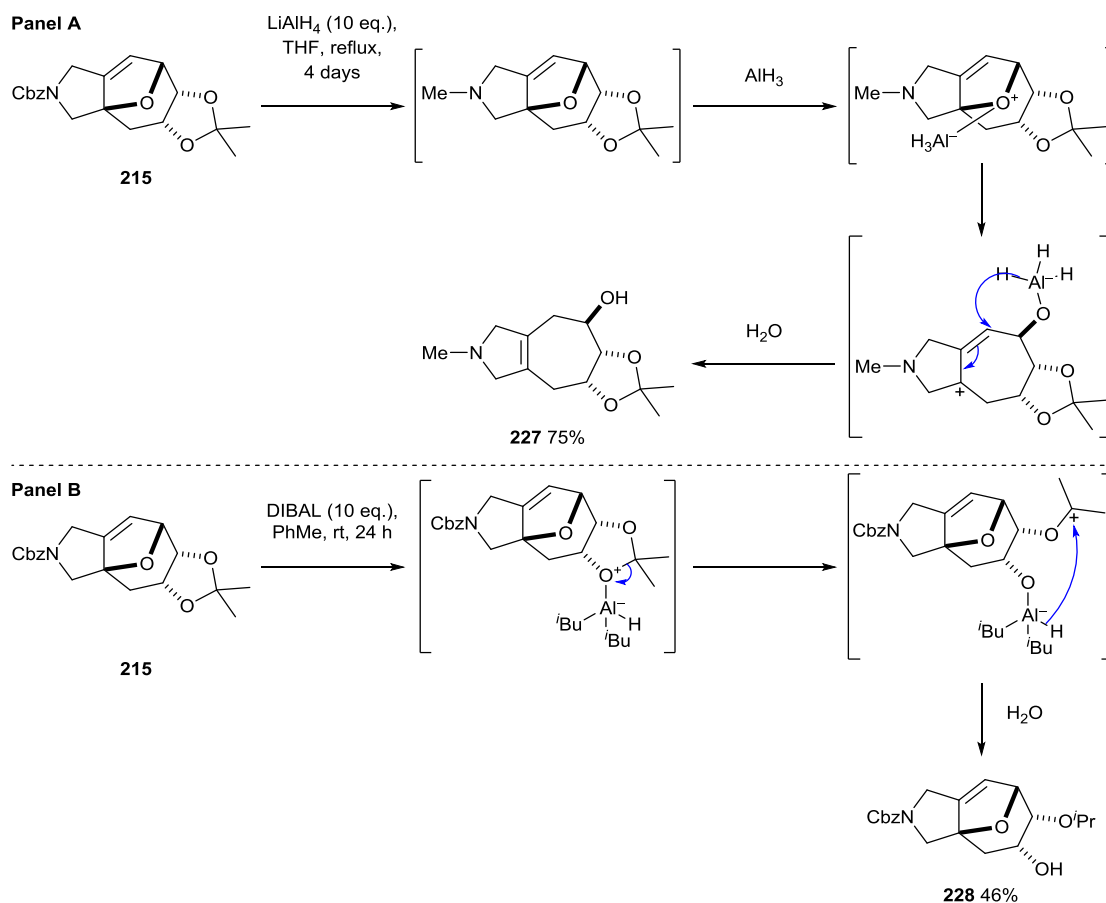
Entry	Substrate	Conditions	Reaction Outcome
			100% conversion to 221
1	 183	1. MeLi (1.05 eq.), THF, -78 °C, 10 min 2. BF ₃ ·OEt ₂ (5.0 eq.), 0.5 h, -78 °C	 221
2	 221	1. LiHMDS (1.5 eq.), THF, -78 °C, 10 min 2. BF ₃ ·OEt ₂ (5.0 eq.), PhMe, -78 °C to reflux	No reaction at -78 °C, 0 °C or rt. Decomposition after 15 h at reflux.
2	 221	1. LiHMDS (1.5 eq.), THF, -78 °C, 10 min 2. -78 °C to reflux	No reaction at -78 °C, 0 °C or rt. After 15 h at reflux: mixture of unreacted starting material and an unknown decomposition product. ^a
4	 221	1. LiHMDS (1.5 eq.), THF, -78 °C, 10 min 2. TMSOTf (5.0 eq.), PhMe, -78 °C to rt	No reaction at -78 °C or 0 °C.
5	 221	NaOH (5.0 eq.), MeOH, reflux, 2 days	Global deprotection only

Table 17 Attempts to open the ether bridge of cycloadduct **183** and derivative **221**.^aThe unknown product did not contain an alkenyl proton (by analysis of the crude reaction mixture by ¹H NMR spectroscopy).

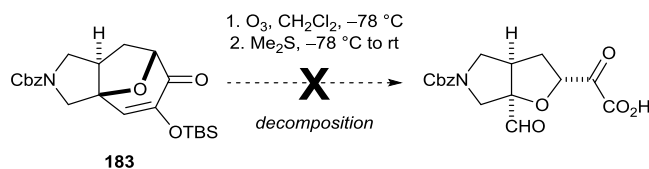
Having exhausted attempts to open the ether bridge of the allylamine-derived cycloadduct **183** we turned our attention to propargylamine-derived cycloadduct **184**. Richard Doveston showed that heating acetonide **215** with excess lithium aluminium hydride at reflux opened the ether bridge (with concurrent reduction of the Cbz group) to give amino alcohol **227**, which was isolated in 75% yield (Scheme 78, Panel A). Interestingly, treatment of acetonide **215** with DIBAL at rt led to formation of the isopropyl ether **228**, which was isolated in 46% yield (Panel B). The reduction using lithium aluminium hydride may take place *via* an internal delivery mechanism. By contrast, DIBAL is Lewis acidic and promotes reduction at the acetonide.



Scheme 78 Opening of the ether bridge of acetonide **215**.⁹⁵

3.2.3.2.2 Oxidative cleavages and subsequent reductive aminations

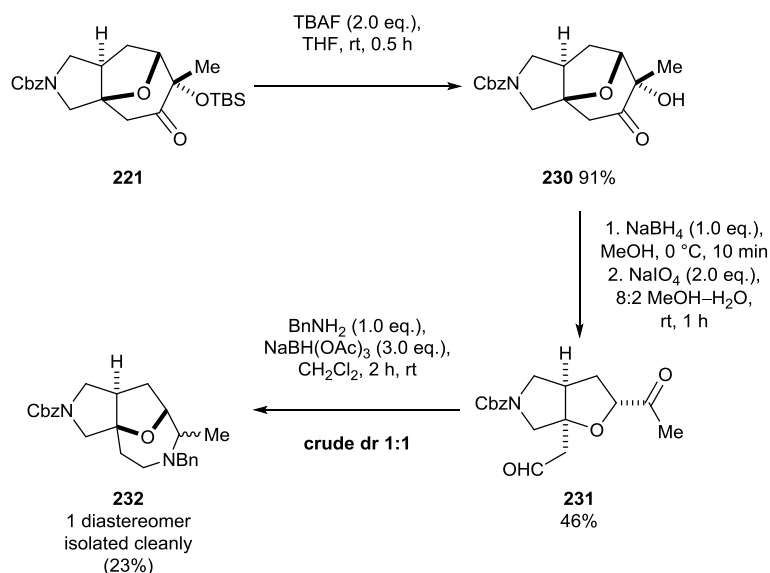
Oxidative cleavage of the polycyclic assemblies was investigated to prepare scaffolds. Initially ozonolysis of the α -silyloxyenone of cycloadduct **183** was attempted, however, this led to decomposition (as judged by analysis of the crude reaction mixture by ¹H NMR spectroscopy, Scheme 79).



Scheme 79 Attempted ozonolysis of cycloadduct **183**.

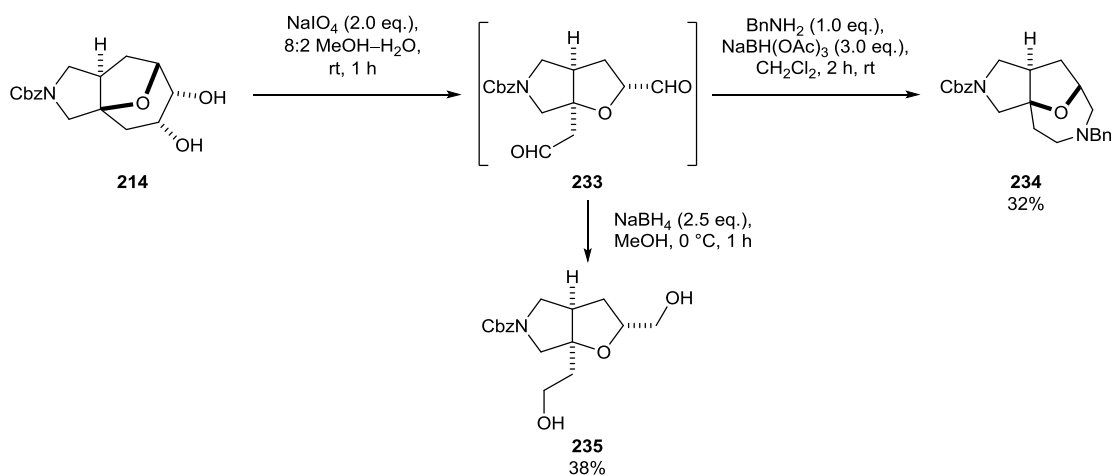
To provide an alternative route to the same bicyclic scaffold core, oxidative cleavage of 1,2-diols was investigated (Scheme 80). First, deprotection of α -silyloxyketone **221** (see Section 3.2.2.1 for preparation) with TBAF gave precursor **230**. Reduction with sodium borohydride, followed by cleavage of the resulting diol with sodium periodate, gave complete conversion to ketoaldehyde **231** (as judged by analysis of the crude product by ¹H NMR

spectroscopy), which was isolated in 46% yield. Double reductive amination of ketoaldehyde **231** using benzylamine and sodium triacetoxyborohydride gave a 1:1 mixture of diastereomers of cyclic amines **232** (as judged by analysis of the crude reaction product using ^1H NMR spectroscopy). However, during purification, only one amine diastereomer was isolated cleanly, in 23% yield. NOESY studies to determine the configuration of amine **232** proved inconclusive.



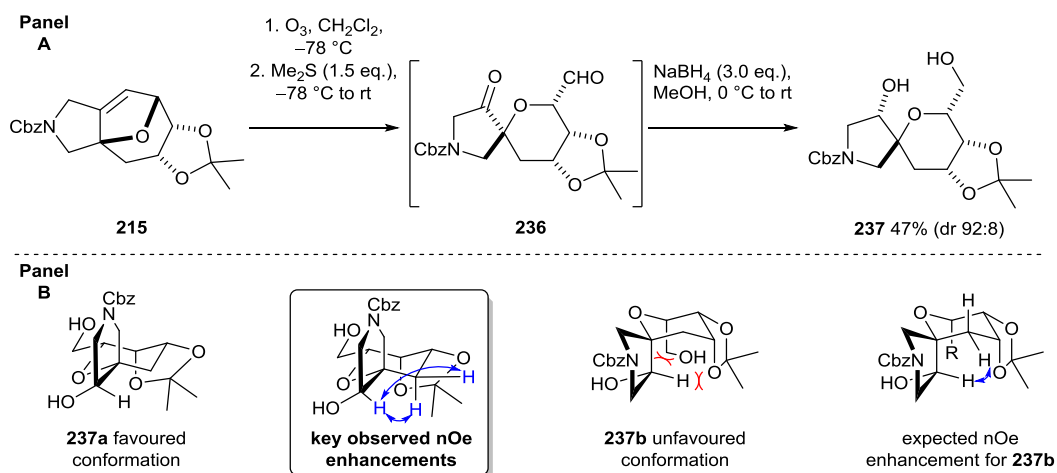
Scheme 80 Preparation of the ketoaldehyde scaffold **231** and subsequent reductive amination to form cyclic amine **232**.

The lack of diastereoselectivity in the reductive amination of ketoaldehyde **231** prompted us to consider reductive amination of the analogous dialdehyde **233** in order to avoid the creation of a new stereocentre. Starting with diol **214** (synthesis described in Section 3.2.2.1), oxidative cleavage with sodium periodate provided access to dialdehyde **233** (Scheme 81). Pleasingly, double reductive amination with benzylamine delivered cyclic amine **234**, which was isolated in 32% yield over two steps. Alternatively, reduction of dialdehyde **233** with sodium borohydride gave access to diol **235**, which was isolated in 38% yield, however, the purification procedure requires optimisation.



Scheme 81 Formation of cyclic amine **234** and diol **235**.

Richard Doveston investigated the oxidative cleavage of acetonide **215** (Scheme 82, Panel A). Ozonolysis gave access to ketoaldehyde **236** which was subsequently reduced with NaBH_4 to give diol **237** as 92:8 mixture of diastereomers. Notably, in order to achieve high diastereoselectivity in the formation of diol **237**, dimethylsulfide had to be used to reduce the intermediate ozonides, as using NaBH_4 to directly reduce the ozonides gave diol **237** as a 2:1 mixture of diastereomers. The erosion of diastereoselectivity presumably arises through the stepwise reduction of the ozonides. The configuration of diol **237** was inferred from the NOESY correlations (Panel B); enhancements between the proton alpha to the secondary alcohol and two tetrahydropyran methylene protons were observed, suggesting that the secondary alcohol points away from the tetrahydropyran ring. The conformation **237a** is presumably preferred over the conformation **237b**, which would lead to a sterically unfavoured 1,3,5-triaxial arrangement of non-hydrogen ring substituents. For conformation **237b** we would not expect to observe an nOe enhancement between the proton alpha to the secondary alcohol and the axial methylene proton on the tetrahydropyran ring.



Scheme 82 Panel A: ozonolysis to form ketoaldehyde **236** and subsequent reduction to diol **237**.
Panel B: configurational and conformational assignment of diol **237**.⁹⁵

3.2.3.3 Scaffold synthesis: A summary

Including the cycloadducts themselves, a total of eight scaffolds (at the graph-node-bond framework level) have been prepared so far using the top-down approach (Figure 51). Four unique scaffolds were prepared from the allylamine-derived cycloadduct **183**, whilst two were prepared from the propargylamine-derived cycloadduct **184**. Notably, each scaffold was delivered in ≤ 3 steps from a preceding scaffold.

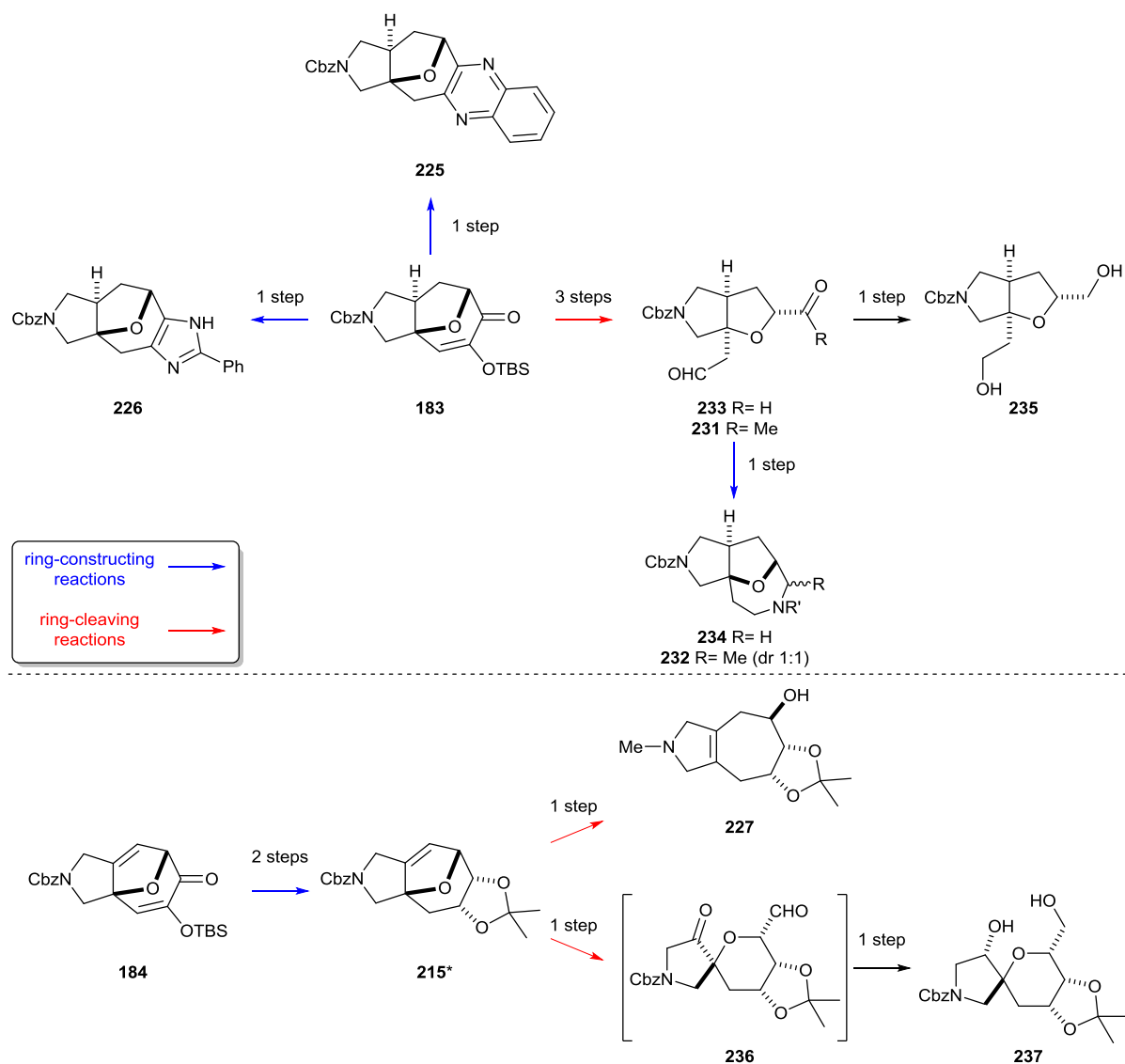


Figure 51 A summary of the scaffolds prepared in this study.
 *Not considered to constitute a new scaffold in our analysis.

3.3 Computational assessment of the scaffolds prepared

To assess the novelty, diversity and lead-likeness of the library, nine compounds were chosen for virtual decoration and computational analysis. This study included six scaffolds (**225**, **226**, **227**, **231**, **234** and **237**) derived from cycloadducts **183-184**, and three representative derivatives (**214**, **216** and **230**) based on the cycloadduct framework **183** (Figure 52). These nine compounds will be collectively referred to as scaffolds herein.

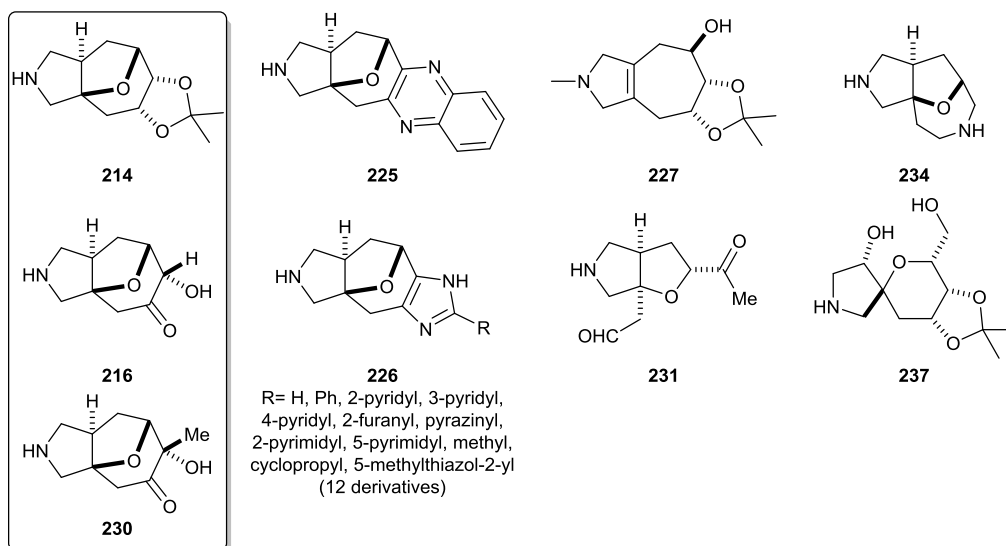


Figure 52 Scaffolds chosen for virtual decoration. Acetonides were included to prevent decoration of any diols. Acetonides were removed following the decoration step in the computational studies (see Section 3.3.3).

3.3.1 Novelty assessment

To assess the novelty of the scaffolds, a structure search was performed for the nine compounds as shown above (Figure 52, acetonide protecting groups were removed). None of the compounds were found in the ZINC database (9×10^6 compounds). In addition, none of the compounds were found in the CAS registry.

The Murcko assemblies⁹⁷ (with alpha attachments) were also generated and compared against the Murcko assemblies (with alpha attachments) of a random 5% sample of the ZINC database (4.5×10^5 compounds). Only the Murcko assembly derived from compound **231** was found as a substructure match (308 hits).

3.3.2 Diversity assessment

The skeletal diversity and relationship between the scaffolds was assessed using the 'scaffold tree' hierarchical analysis developed by Waldmann.¹⁶⁰ By applying Waldmann's prioritisation rules to the graph-node-bond (GNB) frameworks of the nine scaffolds, it was found that the scaffolds were ultimately related to five parental frameworks. The results are summarized in Figure 53 and the frameworks are illustrated in Figure 54. The lack of similarity between the scaffolds is significant given that synthetically all the scaffolds derive from two common cycloadduct frameworks.

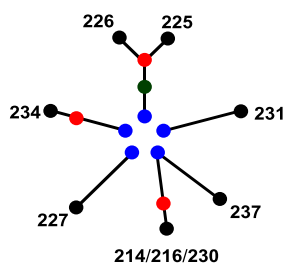


Figure 53 The hierarchical relationship between the seven distinct molecular frameworks at the graph-node-bond level (black) and the five parental frameworks (blue). Daughter frameworks are shown in red and green.

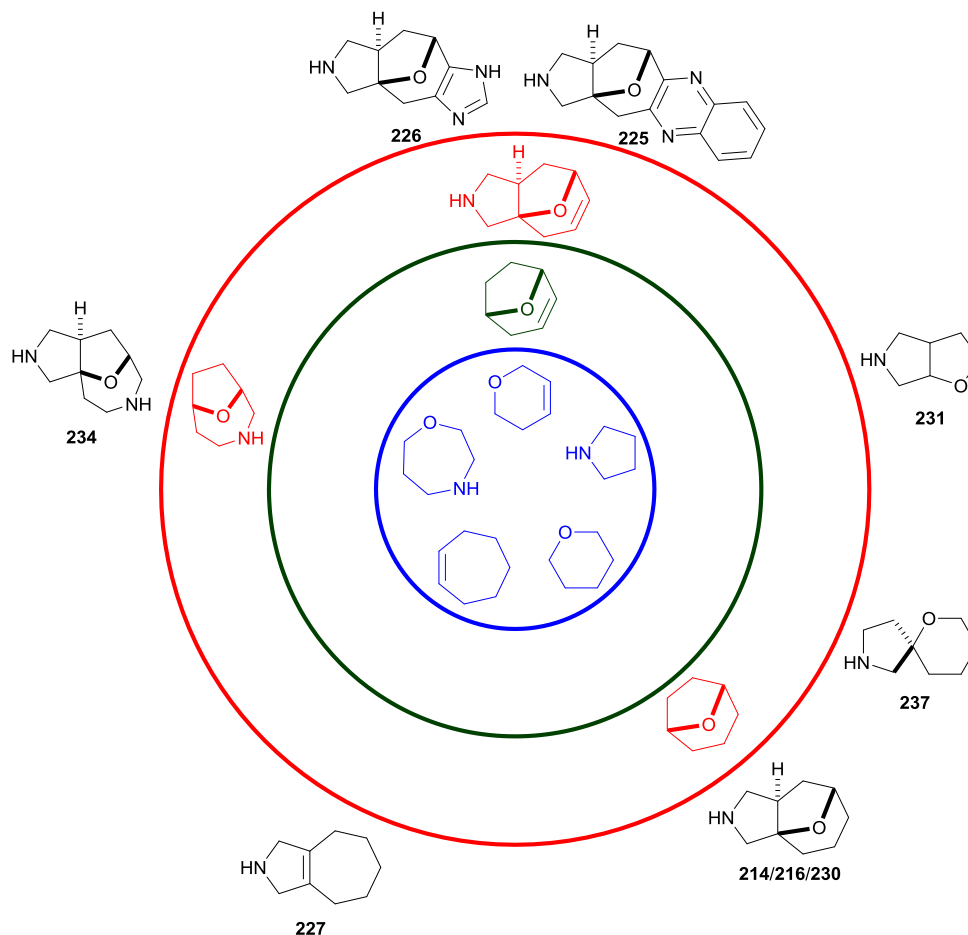


Figure 54 The seven distinct molecular frameworks of the nine scaffolds in the analysis are shown at the graph-node-bond level (black) along with the five parental frameworks (blue). Daughter frameworks are shown in green and red. The scaffolds which represent each framework are indicated. See Figure 27 for the relationship between scaffolds at each level of hierarchy.

3.3.3 Virtual decoration of the scaffolds

To determine the ability of the scaffolds to provide potential access to lead-like screening compounds, a virtual library of compounds was enumerated using Accelrys Pipeline Pilot. The enumeration process is illustrated in Figure 55. Nine scaffolds (Figure 52) were used in the analysis (n.b. acetonides were removed in manipulation 2). Before decoration, ketones and aldehydes were converted to the corresponding alcohols (Table 18, entry 1). Decoration reactions (Table 19) were

performed using the same set of 80 typical medicinal chemistry capping groups as was used for the allylic-alkylation derived scaffolds (Appendix 1). Notably, decoration of alcohols (Table 19, entries 1-3) was included in the enumeration process (cf. the enumeration process for the allylic alkylation-derived scaffolds). The deprotected but underivatised scaffolds (i.e the scaffolds as shown in Figure 52) were also retained in the final virtual library. This process generated a library of 798 virtual screening compounds.

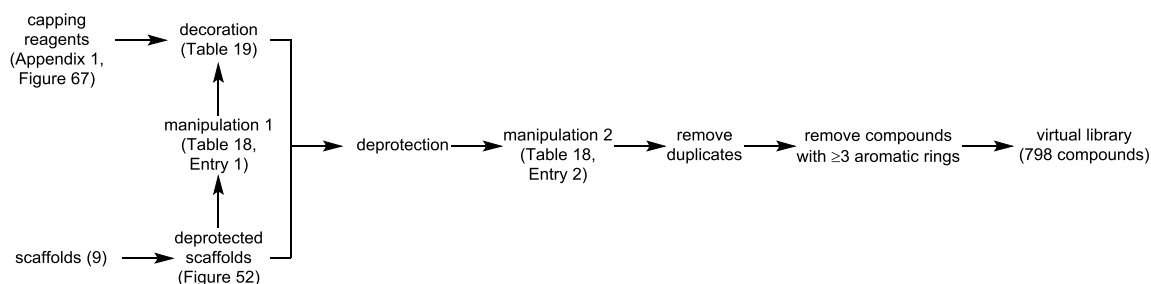


Figure 55 An overview of the process for enumeration of the virtual library.

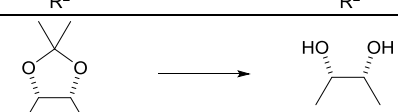
Entry	Manipulation 1 or 2	Synthetic transformation	Description
1	1	$\begin{array}{c} \text{R}^1 \\ \text{C}=\text{O} \\ \text{R}^2 \end{array} \longrightarrow \begin{array}{c} \text{R}^1 \\ \text{C}-\text{OH} \\ \text{R}^2 \end{array}$	Aldehydes and ketones reduced to alcohols
2	2		Acetonides converted to diols

Table 18 Functional group manipulations of the scaffolds (Manipulation 1).

Entry	Functional group decoration	Synthetic transformation	Description
1	Alcohol	$\text{R}-\text{CH}_2-\text{OH} \xrightarrow{\text{R}^1\text{Br}} \text{R}-\text{CH}_2-\text{OR}^1$	Alkylation
2	Alcohol	$\text{R}-\text{CH}_2-\text{OH} \xrightarrow{\text{ArBr}} \text{R}-\text{CH}_2-\text{OAr}$	Arylation
3	Alcohol	$\text{R}-\text{CH}_2-\text{OH} \xrightarrow{\text{R}_2\text{NH}-\text{R}^1} \text{R}-\text{CH}_2-\text{N}(\text{R}^1)(\text{R}^2)$	S _N 2
4	Amine (R ¹ = H, alkyl)	$\text{R}-\text{NH}-\text{R}^1 \xrightarrow{\text{R}^2\text{Br}} \text{R}-\text{N}(\text{R}^1)(\text{R}^2)$	Alkylation
5	Amine (R ¹ = H, alkyl)	$\text{R}-\text{NH}-\text{R}^1 \xrightarrow{\text{R}^2\text{COOH}} \text{R}-\text{N}(\text{R}^1)-\text{C}(=\text{O})-\text{R}^2$	Amide coupling
6	Amine (R ¹ = H, alkyl)	$\text{R}-\text{NH}-\text{R}^1 \xrightarrow{\text{ArBr}} \text{R}-\text{N}(\text{R}^1)(\text{Ar})$	Arylation
7	Amine (R ¹ = H, alkyl)	$\text{R}-\text{NH}-\text{R}^1 \xrightarrow{\text{R}^2\text{COR}^3} \text{R}-\text{N}(\text{R}^1)-\text{CH}(\text{R}^2)-\text{R}^3$	Reductive amination (R ² = H, alkyl, aryl)

Entry	Functional group decoration	Synthetic transformation	Description
8	Amine (R ¹ = H, alkyl)	$R-NH-R^1 \xrightarrow{R^2SO_2Cl} R-N(R^1)-SO_2-R^2$	Sulfonamide formation
9	Amine (R ¹ = H, alkyl)	$R-NH-R^1 \xrightarrow{R^2NCO} R-N(R^1)-C(=O)-NH-R^2$	Urea formation

Table 19 Decoration reactions exploited in the enumeration of the virtual library.

3.3.3.1 Molecular properties analysis

3.3.3.1.1 Lead-likeness assessment

The lead-likeness of the virtual compound library was assessed in accordance with the criteria designated by Churcher (Figure 56, boxed area):¹⁰ 72% of virtual library compounds survived filtering by molecular size ($14 \leq$ heavy atom count ≤ 26), lipophilicity ($-1 < AlogP < 3$) and structural filters – heavy atoms: $\mu = 22.2$, $\sigma = 3.36$; $AlogP$: $\mu = 0.03$, $\sigma = 1.15$. The next chapter will compare the properties of the virtual compound libraries derived from the top-down and bottom-up strategies.

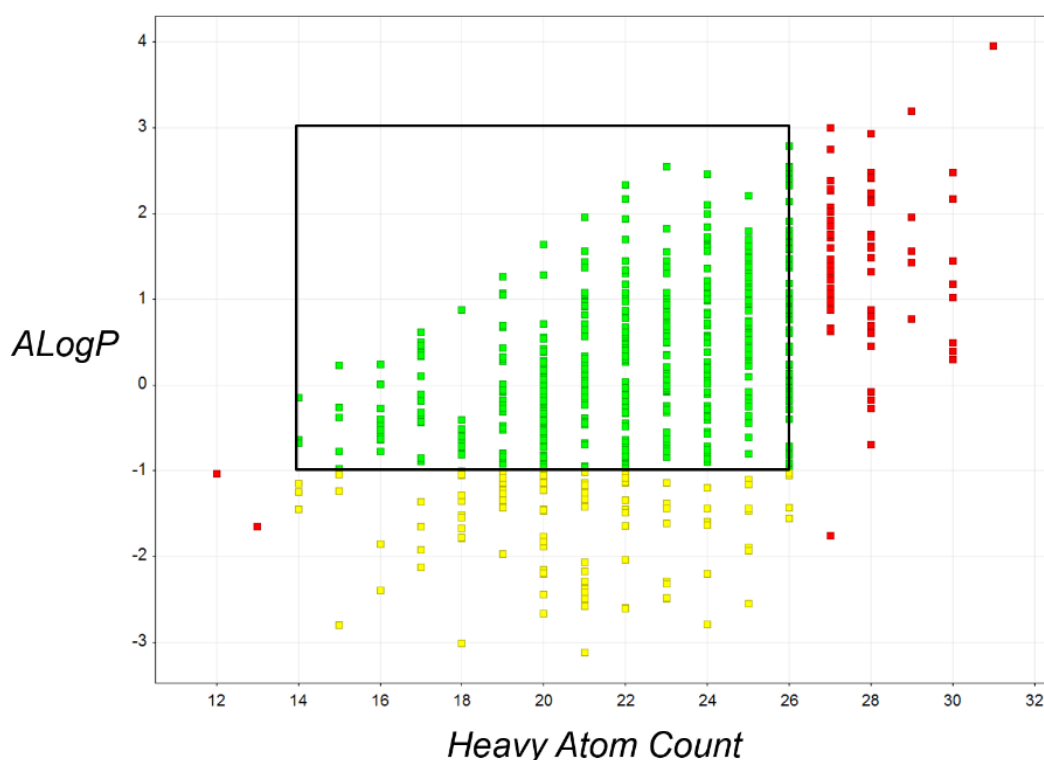


Figure 56 Distribution of the number of heavy atoms and $AlogP$ values for the 798 decorated final compounds derived from the nine scaffolds using the virtual library enumeration process. Compounds that survive successive filtering are shown in green (571 compounds, 72%). Compounds that fail successive filtering by number of heavy atoms (red, 82 compounds, 10%), $AlogP$ (yellow, 145 compounds, 18%) are shown. The black box shows the limit of lead-like space as outlined by Churcher.¹⁰ A larger annotated version of this plot is included in Appendix 1.

When decorated with the same set of 80 capping groups, all nine scaffolds would allow lead-like chemical space to be targeted (Figure 57). Decoration of scaffolds **226** and **234** and would generally give large numbers of high-quality lead-like compounds and would be ideal starting points for compound library synthesis. The versatility of being able to essentially perform a decoration step whilst preparing the imidazole-containing scaffold **226** enables a large library of final compounds to be prepared (294 compounds).

Scaffolds **225** and **237** perform relatively poorly in the lead-likeness assessment (Figure 58, Panel A). Scaffold **225** suffers from having only one site for further decoration, limiting the number of derivatives that can be prepared (15 compounds). Compounds derived from scaffold **237** generally suffer from low AlogP values (78 out of 89 fail the AlogP filter); this is hardly unexpected as some of the final compounds are tetra- and penta-alcohols (Figure 58, Panel B). In practice we could carefully modify these polyalcohol compounds (e.g. global methylation) to tune them within lead-like space. However, it is also worth noting that they may also find use as carbohydrate mimetics.²⁰¹

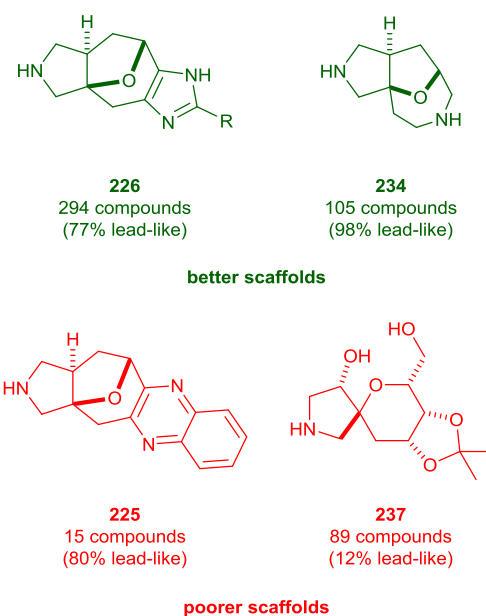
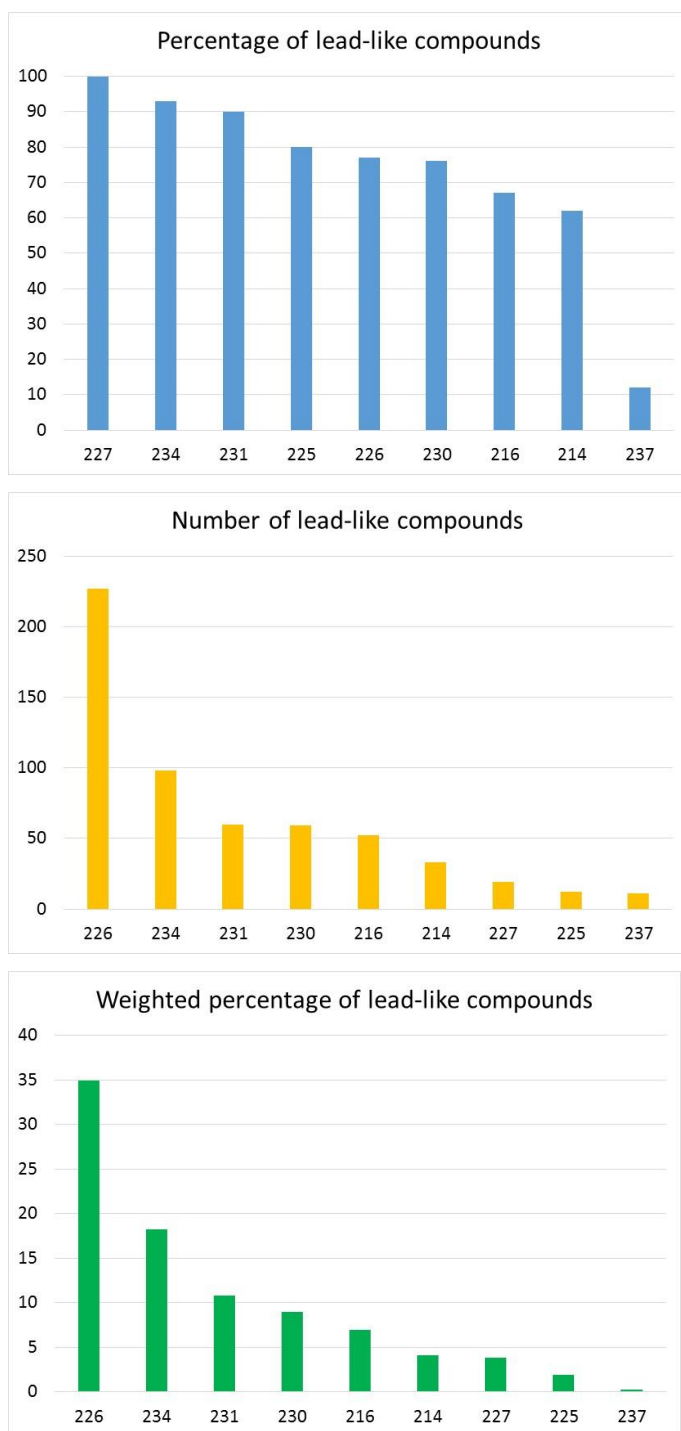


Figure 57 Histograms to show: the percentage of lead-like compounds derived from each scaffold (top); the absolute number of lead-like compounds that may be derived from each scaffold (middle); and the weighted average of the number of lead-like compounds and the percentage of lead-like compounds (bottom).

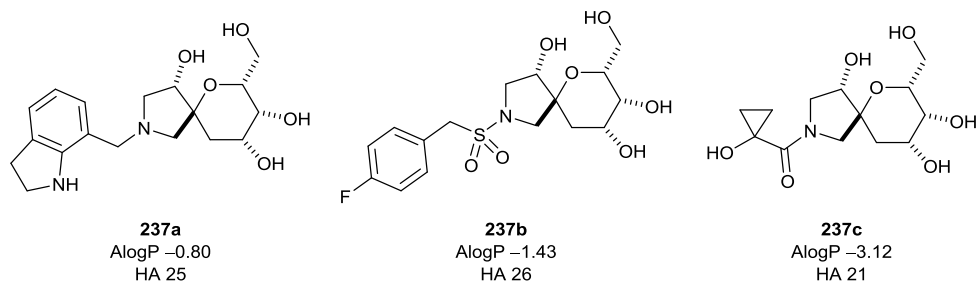


Figure 58 Exemplar final compounds derived from scaffold **237**. Compound **237a** is lead-like, while **237b-c** fail the AlogP filter.

The virtual library derived from the top-down approach had higher sp^3 content (F_{sp^3} : $\mu = 0.68$) than the commercially available compounds in ZINC (F_{sp^3} : $\mu = 0.33$).

3.3.3.2 Principal moments of inertia study

The shape diversity of the virtual library was compared with that of 90911 randomly-selected compounds from the ZINC database (Figure 59). Dividing the PMI plot into 20 bins (as described in Section 2.5.3.2 and Appendix 1, Section 6.3.1, Figure 60) showed that 16% of compounds derived from the top-down approach are found at the extreme flat-linear edge of the plot. However, of the 16% (128 compounds) of the derivatives found in bin 1, 96% are derived from scaffolds containing aromatic rings; the imidazole scaffold **226** (93%, 119 compounds) and quinoxaline scaffold **225** (3%, 4 compounds).

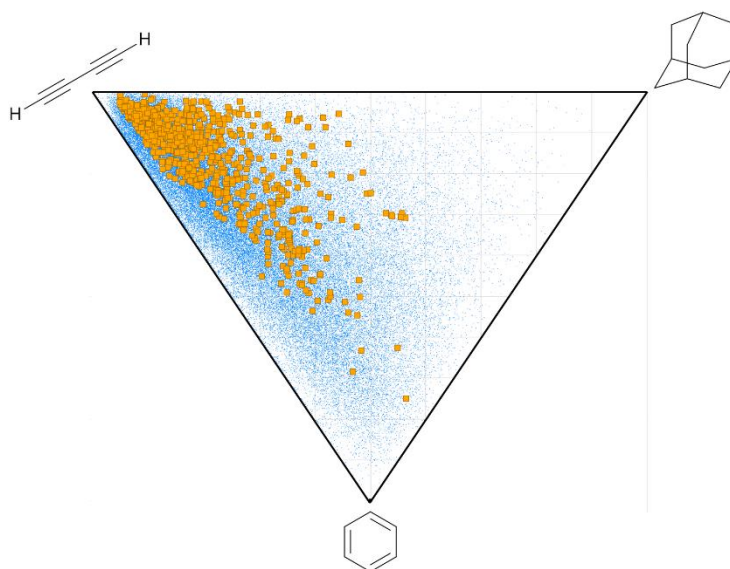


Figure 59 A normalised principal moment of inertia plot to show the shapes of the 798 virtual compounds (orange, enlarged for clarity) compared with 90911 randomly selected compounds from the ZINC database (blue). An annotated version is given in Appendix 1.

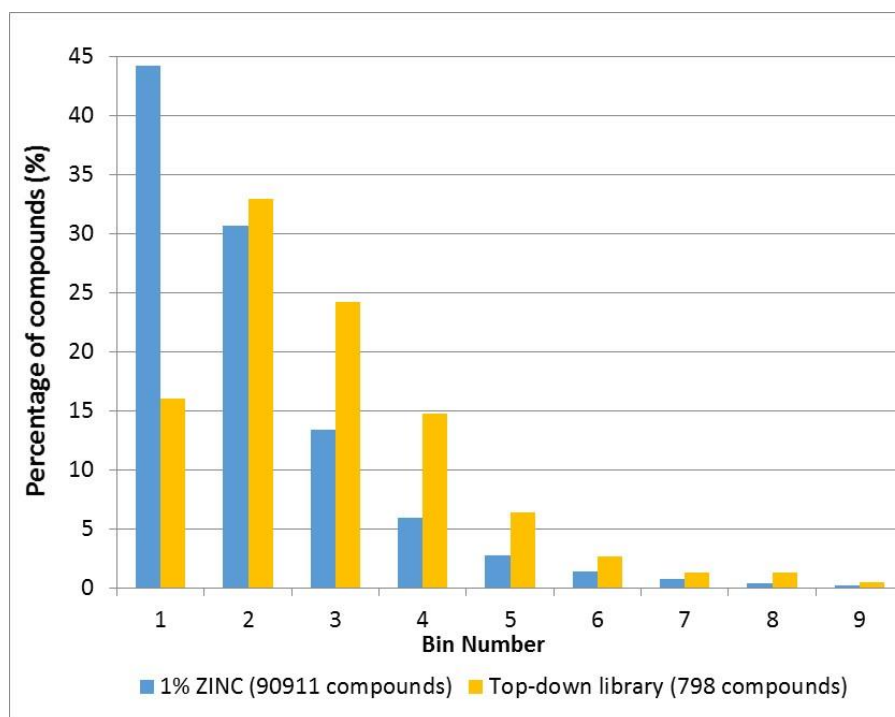


Figure 60 The relative proportions of the compounds found when the PMI was divided into twenty bins for the virtual library versus ZINC and the allylic alkylation-derived compounds (9 of 20 bins shown).

3.3.4 Conclusions and future work

In summary, the preparation of key polyfunctionalised cycloadducts has enabled a downstream synthetic programme in which these precursors are converted into new molecular scaffolds which can systematically target lead-like chemical space.

Two different types of intramolecular oxidopyrylium [5+2] cycloaddition were investigated to prepare polycyclic assemblies. While the [5+2] cycloaddition of an oxidopyrylium generated from an α -acetoxypyranone was successful, it suffered from a long synthetic sequence to prepare the required starting material for the cycloaddition. However, investigation of the [5+2] cycloaddition of oxidopyryliums generated from β -alkoxy- γ -pyrones allowed rapid and scalable preparation of polycyclic assemblies.

We established understanding of the reactivity of the α -silyloxyenone functionality by investigating its reaction with reducing agents and nucleophiles. A strategy to prepare scaffolds was then realised, relying upon both ring-constructing (condensation-aromatisations, double reductive aminations) and ring-cleaving reactions (oxidative cleavage of alkenes, ether bridge opening) providing access

to six unique new scaffolds. Each scaffold was prepared in three or fewer steps from a preceding scaffold, and in several instances just one step was required.

There remain a number of reactivity pathways which could still be investigated in order to prepare new scaffolds. In future it would be particularly interesting to investigate whether some of the methodologies developed could be used in sequence to maximise their utility. For instance, condensation-aromatisation on the propargylamine derived cycloadduct **184**, followed by ozonolysis and reduction, would give access to a unique spirocyclic framework **238** (Figure 61). This methodology would provide a way of removing the prevalence of alcohol functionality found in scaffold **237**.

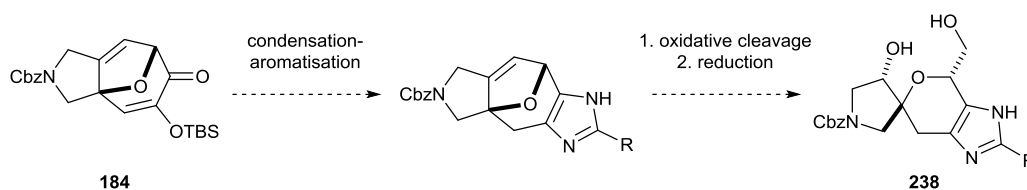


Figure 61 An example of how the established methodologies could be used in sequence.

Application of the established methodologies to the readily accessible maltol-derived cycloadducts may allow rapid access to a complementary, but structurally unique, series of compounds (Figure 62).

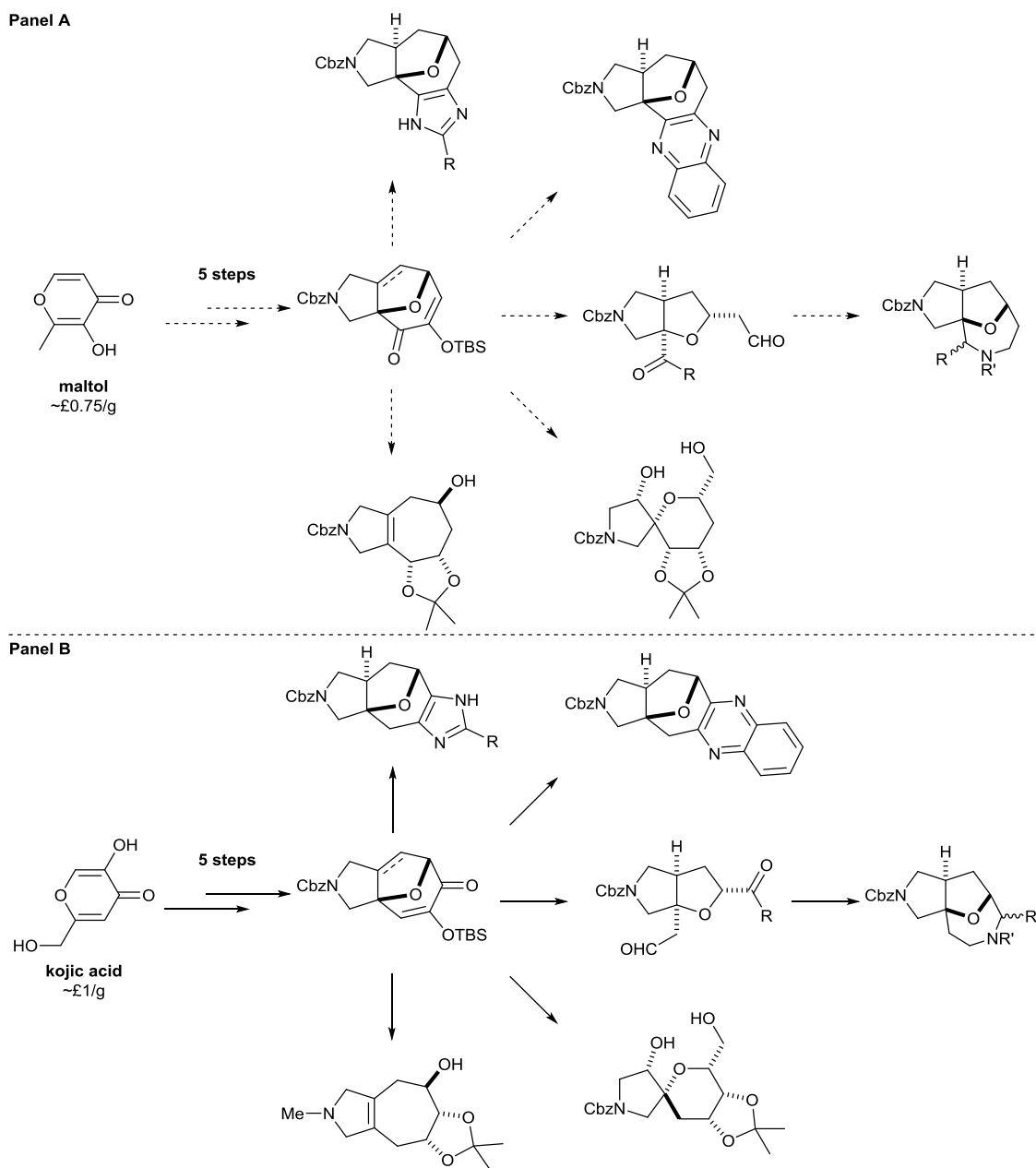


Figure 62 The methodologies applied to the kojic acid series (Panel B) may also be applicable to the isomeric maltol-derived series (Panel A).

It may also be possible to exploit variants of the intramolecular [5+2] oxidopyrylium cycloaddition to provide access to novel scaffolds (Figure 63). For instance, cycloadduct **239**, containing a six-membered ring, could be prepared from the homoallylic starting material **240** (equation 1), and would provide access to a novel set of scaffolds using the established methodologies. Cycloadduct **241**, which contains a benzylic amine, may be cleaved by hydrogenation (equation 2). Alternatively, preparation of cycloadducts **242-243**, containing *N-N* and *N-O* bonds, may allow cleavage by hydrogenation to form aminoalcohols and diamines **244-245** (equations 3 and 4).

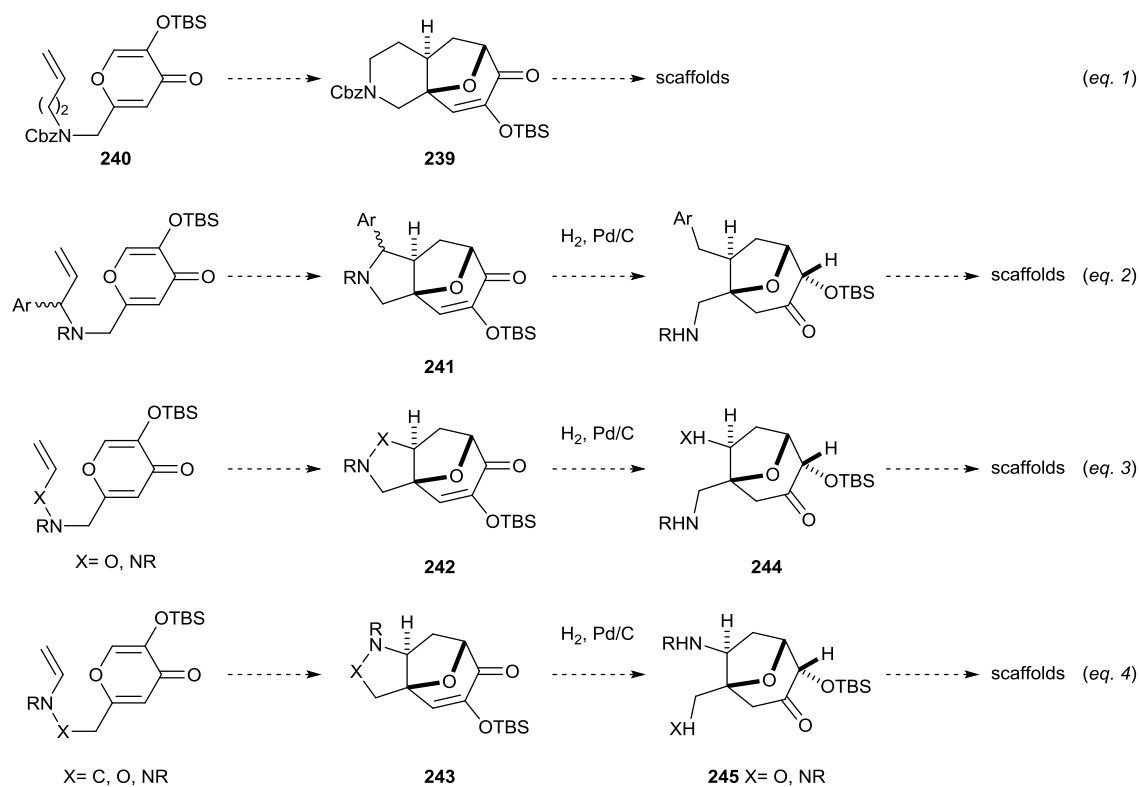


Figure 63 Potential cycloadducts which may be prepared to enable the synthesis of new scaffolds.

It may also be valuable to prepare aza-bridged scaffolds **246a-b** via intramolecular [5+2] oxidopyridinium cycloadditions (Figure 64, Panel A). A similar strategy to that used to prepare the allylic alkylation-derived scaffolds could then be applied (Panel B). This would involve capping the bridging amine with a variety of different functionalised handles, which may then facilitate cyclisation reactions. There would also be the option to apply many of the established methodologies used so far in our top-down approach.

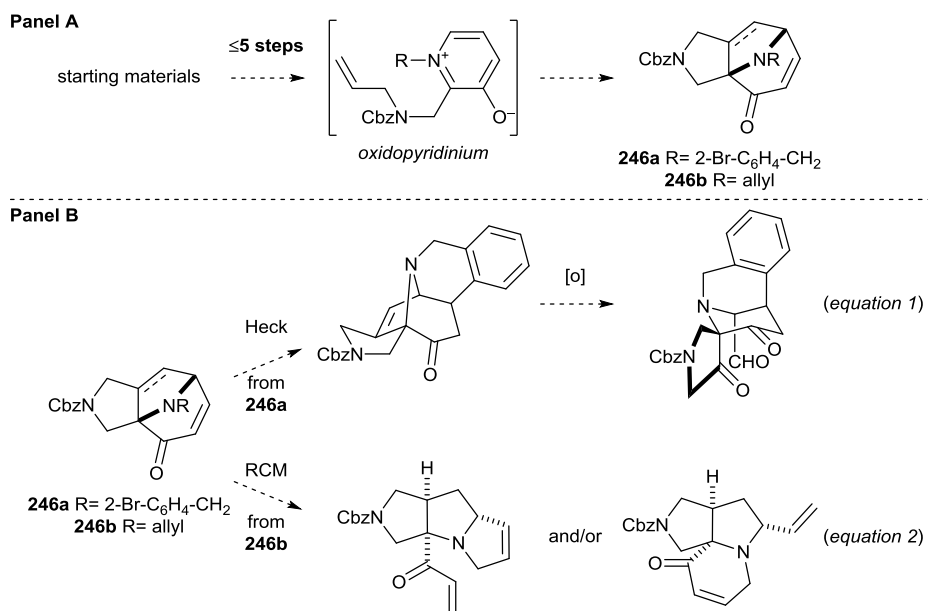


Figure 64 Panel A: the proposed intramolecular oxidopyridinium cycloaddition to prepare cycloadducts **246a-b**. Panel B: a potential strategy to prepare scaffolds from cycloadducts **246a-b**. The amine bridge would be capped with a variety of different functional handles to facilitate cyclisations, such as an intramolecular Heck reaction (equation 1) and/or a ring-closing metathesis reaction (equation 2).

In summary, we have demonstrated the feasibility of a top-down approach to LOS. This paradigm should be applicable to many different classes of polycyclic assemblies in the future and represents a streamlined and synthetically efficient approach to LOS.

4.0 Comparison of approaches to LOS

This chapter compares the LOS strategies developed so far in the Marsden and Nelson groups, and assesses their ability to systematically, and efficiently, target lead-like space. This assessment compares the libraries derived from the two bottom-up approaches to LOS (the allylic amination⁸² [see Section 1.5.3.3] and allylic alkylation connective reactions) with the top-down approach to LOS (intramolecular [5+2] cycloaddition, Table 20).

4.1 Lead-likeness assessment

We have demonstrated that all of the approaches we have developed would allow significant lead-like space to be accessed through the preparation of derivative compound libraries (Table 20, entry 1). The virtual library enumerated from the 'top-down' scaffolds would give the highest proportion of lead-like compounds (72%, 571 compounds), followed by the allylic alkylation-derived compounds (66%, 734 compounds) and the allylic amination-derived virtual compounds⁸² (59%, 11,468 compounds). It is worth noting that the allylic amination-derived compounds were typically decorated twice (except where a diversification step was used in the preparation of a scaffold, e.g. where scaffolds were derived from the Wolfe reaction – see Section 1.5.3.3 for full details) allowing access to a much larger virtual library of compounds.

4.2 PMI assessment

Overall, the allylic alkylation-derived compounds give the best PMI molecular shape distribution (Table 20, entry 2), both systematically avoiding the extreme flat-linear edge of the graph (bin 1, Figure 65) and penetrating further towards more three-dimensional space (compounds found as far as bin 17). In contrast, compounds derived from the top-down approach are weighted towards the rod-like edge of the plot. In addition, 16% of the top-down derived compounds are found at the extreme flat-linear edge (bin 1) of the plot, and are only found as far as bin 9. Compounds derived from the allylic amination are weighted towards the flat-linear edge of the graph (compounds are found as far as bin 12).

Entry	Analysis	Allylic amination* (OBC paper compounds) ⁸²	Allylic alkylation†	[5+2] cycloaddition†
1	AlogP vs. HA			
2	PMI	<p>$\mu F_{sp^3} = 0.58$</p>	<p>$\mu F_{sp^3} = 0.57$</p>	<p>$\mu F_{sp^3} = 0.68$</p>

Table 20 Comparison of AlogP vs. HA and PMI distributions for the three LOS approaches developed so far in the Marsden and Nelson groups. *Virtual library generated by Richard Doveston using 59 capping groups.⁸² Each scaffold was decorated twice except where aminoarylation reactions were used to prepare a scaffold (in which case they were decorated once). †80 capping groups used.

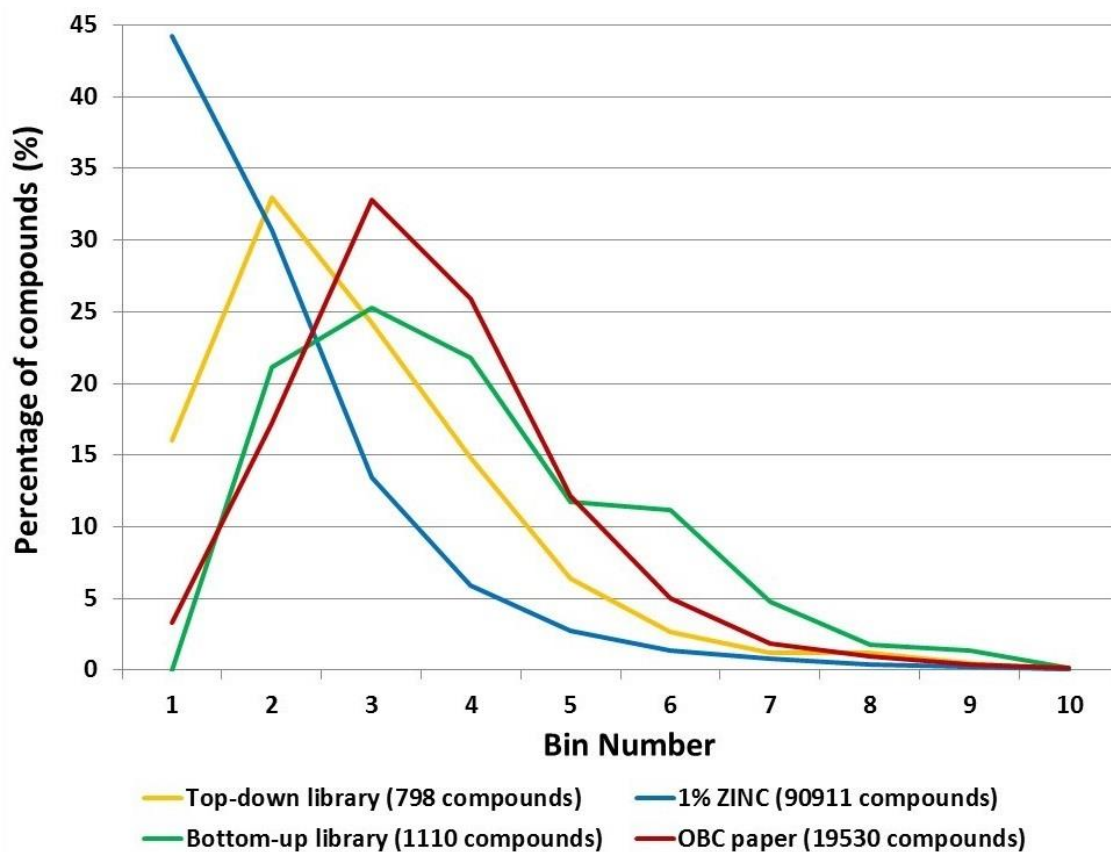


Figure 65 The relative proportions of compounds found when the PMI plots were divided into twenty bins (see Section 2.5.3.2 and Appendix 1, Section 6.3.1 for details). In general, all of the LOS approaches developed exhibit a systematic avoidance of the extreme flat-linear edge of the PMI plot (bin 1).

4.3 Synthetic efficiency

All of the approaches developed by the candidate allow rapid preparation of scaffolds. Including the key coupling step, scaffolds were prepared in an average of two steps, regardless of the synthetic strategy used (Table 21, entry 5). Notably, however, if the key coupling step is not included in the step count, the allylic amination-derived building blocks provide more rapid access to scaffolds (one step per scaffold, entry 7). This is probably due to the large number of aminoarylations (one step) that were carried out post-coupling, but also because some of the coupling products were considered to be scaffolds in their own right (and therefore required zero steps to prepare).

On average the allylic alkylation derived building blocks are predisposed to deliver the most scaffolds (six per building block, entry 3), followed by the allylic amination and the cycloaddition-derived scaffolds (four per building block respectively). Full investigation of the top-down approach may prove this

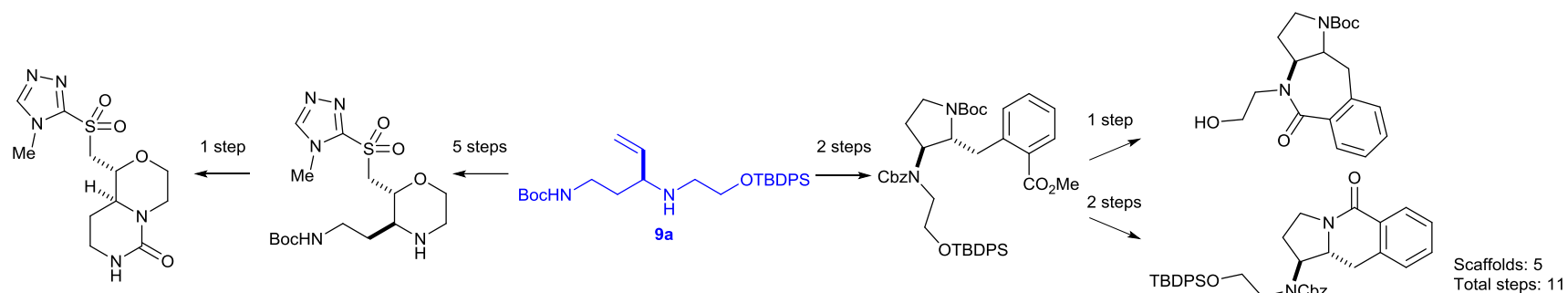
approach to be more productive (i.e. if the proposed future work in Section 3.3.4 can be realised).

Entry	Parameter	Allylic amination	Allylic alkylation	[5+2] Cycloaddition
1	No. building blocks used	13	4	2
2	No. scaffolds	52	22	7 ^a
3	Av. no. scaffolds per building block	4	6	4
4	No. steps ^{b,c} to prepare library including the key coupling step	83	53 ^d	15
5	Av. no. steps per scaffold	2	2	2
6	No. steps ^{a,c} to prepare library post coupling	74	49	13
7	Av. no. steps ^{a,c} per scaffold post coupling	1	2	2

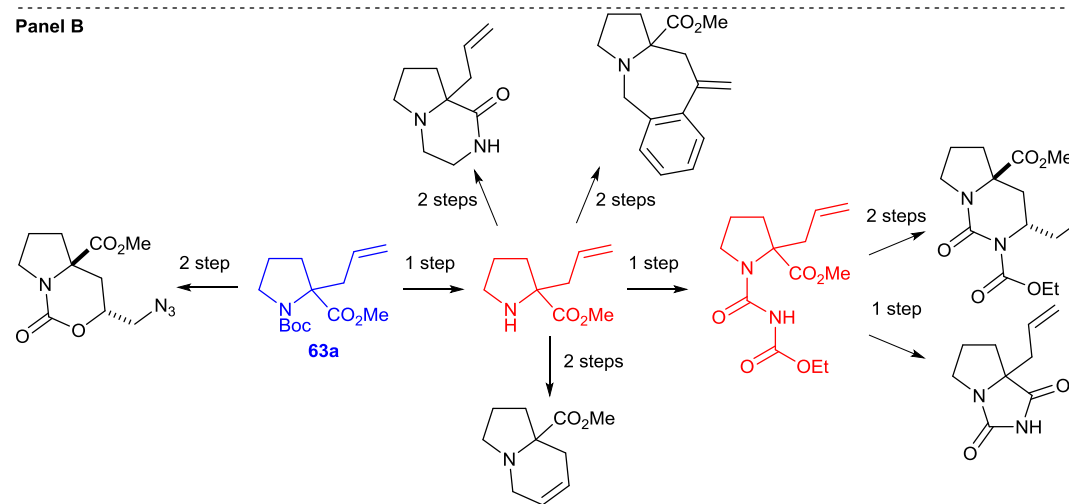
Table 21 Synthetic efficiency parameters for the LOS approaches developed. Numbers are rounded to the nearest integer. ^aCompound **216** was included as a representative derivative of the cycloadduct **183** framework (see Figure 66). ^bFor the purposes of this analysis, a synthetic operation is defined as a process conducted in a single reaction vessel. ^cSteps counted once per linear sequence (for examples of step counting see Figure 66). ^dTotal step count for preparation of the entire library (including synthesis of the building blocks) was 56.

In order to directly compare the synthetic efficiency of the top-down approach with the two bottom-up approaches, it is perhaps fairer to compare the building blocks from each series that give rise to the most scaffolds (Figure 66). This analysis shows that (i) the building block **9a** in the allylic amination series gives access to 5 scaffolds in 11 steps (average 2.2 steps per scaffold, Panel A); (ii) the proline-derived building block **63a** gives 6 scaffolds in 13 steps (average 2.2 steps per scaffold, Panel B); and (iii) the cycloadduct **183** gives 5 scaffolds in 8 steps (average 1.6 steps per scaffold, Panel C).

Panel A

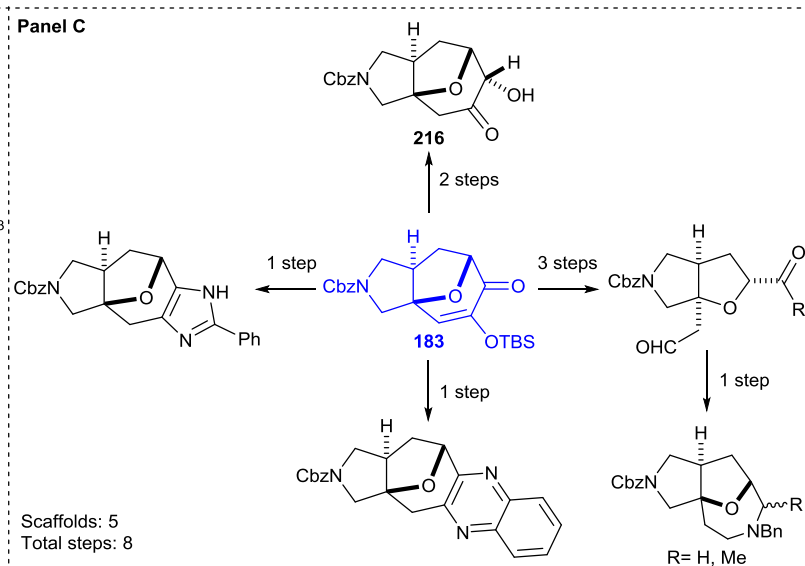


Panel B



Scaffolds: 6
Total steps: 13

Panel C



Scaffolds: 5
Total steps: 8

Figure 66 Examples of the building blocks (blue) which provided access to the most scaffolds (black) from the allylic amination (Panel A),⁸² allylic alkylation (Panel B), and cycloaddition-derived (Panel C) precursors. Common intermediates are shown in red.

The major conclusion that can be drawn from the two synthetic economy analyses above is that at present, there is no significant advantage in synthetic economy between any of the LOS strategies used (all average two steps per scaffold). Whether full exploration of the top-down approach will lead to an increase in synthetic economy can only be determined through full exploration of the strategy by preparing more scaffolds.

4.4 Summary and outlook

All of the LOS strategies developed so far give access to large numbers of scaffolds. Virtual decoration of the scaffolds suggests that ~65% of derivatives from all three approaches would be lead-like. The derivatives also systematically target three-dimensional space. The synthetic economy is excellent, on average it takes two steps to prepare novel scaffolds. Future strategies must focus on streamlined synthetic approaches so that fewer steps are required to access the building blocks for cyclisation. In addition, we aspire to design our syntheses in such a way that diverse scaffolds can be prepared in the fewest number of steps (ideally one) from a minimal number of readily available building blocks.¹¹

5.0 Experimental

5.1 General experimental

All non-aqueous reactions were performed under an atmosphere of nitrogen unless otherwise stated. Water-sensitive reactions were performed in oven-dried glassware, cooled under nitrogen before use. THF, CH₂Cl₂, PhMe and MeCN were dried and purified by means of a Pure Solv MD solvent purification system (Innovative Technology Inc.). Anhydrous DMF was obtained in a SureSeal bottle from Sigma-Aldrich. All other solvents used were of chromatography or analytical grade. Petrol refers to petroleum spirit (b.p. 40-60 °C). Commercially available starting materials were obtained from Sigma-Aldrich, Fluka, Acros, Alfa-Aesar or Fluorochem and were used without purification.

Thin layer chromatography (TLC) was carried out on aluminium backed silica plates (Merck silica gel 60 F254). Visualisation of the plates was achieved using an ultraviolet lamp ($\lambda_{\text{max}} = 254 \text{ nm}$) and KMnO₄. Flash chromatography was carried out using silica gel 60 (60-63 μm particles) supplied by Merck. Columns with solvent gradients were carried out using a Biotage Flashmaster II on pre-packed Redisep normal-phase silica or cyanosilica cartridges (as specified). Strong cation exchange solid phase extraction (SCX-SPE) was carried out using pre-packed Discovery DSC-SCX cartridges supplied by Supelco, see general procedure **R**.

Melting points were measured on a Reichert hot stage apparatus and are uncorrected. Optical rotation measurements were carried out at the sodium D-line (589 nm) on a Schmidt and Haensch H532; concentrations are in g/100 mL, temperatures are given in °C, optical rotations are given in $\text{deg dm}^{-1}\text{cm}^3 \text{g}^{-1}$ (units are omitted). Infrared spectra were recorded on a Perkin-Elmer One FT-IR spectrometer or a Bruker Alpha Platinum-ATR, with absorption reported in wavenumbers (cm^{-1}). High resolution mass spectra (HRMS) were recorded by the candidate or by Tanya Marinko-Covell on a Bruker Daltonics micrOTOF or Bruker MaXis Impact spectrometer with electrospray ionisation (ESI) source. Where EI ionisation was required, a Waters/Micromass GCT Premier spectrometer was used.

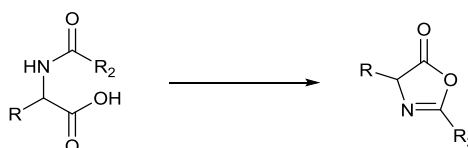
Proton (¹H) and carbon (¹³C) NMR spectral data were collected on a Bruker Advance 500 or Bruker DPX500 or DPX300 spectrometers. Chemical shifts (δ)

are quoted in parts per million (ppm) and referenced to the residual solvent peak. Coupling constants (J) are quoted in Hertz (Hz) and splitting patterns reported in an abbreviated manner: app. (apparent), s (singlet), d (doublet), t (triplet), q (quartet), m (multiplet). All fully characterised products were assigned with the aid of COSY, DEPT-135 and HMQC experiments. Where stated HMBC and NOESY experiments were also used to aid assignments. Compounds are numbered with respect to their IUPAC names. Where necessary, coloured text is used to distinguish similar protons and carbons. Diastereomeric ratios were calculated by analysis of the ^1H NMR spectra and assigned through the interpretation of coupling constants, NOESY spectra, and through crystallographic studies. X-ray crystallography studies were performed by Helena Shepherd and Christopher Pask.

5.2 Experimental for 'bottom-up' approach to LOS

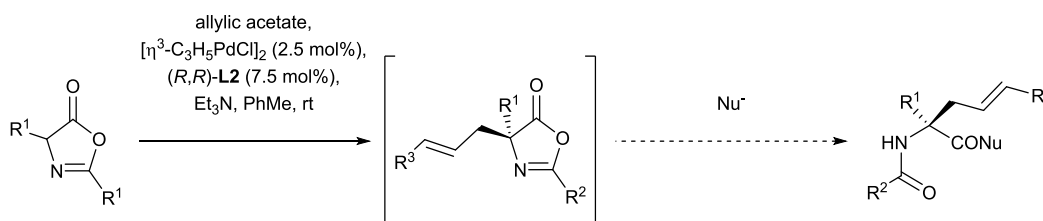
5.2.1 General procedures

General procedure A: synthesis of azlactones



Following a procedure by Taran,¹¹⁰ protected amino acids in acetic anhydride (0.3 M) were heated at 65 °C for 2 h. The resulting reaction mixture was concentrated *in vacuo*. The crude azlactones were used without further purification.

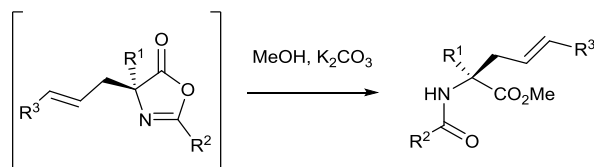
General procedure B: asymmetric allylic alkylation of azlactones



Following a modification of a procedure by Trost,¹⁰⁸ a pre-stirred suspension of $[(\eta^3\text{-C}_3\text{H}_5)\text{PdCl}]_2$ (2.5 mol%) and (*R,R*)-DACH-phenyl **L2** (7.5 mol%) in PhMe (0.02 M) was added *via* cannula to a stirred solution of cinnamyl acetate

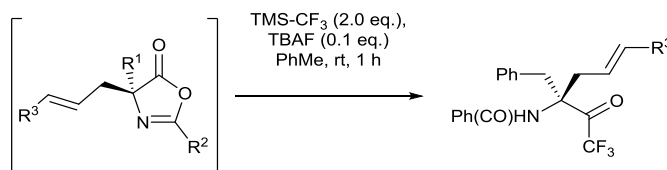
(eq. stated), Et₃N (eq. stated), and azlactone (eq. stated) in PhMe (0.25 M, 1 volume). The reaction mixture was stirred for 3 h. Following complete consumption of the starting material (as determined by TLC and ¹H NMR spectroscopy of an aliquot of the crude reaction mixture) a nucleophilic work-up (general procedures **C-D** or as stated) was then carried out.

General procedure C: methanolysis of quaternary azlactones

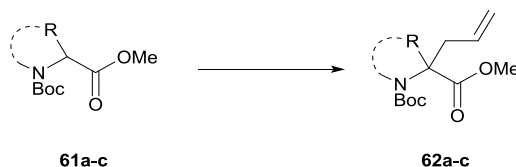


Following completion of general procedure **B**, MeOH (120 eq.) and K₂CO₃ (2.0 eq.) were added to the crude reaction mixture. The resulting mixture was stirred for 15 h. The reaction mixture was concentrated *in vacuo*, diluted in EtOAc (1 volume) and washed with H₂O (1 volume) and brine (1 volume). The combined organic extracts were dried over Na₂SO₄, filtered and concentrated *in vacuo*. Compounds were purified by flash chromatography as stated.

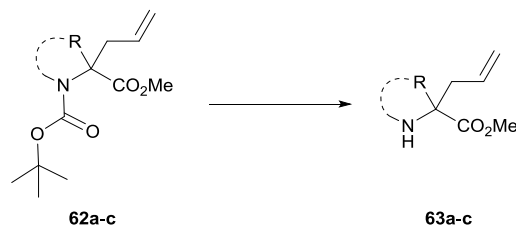
General procedure D: opening the quaternary azlactones with TMS-CF₃



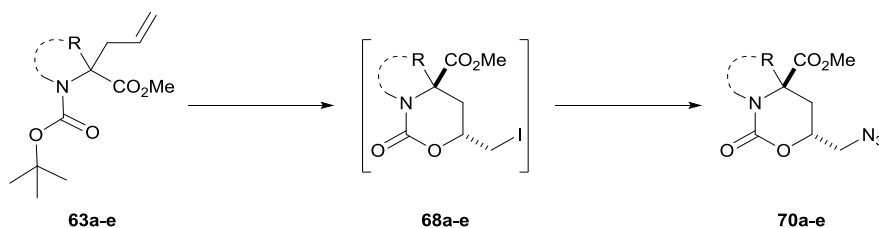
Following completion of general procedure **B**, the reaction mixture was concentrated *in vacuo*, diluted in EtOAc (1 volume), and washed with pH 7 phosphate buffer (1 volume). The organic phase was dried over Na₂SO₄ and concentrated *in vacuo*. Following a modification of a procedure by Bräse,¹¹⁹ the resulting residue was dissolved in PhMe (0.25 M, 1 volume). TBAF (1.0 M in THF, 0.1 eq.) was added to the mixture, followed by TMS-CF₃ (2.0 eq.). The resulting mixture was stirred for 1 h. The reaction mixture was concentrated *in vacuo*, diluted in EtOAc (1 volume) and washed with brine (1 volume). The organic phase was dried over MgSO₄, filtered, then concentrated *in vacuo*. Compounds were purified by flash chromatography or crystallisation as stated.

General procedure E: Alkylation of Boc-protected amino esters

LiHMDS (1.0 M in THF, 1.1 eq.) was added dropwise to a stirred solution of Boc-protected amino ester **61a-c** (1.0 eq.) in THF (0.45 M, 1 volume) at $-78\text{ }^{\circ}\text{C}$. The reaction mixture was stirred for 15 min, then allyl bromide (1.5 eq.) was added dropwise. The reaction mixture was stirred for 1 h, the dry-ice bath was removed and the reaction mixture was warmed to rt and stirred for 15 h. Sat. aq. NH_4Cl solution was added (0.1 volume), then the reaction mixture was partitioned between EtOAc (1 volume) and brine (1 volume). The aqueous layer was extracted with EtOAc (2×1 volume). The combined organic extracts were dried over MgSO_4 and concentrated *in vacuo*. Compounds **62a-c** were purified by flash chromatography.

General procedure F: Boc-carbamate deprotection

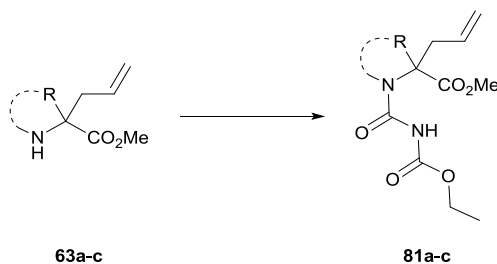
Boc-carbamate **62a-c** (1.0 eq.) was diluted in 2:1 CH_2Cl_2 -TFA (0.5 M) at $0\text{ }^{\circ}\text{C}$. The reaction mixture was stirred for 1 h at rt then concentrated *in vacuo*. Compounds **63a-c** were purified by SCX, according to general procedure **R**.

General procedure G: Cyclic carbamate synthesis

Following a procedure by Licini,¹⁰² iodine (3.0 eq.) was added to Boc-carbamate **62a-e** (1.0 eq.) in 1:1 THF- H_2O (0.04 M, 1 volume) and the reaction mixture was stirred for 2-3 h. Sat. aq. $\text{Na}_2\text{S}_2\text{O}_3$ was added until the reaction mixture turned colourless. The reaction mixture was extracted with CH_2Cl_2 (2×0.25 volumes).

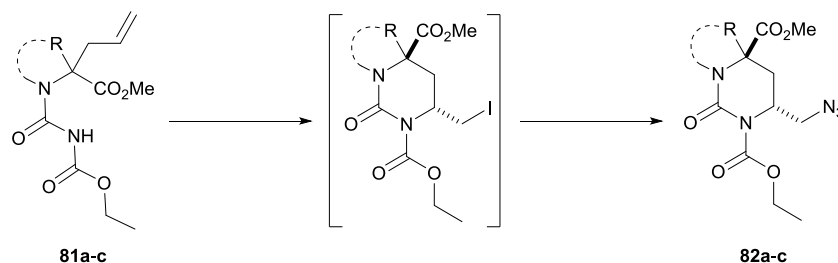
The combined organic phase was washed with brine (0.5 volume) then dried over Na_2SO_4 , filtered, and concentrated *in vacuo* to give the crude iodide **68a-e**. The iodide was diluted in DMF (0.1 M, 1 volume) and NaN_3 (2.0 eq.) was added (*CAUTION: azides are potentially explosive and should be handled with care – this reaction should be performed behind a blast shield. NaN_3 is extremely toxic and should be weighed out inside a fumehood using a non-metal spatula*). The reaction mixture was stirred for 15 h. H_2O (0.5 volume) was added at 0 °C. The reaction mixture was extracted with EtOAc (3 × 0.25 volume). The organics were washed with brine (0.5 volume) then dried over Na_2SO_4 , filtered, and concentrated *in vacuo*. Compounds **70a-e** were purified by flash chromatography.

General procedure H: Carbamoyl urea synthesis



Following a procedure by Taguchi,¹³⁸ ethyl isocyanatoformate (1.2 eq.) was added to a stirred solution of amino ester **63a-c** (1.0 eq.) in CH_2Cl_2 (0.1 M). The reaction mixture was stirred for 0.5 h then concentrated *in vacuo* to give crude urea **81a-c**.

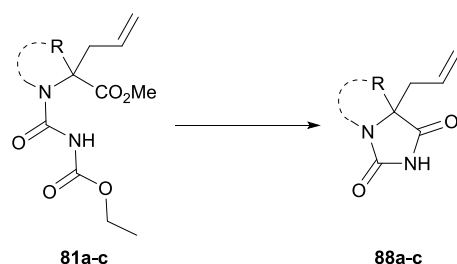
General procedure I: Cyclic urea synthesis



Following a procedure by Taguchi,¹³⁸ $\text{Li}[\text{Al}(\text{O}^t\text{Bu})_4]$ (0.7 M in THF, 1.0 eq., prepared following general procedure **Q**) was added to the crude urea **81a-c** in PhMe (0.1 M, 1 volume) at -5 °C. The reaction mixture was stirred for 0.5 h, then iodine (3.0 eq.) was added. The reaction mixture was stirred for 15 h at -5 °C, then quenched with ice-cold sat. aq. $\text{Na}_2\text{S}_2\text{O}_3$ until colourless. The reaction

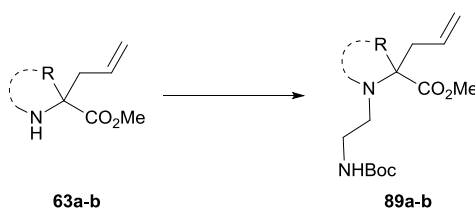
mixture was extracted with ice-cold EtOAc (3 × 0.5 volume). The organics were dried over Na₂SO₄ at 0 °C, filtered, then concentrated *in vacuo* to give the crude iodide. The residue was dissolved in DMF (0.2 M, 1 volume) and NaN₃ (2.0 eq.) was added (*CAUTION: azides are potentially explosive and should be handled with care – this reaction should be performed behind a blast shield. NaN₃ is extremely toxic and should be weighed out inside a fumehood using a non-metal spatula*). The reaction mixture was stirred for 15 h at rt. H₂O (0.5 volume) was added at 0 °C. The reaction mixture was extracted with EtOAc (3 × 0.25 volume). The organics were washed with brine (0.5 volume) then dried, filtered, and concentrated *in vacuo*. Compounds **82a-c** were purified by flash chromatography.

General procedure J: Hydantoin synthesis



NaOMe (25 wt% in MeOH, 1.0 eq.) was added to the crude urea **81a-c** in 85:15 PhMe–MeOH (0.1 M). The reaction mixture was heated at 65 °C for 2 h, then concentrated *in vacuo*. Compounds **88a-c** were purified by SCX eluting with MeOH.

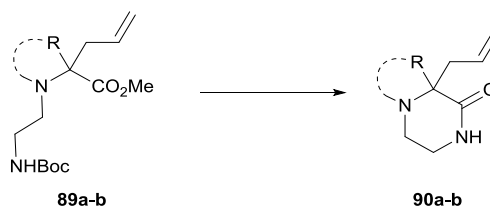
General procedure K: Reductive amination with *N*-Boc glycinal



A suspension of amino ester **63a-b** (1.0 eq.), *N*-Boc glycinal (2.0 eq.) and 4 Å MS (50 mg for 2.5 mmol of amine) in CH₂Cl₂ (0.1 M, 1 volume) was stirred for 1 h. NaBH(OAc)₃ (2.0 eq.) was added in one portion and the reaction mixture was stirred for 15 h. The reaction mixture was filtered through Celite then concentrated *in vacuo*. The residue was dissolved in EtOAc (0.5 volume) and washed with brine (0.5 volume). The aqueous phase was extracted with EtOAc (2 × 0.25 volume). The combined organic phase was dried over MgSO₄, filtered,

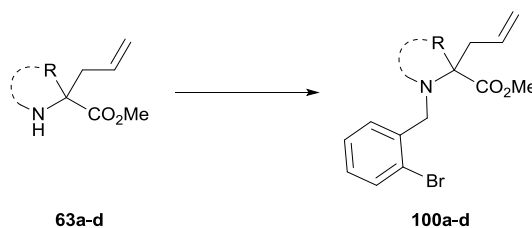
and concentrated *in vacuo*. Compounds **89a-b** were carried on crude without further purification.

General procedure L: Lactamisation

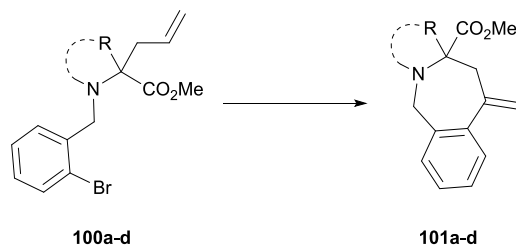


The crude *N*-Boc glycinated amino ester **89a-b** (1.0 eq.) was deprotected, following general procedure **F**. The residue was diluted in DMF (0.04 M) and Cs₂CO₃ (2.0 eq.) was added. The reaction mixture was heated at reflux for 1 h, then concentrated *in vacuo*. Compounds **90a-b** were purified by flash chromatography or by SCX, according to general procedure **R**.

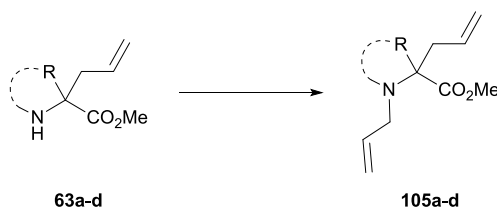
General procedure M: Reductive amination with 2-bromobenzaldehyde



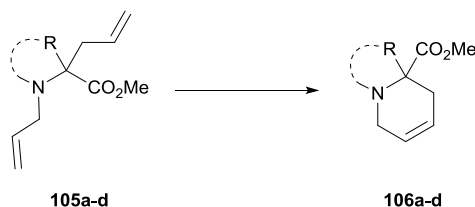
A suspension of amino ester **63a-d** (1.0 eq.), 2-bromobenzaldehyde (2.0 eq.) and 4 Å MS (50 mg for 2.5 mmol of amine) in CH₂Cl₂ (0.1 M) was stirred for 1 h. NaBH(OAc)₃ (2.0 eq.) was added in one portion and the reaction mixture was stirred for 15 h. The reaction mixture was filtered through Celite then concentrated *in vacuo*. The residue was dissolved in EtOAc (0.5 volume) and washed with brine (0.5 volume). The aqueous phase was extracted with EtOAc (2 × 0.25 volume). The combined organic phase was dried over MgSO₄, filtered, and concentrated *in vacuo*. Compounds **100a-d** were purified by flash chromatography or by SCX, according to general procedure **R**.

General procedure N: Intramolecular Heck reaction

Et₃N (2.5 eq.) was added to a stirred solution of amino ester **100a-d** (1.0 eq.) and Pd(PPh₃)₄ (5 mol%) in MeCN (0.1 M). The mixture was heated at 125 °C under microwave irradiation for 1 h, then filtered through celite and concentrated *in vacuo*. Compounds **101a-d** were purified by flash chromatography.

General procedure O: N-Allylation of amines

Allyl bromide (3.0 eq.) and K₂CO₃ (1.1 eq.) were added to a stirred solution of amino ester **63a-d** (1.0 eq.) in DMF (0.2 M, 1 volume) and the reaction mixture was stirred for 15 h. The reaction mixture was diluted with H₂O (0.5 volume) and extracted with EtOAc (3 × 0.25 volume). The organics were washed with brine (0.5 volume) then dried over MgSO₄, filtered, and concentrated *in vacuo*. The compounds **105a-d** were purified by SCX, according to general procedure **R**.

General procedure P: Ring-closing metathesis

Following a procedure by Gracias,¹⁵⁰ *p*-TsOH (2.0 eq.) was added to a stirred solution of *N*-allyl amino ester **105a-d** (1.0 eq.) in CH₂Cl₂ or PhMe as specified (0.03 M). The reaction mixture was heated at reflux for 0.5 h then cooled to rt. GII (2.5-7.5 mol%) was added, the mixture was heated at reflux and monitored by NMR until complete consumption of the starting material was observed. The reaction mixture was cooled to rt. Sat. aq. NaHCO₃ (0.25 volume) solution was added. The reaction mixture was extracted with CH₂Cl₂ (for reactions performed

in CH₂Cl₂, 2 × 0.25 volume) or EtOAc (for reactions performed in PhMe, 2 × 0.25 volume). The organics were washed with brine, dried over Na₂SO₄, filtered, then concentrated *in vacuo*. Compounds **106a-d** were purified by flash chromatography or by SCX, according to general procedure **R**.

General procedure Q: Preparation of a Li[Al(O^tBu)₄] solution in THF

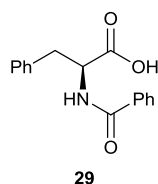
t-BuOH (4.0 eq.) was added dropwise to LiAlH₄ in THF (1.0 M solution) at 0 °C (*CAUTION: gas evolution*). The reaction mixture was stirred for 0.5 h warming to rt and was considered to constitute a 0.7 M solution of Li[Al(O^tBu)₄].

General procedure R: SCX purification

TfOH (0.5 M in MeOH, 10 mL / 5 g SPE-SCX) was dripped through the SPE-SCX cartridge prior to use. MeOH (20 mL) was then washed through using pressurised air (bellows). The crude residue was loaded (3.5 mmol / 5 g SPE-SCX silica) in the minimum amount of MeOH. The cartridge was washed with MeOH and the fractions were collected and monitored by TLC. The cartridge was then washed with sat. NH₃/MeOH and the fractions were collected and monitored by TLC. Fractions containing product were combined and concentrated.

5.2.2 Compound data for 'bottom-up' approach to LOS

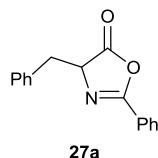
(2S)-3-Phenyl-2-(phenylformamido)propanoic acid **29**



Following a procedure by Richards,²⁰² benzoyl chloride (1.8 mL, 16 mmol, 1.1 eq.) was added dropwise to a stirred solution of L-phenylalanine (2.5 g, 15 mmol, 1.0 eq.) and NaOH (1.8 g, 45 mmol, 3.0 eq.) in H₂O (250 mL) at 0 °C. The mixture was stirred for 3 h then acidified to neutral pH with conc. HCl. Filtration of the resulting solid gave the title compound **29** (2.6 g, 9.8 mmol, 65%) as a colourless powder. **M.p.** 185 °C, microcrystalline, acetone, (lit.²⁰³ 185-186 °C, acetone). **¹H NMR** (300 MHz, CDCl₃, CO₂H not observed): δ 7.73-7.65 (2H, m, Ar-H), 7.57-7.48 (1H, m, Ar-H), 7.47-7.37 (2H, m, Ar-H), 7.37-7.24 (3H, m, Ar-H), 7.24-7.17 (2H, m, Ar-H), 6.57 (1H, d, *J* 7.2, NH), 5.16-5.03 (1H, m, CHCH₂Ph), 3.38 (1H, dd, *J* 14.0, 5.6, CH_AH_BPh), 3.27 (1H, dd, *J* 14.0, 5.9, CH_AH_BPh). **¹³C NMR** (75 MHz, CDCl₃): δ 174.3 (CO₂H), 167.9 (CONH), 135.7 (Ar-C_q), 133.5 (Ar-C_q), 132.3 (Ar-C), 129.6 (Ar-C), 129.0 (Ar-C), 128.9 (Ar-C), 127.5 (Ar-C), 127.2 (Ar-C), 53.8 (CHCH₂), 37.3

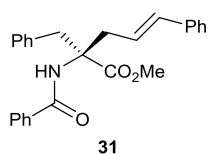
(CHCH₂). **IR** ν_{\max} (film)/cm⁻¹ 3029 (NH), 1725 (CO), 1634 (CO), 1532, 1490, 1216, 755, 700. **HRMS** (ESI): C₁₆H₁₅NNaO₃ [M+Na]⁺; calculated 292.0944, found 292.0939. [α]_D²⁶ +54.0° (c. 1.00, CHCl₃) {lit.²⁰⁴ +45.9° (c. 1.60, dioxane)}. Spectra consistent with the literature values.²⁰²

4-Benzyl-2-phenyl-4,5-dihydro-1,3-oxazol-5-one 27a



General procedure **A** was followed using benzoylated phenylalanine **29** (1.00 g, 3.71 mmol) to give the title compound **27a** (914 mg, 3.60 mmol, 97%) as a colourless amorphous solid. **M.p.** 68-70 °C, colourless needles, petrol (lit.²⁰⁵ 69-70 °C, hexane). **¹H NMR** (300 MHz, CDCl₃): δ 7.95-7.89 (2H, m, Ar-H), 7.59-7.51 (1H, m, Ar-H), 7.50-7.41 (2H, m, Ar-H), 7.31-7.16 (5H, m, Ar-H), 4.70 (1H, dd, *J* 6.7, 5.0, 4-H), 3.38 (1H, dd, *J* 14.0, 5.0, CH_AH_BPh), 3.19 (1H, dd, *J* 14.0, 6.7, CH_AH_BPh). **¹³C NMR** (125 MHz, CDCl₃): δ 177.7 (5-C), 161.9 (2-C), 135.4 (Ar-C), 132.9 (Ar-C), 129.7 (Ar-C), 128.9 (Ar-C), 128.6 (Ar-C), 128.0 (Ar-C), 127.4 (Ar-C), 126.0 (Ar-C), 66.7 (4-C), 37.5 (CH₂Ph). **IR** ν_{\max} (film)/cm⁻¹ 1810, 1645, 1448, 1295, 1161, 1149, 899, 691. **HRMS** (ESI): C₁₆H₁₃NNaO₂ [M+Na]⁺; calculated 274.0838, found 274.0832. Spectra consistent with the literature values.²⁰⁶

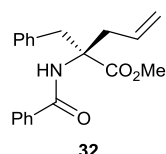
Methyl (2*R*,4*E*)-2-benzyl-5-phenyl-2-(phenylformamido)pent-4-enoate 31



General procedure **B** was followed using cinnamyl acetate (70 μ L, 0.40 mmol, 1.0 eq), Et₃N (60 μ L, 0.40 mmol, 1.0 eq.), and azlactone **27a** (100 mg, 0.400 mmol, 1.00 eq.). General procedure **C** was then followed. Flash chromatography eluting with pentane–EtOAc (95:5) gave the *title compound* **31** (125 mg, 0.313 mmol, 78%, er 95:5) as a colourless oil. **R_f** 0.34 (4:1 pentane–EtOAc). **¹H NMR** (500 MHz, CDCl₃): δ 7.68 (2H, d, *J* 7.4, Ar-H), 7.51-7.46 (1H, m, Ar-H), 7.42-7.38 (2H, m, Ar-H), 7.28-7.23 (4H, m, Ar-H), 7.23-7.15 (4H, m, Ar-H), 7.09-7.04 (2H, m, Ar-H), 6.94 (1H, s, NH), 6.48 (1H, d, *J* 15.6, CH=CHPh), 6.00 (1H, dt, *J* 15.6, 7.6, CH=CHPh), 4.01 (1H, d, *J* 13.5, CH_AH_BPh), 3.84 (3H, s, CO₂CH₃), 3.77 (1H, dd, *J* 14.0, 7.4, CH_AH_BCH=CHPh), 3.25 (1H, d, *J* 13.5, CH_AH_BPh), 2.88 (1H, dd, *J* 14.0, 7.7, CH_AH_BCH=CHPh). **¹³C NMR** (75 MHz, CDCl₃): δ 173.3 (CO₂CH₃), 167.3 (CONH), 137.0 (Ar-C_q), 136.2 (Ar-C_q), 135.2 (Ar-C_q), 134.3 (CH=CHPh), 131.6 (Ar-C), 129.7 (Ar-C), 128.7 (Ar-C), 128.5 (Ar-C), 128.3 (Ar-C), 127.5 (Ar-C), 127.0 (Ar-C), 126.8 (Ar-C), 126.2 (Ar-C), 123.5 (CH=CHPh), 66.7 (C_q), 52.9 (CO₂CH₃), 40.4

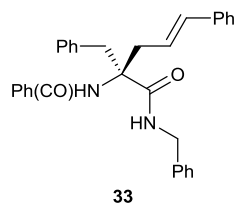
(CH₂Ph), 38.7 (CH₂CH=CH). **IR** ν_{max} (film)/cm⁻¹ 3410 (NH), 3029, 2950, 1737 (CO), 1662 (CO), 1515, 1486, 1114. **HRMS** (ESI): C₂₆H₂₅NNaO₃ [M+Na]⁺; calculated 422.1727, found 422.1738. $[\alpha]^{23}_{\text{D}}$ -2.3° (c. 1.37, MeOH). **HPLC** (Chiralpak AD column, 25 cm, 70:29.9:0.1 ethanol-*n*-heptane-isopropylamine, 1 mL/min flow rate, *R*_t (min) 13.80 (major), 21.44 (minor).

Methyl (2*R*)-2-benzyl-2-(phenylformamido)pent-4-enoate **32**



General procedure **B** was followed using allyl acetate (40 μL, 0.40 mmol, 1.0 eq.), Et₃N (60 μL, 0.40 mmol, 1.0 eq.) and azlactone **27a** (100 mg, 0.400 mmol, 1.00 eq.). General procedure **C** was then followed. Flash chromatography eluting with EtOAc-pentane (4:1) gave the *title compound* **32** (94 mg, 0.29 mmol, 73%) as a colourless oil. **¹H NMR** (300 MHz, CDCl₃): δ 7.73-7.65 (2H, m, Ar-H), 7.53-7.46 (1H, m, Ar-H), 7.46-7.37 (2H, m Ar-H), 7.23-7.15 (3H, m, Ar-H), 7.10-7.00 (2H, m, Ar-H), 6.93 (1H, s, NH), 5.74-5.55 (1H, m, CH=CH₂), 5.13 (1H, dd, *J* 17.0, 2.0, CH=CH_AH_B), 5.07 (1H, dd, *J* 10.1, 2.0, CH=CH_AH_B), 3.96 (1H, d, *J* 13.5, CH_AH_BPh), 3.83 (3H, s, CO₂CH₃), 3.61 (1H, dd, *J* 13.8, 7.2, CH_AH_BCH=CH₂), 3.21 (1H, d, *J* 13.5, CH_AH_BPh), 2.72 (1H, dd, *J* 13.8, 7.6, CH_AH_BCH=CH₂). **¹³C NMR** (75 MHz, CDCl₃): δ 173.5 (CO₂CH₃), 167.0 (CONH), 136.3 (Ar-C_q), 135.4 (Ar-C_q), 132.3 (CH=CH₂), 131.6 (Ar-C), 129.8 (Ar-C), 128.7 (Ar-C), 128.4 (Ar-C), 127.1 (Ar-C), 126.9 (Ar-C), 119.4 (CH=CH₂), 66.6 (C_q), 52.9 (CO₂CH₃), 40.4 (CH₂Ph), 39.6 (CH₂CH=CH₂). **IR** ν_{max} (film)/cm⁻¹ 3412 (NH), 2952, 1738 (CO), 1662, 1519, 1446, 1351, 1082. **HRMS** C₂₀H₂₁NNaO₃ [M+Na]⁺; calculated 346.1414, found 346.1413. $[\alpha]^{24}_{\text{D}}$ -3.9° (c. 0.93, CHCl₃).

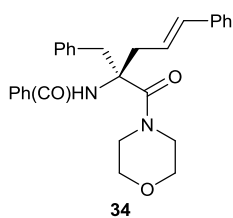
(2*R*,4*E*)-*N*,2-Dibenzyl-5-phenyl-2-(phenylformamido)pent-4-enamide **33**



General procedure **B** was followed using cinnamyl acetate (60 μL, 0.35 mmol, 1.0 eq.), Et₃N (0.10 mL, 0.70 mmol, 2.0 eq.) and azlactone **27a** (200 mg, 0.800 mmol, 2.25 eq.). Following the completion of the reaction, benzylamine (60 μL, 0.53 mmol, 1.5 eq.) was added and the mixture was stirred for 15 h. The reaction mixture was concentrated *in vacuo*, diluted in EtOAc (50 mL) and washed with H₂O (2 × 25 mL) and brine (25 mL). The organic phase was dried over Na₂SO₄, filtered and concentrated *in vacuo*. Flash chromatography eluting with pentane-EtOAc (4:1) gave the *title compound* **33** (145 mg, 0.306 mmol, 87%) as a colourless oil.

R_f 0.15 (4:1 pentane–EtOAc). $^1\text{H NMR}$ (300 MHz, CDCl_3 , one NH not observed): δ 7.68–7.58 (2H, m, Ar-H), 7.48–7.39 (1H, m, Ar-H), 7.39–7.30 (2H, m, Ar-H), 7.29–7.10 (13H, m, Ar-H), 7.10–6.98 (2H, m, Ar-H), 6.83–6.67 (1H, m, NH), 6.40 (1H, d, J 15.8, $\text{CH}=\text{CHPh}$), 6.02 (1H, ddd, J 15.8, 8.3, 7.2, $\text{CH}=\text{CHPh}$), 4.55 (1H, dd, J 14.6, 6.1, $\text{NHCH}_A\text{H}_B\text{Ph}$), 4.40 (1H, dd, J 14.6, 5.4, $\text{NHCH}_A\text{H}_B\text{Ph}$), 3.73 (1H, d, J 13.8, $\text{C}_q\text{CH}_A\text{H}_B\text{Ph}$), 3.42 (1H, dd, J 14.6, 8.3, $\text{CH}_A\text{H}_B\text{CH}=\text{CHPh}$), 3.35 (1H, d, J 13.8, $\text{C}_q\text{CH}_A\text{H}_B\text{Ph}$), 2.87 (1H, ddd, J 14.6, 7.2, 0.7, $\text{CH}_A\text{H}_B\text{CH}=\text{CHPh}$). $^{13}\text{C NMR}$ (75 MHz, CDCl_3): δ 172.1 (CO), 167.6 (CO), 137.8 (Ar- C_q), 136.9 (Ar- C_q), 135.8 (Ar- C_q), 135.2 (Ar- C_q), 134.8 ($\text{CH}=\text{CHPh}$), 131.8 (Ar-C), 130.2 (Ar-C), 128.9 (Ar-C), 128.8 (Ar-C), 128.6 (Ar-C), 128.5 (Ar-C), 128.2 (Ar-C), 127.8 (Ar-C), 127.7 (Ar-C), 127.2 (Ar-C), 127.0 (Ar-C), 126.4 (Ar-C), 123.6 ($\text{CH}=\text{CHPh}$), 64.9 (C_q), 44.3 (NHCH_2Ph), 41.1 ($\text{C}_q\text{CH}_2\text{Ph}$), 39.4 ($\text{CH}_2\text{CH}=\text{CHPh}$). IR $\nu_{\text{max}}(\text{film})/\text{cm}^{-1}$ 3347 (NH), 3062, 3028, 1637 (CO), 1509, 1241, 1217, 966. HRMS (ESI): $\text{C}_{32}\text{H}_{30}\text{N}_2\text{O}_2$ [$\text{M}+\text{Na}$] $^+$; calculated 497.2199, found 497.2200. $[\alpha]_D^{24} +1.9^\circ$ (c. 3.97, CHCl_3).

N*-[(2*R*,4*E*)-2-Benzyl-1-(morpholin-4-yl)-1-oxo-5-phenylpent-4-en-2-yl]benzamide **34*

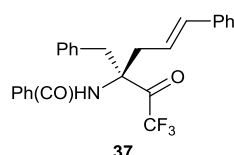


General procedure **B** was followed using cinnamyl acetate (60 μL , 0.35 mmol, 1.0 eq.), Et_3N (0.10 mL, 0.70 mmol, 2.0 eq.) and azlactone **27a** (200 mg, 0.800 mmol, 2.25 eq.). Following the completion of the reaction, morpholine (50 μL , 0.53 mmol, 1.5 eq.) and DMAP (5.0 mg, 41 μmol , 0.1 eq.) were added and the mixture was heated at 90 $^\circ\text{C}$ for 15 h. The reaction mixture was concentrated *in vacuo*, diluted in EtOAc (50 mL) and washed with H_2O (2 \times 25 mL) and brine (25 mL). The organic phase was dried over Na_2SO_4 , filtered and concentrated *in vacuo*. Flash chromatography eluting with a gradient of 0–100% EtOAc in CH_2Cl_2 gave the *title compound* **34** (96 mg, 0.21 mmol, 60%) as a colourless oil. R_f 0.35 (1:1 CH_2Cl_2 –EtOAc). $^1\text{H NMR}$ (300 MHz, CDCl_3 , NH not observed): δ 7.71–7.62 (3H, m, Ar-H), 7.52–7.44 (1H, m, Ar-H), 7.43–7.34 (2H, m, Ar-H), 7.31–7.16 (7H, m, Ar-H), 7.14–7.07 (2H, m, Ar-H), 6.50 (1H, d, J 15.8, $\text{CH}=\text{CHPh}$), 6.06 (1H, dt, J 15.8, 7.2, $\text{CH}=\text{CHPh}$), 4.07 (1H, d, J 14.2, $\text{CH}_A\text{H}_B\text{Ph}$), 3.92–3.68 (9H, m, all morpholine-H and $\text{CH}_A\text{H}_B\text{CH}=\text{CHPh}$), 3.27 (1H, d, J 14.2, $\text{CH}_A\text{H}_B\text{Ph}$), 2.84 (1H, dd, J 15.0, 7.7, $\text{CH}_A\text{H}_B\text{CH}=\text{CHPh}$). $^{13}\text{C NMR}$ (75 MHz, CDCl_3): δ 169.8 (CO), 166.5 (CO), 136.9 (Ar- C_q), 136.2 (Ar- C_q), 135.5 (Ar- C_q), 134.2 ($\text{CH}=\text{CHPh}$),

131.6 (Ar-C), 129.9 (Ar-C), 128.8 (Ar-C), 128.7 (Ar-C), 128.5 (Ar-C), 127.7 (Ar-C), 127.2 (Ar-C), 127.0 (Ar-C), 126.4 (Ar-C), 123.8 (CH=CHPh), 66.8 (C_q), 65.6 (NCH₂), 46.0 (OCH₂), 39.6 (CH₂Ph), 38.3 (CH₂CH=CHPh). **IR** $\nu_{\text{max}}(\text{film})/\text{cm}^{-1}$ 3278, 3027, 2856, 1642 (CO), 1534 (CO), 1421, 1218, 1115. **HRMS** (ESI): C₂₉H₃₀N₂NaO₃ [M+Na]⁺; calculated 477.2149, found 477.2152. $[\alpha]_{\text{D}}^{24}$ -1.3° (c. 1.70, CHCl₃).

N*-[(3*R*,5*E*)-3-Benzyl-1,1,1-trifluoro-2-oxo-6-phenylhex-5-en-3-yl]benzamide **37*

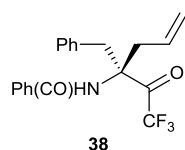
benzamide **37**



General procedure **B** was followed using cinnamyl acetate (210 μL , 1.23 mmol, 1.00 eq.), Et₃N (0.18 mL, 1.3 mmol, 1.0 eq.) and azlactone **27a** (300 mg, 1.20 mmol, 1.00 eq.).

General procedure **D** was then followed using one-sixth (0.20 mmol maximum) of the crude product. Flash chromatography eluting with pentane–EtOAc (4:1) gave the *title compound* **37** (55 mg, 13 μmol , 63%) as a pale oil. R_f 0.35 (4:1 pentane–EtOAc). **¹H NMR** (300 MHz, CDCl₃): δ 7.67–7.58 (2H, m, Ar-H), 7.54–7.46 (1H, m, Ar-H), 7.44–7.35 (2H, m, Ar-H), 7.34–7.18 (8H, m, Ar-H), 7.18–7.09 (2H, m, Ar-H), 6.46 (1H, d, J 15.7, CH=CHPh), 6.32 (1H, s, NH), 5.97 (1H, dt, J 15.7, 7.6, CH=CHPh), 3.51 (1H, d, J 14.0, CH_AH_BPh), 3.39 (1H, d, J 14.0, CH_AH_BPh), 2.88 (2H, app. d, J 7.3, CH₂CH=CHPh). **¹³C NMR** (75 MHz, CDCl₃): δ 189.3 (q, J 32.6, COCF₃), 167.9 (CONH), 136.5 (Ar-C), 136.1 (CH=CHPh), 134.6 (Ar-C), 132.6 (Ar-C), 132.5 (Ar-C), 130.9 (Ar-C), 129.0 (Ar-C), 128.8 (Ar-C), 128.7 (Ar-C), 128.1 (Ar-C), 127.7 (Ar-C), 127.2 (Ar-C), 126.5 (Ar-C), 121.3 (CH=CHPh), 116.3 (q, J 294.2, CF₃), 65.6 (C_q), 37.8 (CH₂Ph), 37.0 (CH₂CH=CHPh). **IR** $\nu_{\text{max}}(\text{film})/\text{cm}^{-1}$ 3281 (NH), 3030, 1746 (CO), 1633, 1532, 1199, 1151, 692. **HRMS** (ESI): C₂₆H₂₂F₃NNaO₂ [M+Na]⁺; calculated 483.1675, found 438.1696. $[\alpha]_{\text{D}}^{25}$ -2.2° (c. 1.73, CHCl₃).

N*-[(3*R*)-3-Benzyl-1,1,1-trifluoro-2-oxohex-5-en-3-yl]benzamide **38*

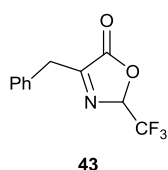


General procedure **B** was followed using allyl acetate (0.45 mL, 4.2 mmol, 1.0 eq.), Et₃N (0.58 mL, 4.2 mmol, 1.0 eq.) and azlactone **27a** (1.00 g, 4.19 mmol, 1.00 eq.). General procedure **D**

was then followed. Crystallisation of the crude residue from pentane–EtOAc (4:1) gave the *title compound* **38** (650 mg, 1.80 mmol, 43%) as a pale yellow solid. **M.p.** 163 °C, microcrystalline, EtOAc. **¹H NMR** (300 MHz, CDCl₃): δ 7.60–7.51

(2H, m, Ar-H), 7.50-7.40 (1H, m, Ar-H), 7.37-7.28 (2H, m, Ar-H), 7.26-7.13 (2H, m, Ar-H), 7.13-6.97 (3H, m, Ar-H), 6.33 (1H, br. s, NH), 5.69-5.51 (1H, m, CH=CH₂), 5.20-5.08 (2H, m, CH=CH₂), 3.42 (1H, d, *J* 14.0, CH_AH_BPh), 3.26 (1H, d, *J* 14.0, CH_AH_BPh), 2.65 (2H, app. d, *J* 7.1, CH₂CH=CH₂). **¹³C NMR** (75 MHz, CDCl₃): δ 189.3 (q, *J* 32.4, COCF₃), 167.8 (CONH), 134.6 (Ar-C_q), 132.6 (Ar-C_q), 132.5 (Ar-C), 130.9 (CH=CH₂), 130.1 (Ar-C), 128.9 (Ar-C), 128.7 (Ar-C), 127.6 (Ar-C), 127.2 (Ar-C), 121.6 (CH=CH₂), 118.2 (q, *J* 294.3, CF₃), 65.3 (C_q), 37.4 (CH₂Ph and CH₂CH=CH₂). **IR** *v*_{max}(film)/cm⁻¹ 3263 (NH), 3031, 1746 (CO), 1626, 1531, 1200, 1139, 701. **HRMS** C₂₀H₁₈F₃NNaO₂ [M+Na]⁺; calculated 384.1182, found 384.1184. [α]_D²³ +1.9° (c. 0.87, CHCl₃).

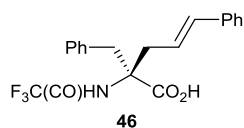
4-Benzyl-2-(trifluoromethyl)-2,5-dihydro-1,3-oxazol-5-one **43**



Following a modification of a procedure by Ries,¹²⁶ L-phenylalanine (2.00 g, 12.0 mmol) in trifluoroacetic anhydride (19 mL) was heated at reflux for 36 h. The reaction mixture was concentrated *in vacuo* and the residue was washed through a pad of silica with EtOAc.

The resulting solution was concentrated *in vacuo*. The residue was distilled at 88-90 °C (5 mmHg) to give the title compound **43** (1.69 g, 6.95 mmol, 58%) as a yellow oil. *R*_f 0.32 (9:1 pentane–EtOAc). **¹H NMR** (500 MHz, CDCl₃): δ 7.38-7.28 (5H, m, Ar-H), 6.11-6.07 (1H, m, 2-H), 4.06 (1H, dd, *J* 15.1, 1.4, CH_AH_BPh), 4.02 (1H, dd, *J* 15.1, 1.8, CH_AH_BPh). **¹³C NMR** (125 MHz, CDCl₃): δ 167.5 (5-C), 163.4 (4-C), 132.6 (Ar-C_q), 129.5 (Ar-C), 129.2 (Ar-C), 128.0 (Ar-C), 120.3 (q, *J* 281.7, CF₃), 93.2 (q, *J* 35.3, 2-C), 34.7 (CH₂Ph). **¹⁹F NMR** (300 MHz, CDCl₃, decoupled) δ 73.7 (CF₃). **IR** *v*_{max}(neat)/cm⁻¹ 3035, 1808 (CO), 1651 (CN), 1497, 1372, 1272, 1196, 1158. **HRMS** (ESI): C₁₁H₈F₃NNaO₂ [M+Na]⁺; calculated 266.0399, found 266.0389. Spectral data consistent with the literature values.²⁰⁷

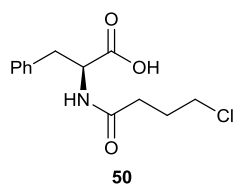
(2*R*,4*E*)-2-Benzyl-5-phenyl-2-(trifluoroacetamido)pent-4-enoic acid **46**



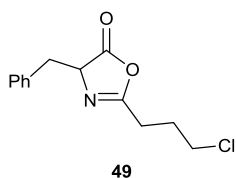
General procedure **B** was followed using cinnamyl acetate (100 μL, 0.570 mmol, 1.0 eq.), Et₃N (0.16 mL, 1.1 mmol, 2.0 eq.) and pseudoazlactone **43** (312 mg, 1.28 mmol, 2.25 eq.). General procedure **C** was then followed. Flash chromatography eluting with EtOAc–AcOH (98.5:1.5) gave the *title compound* **46** (102 mg, 0.270 mmol, 47%) as a yellow oil. *R*_f 0.36 (98.5:1.5 EtOAc–AcOH). **¹H NMR** (300 MHz, CDCl₃, CO₂H and NH not observed): δ 7.34-7.18 (6H, m, Ar-H), 7.15-7.02 (4H, m, Ar-H),

6.52 (1H, d, J 15.8, CH=CHPh), 5.99-5.88 (1H, m, CH=CHPh), 3.77 (1H, d, J 13.8, CH_AH_BPh), 3.54 (1H, dd, J 14.3, 7.4, CH_AH_BCH=CHPh), 3.29 (1H, d, J 13.8, CH_AH_BPh), 2.93 (1H, dd, J 14.3, 7.0, CH_AH_BCH=CHPh). ¹³C NMR (125 MHz, CDCl₃): δ 176.1 (CO₂H), 156.5 (q, J 37.0, NHCOCF₃), 136.8 (Ar-C_q), 135.7 (CH=CHPh), 134.9 (Ar-C_q), 129.6 (Ar-C), 128.7 (Ar-C), 128.7 (Ar-C), 127.9 (Ar-C), 127.7 (Ar-C), 126.5 (Ar-C), 121.7 (CH=CHPh), 115.5 (q, J 288.7, CF₃), 66.6 (C_q), 40.2 (CH₂Ph), 38.3 (CH₂CH=CHPh). IR ν_{\max} (film)/cm⁻¹ 3375 (br., CO₂H), 1714 (CO), 1532, 1448, 1214, 1169, 739, 701. HRMS (ESI): C₂₀H₁₉F₃NO₃ [M+H]⁺; calculated 377.1259, found 377.1239. [α]²⁴_D -0.2° (c. 1.17, MeOH).

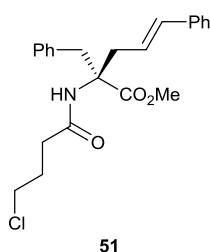
(2S)-2-(4-Chlorobutanamido)-3-phenylpropanoic acid **50**



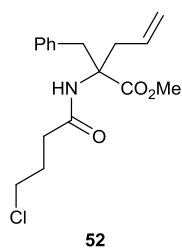
Following a modification of a procedure by Mandić,¹³³ TMSCl (1.8 mL, 15 mmol, 1.2 eq.) was added to a stirred solution of L-phenylalanine (2.0 g, 12 mmol, 1.0 eq.) in CH₂Cl₂ (30 mL). The reaction mixture was cooled to 0 °C and Et₃N (2.0 mL, 15 mmol, 1.2 eq.) was added dropwise. The resulting mixture was heated to reflux for 1 h. The reaction mixture was cooled to rt then further to -10 °C. 4-Chlorobutyryl chloride (1.4 mL, 12 mmol, 1.0 eq.) in CH₂Cl₂ (15 mL) was added dropwise to the reaction mixture. The reaction mixture was stirred at -10 °C for 2 h, at rt for 1 h, then filtered to remove the precipitated Et₃N·HCl. The solution was concentrated *in vacuo*. The resulting residue was diluted in acetone-H₂O (20:80), acidified with conc. HCl to pH 1 (15 mL), and extracted with CH₂Cl₂ (3 × 50 mL). The organic extracts were concentrated *in vacuo* to afford the *title compound* **50** as an off-white amorphous solid (2.1 g, 7.7 mmol, 64%), which was not purified further. **M.p.** 101 °C, microcrystalline, CH₂Cl₂. ¹H NMR (300 MHz, CDCl₃, CO₂H not observed): δ 7.37-7.23 (3H, m, Ar-H), 7.23-7.13 (2H, m, Ar-H), 5.99 (1H, d, J 7.4, NH), 4.90 (1H, app. q, J 6.5, CHCO₂H), 3.61-3.43 (2H, m, CH₂Cl), 3.25 (1H, dd, J 14.0, 5.4, CH_AH_BPh), 3.11 (1H, dd, J 14.0, 6.6, CH_AH_BPh), 2.37 (2H, t, J 7.1, NH(CO)CH₂), 2.13-1.99 (2H, m, CH₂CH₂Cl). ¹³C NMR (75 MHz, CDCl₃, CONH not observed): δ 172.4 (CO₂H), 135.6 (Ar-C_q), 129.4 (Ar-C), 128.9 (Ar-C), 127.5 (Ar-C), 53.2 (CHCH₂Ph), 44.3 (CH₂Cl), 37.4 (CH₂Ph), 33.1 (NH(CO)CH₂), 28.0 (CH₂CH₂Cl). IR ν_{\max} (film)/cm⁻¹ 3313 (br., CO₂H), 2951, 1738, 1660, 1506, 1446, 1228, 991. HRMS (ESI): C₁₃H₁₆³⁵ClNaNO₃ [M+Na]⁺; calculated 292.0711, found 292.0696. [α]²⁴_D +7.7° (c. 0.67, CHCl₃).

4-Benzyl-2-(3-chloropropyl)-4,5-dihydro-1,3-oxazol-5-one 49

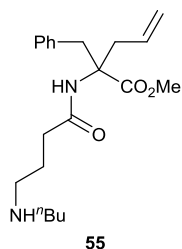
General procedure **A** was followed using protected phenylalanine **50** (2.74 g, 10.1 mmol) to give the *title compound 49* (2.55 g, 10.1 mmol, 99%) as a colourless oil. **¹H NMR** (300 MHz, CDCl₃): δ 7.38-7.21 (3H, m, Ar-H), 7.21-7.13 (2H, m, Ar-H), 4.53-4.41 (1H, m, 4-H), 3.48-3.31 (2H, m, CH₂Cl), 3.27 (1H, dd, *J* 13.9, 5.1, CH_AH_BPh), 3.14 (1H, dd, *J* 13.9, 5.6, CH_AH_BPh), 2.61-2.41 (2H, m, CH₂CH₂CH₂Cl), 2.07-1.89 (2H, m, CH₂CH₂Cl). **¹³C NMR** (75 MHz, CDCl₃): δ 177.9 (5-C), 164.8 (2-C), 134.9 (Ar-C_q), 129.8 (Ar-C), 128.6 (Ar-C), 127.5 (Ar-C), 65.9 (4-C), 43.4 (CH₂Cl), 36.9 (CH₂Ph), 27.6 (CH₂CH₂CH₂Cl), 26.1 (CH₂CH₂Cl). **IR** *v*_{max}(film)/cm⁻¹ 3031, 2928, 1820 (CO), 1678 (CN), 1496, 1454, 1131, 1082. **HRMS** (EI⁺): C₁₃H₁₄³⁵ClNO₂ [M]⁺; calculated 251.0713, found 251.0717.

Methyl (4E)-2-benzyl-2-(4-chlorobutanamido)-5-phenylpent-4-enoate 51

General procedure **B** was followed using cinnamyl acetate (0.23 mL, 1.3 mmol, 1.0 eq.), Et₃N (0.36 mL, 2.6 mmol, 2.0 eq.) and azlactone **49** (738 mg, 2.92 mmol, 2.25 mmol). General procedure **C** was then followed. Flash chromatography eluting with pentane–EtOAc (4:1) gave the *title compound 51* (420 mg, 1.05 mmol, 81%) as a straw-coloured oil. *R_f* 0.2 (4:1 pentane–EtOAc). **¹H NMR** (300 MHz, CDCl₃): δ 7.28-7.10 (8H, m, Ar-H), 7.00-6.91 (2H, m, Ar-H), 6.38 (1H, d, *J* 15.7, CH=CHPh), 6.17 (1H, s, NH), 5.93-5.79 (1H, m, CH=CHPh), 3.80-3.68 (4H, m, includes 1H, m, CH_AH_BPh and at δ 3.75: 3H, s, CO₂CH₃), 3.53-3.43 (3H, m, includes 1H, m, CH_AH_BCH=CHPh and at δ 3.50: 2H, t, *J* 6.3, CH₂Cl), 3.11 (1H, d, *J* 13.5, CH_AH_BPh), 2.72 (1H, dd, *J* 13.9, 7.2, CH_AH_BCH=CHPh), 2.27 (2H, app. dd, *J* 10.6, 4.0, NH(CO)CH₂), 2.06-1.95 (2H, m, CH₂CH₂Cl). **¹³C NMR** (75 MHz, CDCl₃): δ 173.3 (CO₂CH₃), 171.2 (CONH), 137.1 (Ar-C_q), 136.3 (Ar-C_q), 134.3 (CH=CHPh), 129.7 (Ar-C), 128.7 (Ar-C), 128.5 (Ar-C), 127.6 (Ar-C), 127.2 (Ar-C), 126.4 (Ar-C), 123.6 (CH=CHPh), 66.4 (C_q), 53.0 (CO₂CH₃), 44.5 (CH₂Cl), 40.6 (CH₂Ph), 38.9 (CH₂CH=CHPh), 34.0 (NH(CO)CH₂), 28.2 (CH₂CH₂Cl). **IR** *v*_{max}(film)/cm⁻¹ 3402 (NH), 3030, 2249 (C=C), 1737 (CO), 1656 (CO), 1508, 1445, 1220. **HRMS** (ESI): C₂₃H₂₆³⁵ClNaNO₃ [M+Na]⁺; calculated 422.1493, found 422.1495. [*α*]_D²⁵ +0.9° (c. 1.75, MeOH).

Methyl 2-benzyl-2-(4-chlorobutanamido)pent-4-enoate 52

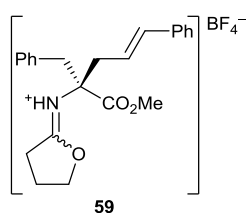
Pd(PPh₃)₄ (500 mg, 5 mol%) was added to a stirred solution of allyl acetate (1.1 mL, 10 mmol, 1.0 eq.), Et₃N (1.4 mL, 10 mmol, 1.0 eq.) and the azlactone **49** (2.55 g, 10.1 mmol, 1.00 eq.) in PhMe (100 mL). The reaction mixture was stirred at rt for 3 h. General procedure **C** was then followed. Flash chromatography eluting with a gradient of 0-100% EtOAc in pentane gave the *title compound* **52** (2.57 g, 7.93 mmol, 79%) as a yellow oil. *R_f* 0.10 (4:1 pentane–EtOAc). **¹H NMR** (300 MHz, CDCl₃): δ 7.35-7.18 (3H, m, Ar-H), 7.13-6.96 (2H, m, Ar-H), 6.26 (1H, s, NH), 5.72-5.49 (1H, m, CH=CH₂), 5.18-5.08 (2H, m, CH=CH₂), 3.82 (3H, s, CO₂CH₃), 3.77 (1H, d, *J* 13.5, CH_AH_BPh), 3.61 (2H, t, *J* 6.3, CH₂Cl), 3.41 (1H, dd, *J* 13.8, 7.4, CH_AH_BCH=CH₂), 3.18 (1H, d, *J* 13.5, CH_AH_BPh), 2.65 (1H, dd, *J* 13.8, 7.3, CH_AH_BCH=CH₂), 2.37 (2H, app. dd, *J* 10.7, 4.3, NH(CO)CH₂), 2.18-2.03 (2H, m, CH₂CH₂Cl). **¹³C NMR** (75 MHz, CDCl₃): δ 173.2 (CO₂CH₃), 171.0 (CONH), 136.2 (Ar-C_q), 132.2 (CH=CH₂), 129.6 (Ar-C), 128.4 (Ar-C), 127.1 (Ar-C), 119.2 (CH=CH₂), 65.9 (C_q), 52.8 (CO₂CH₃), 44.4 (CH₂Cl), 40.3 (CH₂Ph), 39.5 (CH₂CH=CH₂), 33.8 (NH(CO)CH₂), 28.1 (CH₂CH₂Cl). **IR** *v*_{max}(film)/cm⁻¹ 3342 (NH), 2917, 1699 (CO), 1615, 1548, 1268, 1231, 1207. **HRMS** C₁₇H₂₃³⁵ClNO₃ [M+H]⁺; calculated 324.1361, found 324.1361.

Methyl 2-benzyl-2-[4-(butylamino)butanamido]pent-4-enoate 55

4-Chlorobutyryl-protected amino ester **52** (109 mg, 0.340 mmol) in *n*-butylamine (2.5 mL) was heated at reflux for 3 h. The reaction mixture was cooled to rt and concentrated *in vacuo*. The resulting residue was dissolved in CH₂Cl₂ (50 mL) and washed with sat. aq. NaHCO₃ solution (50 mL). The aqueous phase was extracted with CH₂Cl₂ (6 × 10 mL). The combined organic extracts were dried over MgSO₄ then concentrated *in vacuo* to give the *title compound* **55** (124 mg, 0.34 mmol, 99%) as a colourless oil which was not purified further. *R_f* 0.67 (4:1 pentane–EtOAc). **¹H NMR** (300 MHz, CDCl₃, CH₂NHCH₂ not observed): δ 7.23-7.09 (3H, m, Ar-H), 6.97-6.92 (2H, m, Ar-H), 6.39 (1H, s, NH), 5.62-5.41 (1H, m, CH=CH₂), 5.09-4.96 (2H, m, CH=CH₂), 3.71 (3H, s, CO₂CH₃), 3.66 (1H, d, *J* 13.5, CH_AH_BPh), 3.29 (1H, dd, *J* 13.8, 7.3, CH_AH_BCH=CH₂), 3.07 (1H, d, *J* 13.5, CH_AH_BPh), 2.61-2.44 (5H, m, CH_AH_BCH=CH₂, NHCH₂CH₂CH₂CH₃ and NH(CO)CH₂CH₂CH₂NH), 2.16 (2H, t, *J* 7.4, NH(CO)CH₂), 1.81-1.62 (2H, m,

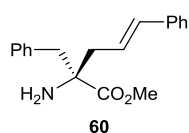
NH(CO)CH₂CH₂CH₂NH), 1.45-1.31 (2H, m, CH₂CH₂CH₃), 1.31-1.15 (2H, m, CH₂CH₃), 0.84 (3H, t, *J* 7.2, CH₂CH₃). **¹³C NMR** (75 MHz, CDCl₃): δ 173.4 (CO), 172.3 (CO), 136.4 (Ar-C_q), 132.4 (CH=CH₂), 129.8 (Ar-C), 128.3 (Ar-C), 127.0 (Ar-C), 119.2 (CH=CH₂), 65.9 (C_q), 52.7 (CO₂CH₃), 49.6 (NHCH₂), 49.3 (NHCH₂), 40.3 (CH₂Ph), 39.5 (CH₂CH=CH₂), 35.3 (NH(CO)CH₂), 32.2 (CH₂CH₂CH₃), 25.8 (NH(CO)CH₂CH₂), 20.6 (CH₂CH₃), 14.1 (CH₂CH₃). **IR** ν_{\max} (film)/cm⁻¹ 3290, 2955, 1739 (CO), 1651, 1539, 1446, 1226, 703. **HRMS** (ESI): C₂₁H₃₃N₂O₃ [M+H]⁺; calculated 361.2486 found 361.2503.

(2Z*)-N-[(2R,4E)-2-Benzyl-1-methoxy-1-oxo-5-phenylpent-4-en-2-yl]oxolan-2-iminium trifluoroborate fluoride **59**



Following a modification of a procedure by Peter,⁸ 4-chlorobutyryl-protected amino ester **52** (20 mg, 50 μmol, 1.0 eq.) in THF (1.0 mL) was added *via* cannula to a stirred solution of AgBF₄ (11 mg, 55 μmol, 1.1 eq.) in THF (1.0 mL) at -20 °C in the dark. The reaction mixture was warmed to rt and stirred 2 h. The reaction mixture was diluted in THF and washed through a plug of Celite. The resulting solution was concentrated *in vacuo* to give the *title compound* **59** (18 mg, 40 μmol, 80%) as a colourless oil. **¹H NMR** (300 MHz, CDCl₃): δ 9.96 (1H, s, NH⁺), 7.33 (2H, d, *J* 7.3, Ar-H), 7.29-7.11 (6H, m, Ar-H), 7.08 (2H, d, *J* 7.0, Ar-H), 6.47 (1H, d, *J* 15.6, CH=CHPh), 6.12-5.92 (1H, m, CH=CHPh), 4.76-4.38 (2H, m, 5-H), 3.71 (3H, s, CO₂CH₃), 3.43 (1H, d, *J* 14.0, CH_AH_BPh), 3.37-3.14 (3H, m, includes 2H, m, 3-H and at δ 3.22: 1H, d, *J* 14.0, CH_AH_BPh), 2.93 (2H, app. d, *J* 7.3, CH₂CH=CHPh), 2.29-2.04 (2H, m, 4-H). **¹³C NMR** (75 MHz, CDCl₃): δ 182.6 (2-C), 168.7 (CO₂CH₃), 136.4 (Ar-C_q), 136.1 (Ar-C_q), 133.9 (CH=CHPh), 130.3 (Ar-C), 128.9 (Ar-C), 128.8 (Ar-C), 128.2 (Ar-C), 128.1 (Ar-C), 126.6 (Ar-C), 121.1 (CH=CHPh), 81.4 (C_q), 70.2 (5-C), 53.5 (CO₂CH₃), 42.1 (CH₂Ph), 40.3 (CH₂CH=CH₂), 32.0 (3-C), 21.8 (4-C). **IR** ν_{\max} (film)/cm⁻¹ 2960, 1744 (CO), 1674, 1449, 1258, 1223, 1065, 752. **HRMS** (ESI): C₂₃H₂₆NO₃ [M]⁺; calculated 364.1907, found 364.1910. **[α]_D²⁵** +6.1° (c. 0.27, CHCl₃).

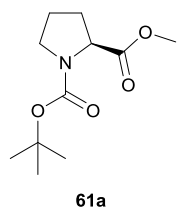
Methyl (2R,4E)-2-amino-2-benzyl-5-phenylpent-4-enoate **60**



Following a modification of a procedure by Peter,¹³² protected amino ester **52** (50 mg, 0.13 mmol, 1.0 eq.) in THF (1.0 mL) was added *via* cannula to a stirred solution of AgBF₄ (28 mg,

0.14 mmol, 1.1 eq.) in THF (1.0 mL) at 0 °C in the dark. The reaction mixture was warmed to rt and stirred for 2 h. The reaction mixture was concentrated *in vacuo*. The residue was dissolved in 1:1 acetone–H₂O (5 mL) and stirred for 15 h. The reaction mixture was concentrated *in vacuo* and purified by flash chromatography, eluting with pentane–EtOAc (4:6), to give the *title compound 60* (35 mg, 0.12 mmol, 95%) as a colourless oil. *R_f* 0.48 (2:3 pentane–EtOAc). **¹H NMR** (300 MHz, CDCl₃, NH₂ not observed): δ 7.43–7.18 (8H, m, Ar-H), 7.18–7.11 (2H, m, Ar-H), 6.53 (1H, d, *J* 15.7, CH=CHPh), 6.21–5.95 (1H, m, CH=CHPh), 3.72 (3H, s, CO₂CH₃), 3.23 (1H, d, *J* 13.1, CH_AH_BPh), 2.92–2.80 (2H, m, includes at δ 2.88: 1H, ddd, *J* 13.5, 6.4, 1.4, CH_AH_BCH=CHPh and at δ 2.83: 1H, d, *J* 13.1, CH_AH_BPh), 2.47 (1H, dd, *J* 13.5, 8.7, CH_AH_BCH=CHPh). **¹³C NMR** (75 MHz, CDCl₃): δ 176.7 (CO₂CH₃), 137.1 (Ar-C_q), 136.3 (Ar-C_q), 134.8 (CH=CHPh), 130.0 (Ar-C), 128.7 (Ar-C), 128.6 (Ar-C), 127.6 (Ar-C), 127.2 (Ar-C), 126.4 (Ar-C), 124.0 (CH=CHPh), 62.4 (C_q), 52.2 (CO₂CH₃), 46.1 (CH₂Ph), 43.9 (CH₂CH=CHPh). **IR** *v*_{max}(film)/cm⁻¹ 3377 (NH₂), 3027, 2949, 1735 (CO), 1494, 1197, 1066, 1026. **HRMS** (ESI): C₁₉H₂₂NO₂ [M+H]⁺; calculated 296.1645, found 296.1653. [α]²⁴_D -0.7° (c. 0.23, CHCl₃).

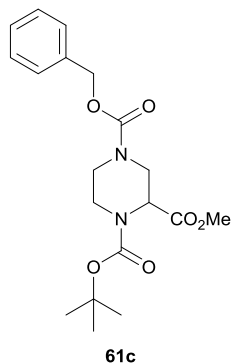
1-*tert*-Butyl 2-methyl (2*S*)-pyrrolidine-1,2-dicarboxylate **61a**



Boc₂O (5.20 g, 23.9 mmol, 1.03 eq.) and Et₃N (9.7 mL, 70 mmol, 2.9 eq.) were added to a stirred solution of L-proline methyl ester hydrochloride (3.84 g, 23.2 mmol, 1.00 eq.) in CH₂Cl₂ (230 mL). The reaction mixture was stirred for 1 h, then concentrated *in vacuo*. The residue was triturated with Et₂O (3 × 50 mL) and filtered to remove the insoluble Et₃N·HCl. The resulting solution was dry-loaded onto silica. Flash chromatography eluting with pentane–EtOAc (4:1) gave the title compound **61a** (5.30 g, 23.1 mmol, 99%) as a colourless oil. *R_f* 0.19 (4:1 petrol–EtOAc). [α]²⁷_D -61.4 (c. 0.83, MeOH) {lit.²⁰⁸ -61.7 (c. 1.15, MeOH)}. **¹H NMR** (300 MHz, CDCl₃, 40:60 mixture of rotamers): δ 4.34 (0.4H, dd, *J* 8.5, 3.1, 2-H), 4.23 (0.6H, dd, *J* 8.5, 4.1, 2-H), 3.73 (3H, s, CO₂CH₃), 3.62–3.33 (2H, m, 5-H), 2.33–2.09 (1H, m, 3-H_A), 2.05–1.77 (3H, m, 3-H_B and 4-H), 1.47 (3.6H, s, C(CH₃)₃), 1.42 (5.4H, s, C(CH₃)₃). **¹³C NMR** (75 MHz, CDCl₃, mixture of two rotamers): δ 173.8 (major, CO₂CH₃), 173.5 (minor, CO₂CH₃), 154.5 (minor, N(CO)O), 153.8 (major, N(CO)O), 79.9 (major and minor, C_q(CH₃)₃), 59.2 (major, 2-C), 58.8 (minor, 2-C), 52.1 (minor, CO₂CH₃), 52.0 (major, CO₂CH₃), 46.6 (minor, 5-C), 46.4 (major,

5-C), 30.9 (major, 3-C), 30.0 (minor, 3-C), 28.5 (minor, C_q(CH₃)₃), 28.3 (major, C_q(CH₃)₃), 24.4 (minor, 4-C), 23.7 (major, 4-C). IR $\nu_{\max}(\text{film})/\text{cm}^{-1}$ 2977, 2882, 1747 (CO), 1694 (CO), 1393, 1201, 1121, 1088. HRMS (ESI): C₁₁H₁₉NNaO₄ [M+Na]⁺; calculated 252.1212, found 252.1206. Spectra consistent with the literature values.²⁰⁹

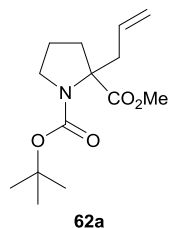
4-Benzyl 1-*tert*-butyl 2-methyl piperazine-1,2,4-tricarboxylate **61c**



Benzyl chloroformate (3.5 mL, 24 mmol, 1.3 eq.) was added dropwise to a stirred solution of 1-*tert*-butyl 2-methyl piperazine-1,2-dicarboxylate* (4.59 g, 18.8 mmol, 1.00 eq.) and Et₃N (3.4 mL, 24 mmol, 1.3 eq.) in CH₂Cl₂ (50 mL) at 0 °C. The reaction mixture was warmed to rt and stirred for 15 h, then partitioned between H₂O (50 mL) and CH₂Cl₂ (50 mL). The organics were dried over MgSO₄, filtered, then concentrated *in vacuo*. Flash chromatography eluting with pentane–EtOAc (4:1) gave the *title compound* **61c** (5.52 g, 14.6 mmol, 85%) as a straw-coloured oil. R_f 0.11 (4:1 petrol–EtOAc). ¹H NMR (500 MHz, d⁶-DMSO, 343 K): δ 7.40-7.29 (5H, m, Cbz Ar-H), 5.11 (1H, d, *J* 12.7, CH_AH_BPh), 5.07 (1H, d, *J* 12.7, CH_AH_BPh), 4.61 (1H, br. s, 2-H), 4.34 (1H, d, *J* 13.8, 3-H_A), 3.92-3.85 (1H, m, NCH_AH_BCH₂N), 3.74 (1H, dt, *J* 13.0, 3.4, NCH_AH_BCH₂N), 3.60 (3H, s, CO₂CH₃), 3.27 (1H, dd, *J* 13.8, 4.5, 3-H_B), 3.16-3.07 (1H, m, NCH_AH_BCH₂N), 3.04-2.03 (1H, m, NCH_AH_BCH₂N), 1.40 (9H, s, C(CH₃)₃). ¹³C NMR (125 MHz, d⁶-DMSO, 373 K): δ 169.9 (CO₂CH₃), 154.0 (N(CO)O), 153.9 (N(CO)O), 136.3 (Ar-C_q), 127.8 (Ar-C), 127.2 (Ar-C), 126.8 (Ar-C), 79.5 (C_q(CH₃)₃), 66.0 (CH₂Ph), 53.7 (2-C), 51.3 (CO₂CH₃), 43.5 (3-C and NCH₂CH₂N), 42.3 (NCH₂CH₂N), 27.4 (C(CH₃)₃). IR $\nu_{\max}(\text{film})/\text{cm}^{-1}$ 2976, 1744 (CO), 1694, 1457, 1431, 1224, 1168, 1106. HRMS (ESI): C₁₉H₂₇N₂O₆ [M+H]⁺; calculated 379.1864, found 379.1866.

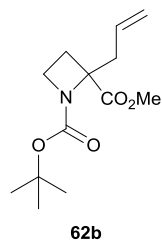
* Purchased from Fluorochem.

1-*tert*-Butyl 2-methyl 2-(prop-2-en-1-yl)pyrrolidine-1,2-dicarboxylate **62a**



General procedure **E** was followed using Boc-protected amino ester **61a** (2.50 g, 10.9 mmol). Flash chromatography eluting with pentane–EtOAc (5:1) gave the title compound **62a** (2.4 g, 8.8 mmol, 81%) as a colourless oil. R_f 0.35 (4:1 petrol–EtOAc). $^1\text{H NMR}$ (300 MHz, CDCl_3 , 33:67 mixture of rotamers): δ 5.89–5.64 (1H, m, $\text{CH}=\text{CH}_2$), 5.22–5.05 (2H, m, $\text{CH}=\text{CH}_2$), 3.76–3.54 (4H, includes 1H, m, 5- H_A and at δ 3.72: 3H, s, CO_2CH_3), 3.50–3.28 (1H, m, 5- H_B), 3.11 (0.33H, dd, J 14.1, 6.5, $\text{CH}_A\text{H}_B\text{CH}=\text{CH}_2$), 2.92 (0.67H, dd, J 14.1, 6.5, $\text{CH}_A\text{H}_B\text{CH}=\text{CH}_2$), 2.61 (1H, dd, J 14.1, 8.1, $\text{CH}_A\text{H}_B\text{CH}=\text{CH}_2$), 2.20–1.96 (2H, m, 3-H), 1.96–1.72 (2H, m, 4-H), 1.46 (3H, s, $\text{C}(\text{CH}_3)_3$), 1.43 (6H, s, $\text{C}(\text{CH}_3)_3$). $^{13}\text{C NMR}$ (75 MHz, CDCl_3 , mixture of two rotamers): δ 175.4 (major and minor, CO_2CH_3), 154.2 (minor, $\text{N}(\text{CO})\text{O}$), 153.8 (major, $\text{N}(\text{CO})\text{O}$), 134.0 (minor, $\text{CH}=\text{CH}_2$), 133.6 (major, $\text{CH}=\text{CH}_2$), 119.3 (major, $\text{CH}=\text{CH}_2$), 119.0 (minor, $\text{CH}=\text{CH}_2$), 79.8 ($\text{C}_q(\text{CH}_3)_3$, major and minor), 67.8 (minor, 2-C), 67.2 (major, 2-C), 52.5 (minor, CO_2CH_3), 52.4 (major, CO_2CH_3), 48.8 (minor, 5-C), 48.7 (major, 5-C), 39.9 (major, $\text{CH}_2\text{CH}=\text{CH}_2$), 38.6 (minor, $\text{CH}_2\text{CH}=\text{CH}_2$), 37.3 (major, 3-C, major), 36.0 (minor, 3-C), 28.7 (minor, $\text{C}(\text{CH}_3)_3$), 28.6 (major, $\text{C}(\text{CH}_3)_3$), 23.4 (minor, 4-C), 22.9 (major, 4-C). $\text{IR } \nu_{\text{max}}(\text{film})/\text{cm}^{-1}$ 2977, 2878, 1742 (CO), 1698 (CO), 1392, 1253, 1162, 1022. HRMS (ESI): $\text{C}_{14}\text{H}_{23}\text{NNaO}_4$ $[\text{M}+\text{Na}]^+$; calculated 292.1525, found 292.1519. Spectra consistent with the literature values.^{209,134}

1-*tert*-Butyl 2-methyl 2-(prop-2-en-1-yl)azetidine-1,2-dicarboxylate **62b**

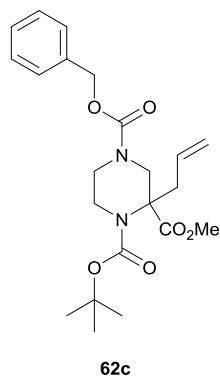


General procedure **E** was followed using 1-*tert*-butyl 2-methyl azetidine-1,2-dicarboxylate* (2.4 g, 11 mmol). The residue was washed through a pad of silica with EtOAc to give the *title compound* **62b** (2.26 g, 8.85 mmol, 80%) as a yellow oil. R_f 0.07 (91:9 pentane–EtOAc). $^1\text{H NMR}$ (500 MHz, CDCl_3 , 33:67 mixture of rotamers): δ 5.97–5.84 (1H, m, $\text{CH}=\text{CH}_2$), 5.23–5.16 (2H, m, $\text{CH}=\text{CH}_2$), 4.00–3.86 (1H, m, 4- H_A), 3.77 (3H, s, CO_2CH_3), 3.69 (1H, m, 4- H_B), 2.96–2.86 (0.33H, m, $\text{CH}_A\text{H}_B\text{CH}=\text{CH}_2$), 2.76 (0.67H, m, dd, J 14.2, 6.0, $\text{CH}_A\text{H}_B\text{CH}=\text{CH}_2$), 2.60 (1H, dd, J 14.2, 8.1, $\text{CH}_A\text{H}_B\text{CH}=\text{CH}_2$), 2.29–2.21 (1H, m, 3- H_A), 2.19–2.11 (1H, m, 3- H_B), 1.40 (9H, s, $\text{C}(\text{CH}_3)_3$). $^{13}\text{C NMR}$ (125 MHz, CDCl_3): δ 173.1 (CO_2CH_3), 155.1

* Purchased from Fluorochem.

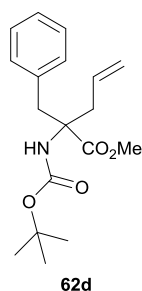
(N(CO)O), 132.6 (CH=CH₂), 119.6 (CH=CH₂), 80.0 (C_q(CH₃)₃), 70.3 (2-C), 52.4 (CO₂CH₃), 44.9 (4-C), 38.8 (C_qCH₂CH=CH₂), 28.4 (C(CH₃)₃), 24.3 (3-C). **IR** ν_{\max} (film)/cm⁻¹ 2977, 2895, 1739 (CO), 1713 (CO), 1392, 1257, 1157, 1112. **HRMS** (ESI): C₁₃H₂₂NO₄ [M+H]⁺; calculated 256.1543, found 256.1541.

4-Benzyl 1-*tert*-butyl 2-methyl 2-(prop-2-en-1-yl)piperazine-1,2,4-tricarboxylate **62c**



General procedure **E** was followed using Boc-protected amino ester **61c** (3.5 g, 9.2 mmol). The residue was washed through a pad of silica with EtOAc to give the *title compound* **62c** (3.7 g, 8.8 mmol, 96%) was isolated as a yellow oil. **¹H NMR** (500 MHz, *d*⁶-DMSO, 340 K): δ 7.41-7.28 (5H, m, Cbz Ar-H), 5.85-5.71 (1H, m, CH=CH₂), 5.17-5.02 (4H, m, CH=CH₂ and OCH₂Ph), 4.01-3.93 (1H, m, NCH_AH_BCH₂N), 3.82-3.77 (1H, m, 3-H_A), 3.66-3.58 (1H, m, 3-H_B), 3.56-3.47 (1H, m, NCH_AH_BCH₂N), 3.43-3.36 (4H, m, includes NCH_AH_BCH₂N and at δ 3.52: 3H, s, CO₂CH₃), 3.35-3.26 (1H, m, NCH_AH_BCH₂N), 2.92 (1H, d, *J* 14.5, CH_AH_BCH=CH₂), 2.53-2.44 (1H, m, CH_AH_BCH=CH₂), 1.37 (9H, s, C(CH₃)₃). **¹³C NMR** (125 MHz, *d*⁶-DMSO, 340 K, one carbamate CO peak not observed): δ 172.0 (CO₂CH₃), 153.1 (N(CO)O), 136.5 (Ar-C_q), 132.1 (CH=CH₂), 128.0 (Ar-C), 127.5 (Ar-C), 127.2 (Ar-C), 118.9 (CH=CH₂), 80.0 (C_q(CH₃)₃), 66.0 (CH₂Ph), 63.1 (2-C), 51.6 (CO₂CH₃), 45.3 (3-C), 43.2 (NCH₂CH₂N), 38.3 (NCH₂CH₂N or CH₂CH=CH₂), 37.6 (NCH₂CH₂N or CH₂CH=CH₂), 27.6 (C(CH₃)₃). **IR** ν_{\max} (film)/cm⁻¹ 2976, 1746 (CO), 1704 (CO), 1417, 1394, 1366, 1270, 1219. **HRMS** (ESI): C₂₂H₃₁N₂O₆ [M+H]⁺; calculated 419.2177, found 419.2181.

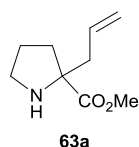
Methyl 2-benzyl-2-[(*tert*-butoxycarbonyl)amino]pent-4-enoate **62d**



To a stirred solution of amino ester **63d** (322 mg, 1.47 mmol, 1.00 eq.) in THF (10 mL) was added Boc₂O (321 mg, 1.47 mmol, 1.00 eq.) and the reaction mixture was heated at reflux for 15 h. The reaction mixture was concentrated *in vacuo*, diluted with EtOAc (50 mL), washed with H₂O (50 mL) then brine (50 mL). The organic phase was dried over MgSO₄, filtered, then concentrated *in vacuo* to give the *title compound* **62d** (470 mg, 1.47 mmol, 99%) as a yellow oil. *R_f* 0.35 (4:1 pentane–EtOAc). **¹H NMR** (500 MHz, CDCl₃): δ 7.27-7.19 (3H, m, Ar-H), 7.07-7.04 (2H, m,

Ar-H), 5.70-5.59 (1H, m, $CH=CH_2$), 5.33 (1H, br. s, NH), 5.14-5.06 (2H, m, $CH=CH_2$), 3.75 (3H, s, CO_2CH_3), 3.61 (1H, d, J 13.6, CH_AH_BPh), 3.21 (1H, dd, J 13.7, 7.1, $CH_AH_BCH=CH_2$), 3.12 (1H, d, J 13.6, CH_AH_BPh), 2.59 (1H, dd, J 13.7, 7.4, $CH_AH_BCH=CH_2$), 1.47 (9H, s, $C(CH_3)_3$). ^{13}C NMR (125 MHz, $CDCl_3$): δ 173.2 (CO_2CH_3), 154.2 ($NH(CO)O$), 136.6 (Ar- C_q), 132.6 ($CH=CH_2$), 130.0 (Ar-C), 128.3 (Ar-C), 127.0 (Ar-C), 119.1 ($CH=CH_2$), 79.4 ($C_q(CH_3)_3$), 65.1 (C_q), 52.6 (CO_2CH_3), 40.9 (CH_2Ph), 40.1 ($CH_2CH=CH_2$), 28.6 ($C(CH_3)_3$). IR $\nu_{max}(\text{film})/\text{cm}^{-1}$ 3430, 2978, 1739 (CO), 1714 (CO), 1495, 1447, 1348, 1232. HRMS (ESI): $C_{18}H_{25}NNaO_4$ $[M+Na]^+$; calculated 342.1681, found 342.1676. Spectra consistent with the literature values.²¹⁰

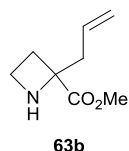
Methyl 2-(prop-2-en-1-yl)pyrrolidine-2-carboxylate **63a**



63a

General procedure **F** was followed using Boc-protected amino ester **62a** (6.7 g, 25 mmol). Purification by SCX cartridge, eluting first with MeOH then sat. $NH_3/MeOH$, gave the *title compound* **63a** (3.10 g, 18.3 mmol, 74%) as an orange oil. 1H NMR (500 MHz, $CDCl_3$, NH not observed): δ 5.78-5.69 (1H, m, $CH=CH_2$), 5.15-5.07 (2H, m, $CH=CH_2$), 3.74 (3H, s, CO_2CH_3), 3.14-3.02 (2H, m, 5-H), 2.61 (1H, ddt, J 13.7, 7.3, 1.1, $CH_AH_BCH=CH_2$), 2.45 (1H, ddt, J 13.7, 7.2, 1.0, $CH_AH_BCH=CH_2$), 2.27-2.18 (1H, m, 3- H_A), 1.91-1.79 (2H, m, 3- H_B and 4- H_A), 1.79-1.68 (1H, m, 4- H_B). ^{13}C NMR (125 MHz, $CDCl_3$): δ 176.3 (CO_2CH_3), 133.3 ($CH=CH_2$), 119.0 ($CH=CH_2$), 70.0 (2-C), 52.6 (CO_2CH_3), 46.5 (5-C), 43.3 ($CH_2CH=CH_2$), 35.2 (3-C), 24.7 (4-C). IR $\nu_{max}(\text{film})/\text{cm}^{-1}$ 3352 (NH), 2953, 1732 (CO), 1435, 1217, 1200, 997, 918. HRMS (ESI): $C_9H_{16}NO_2$ $[M+H]^+$; calculated 170.1181, found 170.1176.

Methyl 2-(prop-2-en-1-yl)azetidine-2-carboxylate **63b**

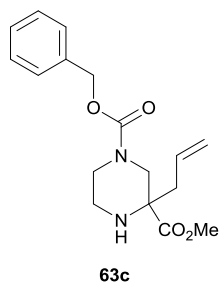


63b

General procedure **F** was followed using Boc-protected amino ester **62b** (1.93 g, 7.53 mmol). Purification by SCX cartridge, eluting first with MeOH then sat. $NH_3/MeOH$, gave the *title compound* **63b** (771 mg, 4.97 mmol, 66%) as an orange oil. 1H NMR (500 MHz, $CDCl_3$, NH not observed): δ 5.80-5.68 (1H, m, $CH=CH_2$), 5.14-5.07 (2H, m, $CH=CH_2$), 3.78 (3H, s, CO_2CH_3), 3.51 (1H, app. q, J 7.9, 4- H_A), 3.37-3.31 (1H, m, 4- H_B), 2.63-2.51 (2H, m, $CH_2CH=CH_2$), 2.49-2.39 (2H, m, 3-H). ^{13}C NMR (125 MHz, $CDCl_3$): δ 176.6 (CO_2CH_3), 132.2 ($CH=CH_2$), 118.5 ($CH=CH_2$), 67.4 (2-C), 52.3 (CO_2CH_3), 43.8 ($CH_2CH=CH_2$), 41.5 (4-C), 30.0 (3-C). IR $\nu_{max}(\text{film})/\text{cm}^{-1}$ 3329, 2954, 2879,

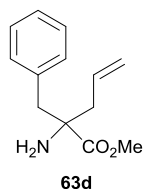
1732 (CO), 1436, 1266, 1216, 1140. **HRMS** (EI): C₈H₁₃NO₂ [M]⁺; calculated 155.0945, found 155.0946.

1-Benzyl 3-methyl 3-(prop-2-en-1-yl)piperazine-1,3-dicarboxylate **63c**



General procedure **F** was followed using Boc-protected amino ester **62c** (3.37 g, 8.05 mmol). Purification by SCX cartridge, eluting first with MeOH then sat. NH₃/MeOH, gave the *title compound* **63c** (2.19 g, 6.88 mmol, 85%) as a colourless oil. **R_f** 0.18 (3:2 pentane–EtOAc). **¹H NMR** (500 MHz, *d*⁶-DMSO, 340 K): δ 7.41-7.28 (5H, m, Cbz Ar-H), 5.74-5.64 (1H, m, CH=CH₂), 5.13-5.03 (4H, m, CH₂Ph and CH=CH₂), 4.19 (1H, d, *J* 12.8, 3-H_A), 3.70 (1H, d, *J* 12.5, NCH_AH_BCH₂N), 3.58 (3H, s, CO₂CH₃), 3.00-2.92 (1H, m, NCH_AH_BCH₂N), 2.90 (1H, d, *J* 12.8, 3-H_B), 2.80-2.74 (1H, m, NCH_AH_BCH₂N), 2.73-2.66 (1H, m, NCH_AH_BCH₂N), 2.65 (1H, br. s, NH), 2.32 (1H, dd, *J* 13.8, 7.2, CH_AH_BCH=CH₂), 2.25 (1H, dd, *J* 13.8, 7.5, CH_AH_BCH=CH₂). **¹³C NMR** (125 MHz, *d*⁶-DMSO, 340 K): δ 173.2 (CO₂CH₃), 154.1 (N(CO)O), 136.7 (Ar-C_q), 131.7 (CH=CH₂), 128.0 (Ar-C), 127.4 (Ar-C), 127.0 (Ar-C), 118.4 (CH=CH₂), 65.9 (CH₂Ph), 61.1 (2-C), 51.1 (CO₂CH₃), 49.0 (3-C), 43.2 (NCH₂CH₂), 41.0 (CH₂CH=CH₂ or NCH₂CH₂N), 40.8 (CH₂CH=CH₂ or NCH₂CH₂N). **IR** *v*_{max}(film)/cm⁻¹ 3564, 3339, 2951, 1731 (CO), 1704 (CO), 1434, 1358, 1229, 1122, 761. **HRMS** (ESI): C₁₇H₂₃N₂O₄ [MH]⁺; calculated 319.1652, found 319.1658.

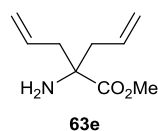
Methyl 2-amino-2-benzylpent-4-enoate **63d**



Benzaldehyde (1.2 mL, 12 mmol, 1.0 eq.) was added to a stirred suspension of L-phenylalanine methyl ester hydrochloride (2.5 g, 12 mmol, 1.0 eq.), Et₃N (1.6 mL, 12 mmol, 1.0 eq.) and 4 Å MS (500 mg) in THF (60 mL). The reaction mixture was stirred for 15 h, then filtered to remove the insoluble Et₃N·HCl and concentrated *in vacuo* to give the crude imine as a pale yellow oil. The residue was diluted in THF (60 mL) and LiHMDS (1.0 M in THF, 17.4 mL, 17.4 mmol, 1.50 eq.) was added dropwise at -78 °C. The reaction mixture was stirred for 15 min then allyl bromide (1.50 mL, 17.4 mmol, 1.50 eq.) was added dropwise. After 1 h the dry-ice bath was removed, the reaction mixture was warmed to rt and stirred for 15 h. Aqueous citric acid (15 wt%, 100 mL) was added and the reaction mixture was stirred for

1 h, then partitioned with Et₂O (100 mL). The aqueous layer was neutralised with solid NaHCO₃, then extracted with CH₂Cl₂ (3 × 50 mL). The combined organics were dried over Na₂SO₄ and concentrated *in vacuo*. The *title compound 63d* (2.26 g, 10.3 mmol, 89%) was isolated as a yellow oil after flushing through a pad of silica with EtOAc–MeOH (9:1). **R_f** 0.14 (4:1 pentane–EtOAc). **¹H NMR** (300 MHz, CDCl₃, NH₂ not observed): δ 7.24–7.10 (3H, m, Ar-H), 7.10–7.02 (2H, m, Ar-H), 5.70–5.54 (1H, m, CH=CH₂), 5.15–5.05 (2H, m, CH=CH₂), 3.62 (3H, s, CO₂CH₃), 3.11 (1H, d, *J* 13.2, CH_AH_BPh), 2.71 (1H, d, *J* 13.2, CH_AH_BPh), 2.65 (1H, ddt, *J* 13.4, 6.4, 1.2, CH_AH_BCH=CH₂), 2.24 (1H, dd, *J* 13.4, 8.5, CH_AH_BCH=CH₂). **¹³C NMR** (75 MHz, CDCl₃): δ 176.6 (CO₂CH₃), 136.2 (Ar-C_q), 132.6 (CH=CH₂), 129.9 (Ar-C), 128.5 (Ar-C), 127.1 (Ar-C), 119.9 (CH=CH₂), 62.0 (C_q), 52.1 (CO₂CH₃), 45.9 (CH₂Ph), 44.6 (CH₂CH=CH₂). **IR** ν_{max}(film)/cm⁻¹ 3378, 2951, 1738 (CO), 1603, 1441, 1218, 1030, 922. **HRMS** C₁₃H₁₈NO₂ [M+H]⁺; calculated 220.1332, found 220.1340. Spectra consistent with the literature values.²¹¹

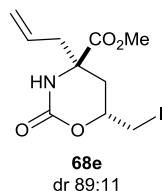
Methyl 2-amino-2-(prop-2-en-1-yl)pent-4-enoate **63e**



Et₃N (5.6 mL, 40 mmol, 1.0 eq.) was added to a stirred solution of glycine methyl ester hydrochloride (5.0 g, 40 mmol, 1.0 eq.), benzaldehyde (4.1 mL, 40 mmol, 1.0 eq.) and 4 Å MS (1.5 g). The reaction mixture was stirred for 4 h, filtered, then concentrated *in vacuo* to give the crude α-imino ester (6.3 g, 62% mass recovery). A sample of the crude residue (2.5 g, 16 mmol, 1.0 eq.) was dissolved in THF (70 mL) and cooled to -78 °C. LiHMDS (1.0 M in THF, 34 mL, 34 mmol, 2.2 eq.) was added dropwise. The reaction mixture was stirred for 20 min then allyl bromide (3.7 mL, 42 mmol, 2.7 eq.) was added dropwise. The reaction mixture was stirred for 1 h then warmed to rt. Aq. citric acid (5 wt%, 100 mL) was added and the reaction mixture was stirred for 2 h. Et₂O (50 mL) was added and the phases were separated. The aqueous phase was neutralised with solid NaHCO₃ then extracted with CH₂Cl₂ (3 × 20 mL). The combined organic extracts were dried over MgSO₄, filtered, then concentrated *in vacuo* to give the title compound **63e** (1.35 g, 7.98 mmol, 51%) as an orange oil which was not purified further. **¹H NMR** (300 MHz, CDCl₃, NH₂ not observed): δ 5.78–5.60 (2H, m, CH=CH₂), 5.19–5.08 (4H, m, CH=CH₂), 3.71 (3H, s, CO₂CH₃), 2.56 (2H, dd, *J* 13.5, 6.5, CH_AH_BCH=CH₂), 2.26 (2H, dd, *J* 13.5, 8.4, CH_AH_BCH=CH₂). **¹³C NMR** (75 MHz, CDCl₃): δ 176.9 (CO₂CH₃),

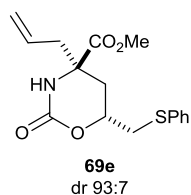
132.6 (CH=CH₂), 119.7 (CH=CH₂), 60.7 (C_q), 52.3 (CO₂CH₃), 44.2 (CH₂CH=CH₂). **IR** $\nu_{\text{max}}(\text{film})/\text{cm}^{-1}$ 3380 (NH₂), 3078, 2980, 2952, 1738 (CO), 1640, 1440, 1213. **HRMS** (ESI): C₉H₁₆NO₂ [M+H]⁺; calculated 170.1176, found 170.1198.

Methyl (4*R,6*R**)-6-(iodomethyl)-2-oxo-4-(prop-2-en-1-yl)-1,3-oxazinane-4-carboxylate **68e****



Boc₂O (1.0 g, 4.6 mmol, 1.0 eq.) was added to a stirred solution of amino ester **63e** (775 mg, 4.60 mmol, 1.00 eq.) in THF (15 mL). The reaction mixture was stirred at rt for 15 h then concentrated *in vacuo*. General procedure **G** was then followed to give the *title compound* **68e** (1.3 g, 3.8 mmol, 85%, dr 89:11) as a colourless amorphous solid which was not purified further. **R_f** 0.14 (4:1 pentane–EtOAc). **¹H NMR** (500 MHz, CDCl₃, *dr* 89:11, major diastereomer peaks assigned): δ 5.66–5.55 (1H, m, CH=CH₂), 5.48 (1H, s, NH), 5.29 (1H, d, *J* 9.9, CH=CH_AH_B), 5.25 (1H, dd, *J* 17.0, 0.7, CH=CH_AH_B), 4.15–4.07 (1H, m, 6-H), 3.80 (3H, s, CO₂CH₃), 3.36 (1H, dd, *J* 10.7, 4.5, CH_AH_BI), 3.28 (1H, dd, *J* 10.7, 6.5, CH_AH_BI), 2.73–2.66 (2H, m, CH_AH_BCH=CH₂ and 5-H_A), 2.38 (1H, dd, *J* 13.7, 8.8, CH_AH_BCH=CH₂), 1.73 (1H, dd, *J* 13.8, 11.8, 5-H_B). Minor diastereomer characteristic peaks: δ 5.69 (1H, s, NH), 5.19 (1H, d, *J* 16.6, CH=CH_AH_B), 4.45–4.33 (1H, m, 6-H). **¹³C NMR** (125 MHz, CDCl₃, major diastereomer peaks assigned): δ 172.6 (CO₂CH₃), 151.9 (2-C), 129.4 (CH=CH₂), 122.4 (CH=CH₂), 73.8 (6-C), 60.4 (4-C), 53.4 (CO₂CH₃), 44.2 (CH₂CH=CH₂), 35.5 (5-C), 5.5 (CH₂I). **IR** $\nu_{\text{max}}(\text{film})/\text{cm}^{-1}$ 3251, 3130, 2953, 2158, 1709, 1397, 1264, 1222. **HRMS** (ESI): C₁₀H₁₅INO₄ [M+H]⁺; calculated 340.0040, found 340.0040.

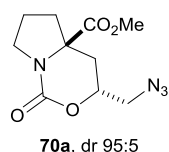
Methyl (4*R,6*R**)-2-oxo-6-[(phenylsulfanyl)methyl]-4-(prop-2-en-1-yl)-1,3-oxazinane-4-carboxylate **69e****



Thiophenol (150 μ L, 1.46 mmol, 1.30 eq.) and DBU (240 μ L, 1.60 mmol, 1.40 eq.) were added to a stirred solution of iodide **68e** (451 mg, 1.12 mmol, 1.00 eq.) in DMF (13 mL). The reaction mixture was diluted in EtOAc (150 mL), washed with H₂O (50 mL) and brine (50 mL). The organic phase was dried over Na₂SO₄, filtered then concentrated *in vacuo*. Flash chromatography eluting with 0–100% EtOAc in pentane gave the *title compound* **69e** (289 mg, 0.899 mmol, 80%, dr 93:7) as a

colourless amorphous solid. R_f 0.10 (3:2 petrol–EtOAc). **M.p.** 116–117 °C, colourless needles, hexane–EtOAc. **$^1\text{H NMR}$** (500 MHz, CDCl_3 , dr 93:7, major diastereomer peaks assigned): δ 7.42–7.37 (2H, m, Ar-H), 7.33–7.28 (2H, m, Ar-H), 7.27–7.22 (1H, m, Ar-H), 5.64–5.53 (1H, m, $\text{CH}=\text{CH}_2$), 5.50 (1H, s, NH), 5.26 (1H, d, J 10.1, $\text{CH}=\text{CH}_A\text{H}_B$), 5.21 (1H, dd, J 16.9, 1.1, $\text{CH}=\text{CH}_A\text{H}_B$), 4.21–4.14 (1H, m, 6-H), 3.70 (3H, s, CO_2CH_3), 3.34 (1 H, dd, J 14.0, 4.4, $\text{CH}_A\text{H}_B\text{SPh}$), 2.95 (1H, dd, J 14.0, 8.4, $\text{CH}_A\text{H}_B\text{SPh}$), 2.77 (1H, dt, J 13.9, 1.8, 5- H_A), 2.67 (1H, dd, J 13.7, 6.0, $\text{CH}_A\text{H}_B\text{CH}=\text{CH}_2$), 2.34 (1H, dd, J 13.7, 8.9, $\text{CH}_A\text{H}_B\text{CH}=\text{CH}_2$), 1.67 (1H, dd, J 13.9, 12.0, 5- H_B). Minor diastereomer characteristic peaks: 5.17 (1H, d, J 10.0, $\text{CH}=\text{CH}_A\text{H}_B$), 5.10 (1H, dd, J 17.3, 1.3, $\text{CH}=\text{CH}_A\text{H}_B$), 4.43–4.36 (1H, m, 6-H), 3.40 (1H, dd, J 14.0, 4.5, $\text{CH}_A\text{H}_B\text{SPh}$), 3.10 (1H, dd, J 14.0, 7.4, $\text{CH}_A\text{H}_B\text{SPh}$), 2.54–2.40 (3H, m), 1.96 (1H, dd, J 14.3, 11.3). **$^{13}\text{C NMR}$** (75 MHz, CDCl_3 , major diastereomer peaks assigned): δ 172.6 (CO_2CH_3), 152.7 (2-C), 134.5 (Ar- C_q), 130.9 ($\text{CH}=\text{CH}_2$), 129.7 (Ar-C), 129.3 (Ar-C), 127.3 (Ar-C), 121.9 ($\text{CH}=\text{CH}_2$), 73.9 (6-C), 60.7 (4-C), 53.1 (CO_2CH_3), 43.9 ($\text{CH}_2\text{CH}=\text{CH}_2$), 38.3 (CH_2SPh), 33.8 (5-C). **IR** $\nu_{\text{max}}(\text{film})/\text{cm}^{-1}$ 3245, 3121, 1711 (CO), 1403, 1288, 1221, 1089, 742. **HRMS** (ESI): $\text{C}_{16}\text{H}_{19}\text{NNaO}_4\text{S}$ [$\text{M}+\text{Na}$] $^+$; calculated 344.0927, found 344.0934.

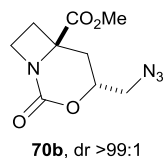
Methyl (3*R,4*aR**)-3-(azidomethyl)-1-oxo-hexahydro-1*H*-pyrrolo[1,2-*c*][1,3]oxazine-4*a*-carboxylate 70a**



General procedure **G** was followed using Boc-carbamate **62a** (200 mg, 0.740 mmol). Flash chromatography eluting with 0–100% EtOAc in pentane gave the *title compound* **70a** (99 mg, 0.39 mmol, 53%, 95:5 mixture of diastereomers) as a yellow oil. R_f 0.05 (1:1 petrol–EtOAc). **$^1\text{H NMR}$** (500 MHz, CDCl_3): δ 4.30–4.21 (1H, m, 3-H), 3.79 (3H, s, CO_2CH_3), 3.77–3.71 (1H, m, 7- H_A), 3.67–3.61 (1H, m, 7- H_B), 3.57 (1H, dd, J 13.0, 4.6, $\text{CH}_A\text{H}_B\text{N}_3$), 3.46 (1H, dd, J 13.0, 4.5, $\text{HCH}_A\text{H}_B\text{N}_3$), 2.63 (1H, dd, J 13.5, 2.6, 4- H_A), 2.55–2.43 (1H, m, 5- H_A), 2.07–1.96 (1H, m, 6- H_A), 1.90–1.79 (2H, m, 5- H_B and 6- H_B), 1.74 (1H, dd, J 13.5, 12.3, 4- H_B). **$^{13}\text{C NMR}$** (125 MHz, CDCl_3): δ 173.5 (CO_2CH_3), 151.5 (1-C), 74.1 (3-C), 67.1 (4a-C), 54.1 (CH_2N_3), 53.6 (CO_2CH_3), 47.4 (7-C), 38.5 (5-C), 33.9 (4-C), 21.7 (6-C). **IR** $\nu_{\text{max}}(\text{film})/\text{cm}^{-1}$ 2955, 2898, 2106 (N_3), 1738 (CO), 1416, 1302, 1210, 1171. **HRMS** (ESI): $\text{C}_{10}\text{H}_{15}\text{N}_4\text{O}_4$ [$\text{M}+\text{H}$] $^+$; calculated 255.1093, found 255.1088. **X-Ray Crystallography**: CCDC 1008922 contains the supplementary crystallographic data for this compound. Crystals

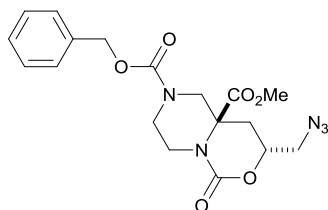
were grown by slow diffusion of Et₂O into the sample dissolved in the minimum amount of CHCl₃.

Methyl (4*R,6*R**)-4-(azidomethyl)-2-oxo-3-oxa-1-azabicyclo[4.2.0]octane-6-carboxylate **70b****



Following a procedure by Licini,¹⁰² NIS (160 mg, 0.710 mmol, 1.20 eq.) was added to a stirred solution of Boc-carbamate **62b** (150 mg, 0.560 mmol, 1.00 eq.) in CHCl₃ (6.0 mL). The reaction mixture was stirred for 4 days and monitored by TLC until complete. The reaction mixture was concentrated *in vacuo*, extracted with EtOAc (25 mL) and washed with sat. aq. Na₂S₂O₃ until colourless. The aqueous layer was extracted with EtOAc (2 × 25 mL). The combined organics were dried over Na₂SO₄, filtered, then concentrated *in vacuo* to give the crude iodide. The iodide was dissolved in DMF (6.0 mL). NaN₃ (114 mg, 1.76 mmol, 3.0 eq.) was added and the reaction mixture was stirred for 48 h. H₂O (25 mL) was added at 0 °C. The reaction mixture was extracted with EtOAc (3 × 25 mL). The combined organic extracts were washed with brine (25 mL), dried over Na₂SO₄, filtered, then concentrated *in vacuo*. Flash chromatography eluting with 0-100% EtOAc in pentane gave co-elution of the title compound with succinimide. Trituration of the residue with Et₂O gave the *title compound* **70b** (53 mg, 0.22 mmol, 37%) as a colourless solid. **R_f** 0.09 (4:1 pentane–EtOAc). **¹H NMR** (500 MHz, CDCl₃): δ 4.44-4.37 (1H, m, 4-H), 4.33-4.25 (1H, m, 8-H_A), 4.15 (1H, td, *J* 9.6, 4.8, 8-H_B), 3.87 (3H, s, CO₂CH₃), 3.56 (1H, dd, *J* 13.1, 4.5, CH_AH_BN₃), 3.45 (1H, dd, *J* 13.1, 4.5, CH_AH_BN₃), 2.72-2.58 (2H, m, 7-H), 2.48 (1H, dd, *J* 13.5, 2.2, 5-H_A), 2.02 (1H, dd, *J* 13.5, 11.9, 5-H_B). **¹³C NMR** (125 MHz, CDCl₃): δ 172.3 (CO₂CH₃), 154.0 (2-C), 75.9 (4-C), 69.3 (6-C), 53.9 (CH₂N₃), 53.4 (CO₂CH₃), 50.3 (8-C), 33.3 (7-C), 31.6 (5-C). **IR** ν_{max}(film)/cm⁻¹ 2959, 2107 (N₃), 1713 (CO), 1392, 1293, 1208, 1155, 762. **HRMS** (ESI): C₉H₁₃N₄O₄ [M+H]⁺; calculated 241.0931, found 241.0930.

2-Benzyl 9a-methyl (8R*,9aS*)-8-(azidomethyl)-6-oxo-octahydropiperazino[1,2-c][1,3]oxazine-2,9a-dicarboxylate 70c

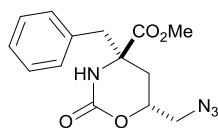


70c, dr 93:7

General procedure **G** was followed using Boc-carbamate **62c** (314 mg, 0.750 mmol). Flash chromatography eluting with 0-100% EtOAc in pentane gave the *title compound* **70c** (195 mg, 0.480 mmol, 64%, 93:7 mixture of diastereomers) as a brown oil.

R_f 0.04 (4:1 petrol–EtOAc). $^1\text{H NMR}$ (500 MHz, d^6 -DMSO, 319 K, major diastereomer peaks assigned): δ 7.42-7.29 (5H, m, Cbz Ar-H), 5.12 (1H, d, J 12.7, $\text{CH}_\text{A}\text{H}_\text{B}\text{Ph}$), 5.08 (1H, d, J 12.7, $\text{CH}_\text{A}\text{H}_\text{B}\text{Ph}$), 4.55 (1H, dd, J 13.4, 1.7, 1- H_A), 4.34-4.28 (1H, m, 8-H), 4.13-4.07 (1H, m, $\text{NCH}_\text{A}\text{H}_\text{B}\text{CH}_2\text{N}$), 4.03-3.97 (1H, m, $\text{NCH}_\text{A}\text{H}_\text{B}\text{CH}_2\text{N}$), 3.66 (3H, s, CO_2CH_3), 3.61 (1H, dd, J 13.5, 3.2, $\text{CH}_\text{A}\text{H}_\text{B}\text{N}_3$), 3.44 (1H, dd, J 13.5, 5.3, $\text{CH}_\text{A}\text{H}_\text{B}\text{N}_3$), 3.01 (1H, d, J 13.4, 1- H_B), 2.98-2.86 (2H, m, $\text{NCH}_\text{A}\text{H}_\text{B}\text{CH}_2\text{N}$ and $\text{NCH}_\text{A}\text{H}_\text{B}\text{CH}_2\text{N}$), 2.26 (1H, dd, J 14.0, 2.6, 9- H_A), 2.02 (1H, dd, J 14.0, 12.4, 9- H_B). $^{13}\text{C NMR}$ (125 MHz, d^6 -DMSO, 319 K): δ 170.8 (CO_2CH_3), 153.7 (N(CO)O), 151.0 (N(CO)O), 136.4 (Ar- C_q), 128.2 (Ar-C), 127.7 (Ar-C), 127.3 (Ar-C), 71.8 (8-C), 66.4 (CH_2Ph), 61.6 (9a-C), 53.0 (CO_2CH_3), 52.8 (CH_2N_3), 49.9 (1-C), 42.4 ($\text{NCH}_2\text{CH}_2\text{N}$), 41.0 ($\text{NCH}_2\text{CH}_2\text{N}$), 30.8 (9-C). $\text{IR } \nu_{\text{max}}(\text{film})/\text{cm}^{-1}$ 2953, 2107 (N_3), 1741 (CO), 1701 (CO), 1432, 1421, 1280, 1230. HRMS (ESI): $\text{C}_{18}\text{H}_{22}\text{N}_5\text{O}_6$ $[\text{M}+\text{H}]^+$; calculated 404.1565, found 404.1580.

Methyl (4R*,6R*)-6-(azidomethyl)-4-benzyl-2-oxo-1,3-oxazinane-4-carboxylate 70d

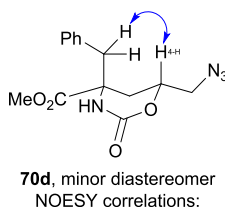


70d, dr 87:13

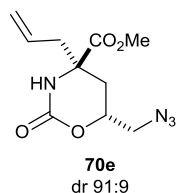
General procedure **G** was followed using Boc-carbamate **62d** (100 mg, 0.310 mmol). The residue was washed through a pad of silica with EtOAc–MeOH (9:1) to give the *title compound* **70d** (84 mg, 0.28 mmol, 88%, 87:13 mixture of diastereomers) as a yellow oil.

R_f 0.08 (3:2 petrol–EtOAc). $^1\text{H NMR}$ (500 MHz, CDCl_3 , dr 87:13, diastereomers assigned by NOESY) major diastereomer peaks: δ 7.37-7.30 (3H, m, Ar-H), 7.13-7.07 (2H, m, Ar-H), 5.42 (1H, br. s, NH), 4.29-4.22 (1H, m, 6-H), 3.73 (3H, s, CO_2CH_3), 3.55 (1H, dd, J 13.2, 4.4, $\text{CH}_\text{A}\text{H}_\text{B}\text{N}_3$), 3.45 (1H, dd, J 13.2, 4.7, $\text{CH}_\text{A}\text{H}_\text{B}\text{N}_3$), 3.31 (1H, d, J 13.4, $\text{CH}_\text{A}\text{H}_\text{B}\text{Ph}$), 2.90 (1H, d, J 13.4, $\text{CH}_\text{A}\text{H}_\text{B}\text{Ph}$), 2.51 (1H, app. dt, J 13.9, 2.0, 5- H_A), 1.94 (1H, dd, J 13.9, 12.2, 5- H_B). Minor diastereomer characteristic peaks: 5.55 (1H, br. s, NH), 4.43-4.37 (1H, m, 6-H), 3.74 (3H, s, CO_2CH_3), 3.58-3.47 (2H, m, CH_2N_3), 3.14 (1H, d, J 13.3, $\text{CH}_\text{A}\text{H}_\text{B}\text{Ph}$),

3.04 (1H, d, J 13.3, $\text{CH}_A\text{H}_B\text{Ph}$), 2.30 (1H, ddd, J 14.3, 2.5, 1.3, 5- H_A), 2.14 (1H, dd, J 14.3, 11.6, 5- H_B). ^{13}C NMR (125 MHz, CDCl_3 , peaks of major diastereomer assigned): δ 172.6 (CO_2CH_3), 151.9 (2-C), 133.0 (Ar-C_q), 129.9 (Ar-C), 129.3 (Ar-C), 128.3 (Ar-C), 73.6 (6-C), 61.9 (4-C), 53.7 (CH_2N_3), 53.2 (CO_2CH_3), 46.2 (CH_2Ph), 33.0 (5-C). IR $\nu_{\text{max}}(\text{film})/\text{cm}^{-1}$ 3247, 2927, 2105 (N_3), 1713 (CO), 1435, 1403, 1284, 1214. HRMS (ESI): $\text{C}_{14}\text{H}_{16}\text{N}_4\text{NaO}_4$ $[\text{M}+\text{Na}]^+$; calculated 327.1064, found 327.1076. The relative configuration of the minor diastereomer was determined by interpretation of the NOESY correlations.

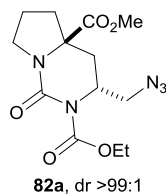


Methyl (4*R**,6*R**)-6-(azidomethyl)-2-oxo-4-(prop-2-en-1-yl)-1,3-oxazinane-4-carboxylate 70e



General procedure **G** was followed for iodide **68e** (200 mg, 0.49 mmol). Flash chromatography eluting with pentane–EtOAc (3:2) gave the *title compound* **70e** (97 mg, 0.38 mmol, 78%, dr 91:9) as a yellow oil. R_f 0.05 (3:2 petrol–EtOAc). ^1H NMR (500 MHz, CDCl_3 , dr 91:9, major diastereomer peaks assigned): δ 5.67 (1H, s, NH), 5.65–5.56 (1H, m, $\text{CH}=\text{CH}_2$), 5.28 (1H, d, J 10.1, $\text{CH}=\text{CH}_A\text{H}_B$), 5.24 (1H, dd, J 16.9, 1.1, $\text{CH}=\text{CH}_A\text{H}_B$), 4.35–4.23 (1H, m, 6-H), 3.79 (3H, s, CO_2CH_3), 3.55 (1H, dd, J 13.1, 4.4, $\text{CH}_A\text{H}_B\text{N}_3$), 3.45 (1H, dd, J 13.1, 4.7, $\text{CH}_A\text{H}_B\text{N}_3$), 2.68 (1H, dd, J 13.7, 6.1, $\text{CH}_A\text{H}_B\text{CH}=\text{CH}_2$), 2.44–2.36 (2H, m, 5- H_A and $\text{CH}_A\text{H}_B\text{CH}=\text{CH}_2$), 1.84 (1H, dd, J 13.9, 12.2, 5- H_B). Minor diastereomer characteristic peaks: 5.78 (1H, s, NH), 5.18 (1H, dd, J 16.9, 1.4, $\text{CH}=\text{CH}_A\text{H}_B$), 4.52–4.46 (1H, m, 6-H), 3.80 (3H, s, CO_2CH_3), 3.36 (1H, dd, J 10.7, 4.5, $\text{CH}_A\text{H}_B\text{N}_3$), 3.28 (1H, dd, J 10.7, 6.4, $\text{CH}_A\text{H}_B\text{N}_3$), 2.59–2.50 (2H, m), 2.18 (1H, ddd, J 14.2, 3.0, 1.3, $\text{CH}_A\text{H}_B\text{CH}=\text{CH}_2$), 2.11 (1H, dd, J 14.2, 11.2, $\text{CH}_A\text{H}_B\text{CH}=\text{CH}_2$), 1.73 (1H, dd, J 13.9, 11.8, 5- H_B). ^{13}C NMR (75 MHz, CDCl_3): δ 172.6 (CO_2CH_3), 152.5 (2-C), 129.7 ($\text{CH}=\text{CH}_2$), 121.9 ($\text{CH}=\text{CH}_2$), 73.5 (6-C), 60.4 (4-C), 53.7 (CO_2CH_3), 53.2 (CH_2N_3), 43.8 ($\text{CH}_2\text{CH}=\text{CH}_2$), 31.6 (5-C). IR $\nu_{\text{max}}(\text{film})/\text{cm}^{-1}$ 3252, 2954, 2106 (N_3), 1715 (CO), 1403, 1291, 1224, 1109. HRMS (ESI): $\text{C}_{10}\text{H}_{15}\text{N}_4\text{O}_4$ $[\text{M}+\text{H}]^+$; calculated 255.1093, found 255.1088.

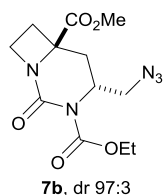
2-Ethyl 4a-methyl (3*R,4*aR**)-3-(azidomethyl)-1-oxo-octahydropyrrolo[1,2-c]pyrimidine-2,4a-dicarboxylate **82a****



82a, dr >99:1

General procedures **H** and **I** were followed using amino ester **63a** (1.1 g, 6.7 mmol). Flash chromatography on cyanosilica eluting with a gradient of 0-100% EtOAc in pentane gave the *title compound* **82a** (1.17 g, 3.60 mmol, 54%) as a colourless oil. R_f 0.11 (1:1 pentane–EtOAc). $^1\text{H NMR}$ (500 MHz, CDCl_3): δ 4.34-4.20 (3H, m, CH_2CH_3 and 3-H), 3.75-3.67 (5H, includes 2H, m, 7-H and at δ 3.72: 3H, s, CO_2CH_3), 3.65 (1H, dd, J 12.3, 5.6, $\text{CH}_\text{A}\text{H}_\text{B}\text{N}_3$), 3.50 (1H, dd, J 12.3, 2.9, $\text{CH}_\text{A}\text{H}_\text{B}\text{N}_3$), 2.89 (1H, dd, J 13.2, 8.5, 4- H_A), 2.37-2.30 (1H, m, 5- H_A), 2.06-1.92 (3H, m, 5- H_B and 6-H), 1.83 (1H, dd, J 13.2, 9.7, 4- H_B), 1.31 (3H, t, J 7.1, CH_2CH_3). $^{13}\text{C NMR}$ (125 MHz, CDCl_3): δ 173.1 (CO_2CH_3), 154.3 (CO), 150.4 (CO), 65.8 (4a-C), 63.1 (OCH_2CH_3), 54.5 (CH_2N_3), 53.1 (CO_2CH_3), 52.5 (3-C), 46.7 (7-C), 38.1 (5-C), 37.6 (4-C), 22.8 (6-C), 14.5 (OCH_2CH_3). $\text{IR } \nu_{\text{max}}(\text{film})/\text{cm}^{-1}$ 3597, 3507, 2981, 2106 (N_3), 1708 (CO), 1420, 1296, 1018. HRMS (ESI): $\text{C}_{13}\text{H}_{20}\text{N}_5\text{O}_5$ [$\text{M}+\text{H}$] $^+$; calculated 326.1459, found 326.1462.

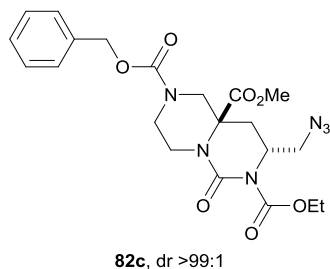
3-Ethyl 6-methyl (4*R,6*R**)-4-(azidomethyl)-2-oxo-1,3-diazabicyclo[4.2.0]octane-3,6-dicarboxylate **82b****



7b, dr 97:3

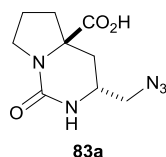
General procedures **H** and **I** were followed using amino ester **63b** (150 mg, 0.970 mmol, 1.00 eq.). Flash chromatography eluting with a gradient of 0-100% EtOAc in pentane gave the *title compound* **82b** (98 mg, 0.31 mmol, 32%, 97:3 mixture of diastereomers) as a pale yellow oil. R_f 0.17 (1:1 pentane–EtOAc). $^1\text{H NMR}$ (500 MHz, CDCl_3): δ 4.32-4.19 (3H, m, CH_2CH_3 and 4-H), 4.16 (1H, td, J 9.4, 6.8, 8- H_A), 4.05 (1H, td, J 9.4, 5.7, 8- H_B), 3.82-3.76 (4H, m, includes 1H, m, $\text{CH}_\text{A}\text{H}_\text{B}\text{N}_3$ and at δ 3.80: 3H, s, CO_2CH_3), 3.53 (1H, dd, J 12.4, 2.5, $\text{CH}_\text{A}\text{H}_\text{B}\text{N}_3$), 2.75-2.68 (1H, m, 7- H_A), 2.63 (1H, dd, J 13.6, 6.5, 5- H_A), 2.42-2.34 (1H, m, 7- H_B), 2.25 (1H, dd, J 13.6, 11.7, 5- H_B), 1.31 (3H, t, J 7.1, CH_2CH_3). $^{13}\text{C NMR}$ (125 MHz, CDCl_3): δ 171.4 (CO_2CH_3), 153.8 (CO), 153.3 (CO), 68.5 (6-C), 63.2 (OCH_2CH_3), 55.1 (4-C), 54.0 (CH_2N_3), 53.2 (CO_2CH_3), 47.2 (8-C), 35.9 (5-C), 28.8 (7-C), 14.4 (OCH_2CH_3). $\text{IR } \nu_{\text{max}}(\text{film})/\text{cm}^{-1}$ 2978, 2108 (N_3), 1712 (CO), 1390, 1372, 1289, 1245, 1033. HRMS (ESI): $\text{C}_{12}\text{H}_{18}\text{N}_5\text{O}_5$ [$\text{M}+\text{H}$] $^+$; calculated 312.1303, found 312.1307.

2-Benzyl 7-ethyl 9a-methyl (8*R,9*aS**)-8-(azidomethyl)-6-oxo-octahydro-1*H*-pyrimido[1,6-*a*]piperazine-2,7,9*a*-tricarboxylate **82c****



General procedures **H** and **I** were followed using amino ester **63c** (150 mg, 0.470 mmol, 1.00 eq.). Flash chromatography eluting with a gradient of 0-100% EtOAc in pentane gave the *title compound* **82c** (98 mg, 0.21 mmol, 44%) as a pale yellow oil. R_f 0.15 (1:1 pentane–EtOAc). $^1\text{H NMR}$ (500 MHz, d^6 -DMSO, 348 K): δ 7.40-7.30 (5H, m, Cbz Ar-H), 5.11 (2H, s, CH_2Ph), 4.33-4.26 (1H, m, 8-H), 4.22 (1H, d, J 13.8, 1- H_A), 4.17 (2H, q, J 7.1, CH_2CH_3), 3.91-3.79 (2H, m, $\text{NCH}_A\text{H}_B\text{CH}_2\text{N}$ and $\text{NCH}_A\text{H}_B\text{CH}_2\text{N}$), 3.62-3.57 (4H, m, includes 1H, m, $\text{CH}_A\text{H}_B\text{N}_3$ and at δ 3.59: 3H, s, CO_2CH_3), 3.49 (1H, dd, J 12.7, 5.5, $\text{CH}_A\text{H}_B\text{N}_3$), 3.35 (1H, d, J 13.8, 1- H_B), 3.35 (1H, d, J 13.9, $\text{NCH}_A\text{H}_B\text{CH}_2\text{N}$) 3.33-3.25 (1H, m, $\text{NCH}_A\text{H}_B\text{CH}_2\text{N}$), 2.57 (1H, dd, J 14.1, 8.5, 9- H_A), 1.96 (1H, dd, J 14.1, 6.7, 9- H_B), 1.22 (3H, t, J 7.1, CH_2CH_3). $^{13}\text{C NMR}$ (125 MHz, d^6 -DMSO, 348 K): δ 171.1 (CO_2CH_3), 154.0 (CO), 153.0 (CO), 151.1 (CO), 136.3 (Ar- C_q), 128.0 (Ar-C), 127.5 (Ar-C), 127.1 (Ar-C), 66.2 (CH_2Ph), 61.9 (OCH_2CH_3), 60.9 (9*a*-C), 53.0 (CH_2N_3), 52.4 (CO_2CH_3), 50.1 (8-C), 48.0 (1-C), 42.4 ($\text{NCH}_2\text{CH}_2\text{N}$), 38.6 ($\text{NCH}_2\text{CH}_2\text{N}$), 33.5 (9-C), 13.6 (OCH_2CH_3). **IR** ν_{max} (film)/ cm^{-1} 2106 (N_3), 1740 (CO), 1705 (CO), 1416, 1290, 1226, 1145, 769. **HRMS** (ESI): $\text{C}_{21}\text{H}_{27}\text{N}_6\text{O}_7$ [$\text{M}+\text{H}$] $^+$; calculated 475.1936, found 475.1950.

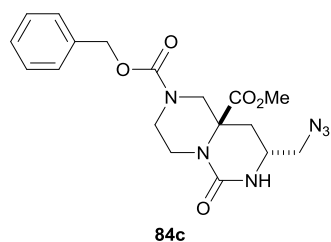
(3*R,4*aR**)-3-(Azidomethyl)-1-oxo-octahydropyrrolo[1,2-*c*]pyrimidine-4*a*-carboxylic acid **83a****



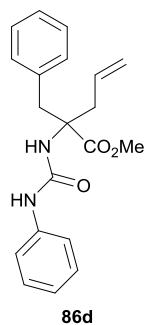
NaOH (14 mg, 0.35 mmol, 2.2 eq.) was added to a solution of urea **82a** (50 mg, 0.15 mmol, 1.0 eq.) in MeOH (0.3 mL) and the reaction mixture was stirred for 2 h by which point a colourless precipitate had formed. The reaction mixture was diluted with MeOH (10 mL), then Amberlite IR-120 (hydrogen form, 94 mg) was added at 0 °C. The reaction mixture was stirred for 0.5 h, then filtered through celite and concentrated *in vacuo*. The resulting residue was triturated with CHCl_3 to give the *title compound* **83a** (37 mg, 0.15 mmol, 99%) as a colourless solid. $^1\text{H NMR}$ (500 MHz, d^6 -DMSO, 343 K, CO_2H not observed): δ 6.13 (1H, s, NH), 3.52-3.41 (2H, m, $\text{CH}_A\text{H}_B\text{N}_3$, 7- H_A), 3.40-3.29 (3H, m, $\text{CH}_A\text{H}_B\text{N}_3$, 3-H, 7- H_B), 2.46-2.40 (1H, m, 4- H_A), 2.34-2.28 (1H, m, 5- H_A), 1.89-1.76 (2H, m, 5- H_B and 6- H_A), 1.75-1.63 (1H, m, 6- H_B), 1.46 (1H,

app. t, J 12.2, 4- H_B). **^{13}C NMR** (125 MHz, d^6 -DMSO): δ 175.1 (CO₂H), 153.8 (1-C), 65.6 (4a-C), 53.5 (CH₂N₃), 48.5 (3-C), 44.9 (7-C), 37.4 (5-C), 33.6 (4-C), 21.1 (6-C). **IR** ν_{max} (film)/cm⁻¹ 3265, 2105 (N₃), 1685 (CO), 1530, 1453, 1308, 1233, 1078. **HRMS** (ESI): C₉H₁₄N₅O₃ [M+H]⁺; calculated 240.1091, found 240.1091. **X-Ray Crystallography**: CCDC 1008923 contains the supplementary crystallographic data for this compound. Crystals were grown by slow diffusion of Et₂O into the sample dissolved in the minimum amount of CHCl₃.

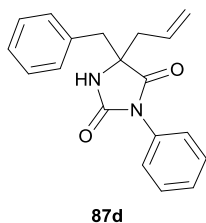
2-Benzyl 9a-methyl (8*R,9a*S**)-8-(azidomethyl)-6-oxo-octahydro-1H-pyrimido[1,6 a]piperazine-2,9a-dicarboxylate **84c****



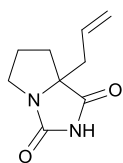
NaOMe (25 wt% in MeOH, 18 μ L, 80 μ mol, 1.0 eq.) was added to a stirred solution of urea **82c** (37 mg, 80 μ mol, 1.0 eq.) in MeOH (0.8 mL). The reaction mixture was stirred at rt for 0.5 h, then concentrated *in vacuo*. The residue was redissolved in MeOH (10 mL) and Amberlite IR-120 (hydrogen form, 50 mg) was added. After stirring for 1 h the reaction mixture was filtered and concentrated to give the *title compound* **84c** (28 mg, 70 μ mol, 88%) as a pale yellow oil. R_f 0.16 (4:1 pentane–EtOAc). **1H NMR** (500 MHz, d^6 -DMSO, 319 K): δ 7.42-7.28 (5H, m, Cbz Ar-H), 6.68 (1H, s, NH), 5.11 (1H, d, J 12.7, CH_AH_BPh), 5.06 (1H, d, J 12.7, CH_AH_BPh), 4.50 (1H, d, J 13.2, 1- H_A), 4.04 (1H, d, J 12.1, $NCH_AH_BCH_2N$), 3.96 (1H, d, J 13.1, $NCH_AH_BCH_2N$), 3.60 (3H, s, CO₂CH₃), 3.53-3.45 (1H, m, $CH_AH_BN_3$), 3.33-3.24 (2H, m, 8-H and $CH_AH_BN_3$), 3.01-2.84 (2H, m, 1- H_B and $NCH_AH_BCH_2N$), 2.83-2.73 (1H, m, $NCH_AH_BCH_2N$), 2.14 (1H, d, J 12.7, 9- H_A), 1.78 (1H, app. t, J 12.7, 9- H_B). **^{13}C NMR** (125 MHz, d^6 -DMSO, 319 K): δ 171.5 (CO₂CH₃), 154.9 (CO), 153.8 (CO), 136.5 (Ar-C_q), 128.2 (Ar-C), 127.7 (Ar-C), 127.3 (Ar-C), 66.3 (CH₂Ph), 61.3 (9a-C), 53.2 (CH₂N₃), 52.5 (CO₂CH₃), 50.2 (1-C), 46.6 (8-C), 42.8 (NCH_2CH_2N), 39.3 (NCH_2CH_2N), 32.2 (9-C). **IR** ν_{max} (film)/cm⁻¹ 2107 (N₃), 1738 (CO), 1704 (CO), 1664 (CO), 1432, 1284, 1234, 1122. **HRMS** (ESI): C₁₈H₂₃N₆O₅ [M+H]⁺; calculated 403.1724, found 403.1728. **X-Ray Crystallography**: CCDC 1008924 contains the supplementary crystallographic data for this compound. Crystals were grown by slow diffusion of Et₂O into the sample dissolved in the minimum amount of CHCl₃.

Methyl 2-benzyl-2-[(phenylcarbamoyl)amino]pent-4-enoate 86d

Phenyl isocyanate (180 μL , 1.61 mmol, 1.05 eq.) was added to a stirred solution of amino ester **63d** (337 mg, 1.54 mmol, 1.0 eq.) in PhMe (20 mL). Flash chromatography eluting with pentane–EtOAc (4:1) gave the *title compound* **86d** (271 mg, 0.80 mmol, 52%) as a colourless solid. R_f 0.46 (4:1 pentane–EtOAc). $^1\text{H NMR}$ (500 MHz, CDCl_3): δ 7.32–7.18 (7H, m, Ar-H), 7.13–7.04 (3H, m, Ar-H), 6.23 (1H, br. s., NH), 5.75–5.61 (1H, m, $\text{CH}=\text{CH}_2$), 5.5 (1H, br. s., NH), 5.17–5.03 (2H, m, $\text{CH}=\text{CH}_2$), 3.84–3.75 (4H, m, includes 1H, m, $\text{CH}_\text{A}\text{H}_\text{B}\text{Ph}$ and at δ 3.78: 3H, s, CO_2CH_3), 3.42 (1H, dd, J 13.9, 7.1, $\text{CH}_\text{A}\text{H}_\text{B}\text{CH}=\text{CH}_2$), 3.18 (1H, d, J 13.5, $\text{CH}_\text{A}\text{H}_\text{B}\text{Ph}$), 2.65 (1H, dd, J 13.9, 7.6, $\text{CH}_\text{A}\text{H}_\text{B}\text{CH}=\text{CH}_2$). $^{13}\text{C NMR}$ (125 MHz, CDCl_3): δ 173.8 (CO_2CH_3), 154.3 (CO), 138.6 (Ar- C_q), 136.6 (Ar- C_q), 132.7 ($\text{CH}=\text{CH}_2$), 130.0 (Ar-C), 129.4 (Ar-C), 128.4 (Ar-C), 127.0 (Ar-C), 124.0 (Ar-C), 121.1 (Ar-C), 119.1 ($\text{CH}=\text{CH}_2$), 65.8 (C_q), 52.7 (CO_2CH_3), 41.1 (CH_2Ph), 40.3 ($\text{CH}_2\text{CH}=\text{CH}_2$). $\text{IR } \nu_{\text{max}}(\text{film})/\text{cm}^{-1}$ 3355, 3030, 1742 (CO), 1651 (CO), 1599, 1549, 1497, 1441. HRMS (ESI): $\text{C}_{20}\text{H}_{22}\text{N}_2\text{NaO}_3$ [$\text{M}+\text{Na}$] $^+$; calculated 361.1523, found 361.1525.

5-Benzyl-3-phenyl-5-(prop-2-en-1-yl)imidazolidine-2,4-dione 87d

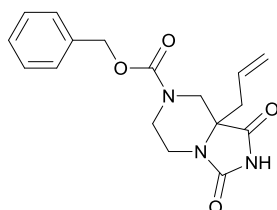
To a solution of urea **86d** (47 mg, 0.14 mmol, 1.0 eq.) in PhMe (1.5 mL) was added NaO^tBu (14 mg, 0.14 mmol, 1.0 eq.) and the reaction mixture was heated at 100 $^\circ\text{C}$ for 15 h. The reaction mixture was cooled to rt then concentrated *in vacuo*. Flash chromatography eluting with 0–100% EtOAc in pentane gave the *title compound* **87d** (36 mg, 0.12 mmol, 85%) as a colourless oil. $^1\text{H NMR}$ (500 MHz, CDCl_3): δ 7.41–7.36 (2H, m, Ar-H), 7.35–7.29 (4H, m, Ar-H), 7.24–7.18 (2H, m, Ar-H), 6.99–6.94 (2H, m, Ar-H), 6.30 (1H, s, NH), 5.94–5.84 (1H, m, $\text{CH}=\text{CH}_2$), 5.31–5.21 (2H, m, $\text{CH}=\text{CH}_2$), 3.21 (1H, d, J 13.6, $\text{CH}_\text{A}\text{H}_\text{B}\text{Ph}$), 2.96 (1H, d, J 13.6, $\text{CH}_\text{A}\text{H}_\text{B}\text{Ph}$), 2.75 (1H, dd, J 13.9, 7.7, $\text{CH}_\text{A}\text{H}_\text{B}\text{CH}=\text{CH}_2$), 2.56 (1H, dd, J 13.9, 7.1, $\text{CH}_\text{A}\text{H}_\text{B}\text{CH}=\text{CH}_2$). $^{13}\text{C NMR}$ (125 MHz, CDCl_3): δ 174.2 (4-C), 155.9 (2-C), 134.1 (Ar- C_q), 131.4 (Ar- C_q), 130.4 (2 \times C; $\text{CH}=\text{CH}_2$ and Ar-C); 129.2 (Ar-C), 128.7 (Ar-C), 128.5 (Ar-C), 127.7 (Ar-C), 126.5 (Ar-C), 121.4 ($\text{CH}=\text{CH}_2$), 66.0 (5-C), 42.9 (CH_2Ph), 41.1 ($\text{CH}_2\text{CH}=\text{CH}_2$). $\text{IR } \nu_{\text{max}}(\text{film})/\text{cm}^{-1}$ 3290, 1778, 1715 (CO), 1502, 1414, 1123, 919, 703. HRMS (ESI): $\text{C}_{19}\text{H}_{19}\text{N}_2\text{O}_2$ [$\text{M}+\text{H}$] $^+$; calculated 307.1441, found 307.142

7a-(Prop-2-en-1-yl)-hexahydro-1H-pyrrolo[1,2-c]imidazolidine-1,3-dione**88a**

88a

General procedures **H** and **J** were followed using amino ester **63a** (200 mg, 1.18 mmol). Purification by SCX, eluting with MeOH, gave the *title compound* **88a** (200 mg, 1.11 mmol, 94%) as a colourless oil.

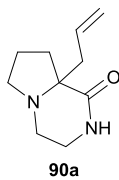
¹H NMR (500 MHz, CDCl₃): δ 8.14 (1H, br. s, NH), 5.81-5.71 (1H, m, CH=CH₂), 5.22-5.15 (2H, m, CH=CH₂), 3.83-3.75 (1H, m, 5-H_A), 3.21-3.14 (1H, m, 5-H_B), 2.58 (1H, dd, *J* 14.0, 7.7, CH_AH_BCH=CH₂), 2.41 (1H, dd, *J* 14.0, 6.8, CH_AH_BCH=CH₂), 2.17-2.03 (2H, m, 6-H), 2.02-1.89 (2H, m, 7-H). **¹³C NMR** (125 MHz, CDCl₃): δ 176.3 (1-C), 159.5 (3-C), 131.0 (CH=CH₂), 120.6 (CH=CH₂), 73.8 (7a-C), 44.9 (5-C), 39.6 (CH₂CH=CH₂), 32.2 (7-C), 26.3 (6-C). **IR** ν_{\max} (film)/cm⁻¹ 3210, 3074, 2978, 1771 (CO), 1715 (CO), 1391, 1332, 1208. **HRMS** (EI): C₉H₁₂N₂O₂ [M]⁺; calculated 180.0899, found 180.0897.

Benzyl 1,3-dioxo-8a-(prop-2-en-1-yl)-octahydroimidazolidino[1,5-a]piperazine-7-carboxylate 88c

88c

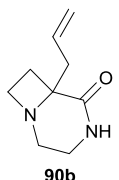
General procedures **H** and **J** were followed using amino ester **63c** (141 mg, 0.440 mmol). Purification by SCX, eluting with MeOH, gave the *title compound* **88c** (139 mg, 0.420 mmol, 96%). **¹H NMR** (500 MHz, *d*⁶-DMSO, 319 K):

δ 10.98 (1H, s, NH), 7.42-7.28 (5H, m, Cbz Ar-H), 5.57-5.44 (1H, m, CH=CH₂), 5.18-5.03 (4H, m, CH=CH₂ and CH₂Ph), 4.02-3.91 (1H, m, NCH_AH_BCH₂N), 3.93 (1H, d, *J* 13.1, 8-H_A), 3.83 (1H, dd, *J* 13.2, 3.0, NCH_AH_BCH₂N), 3.19-3.01 (1H, m, 8-H_B), 2.98-2.92 (2H, m, NCH_AH_BCH₂N and NCH_AH_BCH₂N), 2.56 (1H, dd, *J* 14.3, 7.3, CH_AH_BCH=CH₂), 2.34 (1H, dd, *J* 14.3, 6.9, CH_AH_BCH=CH₂). **¹³C NMR** (125 MHz, *d*⁶-DMSO, 319 K, one C_q peak not observed): δ 174.1 (1-C), 154.4 (CO), 136.4 (Ar-C_q), 130.4 (CH=CH₂), 128.2 (Ar-C), 127.8 (Ar-C), 127.5 (Ar-C), 119.7 (CH=CH₂), 66.7 (CH₂Ph), 62.8 (8a-C), 47.5 (8-C), 42.8 (NCH₂CH₂N), 35.8 (NCH₂CH₂N), 34.0 (CH₂CH=CH₂). **IR** ν_{\max} (film)/cm⁻¹ 3199, 1772 (CO), 1708 (CO), 1455, 1428, 1353, 1267, 1244. **HRMS** (ESI): C₁₇H₂₀N₃O₄ [M+H]⁺; calculated 330.1448, found 330.1449.

8a-(Prop-2-en-1-yl)-octahydropyrrolo[1,2-a]piperazin-1-one 90a

90a

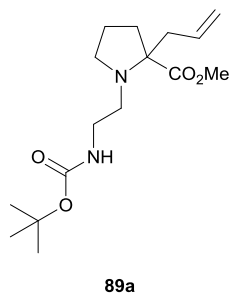
General procedures **K** and **L** were followed using amino ester **63a** (400 mg, 2.36 mmol). The residue was purified by SCX, eluting first with MeOH then sat. NH_3/MeOH , to give the *title compound 90a* (270 mg, 1.50 mmol, 62%) as a brown oil. **$^1\text{H NMR}$** (500 MHz, CDCl_3): δ 5.95-5.84 (1H, m, $\text{CH}=\text{CH}_2$), 5.76 (1H, br. s, NH), 5.16-5.07 (2H, m, $\text{CH}=\text{CH}_2$), 3.72-3.62 (1H, m, 3- H_A), 3.32-3.18 (2H, m, 3- H_B and 4- H_A), 3.09-3.02 (1H, m, 6- H_A), 2.96-2.82 (2H, m, 4- H_B and 6- H_B), 2.62 (1H, dd, J 13.9, 6.6, $\text{CH}_\text{A}\text{H}_\text{B}\text{CH}=\text{CH}_2$), 2.43 (1H, dd, J 13.9, 7.9, $\text{CH}_\text{A}\text{H}_\text{B}\text{CH}=\text{CH}_2$), 2.20-2.12 (1H, m, 8- H_A), 2.01-1.93 (1H, m, 8- H_B), 1.83-1.69 (2H, m, 7-H). **$^{13}\text{C NMR}$** (125 MHz, CDCl_3): δ 176.3 (1-C), 134.4 ($\text{CH}=\text{CH}_2$), 117.8 ($\text{CH}=\text{CH}_2$), 68.4 (8a-C), 51.9 (6-C), 43.4 (4-C), 42.6 ($\text{CH}_2\text{CH}=\text{CH}_2$), 38.5 (3-C), 34.9 (8-C), 22.8 (7-C). **IR** $\nu_{\text{max}}(\text{film})/\text{cm}^{-1}$ 3218, 3074, 2944, 1655 (CO), 1487, 1447, 915, 753. **HRMS** (ESI): $\text{C}_{10}\text{H}_{17}\text{N}_2\text{O}$ [$\text{M}+\text{H}$] $^+$; calculated 181.1341, found 181.1335.

6-(Prop-2-en-1-yl)-1,4-diazabicyclo[4.2.0]octan-5-one 90b

90b

General procedures **K** and **L** were followed using the TFA salt of the amino ester **63b** (404 mg, 1.50 mmol). Flash chromatography on eluting with a gradient of 0-100% EtOAc in pentane containing 1% Et_3N gave the *title compound 90b* (54 mg, 0.32 mmol, 22%) as a pale yellow oil. **R_f** 0.19 (1:1 petrol-EtOAc). **$^1\text{H NMR}$** (500 MHz, CDCl_3): δ 6.97 (1H, br. s, NH), 5.83-5.72 (1H, m, $\text{CH}=\text{CH}_2$), 5.29-5.19 (2H, m, $\text{CH}=\text{CH}_2$), 4.39-4.32 (1H, m, 8- H_A), 4.28-4.20 (1H, m, 8- H_B), 3.47-3.34 (2H, m, 3-H), 2.94-2.86 (1H, m, 2- H_A), 2.77-2.70 (1H, m, 2- H_B), 2.52 (1H, dd, J 14.0, 7.2, $\text{CH}_\text{A}\text{H}_\text{B}\text{CH}=\text{CH}_2$), 2.38 (1H, dd, J 14.0, 7.5, $\text{CH}_\text{A}\text{H}_\text{B}\text{CH}=\text{CH}_2$), 2.29-2.19 (2H, m, 7-H). **$^{13}\text{C NMR}$** (125 MHz, CDCl_3): δ 178.4 (5-C), 131.1 ($\text{CH}=\text{CH}_2$), 121.0 ($\text{CH}=\text{CH}_2$), 65.0 (8-C), 61.8 (6-C), 41.6 (2-C), 40.1 (2 \times C; 3-C and $\text{CH}_2\text{CH}=\text{CH}_2$), 32.1 (7-C). **IR** $\nu_{\text{max}}(\text{film})/\text{cm}^{-1}$ 3325 (NH), 2982, 1763 (CO), 1719, 1560, 1183, 1024, 927. **HRMS** (EI): $\text{C}_9\text{H}_{14}\text{N}_2\text{O}$ [M] $^+$; calculated 166.1106, found 166.1133.

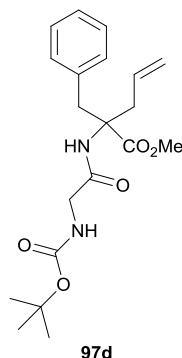
Methyl 1-(2-[[[(tert-butoxy)carbonyl]amino]ethyl]-2-(prop-2-en-1-yl)pyrrolidine-2-carboxylate **89a**



3-Boc-1,2,3-oxathiazolidine 2,2-dioxide* (1.19 g, 5.32 mmol, 1.20 eq.) was added to a stirred solution of the amino ester **63a** (750 mg, 4.43 mmol, 1.00 eq.) and K₂CO₃ (674 mg, 4.87 mmol, 1.10 eq.) in DMF (22 mL). The reaction mixture was stirred for 15 h. 1 N HCl (25 mL) was added and the reaction mixture was stirred for 1 h. The reaction mixture was neutralised with solid NaHCO₃. EtOAc (75 mL) was added and the phases were separated. The organic phase was washed with brine (25 mL), dried over MgSO₄, filtered, and concentrated *in vacuo*. Purification by SCX, eluting first with MeOH then NH₃/MeOH, gave the *title compound* **89a** (566 mg, 1.81 mmol, 37%) as an orange oil. **R_f** 0.48 (1:4:0.05 petrol–EtOAc–Et₃N). **¹H NMR** (500 MHz, CDCl₃): δ 5.85-5.72 (1H, m, CH=CH₂), 5.16-5.03 (2H, m, CH=CH₂), 4.98 (1H, br. s, NH), 3.67 (3H, s, CO₂CH₃), 3.31-3.20 (1H, m, NHCH_AH_B), 3.11-3.02 (2H, m, NHCH_AH_B and 5-H_A), 2.82-2.73 (1H, m, NHCH₂CH_AH_B), 2.68-2.61 (1H, m, 5-H_B), 2.58 (1H, dd, *J* 14.2, 6.9, CH_AH_BCH=CH₂), 2.51-2.43 (1H, m, NHCH₂CH_AH_B), 2.31 (1H, dd, *J* 14.2, 7.3, CH_AH_BCH=CH₂), 2.15-2.07 (1H, m, 3-H_A), 1.90-1.71 (3H, m, 3-H_B and 4-H), 1.44 (9H, s, C(CH₃)₃). **¹³C NMR** (125 MHz, CDCl₃): δ 175.0 (CO₂CH₃), 156.2 (NH(CO)O), 134.2 (CH=CH₂), 118.3 (CH=CH₂), 79.1 (C_q(CH₃)₃), 70.3 (2-C), 51.4 (5-C), 51.1 (CO₂CH₃), 48.6 (NCH₂CH₂), 39.1 (2 peaks, CH₂CH=CH₂ and NHCH₂), 34.1 (3-C), 28.6 (C(CH₃)₃), 22.1 (4-C). **IR** ν_{max} (film)/cm⁻¹ 3076, 2821, 1712 (CO), 1502, 1365, 1245, 1165, 754. **HRMS** (ESI): C₁₆H₂₉N₂O₄ [M+H]⁺; calculated 313.2122, found 313.2126.

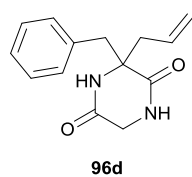
* Purchased from Sigma Aldrich.

Methyl 2-benzyl-2-(2-[[*tert*-butoxy]carbonyl]amino)acetamido)pent-4-enoate **97d**



Amino ester **63d** (535 mg, 2.44 mmol, 1.0 eq.) was added to a stirred solution of *N*-Boc-glycine (855 mg, 4.88 mmol, 2.0 eq.), EDCI (936 mg, 4.88 mmol, 2.0 eq.) and Et₃N (0.85 mL, 6.10 mmol, 2.50 eq.) in CH₂Cl₂ (20 mL). The reaction mixture was stirred for 15 h. Additional *N*-Boc-glycine (855 mg, 4.88 mmol, 2.00 eq.) and EDCI (936 mg, 4.88 mmol, 2.00 eq.) were added and the reaction mixture was stirred for 3 h, then concentrated *in vacuo*. The residue was diluted with EtOAc (50 mL) and washed with H₂O (50 mL) and brine (50 mL). The organic layer was dried over MgSO₄, filtered, then concentrated *in vacuo*. Flash chromatography eluting with pentane–EtOAc–Et₃N (80:20:1) gave the *title compound* **97d** (790 mg, 2.09 mmol, 86%) as a colourless oil. *R*_f 0.22 (4:1 petrol–EtOAc). ¹H NMR (500 MHz, CDCl₃): δ 7.28–7.20 (3H, m, Ar-H), 7.01 (2H, dd, *J* 7.9, 1.4, Ar-H), 6.66 (1H, br. s, NH), 5.65–5.55 (1H, m, CH=CH₂), 5.13–5.06 (2H, m, CH=CH₂), 5.03 (1H, br. s, NH), 3.78 (3H, s, CO₂CH₃), 3.76–3.72 (3H, m, includes 2H, m, CH₂NHBoc and at δ 3.74: 1H, d, *J* 13.6, CH_AH_BPh), 3.38 (1H, dd, *J* 13.9, 7.1, CH_AH_BCH=CH₂), 3.14 (1H, d, *J* 13.6, CH_AH_BPh), 2.64 (1H, dd, *J* 13.9, 7.7, CH_AH_BCH=CH₂), 1.44 (9H, s, C(CH₃)₃). ¹³C NMR (125 MHz, CDCl₃): δ 172.9 (CO₂CH₃), 168.8 (NH(CO)CH₂), 155.9 (NH(CO)O), 136.1 (Ar-C_q), 132.1 (CH=CH₂), 129.7 (Ar-C), 128.4 (Ar-C), 127.1 (Ar-C), 119.3 (CH=CH₂), 80.1 (C_q(CH₃)₃), 66.0 (C_q), 52.7 (CO₂CH₃), 44.9 (CH₂NHBoc), 40.5 (CH₂CH=CH₂), 39.6 (CH₂Ph), 28.3 (C(CH₃)₃). IR *v*_{max}(film)/cm⁻¹ 3385, 2978, 1740 (CO), 1716 (CO), 1679, 1514, 1448, 1367. HRMS (ESI): C₂₀H₂₈N₂NaO₅ [M+Na]⁺; calculated 399.1890, found 399.1895.

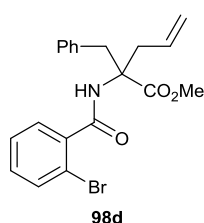
3-Benzyl-3-(prop-2-en-1-yl)piperazine-2,5-dione **96d**



General procedure **L** was followed using amide **97d** (50 mg, 0.13 mmol, 1.0 eq.). Flash chromatography eluting with a gradient of 0–10% MeOH in CH₂Cl₂ gave the *title compound* **96d** (30 mg, 0.12 mmol, 93%) as a colourless solid. *R*_f 0.33 (5:95 CH₂Cl₂–MeOH). ¹H NMR (500 MHz, CD₃OD, 2 × NH not observed): δ 7.34–7.30 (3H, m, Ar-H), 7.27–7.22 (2H, m, Ar-H), 5.85–5.75 (1H, m, CH=CH₂), 5.28–5.18 (2H, m, CH=CH₂), 3.46 (1H, d, *J* 17.9, 6-H_A), 3.27 (1H, d, *J* 13.3, CH_AH_BPh), 2.95 (1H, dd, *J* 13.8, 6.6, CH_AH_BCH=CH₂), 2.80 (1H, d, *J* 13.3,

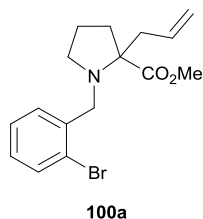
CH_AH_BPh), 2.62 (1H, d, *J* 17.9, 6-H_B), 2.43 (1H, dd, *J* 13.8, 7.8, CH_AH_BCH=CH₂). **¹³C NMR** (125 MHz, CD₃OD): δ 170.8 (CO), 168.8 (CO), 136.5 (CH=CH₂), 133.1 (Ar-C_q), 131.8 (Ar-C), 129.4 (Ar-C), 128.4 (Ar-C), 120.4 (CH=CH₂), 65.4 (3-C), 47.4 (6-C), 44.9 (CH₂Ph), 44.6 (CH₂CH=CH₂). **IR** ν_{max}(film)/cm⁻¹ 3192, 3071, 2917, 2332, 1673 (CO), 1451, 1316, 1108. **HRMS** (ESI): C₁₄H₁₆N₂NaO₂ [M+Na]⁺; calculated 267.1104, found 267.1092.

Methyl 2-benzyl-2-[(2-bromophenyl)formamido]pent-4-enoate **98d**



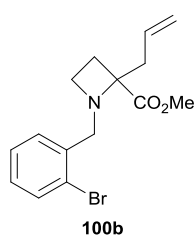
Oxalyl chloride (51 μL, 0.60 mmol, 1.2 eq.) was added to a stirred solution of 2-bromobenzoic acid (100 mg, 0.500 mmol, 1.00 eq.) and DMF (4 drops) in CH₂Cl₂ (3.3 mL) (**CAUTION: gas evolution**). The reaction mixture was stirred at rt for 3 h then concentrated *in vacuo* to give the crude acid chloride. The residue was dissolved in CH₂Cl₂ (3.3 mL) and amino ester **63d** (110 mg, 0.500 mmol, 1.00 eq.) and Et₃N (77 μL, 0.55 mmol, 1.1 eq.) were added. The reaction mixture was stirred for 15 h then the reaction mixture was quenched with sat. aq. NaHCO₃ solution (50 mL). The phases were separated and the aqueous phase was extracted with CH₂Cl₂ (2 × 50 mL). The combined organic phase was washed with brine (50 mL), dried over MgSO₄ and concentrated *in vacuo*. The residue was filtered through a pad of silica with EtOAc to give the *title compound* **98d** (200 mg, 0.50 mmol, 99%) as a colourless oil. **¹H NMR** (500 MHz, CDCl₃): δ 7.49 (1H, dd, *J* 7.9, 1.2, Ar-H), 7.27-7.11 (6H, m, Ar-H), 7.10-7.05 (2H, m, Ar-H), 6.67 (1H, s, NH), 5.75-5.64 (1H, m, CH=CH₂), 5.12 (1H, ddd, *J* 17.0, 2.0, 1.2, CH=CH_AH_B), 5.05 (1H, dd, *J* 10.1, 2.0, CH=CH_AH_B), 3.86 (1H, d, *J* 13.6, CH_AH_BPh), 3.75 (3H, s, CO₂CH₃), 3.53 (1H, dd, *J* 13.9, 7.2, CH_AH_BCH=CH₂), 3.19 (1H, d, *J* 13.6, CH_AH_BPh), 2.65 (1H, dd, *J* 13.9, 7.6, CH_AH_BCH=CH₂). **¹³C NMR** (125 MHz, CDCl₃): δ 173.2 (CO₂CH₃), 166.8 (CONH), 137.9 (Ar-C_q), 136.2 (Ar-C_q), 133.8 (Ar-C), 132.4 (CH=CH₂), 131.4 (Ar-C), 129.9 (Ar-C), 129.4 (Ar-C), 128.5 (Ar-C), 127.5 (Ar-C), 127.2 (Ar-C), 119.8 (Ar-C_q-Br), 119.6 (CH=CH₂), 67.0 (C_q), 52.9 (CO₂CH₃), 40.7 (CH₂Ph), 39.7 (CH₂CH=CH₂). **IR** ν_{max}(film)/cm⁻¹ 3393 (NH), 3029, 2951, 1738 (CO), 1664, 1507, 1230, 748. **HRMS** (ESI): C₂₀H₂₁BrNO₃ [M+H]⁺; calculated 402.0705, found 402.0699.

Methyl 1-[(2-bromophenyl)methyl]-2-(prop-2-en-1-yl)pyrrolidine-2-carboxylate 100a



General procedure **M** was followed using amino ester **63a** (250 mg, 1.48 mmol). The residue was purified by SCX cartridge, eluting first with MeOH then sat. NH_3/MeOH , to give the *title compound* **100a** (392 mg, 1.16 mmol, 78%) as a colourless oil. R_f 0.26 (4:1 pentane–EtOAc). $^1\text{H NMR}$ (300 MHz, CDCl_3): δ 7.52 (1H, dd, J 7.9, 1.1, Ar-H), 7.47 (1H, dd, J 7.6, 1.1, Ar-H), 7.31–7.23 (1H, m, Ar-H), 7.09 (1H, td, J 7.6, 1.6, Ar-H), 5.96–5.78 (1H, $\text{CH}=\text{CH}_2$), 5.14–5.06 (2H, $\text{CH}=\text{CH}_2$), 3.98 (1H, d, J 15.0, $\text{CH}_\text{A}\text{H}_\text{B}\text{Ar}$), 3.76 (3H, s, CO_2CH_3), 3.67 (1H, d, J 15.0, $\text{CH}_\text{A}\text{H}_\text{B}\text{Ar}$), 2.97 (1H, td, J 8.5, 3.5, 5- H_A), 2.77–2.58 (2H, m, 5- H_B and $\text{CH}_\text{A}\text{H}_\text{B}\text{CH}=\text{CH}_2$), 2.46 (1H, dd, J 14.1, 6.6, $\text{CH}_\text{A}\text{H}_\text{B}\text{CH}=\text{CH}_2$), 2.24–2.16 (1H, m, 3- H_A), 1.95–1.82 (2H, m, 3- H_B and 4- H_A), 1.81–1.72 (1H, m, 4- H_B). $^{13}\text{C NMR}$ (125 MHz, CDCl_3): δ 174.9 (CO_2CH_3), 139.1 (Ar- C_q), 134.4 ($\text{CH}=\text{CH}_2$), 132.7 (Ar-C), 130.2 (Ar-C), 128.2 (Ar-C), 127.3 (Ar-C), 124.0 (Ar- C_q -Br), 118.1 ($\text{CH}=\text{CH}_2$), 70.7 (2-C), 53.2 (CH_2Ar), 51.9 (5-C), 51.4 (CO_2CH_3), 39.7 ($\text{CH}_2\text{CH}=\text{CH}_2$), 34.0 (3-C), 22.0 (4-C). **IR** ν_{max} (film)/ cm^{-1} 2949, 1727 (CO), 1439, 1219, 1193, 1171, 1025, 916. **HRMS** (ESI): $\text{C}_{16}\text{H}_{21}^{79}\text{BrNO}_2$ [$\text{M}+\text{H}$] $^+$; calculated 338.0756, found 338.0750.

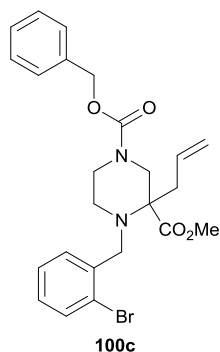
Methyl 1-[(2-bromophenyl)methyl]-2-(prop-2-en-1-yl)azetidine-2-carboxylate 100b



Method 1: General procedure **M** was followed using amino ester **63b** (175 mg, 1.13 mmol). The residue was purified by SCX cartridge, eluting first with MeOH then sat. NH_3/MeOH , to give the *title compound* **100b** (246 mg, 0.759 mmol, 67%) as a colourless oil. **Method 2:** To a stirred solution of the TFA salt of the amino ester **63b** (404 mg, 1.50 mmol, 1.00 eq.) in DMF (7.5 mL) was added 2-bromobenzyl bromide (0.01 M in THF, 0.45 mL, 0.45 mmol, 3.00 eq.) and K_2CO_3 (456 mg, 3.30 mmol, 2.20 eq.) and the reaction mixture was heated at 60 °C for 15 h. The reaction mixture was diluted with H_2O (20 mL) and extracted with EtOAc (2 x 20 mL). The combined organics were washed with brine (20 mL) then dried over MgSO_4 , filtered, and concentrated *in vacuo*. Purification by SCX cartridge, eluting first with MeOH then sat. NH_3/MeOH , gave the *title compound* **100b** (358 mg, 1.10 mmol, 74%) as a colourless oil. $^1\text{H NMR}$

(500 MHz, CDCl₃): δ 7.51 (1H, dd, J 8.0, 1.2, Ar-H), 7.43 (1H, dd, J 7.7, 1.2, Ar-H), 7.28-7.24 (1H, m, Ar-H), 7.08 (1H, td, J 7.7, 1.7, Ar-H), 5.84-5.74 (1H, m, CH=CH₂), 5.17-5.07 (2H, m, CH=CH₂), 3.86-3.76 (5H, m includes 2H, dd, J 14.3, CH₂Ar and at δ 3.77: 3H, s, CO₂CH₃), 3.31-3.25 (1H, m, 4-H_A), 3.25-3.19 (1H, m, 4-H_B), 2.71 (1H, dd, J 13.7, 7.3, CH_AH_BCH=CH₂), 2.65 (1H, dd, J 13.7, 6.9, CH_AH_BCH=CH₂), 2.58-2.51 (1H, m, 3-H_A), 2.15-2.07 (1H, m, 3-H_B). ¹³C NMR (125 MHz, CDCl₃): δ 173.7 (CO₂CH₃), 138.0 (Ar-C_q), 132.9 (Ar-C or CH=CH₂), 132.8 (Ar-C or CH=CH₂), 130.3 (Ar-C), 128.4 (Ar-C), 127.4 (Ar-C), 124.2 (Ar-C_q-Br), 118.6 (CH=CH₂), 72.0 (2-C), 55.6 (CH₂Ar), 51.7 (CO₂CH₃), 50.3 (4-C), 38.9 (CH₂CH=CH₂), 25.9 (3-C). IR ν_{max} (film)/cm⁻¹ 2950, 2843, 1728 (CO), 1440, 1214, 1146, 1025, 751. HRMS (ESI): C₁₅H₁₉⁷⁹BrNO₂ [M+H]⁺; calculated 324.0594, found 324.0598.

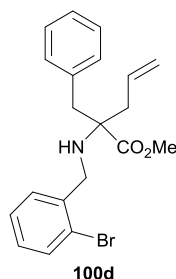
1-Benzyl 3-methyl 4-[(2-bromophenyl)methyl]-3-(prop-2-en-1-yl)piperazine-1,3-dicarboxylate **100c**



To a stirred solution amino ester **63c** (225 mg, 0.71 mmol, 1.00 eq.) in DMF (3.6 mL) was added 2-bromobenzyl bromide (10.4 M in THF, 200 μ L, 2.13 mmol, 3.00 eq.) and K₂CO₃ (108 mg, 0.780 mmol, 1.10 eq.). The reaction mixture was heated at 60 °C for 24 h, then diluted with H₂O (20 mL) and extracted with EtOAc (2 x 20 mL). The combined organics were washed with brine (20 mL) then dried over MgSO₄, filtered, and concentrated *in vacuo*. Purification by SCX cartridge, eluting first with MeOH then sat. NH₃/MeOH, gave the *title compound* **100c** (288 mg, 0.591 mmol, 83%) as an orange oil. ¹H NMR (500 MHz, *d*⁶-DMSO, 319 K): δ 7.61 (1H, d, J 7.0, Ar-H), 7.57 (1H, dd, J 7.9, 0.9, Ar-H), 7.42-7.29 (6H, m, Ar-H), 7.19 (1H, td, J 7.9, 1.5, Ar-H), 5.82-5.71 (1H, m, CH=CH₂), 5.14-5.01 (4H, m, CH=CH₂ and OCH₂Ph), 4.27 (1H, d, J 13.4, 2-H_A), 4.12 (1H, d, J 16.6, NCH_AH_BAr), 3.84 (1H, d, J 12.9, NCH_AH_BCH₂N), 3.79 (1H, d, J 16.6, NCH_AH_BAr), 3.59 (3H, s, CO₂CH₃), 3.09 (1H, d, J 13.4, 2-H_B), 3.05-2.95 (1H, m, NCH_AH_BCH₂N), 2.71 (1H, td, J 11.8, 3.5, NCH_AH_BCH₂N), 2.65-2.53 (2H, m, CH₂CH=CH₂), 2.53-2.46 (1H, m, NCH_AH_BCH₂N). ¹³C NMR (125 MHz, *d*⁶-DMSO, 319 K): δ 172.5 (CO₂CH₃), 154.0 (N(CO)O), 138.1 (Ar-C_q), 136.8 (Ar-C_q), 132.3 (Ar-C or CH=CH₂), 132.2 (Ar-C or CH=CH₂), 129.2 (Ar-C), 128.3 (Ar-C), 128.2 (Ar-C), 127.6 (Ar-C), 127.5 (Ar-C), 127.2 (Ar-C), 122.9 (Ar-C_q-Br), 118.7 (CH=CH₂), 66.0 (OCH₂Ph), 64.5 (3-C), 53.3

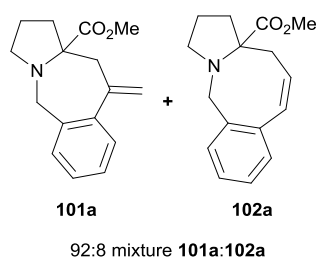
(NCH₂Ar), 51.2 (CO₂CH₃), 49.6 (2-C), 46.6 (NCH₂CH₂N), 43.2 (NCH₂CH₂N), 38.0 (CH₂CH=CH₂). IR ν_{max} (film)/cm⁻¹ 2950, 1732 (CO), 1704, 1456, 1435, 1284, 1228, 1212. HRMS (ESI): C₂₄H₂₈⁷⁹BrN₂O₄ [M+H]⁺; calculated 487.1227, found 487.1233.

Methyl 2-benzyl-2-[(2-bromobenzyl)amino]pent-4-enoate **100d**



General procedure **M** was followed using amino ester **63d** (268 mg, 1.22 mmol) with two changes; the reaction was performed in THF at 45 °C. After heating for 3 days, additional NaBH(OAc)₃ (518 mg, 2.44 mmol, 2.0 eq.) was added and the reaction mixture was stirred for 3 h. Flash chromatography eluting with a gradient of 0-20% EtOAc in hexane gave the *title compound* **100d** (327 mg, 0.842 mmol, 69%) as a colourless oil. *R_f* 0.68 (4:1 petrol–EtOAc). ¹H NMR (500 MHz, CDCl₃): δ 7.53 (1H, dd, *J* 8.0, 1.2, Ar-H), 7.47 (1H, d, *J* 7.5, Ar-H), 7.26 (4H, m, Ar-H), 7.16 (2H, d, *J* 6.9, Ar-H), 7.11 (1H, td, *J* 7.7, 1.6, Ar-H), 6.00-5.88 (1H, m, CH=CH₂), 5.23-5.13 (2H, m, CH=CH₂), 3.89-3.79 (2H, m, NHCH₂Ar), 3.67 (3H, s, CO₂CH₃), 3.09 (1H, d, *J* 13.7, CH_AH_BPh), 3.01 (1H, d, *J* 13.7, CH_AH_BPh), 2.65 (1H, dd, *J* 14.8, 6.1, CH_AH_BCH=CH₂), 2.52 (1H, dd, *J* 14.8, 7.6, CH_AH_BCH=CH₂). ¹³C NMR (125 MHz, CDCl₃, one Ar-C peak not observed): δ 175.3 (CO₂CH₃), 139.5 (Ar-C_q), 136.4 (Ar-C_q), 133.3 (Ar-C), 132.8 (CH=CH₂), 130.3 (Ar-C), 128.7 (Ar-C), 128.3 (Ar-C), 127.7 (Ar-C), 127.0 (Ar-C), 124.0 (Ar-C_q-Br), 118.8 (CH=CH₂), 66.2 (C_q), 51.8 (CO₂CH₃), 47.3 (NHCH₂Ar), 42.3 (CH₂Ph), 38.1 (CH₂CH=CH₂). IR ν_{max} (film)/cm⁻¹ 2949, 1732 (CO), 1465, 1439, 1213, 1197, 1206, 750. HRMS (ESI): C₂₀H₂₃⁷⁹BrNO₂ [M+H]⁺; calculated 388.0907, found 388.0913.

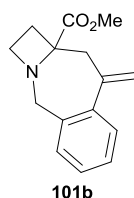
Methyl 9-methylidene-3-azatricyclo[8.4.0.0^{3,7}]tetradeca-1(10),11,13-triene-7-carboxylate **101a** and methyl (9Z)-3-azatricyclo[9.4.0.0^{3,7}]pentadeca-1(11),9,12,14-tetraene-7-carboxylate **102a**



General procedure **N** was followed using amino ester **100a** (105 mg, 0.310 mmol, 1.0 eq.). Flash chromatography eluting with pentane–EtOAc (4:1) gave the *title compound* **101a** (43 mg, 0.17 mmol, 54%, 92:8 mixture of **101a**:**102a**) as a yellow oil. *R_f* 0.21 (4:1 petrol–EtOAc). ¹H NMR (500 MHz, CDCl₃, peaks for **101a**): δ 7.37-7.30 (1H, m, Ar-H),

7.25-7.18 (2H, m, Ar-H), 7.17-7.11 (1H, m, Ar-H), 5.33 (1H, d, J 1.6, C=CH_AH_B), 5.12 (1H, s, C=CH_AH_B), 4.54 (1H, d, J 16.0, 2-H_A), 3.89 (1H, d, J 16.0, 2-H_B), 3.73 (3H, s, CO₂CH₃), 3.13 (1H, d, J 13.6, 8-H_A), 3.05 (1H, td, J 8.4, 2.4, 4-H_A), 2.76 (1H, app. q, J 8.4, 4-H_B), 2.58 (1H, d, J 13.6, 8-H_B), 2.26-2.16 (1H, m, 6-H_A), 2.10-2.00 (1H, m, 6-H_B), 1.95-1.83 (1H, m, 5-H_A), 1.81-1.69 (1H, m, 5-H_B). Characteristic peaks for **102a**: 6.79 (1H, d, J 10.6, 10-H), 5.94-5.87 (1H, m, 9-H), 4.09 (1H, d, J 14.8, 2-H_A), 4.02 (1H, d, J 14.8, 2-H_B), 3.77 (3H, s, CO₂CH₃), 2.74-2.67 (1H, m), 2.46 (1H, dd, J 13.4, 7.5, 8-H_A), 2.37-2.30 (1H, m). **¹³C NMR** (125 MHz, CDCl₃, peaks for **101a** assigned): δ 175.7 (CO₂CH₃), 145.5 (9-C), 141.3 (Ar-C_q), 136.8 (Ar-C_q), 129.3 (Ar-C), 127.5 (Ar-C), 127.4 (Ar-C), 127.2 (Ar-C), 116.9 (C=CH₂), 69.9 (7-C), 52.9 (2-C), 52.0 (CO₂CH₃), 50.7 (4-C), 41.8 (8-C), 36.1 (6-C), 22.3 (5-C). **IR** ν_{\max} (film)/cm⁻¹ 2949, 2902, 1727 (CO), 1433, 1256, 1209, 1157, 1111. **HRMS** (EI): C₁₆H₁₉N₂O [M]⁺; calculated 257.1409, found 257.1416.

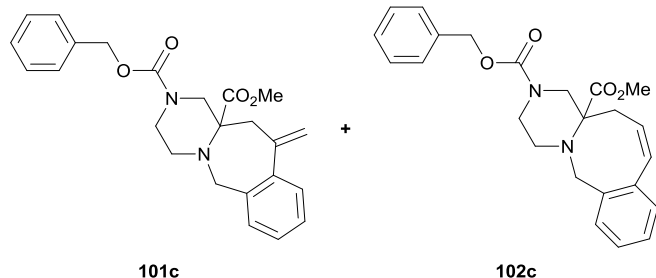
Methyl 8-methylidene-3-azatricyclo[7.4.0.0^{3,6}]trideca-1(9),10,12-triene-6-carboxylate **101b**



101b

General procedure **N** was followed using amino ester **100b** (163 mg, 0.500 mmol). After heating at 125 °C under microwave irradiation for 2 h, additional Pd(PPh₃)₄ (29 mg, 25 μ mol, 5.0 mol%) was added and the reaction mixture heated for a further 2 h. Flash chromatography eluting with a gradient of 0-100% EtOAc in pentane (containing 1% Et₃N) gave the *title compound* **101b** (35 mg, 0.14 mmol, 29%) as a yellow oil. **R_f** 0.07 (4:1 petrol–EtOAc). **¹H NMR** (500 MHz, CDCl₃): δ 7.49-7.43 (1H, m, Ar-H), 7.30-7.18 (2H, m, Ar-H), 7.15-7.10 (1H, m, Ar-H), 5.50 (1H, s, C=CH_AH_B), 5.23 (1H, d, J 1.0, C=CH_AH_B), 4.22 (1H, d, J 15.2, 2-H_A), 3.89 (1H, d, J 15.2, 2-H_B), 3.60 (3H, s, CO₂CH₃), 3.35-3.28 (1H, m, 4-H_A), 3.25-3.15 (2H, m, 4-H_B and 7-H_A), 3.06 (1H, d, J 15.1, 7-H_B), 2.65-2.55 (1H, m, 5-H_A), 2.29-2.26 (1H, m, 5-H_B). **¹³C NMR** (125 MHz, CDCl₃): δ 175.5 (CO₂CH₃), 144.7 (8-C), 139.8 (Ar-C_q), 135.8 (Ar-C_q), 129.8 (Ar-C), 128.2 (Ar-C), 127.8 (Ar-C), 127.6 (Ar-C), 117.2 (C=CH₂), 69.2 (6-C), 54.9 (2-C), 52.2 (CO₂CH₃), 46.6 (4-C), 39.6 (7-C), 26.7 (5-C). **IR** ν_{\max} (film)/cm⁻¹ 2921, 1736 (CO), 1484, 1435, 1257, 1235, 1104, 775. **HRMS** (ESI): C₁₅H₁₈NO₂ [M+H]⁺; calculated 244.1332, found 244.1335.

13-Benzyl 11-methyl 9-methylidene-1,13-diazatricyclo[9.4.0.0^{3,8}]pentadeca-3(8),4,6-triene-11,13-dicarboxylate 101c and 14-benzyl 12-methyl (9Z)-1,14-diazatricyclo[10.4.0.0^{3,8}]hexadeca-3(8),4,6,9-tetraene-12,14-dicarboxylate 102c



General procedure **N** was followed using amino ester **100c** (280 mg, 0.570 mmol, 1.00 eq.). Flash chromatography eluting with a gradient of 0-100% EtOAc in

pentane gave the separable *title compounds* **101c** (74 mg, 0.18 mmol, 32%) and **102c** (72 mg, 0.18 mmol, 31%) as pale yellow oils.*

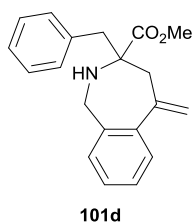
13-Benzyl 11-methyl 9-methylidene-1,13-diazatricyclo[9.4.0.0^{3,8}]pentadeca-3(8),4,6-triene-11,13-dicarboxylate 101c: R_f 0.11 (4:1 petrol–EtOAc). $^1\text{H NMR}$ (500 MHz, d^6 -DMSO, 319 K): δ 7.42-7.29 (6H, m, Ar-H), 7.21-7.14 (2H, m, Ar-H), 7.13-7.08 (1H, m, Ar-H), 5.40 (1H, s, $\text{C}=\text{CH}_\text{A}\text{H}_\text{B}$), 5.12 (1H, s, $\text{C}=\text{CH}_\text{A}\text{H}_\text{B}$), 5.12-5.03 (2H, m, OCH_2Ph), 4.49 (1H, d, J 17.0, 2- H_A), 4.22 (1H, d, J 12.8, 12- H_A), 3.79 (1H, d, J 12.8, $\text{NCH}_\text{A}\text{H}_\text{B}\text{CH}_2\text{N}$), 3.64 (1H, d, J 17.0, 2- H_B), 3.58 (3H, s, CO_2CH_3), 3.28-3.18 (1H, m, $\text{NCH}_\text{A}\text{H}_\text{B}\text{CH}_2\text{N}$), 3.15 (1H, d, J 12.8, 12- H_B), 2.90 (1H, br. s, $\text{NCH}_\text{A}\text{H}_\text{B}\text{CH}_2\text{N}$), 2.78 (1H, d, J 13.8, 10- H_A), 2.69 (1H, d, J 11.4, $\text{NCH}_\text{A}\text{H}_\text{B}\text{CH}_2\text{N}$), 2.63 (1H, d, J 13.8, 10- H_B). $^{13}\text{C NMR}$ (125 MHz, d^6 -DMSO, 319 K): δ 172.7 (CO_2CH_3), 154.2 ($\text{N}(\text{CO})\text{O}$), 143.9 (9-C), 139.4 (Ar- C_q), 139.1 (Ar- C_q), 136.7 (Ar- C_q), 128.2 (Ar-C), 127.6 (Ar-C), 127.5 (Ar-C), 127.3 (Ar-C), 127.0 (Ar-C), 126.8 (Ar-C), 126.2 (Ar-C), 115.9 ($\text{C}=\text{CH}_2$), 66.1 (OCH_2Ph), 64.8 (11-C), 56.6 (2-C), 51.2 (CO_2CH_3), 49.0 (12-C), 48.8 ($\text{NCH}_2\text{CH}_2\text{N}$), 43.4 ($\text{NCH}_2\text{CH}_2\text{N}$), 41.2 (10-C). **IR** ν_{max} (film)/ cm^{-1} 2946, 1732 (CO), 1702, 1461, 1432, 1277, 1223, 1128. **HRMS** (ESI): $\text{C}_{24}\text{H}_{27}\text{N}_2\text{O}_4$ $[\text{M}+\text{H}]^+$; calculated 407.1965, found 407.1975.

14-Benzyl 12-methyl (9Z)-1,14-diazatricyclo[10.4.0.0^{3,8}]hexadeca-3(8),4,6,9-tetraene-12,14-dicarboxylate 102c: R_f 0.21 (4:1 petrol–EtOAc). $^1\text{H NMR}$ (500 MHz, d^6 -DMSO, 319 K): δ 7.45 (1H, d, J 7.0, Ar-H), 7.40-7.30 (5H, m, Ar-H), 7.29-7.22 (2H, m, Ar-H), 7.16 (1H, d, J 7.1, Ar-H), 6.78 (1H, d, J 10.7, 9-H), 5.78 (1H, app. q, J 9.1, 10-H), 5.13-5.00 (2H, m, OCH_2Ph), 4.23 (1H, d, J 13.0, 13- H_A), 3.93-3.81 (2H, m, $\text{NCH}_\text{A}\text{H}_\text{B}\text{CH}_2\text{N}$)

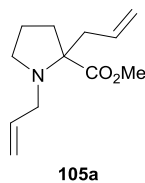
* Analysis of the crude product by 500 MHz NMR spectroscopy showed 100% conversion to a 42:58 mixture of **101c**:**102c**.

and 2-H_A), 3.65-3.51 (4H, m, includes 1H, m, 2-H_B and at δ 3.57: 3H, s, CO₂CH₃), 3.42 (1H, td, J 11.5, 3.3, NCH_AH_BCH₂N), 3.06-2.90 (2H, m, NCH_AH_BCH₂N and NCH_AH_BCH₂N), 2.73 (1H, d, J 13.0, 13-H_B), 2.40 (1H, dd, J 13.2, 7.6, 11-H_A), 1.66 (1H, dd, J 13.2, 9.3, 11-H_B). **¹³C NMR** (125 MHz, *d*⁶-DMSO, 319 K): δ 171.6 (CO₂CH₃), 153.8 (N(CO)O), 138.7 (Ar-C_q), 136.6 (Ar-C_q), 135.3 (Ar-C_q), 132.5 (9-C), 130.9 (Ar-C), 128.2 (2 × Ar-C), 127.6 (Ar-C), 127.2 (3 peaks, 3 × C; 10-C and 2 × Ar-C), 126.5 (Ar-C), 66.1 (OCH₂Ph), 60.4 (12-C), 55.8 (2-C), 52.4 (13-C), 51.1 (NCH₂CH₂N and CO₂CH₃), 44.0 (NCH₂CH₂N), 35.3 (11-C). **IR** ν_{max} (film)/cm⁻¹ 3010, 2948, 1733 (CO), 1701, 1456, 1432, 1284, 1232. **HRMS** (ESI): C₂₄H₂₇N₂O₄ [M+H]⁺; calculated 407.1965, found 407.1980.

Methyl 3-benzyl-5-methyldene-2,3,4,5-tetrahydro-1H-2-benzazepine-3-carboxylate **101d**

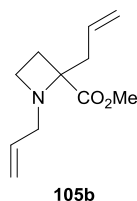


Et₃N (90 μ L, 0.65 mmol, 2.5 eq.) was added to a stirred solution of amino ester **100d** (100 mg, 0.260 mmol, 1.00 eq.), Pd(OAc)₂ (3.0 mg, 13 μ mol, 5.0 mol%) and PPh₃ (7.0 mg, 27 μ mol, 10 mol%) in MeCN (4 mL). The reaction mixture was heated at 125 °C under microwave irradiation for 1 h. Additional Pd(OAc)₂ (3.0 mg, 13 μ mol, 5.0 mol%) and PPh₃ (7.0 mg, 27 μ mol, 10 mol%) was added and the reaction mixture heated for 1 h. The reaction mixture was filtered through celite then concentrated *in vacuo*. Flash chromatography eluting with 80:20:1 pentane–EtOAc–Et₃N gave the *title compound* **101d** (72 mg, 0.23 mmol, 90%) as a colourless oil. R_f 0.29 (4:1 petrol–EtOAc). **¹H NMR** (500 MHz, CDCl₃): δ 7.38-7.29 (1H, m, Ar-H), 7.24-7.14 (4H, m, Ar-H), 7.13-7.04 (4H, m, Ar-H), 7.00-6.95 (1H, m, NH), 5.37 (1H, s, C=CH_AH_B), 5.06 (1H, s, C=CH_AH_B), 3.97-3.87 (2H, m, 1-H), 3.59 (3H, s, CO₂CH₃), 3.02-2.97 (3H, m, 4-H and CH_AH_BPh), 2.72 (1H, d, J 13.5, CH_AH_BPh). **¹³C NMR** (125 MHz, CDCl₃): δ 175.4 (CO₂CH₃), 144.8 (5-C), 140.3 (Ar-C_q), 139.8 (Ar-C_q), 136.3 (Ar-C_q), 130.1 (Ar-C), 128.4 (Ar-C), 128.1 (Ar-C), 128.0 (Ar-C), 127.5 (Ar-C), 127.1 (Ar-C), 126.9 (Ar-C), 116.0 (C=CH₂), 67.5 (3-C), 51.9 (CO₂CH₃), 48.8 (1-C), 44.3 (4-C or CH₂Ph), 43.8 (4-C or CH₂Ph). **IR** ν_{max} (film)/cm⁻¹ 2949, 1733 (CO), 1454, 1435, 1196, 909, 735, 701. **HRMS** (ESI): C₂₀H₂₂NO₂ [M+H]⁺; calculated 308.1645, found 308.1635.

Methyl 1,2-bis(prop-2-en-1-yl)pyrrolidine-2-carboxylate 105a

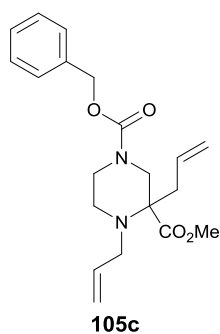
105a

General procedure **O** was followed using amino ester **63a** (1.0 g, 5.9 mmol). Purification by SCX cartridge, eluting first with MeOH then sat. NH₃/MeOH, gave the *title compound* **105a** (1.0 g, 4.8 mmol, 81%) as an orange oil. *R_f* 0.27 (1:1 pentane–EtOAc). **¹H NMR** (300 MHz, CDCl₃): δ 5.92–5.67 (2H, m, C_qCH₂CH=CH₂ and NCH₂CH=CH₂), 5.22–4.96 (4H, m, C_qCH₂CH=CH₂ and NCH₂CH=CH₂), 3.67 (3H, s, CO₂CH₃), 3.38 (1H, dd, *J* 13.7, 5.0, NCH_AH_BCH=CH₂), 3.15–2.97 (1H, m, 5-H_A), 2.84 (1H, dd, *J* 13.7, 7.5, NCH_AH_BCH=CH₂), 2.69–2.48 (2H, m, 5-H_B and C_qCH_AH_BCH=CH₂), 2.31 (1H, dd, *J* 14.0, 6.8, C_qCH_AH_BCH=CH₂), 2.19–1.99 (1H, m, 3-H_A), 1.92–1.65 (3H, m, 3-H_B and 4-H). **¹³C NMR** (75 MHz, CDCl₃): δ 174.6 (CO₂CH₃), 136.9 (NCH₂CH=CH₂ or C_qCH₂CH=CH₂), 134.3 (NCH₂CH=CH₂ or C_qCH₂CH=CH₂), 118.0 (NCH₂CH=CH₂ or C_qCH₂CH=CH₂), 116.2 (NCH₂CH=CH₂ or C_qCH₂CH=CH₂), 70.2 (2-C), 52.5 (NCH₂CH=CH₂), 51.8 (5-C), 51.2 (CO₂CH₃), 39.4 (C_qCH₂CH=CH₂), 33.9 (3-C), 21.6 (4-C). **IR** *v*_{max}(film)/cm⁻¹ 3077, 2978, 2951, 2814, 1738 (CO), 1642, 1445, 1434. **HRMS** (ESI): C₁₂H₂₀NO₂ [M+H]⁺; calculated 210.1494, found 210.1489.

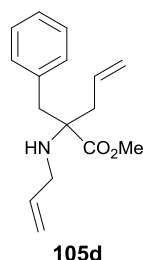
Methyl 1,2-bis(prop-2-en-1-yl)azetidine-2-carboxylate 105b

105b

General procedure **O** was followed using the TFA salt of the amino ester **63b** (404 mg, 1.50 mmol, 1.0 eq.) and K₂CO₃ (2.2 eq.). Purification by SCX cartridge, eluting first with MeOH then sat. NH₃/MeOH, gave the *title compound* **105b** (183 mg, 0.937 mmol, 62%) as an orange oil. **¹H NMR** (500 MHz, CDCl₃): δ 5.81–5.65 (2H, m, NCH₂CH=CH₂ and C_qCH₂CH=CH₂), 5.19–5.02 (4H, m, NCH₂CH=CH₂ and C_qCH₂CH=CH₂), 3.74 (3H, s, CO₂CH₃), 3.25–3.18 (1H, m, 4-H_A), 3.18–3.12 (3H, m, 4-H_B and NCH₂CH=CH₂), 2.66 (1H, dd, *J* 13.6, 7.3, C_qCH_AH_BCH=CH₂), 2.55 (1H, m, C_qCH_AH_BCH=CH₂), 2.52–2.47 (1H, m, 3-H_A), 2.08–2.00 (1H, m, 3-H_B). **¹³C NMR** (125 MHz, CDCl₃): δ 173.7 (CO₂CH₃), 134.9 (NCH₂CH=CH₂ or C_qCH₂CH=CH₂), 132.8 (NCH₂CH=CH₂ or C_qCH₂CH=CH₂), 118.5 (NCH₂CH=CH₂ or C_qCH₂CH=CH₂), 117.1 (NCH₂CH=CH₂ or C_qCH₂CH=CH₂), 71.5 (2-C), 54.9 (NCH₂CH=CH₂), 51.6 (CO₂CH₃), 49.4 (4-C), 38.7 (C_qCH₂CH=CH₂), 25.8 (3-C). **IR** *v*_{max}(film)/cm⁻¹ 2952, 2848, 1728 (CO), 1640 (CO), 1435, 1259, 1200, 1146. **HRMS** (ESI): C₁₁H₁₈NO₂ [M+H]⁺; calculated 196.1338, found 196.1328.

1-Benzyl 3-methyl 3,4-bis(prop-2-en-1-yl)piperazine-1,3-dicarboxylate 105c

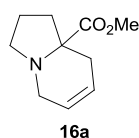
General procedure **O** was followed using amino ester **63c** (230 mg, 0.720 mmol). Purification by SCX cartridge, eluting first with MeOH then sat. NH_3/MeOH , gave the *title compound* **105c** (212 mg, 0.591 mmol, 82%) as an orange oil. **^1H NMR** (500 MHz, d^6 -DMSO, 319 K): δ 7.42-7.27 (5H, m, Cbz Ar-H), 5.86-5.66 (2H, m, $\text{NCH}_2\text{CH}=\text{CH}_2$ and $\text{C}_q\text{CH}_2\text{CH}=\text{CH}_2$), 5.22-5.01 (6H, m, CH_2Ph , $\text{NCH}_2\text{CH}=\text{CH}_2$ and $\text{C}_q\text{CH}_2\text{CH}=\text{CH}_2$), 4.15 (1H, dd, J 13.3, 1.5, 2- H_A), 3.85 (1H, d, J 13.0, $\text{NCH}_A\text{H}_B\text{CH}_2\text{N}$), 3.62-3.56 (1H, m, $\text{NCH}_A\text{H}_B\text{CH}=\text{CH}_2$), 3.54 (3H, s, CO_2CH_3), 3.00-2.85 (3H, m, 2- H_B , $\text{NCH}_A\text{H}_B\text{CH}=\text{CH}_2$ and $\text{NCH}_A\text{H}_B\text{CH}_2\text{N}$), 2.72-2.54 (3H, m, $\text{NCH}_2\text{CH}_2\text{N}$, and $\text{C}_q\text{CH}_A\text{H}_B\text{CH}=\text{CH}_2$), 2.50 (1H, m, $\text{C}_q\text{CH}_A\text{H}_B\text{CH}=\text{CH}_2$). **^{13}C NMR** (125 MHz, d^6 -DMSO, 319 K): δ 172.5 (CO_2CH_3), 154.0 ($\text{N}(\text{CO})\text{O}$), 136.8 (Ar- C_q), 136.5 ($\text{NCH}_2\text{CH}=\text{CH}_2$ or $\text{C}_q\text{CH}_2\text{CH}=\text{CH}_2$), 132.6 ($\text{NCH}_2\text{CH}=\text{CH}_2$ or $\text{C}_q\text{CH}_2\text{CH}=\text{CH}_2$), 128.2 (Ar-C), 127.6 (Ar-C), 127.2 (Ar-C), 118.1 ($\text{NCH}_2\text{CH}=\text{CH}_2$ or $\text{C}_q\text{CH}_2\text{CH}=\text{CH}_2$), 116.0 ($\text{NCH}_2\text{CH}=\text{CH}_2$ or $\text{C}_q\text{CH}_2\text{CH}=\text{CH}_2$), 66.0 (CH_2Ph), 63.9 (3-C), 52.4 ($\text{NCH}_2\text{CH}=\text{CH}_2$), 51.0 (CO_2CH_3), 49.2 (2-C), 45.6 ($\text{NCH}_2\text{CH}_2\text{N}$), 43.2 ($\text{NCH}_2\text{CH}_2\text{N}$), 37.8 ($\text{C}_q\text{CH}_2\text{CH}=\text{CH}_2$). **IR** $\nu_{\text{max}}(\text{film})/\text{cm}^{-1}$ 2950, 1734 (CO), 1706 (CO), 1458, 1431, 1283, 1225, 1124. **HRMS** (ESI): $\text{C}_{20}\text{H}_{27}\text{N}_2\text{O}_4$ [$\text{M}+\text{H}$] $^+$; calculated 359.1965, found 359.1975.

Methyl 2-benzyl-2-[(prop-2-en-1-yl)amino]pent-4-enoate 105d

General procedure **O** was followed using amino ester **63d** (400 mg, 1.82 mmol) and allyl bromide (0.8 mL, 9 mmol, 5 eq.). The reaction mixture was stirred for 2 days at rt. Purification by SCX cartridge, eluting first with MeOH then sat. NH_3/MeOH , gave the *title compound* **105d** (297 mg, 1.15 mmol, 63%) as a pale yellow oil. **^1H NMR** (500 MHz, CDCl_3 , NH not observed): δ 7.18-7.07 (3H, m, Ar-H), 6.99 (2H, m, Ar-H), 5.87-5.67 (2H, m, $\text{NHCH}_2\text{CH}=\text{CH}_2$ and $\text{C}_q\text{CH}_2\text{CH}=\text{CH}_2$), 5.16-5.02 (4H, m, $\text{NHCH}_2\text{CH}=\text{CH}_2$ and $\text{C}_q\text{CH}_2\text{CH}=\text{CH}_2$), 3.52 (3H, s, CO_2CH_3), 3.12 (1H, dd, J 13.0, 5.8, $\text{NHCH}_A\text{H}_B\text{CH}=\text{CH}_2$), 3.05 (1H, dd, J 13.0, 6.1, $\text{NHCH}_A\text{H}_B\text{CH}=\text{CH}_2$), 2.88 (1H, d, J 13.6, $\text{CH}_A\text{H}_B\text{Ph}$), 2.81 (1H, d, J 13.6, $\text{CH}_A\text{H}_B\text{Ph}$), 2.41 (1H, dd, J 14.8, 6.5, $\text{C}_q\text{CH}_A\text{H}_B\text{CH}=\text{CH}_2$), 2.31 (1H, dd, J 14.8, 7.8, $\text{C}_q\text{CH}_A\text{H}_B\text{CH}=\text{CH}_2$). **^{13}C NMR** (125 MHz, CDCl_3 , Ar- C_q not observed): δ 175.3 (CO_2CH_3), 136.4 ($\text{NCH}_2\text{CH}=\text{CH}_2$ or $\text{C}_q\text{CH}_2\text{CH}=\text{CH}_2$), 133.0 ($\text{NCH}_2\text{CH}=\text{CH}_2$ or

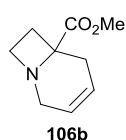
$C_qCH_2CH=CH_2$), 130.0 (Ar-C), 128.2 (Ar-C), 126.8 (Ar-C), 118.7 (NCH₂CH=CH₂ or $C_qCH_2CH=CH_2$), 116.0 (NCH₂CH=CH₂ or $C_qCH_2CH=CH_2$), 66.0 (C_q), 51.7 (CO₂CH₃), 46.0 (NHCH₂CH=CH₂), 41.8 (CH₂Ph), 38.1 ($C_qCH_2CH=CH_2$). **IR** ν_{max} (film)/cm⁻¹ 2949 (NH), 1731 (CO), 1495, 1454, 1119, 917, 701, 614. **HRMS** (ESI): C₁₆H₂₂NO₂ [M+H]⁺; calculated 260.1645, found 260.1647.

Methyl 1,2,3,5,8,8a-hexahydroindolizine-8a-carboxylate **106a**



Method A: General procedure **P** was followed using amino ester **105a** (266 mg, 1.27 mmol) with GII (27 mg, 32 μ mol, 2.5 mol%) in PhMe. The residue was washed through a pad of silica with EtOAc–MeOH (9:1) to give the title compound **106a** (191 mg, 1.05 mmol, 83%) as a red-brown oil. **Method B:** General procedure **P** was followed using amino ester **105a** (1.89 g, 9.03 mmol) with two changes; the addition of *p*-TsOH was omitted and HGII (245 mg, 0.290 mmol, 3.20 mol%) was used as the catalyst. The residue was washed through a pad of silica with EtOAc–MeOH (9:1) to give the *title compound* **106a** (1.12 g, 6.18 mmol, 69% [100% conversion based on crude ¹H NMR study]) as a red-brown oil. *R_f* 0.28 (1:1 pentane–EtOAc). **¹H NMR** (500 MHz, CDCl₃): δ 5.74–5.67 (2H, m, 6-H and 7-H), 3.67 (3H, s, CO₂CH₃), 3.55–3.48 (1H, m, 5-H_A), 3.40–3.33 (1H, m, 5-H_B), 3.18–2.98 (2H, m, 3-H), 2.86–2.71 (1H, m, 8-H_A), 2.23–2.08 (2H, m, 1-H_A and 8-H_B), 1.98–1.70 (3H, m, 1-H_B and 2-H). **¹³C NMR** (125 MHz, CDCl₃): δ 175.6 (CO₂CH₃), 125.9 (6-C or 7-C), 123.9 (6-C or 7-C), 65.5 (8a-C), 51.5 (CO₂CH₃), 50.9 (3-C), 47.4 (5-C), 36.8 (1-C), 33.8 (8-C), 20.6 (2-C). **IR** ν_{max} (film)/cm⁻¹ 3033, 2949, 2853, 1935 (C=C), 1731 (CO), 1447, 1192, 1175. **HRMS** (ESI): C₁₀H₁₆NO₂ [M+H]⁺; calculated 182.1181, found 182.1176.

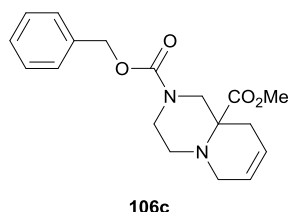
Methyl 1-azabicyclo[4.2.0]oct-3-ene-6-carboxylate **106b**



General procedure **P** was followed using amino ester **105b** (100 mg, 0.510 mmol) with GII (33 mg, 38 μ mol, 7.5 mol%) in PhMe. Flash chromatography eluting with a gradient of 0–10% MeOH in CH₂Cl₂, gave the *title compound* **106b** (49 mg, 0.29 mmol, 57%) as a red-brown oil. *R_f* 0.35 (10:1 CH₂Cl₂–MeOH). **¹H NMR** (500 MHz, CDCl₃): δ 6.05–5.98 (1H, m, 3-H), 5.94–5.88 (1H, m, 4-H), 3.73 (3H, s, CO₂CH₃), 3.48–3.37 (2H, m, 2-H_A and 8-H_A), 3.18–3.11 (1H, m, 8-H_B), 2.95–2.88 (1H, m, 2-H_B), 2.69–2.60 (1H, m, 7-H_A), 2.43–2.39 (2H, m, 5-H), 2.03–1.96 (1H, m, 7-H_B). **¹³C NMR** (125 MHz, CDCl₃):

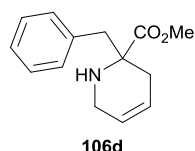
δ 175.8 (CO₂CH₃), 127.0 (4-C), 124.1 (3-C), 64.2 (6-C), 52.3 (CO₂CH₃), 49.0 (8-C), 47.4 (2-C), 30.5 (7-C), 28.5 (5-C). **IR** $\nu_{\text{max}}(\text{film})/\text{cm}^{-1}$ 2952, 2928, 1734 (CO), 1437, 1267, 1225, 1202, 1156. **HRMS** (ESI): C₉H₁₄NO₂ [M+H]⁺; calculated 168.1019, found 168.1022.

2-Benzyl 9a-methyl 1H,2H,3H,4H,6H,9H,9aH-pyrido[1,2-a]piperazine-2,9a-dicarboxylate **106c**



General procedure **P** was followed using amino ester **105c** (211 mg, 0.590 mmol) with GII (13 mg, 15 μmol , 2.5 mol%) in PhMe. Flash chromatography eluting with a gradient of 0-100% EtOAc in pentane (containing 1% Et₃N) gave the *title compound* **106c** (176 mg, 0.533 mmol, 90%) as a pale yellow oil. **R_f** 0.15 (3:2 petrol–EtOAc). **¹H NMR** (500 MHz, *d*⁶-DMSO, 319 K): δ 7.42-7.26 (5H, m, Cbz Ar-H), 5.69-5.58 (2H, m, 7-H and 8-H), 5.12-4.99 (2H, m, CH₂Ph), 4.25 (1H, dd, *J* 13.1, 2.1, 1-H_A), 3.98-3.90 (1H, m, NCH_AH_BCH₂N), 3.47 (3H, s, CO₂CH₃), 3.38-3.30 (1H, m, 6-H_A), 3.19-3.13 (1H, m, 6-H_B), 3.10-2.99 (2H, m, NCH_AH_BCH₂N and NCH_AH_BCH₂N), 2.86 (1H, d, *J* 13.1, 1-H_B), 2.65-2.55 (1H, m, NCH_AH_BCH₂N), 2.44-2.33 (1H, m, 9-H_A), 2.11-2.02 (1H, m, 9-H_B). **¹³C NMR** (125 MHz, *d*⁶-DMSO, 319 K): δ 172.3 (CO₂CH₃), 153.8 (N(CO)O), 136.7 (Ar-C_q), 128.2 (Ar-C), 127.6 (Ar-C), 127.2 (Ar-C), 125.1 (7-C or 8-C), 121.2 (7-C or 8-C), 66.1 (CH₂Ph), 59.8 (9a-C), 51.6 (1-C), 50.9 (CO₂CH₃), 49.8 (6-C), 47.6 (NCH₂CH₂N), 43.4 (NCH₂CH₂N), 32.2 (9-C). **IR** $\nu_{\text{max}}(\text{film})/\text{cm}^{-1}$ 3034, 2949, 1732 (CO), 1704 (CO), 1463, 1434, 1286, 1228. **HRMS** (ESI): C₁₈H₂₃N₂O₄ [M+H]⁺; calculated 331.1652, found 331.1652.

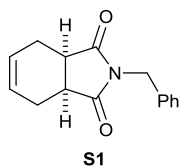
Methyl 2-benzyl-1,2,3,6-tetrahydropyridine-2-carboxylate **106d**



General procedure **P** was followed using amino ester **105d** (38 mg, 0.15 mmol) with GII (7.0 mg, 7.5 μmol , 5.0 mol%) in CH₂Cl₂. Flash chromatography eluting with pentane–EtOAc (4:1) gave the *title compound* **106d** (24 mg, 0.10 mmol, 69%) as an orange oil. **R_f** 0.06 (4:1 petrol–EtOAc). **¹H NMR** (500 MHz, CDCl₃): δ 7.31-7.22 (3H, m, Ar-H), 7.12-7.08 (2H, m, Ar-H), 5.74-5.69 (1H, m, 4-H), 5.69-5.64 (1H, m, 5-H), 3.62 (3H, s, CO₂CH₃), 3.54-3.48 (1H, m, 6-H_A), 3.43-3.36 (1H, m, 6-H_B), 3.04 (1H, d, *J* 13.2, CH_AH_BPh), 2.91 (1H, d, *J* 13.2, CH_AH_BPh), 2.68-2.61 (1H, m, 3-H_A), 2.31-2.24 (1H, m, 3-H_B). **¹³C NMR** (125 MHz, CDCl₃): δ 175.3 (CO₂CH₃), 135.7 (Ar-C_q),

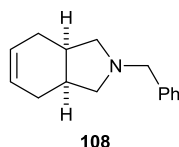
130.0 (Ar-C), 128.5 (Ar-C), 127.2 (Ar-C), 125.3 (5-C), 123.3 (4-C), 61.7 (2-C), 51.8 (CO₂CH₃), 46.5 (CH₂Ph), 42.7 (6-C), 33.3 (3-C). **IR** $\nu_{\text{max}}(\text{film})/\text{cm}^{-1}$ 3030 (NH), 2949, 1730, (CO), 1454, 1435, 1200, 1110, 1084, 1041. **HRMS** (ESI): C₁₄H₁₈NO₂ [M+H]⁺; calculated 232.1332, found 232.1342.

2-Benzyl-2,3,3a,4,7,7a-hexahydro-1H-isoindole-1,3-dione **S1**



Benzylamine (3.8 mL, 36 mmol, 1.1 eq.) was added to a stirred solution of *cis*-1,2,3,6-tetrahydrophthalic anhydride (5.0 g, 33 mmol, 1.0 eq.) and Et₃N (2.75 mL, 37.4 mmol, 1.10 mmol) in PhMe (27 mL). The reaction mixture was heated at reflux for 15 h then concentrated *in vacuo*. The crude residue was diluted in EtOAc (50 mL) and washed with sat. aq. NaHCO₃ (50 mL) and brine (50 mL). The organic phase was dried over MgSO₄, filtered and concentrated *in vacuo*. The residue was filtered through a pad of silica, washed with 9:1 EtOAc–MeOH to give the title compound **S1** (6.86 g, 28.4 mmol, 86%) as a colourless solid. R_f 0.57 (1:1 pentane–EtOAc). **¹H NMR** (500 MHz, CDCl₃): δ 7.32–7.22 (5H, m, Ar-H), 5.92–5.82 (2H, m, 5-H and 6-H), 4.63 (2H, s, CH₂Ph), 3.13–3.05 (2H, m, 3a-H and 7a-H), 2.64–2.57 (2H, m, 4-H_A and 7-H_A), 2.28–2.18 (2H, m, 4-H_B and 7-H_B). **¹³C NMR** (125 MHz, CDCl₃): δ 179.9 (1-C and 3-C), 136.0 (Ar-C_q), 128.7 (Ar-C), 128.5 (Ar-C), 127.9 (2 peaks, Ar-C, 5-C and 6-C), 42.6 (CH₂Ph), 39.3 (3a-C and 7a-C), 23.7 (4-C and 7-C). **IR** $\nu_{\text{max}}(\text{film})/\text{cm}^{-1}$ 1689 (CO), 1399, 1367, 1313, 1195, 928, 901, 737. **HRMS** (ESI): C₁₅H₁₆NO₂ [M+H]⁺; calculated 242.1176, found 242.1176. Spectral data consistent with the literature values.²¹²

2-Benzyl-2,3,3a,4,7,7a-hexahydro-1H-isoindole **108**

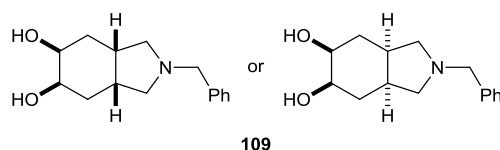


LiAlH₄ (3.2 g, 85 mmol, 6.0 eq.) was added to a stirred solution of imide **S1** (3.4 g, 14 mmol, 1.0 eq.) in THF (200 mL) at –78 °C. The reaction mixture was warmed to rt over 0.5 h, then heated at 60 °C for 2 h. The reaction mixture was cooled to rt and H₂O (5 mL) was added dropwise followed by 1 N NaOH (5 mL) and H₂O (10 mL). The resulting suspension was stirred vigorously for 1 h. MgSO₄ (ca. 15 g) was added and the reaction mixture was filtered through a pad of Celite, washed with EtOAc. The filtrate was washed with EtOAc (2 × 50 mL). The resulting solution was concentrated *in vacuo*. The residue was filtered through a pad of silica, washed with 9:1 EtOAc–MeOH to give the *title compound* **108** (3.0 g, 41 mmol, 99%) as a pale yellow oil. R_f 0.06

(1:1 pentane–EtOAc). **¹H NMR** (500 MHz, CDCl₃): δ 7.35–7.20 (5H, m, Ar-H), 5.86–5.78 (2H, m, 5-H and 6-H), 3.62 (2H, s, CH₂Ph), 2.92 (2H, dd, *J* 8.8, 7.0, 1-H_A and 3-H_A), 2.44–2.34 (2H, m, 3a-H and 7a-H), 2.21 (1H, dd, *J* 8.8, 7.0, 1-H_B and 3-H_B), 2.15 (2H, dd, *J* 15.2, 4.6, 4-H_A and 7-H_A), 1.87 (2H, d, *J* 15.2, 2.7, 4-H_B and 7-H_B). **¹³C NMR** (125 MHz, CDCl₃, one Ar-C_q not observed): δ 128.9 (Ar-C), 128.3 (Ar-C), 128.0 (5-C and 6-C), 126.9 (Ar-C), 61.2 (CH₂Ph or 1-C and 3-C), 61.0 (CH₂Ph or 1-C and 3-C), 35.9 (3a-C and 7a-C), 26.6 (4-C and 7-C). **IR** ν_{\max} (film)/cm⁻¹ 3085, 2920, 2783, 1494, 1452, 1147, 1130, 908. **HRMS** (ESI): C₁₅H₁₉NNa [M+Na]⁺; calculated 236.1410, found 236.1401.

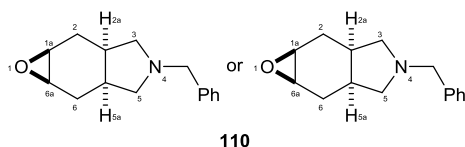
(3aR*,5R*,6S*,7aS*)-2-benzyl-octahydro-1H-isoindole-5,6-diol

or (3aR*,5S*,6R*,7aS*)-2-benzyl-octahydro-1H-isoindole-5,6-diol 109



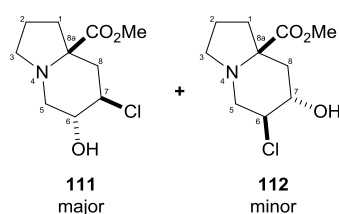
4-Methylmorpholine *N*-oxide monohydrate (254 mg, 1.88 mmol, 2.00 eq.) and OsO₄ (0.1 M in ^tBuOH, 0.47 mL, 47 μmol, 2.5 mol%) were added to a stirred solution of alkene **108** (200 mg, 0.940 mmol, 1.00 eq.) in 25:1 THF–H₂O at 0 °C. The reaction mixture was stirred at this temperature for 8 h, by which time all of the starting material had been consumed (TLC monitoring). Sat. aq. Na₂SO₃ (2 mL) was added and the reaction mixture was stirred for 30 min. EtOAc (20 mL) and H₂O (10 mL) were added and the phases were separated. The aqueous phase was washed with EtOAc (2 × 25 mL). The combined organic extracts were dried over MgSO₄ and concentrated *in vacuo*. The residue was filtered through a pad of silica, washed with 9:1 EtOAc–MeOH to give the *title compound* **109** (160 mg, 0.65, 69%) as a pale yellow oil. **R_f** 0.25 (9:1 CH₂Cl₂–MeOH). **¹H NMR** (500 MHz, CDCl₃): δ 7.37–7.17 (5H, m, Ar-H), 3.89 (2H, dd, *J* 5.8, 3.1, 5-H and 6-H), 3.70 (2H, s, CH₂Ph), 2.73 (2H, dd, *J* 9.3, 7.2, 1-H_A and 3-H_A), 2.58 (2H, dd, *J* 9.3, 5.0, 1-H_B and 3-H_B), 2.43–2.35 (2H, m, 3a-H and 7a-H), 1.95–1.87 (2H, m, 4-H_A and 7-H_A), 1.68 (2H, ddd, *J* 14.1, 6.4, 3.9, 4-H_B and 7-H_B). **¹³C NMR** (125 MHz, CDCl₃): δ 140.1 (Ar-C_q), 128.6 (Ar-C), 128.3 (Ar-C), 126.9 (Ar-C), 68.9 (5-C and 6-C), 61.0 (CH₂Ph), 57.8 (1-C and 3-C), 34.5 (3a-C and 7a-C), 31.0 (4-C and 7-C). **IR** ν_{\max} (film)/cm⁻¹ 3303 (OH), 2898, 2798, 1685, 1451, 1073, 1027, 698. **HRMS** (ESI): C₁₅H₂₂NO₂ [M+H]⁺; calculated 248.1646, found 248.1648.

(1aR*,2aR*,5aS*,6aS*)-4-benzyl-octahydro-1aH-oxireno[2,3-f]isoindole or (1aR*,2aS*,5aR*,6aS*)-4-benzyl-octahydro-1aH-oxireno[2,3-f]isoindole 110



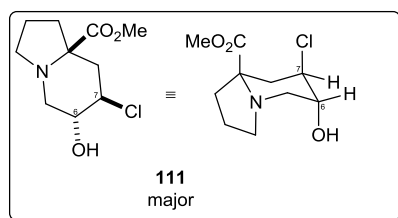
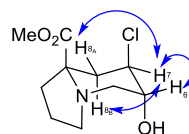
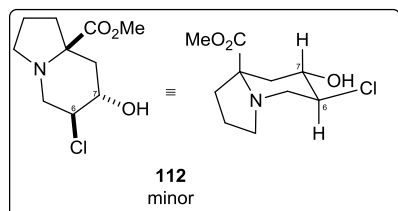
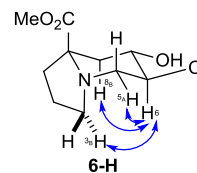
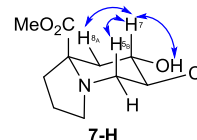
Following a procedure by Young,¹⁵⁶ TFA (90 μ L, 1.2 mmol, 1.3 eq.) was added to a stirred suspension of the alkene **108** (200 mg, 0.94 mmol, 1.00 eq.) in H₂O (1.0 mL) in a sealed screw-topped vial. NCS (150 mg, 1.13 mmol, 1.20 eq.) was added and the reaction mixture was heated at 70 °C for 4 h. The reaction mixture was cooled to rt and quenched with sat. aq. NaHCO₃ (2 mL), then extracted with EtOAc (25 mL). The organic phase was washed with brine (25 mL). The combined aqueous phase was extracted with EtOAc (2 \times 25 mL). The combined organic extracts were dried over MgSO₄, filtered and concentrated *in vacuo* to give a colourless oil (232 mg). The residue was dissolved in MeOH (10 mL) and K₂CO₃ (260 mg, 1.88 mmol, 2.00 eq.) was added. The reaction mixture was stirred for 24 h then concentrated *in vacuo*. The residue was diluted in EtOAc (25 mL) and washed with sat. aq. NaHCO₃ (25 mL). The aqueous phase was extracted with EtOAc (2 \times 25 mL). The combined organic phase was dried over MgSO₄, filtered and concentrated *in vacuo* to give the *title compound 110* (90 mg, 0.39 mmol, 42%) as a yellow oil which was not purified further. *R*_f 0.11 (9:1 CH₂Cl₂–MeOH). **¹H NMR** (500 MHz, CDCl₃): δ 7.35–7.20 (5H, m, Ar-H), 3.63 (2H, s, CH₂Ph), 3.17–3.10 (2H, m, 1a-H and 6a-H), 2.98–2.86 (2H, m, 3-H_A and 5-H_A), 2.38–2.26 (4H, m, 2a-H, 3-H_B, 5-H_B and 5a-H), 2.00 (2H, dd, *J* 15.3, 5.4, 2-H_A and 6-H_A), 1.83 (2H, dd, *J* 15.3, 1.4, 2-H_B and 6-H_B). **¹³C NMR** (125 MHz, CDCl₃): δ 139.2 (Ar-C_q), 129.1 (Ar-C), 128.4 (Ar-C), 127.1 (Ar-C), 61.8 (3-C and 5-C), 60.6 (CH₂Ph), 50.7 (1a-C and 6a-C), 31.1 (2a-C and 5a-C), 24.3 (2-C and 6-C). **IR** ν_{max} (film)/cm⁻¹ 2910, 2809, 1495, 1453, 1229, 1155, 936, 699. **HRMS** (ESI): C₁₅H₂₀NO [M+H]⁺; calculated 230.1539, found 230.1543.

Methyl (6R*,7R*,8aR*)-7-chloro-6-hydroxy-octahydroindolizine-8a-carboxylate 111 and methyl (6S*,7S*,8aR*)-6-chloro-7-hydroxy-octahydroindolizine-8a-carboxylate 112

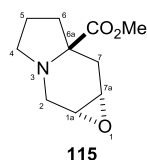


Following a procedure by Young,¹⁵⁶ TFA (0.21 mL, 2.8 mmol, 1.0 eq.) was added to a stirred suspension of amine **106a** (500 mg, 2.76 mmol, 1.00 eq.) in H₂O (2.8 mL) in a sealed screw-topped vial. NCS (442 mg, 3.31 mmol, 1.2 eq.) was added and the reaction

mixture was heated at 70 °C for 24 h. Additional NCS (300 mg, 2.25 mmol, 0.80 eq.) was added and the reaction mixture was heated for a further 15 h. The reaction mixture was cooled to rt and quenched with solid NaHCO₃ until neutralised. NaCl was added until the solution was saturated, then the mixture was extracted with EtOAc (5 × 2 mL). The combined organics were dried, filtered, and concentrated. Flash chromatography on cyanosilica eluting with a gradient of 0-10% EtOAc in pentane, gave the *title compounds* **111** (231 mg, 0.988 mmol, 36%) and **112** (52 mg, 0.22 mmol, 8%) as colourless oils. **Methyl (6R*,7R*,8aR*)-7-chloro-6-hydroxy-octahydroindolizine-8a-carboxylate 111**: R_f 0.11 (1:1 petrol–EtOAc). ¹H NMR (500 MHz, CDCl₃, OH not observed): δ 4.11 (1H, dd, J 3.3, 3.0, 7-H), 3.79 (1H, app. br. s, 6-H), 3.73 (1H, d, J 12.7, 5-H_A), 3.68 (3H, s, CO₂CH₃), 3.25-3.12 (1H, m, 3-H_A), 3.05-2.98 (1H, m, 3-H_B), 2.79 (1H, dd, J 12.7, 2.7, 5-H_B), 2.72 (1H, dd, J 14.7, 2.8, 8-H_A), 2.19-2.06 (2H, m, 1-H_A and 8-H_B), 1.94-1.78 (1H, m, 2-H_A), 1.77-1.64 (2H, m, 1-H_B and 2-H_B). ¹³C NMR (125 MHz, CDCl₃): 175.4 (CO₂CH₃), 69.0 (6-C), 64.3 (8a-C), 57.2 (7-C), 51.6 (CO₂CH₃), 50.5 (3-C), 47.3 (5-C), 38.2 (1-C), 37.0 (8-C), 20.4 (2-C). IR ν_{max}(film)/cm⁻¹ 2952, 2855, 1731 (CO), 1309, 1196, 1068, 907, 725. HRMS (ESI): C₁₀H₁₇³⁵CINO₃ [M+H]⁺; calculated 234.0891, found 234.0896. **Methyl (6S*,7S*,8aR*)-6-chloro-7-hydroxy-octahydroindolizine-8a-carboxylate 112**: R_f 0.18 (1:1 petrol–EtOAc). ¹H NMR (500 MHz, CDCl₃): δ 3.86 (1H, ddd, J 11.2, 9.9, 5.1, 6-H), 3.74 (3H, s, CO₂CH₃), 3.52 (1H, ddd, J 11.8, 9.9, 4.5, 7-H), 3.28 (1H, dd, J 13.3, 5.1, 5-H_A), 3.19-3.12 (1H, m, 3-H_A), 3.09-2.97 (2H, m, includes 1H, m, 3-H_B and at δ 3.06: 1H, dd, J 13.3, 11.2, 5-H_B) 2.61 (1H, dd, J 13.0, 4.5, 8-H_A), 2.53 (1H, br. s, OH), 2.15-2.05 (1H, m, 1-H_A), 1.95-1.77 (3H, m, 1-H_B and 2-H), 1.49 (1H, dd, J 13.0, 11.8, 8-H_B). ¹³C NMR (125 MHz, CDCl₃): δ 174.8 (CO₂CH₃), 72.9 (7-C), 67.8 (8a-C), 61.2 (6-C), 52.3 (CO₂CH₃), 51.4 (5-C), 50.0 (3-C), 38.7 (8-C), 37.3 (1-C), 21.9 (2-C). IR ν_{max}(film)/cm⁻¹ 2951, 2853, 1727 (CO), 1447, 1194, 1174, 1149, 1023. HRMS (ESI): C₁₀H₁₇³⁵CINO₃ [M+H]⁺; calculated 234.0891, found 234.0888.

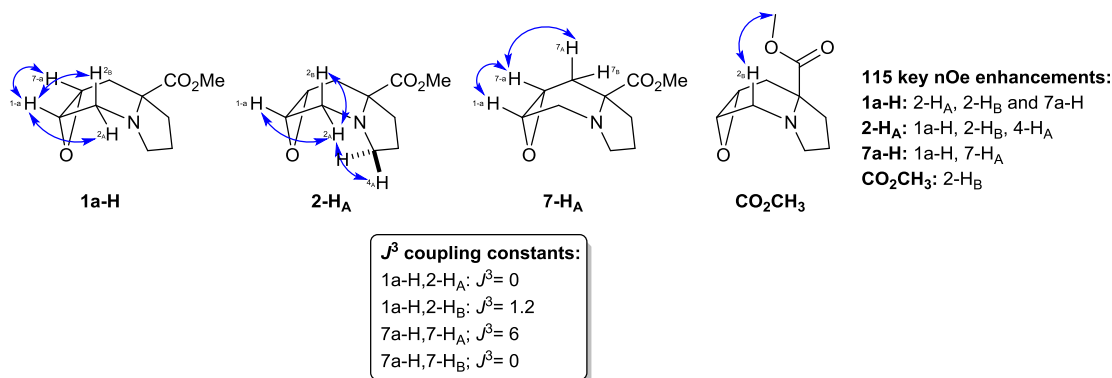
**¹³C NMR shifts:****6-C:** 69.0 ppm**7-C:** 57.2 ppm**J^β coupling constants:**6-H,5-H_A; J^β= 06-H,5-H_B; J^β= 2.77-H,8-H_A; J^β= 2.8**key nOe enhancements:****6-H:** 7-H**7-H:** 6-H; 8-H_A; 8-H_B**¹³C NMR shifts:****6-C:** 61.2 ppm**7-C:** 72.9 ppm**J^β coupling constants:**6-H,7-H; J^β= 9.9**J^β coupling constants:**6-H,5-H_A; J^β= 5.16-H,5-H_B; J^β= 11.27-H,8-H_A; J^β= 4.57-H,8-H_B; J^β= 11.8**key nOe enhancements:****6-H:** 3-H_B; 5-H_A; 8-H_B**7-H:** OH, 5-H_B, 8-H_A

Methyl (1aR*,6aR*,7aS*)-octahydrooxireno[2,3-f]indolizine-6a-carboxylate **115**

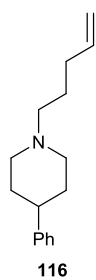


NaOMe (25 wt% in MeOH, 146 μ L, 0.640 mmol, 2.00 eq.) was added to a stirred solution of the major chlorohydrin **111** (75 mg, 0.32 mmol, 1.0 eq.) in MeOH (3.2 mL). The reaction mixture was stirred for 15 h then concentrated *in vacuo*. The residue was washed through a pad

of silica with 9:1 EtOAc–MeOH. Flash chromatography on cyanosilica eluting with a gradient of 0–100% EtOAc in pentane, gave the *title compound* **115** (27 mg, 0.14 mmol, 43%) as a colourless oil. *R_f* 0.17 (1:1 petrol–EtOAc). **¹H NMR** (500 MHz, CDCl₃): δ 3.70 (3H, s, CO₂CH₃), 3.39 (1H, d, *J* 13.9, 2-H_A), 3.33 (1H, dd, *J* 5.8, 4.1, 7a-H), 3.15 (1H, app. d, *J* 4.1, 1a-H), 3.07 (1H, td, *J* 8.5, 3.9, 4-H_A), 2.86–2.78 (2H, m, includes 1H, m, 4-H_B and at δ 2.81: 1H, d, *J* 13.9, 1.2, 2-H_B), 2.63 (1H, dd, *J* 14.9, 5.8, 7-H_A), 2.12–2.05 (1H, m, 6-H_A), 1.95–1.80 (2H, m, 5-H), 1.77 (1H, app. d, *J* 14.9, 7-H_B), 1.67–1.59 (1H, m, 6-H_B). **¹³C NMR** (125 MHz, CDCl₃): δ 174.8 (CO₂CH₃), 64.7 (6a-C), 51.5 (2 \times C, 1a-C and CO₂CH₃), 51.1 (4-C), 50.8 (7a-C), 46.2 (2-C), 36.4 (6-C), 33.1 (7-C), 21.4 (5-C). **IR** ν_{\max} (film)/cm⁻¹ 2951, 2841, 1723 (CO), 1447, 1433, 1195, 1173, 1111. **HRMS** (ESI): C₁₀H₁₆NO₃ [M+H]⁺; calculated 198.1125, found 198.1127.

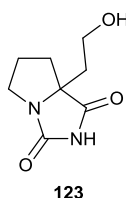


1-(Pent-4-en-1-yl)-4-phenylpiperidine **116**



NaBH(OAc)₃ (4.2 g, 30 mmol, 2.0 eq.) was added to a stirred solution of 4-phenylpiperidine (1.6 g, 9.9 mmol, 1.0 eq.), 4-penten-1-al (1.2 mL, 12 mmol, 1.2 eq.) and 4 Å MS in CH₂Cl₂ (50 mL). The reaction mixture was stirred for 2 days then filtered. The resulting solution was washed with sat. aq. NaHCO₃ (50 mL) and brine (50 mL). The organic phase was dried over MgSO₄ and filtered through Celite, washed with EtOAc. The residue was filtered through a pad of silica, washed with 9:1 EtOAc–MeOH to give the *title compound* **116** (2.1 g, 9.0 mmol, 91%) as a pale brown oil which was not purified further. **¹H NMR** (500 MHz, CDCl₃): δ 7.34-7.16 (5H, m, Ar-H), 5.91-5.72 (1H, m, CH=CH₂), 5.03 (1H, dd, *J* 17.1, 1.6, CH=CH_AH_B), 4.97 (1H, d, *J* 10.2, CH=CH_AH_B), 3.06 (2H, app. d, *J* 11.5, 2-H_A and 6-H_A), 2.57-2.44 (1H, m, 4-H), 2.43-2.33 (2H, m, NCH₂), 2.12-2.00 (4H, m, 2-H_B, 6-H_B and CH₂CH=CH₂), 1.87-1.75 (4H, m, 3-H and 5-H), 1.68-1.60 (2H, m, NCH₂CH₂). **¹³C NMR** (125 MHz, CDCl₃): δ 146.6 (Ar-C_q), 138.7 (CH=CH₂), 128.5 (Ar-C), 127.0 (Ar-C), 126.2 (Ar-C), 114.7 (CH=CH₂), 58.7 (NCH₂), 54.6 (2-C and 6-C), 43.0 (4-C), 33.6 (3-C and 5-C), 32.0 (CH₂CH=CH₂), 26.4 (NCH₂CH₂). **IR** ν_{max}(film)/cm⁻¹ 2933, 2801, 2763, 1130, 992, 908, 754, 697. **HRMS** (ESI): C₁₆H₂₃NNa [M+Na]⁺; calculated 252.1723, found 252.1717.

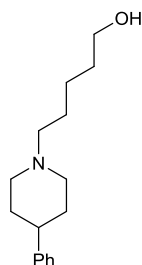
7a-(2-Hydroxyethyl)-hexahydro-1H-pyrrolo[1,2-c]imidazolidine-1,3-dione **123**



NaIO₄ (193 mg, 0.900, 2.00 eq.) and K₂OsO₄·2H₂O (4.0 mg, 1.0 μmol, 2.5 mol%) were added to a stirred solution of hydantoin **88a** (81 mg, 0.45 mmol, 1.0 eq.) in 4:1 acetone–H₂O (5.0 mL). The reaction mixture was stirred at rt for 24 h. Na₂SO₃ (500 mg) was added and the reaction

mixture stirred for 0.5 h, then diluted with acetone (25 mL) and filtered through Celite. The solution was concentrated *in vacuo* to give a brown oil. The residue was dissolved in MeOH (5.0 mL) and NaBH₄ (34 mg, 0.90 mmol, 2.0 eq.) was added at 0 °C. The reaction mixture was stirred for 5 h. Sat. aq. NH₄Cl (0.2 mL) was added and the reaction mixture was filtered through Celite then concentrated *in vacuo*. Flash chromatography eluting with 85:14:1 CH₂Cl₂-EtOH-NH₃^{*} gave the *title compound* **123** (22 mg, 0.12 mmol, 27%) as a colourless oil. *R_f* 0.44 (1:1 85:14:1 CH₂Cl₂-EtOH-NH₃). **¹H NMR** (500 MHz, CD₃OD, NH and OH not observed): δ 3.78-3.71 (1H, m, CH_AH_BOH), 3.70-3.60 (2H, m, 5-H), 3.27-3.19 (1H, m, CH_AH_BOH), 2.27-2.09 (3H, m, 6-H and CH_AH_BCH₂OH), 2.01-1.85 (3H, m, 7-H and CH_AH_BCH₂OH). **¹³C NMR** (125 MHz, CD₃OD): δ 179.7 (1-C), 162.8 (3-C), 73.4 (7a-C), 58.7 (CH₂OH), 45.6 (5-H), 37.9 (CH₂CH₂OH), 34.1 (7-C), 26.8 (6-C). **IR** *v*_{max}(film)/cm⁻¹ 3418, 3233, 1766 (CO), 1714, 1393, 1094, 1044, 773. **HRMS** (ESI): C₈H₁₃N₂O₃ [M+H]⁺; calculated 185.0921, found 185.0915.

5-(4-Phenylpiperidin-1-yl)pentan-1-ol **124**



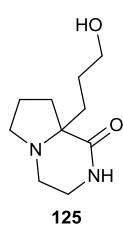
124

9-BBN dimer (106 mg, 0.440 mmol, 0.50 eq.) was added to a stirred solution of alkene **116** (200 mg, 0.870 mmol, 1.00 eq.) in 1,4-dioxane (1.6 mL) in a screw-topped vial. The reaction mixture was heated at 60 °C for 15 h. Additional 9-BBN dimer (53 mg, 0.22 mmol, 0.25 eq.) was added and the reaction mixture was stirred for a further 3 h. H₂O (1.6 mL) was added, followed by NaBO₃·4H₂O (400 mg, 2.60 mmol, 3.00 eq.). The reaction mixture was stirred for 15 h, then partitioned between EtOAc (25 mL) and brine (25 mL). The phases were separated and the aqueous phase was extracted with EtOAc (2 × 25 mL). The combined organic phase was dried over MgSO₄, filtered and concentrated *in vacuo*. The residue was purified by SCX, eluting first with MeOH then sat. NH₃/MeOH, to give the *title compound* **124** (138 mg, 0.56 mmol, 64%) as a yellow wax. **¹H NMR** (500 MHz, CDCl₃, OH not observed): 7.35-7.13 (5H, m, Ar-H), 3.66 (2H, t, *J* 6.4, CH₂OH), 3.06 (2H, app. d, *J* 11.3, 2-H_A and 6-H_A), 2.57-2.43 (1H, m, 4-H), 2.39 (2H, t, *J* 7.6, NCH₂), 2.04 (2H, app. td, *J* 11.3, 4.1, 2-H_B and 6-H_B), 1.87-1.76 (5H, m, 3-H and 5-H and NCH₂CH_AH_B), 1.65-1.54 (3H, m, NCH₂CH_AH_B, NCH₂CH₂CH_AH_B and NCH₂CH₂CH₂CH_AH_B), 1.47-1.39 (2H, m, NCH₂CH₂CH_AH_B and

* Sat. NH₃ in MeOH used.

NCH₂CH₂CH₂CH_AH_B). ¹³C NMR (125 MHz, CDCl₃): δ 146.5 (Ar-C_q), 128.5 (Ar-C), 127.0 (Ar-C), 126.3 (Ar-C), 62.8 (CH₂OH), 59.0 (NCH₂), 54.6 (2-C and 6-C), 42.9 (4-C), 33.5 (3-C and 5-C), 32.5 (NCH₂CH₂) 26.7 (NCH₂CH₂CH₂CH₂), 23.8 (NCH₂CH₂CH₂). IR ν_{\max} (film)/cm⁻¹ 2929, 2765, 1450, 1374, 1119, 1066, 754, 697. HRMS (ESI): C₁₆H₂₆NO [M+H]⁺; calculated 248.2009, found 248.2017.

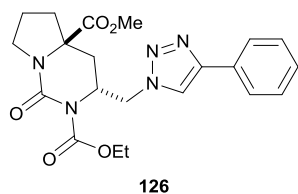
8a-(3-Hydroxypropyl)-octahydropyrrolo[1,2-a]piperazin-1-one **125**



9-BBN (0.5 M in THF, 5.0 mL, 2.5 mmol, 3.0 eq.) was added to a stirred solution of lactam **90a** (147 mg, 0.820 mmol, 1.00 eq.) in THF (0.8 mL). The reaction mixture was heated at reflux for 24 h then cooled to rt. NaBO₃·4H₂O (630 mg, 4.10 mmol, 5.00 eq.) and H₂O (1.0 mL) were added and the reaction mixture was stirred for 15 h, then cooled to 0 °C, dried over MgSO₄, filtered through Celite and concentrated *in vacuo*. Flash chromatography on cyanosilica eluting with a gradient of 0-100% EtOAc in pentane, gave the *title compound* **125** (84 mg, 0.42 mmol, 52%) as a yellow oil. R_f 0.02 (9:1 EtOAc–MeOH). ¹H NMR (500 MHz, CDCl₃, OH not observed): δ 5.81 (1H, s, NH), 3.58 (2H, t, *J* 5.3, CH₂OH), 3.56-3.49 (1H, m, CH_AH_B), 3.45-3.37 (1H, m, CH_AH_B), 3.19-3.08 (2H, m, CH_AH_B and CH_AH_B), 2.95-2.86 (2H, m, CH_AH_B and CH_AH_B), 2.24-2.16 (1H, m, CH_AH_B), 2.14-2.06 (1H, m, CH_AH_BCH₂CH₂OH), 2.03-1.96 (1H, m, CH_AH_B), 1.93-1.79 (3H, m, CH_AH_BCH₂CH₂OH and CH₂), 1.79-1.59 (2H, m, CH₂CH₂OH). ¹³C NMR (125 MHz, CDCl₃): δ 175.5 (CONH), 69.6 (8a-C), 63.5 (CH₂OH), 52.1 (CH₂), 44.5 (CH₂), 39.0 (CH₂), 36.4 (CH₂), 34.5 (CH₂CH₂CH₂OH), 28.3 (CH₂), 22.3 (CH₂CH₂OH). IR ν_{\max} (film)/cm⁻¹ 3290 (NH), 2936, 2874, 1645 (CO), 1487, 1446, 1358, 1059. HRMS (ESI): C₁₀H₁₉N₂O₂ [M+H]⁺; calculated 199.1441, found 199.1442.

5.2.3 Synthesis of scaffold derivatives

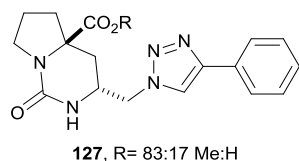
2-Ethyl 4a-methyl (3*R**,4*aR**)-1-oxo-3-[(4-phenyl-1*H*-1,2,3-triazol-1-yl)methyl]-octahydropyrrolo[1,2-*c*]pyrimidine-2,4a-dicarboxylate **126**



Phenyl acetylene (70 μL, 0.62 mmol, 2.0 eq) was added to a stirred solution of azide **82a** (100 mg, 0.31 mmol, 1.0 eq.), Cu(OAc)₂ (11 mg, 60 μmol, 20 mol%) and sodium

ascorbate (24 mg, 0.12 mmol, 40 mol%) in degassed* ^tBuOH–H₂O (1:1, 2.0 mL). After 15 h the reaction mixture was extracted with EtOAc (25 mL) and washed with brine (25 mL). The aqueous layer was extracted with EtOAc (2 × 10 mL). The combined organics were dried over MgSO₄, filtered and concentrated *in vacuo*. Flash chromatography on cyanosilica eluting with a gradient of 0-100% EtOAc in pentane, gave the *title compound* **126** (117 mg, 0.27 mmol, 88%) as colourless oil. *R_f* 0.29 (EtOAc). ¹H NMR (500 MHz, CDCl₃): δ 7.88 (1H, s, triazole 5-H), 7.83 (2H, d, *J* 7.1, Ar-H), 7.41 (2H, t, *J* 7.6, Ar-H), 7.35-7.30 (1H, m, Ar-H), 4.69 (2H, app. d, *J* 4.4, CH₂Ar), 4.59-4.51 (1H, m, 3-H), 4.39-4.20 (2H, m, CH₂CH₃), 3.70 (3H, s, CO₂CH₃), 3.58-3.51 (1H, m, 7-H_A), 3.43-3.37 (1H, m, 7-H_B), 2.86 (1H, dd, *J* 13.6, 8.7, 4-H_A), 2.28-2.21 (1H, m, 5-H_A), 1.96-1.72 (4H, m, 4-H_B; 5-H_B and 6-H), 1.33 (3H, t, *J* 7.1, CH₂CH₃). ¹³C NMR (125 MHz, CDCl₃): δ 172.8 (CO₂CH₃), 154.5 (CO), 150.0 (CO), 148.5 (triazole 4-C), 130.5 (Ar-C_q), 129.0 (Ar-C), 128.4 (Ar-C), 126.1 (Ar-C), 121.2 (triazole 5-C), 65.6 (4a-C), 63.4 (CH₂CH₃), 53.2 (CH₂Ar), 53.2 (3-C), 53.1 (CO₂CH₃), 46.7 (7-C), 37.8 (5-C), 36.7 (4-C), 22.7 (6-C), 14.5 (CH₂CH₃). IR *v*_{max}(film)/cm⁻¹ 2981, 1703 (CO), 1419, 1288, 1230, 1171, 835, 767. HRMS (ESI): C₂₁H₂₆N₅O₅ [M+H]⁺; calculated 428.1928, found 428.1930.

(3*R,4*aR**)-1-oxo-3-[(4-phenyl-1*H*-1,2,3-triazol-1-yl)methyl]-octahydropyrrolo[1,2-*c*]pyrimidine-4*a*-carboxylic acid **127****

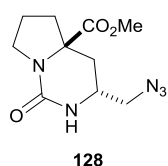


NaOH (6.0 mg, 0.14 mmol, 2.0 eq.) was added to a stirred solution of urea **126** (30 mg, 70 μmol, 1.0 eq.) in MeOH (0.3 mL). The reaction mixture was stirred for 2 h, by which point a colourless solid had precipitated from the solution. The reaction mixture was diluted with MeOH (15 mL). Amberlite IR-120 (hydrogen form, 100 mg) was added and the mixture was stirred for 0.5 h, then filtered and concentrated. The residue was triturated with CHCl₃ to give the *title compound* **127** (20 mg, 83:17 mixture of ester:acid, 56 μmol, 80%) as colourless solid. ¹H NMR (500 MHz, *d*⁶-DMSO, 318 K, ester peaks assigned): δ 8.52 (1H, s, triazole 5-H), 7.85-7.81 (2H, m, Ar-H), 7.46 (2H, t, *J* 7.7, Ar-H), 7.34 (1H, t, *J* 7.4, Ar-H), 6.49 (1H, s, NH), 4.56 (1H, dd, *J* 14.0, 4.5, CH_AH_BAr), 4.44 (1H, dd, *J* 14.0, 6.3, NCH_AH_BAr), 3.66 (3H, s, CO₂CH₃), 3.64-3.56 (1H, m, 3-H), 3.43-3.34 (1H,

* Degassed by bubbling N₂ through the solvent.

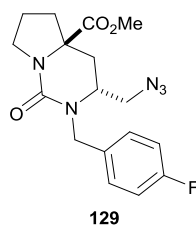
m, 7-H_A), 3.33-3.26 (1H, m, 7-H_B), 2.40-2.33 (1H, m, 4-H_A), 2.30-2.23 (1H, m, 5-H_A), 1.85-1.75 (2H, m, 5-H_B and 6-H_A), 1.68-1.57 (1H, m, 6-H_B), 1.40 (1H, t, *J* 12.4, 4-H_B). Carboxylic acid characteristic peaks: δ 8.53 (1H, s, triazole 5-H), 6.40 (1H, s, NH). ¹³C NMR (125 MHz, *d*⁶-DMSO, 318 K, ester peaks assigned): δ 173.6 (CO₂CH₃), 153.3 (1-C), 146.3 (triazole 4-C), 130.5 (Ar-C_q), 128.7 (Ar-C), 127.7 (Ar-C), 125.0 (Ar-C), 122.1 (triazole 5-C), 65.8 (4a-C), 52.5 (CH₂Ar and CO₂CH₃), 48.5 (3-C), 44.9 (7-C), 37.3 (5-C), 33.8 (4-C), 20.8 (6-C). IR ν_{max} (film)/cm⁻¹ 1737 (CO), 1649 (CO), 1488, 1473, 1221, 1170, 712, 693. HRMS (ESI): C₁₈H₂₂N₅O₃ [M+H]⁺; calculated 356.1717, found 356.1723.

Methyl (3*R**,4*aR**)-3-(azidomethyl)-1-oxo-octahydropyrrolo[1,2-c]pyrimidine-4a-carboxylate **128**



NaOMe (25 wt% in MeOH, 82 μ L, 37 μ mol, 1.0 eq.) was added to a stirred solution of urea **82a** (120 mg, 0.370 mmol, 1.00 eq.) in MeOH (3.0 mL). The reaction mixture was stirred at rt for 1.5 h, then concentrated *in vacuo*. The residue was redissolved in MeOH (10 mL) and Amberlite IR-120 (hydrogen form, 240 mg) was added. After stirring for 0.5 h the reaction mixture was filtered and concentrated to give the *title compound* **128** (72 mg, 0.28 mmol, 76%) as a white solid which was carried on crude to the next step. *R*_f 0.84 (9:1EtOAc–MeOH). ¹H NMR (300 MHz, CDCl₃, characteristic peaks): δ 5.47 (1H, s, NH), 3.74 (3H, s, CO₂CH₃), 3.67-3.53 (2H, m), 3.49 (1H, dd, *J* 11.5, 4.2), 3.44-3.34 (1H, m), 3.25 (1H, dd, *J* 11.5, 7.1), 2.57 (1H, dd, *J* 12.8, 2.4), 2.48-2.32 (1H, m), 2.01-1.69 (3H, m), 1.47-1.34 (1H, m).

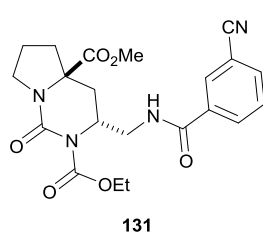
Methyl (3*R**,4*aR**)-3-(azidomethyl)-2-[(4-fluorophenyl)methyl]-1-oxo-octahydropyrrolo[1,2-c]pyrimidine-4a-carboxylate **129**



To a stirred solution of urea **128** (72 mg, 0.28 mmol, 1.0 eq.) in DMF (2.0 mL) was added NaH (60% dispersion in oil, 13 mg, 0.31 mmol, 1.1 eq.). The reaction mixture was stirred for 10 min then 4-fluorobenzyl bromide (70 μ L, 0.56 mmol, 2.0 eq.) was added. The reaction mixture was stirred for 1 h then H₂O (0.1 mL) was added. The reaction mixture was diluted with Et₂O (10 mL) and washed with brine (10 mL). The aqueous layer was extracted with Et₂O (10 mL), then the combined organic layers were dried over MgSO₄, filtered, and concentrated *in vacuo*. Flash chromatography on cyanosilica eluting with a gradient of 0-100%

EtOAc in pentane, gave the *title compound 129* (53 mg, 0.15 mmol, 52%) as colourless oil. R_f 0.26 (EtOAc–petrol). $^1\text{H NMR}$ (500 MHz, CDCl_3): δ 7.21 (2H, app. dd, J 8.4, 5.5, Ar 2-H), 6.99 (2H, app. t, J 8.7, Ar 3-H), 5.32 (1H, d, J 15.9, $\text{CH}_\text{A}\text{H}_\text{B}\text{Ar}$), 3.99 (1H, d, J 15.9, $\text{CH}_\text{A}\text{H}_\text{B}\text{Ar}$), 3.74–3.63 (5H, m includes 2H, m, 7-H and at δ 3.66: 3H, s, CO_2CH_3), 3.48 (1H, dd, J 12.9, 5.2, $\text{CH}_\text{A}\text{H}_\text{B}\text{N}_3$), 3.31 (1H, dd, J 12.9, 2.8, $\text{CH}_\text{A}\text{H}_\text{B}\text{N}_3$), 3.23–3.17 (1H, m, 3-H), 2.60 (1H, dd, J 13.0, 5.0, 4- H_A), 2.42–2.36 (1H, m, 5- H_A), 1.98–1.75 (4H, m, 4- H_B ; 5- H_B and 6-H). $^{13}\text{C NMR}$ (125 MHz, CDCl_3): δ 174.3 (CO_2Me), 162.1 (d, J 245.6, Ar 4-C), 155.3 (1-C), 133.5 (Ar 1-C), 129.4 (d, J 7.8, Ar 2-C), 115.5 (d, J 21.3, Ar 3-C), 65.0 (4a-C), 52.8 (CO_2CH_3), 52.4 (CH_2N_3), 51.2 (3-C), 46.5 (7-C or CH_2Ar), 46.3 (7-C or CH_2Ar), 38.6 (5-C), 35.8 (4-C), 21.7 (6-C). $\text{IR } \nu_{\text{max}}(\text{film})/\text{cm}^{-1}$ 2953, 2101 (N_3), 1733 (CO), 1635, 1509, 1450, 1350, 1218. HRMS (ESI): $\text{C}_{17}\text{H}_{21}\text{FN}_5\text{O}_3$ $[\text{M}+\text{H}]^+$; calculated 362.1623, found 362.1630.

2-Ethyl 4a-methyl (3*R,4a*R**)-3-[[3-cyanophenyl]formamido]methyl]-1-oxo-octahydropyrrolo[1,2-c]pyrimidine-2,4a-dicarboxylate **131****



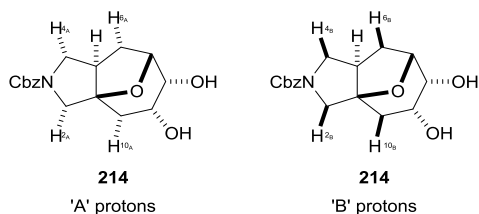
To a stirred solution of azide **82a** (50 mg, 0.15 mmol, 1.0 eq.) in THF– H_2O (1.0 mL) was added PPh_3 (43 mg, 0.17 mmol, 1.1 eq.). The reaction mixture was stirred for 15 h then concentrated *in vacuo* to give the crude amine **130** [characteristic $^1\text{H NMR}$ peaks (300 MHz, CDCl_3): δ 6.45 (1H, s), 5.98–5.88 (1H, m, 3-H), 4.12 (2H, q, J 6.9, $\text{CO}_2\text{CH}_2\text{CH}_3$), 3.76 (3H, s, CO_2CH_3), 3.68–3.58 (2H, m), 3.50 (1H, dd, J 14.0, 7.1), 3.44–3.33 (1H, m), 3.13–2.99 (1H, m), 2.55 (1H, dd, J 12.5, 3.0), 2.49–2.41 (1H, m), 1.99–1.88 (1H, m), 1.81 (2H, dd, J 6.6, 4.1), 1.38 (1H, t, J 12.5), 1.25 (3H, t, J 6.9, $\text{CO}_2\text{CH}_2\text{CH}_3$)]. The residue was dissolved in CH_2Cl_2 (1.0 mL). A pre-stirred solution of 3-cyanobenzoyl chloride (55 mg, 0.33 mmol, 2.2 eq.) and Et_3N (0.12 mL, 0.60 mmol, 4.0 eq.) was added *via* cannula. The reaction mixture was stirred for 15 h. The reaction mixture was concentrated *in vacuo* to give the crude benzamide **131** [characteristic $^1\text{H NMR}$ peaks (300 MHz, CDCl_3): δ 8.41–8.25 (m), 7.95–7.81 (m), 5.24–5.10 (1H, m, NH), 4.51–4.36 (1H, m, 3-H), 4.11 (2H, q, J 7.1, $\text{CO}_2\text{CH}_2\text{CH}_3$), 3.84 (3H, s, CO_2CH_3), 3.75–3.61 (1H, m), 3.54 (1H, ddd, J 14.4, 7.1, 3.5), 3.03 (1H, dd, J 13.8, 8.9), 2.51–2.31 (1H, m), 2.22–1.89 (5H, m), 1.35–1.17 (4H, m, includes at δ 1.23: 3H, t, J 7.1, $\text{CO}_2\text{CH}_2\text{CH}_3$). Attempted purification using flash chromatography and SCX

failed to remove the triphenylphosphine oxide biproduct (optimisation of the purification step is required).

5.3 Experimental for 'top-down' approach to LOS

5.3.1 A note on NMR assignments

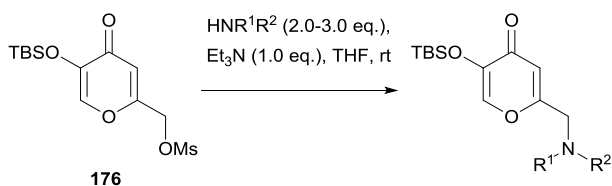
For polycyclic assemblies that were assigned using NOESY, protons labelled 'A' are on the bottom face of the molecule, while protons labelled 'B' are on the top face of the molecule, e.g. see compound **214** below as an example.



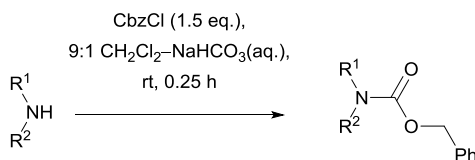
Where polycyclic assemblies **were not** assigned using NOESY the 'A' and 'B' descriptors are reported arbitrarily.

5.3.2 General procedures

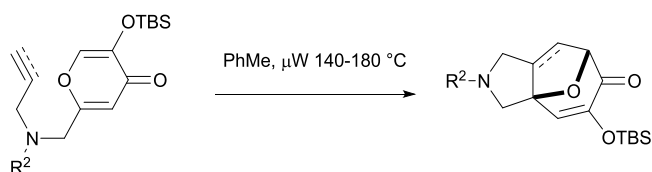
General procedure S: Amination of mesylate **176**



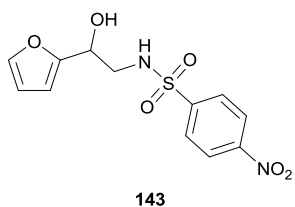
Et₃N (1.0 eq.) was added to a stirred solution of the mesylate **176** (1.0 eq.) in THF (0.5 M, 1 volume). Amine (2.0-3.0 eq., as specified) was added and the reaction mixture was stirred for 15 h, then concentrated *in vacuo*. The resulting residue was diluted in EtOAc (1 volume) and washed with sat. aq. NaHCO₃ (1 volume). The phases were separated and the aqueous phase was extracted with EtOAc (2 volumes). The combined organics were washed with brine, dried over MgSO₄, filtered and concentrated *in vacuo*. Compounds were purified by flash chromatography.

General procedure T: Carboxybenzyl protection of amines

Benzyl chloroformate (1.5 eq.) was added dropwise to a stirred solution of the amine (1.0 eq.) in 9:1 CH₂Cl₂-NaHCO₃ (sat. aq., 0.2 M, 1 volume). The reaction mixture stirred for 0.25 h. Sat. NaHCO₃ (0.5 volume) was then added and the phases separated. The aqueous phase was extracted with CH₂Cl₂ (0.5 volume). The combined organic phase was dried over Na₂SO₄ and concentrated *in vacuo*. Compounds were purified by flash chromatography.

General procedure U: Intramolecular [5+2] cycloaddition of oxidopyryliums generated from β-alkoxy-γ-pyrones

A stirred solution of the starting material in PhMe (1.0 M) was heated at 140-180 °C (as specified) under microwave irradiation for 2-6 h (as specified). The reaction mixture was concentrated *in vacuo*. Compounds were purified by flash chromatography.

5.3.3 Compound data for ‘top-down’ approach to LOS**2-Amino-1-(furan-2-yl)ethan-1-ol 143**

Following a procedure by O’Doherty,¹⁷⁵ nitromethane (27.1 mL, 500 mmol, 5.00 eq.) was added to a stirred solution of LiAlH₄ (380 mg, 10.0 mmol, 0.10 eq.) in THF (200 mL) at 0 °C. The reaction mixture was stirred at 0 °C for 0.5 h, then furfural (8.30 mL, 100 mmol, 1.00 eq.) was added. The reaction mixture was warmed to rt and stirred for 3 days. The reaction mixture was filtered through Celite. The resulting solution was partitioned with sat. aq. NaHCO₃ (200 mL) and the phases were separated. The aqueous phase was extracted with EtOAc (2 × 100 mL). The combined organic phase was washed with brine (100 mL), then dried over MgSO₄, filtered and concentrated *in vacuo* to give the

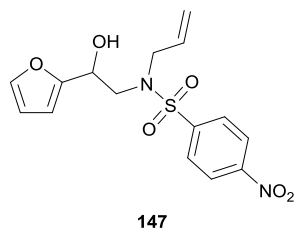
crude Henry adduct **144** as a brown oil (15.2 g, 96% mass recovery) which was not purified further [characteristic $^1\text{H NMR}$ peaks (300 MHz, CDCl_3): δ 7.44-7.41 (1H, m, 5-H), 6.41 (1H, d, J 3.3, 3-H), 6.39 (1H, dd, J 3.3, 1.8, 4-H), 5.53-5.45 (1H, m, $\text{CH}(\text{OH})$), 4.81 (1H, dd, J 13.4, 9.2, $\text{CH}_\text{A}\text{H}_\text{B}\text{NO}_2$), 4.68 (1H, dd, J 13.4, 3.5, $\text{CH}_\text{A}\text{H}_\text{B}\text{NO}_2$), 2.79 (1H, m, OH). Spectrum consistent with the literature values].¹⁷⁵

Following the modification of a procedure by Dixon,²¹³ $\text{NiCl}_2 \cdot 6\text{H}_2\text{O}$ (75 mg, 0.32 mmol, 5.0 mol%) was added to a stirred solution of Henry adduct **144** (1.0 g, 6.4 mmol, 1.0 eq.) in 1:1 THF–MeOH (65 mL) at rt. The reaction mixture was stirred for 10 min then cooled to 0 °C. NaBH_4 (962 mg, 25.4 mmol, 4.00 eq.) was added portionwise. The reaction mixture was stirred for 10 min then warmed to rt and stirred for 1 h. Purification by SCX cartridge, eluting first with MeOH then sat. NH_3/MeOH , gave aminoalcohol **145** (588 mg) as a brown oil which was carried on to the next step without further purification [characteristic $^1\text{H NMR}$ peaks (300 MHz, CDCl_3 , NH_2 and OH not observed): δ 7.37 (1H, app. br. s, 5-H), 6.33 (1H, app. br. s, 4-H), 6.26 (1H, d, J 2.7, 3-H), 4.63 (1H, br. s, $\text{CH}(\text{OH})$), 3.04 (2H, br. s, CH_2NH_2). Spectrum consistent with the literature values].²¹⁴

Et_3N (1.0 mL, 6.9 mmol, 1.5 eq.) was added to a stirred solution of aminoalcohol **145** (588 mg, 4.62 mmol, 1.00 eq.) in CH_2Cl_2 (10 mL). The reaction mixture was stirred for 5 min then cooled to 0 °C. 4-Nitrobenzenesulfonyl chloride (1.23 g, 5.54 mmol, 1.20 eq.) was added and the reaction mixture was stirred for 15 h at rt. The reaction partitioned with sat. aq. NaHCO_3 (10 mL) and the phases were separated. The aqueous phase was extracted with CH_2Cl_2 (2 \times 10 mL). The combined organic phases were washed with brine (20 mL), then dried over MgSO_4 , filtered and concentrated *in vacuo*. Flash chromatography eluting with 0-100% EtOAc in pentane gave the *title compound* **143** (627 mg, 2.00 mmol, 32% over three steps) as a pale brown oil. R_f 0.65 (1:1 petrol–EtOAc). $^1\text{H NMR}$ (500 MHz, CDCl_3): δ 8.37 (2H, d, J 8.9, Ar 3-H), 8.05 (2H, d, J 8.9, Ar 2-H), 7.36-7.35 (1H, m, furyl 5-H), 6.34 (1H, dd, J 3.3, 1.8, furyl 4-H), 6.30 (1H, d, J 3.3, furyl 3-H), 5.08-5.03 (1H, m, NH), 4.86-4.81 (1H, m, $\text{CH}(\text{OH})\text{CH}_2$), 3.50-3.44 (1H, m, $\text{CH}_\text{A}\text{H}_\text{B}\text{NH}$), 3.37-3.30 (1H, m, $\text{CH}_\text{A}\text{H}_\text{B}\text{NH}$), 2.22 (1H, d, J 4.4, OH). $^{13}\text{C NMR}$ (125 MHz, CDCl_3): δ 152.9 (furyl 2-C), 150.4 (Ar- C_q - NO_2), 146.0 (Ar- C_q - SO_2), 142.9 (furyl 5-C), 128.5 (Ar 2-C), 124.6 (Ar 3-C), 110.7 (furyl 4-C), 107.8 (furyl 3-C), 66.6 ($\text{CH}(\text{OH})$), 47.3 (CH_2NH). IR $\nu_{\text{max}}(\text{film})/\text{cm}^{-1}$ 3296 (OH),

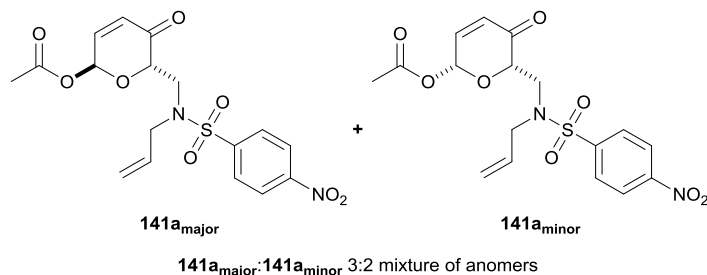
3107, 1529, 1350, 1310, 1163, 1092, 1012. **HRMS** (ESI): C₁₂H₁₁N₂O₆S [M-H]⁻; calculated 311.0343, found 311.0339.

N*-Allyl-*N*-[2-(furan-2-yl)-2-hydroxyethyl]-4-nitrobenzenesulfonamide **147*



Following a procedure by Moitessier,²¹⁵ allyl bromide (39 μ L, 0.44 mmol, 1.20 eq.) was added to a stirred solution of the protected aminoalcohol **143** (115 mg, 0.370 mmol, 1.00 eq.) and K₂CO₃ (512 mg, 3.70 mmol, 10.0 eq.) in acetone (20 mL). The reaction mixture was stirred for 15 h then concentrated *in vacuo*. The resulting residue was extracted with CH₂Cl₂ (20 mL) and washed with H₂O (20 mL). The organic phase was dried over MgSO₄, filtered, then concentrated *in vacuo*. Flash chromatography eluting with 0-100% EtOAc in pentane gave the *title compound* **147** (65 mg, 2.0 mmol, 50%) as a colourless oil. *R_f* 0.69 (1:1 petrol–EtOAc). **¹H NMR** (500 MHz, CDCl₃): δ 8.36 (2H, d, *J* 8.9, Ar 3-H), 8.04 (2H, d, *J* 8.9, Ar 2-H), 7.38 (1H, m, furyl 5-H), 6.36 (1H, dd, *J* 3.2, 1.8, furyl 4-H), 6.33 (1H, d, *J* 3.2, furyl 3-H), 5.62-5.52 (1H, m, CH₂CH=CH₂), 5.23-5.15 (2H, m, includes at δ 5.19: 1H, dd, *J* 10.1, 1.0, CH=CH_AH_B; and at δ 5.18: 1H, dd, *J* 17.0, 1.0, CH=CH_AH_B), 4.99-4.92 (1H, m, CH(OH)), 3.91 (1H, dd, *J* 15.8, 6.5, CH_AH_BCH=CH₂), 3.86 (1H, dd, *J* 15.8, 6.4, CH_AH_BCH=CH₂), 3.62 (1H, dd, *J* 14.9, 8.3, NCH_AH_BCH(OH)), 3.48 (1H, dd, *J* 14.9, 4.2, NCH_AH_BCH(OH)), 2.52 (1H, s, OH). **¹³C NMR** (125 MHz, CDCl₃): δ 153.4 (furyl 2-C), 150.2 (Ar-C_q-NO₂), 145.9 (Ar-C_q-SO₂), 142.6 (furyl 5-C), 131.9 (CH=CH₂), 128.7 (Ar 2-C), 124.5 (Ar 3-C), 120.4 (CH=CH₂), 110.7 (furyl 4-C), 107.7 (furyl 3-C), 66.8 (CH(OH)), 52.0 (CH₂CH=CH₂), 51.6 (NCH₂CH(OH)). **IR** ν_{max} (film)/cm⁻¹ 1529, 1350, 1311, 1160, 1090, 1011, 922, 743. **HRMS** (ESI): C₁₅H₁₅N₂O₆S [M-H]⁻; calculated 351.0647, found 351.0656.

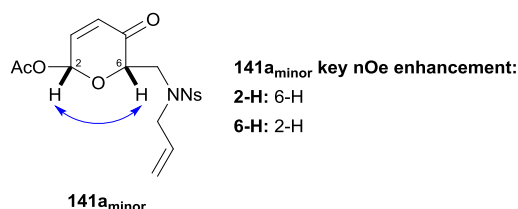
(2*R,6*R**)-5-Oxo-6-[[*N*-(prop-2-en-1-yl)4-nitrobenzenesulfonamido]methyl]-5,6-dihydro-2H-pyran-2-yl acetate **141a_{major}** and (2*R**,6*S**)-5-oxo-6-[[*N*-(prop-2-en-1-yl)4-nitrobenzenesulfonamido]methyl]-5,6-dihydro-2H-pyran-2-yl acetate **141a_{minor}****



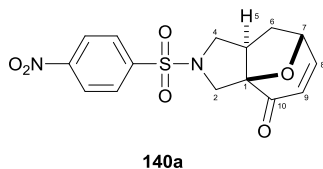
Following a procedure by O'Doherty,¹⁷⁵ NBS (50 mg, 0.28 mmol, 1.0 eq.) was added to a stirred solution of furan **147** (100 mg, 0.28 mmol, 1.0 eq.),

NaHCO₃ (47 mg, 0.56 mmol, 2.0 eq.) and NaOAc·3H₂O (38 mg, 0.28 mmol, 1.0 eq.) in 5:1 THF–H₂O (6.0 mL) at 0 °C. The reaction mixture was stirred at this temperature for 1 h then diluted with sat. aq. NaHCO₃ solution (10 mL). The reaction mixture was extracted with EtOAc (3 × 10 mL). The combined organic phases were washed with sat. aq. Na₂SO₃ (10 mL) and brine (10 mL). The organic phases was then dried, filtered and concentrated *in vacuo* to give a yellow oil (115 mg). The crude residue was dissolved in pyridine (5.0 mL) and Ac₂O (0.1 mL, 1.0 mmol, 3.8 eq.) was added at 0 °C. The reaction mixture was stirred at 0 °C for 0.5 h then warmed to rt and concentrated *in vacuo*. Flash chromatography eluting with 0-100% EtOAc in pentane gave coelution of the *title compounds* **141a_{major}** and **141a_{minor}** (52 mg, 0.13 mmol, 45% over two steps, 3:2 mixture of anomers) as a pale brown oil. *R_f* 0.22 (1:1 petrol–EtOAc). **¹H NMR** (500 MHz, CDCl₃, 60:40 mixture of anomers): δ 8.36 (2H, 2 × d, *J* 9.0, *major* and *minor* Ar 3-H), 8.05 (2H, app. t, *J* 9.0, *major* and *minor* Ar 2-H), 6.91-6.85 (1H, m, *major* and *minor* 4-H), 6.52-6.50 (0.4H, m, *minor* 2-H), 6.40 (0.6H, d, *J* 3.6, *major* 2-H), 6.25 (0.4H, dd, *J* 10.4, 1.2, *minor* 3-H), 6.20 (0.6H, app. d, *J* 10.3, *major* 3-H), 5.66-5.53 (1H, m, *major* and *minor* CH₂CH=CH₂), 5.23-5.15 (2H, m, *major* and *minor* CH₂CH=CH₂), 4.76 (0.6H, dd, *J* 8.6, 2.8, *major* 6-H), 4.42 (0.4H, dd, *J* 8.6, 3.2, *minor* 6-H), 4.04-3.92 (2.6H, m, includes 2H, *major* and *minor* CH₂CH=CH₂; and 0.6H, *major* CHCH_AH_BN), 3.90 (0.4H, dd, *J* 15.3, 3.2, *minor* CHCH_AH_BN), 3.65 (0.4H, dd, *J* 15.3, 8.6, *minor* CHCH_AH_BN), 3.42 (0.6H, dd, *J* 15.5, 8.6, *major* CHCH_AH_BN), 2.17 (1.2H, s, *minor* CH₃), 2.12 (1.8H, s, *major* CH₃). **¹³C NMR** (125 MHz, CDCl₃, mixture of two rotamers): δ 192.9 (*major*, 5-C), 192.8 (*minor*, 5-C), 169.4 (*major*, (CO)CH₃), 169.2 (*minor*, (CO)CH₃), 150.2 (*major* and *minor*, Ar-C_q-NO₂), 146.2 (*minor*, Ar-C_q-SO₂), 146.0 (*major*,

Ar-C_q-SO₂), 144.6 (minor, 4-C), 142.0 (major, 4-C), 132.0 (major, CH=CH₂), 131.9 (minor, CH=CH₂), 129.1 (minor, 3-C), 128.8 (major, 3-C or Ar 2-C), 128.7 (major, 3-C or Ar 2-C), 128.4 (minor, Ar 2-C), 124.5 (minor, Ar 3-C), 124.4 (major, Ar 3-C), 120.2 (minor, CH=CH₂), 120.1 (major, CH=CH₂), 88.0 (minor, 2-C), 86.0 (major, 2-C), 78.3 (minor, 6-C), 75.5 (major, 6-C), 51.7 (major, CH₂CH=CH₂), 51.3 (minor, CH₂CH=CH₂), 48.0 (minor, C_qCH₂N), 46.6 (major, C_qCH₂N), 21.1 (minor, CH₃), 21.0 (major, CH₃). IR $\nu_{\max}(\text{film})/\text{cm}^{-1}$ 1755 (CO), 1697 (CO), 1531, 1312, 1217, 1162, 1090, 1010. HRMS (APCI): C₁₅H₁₅N₂O₆S⁺ [M+H]⁺; calculated 351.0651, found 351.0645.

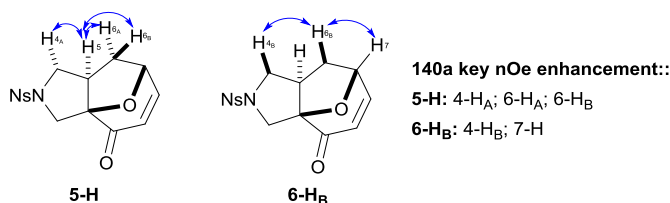


(1R*,5R*,7R*)-3-(4-Nitrobenzenesulfonyl)-11-oxa-3-azatricyclo[5.3.1.0^{1,5}]undec-8-en-10-one 140a

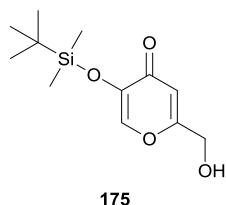


Following a modified procedure by Mitchell,¹⁷⁹ quinuclidine (15 mg, 0.13 mmol, 4.0 eq.) was added to a stirred solution of acetoxypyranone **141a** (14 mg, 34 μmol , 1.0 eq.) in MeCN (0.3 mL) in a 1 mL screw-topped vial. The reaction mixture was heated at 80 °C for 15 h then concentrated *in vacuo*. Flash chromatography eluting with 0-100% EtOAc in pentane gave the *title compound* **140a** (10 mg, 29 μmol , 84%) as a colourless oil. R_f 0.69 (1:1 petrol–EtOAc). ¹H NMR (500 MHz, CDCl₃): δ 8.40 (2H, d, *J* 8.7, Ar 3-H), 8.04 (2H, d, *J* 8.7, Ar 2-H), 7.20 (1H, dd, *J* 9.8, 4.5, 8-H), 5.97 (1H, d, *J* 9.8, 9-H), 4.92 (1H, dd, *J* 6.7, 4.5, 7-H), 4.12 (1H, d, *J* 12.0, 2-H_A), 3.72 (1H, dd, *J* 10.5, 8.7, 4-H_A), 3.46 (1H, d, *J* 12.0, 2-H_B), 3.22 (1H, dd, *J* 10.5, 6.7, 4-H_B), 2.60-2.53 (1H, m, 5-H), 2.13 (1H, dd, *J* 12.3, 8.5, 6-H_A), 1.99-1.93 (1H, m, 6-H_B). ¹³C NMR (125 MHz, CDCl₃): δ 192.8 (10-C), 152.8 (9-C), 150.5 (Ar-C_q-NO₂), 142.5 (Ar-C_q-SO₂), 129.1 (Ar 2-C), 125.8 (8-C), 124.5 (Ar 3-C), 96.2 (1-C), 76.9 (7-C), 54.2 (4-C), 51.1 (2-C), 44.3 (5-C), 35.5 (6-C). IR $\nu_{\max}(\text{film})/\text{cm}^{-1}$ 1693 (CO), 1528, 1350, 1307, 1164, 1100, 1013, 856. HRMS (APCI): C₁₅H₁₅N₂O₆S [M+H]⁺; calculated 351.0651, found 351.0643.

[†] N.b. The pyran underwent [5 + 2] cycloaddition under all attempted MS conditions to give cycloadduct **140a**.

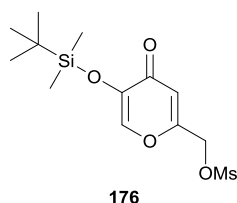


5-[(*tert*-Butyldimethylsilyl)oxy]-2-(hydroxymethyl)-4*H*-pyran-4-one **175**



Following a procedure by Miyazaki,¹⁹¹ TBSCl (5.3 g, 35 mmol, 1.0 eq.) was added to a stirred suspension of kojic acid (5.0 g, 35 mmol, 1.0 eq.), Et₃N (7.4 mL, 100 mmol, 2.90 eq.) and DMAP (5 mg, 0.04 mmol, 0.001 eq.) in CHCl₃ at 0 °C. The reaction mixture was stirred at this temperature for 1 h then aqueous 5 wt% KHSO₄ (50 mL) was added. The phases were separated and the organic phase was washed with brine (50 mL), dried, filtered and concentrated *in vacuo*. Flash chromatography eluting with 1:1 pentane–EtOAc gave the title compound **175** (8.08 g, 31.5 mmol, 90%) as a colourless amorphous solid.* *R*_f 0.57 (1:1 petrol–EtOAc). ¹H NMR (500 MHz, CDCl₃): δ 7.65 (1H, s, 6-H), 6.47 (1H, s, 3-H), 4.46 (2H, d, *J* 6.3, CH₂OH), 3.13 (1H, t, *J* 6.3, OH), 0.95 (9H, s, SiC(CH₃)₃), 0.21 (6H, s, 2 × SiCH₃). ¹³C NMR (125 MHz, CDCl₃): δ 176.1 (4-C), 166.6 (2-C), 144.6 (5-C), 144.2 (6-C), 112.4 (3-C), 61.1 (CH₂), 25.8 (SiC(CH₃)₃), 18.7 (SiC_q), –4.4 (2 × SiCH₃). IR *v*_{max}(film)/cm^{–1} 3358 (br., OH), 2954, 2857, 1651 (CO), 1629, 1268, 1211, 874. LRMS[†] (HPLC-MS): C₁₂H₂₁O₄Si; found 257.1 [M+H]⁺. Spectral data are consistent with the literature values.²¹⁶

{5-[(*tert*-Butyldimethylsilyl)oxy]-4-oxo-4*H*-pyran-2-yl}methyl methanesulfonate **176**



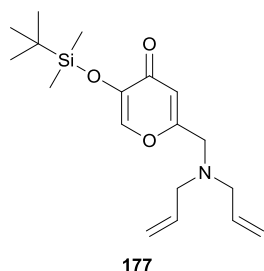
Et₃N (3.3 mL, 23.4 mmol, 2.0 eq.) was added to a stirred solution of silyl protected kojic acid **175** (3.00 g, 11.7, 1.00 eq.) in CH₂Cl₂ (24 mL). The reaction mixture was cooled to 0 °C and MsCl (1.1 mL, 14 mmol, 1.2 eq.) was added dropwise. The reaction mixture was stirred at 0 °C for 0.5 h, then warmed to rt and partitioned with H₂O (25 mL). The phases were separated and the aqueous phase was

* This compound and all derivatives slowly decomposed in mildly acidic solvents (e.g. CHCl₃) and should be stored in a freezer. N.b. the derived cycloadducts **181**, **183**, **184** were bench stable for weeks.

† Compound decomposed before HRMS could be performed.

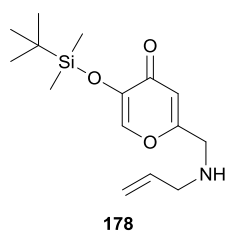
extracted with CH_2Cl_2 (25 mL). The combined organic phases were dried over MgSO_4 , filtered and concentrated *in vacuo* to give the *title compound* **176** (3.31 g, 9.89 mmol, 85% mass recovery) which was used subsequently without further purification. R_f 0.62 (1:1 petrol–EtOAc). $^1\text{H NMR}$ (300 MHz, CDCl_3 , characteristic peaks): δ 7.69 (1H, s, 6-H), 6.48 (1H, s, 3-H), 4.97 (2H, s, CH_2), 3.11 (3H, s, SO_2CH_3), 0.95 (9H, s, $\text{SiC}(\text{CH}_3)_3$), 0.23 (6H, s, $2 \times \text{SiCH}_3$).

2-[[bis(Prop-2-en-1-yl)amino]methyl]-5-[(*tert*-butyldimethylsilyl)oxy]-4H-pyran-4-one **177**



General procedure **S** was followed using mesylate **176** (650 mg, 1.95 mmol, 1.00 eq.) and diallylamine (0.48 mL, 3.9 mmol, 2.0 eq). Flash chromatography on cyanosilica, eluting with 0-50% EtOAc in pentane gave the *title compound* **177** (498 mg, 1.48 mmol, 76%) as a colourless oil. R_f 0.11 (95:5 petrol–EtOAc). $^1\text{H NMR}$ (500 MHz, CDCl_3): δ 7.64 (1H, s, 6-H), 6.40 (1H, s, 3-H), 5.87-5.77 (2H, m, $2 \times \text{NCH}_2\text{CH}=\text{CH}_2$), 5.23-5.15 (4H, m, $2 \times \text{CH}=\text{CH}_2$), 3.42 (2H, s, $\text{C}_q\text{CH}_2\text{N}$), 3.14 (4H, dt, J 6.3, 1.1, $2 \times \text{NCH}_2\text{CH}=\text{CH}_2$), 0.96 (9H, s, $\text{SiC}(\text{CH}_3)_3$), 0.23 (6H, s, $2 \times \text{SiCH}_3$). $^{13}\text{C NMR}$ (125 MHz, CDCl_3): δ 175.7 (4-C), 165.6 (2-C), 145.5 (5-C), 144.2 (6-C), 134.9 ($2 \times \text{CH}=\text{CH}_2$), 118.5 ($2 \times \text{CH}=\text{CH}_2$), 114.6 (3-C), 57.2 ($2 \times \text{NCH}_2\text{CH}=\text{CH}_2$), 54.2 ($\text{C}_q\text{CH}_2\text{N}$), 25.8 ($\text{SiC}(\text{CH}_3)_3$), 18.7 (SiC_q), -4.3 ($2 \times \text{SiCH}_3$). **IR** $\nu_{\text{max}}(\text{film})/\text{cm}^{-1}$ 2954, 2929, 2857, 1652 (CO), 1279, 1252, 1010, 922. **HRMS** (ESI): $\text{C}_{18}\text{H}_{30}\text{NO}_3\text{Si}$ $[\text{M}+\text{H}]^+$; calculated 336.1989, found 336.1994.

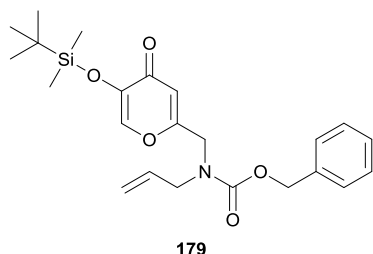
5-[(*tert*-Butyldimethylsilyl)oxy]-2-[[prop-2-en-1-yl]amino]methyl]-4H-pyran-4-one **178**



General procedure **S** was followed using mesylate **176** (10 g, 35 mmol, 1.0 eq.) and Et_3N (3.5 mL, 35 mmol) and allylamine (8.0 mL, 0.1 mol, 3.0 eq.). The residue was washed through a pad of silica with 9:1 EtOAc–MeOH to give the *title compound* **178** (5.9 g, 20.0 mmol, 56%) as a dark brown oil. R_f 0.57 (1:1 petrol–EtOAc). $^1\text{H NMR}$ (500 MHz, CDCl_3): δ 7.64 (1H, s, 6-H), 6.36 (1H, s, 3-H), 5.91-5.81 (1H, m, $\text{CH}=\text{CH}_2$), 5.20 (1H, app. dq, J 17.2, 1.4, $\text{CH}=\text{CH}_A\text{H}_B$), 5.14 (1H, ddd, J 10.3, 2.7, 1.4, $\text{CH}=\text{CH}_A\text{H}_B$), 3.62 (2H, s, $\text{C}_q\text{CH}_2\text{NH}$), 3.27 (2H, dt, J 6.0, 1.4, $\text{NHCH}_2\text{CH}=\text{CH}_2$), 0.96 (9H, s, $\text{SiC}(\text{CH}_3)_3$), 0.23 (6H, s,

2 × SiCH₃). ¹³C NMR (125 MHz, CDCl₃): δ 175.7 (4-C), 165.7 (2-C), 145.5 (5-C), 144.2 (6-C), 135.9 (CH=CH₂), 117.1 (CH=CH₂), 113.7 (3-C), 51.5 (CH₂CH=CH₂), 49.8 (C_qCH₂NH), 25.8 (SiC(CH₃)₃), 18.7 (SiC_q), -4.3 (2 × SiCH₃). IR ν_{max}(film)/cm⁻¹ 2954, 2930, 2857, 1651 (CO), 1232, 919, 879, 786. LRMS* (HPLC-MS): C₁₅H₂₅NO₃Si; found 296.1 [M+H]⁺.

Benzyl N-({5-[(*tert*-butyldimethylsilyl)oxy]-4-oxo-4*H*-pyran-2-yl)methyl}-N-(prop-2-en-1-yl)carbamate **179**



Method A (from amine **178):** Benzyl chloroformate (180 μL, 1.28 mmol, 2.6 eq.) was added to a stirred solution of the amine **178** (145 mg, 0.49 mmol, 1.0 eq.) and Et₃N (180 μL, 1.28 mmol, 2.6 eq.) in CH₂Cl₂ (5.0 mL) at 0 °C. The reaction mixture

warmed to rt and stirred for 15 h, then concentrated *in vacuo*. Flash chromatography eluting with 9:1 EtOAc–MeOH gave the *title compound* **179** (145 mg, 0.34 mmol, 69%) as a pale yellow oil.

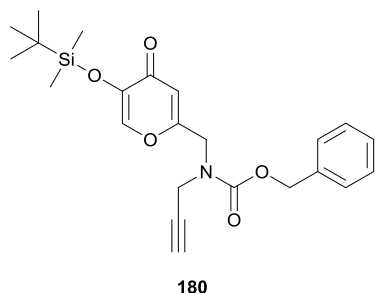
Method B (four-step telescoped procedure): Starting with kojic acid (5.0 g, 35 mmol) the procedure to prepare 5-[(*tert*-butyldimethylsilyl)oxy]-2-(hydroxymethyl)-4*H*-pyran-4-one **175** was followed. The crude silylated kojic acid **175** (35 mmol) was carried forward without further purification following the work-up. The procedure to prepare {5-[(*tert*-butyldimethylsilyl)oxy]-4-oxo-4*H*-pyran-2-yl)methyl methanesulfonate **176** was then followed. The crude mesylate **176** was carried on to the next step without further purification. General procedure **S** was followed using mesylate **176** (35 mmol) and allylamine (8.0 mL, 106 mmol, 3.00 eq.) to give crude amine **178**. General procedure **T** was followed using amine **178** (35 mmol). Flash chromatography eluting with 1:1 pentane–EtOAc gave the *title compound* **179** (4.4 g, 10 mmol, 29% [over four steps]) as a pale yellow oil.† R_f 0.82 (1:1 petrol–EtOAc). ¹H NMR (500 MHz, CDCl₃, 330 K): δ 7.56 (1H, s, 6-H), 7.39-7.27 (5H, m, Cbz Ar-H), 6.23 (1H, s, pyran 3-H), 5.81-5.70 (1H, m, CH=CH₂), 5.21-5.10 (4H, m, CH=CH₂ and CH₂Ph), 4.26 (2H, s, C_qCH₂NH), 3.96 (2H, s, NCH₂CH=CH₂), 0.97 (9H, s, SiC(CH₃)₃), 0.24 (6H, s, 2 × SiCH₃). ¹³C NMR (125 MHz, CDCl₃, 330 K): δ 175.3 (4-C), 163.3 (2-C), 156.1

* Compound decomposed before HRMS could be performed.

† This compound slowly decomposed in mildly acidic solvents (e.g. CHCl₃) and should be stored in a freezer.

(N(CO)O), 145.8 (5-C), 144.0 (6-C), 136.5 (CH=CH₂), 132.9 (Ar-C_q), 128.7 (Ar-C), 128.4 (Ar-C), 128.2 (Ar-C), 118.2 (CH=CH₂), 113.7 (3-C), 65.6 (CH₂Ph), 50.3 (CH₂CH=CH₂), 47.6 (C_qCH₂NH), 25.8 (SiC(CH₃)₃), 18.7 (SiC_q), -4.3 (2 × SiCH₃). IR ν_{max} (film)/cm⁻¹ 2953, 2929, 2857, 1702 (CO), 1649, 1460, 1410, 1210. HRMS (ESI): C₂₃H₃₂NO₅Si [M+H]⁺; calculated 430.2058, found 430.2044.

Benzyl N-({5-[(*tert*-butyldimethylsilyl)oxy]-4-oxo-4*H*-pyran-2-yl)methyl)-N-(prop-2-yn-1-yl)carbamate **180**

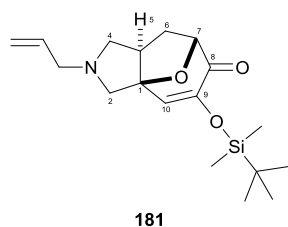


Starting with kojic acid (5.0 g, 35 mmol) the procedure to prepare 5-[(*tert*-butyldimethylsilyl)oxy]-2-(hydroxymethyl)-4*H*-pyran-4-one **175** was followed. The crude silylated kojic acid **175** (35 mmol) was carried forward without further purification following the work-up. The procedure to prepare {5-[(*tert*-butyldimethylsilyl)oxy]-4-oxo-4*H*-pyran-2-yl)methyl methanesulfonate **176** was then followed. The crude mesylate **176** was carried on to the next step without further purification. General procedure **S** was followed using mesylate **176** (35 mmol) and propargylamine (6.8 mL, 106 mmol, 3.00 eq.) to give the crude amine **S2** [characteristic **¹H NMR** peaks (300 MHz, CDCl₃): δ 7.65 (1H, s, 6-H), 6.39 (1H, s, 3-H), 3.73 (2H, s, C_qCH₂N), 3.47 (2H, d, *J* 2.4, NCH₂C≡CH), 2.27 (1H, t, *J* 2.4, C≡CH), 0.95 (9H, s, SiC(CH₃)₃), 0.23 (6H, s, 2 × SiCH₃)]. General procedure **T** was followed using amine **S2** (35 mmol). Flash chromatography eluting with 1:1 pentane–EtOAc gave the *title compound* **180** (2.7 g, 6.3 mmol, 18% [over four steps]) as a pale yellow oil.* **R_f** 0.20 (4:1 petrol–EtOAc). **¹H NMR** (500 MHz, CDCl₃, 329 K): δ 7.57 (1H, s, 6-H), 7.38–7.29 (5H, m, Cbz Ar-H), 6.28 (1H, s, 3-H), 5.19 (2H, s, OCH₂Ph), 4.42 (2H, s, C_qCH₂N), 4.18 (2H, br. s, NCH₂C≡CH), 2.26 (1H, t, *J* 2.5, C≡CH), 0.97 (9H, s, SiC(CH₃)₃), 0.24 (6H, s, 2 × SiCH₃). **¹³C NMR** (125 MHz, CDCl₃, 329 K): δ 175.3 (4-C), 162.7 (2-C), 155.5 (N(CO)O), 145.9 (5-C), 144.0 (6-C), 136.2 (Ar-C_q), 128.8 (Ar-C), 128.5 (Ar-C), 128.3 (Ar-C), 114.0 (3-C), 78.1 (CH₂C≡CH), 73.3 (CH₂C≡CH), 68.5 (CH₂Ph), 47.5 (C_qCH₂N), 37.2 (CH₂C≡CH), 25.9 (SiC(CH₃)₃), 18.7 (SiC_q), -4.3 (2 × SiCH₃). IR ν_{max} (film)/cm⁻¹ 2953, 2930, 2857, 1708 (CO), 1650, 1498,

* This compound slowly decomposed in mildly acidic solvents (e.g. CHCl₃) and should be stored in a freezer.

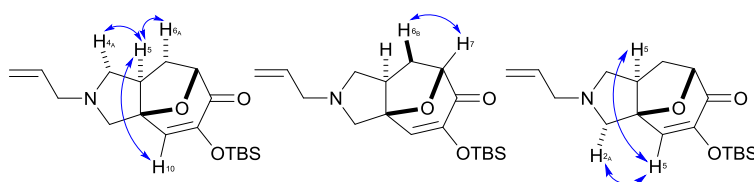
1455, 1216. **HRMS** (ESI): C₂₃H₃₀NO₅Si [M+H]⁺; calculated 428.1888, found 428.1889.

(1R*,5S*,7S*)-9-[(*tert*-Butyldimethylsilyl)oxy]-3-(prop-2-en-1-yl)-11-oxa-3-azatricyclo[5.3.1.0^{1,5}]undec-9-en-8-one **181**



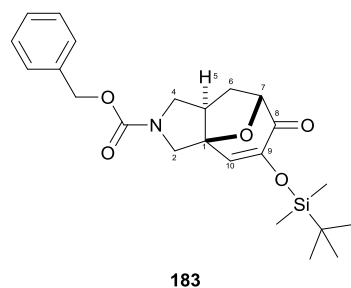
General procedure **U** was followed using amine **177** (174 mg, 0.520 mmol), which was heated at 140 °C under microwave irradiation for 2 h. Flash chromatography eluting with 0-100% EtOAc in pentane gave the *title compound* **181** (127 mg, 0.379 mmol, 73%) as a colourless

oil. *R_f* 0.31 (1:1 petrol–EtOAc). **¹H NMR** (500 MHz, CDCl₃): δ 6.46 (1H, s, 10-H), 5.95-5.85 (1H, m, CH₂CH=CH₂), 5.21 (1H, dd, *J* 17.1, 1.3, CH₂CH=CH_AH_B), 5.13 (1H, d, *J* 10.0, CH₂CH=CH_AH_B), 4.76 (1H, d, *J* 8.0, 7-H), 3.21-3.12 (2H, m, CH₂CH=CH₂), 3.08-2.98 (2H, m, includes at δ 3.04, 1H, d, *J* 11.2, 2-H_A; and at δ 3.00, 1H, d, *J* 8.5, 4-H_A), 2.86 (1H, d, *J* 11.2, 2-H_B), 2.75-2.67 (1H, m, 5-H), 2.39 (1H, app. t, *J* 8.5, 4-H_B), 2.20-2.08 (1H, m, 6-H_B), 1.86 (1H, dd, *J* 13.1, 8.7, 6-H_A), 0.93 (9H, s, SiC(CH₃)₃), 0.15 (6H, s, 2 × SiCH₃). **¹³C NMR** (125 MHz, CDCl₃): δ 194.3 (8-C), 147.7 (9-C), 134.9 (10-C), 131.1 (CH=CH₂), 118.1 (CH=CH₂), 90.7 (1-C), 84.3 (7-C), 61.5 (2-C), 59.6 (4-C), 58.7 (CH₂CH=CH₂), 49.0 (5-C), 30.7 (6-C), 25.7 (SiC(CH₃)₃), 18.5 (SiC_q), -4.6 (2 peaks, 2 × SiCH₃). **IR** *v*_{max}(film)/cm⁻¹ 2952, 2929, 2857, 1702 (CO), 1613, 1471, 1341, 1252. **HRMS** (ESI): C₁₈H₃₀NO₃Si [M+H]⁺; calculated 336.1989, found 336.1990.



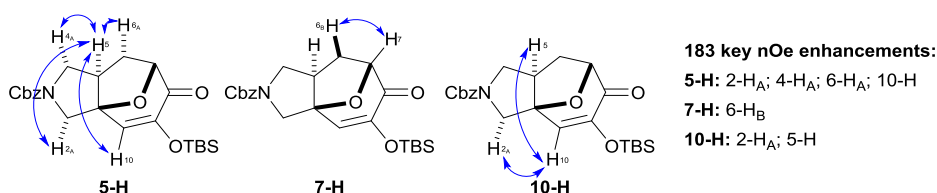
181 key nOe enhancements:
5-H: 4-H_A; 6-H_A; 10-H
7-H: 6-H_B
10-H: 2-H_A; 5-H

Benzyl (1R*,5S*,7S*)-9-[(*tert*-butyldimethylsilyl)oxy]-8-oxo-11-oxa-3-zatricyclo[5.3.1.0^{1,5}]undec-9-ene-3-carboxylate **183**

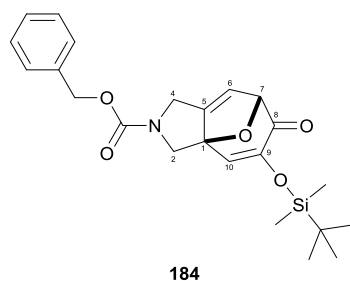


General procedure **U** was followed using carbamate **179** (1.0 g, 2.3 mmol), which was heated at 140 °C under microwave irradiation for 6 h. Flash chromatography eluting with EtOAc gave the *title compound* **183** (890 mg, 2.05 mmol, 89%) as a colourless amorphous solid. **M.p.** 96-98 °C, colourless

plates, hexane–EtOAc. R_f 0.18 (4:1 petrol–EtOAc). $^1\text{H NMR}$ (500 MHz, CDCl_3 , 50:50 mixture of rotamers): δ 7.41–7.29 (5H, m, Cbz Ar-H), 6.29 (0.5H, s, 10-H), 6.26 (0.5H, s, 10-H), 5.15 (1H, d, J 12.0, $\text{OCH}_A\text{H}_B\text{Ph}$), 5.12 (1H, d, J 12.0, $\text{OCH}_A\text{H}_B\text{Ph}$), 4.78 (1H, d, J 8.2, 7-H), 4.04–3.90 (2H, m, 2- H_B and 4- H_A), 3.68 (0.5H, d, J 12.8, 2- H_A), 3.64 (0.5H, d, J 12.8, 2- H_A), 3.22–3.13 (1H, m, 4- H_B), 2.84–2.74 (1H, m, 5-H), 2.34–2.21 (1H, m, 6- H_B), 1.89 (1H, td, J 13.2, 8.2, 6- H_A), 0.94 (4H, s, $\text{SiC}(\text{CH}_3)_3$), 0.93 (5H, s, $\text{SiC}(\text{CH}_3)_3$), 0.16 (6H, m, 2 \times SiCH_3). $^{13}\text{C NMR}$ (125 MHz, CDCl_3 , mixture of two rotamers): δ 193.7 (8-C), 154.5 (N(CO)O), 154.3 (N(CO)O), 148.1 (9-C), 136.8 (Ar 1-C), 138.7 (Ar 1-C), 128.7 (Ar-C), 128.3 (Ar-C), 128.2 (Ar-C), 128.1 (Ar-C), 127.3 (10-C), 127.2 (10-C), 90.6 (1-C), 89.8 (1-C), 83.4 (7-C), 67.2 (OCH_2Ph), 53.9 (2-C or 4-C), 53.5 (2-C or 4-C), 53.1 (2-C or 4-C), 52.7 (2-C or 4-C), 47.1 (5-C), 46.2 (5-C), 31.6 (6-C), 31.5 (6-C), 25.7 ($\text{SiC}(\text{CH}_3)_3$), 18.6 (SiC_q), -4.5 (2 \times SiCH_3) [27 of 36 expected peaks observed]. IR $\nu_{\text{max}}(\text{film})/\text{cm}^{-1}$ 2954, 2953, 1703 (CO), 1652, 1419, 1347, 1163, 919. HRMS (ESI): $\text{C}_{23}\text{H}_{32}\text{NO}_5\text{Si}$ [$\text{M}+\text{H}$] $^+$; calculated 430.2044, found 430.2048.



Benzyl (1*R,7*R**)-9-[(*tert*-butyldimethylsilyl)oxy]-8-oxo-11-oxa-3-azatricyclo[5.3.1.0^{1,5}]undeca-5,9-diene-3-carboxylate **184****

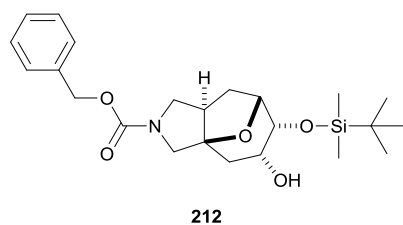
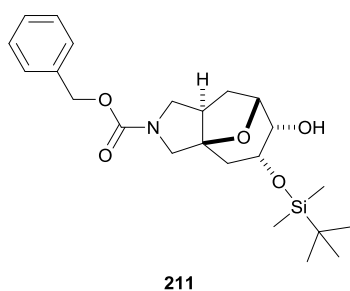


General procedure **U** was followed using carbamate **180** (377 g, 0.88 mmol), which was heated at 180 °C under microwave irradiation for 6 h. Flash chromatography eluting with 0–100% EtOAc in pentane gave the *title compound* **184** (240 mg, 0.56 mmol, 64%) as a colourless powder. R_f 0.39

(4:1 petrol–EtOAc). $^1\text{H NMR}$ (500 MHz, CDCl_3 , 329 K): δ 7.40–7.30 (5H, m, Cbz Ar-H), 6.36 (1H, s, 10-H), 6.04 (1H, s, 6-H), 5.19 (2H, s, OCH_2Ph), 5.17–5.15 (1H, m, 7-H), 4.25 (1H, d, J 16.7, 2- H_A), 4.14 (1H, app. dd, J 16.7, 1.4, 2- H_B), 4.05–3.87 (1H, m, 4- H_A), 3.51 (1H, d, J 11.3, 4- H_B), 0.94 (9H, s, $\text{SiC}(\text{CH}_3)_3$), 0.17 (3H, s, SiCH_3), 0.16 (3H, s, SiCH_3). $^{13}\text{C NMR}$ (125 MHz, CDCl_3 , mixture of two rotamers): δ 190.8 (2 peaks, 8-C), 156.4 (9-C), 155.6 (9-C), 154.7 (N(CO)O), 154.5 (N(CO)O), 143.7 (5-C), 136.3 (Ar- C_q), 128.6 (Ar-C), 128.3 (Ar-C),

128.1 (Ar-C), 127.5 (10-C), 127.4 (10-C), 118.0 (6-C), 93.9 (7-C), 92.2 (1-C), 91.4 (1-C), 67.4 (OCH₂Ph), 51.9 (2 peaks, 4-C), 43.6 (2-C), 43.5 (2-C), 25.5 (SiC(CH₃)₃), 18.4 (SiC_q), -4.6 (SiCH₃), -4.7 (SiCH₃) [26 of 36 expected peaks observed]. IR ν_{max} (film)/cm⁻¹ 2955, 2930, 2887, 2856, 1704, 1606, 1412, 1358. HRMS (ESI): C₂₃H₃₀NO₅Si [M+H]⁺; calculated 428.1888, found 428.1889.

Benzyl (1*R,5*R**,7*R**,8*S**,9*R**)-9-[(*tert*-butyldimethylsilyl)oxy]-8-hydroxy-11-oxa-3-azatricyclo[5.3.1.0^{1,5}]undecane-3-carboxylate **211** and benzyl (1*R**,5*R**,7*R**,8*R**,9*R**)-8-[(*tert*-butyldimethylsilyl)oxy]-9-hydroxy-11-oxa-3-azatricyclo[5.3.1.0^{1,5}]undecane-3-carboxylate **212****

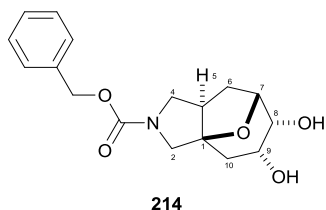


NaBH₄ (44 mg, 1.2 mmol, 2.0 eq.) was added to a stirred solution of cycloadduct **183** (250 mg, 0.58 mmol, 1.0 eq.) in MeOH (10 mL) at 0 °C. The reaction mixture was stirred at 0 °C for 0.5 h. H₂O (1 mL) was added and the reaction mixture was warmed to rt. The reaction mixture was concentrated *in vacuo* to give a colourless oil which was carried on to the next step without further purification [*R*_f 0.29 and 0.45 (7:3 pentane–EtOAc). Characteristic ¹H NMR peaks (500 MHz,

CDCl₃, 40:60* mixture of regioisomers): δ 7.38-7.28 (major and minor, 5H, m, Cbz Ar-H), 5.15-5.07 (major and minor, 2H, m, OCH₂Ph), 4.36 (minor, 0.4H, dd, *J* 7.3, 4.6), 4.25-4.20 (major, 0.6H, dd, *J* 6.9, 5.2), 4.13-4.09 (minor, 0.4H, m), 3.98-3.93 (major, 0.6H, m), 3.93-3.86 (major and minor, 1H, m), 3.84-3.79 (major, 0.6H, m), 3.77-3.68 (major and minor, 1.4H, m), 3.44-3.32 (major and minor, 1H, m), 3.24-3.13 (major and minor, 1H, m), 3.09-3.01 (major, 0.6H, m), 2.95-2.86 (minor, 0.4H, m), 2.77 (major, 0.6H, d, *J* 4.5), 2.62 (major, 0.6H, td, *J* 13.2, 8.5), 2.57-2.50 (minor, 0.4H, m), 2.49 (minor, 0.4H, d, *J* 10.6), 2.24-2.10 (major, 0.6H, m), 2.07 (minor, 0.4H, dd, *J* 14.6, 3.7), 1.98 (major, 0.6H, dd, *J* 14.5, 7.9), 1.80 (minor, 0.4H, dd, *J* 14.6, 9.3), 1.76-1.56 (major and minor, 1H, m), 0.94 (minor, 3.6H, s, SiC(CH₃)₃), 0.91 (major, 5.4H, s, SiC(CH₃)₃), 0.13-0.10 (major and minor, 6H, m, SiCH₃).

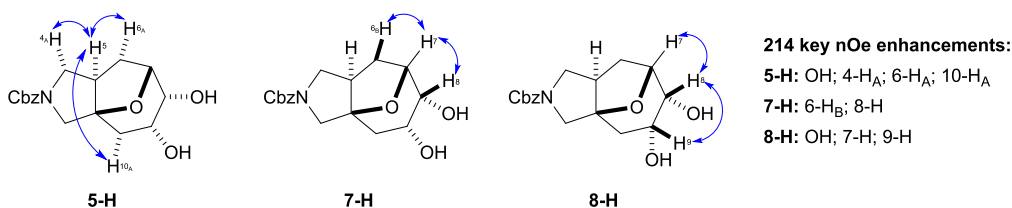
* The identity of the major/minor regioisomers (with respect to the structures **211/212**) has not been determined.

Benzyl (1*R,5*R**,7*R**,8*R**,9*R**)-8,9-dihydroxy-11-oxa-3-azatricyclo[5.3.1.0^{1,5}]undecane-3-carboxylate **214****

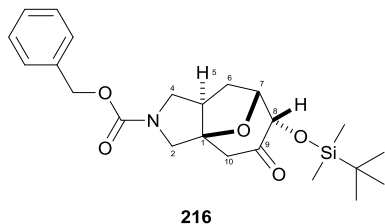


TBAF (1.0 M in THF, 1.2 mL, 1.2 mmol, 2.0 eq.) was added to a stirred solution of the crude silylated alcohols **211-212** (0.58 mmol) in THF. The reaction mixture was stirred for 2 h then concentrated *in vacuo*.

Flash chromatography eluting with 0-10% MeOH in EtOAc gave a mixture of the title compound with TBAF. Further purification by SCX following general procedure **R**, eluting with MeOH gave the *title compound* **214** (76 mg, 0.24 mmol, 41%) as a colourless oil. R_f 0.58 (9:1 EtOAc–MeOH). $^1\text{H NMR}$ (500 MHz, CDCl_3 , 50:50 mixture of rotamers): δ 7.41-7.27 (5H, m, Cbz Ar-H), 5.11 (2H, s, CH_2Ph), 4.35 (1H, dd, J 7.2, 4.8, 7-H), 4.15-4.10 (1H, m, 9-H), 3.93-3.85 (1H, m, includes at δ 3.91: 0.5H, d, J , 10.5; and at δ 3.87: 0.5H, d, J , 10.5, 4- H_A), 3.86-3.80 (1H, m, 8-H), 3.79-3.71 (1H, m, includes at δ 3.76: 0.5H, d, J , 12.6; and at δ 3.74: 0.5H, d, J , 12.6, 2- H_A), 3.41 (0.5H, d, J 12.6, 2- H_B), 3.36 (0.5H, d, J 12.6, 2- H_B), 3.24-3.15 (1H, m, 4- H_B), 3.08-3.00 (1H, m, 5-H), 2.63 (1H, td, J 12.7, 8.5, 6- H_A), 2.49 (2H, br. s, 2 x OH), 2.19 (0.5H, dd, J 14.7, 4.3, 10- H_B), 2.13 (0.5H, dd, J 14.7, 4.3, 10- H_B), 1.97-1.90 (1H, m, includes at δ 1.95: 0.5H, d, J 14.7; and at δ 1.93: 0.5H, d, J 14.7, 10- H_A), 1.78-1.66 (1H, m, 6- H_B). $^{13}\text{C NMR}$ (125 MHz, d^6 -DMSO, mixture of two rotamers): δ 153.5 (N(CO)O), 153.4 (N(CO)O), 137.1 (Ar- C_q), 128.4 (Ar-C), 127.7 (Ar-C), 127.5 (Ar-C), 88.7 (1-C), 87.7 (1-C), 79.0 (7-C), 68.0 (8-C), 65.9 (9-C), 65.7 (CH_2Ph), 54.8 (2-C or 4-C), 54.5 (2-C or 4-C), 54.2 (2-C or 4-C), 54.0 (2-C or 4-C), 44.2 (5-C), 43.2 (5-C), 38.0 (10-C), 37.9 (10-C), 32.7 (6-C), 32.6 (6-C) [22 of 30 expected peaks observed]. $\text{IR } \nu_{\text{max}}(\text{film})/\text{cm}^{-1}$ 3423 (OH), 2948, 2884, 1683 (CO), 1425, 1350, 1149, 1107. HRMS (ESI): $\text{C}_{17}\text{H}_{22}\text{NO}_5$ $[\text{M}+\text{H}]^+$; calculated 320.1495, found 320.1496.

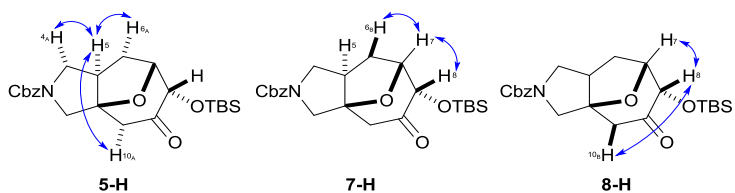


Benzyl (1*R,5*R**,7*R**,8*S**)-8-[(*tert*-butyldimethylsilyl)oxy]-9-oxo-11-oxa-3-azatricyclo[5.3.1.0^{1,5}]undecane-3-carboxylate **216****



L-Selectride® (1.0 M in THF, 0.25 mL, 0.25 mmol, 1.1 eq.) was added dropwise to a stirred solution of cycloadduct **183** (100 mg, 0.230 mmol, 1.00 eq.) in THF (10 mL) at $-78\text{ }^{\circ}\text{C}$. The reaction mixture was stirred for 3.5 h at $-78\text{ }^{\circ}\text{C}$, then quenched with sat.

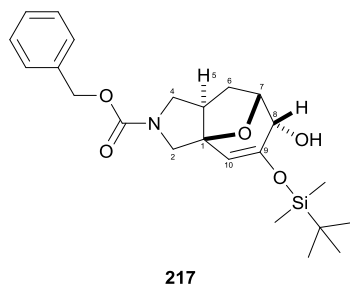
aq. NH_4Cl (1 mL). The reaction mixture was warmed to rt then concentrated *in vacuo*. The resulting residue was dissolved in EtOAc (25 mL) and washed with brine (25 mL). The aqueous phase was extracted with EtOAc (2 \times 10 mL). The combined organic extracts were dried over MgSO_4 , filtered and concentrated *in vacuo*. Flash chromatography eluting with 0-100% EtOAc in pentane gave the *title compound* **216** (61 mg, 0.14 mmol, 61%) as a colourless oil. R_f 0.77 (3:2 petrol–EtOAc). $^1\text{H NMR}$ (500 MHz, CDCl_3 , 50:50 mixture of rotamers): δ 7.38-7.28 (5H, m, Cbz Ar-H), 5.13 (1H, d, J 11.7, $\text{CH}_A\text{H}_B\text{Ph}$), 5.11 (1H, d, J 11.7, $\text{CH}_A\text{H}_B\text{Ph}$), 4.56 (1H, app. t, J 6.4, 7-H), 4.24-4.19 (1H, m, 8-H), 3.95-3.86 (2H, m, 2- H_A and 4- H_A), 3.44 (0.5H, d, J 12.7, 2- H_B), 3.39 (0.5H, d, J 12.7, 2- H_B), 3.21-3.11 (1H, m, 4- H_B), 2.87 (0.5H, dd, 15.1, 10- H_B), 2.86 (0.5H, dd, 15.1, 10- H_B), 2.60-2.50 (1H, m, 5-H), 2.44 (1H, m, includes at δ 2.45: d, J 15.1; and at δ 2.44: d, J 15.1, 10- H_A), 2.20 (1H, td, J 15.0, 8.6, 6- H_A), 1.92-1.79 (1H, m, 6- H_B), 0.89 (9H, s, $\text{SiC}(\text{CH}_3)_3$), 0.14 (3H, s, SiCH_3), 0.04 (3H, s, SiCH_3). $^{13}\text{C NMR}$ (125 MHz, CDCl_3 , mixture of two rotamers): δ 204.6 (9-C), 154.4 (N(CO)O), 136.8 (Ar- C_q), 128.6 (Ar-C), 128.2 (Ar-C), 128.1 (Ar-C), 91.5 (1-C), 90.7 (1-C), 80.8 (7-C), 77.6 (8-C), 67.2 (CH_2Ph), 54.2 (2-C or 4-C), 53.9 (2-C or 4-C), 48.7 (10-C), 45.9 (5-C), 45.0 (5-C), 31.9 (6-C), 31.7 (6-C), 25.9 ($\text{SiC}(\text{CH}_3)_3$), 18.5 (SiC_q), -4.5 (SiCH_3), -5.3 (SiCH_3) [22 of 38 expected peaks observed]. $\text{IR } \nu_{\text{max}}(\text{film})/\text{cm}^{-1}$ 2953, 2856, 1701 (CO), 1417, 1347, 1251, 1104, 836. HRMS (ESI): $\text{C}_{23}\text{H}_{34}\text{NO}_5\text{Si}$ $[\text{M}+\text{H}]^+$; calculated 432.2201, found 432.2205.



216 key nOe enhancements:

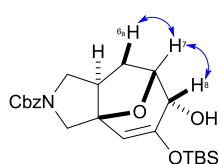
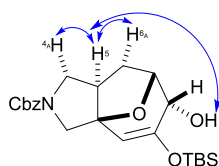
- 5-H:** 4- H_A ; 6- H_A ; 10- H_A
- 7-H:** 6- H_B ; 8-H
- 8-H:** 7-H; 10- H_B

Benzyl (1*R,5*S**,7*S**,8*R**)-9-[(*tert*-butyldimethylsilyl)oxy]-8-hydroxy-11-oxa-3-azatricyclo[5.3.1.0^{1,5}]undec-9-ene-3-carboxylate **217****



NaBH₄ (9 mg, 0.23 mmol, 1.0 eq.) was added to a stirred solution of cycloadduct **183** (100 mg, 0.23 mmol, 1.00 eq.) and CeCl₃·7H₂O (95 mg, 0.25 mmol, 1.1 eq.) in 2:1 CH₂Cl₂–MeOH (9 mL). The reaction mixture was stirred for 0.5 h. H₂O (0.5 mL) was added then the mixture was concentrated *in vacuo*.

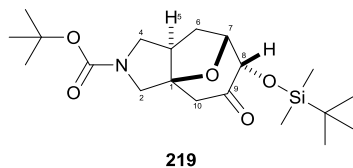
The resulting residue was diluted in EtOAc (30 mL) and washed with brine (20 mL). The aqueous phase was extracted with EtOAc (2 × 10 mL). The combined organic phase was dried over MgSO₄, filtered and concentrated *in vacuo*. Flash chromatography eluting with 0–10% MeOH in EtOAc gave the *title compound* **217** (80 mg, 0.19 mmol, 81%) as a colourless oil. **¹H NMR** (500 MHz, CDCl₃, 50:50 mixture of rotamers): δ 7.38–7.27 (5H, m, Cbz Ar-H), 5.13 (1H, app. dd, *J* 12.5, 1.8, CH_AH_BPh), 5.10 (1H, d, *J* 12.5, CH_AH_BPh), 4.99 (0.5H, s, 10-H), 4.99 (0.5H, s, 10-H), 4.70 (1H, app. t, *J* 6.4, 7-H), 4.51 (1H, app. t, *J* 5.4, 8-H), 3.86–3.75 (2H, m, 2-H_B and 4-H_A), 3.43 (0.5H, d, *J* 12.6, 2-H_A), 3.38 (0.5H, d, *J* 12.6, 2-H_A), 3.12 (0.5H, d, *J* 10.5, 4-H_B), 3.08 (0.5H, d, *J* 10.5, 4-H_B), 2.75–2.65 (1H, m, 5-H), 2.57–2.49 (1H, m, 6-H_A), 2.35–2.26 (1H, m, OH), 1.87 (0.5H, dd, *J* 13.6, 7.6, 6-H_B), 1.82 (0.5H, dd, *J* 13.6, 7.6, 6-H_B), 0.94 (4.5H, SiC_q(CH₃)₃), 0.93 (4.5H, SiC(CH₃)₃), 0.21–0.16 (6H, m, 2 × SiCH₃). **¹³C NMR** (125 MHz, *d*⁶-DMSO, mixture of two rotamers): 153.6 (N(CO)O), 153.5 (N(CO)O), 151.8 (2 peaks, 9-C), 137.0 (Ar-C_q), 128.4 (Ar-C), 127.7 (Ar-C), 127.5 (2 peaks, Ar-C), 107.3 (10-C), 107.2 (10-C), 88.2 (1-C), 87.3 (1-C), 79.0 (7-C), 67.9 (8-C), 65.8 (2 peaks, CH₂Ph), 53.1 (2-C or 4-C), 52.7 (2-C or 4-C), 52.6 (2-C or 4-C), 52.2 (2-C or 4-C), 49.5 (5-C), 48.5 (5-C), 28.1 (6-C), 25.6 (SiC(CH₃)₃), 17.9 (SiC_q), –4.4 (2 peaks, SiCH₃), –4.6 (SiCH₃), –4.7 (SiCH₃) [30 of 38 expected peaks observed]. **IR** *v*_{max}(film)/cm^{–1} 3443, (OH), 2952, 2884, 2857, 1686 (CO), 1650, 1419, 1358. **HRMS** (ESI): C₂₃H₃₄NO₅Si [M+H]⁺; calculated 432.2201, found 432.2200.



217 key nOe enhancements:

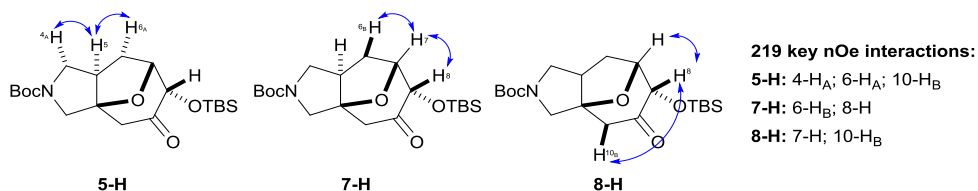
- OH:** 6-H_B; 8-H
- 5-H:** OH, 4-H_A; 6-H_A
- 7-H:** 6-H_B; 8-H
- 8-H:** OH; 7-H

tert*-Butyl (1*R**,5*R**,7*R**,8*S**)-8-[(*tert*-butyldimethylsilyl)oxy]-9-oxo-11-oxa-3-azatricyclo[5.3.1.0^{1,5}]undecane-3-carboxylate **219*

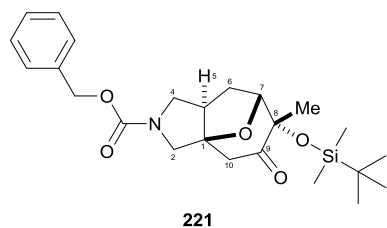


A stirred solution of cycloadduct **183** (100 mg, 0.230 mmol, 1.00 eq.) and 10% Pd/C (10 mg) in MeOH (10 mL) was exposed to an atmosphere of H₂ (balloon) for 24 h. The reaction mixture was filtered through Celite then concentrated *in vacuo* to give amine **218** (69 mg) [characteristic ¹H NMR peaks (300 MHz, CDCl₃): δ 4.49 (1H, t, *J* 6.3), 4.16 (1H, d, *J* 5.9), 3.27 (1H, d, *J* 12.7), 3.09 (1H, dd, *J* 12.0, 8.4), 2.85 (1H, d, *J* 14.8), 2.72 (1H, dd, *J* 12.1, 3.6), 2.63 (1H, d, *J* 12.7), 2.51-2.38 (3H, m), 2.37-2.19 (1H, m), 1.77-1.61 (1H, m), 0.89 (9H, s, SiC(CH₃)₃), 0.14 (3H, s, Si(CH₃)_A), 0.03 (3H, s, Si(CH₃)_B)]. Boc₂O (53 mg, 0.24 mmol, 1.1 eq.) Et₃N (0.1 mL, 0.7 mmol, 3.0 eq.) and DMAP (5 mg, 0.04 mmol, 0.17 eq.) were added to a stirred solution of the crude amine **218** (0.23 mmol) in CH₂Cl₂ (10 mL). The reaction mixture was stirred for 15 h then concentrated *in vacuo*.^{*} Flash chromatography eluting with 0-100% EtOAc in pentane gave the *title compound* **219** (48 mg, 0.12 mmol, 52%) as a colourless oil. *R_f* 0.85 (89:11 petrol–EtOAc). ¹H NMR (500 MHz, CDCl₃, 50:50 mixture of rotamers): δ 4.56 (1H, app. t, *J* 6.3, 7-H), 4.25-4.17 (1H, m, 8-H), 3.88-3.74 (2H, m, 2-H_B and 4-H_A), 3.38 (0.5H, d, *J* 12.5, 2-H_A), 3.32 (0.5H, d, *J* 12.5, 2-H_A), 3.13-3.01 (1H, m, 4-H_B), 2.86 (0.5H, d, *J* 15.2, 10-H_B), 2.81 (0.5H, d, *J* 15.2, 10-H_B), 2.57-2.47 (1H, m, 5-H), 2.44 (1H, d, *J* 15.2, 10-H_A), 2.24-2.14 (1H, m, 6-H_A), 1.91-1.78 (1H, m, 6-H_B), 1.45 (9H, s, OC(CH₃)₃), 0.90 (9H, s, SiC(CH₃)₃), 0.14 (3H, s, SiCH₃), 0.04 (3H, s, SiCH₃). ¹³C NMR (125 MHz, CDCl₃, mixture of two rotamers): δ 204.7 (9-C), 153.9 (N(CO)O), 91.5 (1-C), 90.7 (1-C), 80.7 (7-C), 79.8 (C_q^tBu), 77.5 (8-C), 54.0 (2-C or 4-C), 53.7 (2-C or 4-C), 48.7 (10-C), 45.7 (5-C), 44.8 (5-C), 31.8 (6-C), 31.5 (6-C), 28.5 (OC(CH₃)₃), 25.7 (SiC(CH₃)₃), 18.4 (SiC_q), -4.6 (SiCH₃), -5.4 (SiCH₃) [19 of 32 expected peaks observed]. IR *v*_{max}(film)/cm⁻¹ 2955, 2930, 2886, 2857, 1732, 1697 (CO), 1402, 1365. HRMS (ESI): C₂₀H₃₅NNaO₅Si [M+Na]⁺; calculated 420.2177, found 420.2180.

^{*} n.b. incomplete conversion.

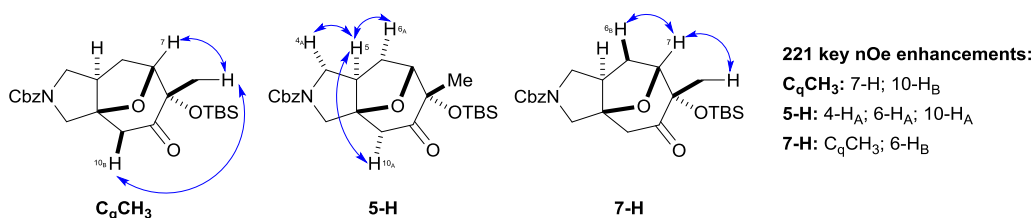


Benzyl (1*R,5*R**,7*R**,8*S**)-8-[(*tert*-butyldimethylsilyl)oxy]-8-methyl-9-oxo-11-oxa-3-azatricyclo[5.3.1.0^{1,5}]undecane-3-carboxylate **221****

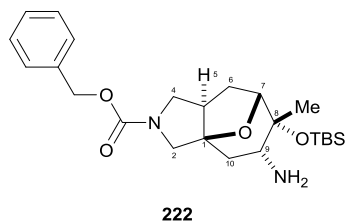


MeLi (1.6 M in Et₂O, 0.37 mL, 0.60 mmol, 1.30 eq.) was added to a stirred solution of cycloadduct **183** (200 mg, 0.460 mmol, 1.00 eq.) in THF (15 mL) at -78 °C. The reaction mixture was stirred at this temperature for 0.5 h, then sat. aq. brine (1 mL). The

reaction mixture was warmed to rt, then partitioned between EtOAc (25 mL) and brine (25 mL). The aqueous phase was extracted with EtOAc (2 × 10 mL). The combined organic extracts were dried, filtered and concentrated *in vacuo*. Flash chromatography eluting with 95:5 pentane–EtOAc gave the *title compound* **221** (187 mg, 0.420 mmol, 91%) as a yellow oil. *R_f* 0.30 (3:1 petrol–EtOAc). **¹H NMR** (500 MHz, CDCl₃, 50:50 mixture of rotamers): δ 7.39-7.28 (5H, m, Cbz Ar-H), 5.12 (2H, s, OCH₂Ph), 4.21-4.15 (1H, m, 7-H), 3.95-3.83 (2H, m, 2-H_B and 4-H_A), 3.43 (0.5H, d, *J* 12.6, 2-H_A), 3.38 (0.5H, d, *J* 12.6, 2-H_A), 3.20-3.09 (1H, m, 4-H_B), 2.92 (0.5H, d, *J* 15.3, 10-H_B), 2.86 (0.5H, d, *J* 15.3, 10-H_B), 2.55-2.46 (1H, m, 5-H), 2.37 (0.5H, d, *J* 3.3, 10-H_A), 2.34 (0.5H, d, *J* 3.3, 10-H_A), 2.27-2.14 (1H, m, 6-H_A), 1.91-1.76 (1H, m, 6-H_B), 1.46 (1.5H, s, C_qCH₃), 1.45 (1.5H, s, C_qCH₃), 0.85 (9H, s, SiC(CH₃)₃), 0.17 (3H, s, SiCH₃), 0.13 (3H, s, SiCH₃). **¹³C NMR** (125 MHz, CDCl₃, mixture of two rotamers): δ 208.0 (9-C), 207.9 (9-C), 154.4 (N(CO)O), 136.8 (Ar-C_q), 128.6 (Ar-C), 128.2 (Ar-C), 128.12 (Ar-C), 91.5 (1-C), 90.7 (1-C), 85.4 (7-C), 81.4 (8-C), 67.1 (OCH₂Ph), 54.2 (2-C or 4-C), 53.8 (2-C or 4-C), 53.7 (2-C or 4-C), 47.3 (10-C), 45.7 (5-C), 44.8 (5-C), 31.7 (6-C), 31.4 (6-C), 26.0 (SiC(CH₃)₃), 24.4 (C_qCH₃), 18.5 (SiC_q), -2.3 (SiCH₃), -2.6 (SiCH₃) [25 of 38 expected peaks observed]. **IR** *v*_{max}(film)/cm⁻¹ 2954, 2953, 2930, 2887, 1702 (CO), 1629, 1593, 1419 **HRMS** (ESI): C₂₄H₃₆NO₅Si [M+H]⁺; calculated 446.2357, found 446.2360.



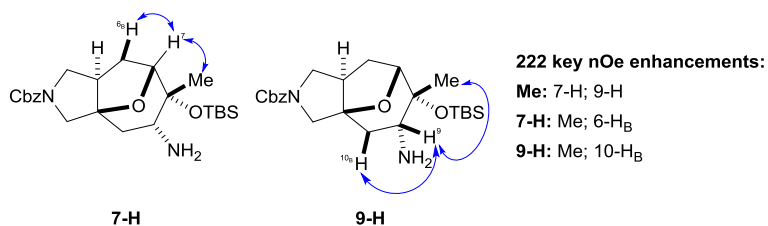
Benzyl (1*R,5*R**,7*R**,8*R**,9*R**)-9-amino-8-[(*tert*-butyldimethylsilyl)oxy]-8-methyl-11-oxa-3-azatricyclo[5.3.1.0^{1,5}]undecane-3-carboxylate **222****



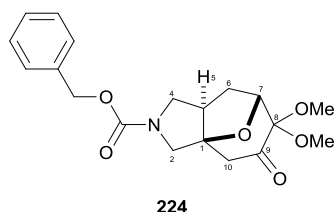
Ti(O^{*i*}Pr)₄ (0.27 mL, 0.92 mmol, 2.0 eq.) was added to a stirred solution of ketone **221** (204 mg, 0.46 mmol, 1.00 eq.) in sat. NH₃/MeOH. The reaction mixture was stirred for 15 h then NaBH₄ (26 mg, 0.7 mmol, 1.5 eq.) was added at 0 °C. The reaction mixture was warmed

to rt, stirred for 2 h then concentrated *in vacuo*. The residue was diluted in EtOAc (10 mL) and sat. aq. brine (10 mL) and stirred vigorously. The phases were separated and the aqueous phase was extracted with EtOAc (2 × 10 mL). The combined organic phase was dried over MgSO₄, filtered, and concentrated *in vacuo*. Flash chromatography eluting with 0-10% MeOH in EtOAc gave the *title compound* **222** (184 mg, 0.410 mmol, 90%) as a colourless oil. **¹H NMR** (500 MHz, CDCl₃, 50:50 mixture of rotamers, NH₂ not observed): δ 7.38-7.27 (5H, m, Cbz Ar-H), 5.10 (2H, s, CH₂Ph), 4.00 (1H, d, *J* 7.5, 7-H), 3.92-3.82 (1H, m, 4-H_A), 3.75-3.68 (1H, m, includes at δ 3.72: d, *J* 12.5; and at δ 3.71: d, *J* 12.5, 2-H_B), 3.38 (0.5H, d, *J* 12.5, 2-H_A), 3.33 (0.5H, d, *J* 12.5, 2-H_A), 3.23-3.12 (2H, m, 4-H_B and 9-H), 3.11-3.03 (1H, m, 5-H), 2.96-2.87 (1H, m, 6-H_A), 2.16 (0.5H, dd, *J* 14.2, 5.4, 10-H_B), 2.11 (0.5H, dd, *J* 14.2, 5.4, 10-H_B), 1.72-1.60 (1H, m, 6-H_B), 1.57-1.50 (1H, m, includes at δ 1.54: 0.5H, d, *J* 14.2; and at δ 1.53: 0.5H, d, *J* 14.2, 10-H_A), 1.37 (1.5H, s, C_qCH₃), 1.36 (1.5H, s, C_qCH₃), 0.91 (9H, s, SiC(CH₃)₃), 0.13 (3H, s, SiCH₃), 0.12-0.10 (3H, m, SiCH₃). **¹³C NMR** (125 MHz, *d*⁶-DMSO, mixture of two rotamers): δ 153.6 (N(CO)O), 153.4 (N(CO)O), 137.1 (Ar-C_q), 128.4 (Ar-C), 127.7 (Ar-C), 127.5 (Ar-C), 89.3 (1-C), 88.4 (1-C), 83.2 (7-C), 73.1 (8-C), 65.7 (CH₂Ph), 54.7 (2-C or 4-C), 54.6 (2-C or 4-C), 54.1 (2-C or 4-C), 54.0 (2-C or 4-C), 53.8 (9-C), 44.4 (5-C), 43.4 (5-C), 36.7 (10-C), 36.6 (10-C), 32.9 (6-C), 32.8 (6-C), 27.5 (C_qCH₃), 25.8 (SiC(CH₃)₃), 18.0 (SiC_q), -2.0 (SiCH₃), -2.2 (SiCH₃) [27 of 38 expected peaks observed]. **IR** *v*_{max}(film)/cm⁻¹ 2952, 2931,

2882, 2856, 1704 (CO), 1419, 1362, 1346. **HRMS** (ESI): C₂₄H₃₉N₂O₄Si [M+H]⁺; calculated 447.2674, found 447.2679.

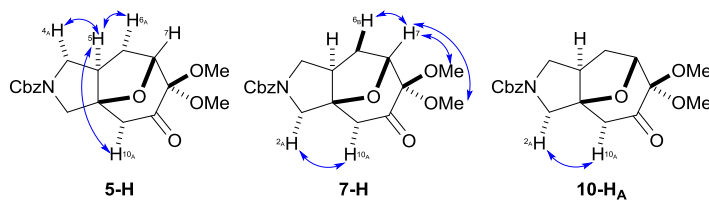
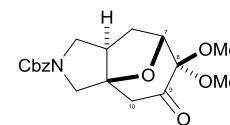
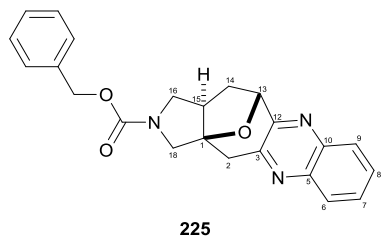


Benzyl (1*R,5*R**,7*R**)-8,8-dimethoxy-9-oxo-11-oxa-3-azatricyclo[5.3.1.0^{1,5}]undecane-3-carboxylate **224****



(±)-Camphorsulfonic acid (196 mg, 0.844 mmol, 1.20 eq.) was added to a stirred suspension of cycloadduct **183** (303 mg, 0.705 mmol, 1.00 eq.) in MeOH (10 mL).

The reaction mixture heated at 45 °C for 15 h, then concentrated *in vacuo*. The residue was partitioned between CH₂Cl₂ (20 mL) and sat. aq. NaHCO₃ (20 mL) and the phases were separated. The aqueous phase was extracted with CH₂Cl₂ (2 × 20 mL). The combined organic phase was dried over Na₂SO₄ and concentrated *in vacuo*. Flash chromatography eluting with 7:3 pentane–EtOAc gave the *title compound* **224** (201 mg, 0.556 mmol, 79%) as a colourless oil. *R_f* 0.46 (1:1 petrol–EtOAc). **¹H NMR** (500 MHz, CDCl₃, 50:50 mixture of rotamers): δ 7.38–7.29 (5H, m, Cbz Ar-H), 5.15–5.07 (2H, m, OCH₂Ph), 4.68 (1H, d, *J* 7.6, 7-H), 3.96 (1H, d, *J* 12.8, 2-H_B), 3.95–3.88 (1H, m, 4-H_A), 3.47–3.35 (4H, m, includes 1H, m, 2-H_A; and at δ 3.37: 3H, s, (OCH₃), 3.26 (3H, s, (OCH₃), 3.24–3.09 (1H, m, 4-H_B), 3.09 (0.5H, d, 14.9, 10-H_B), 3.02 (0.5H, d, 14.9, 10-H_B), 2.62–2.51 (1H, m, 5-H), 2.45–2.38 (1H, m, includes at δ 2.42: 0.5H, d, *J* 14.9; and at δ 2.41: 0.5H, d, *J* 14.9, 10-H_A), 2.16–2.06 (1H, m, 6-H_A), 2.02–1.89 (1H, m, 6-H_B). **¹³C NMR** (125 MHz, CDCl₃, mixture of two rotamers): δ 201.5 (9-C), 201.3 (9-C), 154.3 (N(CO)O), 136.8 (Ar-C_q), 128.6 (Ar-C), 128.2 (Ar-C), 128.1 (2 peaks, Ar-C), 99.7 (8-C), 91.5 (1-C), 90.8 (1-C), 79.3 (7-C), 67.2 (OCH₂Ph), 54.1 (2-C or 4-C), 54.0 (2-C or 4-C), 53.7 (2-C or 4-C), 53.6 (2-C or 4-C), 50.6 (OCH₃), 49.9 (OCH₃), 48.3 (10-C), 48.2 (10-C), 45.4 (5-C), 44.5 (5-C), 31.0 (6-C), 30.7 (6-C) [25 of 34 expected peaks observed]. **IR** *v*_{max}(film)/cm⁻¹ 2947, 2886, 1734, 1698 (CO), 1416, 1347, 1143, 1107 **HRMS** (ESI): C₁₉H₂₄NO₆ [M+H]⁺; calculated 362.1598, found 362.1601.

224 key nOe enhancements:5-H: 4-H_A; 6-H_A; 10-H_A7-H: 2 × OCH₃; 6-H_B10-H: 2-H_A**224 key HMBC correlations:**8-C: ²J with 7-H, 2 × OCH₃; ³J with 10-H_B9-C: ²J with 10-H_A; ³J with 7-H**Benzyl (1*R**, 13*R**, 15*R**)-19-oxa-4,11,17-triazapentacyclo****[11.5.1.0^{1,15}.0^{3,12}.0^{5,10}]nonadeca-3,5(10),6,8,11-pentaene-17-carboxylate 225**

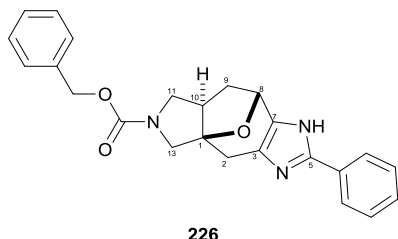
225

1,2-Diaminobenzene (270 mg, 2.50 mmol, 1.1 eq.)

was added to a stirred suspension of cycloadduct **183** (1.0 g, 2.3 mmol, 1.0 eq.) in AcOH (10 mL). The reaction mixture was heated under microwave irradiation at 180 °C for 10 min. Thereaction mixture was concentrated *in vacuo* then partitioned between CH₂Cl₂

(25 mL) and sat. aq. NaHCO₃ (25 mL). The aqueous phase was extracted with CH₂Cl₂ (2 × 10 mL). The combined organic phases were dried, filtered and concentrated *in vacuo*. Flash chromatography eluting with 0-100% EtOAc in pentane gave the *title compound* **225** (789 mg, 2.04 mol, 89%) as a colourless oil. **R_f** 0.51 (1:2 petrol–EtOAc). **¹H NMR** (500 MHz, CDCl₃): δ 8.02-7.97 (2H, m, 6-H and 9-H), 7.75-7.69 (2H, m, 7-H and 8-H), 7.42-7.30 (5H, m, Cbz Ar-H), 5.50 (1H, d, *J* 6.8, 13-H), 5.18 (1H, d, *J* 12.9, CH_AH_BPh), 5.14 (1H, d, *J* 12.9, CH_AH_BPh), 4.14 (1H, d, *J* 12.7, 18-H_A), 3.93 (1H, dd, *J* 11.3, 9.4, 16-H_A), 3.71-3.53 (2H, m, 2-H_A and 18-H_B), 3.53-3.37 (1H, m, 16-H_B), 3.15 (1H, d, *J* 17.8, 2-H_B), 2.83-2.70 (1H, m, 15-H), 2.49-2.30 (2H, m, 14-H). **¹³C NMR** (125 MHz, CDCl₃, mixture of two rotamers): δ 154.9 (2 × Ar-C_q), 154.7 (N(CO)O), 150.0 (Ar-C_q), 142.3 (Ar-C_q), 140.7 (Ar-C_q), 136.8 (Ar-C_q), 129.9 (2 peaks, 2 × Ar-C), 129.0 (Ar-C), 128.7 (2 peaks, 2 × Ar-C), 128.2 (2 peaks, 2 × Ar-C), 91.4 (1-C), 90.5 (1-C), 81.3 (13-C), 67.2 (CH₂Ph), 55.3 (16-C or 18-C), 54.9 (16-C or 18-C), 54.5 (16-C or 18-C), 54.2 (16-C or 18-C), 46.6 (15-C), 45.6 (15-C), 42.8 (2-C), 42.4 (2-C), 40.4 (14-C) [27 of 42 expected peaks observed]. **IR** ν_{\max} (film)/cm⁻¹ 2952, 2884, 1702 (CO), 1421, 1358, 1274, 1112, 769. **HRMS** (ESI): C₂₃H₂₂N₃O₃ [M+H]⁺; calculated 388.1656, found 388.1660.

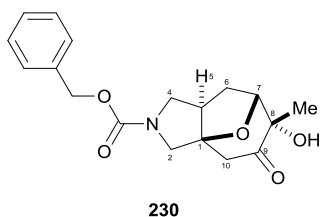
Benzyl (1*R,8*R**)-5-phenyl-14-oxa-4,6,12-triazatetracyclo[6.5.1.0^{1,10}.0^{3,7}]tetradeca-3(7),4-diene-12-carboxylate **226****



PhCHO (18 μ L, 0.17 mmol, 1.0 eq.) and NH₄OAc (135 mg, 1.70 mmol, 10.0 eq.) were added to a suspension of **183** (75 mg, 0.17 mmol, 1.0 eq.) in AcOH (3.0 mL). The resulting mixture was heated under microwave irradiation at 180 °C for 5 min.

The reaction mixture was concentrated *in vacuo*, then partitioned between CH₂Cl₂ (25 mL) and NaHCO₃ (25 mL). The phases were separated and the aqueous phase was extracted with CH₂Cl₂ (2 \times 10 mL). The combined organic extracts were dried, filtered and concentrated *in vacuo*. Flash chromatography eluting with 0-100% EtOAc in pentane gave the *title compound* **226** (64 mg, 0.16 mmol, 91%) as a pale brown oil. *R_f* 0.12 (1:1 petrol–EtOAc). **¹H NMR** (500 MHz, CDCl₃, imidazole NH not observed): δ 7.76 (2H, d, *J* 7.3, Ar-H), 7.43-7.28 (8H, m, Ar-H), 5.28 (1H, d, *J* 5.7, 8-H), 5.17 (1H, d, *J* 15.9, CH_AH_BPh), 5.14 (1H, d, *J* 15.9, CH_AH_BPh), 4.07 (1H, d, *J* 12.6, 13-H_A), 3.85-3.73 (1H, m, 11-H_A), 3.55-3.36 (2H, m, 11-H_B and 13-H_B), 3.28-3.16 (1H, m, 2-H_A), 2.73-2.64 (1H, m, 10-H), 2.61 (1H, d, *J* 15.4, 2-H_B), 2.58-2.47 (1H, m, 9-H_A), 2.16-2.05 (1H, m, 9-H_B). **¹³C NMR** (125 MHz, CDCl₃, mixture of two rotamers, 2 \times imidazole C_q not observed): δ 154.9 (N(CO)O), 145.6 (5-C), 136.7 (Ar-C_q), 130.4 (Ar-C_q), 129.1 (Ar-C), 128.6 (Ar-C), 128.2 (Ar-C), 128.0 (2 peaks, Ar-C), 125.1 (Ar-C), 91.1 (1-C), 90.1 (1-C), 77.4 (8-C), 67.2 (CH₂Ph), 55.4 (13-C), 55.0 (13-C), 53.6 (11-C), 53.5 (11-C), 47.1 (10-C), 46.1 (10-C), 45.8 (9-C), 45.6 (9-C), 32.8 (2-C) [23 of 40 expected peaks observed]. **IR** ν_{max} (film)/cm⁻¹ 3274, 2241, 1682 (CO), 1448, 1418, 1348, 1116, 909. **HRMS** (ESI): C₂₄H₂₄N₃O₃ [M+H]⁺; calculated 402.1812, found 402.1825.

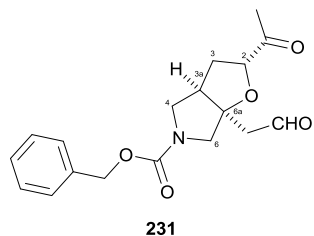
Benzyl (1*R,5*R**,7*R**,8*S**)-8-hydroxy-8-methyl-9-oxo-11-oxa-3-azatricyclo[5.3.1.0^{1,5}]undecane-3-carboxylate **230****



TBAF (1.0 M in THF, 0.46 mL, 0.46 mmol, 2.0 eq.) was added to a stirred solution of compound **221** (102 mg, 0.230 mmol, 1.0 eq.) in THF (10 mL). The reaction mixture was stirred 0.5 h then concentrated *in vacuo*. Flash chromatography eluting with 0-100% EtOAc in pentane gave the *title compound* **230** (69 mg, 0.21 mmol, 91%) as a colourless oil. *R_f* 0.25

(1:1 petrol–EtOAc). **¹H NMR** (500 MHz, CDCl₃, 50:50 mixture of rotamers): δ 7.39-7.28 (5H, m, Cbz Ar-H), 5.12 (2H, s, OCH₂Ph), 4.39 (1H, d, *J* 7.4, 7-H), 3.99-3.92 (1H, m, includes at δ 3.96: 0.5H, d, *J* 12.8; and at δ 3.94: 0.5H, d, *J* 12.8, 2-H_A), 3.92-3.84 (1H, m, 4-H_A), 3.72 (1H, s, OH), 3.45 (0.5H, d, *J* 12.7, 2-H_B), 3.40 (0.5H, d, *J* 12.7, 2-H_B), 3.21-3.10 (1H, m, 4-H_B), 3.05 (0.5H, d, *J* 15.0, 10-H_A), 2.99 (0.5H, d, *J* 15.0, 10-H_A), 2.54-2.42 (2H, m, 5-H and 10-H_B), 2.15 (1H, td, *J* 14.5, 8.7, 6-H_A), 1.91-1.78 (1H, m, 6-H_B), 1.48 (1.5H, s, CH₃), 1.47 (1.5H, s, CH₃). **¹³C NMR** (125 MHz, CDCl₃, 329 K, mixture of two rotamers): δ 210.0 (9-C), 154.4 (N(CO)O), 137.0 (Ar-C_q), 128.7 (Ar-C), 128.2 (Ar-C), 128.1 (Ar-C), 91.5 (1-C), 91.4 (1-C), 84.7 (7-C), 78.5 (8-C), 67.2 (OCH₂Ph), 54.1 (2-C and 4-C), 46.5 (10-C), 45.9 (5-C), 45.0 (5-C), 31.5 (6-C), 24.5 (CH₃) [17 of 34 expected peaks observed]. **IR** ν_{\max} (film)/cm⁻¹ 2954, 2887, 1703 (CO), 1454, 1422, 1350, 1108, 771. **HRMS** (ESI): C₁₈H₂₂NO₅ [M+H]⁺; calculated 332.1492, found 332.1491.

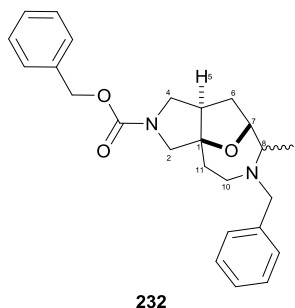
Benzyl (2*R,3*aR**,6*aR**)-2-acetyl-6*a*-(2-oxoethyl)-hexahydro-2*H*-furo[2,3-*c*]pyrrole-5-carboxylate **231****



NaBH₄ (21 mg, 0.54 mmol, 1.0 eq.) was added to a stirred solution of α -hydroxyketone **230** (180 mg, 0.54 mmol, 1.0 eq.) in MeOH at 0 °C. The reaction mixture was stirred for 2 h, warming to rt, then H₂O (1 mL) was added. The reaction mixture was concentrated *in vacuo* then diluted in EtOAc (25 mL) and washed with brine (25 mL). The aqueous phase was extracted with EtOAc (2 × 10 mL). The combined organic phase was dried over MgSO₄, filtered and concentrated *in vacuo*. Flash chromatography on cyanosilica eluting with 0-100% EtOAc in pentane gave the *title compound* **231** (82 mg, 0.25 mmol, 46%) as a colourless oil. **R_f** 0.14 (1:1 petrol–EtOAc). **¹H NMR** (500 MHz, CDCl₃): δ 9.81 (1H, t, *J* 2.0, CHO), 7.37-7.27 (5H, m, Cbz Ar-H), 5.15-5.10 (2H, m, CH₂Ph), 4.54 (1H, t, *J* 8.2, 2-H), 3.88 (1H, d, *J* 12.4, 6-H_A), 3.75 (1H, dd, *J* 11.7, 8.7, 4-H_A), 3.52 (1H, d, *J* 12.4, 6-H_B), 3.39 (1H, dd, *J* 11.7, 5.4, 4-H_B), 2.82 (1H, dd, *J* 16.0, 2.0, CH_AH_BCHO), 2.79-2.65 (2H, m, 3*a*-H and CH_AH_BCHO), 2.18-2.12 (5H, m, includes 2H, m, 3-H; and at δ 2.16: 3H, s, CH₃). **¹³C NMR** (125 MHz, CDCl₃, 329 K): δ 207.5 (CHO), 199.2 (COCH₃), 154.7 (N(CO)O), 136.7 (Ar-C_q), 128.7 (Ar-C), 128.2 (Ar-C), 128.1 (Ar-C), 91.3 (6*a*-C), 83.9 (2-C), 67.3 (CH₂Ph), 56.6 (6-C), 51.2 (4-C or CH₂CHO), 50.7 (4-C or CH₂CHO), 46.5 (3*a*-C), 34.4 (3-C), 25.9 (CH₃). **IR** ν_{\max} (film)/cm⁻¹ 2952, 2885,

1704 (CO), 1498, 1422, 1217, 1099, 769. **HRMS** (ESI): $C_{18}H_{21}NNaO_5$ $[M+Na]^+$; calculated 354.1312, found 354.1314.

Benzyl (1*R,5*R**,7*R**)-9-benzyl-8-methyl-12-oxa-3,9-diazatricyclo[5.4.1.0^{1,5}]dodecane-3-carboxylate **232****

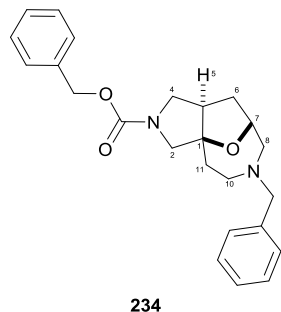


BnNH₂ (18 μ L, 0.16 mmol, 1.0 eq.) was added to a stirred solution of ketoaldehyde **231** (53 mg, 0.16 mmol, 1.0 eq.). The reaction mixture was stirred for 5 min then NaBH(OAc)₃ (102 mg, 0.48 mmol, 3.0 eq.) was added. The reaction mixture was stirred for 2 h, by which time complete consumption of the starting material was observed by TLC. The reaction mixture was diluted in CH₂Cl₂ (15 mL) and washed with brine (25 mL). The aqueous phase was extracted with CH₂Cl₂ (2 \times 20 mL). The combined organic phases were dried over MgSO₄, filtered and concentrated *in vacuo*. Analysis of the crude reaction product by ¹H NMR spectroscopy identified a 1:1 mixture of diastereomers. Flash chromatography eluting with 0-100% EtOAc in pentane gave one diastereomer* of the *title compound* **232** (15 mg, 37 μ mol, 23%) as a colourless oil. *R_f* 0.18 (3:2 petrol–EtOAc). **¹H NMR** (300 MHz, CDCl₃, 50:50 mixture of rotamers): 7.34-7.11 (10H, m, Ar-H), 5.03 (2H, s, OCH₂Ph), 4.33-4.17 (1H, m, 7-H), 3.97 (1H, d, *J* 13.8, NCH_AH_BPh), 3.76 (1H, d, *J* 12.3, 2-H_A), 3.71-3.62 (1H, m, includes at δ 3.68: 0.5H, d, *J* 11.0; and at δ 3.65: 0.5H, d, *J* 11.0, 4-H_A), 3.33-3.05 (3H, m, 2-H_B, 4-H_B and NCH_AH_BPh), 2.77-2.64 (1H, m, 8-H), 2.61-2.46 (3H, m, 5-H and 10-H), 2.46-2.33 (1H, m, 6-H_A), 1.84-1.64 (2H, m, 6-H_B and 11-H_A), 1.64-1.45 (1H, m, 11-H_B), 0.92 (3H, d, *J* 6.6, CH₃). Characteristic peaks for the other diastereomer, as judged by analysis of crude product using ¹H NMR spectroscopy (300 MHz, CDCl₃): 4.16-4.07 (1H, m, 7-H), 3.80 (1H, d, *J* 12.5), 3.65-3.59 (1H, m), 2.94-2.78 (1H, m), 2.30 (1H, ddd, *J* 11.7, 8.2, 3.3), 2.22-2.11 (1H, m), 0.91 (1H, d, *J* 6.5, CH₃). **¹³C NMR** (125 MHz, CDCl₃, mixture of two rotamers, one Ar-C peak not observed): δ 154.8 (CO), 141.0 (Ar-C_q), 137.1 (Ar-C_q), 128.6 (Ar-C), 128.5 (Ar-C), 128.4 (Ar-C), 128.0 (Ar-C), 126.9 (Ar-C), 90.7 (1-C), 89.7 (1-C), 85.3 (7-C), 66.9 (OCH₂Ph), 63.0 (8-C), 62.8 (8-C), 58.3 (NCH₂Ph), 57.4 (2-C), 57.0 (2-C), 53.7 (4-C), 53.4 (4-C), 51.1 (5-C), 50.1 (5-C), 49.4 (10-C), 38.2 (11-C), 30.3 (6-C).

* Optimisation of the purification step is required in order to isolate the other diastereomer cleanly.

29.9 (6-C), 16.5 (CH₃) [26 of 44 expected peaks observed]. IR ν_{max} (film)/cm⁻¹ 2943, 1699 (CO), 1416, 1348, 1099, 1029, 734, 700. HRMS (ESI): C₂₅H₃₁N₂O₃ [M+H]⁺; calculated 407.2329, found 407.2334.

Benzyl (1*R,5*R**,7*R**)-9-benzyl-12-oxa-3,9-diazatricyclo[5.4.1.0^{1,5}]dodecane-3-carboxylate **234****

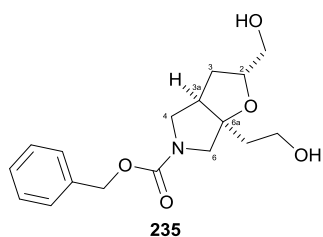


NaIO₄ (105 mg, 0.490 mmol, 2.00 eq.) was added to a stirred solution of diol **214** (78 mg, 0.24 mmol, 1.0 eq.) in 8:2 MeOH–H₂O (10 mL) at 0 °C. The reaction mixture was warmed to rt and stirred for 2 h. The reaction mixture was concentrated *in vacuo* then the resulting crude dialdehyde **233**^{*} was dissolved in CH₂Cl₂ (10 mL). BnNH₂ (26 μ L, 0.25 mmol, 1.0 eq.), NaBH(OAc)₃ (153 mg, 0.72 mmol, 3.0 eq.) and 4 Å MS (10 mg) were added. The reaction mixture was stirred 15 h then filtered through Celite and concentrated *in vacuo*. The resulting residue was diluted in EtOAc (25 mL) and washed with brine (25 mL). The aqueous phase was extracted with EtOAc (2 \times 10 mL). The combined organic phase was dried over MgSO₄, filtered and concentrated *in vacuo*. Flash chromatography eluting with 0-100% EtOAc in pentane gave the *title compound* **234** (30 mg, 76 μ mol, 32%) as a colourless oil. *R_f* 0.74 (1:1 petrol–EtOAc). ¹H NMR (500 MHz, CDCl₃, 50:50 mixture of diastereomers): δ 7.39-7.21 (10H, m, Ar-H), 5.15-5.06 (2H, m, OCH₂Ph), 4.43-4.38 (1H, m, includes at δ 4.41: d, *J* 8.1; and at δ 4.40: d, *J* 8.1, 7-H), 3.89 (1H, d, *J* 12.3, 2-H_A), 3.64-3.53 (3H, includes: 1H, m, 4-H_A; at δ 3.61, 1H, d, *J* 13.3, NCH_AH_BPh; and at δ 3.55, 1H, d, *J* 13.3, NCH_AH_BPh), 3.52-3.33 (1H, m, 4-H_B), 3.22-3.06 (1H, m, 2-H_B), 2.90-2.80 (1H, m, 5-H), 2.77-2.68 (1H, m, 10-H_A), 2.58-2.44 (2H, includes: 1H, m, 10-H_B; and at δ 2.52, 1H, d, *J* 12.4, 8-H_A), 2.43-2.36 (1H, m, includes at δ 2.40: d, *J* 12.4; and at δ 2.39: d, *J* 12.4, 8-H_B), 2.28-2.21 (1H, m, 6-H_A), 1.92-1.74 (3H, m, 6-H_B and 11-H). ¹³C NMR (125 MHz, CDCl₃, mixture of two rotamers): δ 155.1 (N(CO)O), 139.9 (Ar-C_q) 137.1 (Ar-C_q), 128.8 (Ar-C), 128.6 (Ar-C), 128.5 (Ar-C), 128.0 (2 peaks, 2 \times Ar-C), 127.2 (Ar-C), 93.2 (1-C), 92.2 (1-C), 80.2 (7-C), 66.9 (OCH₂Ph), 64.3 (NCH₂Ph), 63.6 (8-C), 57.9 (2-C), 57.5 (2-C), 54.0 (4-C), 53.8 (4-C), 53.6 (10-C), 50.1 (5-C), 38.3 (11-C), 36.6 (6-C) [23 of 40 expected peaks observed]. IR ν_{max} (film)/cm⁻¹ 2930, 2865,

^{*} Characteristic ¹H NMR peaks for the crude aldehyde **233** are given in the procedure for **235**.

1702 (CO), 1451, 1419, 1360, 1217, 1143. **HRMS** (ESI): C₂₄H₂₉N₂O₃ [M+H]⁺; calculated 393.2173, found 393.2185.

Benzyl (2*R,3*aR**,6*aR**)-6a-(2-hydroxyethyl)-2-(hydroxymethyl)-hexahydro-2H-furo[2,3-c]pyrrole-5-carboxylate **235****



NaIO₄ (56 mg, 0.26 mmol, 2.0 eq.) was added to a stirred solution of diol **214** (41 mg, 0.13 mmol, 1.0 eq.) in 8:2 MeOH–H₂O (5 mL) at 0 °C. The reaction mixture was warmed to rt, stirred for 2 h, then concentrated *in vacuo*. The residue was diluted in EtOAc (10 mL) and washed with brine (10 mL). The aqueous phase was extracted with EtOAc (2 × 10 mL). The combined organic extracts were dried over MgSO₄, filtered and concentrated *in vacuo* to give crude aldehyde **233** [characteristic ¹H NMR peaks (300 MHz, CDCl₃): δ 9.82 (1H, t, *J* 1.9, CH₂CHO), 9.64 (1H, d, *J* 1.4, CHCHO), 7.42–7.28 (5H, m, Cbz Ar-H), 5.13 (2H, s, OCH₂Ph)]. NaBH₄ (12 mg, 0.33 mmol, 2.5 eq.) was added to a stirred solution of the crude aldehyde **234** in MeOH (5 mL) at 0 °C. The reaction mixture was warmed to rt, stirred 1 h, then concentrated *in vacuo*. The residue was diluted in EtOAc (10 mL) and washed with brine (10 mL). The aqueous phase was extracted with EtOAc (2 × 10 mL). The combined organic phase was dried over MgSO₄, filtered and concentrated *in vacuo*. Flash chromatography eluting with 9:1 EtOAc–MeOH gave the *title compound* **235** (16 mg, 50 μmol, 38%) as a colourless oil. *R_f* 0.43 (9:1 EtOAc–MeOH). ¹H NMR (500 MHz, CDCl₃, 2 × OH not observed): δ 7.40–7.28 (5H, m, Cbz Ar-H), 5.13 (2H, s, CH₂Ph), 4.33–4.26 (1H, m, 2-H), 3.93–3.79 (4H, m, 6-H_A, CHCH_AH_BOH and CH₂CH₂OH), 3.74 (1H, dd, *J* 11.4, 9.1, 4-H_A), 3.50 (1H, dd, *J* 12.5, 3.0, CHCH_AH_BOH), 3.47–3.28 (2H, m, 4-H_B and 6-H_B), 2.71–2.64 (1H, m, 3a-H), 2.21 (1H, ddd, *J* 12.8, 9.7, 7.3, 3-H_A), 2.03–1.95 (1H, m, CH_AH_BCH₂OH), 1.89–1.76 (2H, m, 3-H_B and CH_AH_BCH₂OH). ¹³C NMR (125 MHz, CDCl₃, one C_q not observed): δ 154.9 (N(CO)O), 137.1 (Ar-C_q), 128.7 (Ar-C), 128.2 (Ar-C), 128.1 (Ar-C), 80.1 (2-C), 67.2 (CH₂Ph), 64.1 (CHCH₂OH), 60.2 (CH₂CH₂OH), 57.1 (6-C), 51.6 (4-C), 47.2 (3a-C), 39.8 (3-C), 33.0 (CH₂CH₂OH). **IR** ν_{max}(film)/cm⁻¹ 3401 (OH), 2938, 2880, 1684 (CO), 1422, 1351, 1217, 1100. **HRMS** (ESI): C₁₇H₂₄NO₅ [M+H]⁺; calculated 322.1649, found 322.1649.

6.0 Appendix 1: Computational tools and related data

6.1 Capping groups for virtual library enumeration

Decoration reactions were performed using the 80 capping groups shown in Figure 67.

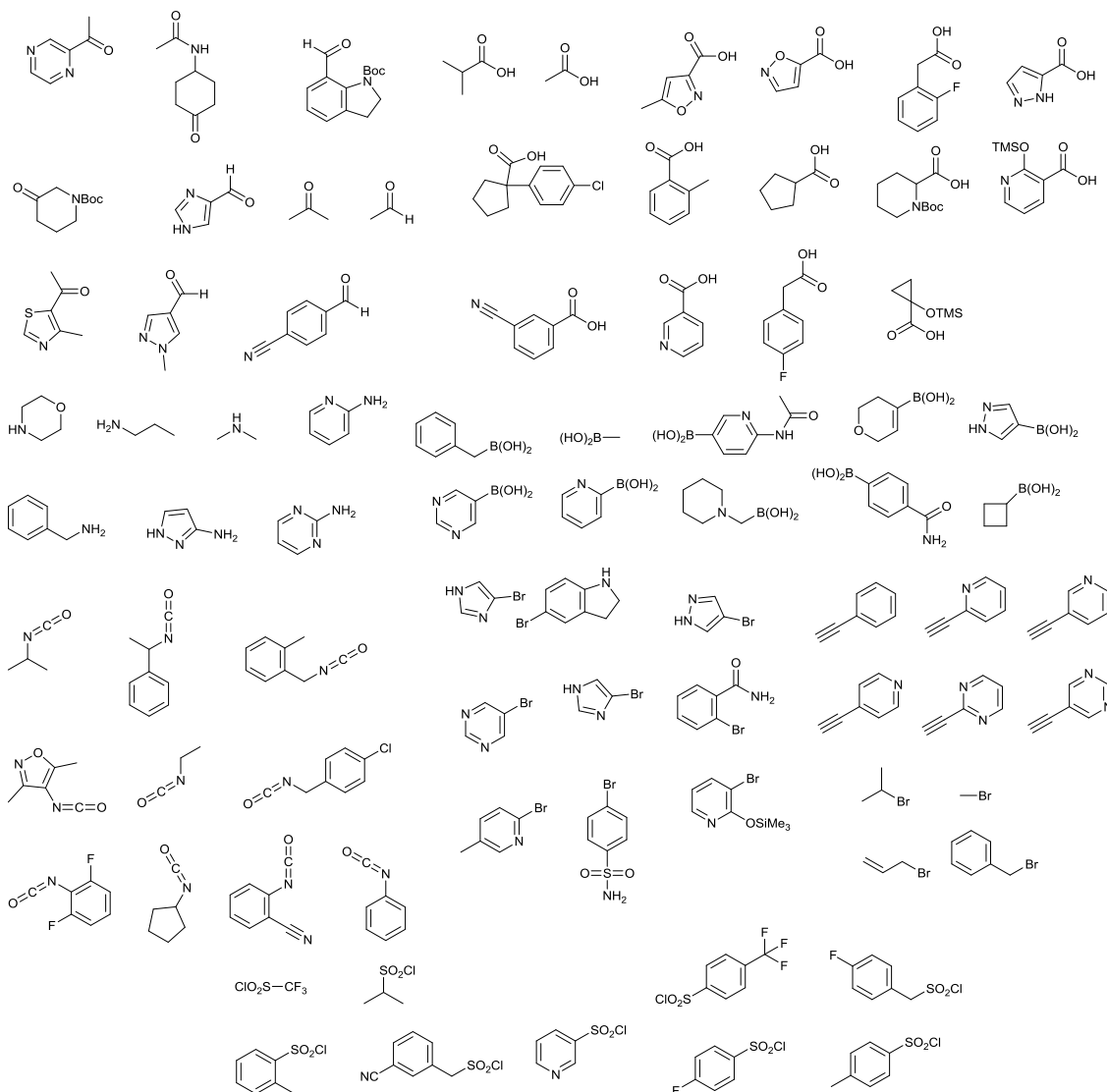


Figure 67 80 capping reagents used in the enumeration of the virtual libraries.

6.2 Lead-likeness analysis

Structural filtering was performed by interrogating SMARTS definitions against each of the final compounds using the substructure search tool within Pipeline Pilot. For full information on the filters used for our assessments see *Org. Biomol. Chem.* **2015**, *13*, 859 (filters can be found in the Supporting Information, Section S5, **Tables S1-S3**, pages 7-13).

AlogP and number of heavy atoms (HA) were calculated using the tools within Pipeline Pilot. The fraction of sp^3 -hybridised carbon atoms (F_{sp^3}) was calculated using Dotmatics Vortex (Vortex v2013.12.25046). The data were visualized and analysed using Vortex.

6.3 Shape analysis: Principal moments of inertia

George Burslem generated the 3D structures from the 2D Pipeline Pilot output using OpenEye OMEGA (OMEGA 2.4.3, OpenEye Scientific Software, 2010) and the lowest energy conformer was selected.²¹⁷ The 3D structures were used to generate the three principal moments of inertia (I_1 , I_2 and I_3) by the candidate, using Accelrys Pipeline Pilot (Pipeline Pilot v8.5.0.200, Accelrys© Software Inc., 2011), which were then normalised by dividing the two lower values by the largest (I_1/I_3 and I_2/I_3). Normalised PMI plots were generated by the candidate to give triangular plots with the corners defined by a perfect sphere, a perfect disk and a perfect rod shape.¹⁶²

6.3.1 PMI plot binning

This section describes how the PMI plots were divided in to 20 bins (see also Section 2.5.3.2) in which the number of virtual compounds were counted. The equations below were derived by the candidate and Stuart Warriner.

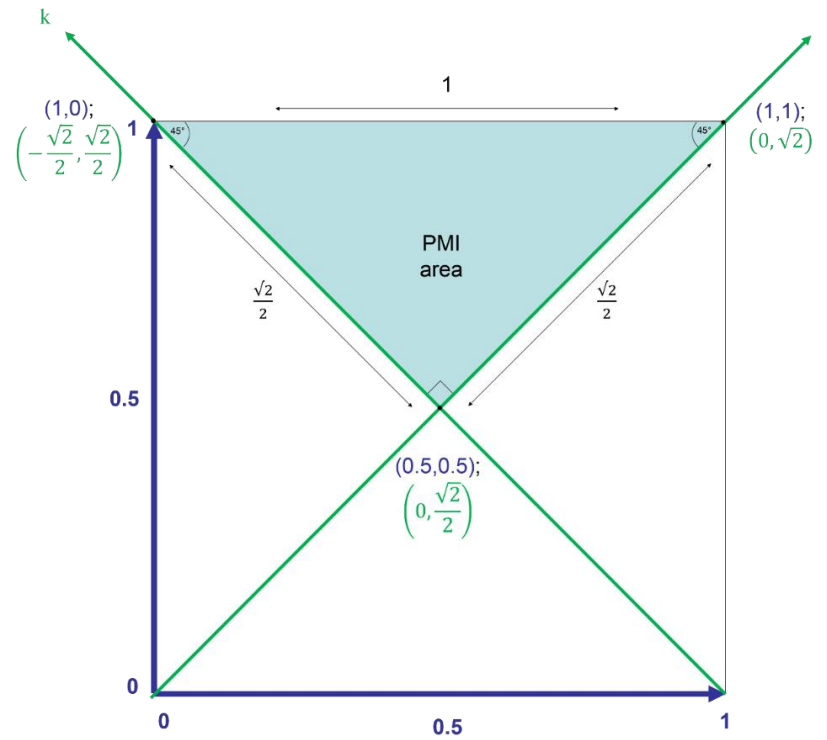


Figure 68 A PMI plot shown on an x,y axis. x,y coordinates are shown in blue; the calculated k,l coordinates (see below) are shown in green.

An axis rotation was applied to the PMI plot (Figure 68); x,y coordinates were converted to k,l coordinates as follows:

$$-\frac{\sqrt{2}}{2}k + \frac{\sqrt{2}}{2}l = 0x + y$$

$$y = \frac{-\sqrt{2}}{2}k + \frac{\sqrt{2}}{2}l$$

$$0k + \sqrt{2}l = x + y$$

$$l = \frac{x}{\sqrt{2}} + \frac{y}{\sqrt{2}} = \frac{1}{2}(x + y)$$

$$y = \frac{-\sqrt{2}}{2}k + \frac{\sqrt{2}}{2} \left(\frac{1}{\sqrt{2}}x + y \right) = \frac{-\sqrt{2}}{2}k + \frac{1}{2}x + \frac{1}{2}y$$

$$\frac{1}{2}y - \frac{1}{2}x = \frac{-\sqrt{2}}{2}k$$

$$y - x = -\sqrt{2}k$$

$$x - y = \sqrt{2}k$$

Equation 1: $k = \frac{x-y}{\sqrt{2}}$

Equation 2: $l = \frac{x+y}{\sqrt{2}}$

$x=I1$ and $y=I2$ were substituted into equations 1 and 2 and k,l coordinates were calculated for all $I1$ and $I2$ values using Microsoft Excel (Figure 69, left hand side). The l axis was divided into 40 bins, of which 20 actually intersect the PMI plot (Figure 69, right hand side).

Since $l_{\max} = \sqrt{2}$; the upper limit of each bin is $(n-1)*\sqrt{2}/40$ (where $n = 0, 1, 2 \dots 40$).

The number of compounds in each bin was counted using an array formula in Microsoft Excel. This was converted to a percentage as a fraction of the total number of compounds, allowing the generation of histogram plots (e.g. Figure 32).

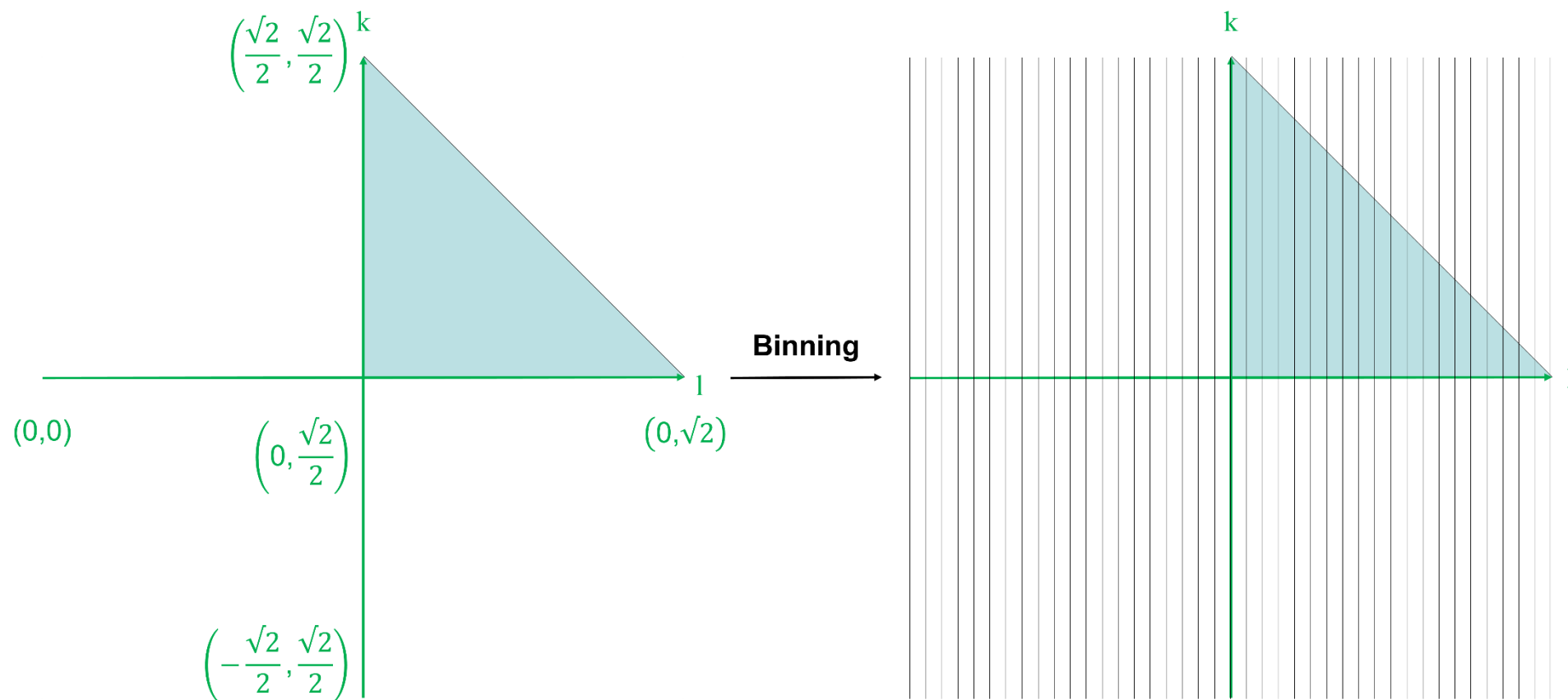


Figure 69 An axis rotation was applied to convert the PMI plot from x,y to k,l coordinates. The l axis was then divided into bins and the number of compounds in each bin were counted.

6.4 Data for the 'bottom-up' compound library

6.4.1 Lead-likeness assessment: Per scaffold basis

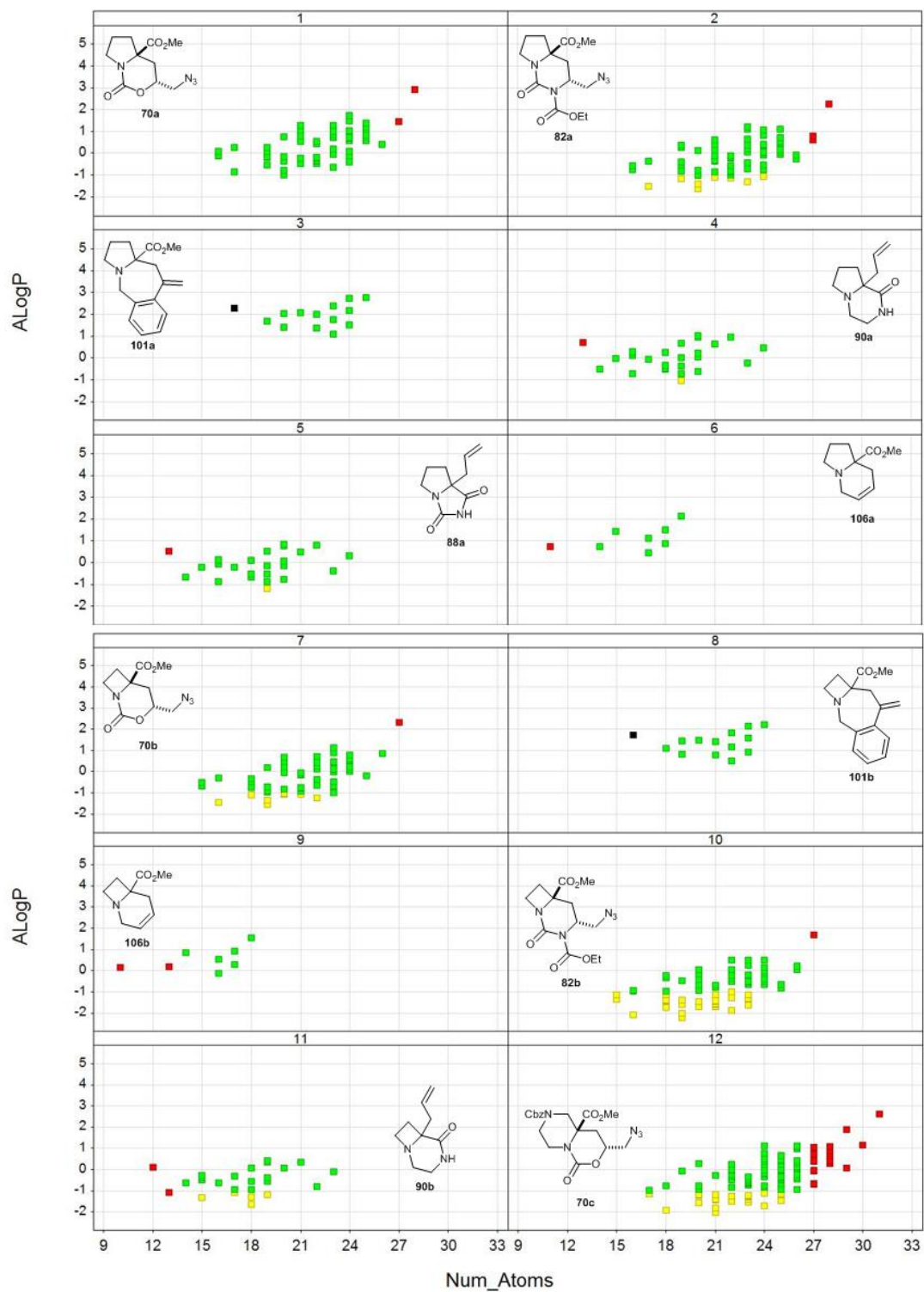
Filter	ZINC Database (9046036)		Random 1% of ZINC Database (90911)		Virtual Library (1110)	
	Successive Filtering	Parallel Filtering	Successive Filtering	Parallel Filtering	Successive Filtering	Parallel Filtering
Fail $14 \leq nHA \leq 26$	4395739	4395739 (48%)	43971	43971 (48%)	173	173 (16%)
Fail $-1 \leq AlogP \leq 3$	1768807	4478982 (49%)	17828	44746 (49%)	200	220 (20%)
Fail Structural	819652	2805505 (31%)	8180	28147 (31%)	3	5 (0.5%)
Pass All	2061838 (23%)	n/a	20932 (23%)	n/a	734 (66%)	n/a

Table 22 Filtering assessment data for the allylic alkylation-derived virtual library and the ZINC database. For comparison, data obtained from parallel filtering of all compounds using each filter in isolation is shown.

Entry	Scaffold	No. final compounds	No. lead-like compounds	% Lead-like Compounds	Average number of lead-like compounds per scaffold	Fail HA	Fail AlogP	Fail SS	Most likely reason(s) for compound failure	Average heavy atom count (standard deviation)	Average AlogP (standard deviation)	Average Fsp ³ (standard deviation)
1	70a	64	62	97	N/A	2	0	0	HA too high	22.3 (2.54)	0.42 (0.75)	0.66 (0.15)
2	70b	64	55	86		1	8	0	AlogP too low	21.3 (2.54)	-0.17 (0.75)	0.63 (0.16)
3	70c	116	68	59		23	25	0	AlogP too low/ HA too high	24.2 (2.73)	-0.28 (0.85)	0.68 (0.14)
4	70d	71	37	52		34	0	0	HA too high	26.1 (2.65)	1.69 (0.74)	0.42 (0.10)
5	82a	76	62	82		3	11	0	AlogP too low	22.2 (2.59)	-0.15 (0.75)	0.67 (0.14)
6	82b	75	46	61		1	28	0	AlogP too low	21.2 (2.61)	-0.75 (0.74)	0.64 (0.15)
7	82c	127	47	37		25	55	0	AlogP too low	24.1 (2.77)	-0.92 (0.83)	0.68 (0.14)
8	88a	26	24	92		1	1	0	-	18.5 (2.63)	-0.12 (0.57)	0.58 (0.15)
9	88c	78	39	50		2	37	0	AlogP too low	21.3 (2.90)	-0.92 (0.72)	0.57 (0.15)
10	87d	10	4	40		3	3	0	AlogP too high/ HA too high	26.0 (1.76)	2.72 (0.52)	0.28 (0.06)
11	90a	26	24	92		1	1	0	-	18.5 (2.63)	0.03 (0.57)	0.69 (0.15)
12	90b	26	18	69		2	6	0	AlogP too low	17.5	-0.55	0.66

Entry	Scaffold	No. final compounds	No. lead-like compounds	% Lead-like Compounds	Average number of lead-like compounds per scaffold	Fail HA	Fail AlogP	Fail SS	Most likely reason(s) for compound failure	Average heavy atom count (standard deviation)	Average AlogP (standard deviation)	Average Fsp ³ (standard deviation)
										(2.63)	(0.57)	(0.16)
13	96d	37	31	84		6	0	0	HA too high	23.6 (2.75)	0.40 (0.57)	0.34 (0.09)
14	101a	15	14	93		0	0	1	Substructure	22.0 (2.20)	1.94 (0.49)	0.47 (0.12)
15	101b	15	14	93		0	0	1	Substructure	21.0 (2.20)	1.36 (0.49)	0.44 (0.12)
16	101c	67	40	60		26	0	1	HA too high	25.6 (2.83)	1.33 (0.75)	0.45 (0.10)
17	101d	21	7	33		10	4	0	HA too high	26.0 (2.41)	2.86 (0.58)	0.37 (0.05)
18	102c	60	33	55		26	1	0	HA too high	25.9 (2.77)	2.23 (0.78)	0.42 (0.09)
19	106a	8	7	88		1	0	0	HA too low	16.1 (2.64)	1.12 (0.54)	0.61 (0.16)
20	106b	8	6	75		2	0	0	HA too low	15.1 (2.64)	0.54 (0.54)	0.57 (0.17)
21	106c	60	58	97		1	1	0	–	19.9 (2.77)	0.71 (0.78)	0.59 (0.14)
22	106d	60	38	63		3	19	0	AlogP too high	22.9 (2.77)	2.66 (0.78)	0.35 (0.09)
10	Sum (22 scaffolds)	1110	734	66	33	173	200	3	AlogP too low	22.8 (3.57)	0.38 (1.38)	0.57 (0.18)

Table 23 Lead-likeness assessment data for the allylic alkylation-derived virtual library.



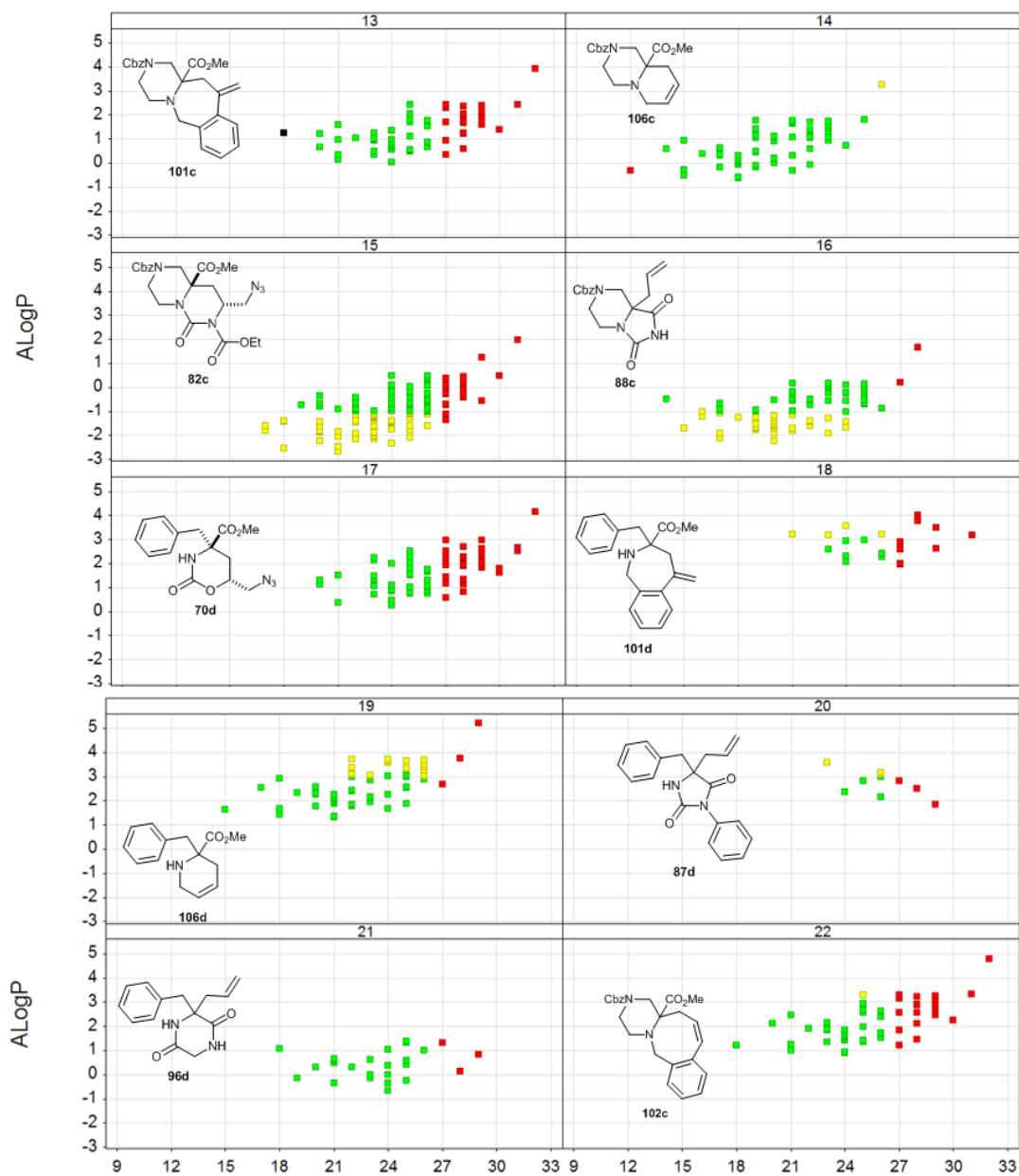
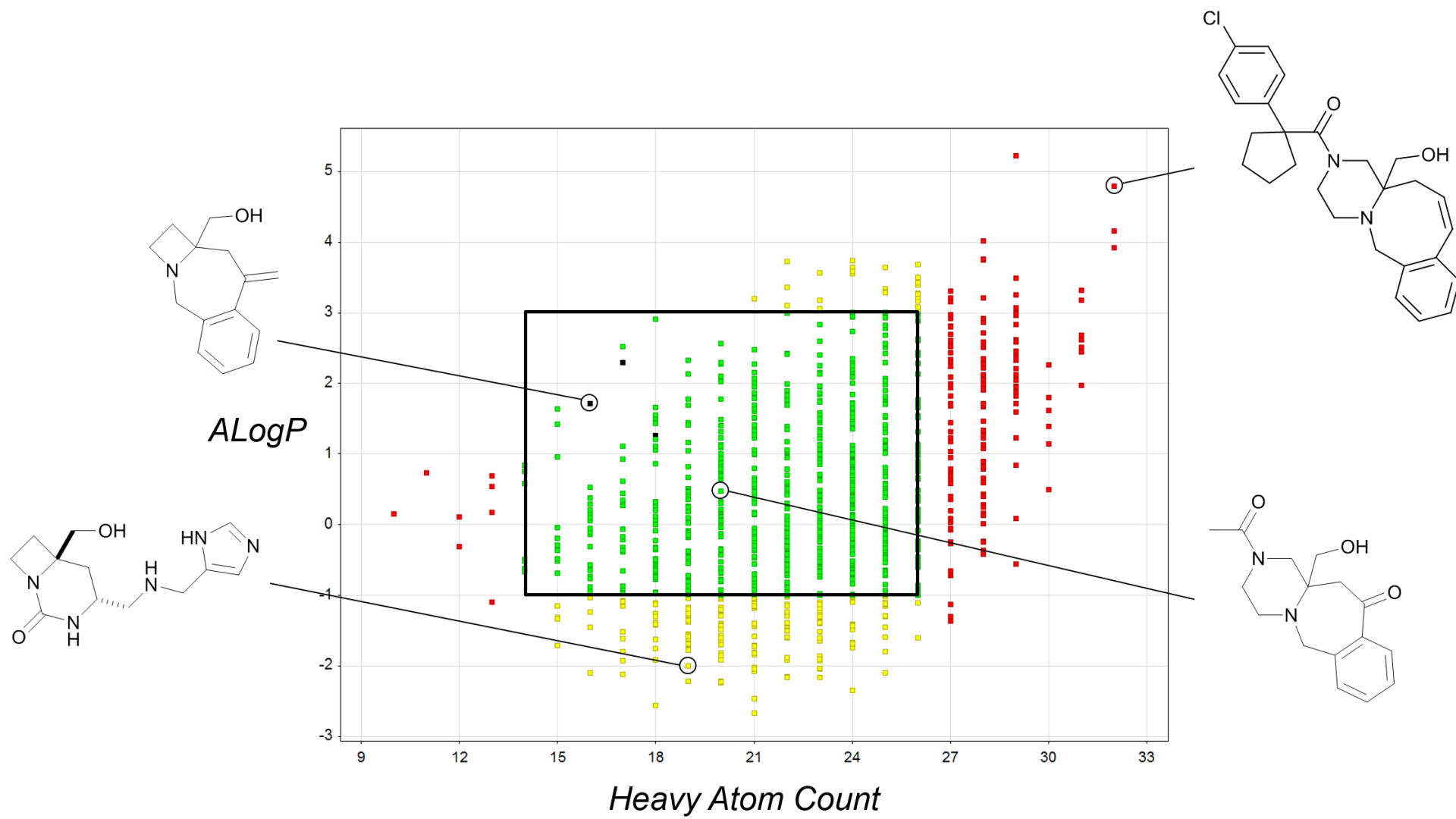


Figure 70 Distribution of number of heavy atoms (Num_Atoms) and ALogP for the virtual library based upon each scaffold. Compounds that survive successive filtering are shown in green. Compounds that fail successive filtering by number of heavy atoms (red), ALogP (yellow) and structural features (black) are shown as appropriate.



6.4.2 Lead-likeness assessment: Per building block basis

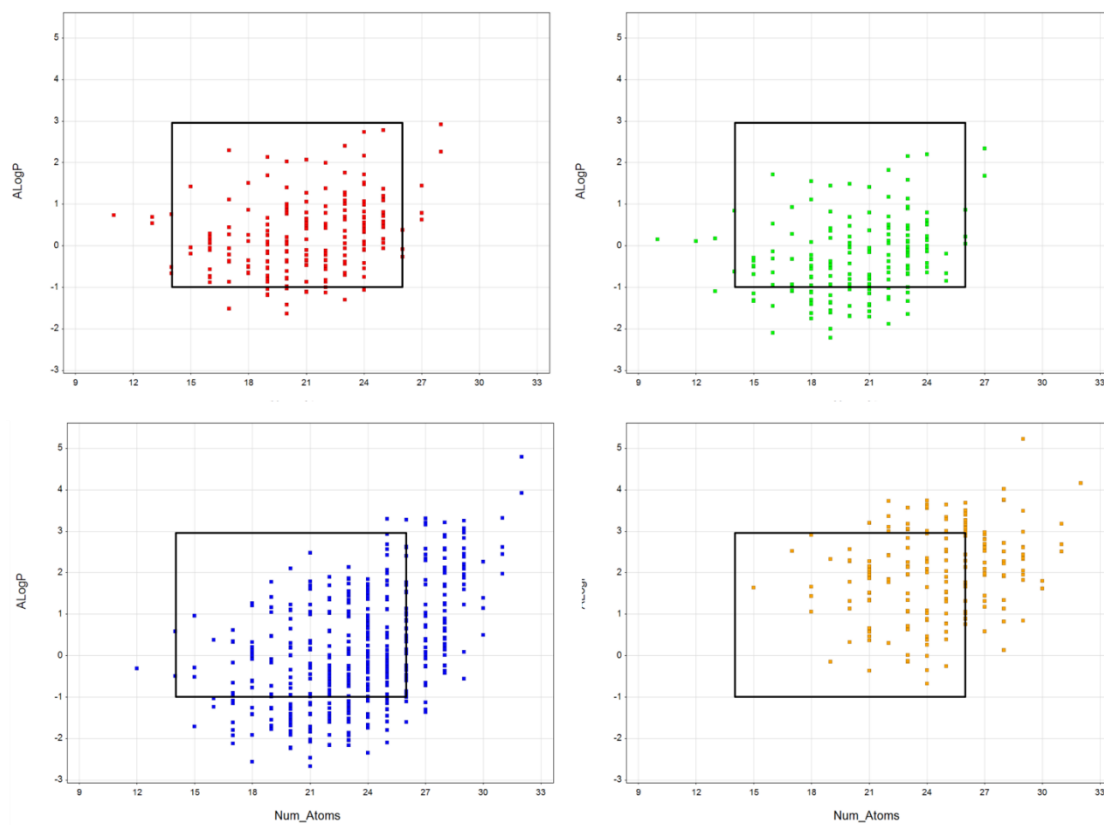
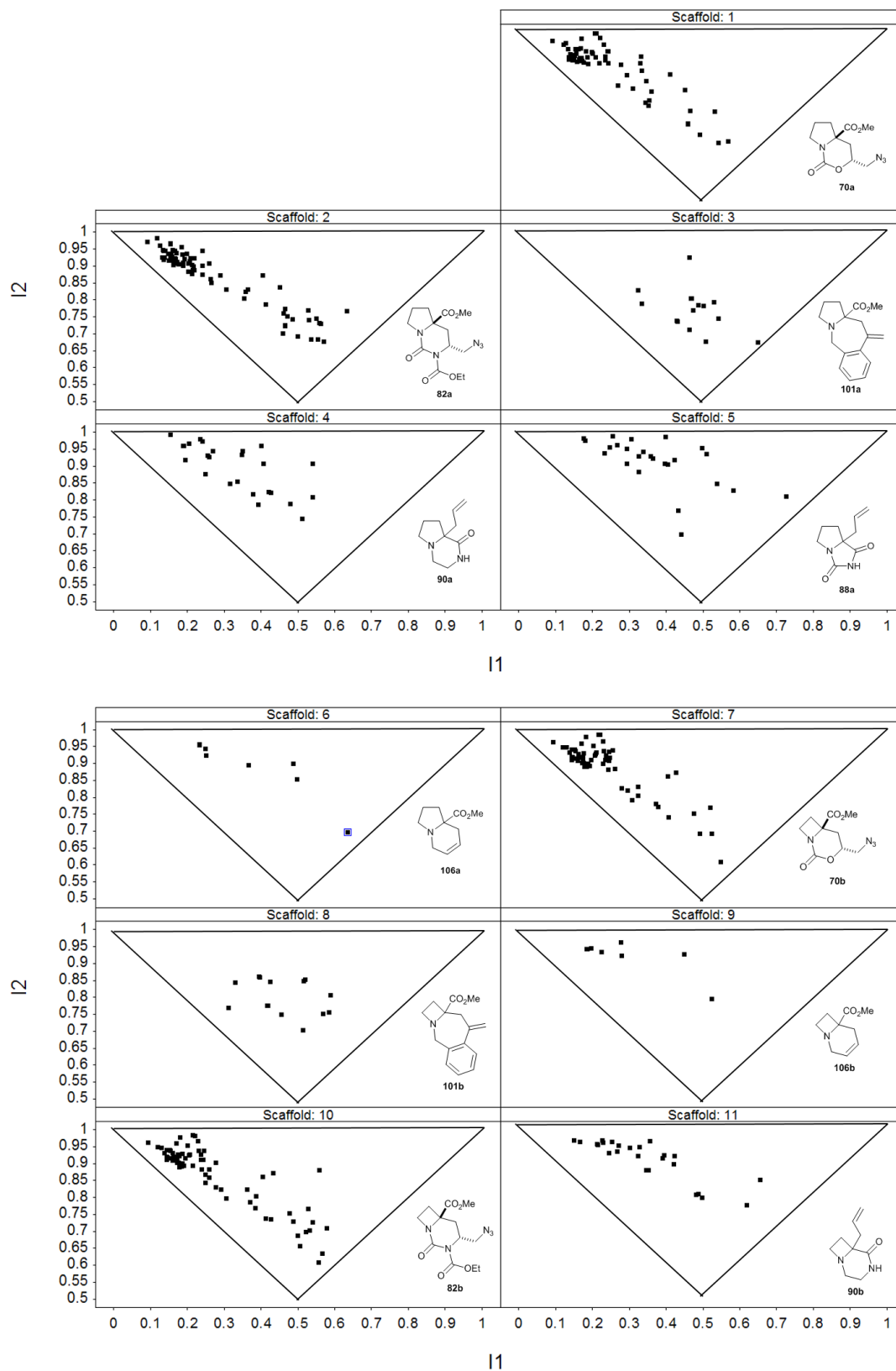


Figure 71 Distribution of the number of heavy atoms (Num_Atoms) and AlogP for the allylic alkylation-derived virtual compound library based upon each building block. Red= pyrrolidine-derived; green= azetidine derived; blue= piperazine-derived; orange= phenylalanine derived.

Entry	Building block	No. scaffolds	No. final compounds	No. lead-like compounds	% Lead-like Compounds	Average number of lead-like compounds per scaffold	Fail HA	Fail AlogP	Fail SS	Most likely reason for compound failure	Average heavy atom count (standard deviation)	Average AlogP (standard deviation)	Average Fsp ³ (standard deviation)
1	Pyrrolidine-derived 63a	6	215	193	90	32	8	13	1	No significant trend*	21.1 (3.15)	0.24 (0.88)	0.64 (0.15)
2	Azetidine-derived 63b	5	188	139	74	28	6	42	1	Alogp too low	20.4 (3.06)	-0.30 (0.91)	0.62 (0.16)
3	Piperazine-derived 63c	6	508	285	56	48	103	119	1	Alogp too low	23.6 (3.37)	0.09 (1.36)	0.57 (0.18)
4	Phenylalanine-derived 63d	5	199	117	59	23	56	26	0	Heavy atoms too high	24.7 (3.01)	1.92 (1.11)	0.37 (0.10)
5	All	22	1110	734	66	33	173	200	3	AlogP too low	22.8 (3.57)	0.38 (1.38)	0.57 (0.18)

Table 24 Lead-likeness assessment data for the allylic alkylation-derived virtual library compounds with respect to the starting building block. *Where logP fails it was always because it was too low.

6.4.3 PMI assessment: Per scaffold basis



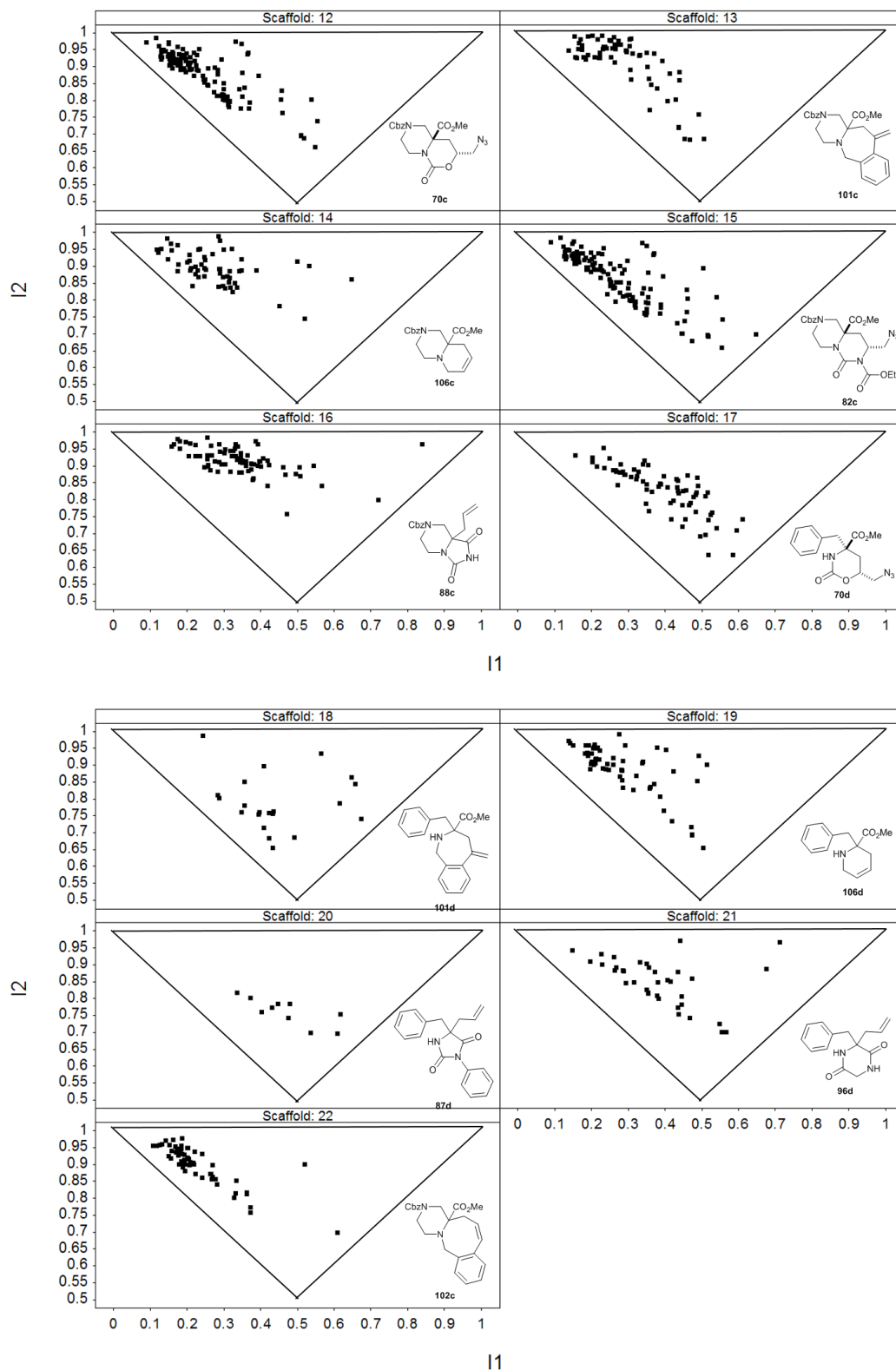


Figure 72 Normalised principal moment of inertia plots to show the shapes of the 1110 allylic alkylation-derived virtual compounds with respect to each scaffold.

6.4.4 PMI assessment: Per building block basis

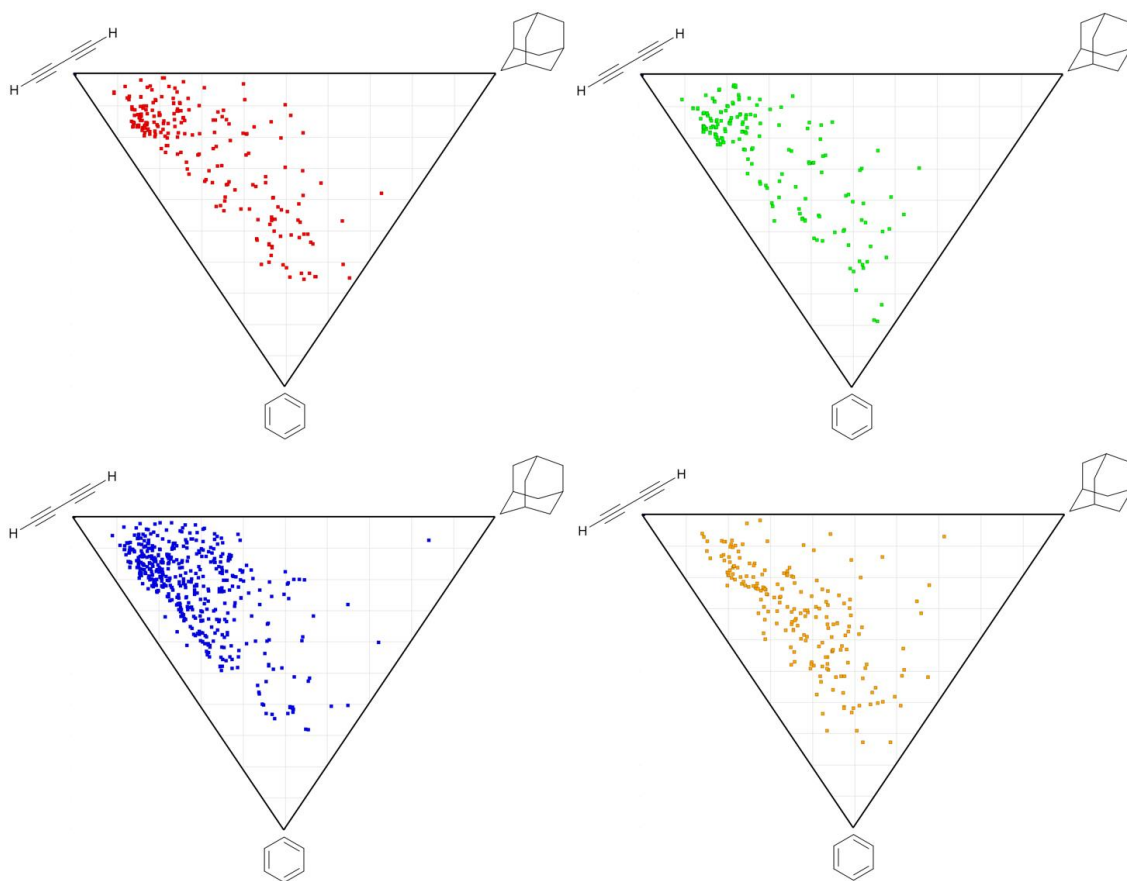
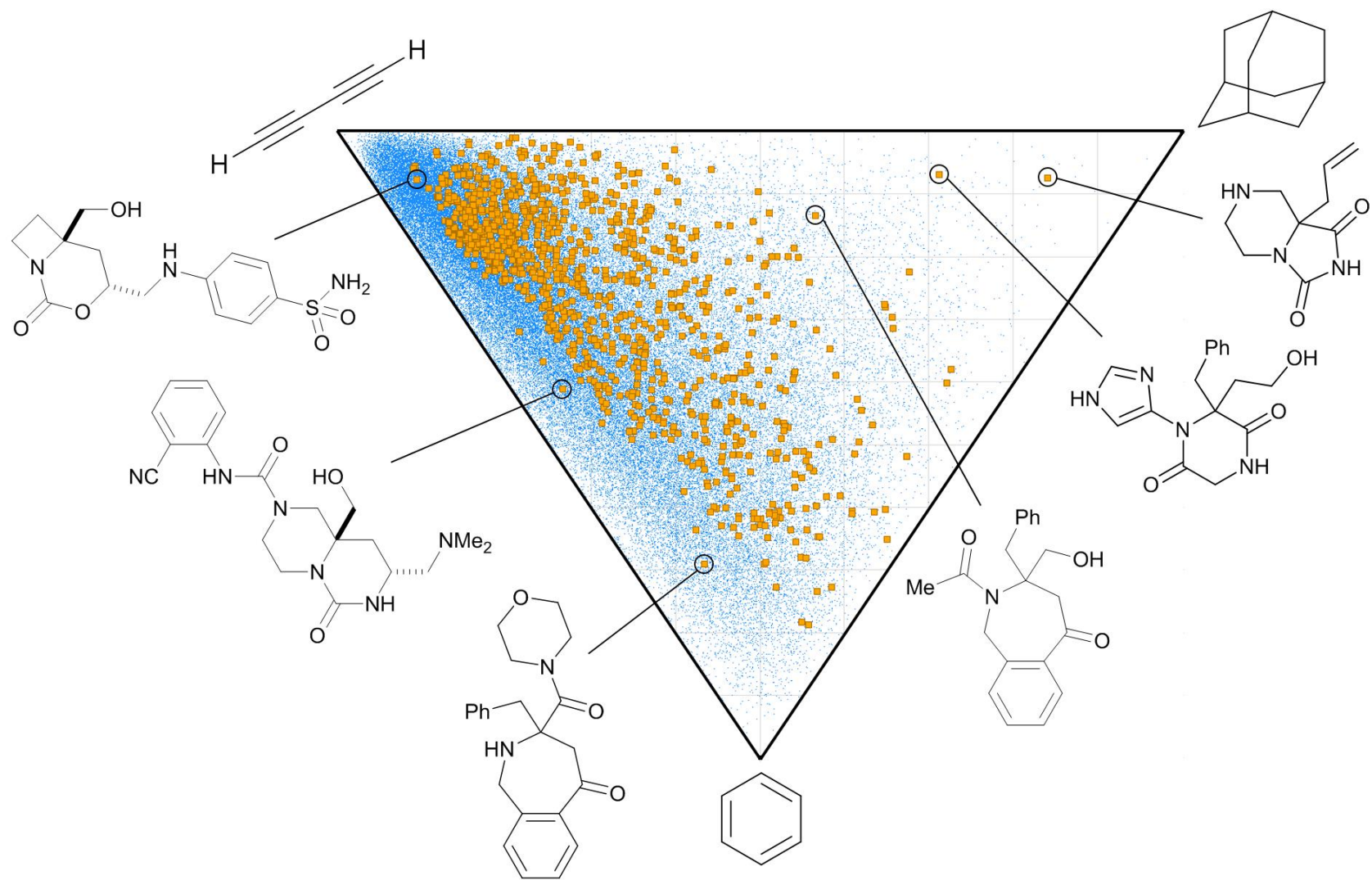


Figure 73 Normalised principal moment of inertia plots to show the shapes of the 1110 for the allylic alkylation-derived virtual library compounds, coloured by initial building block. Red= pyrrolidine-derived; green= azetidine derived; blue= piperazine-derived; orange= phenylalanine derived.

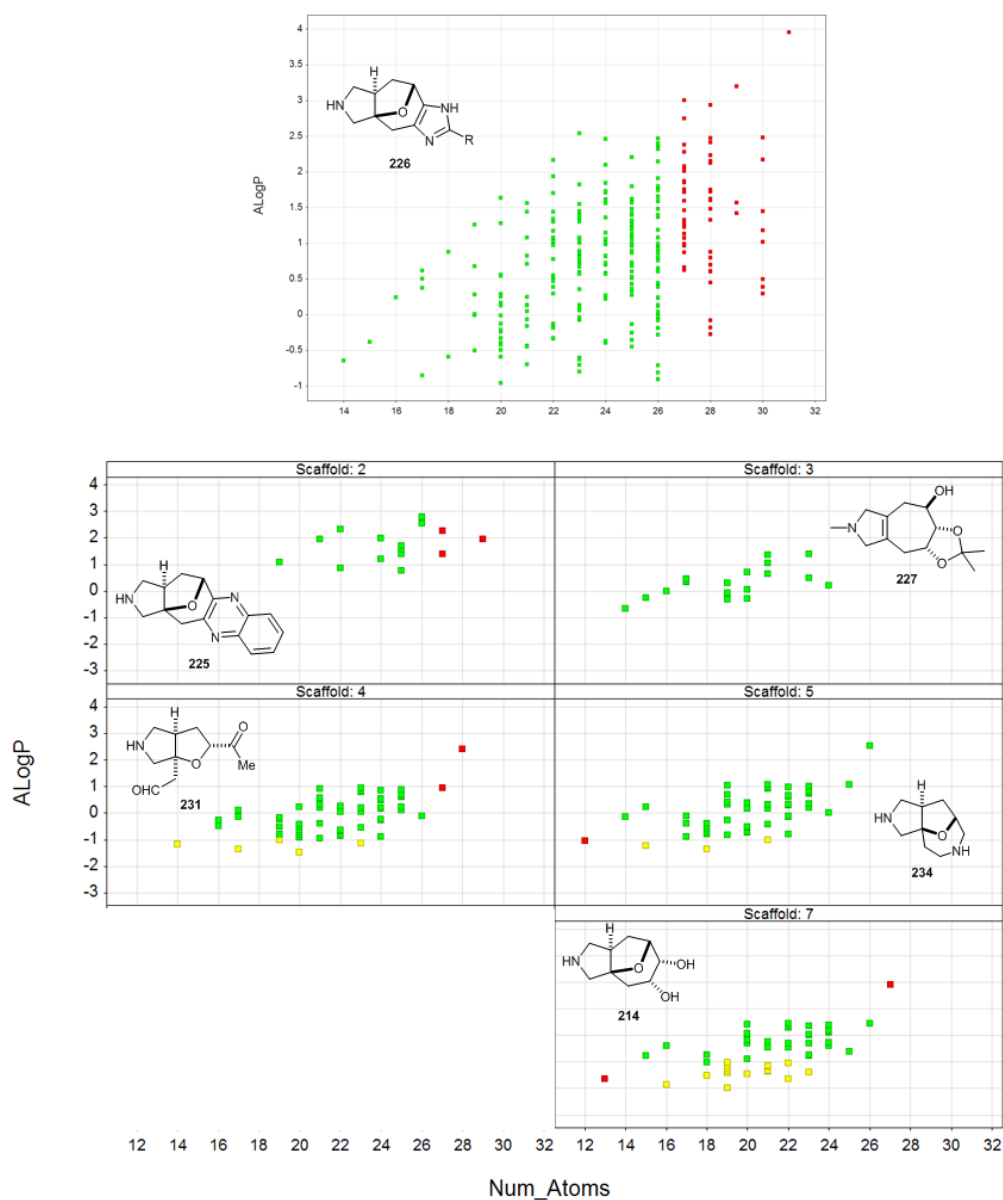


6.5 Data for the 'top-down' compound library

6.5.1 Lead-likeness assessment: Per scaffold basis

Filter	Virtual Library (1110)	
	Successive Filtering	Parallel Filtering
Fail $14 \leq nHA \leq 26$	82	82 (10%)
Fail $-1 \leq AlogP \leq 3$	145	151 (19%)
Fail Structural	0	0
Pass All	571 (72%)	n/a

Table 25 Filtering assessment data for cycloaddition-derived virtual library and the ZINC database. For comparison, data obtained from parallel filtering of all compounds using each filter in isolation is shown.



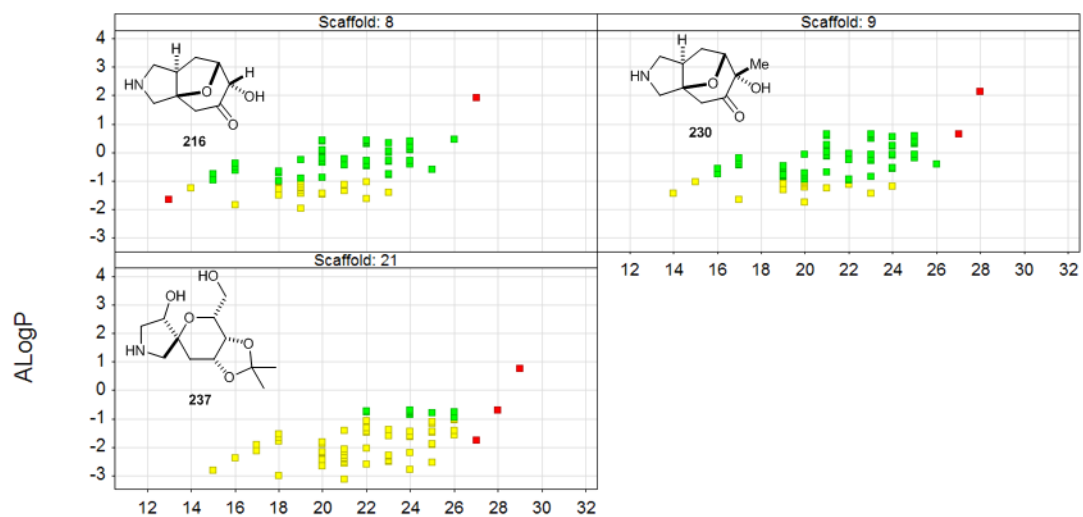
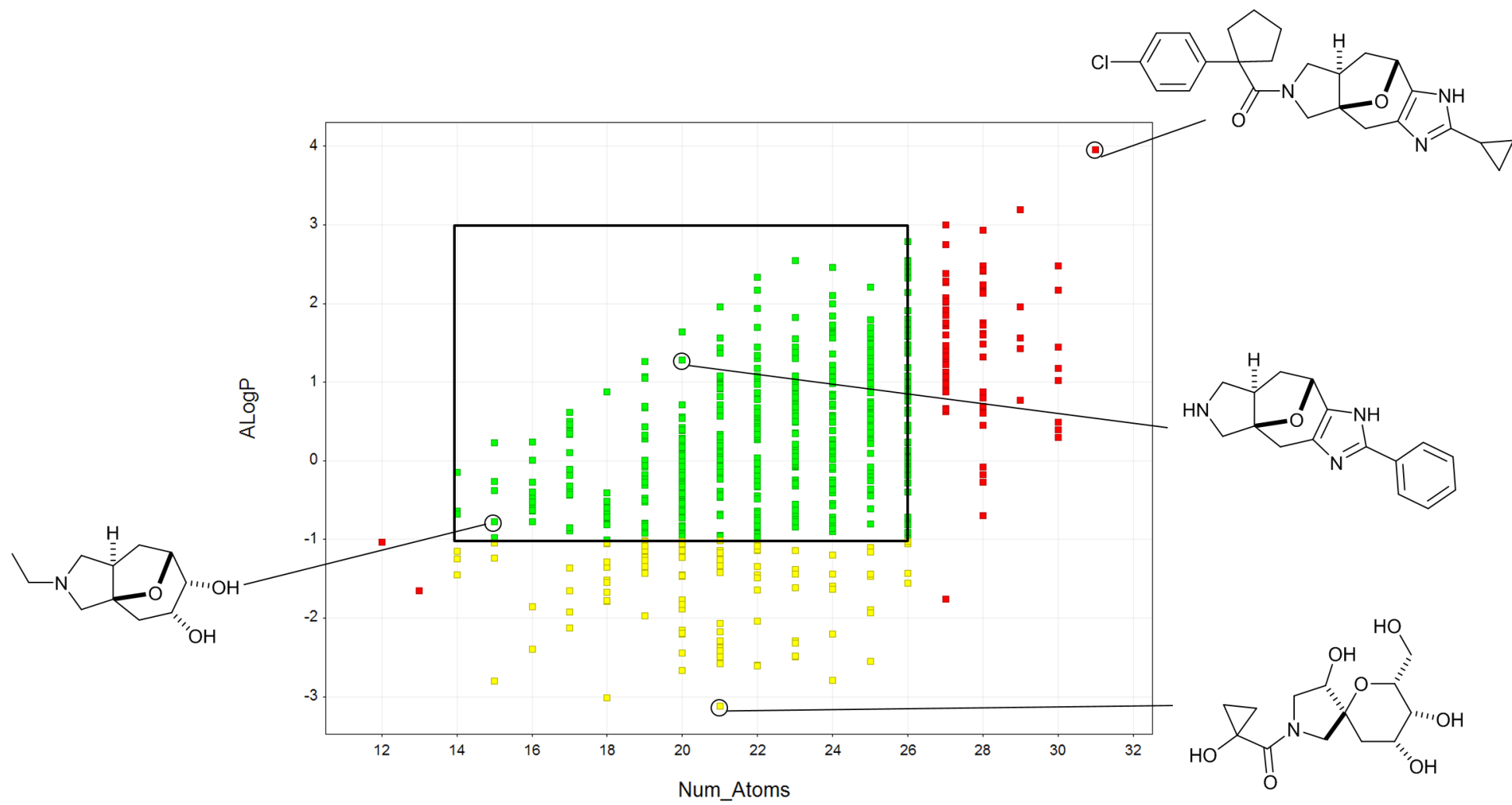


Figure 74 Distribution of number of heavy atoms (Num_Atoms) and AlogP for the virtual library based upon each scaffold. Compounds that survive successive filtering are shown in green. Compounds that fail successive filtering by number of heavy atoms (red), AlogP (yellow) are shown.

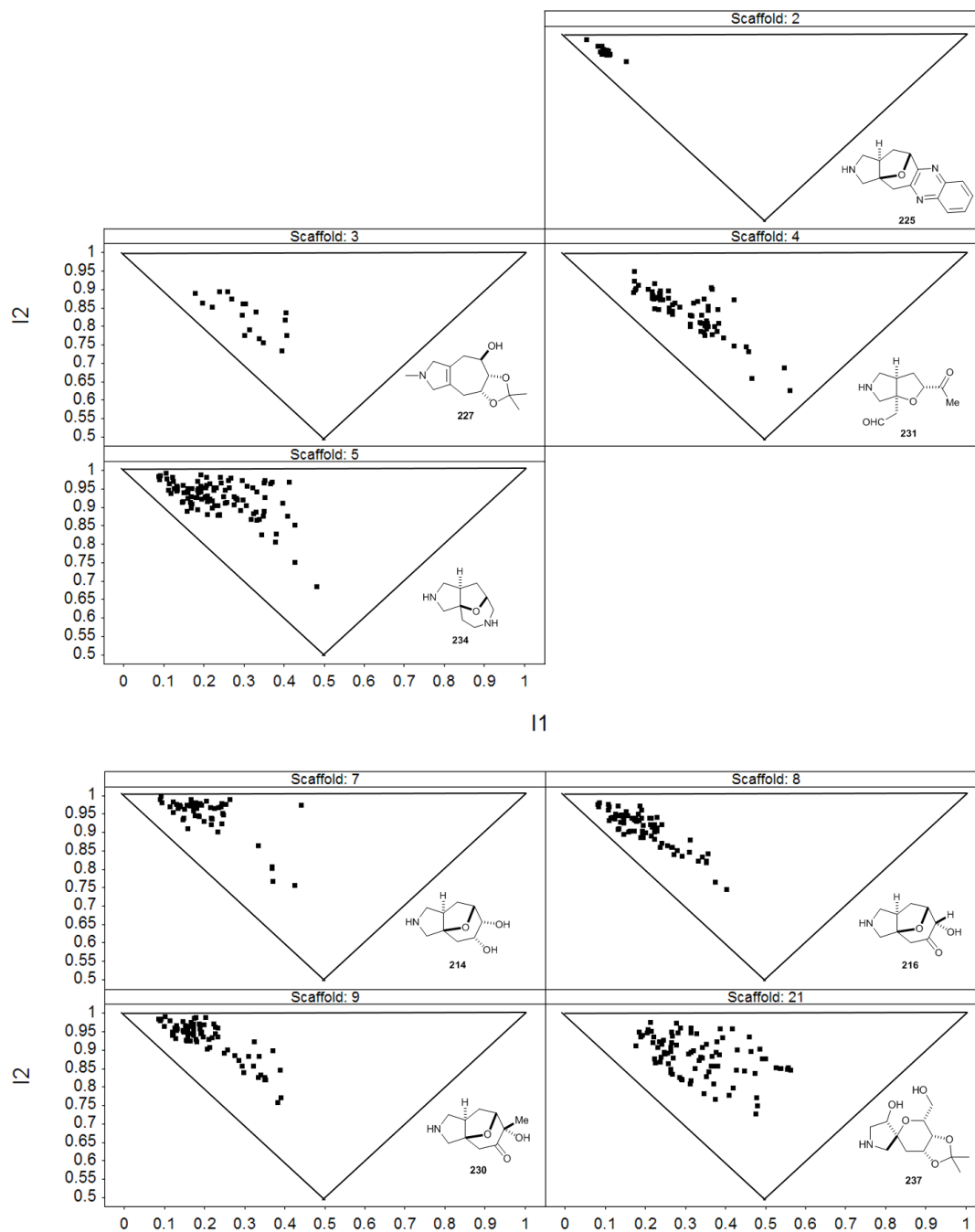


Entry	Scaffold	No. final compounds	No. lead-like compounds	% Lead-like Compounds	Average number of lead-like compounds per scaffold	Fail HA	Fail AlogP	Fail SS	Most likely reason for compound failure	Average heavy atom count (standard deviation)	Average AlogP (standard deviation)	Average Fsp ³ (standard deviation)
1	214	53	33	62	N/A	2	18	0	AlogP too low	21.1 (2.75)	-0.57 (0.77)	0.73 (0.16)
2	216	78	52	67		2	24	0	AlogP too low	20.2 (2.91)	-0.59 (0.69)	0.75 (0.16)
3	225	15	12	80		3	0	0	HA too high	24.5 (2.59)	1.72 (0.61)	0.54 (0.04)
4	226	294	227	77		67	0	0	HA too high	24.3 (2.96)	0.85 (0.86)	0.57 (0.01)
5	227	19	19	100		0	0	0	N/A	19.2 (2.72)	0.30 (0.56)	0.65 (0.14)
6	230	78	59	76		2	17	0	AlogP too low	21.2 (2.91)	-0.39 (0.69)	0.76 (0.15)
7	231	67	60	90		2	5	0	HA too high	21.4 (2.88)	-0.09 (0.71)	0.77 (0.15)
8	234	105	98	93		1	6	0	AlogP too low	20.2 (2.64)	0.07 (0.76)	0.73 (0.15)
9	237	89	11	12		3	75	0	AlogP too low	22.0 (2.92)	-1.7 (0.68)	0.75 (0.16)
10	Sum (9 scaffolds)	798	571	72	63	82	145	0	AlogP too low*	22.2 (3.36)	0.03 [†] (1.15)	0.68 (0.16)

Table 26 Lead-likeness assessment data for the cycloaddition-derived compounds.

*There were 171 failures for too low AlogP and 76 of these can be attributed to scaffold **237**. [†]Excluding scaffold **237** the average AlogP is 0.25.

6.5.2 PMI assessment: Per scaffold basis



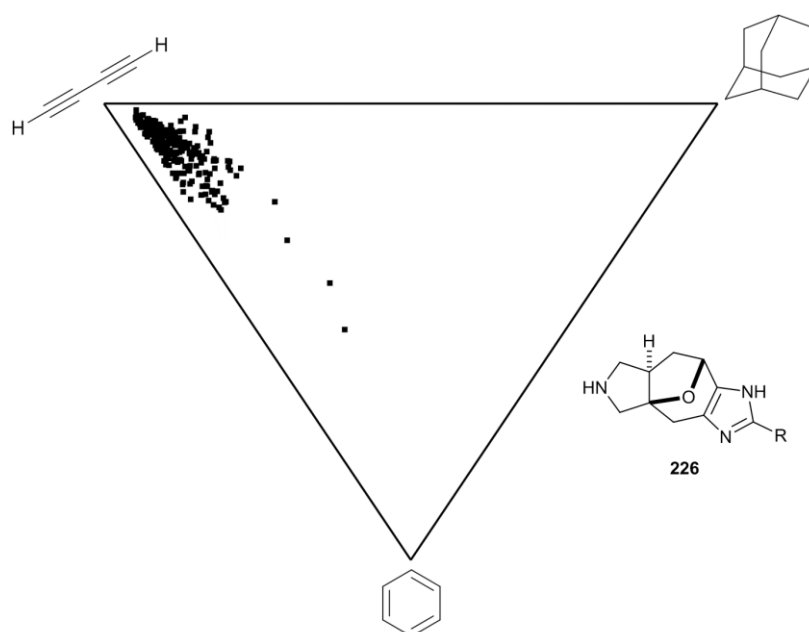
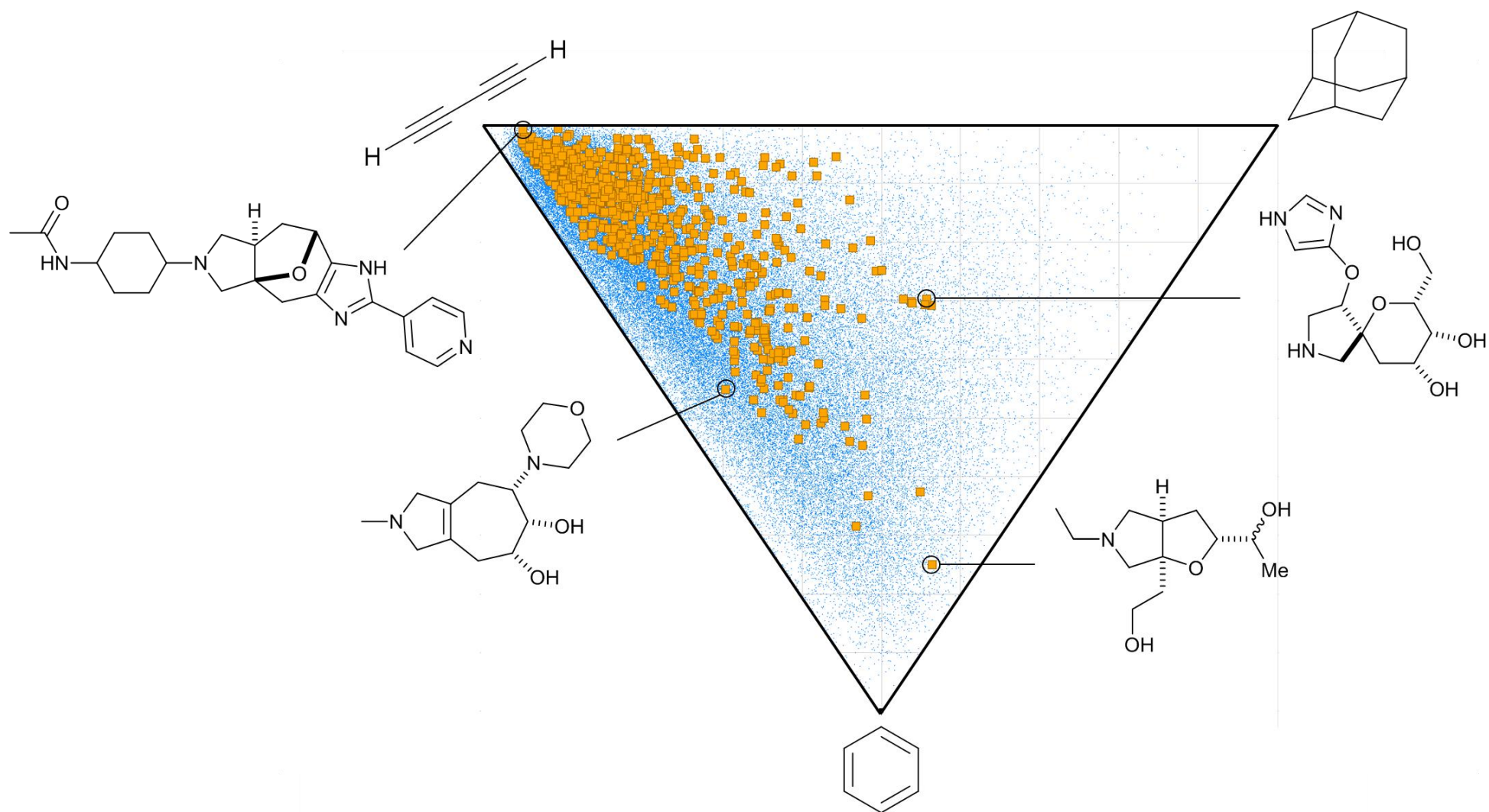
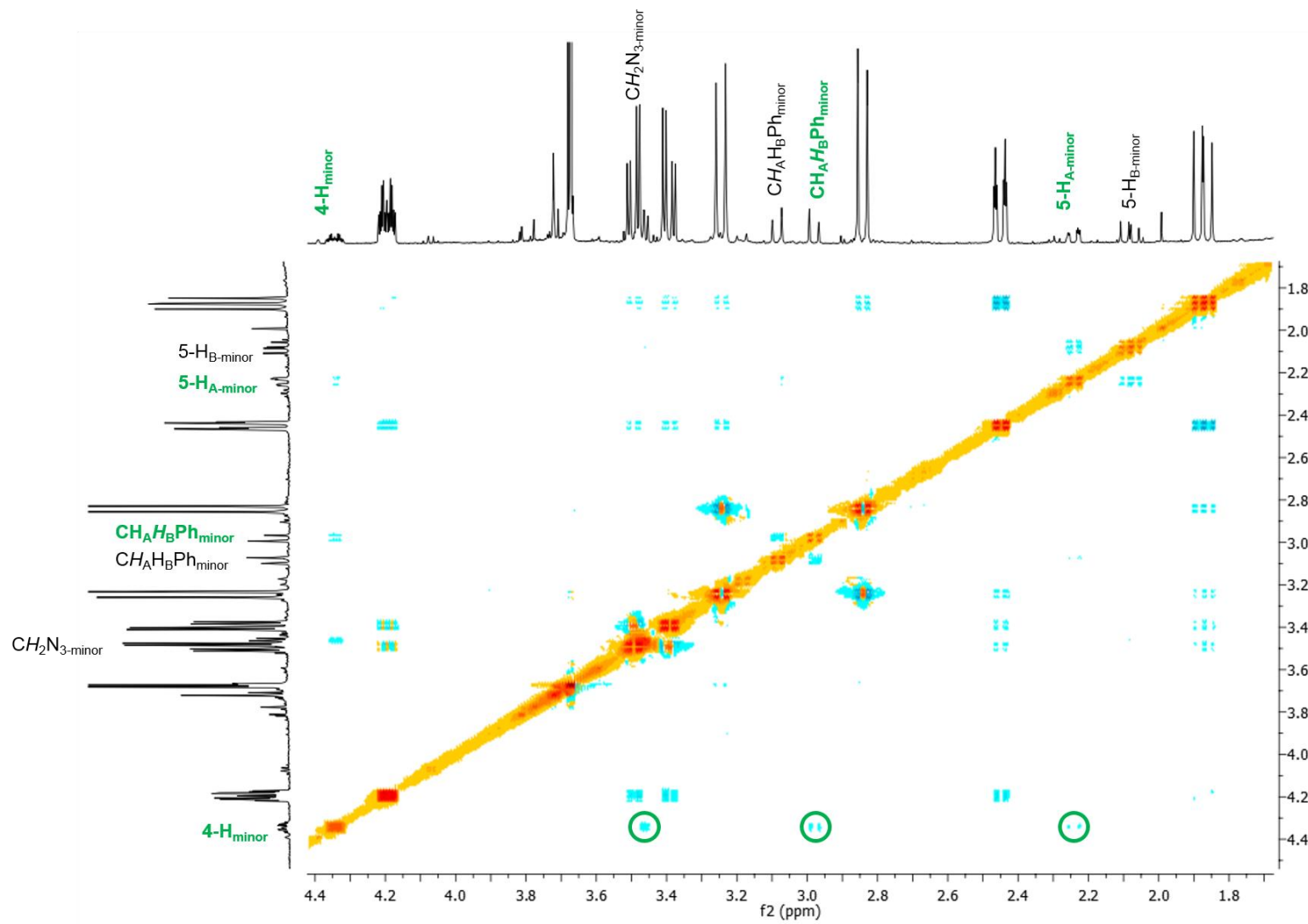


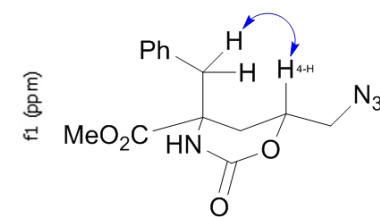
Figure 75 Normalised principal moment of inertia plots to show the shapes of the 798 cycloaddition-derived virtual library compounds with respect to each scaffold.

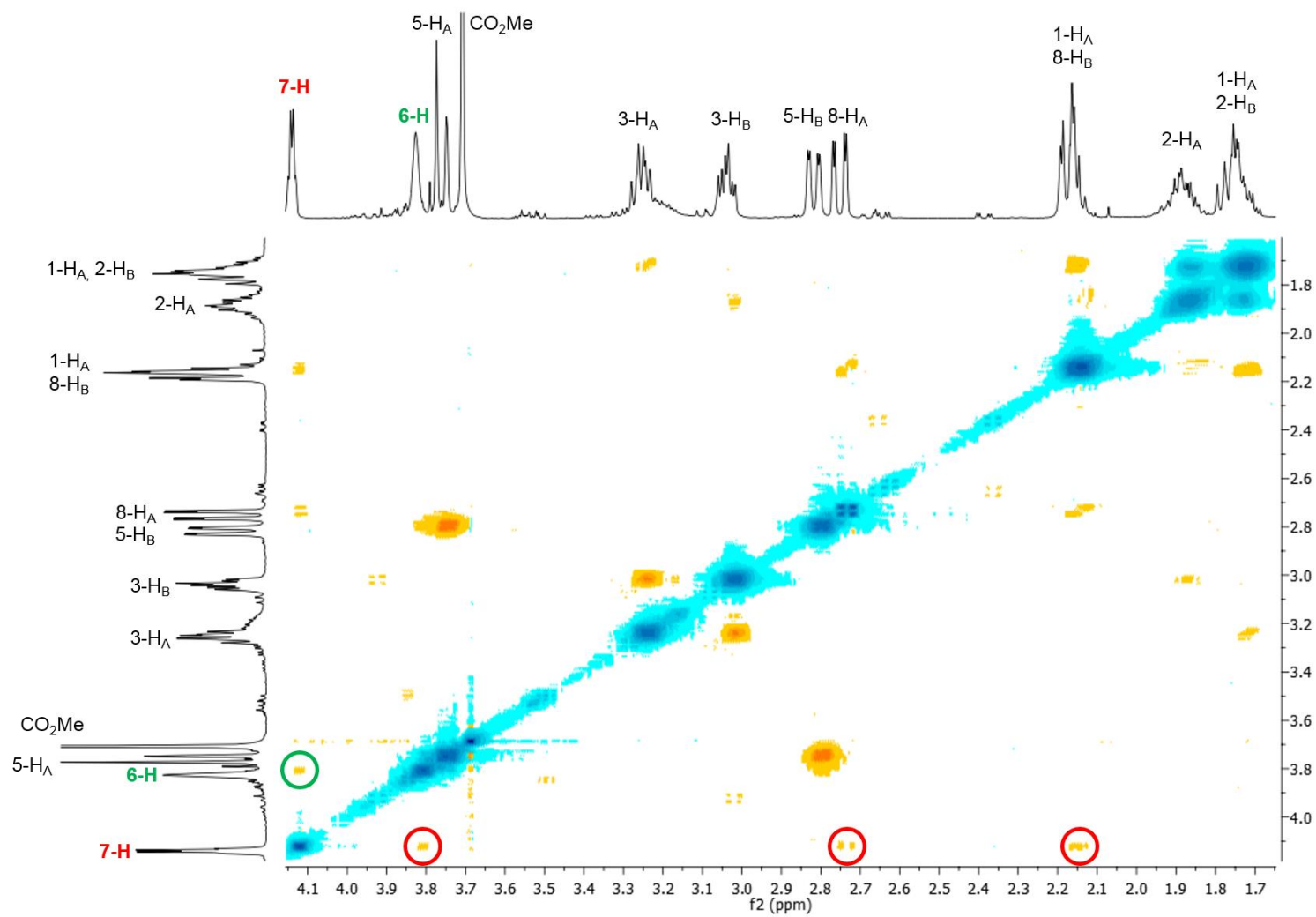


7.0 Appendix 2: NOESY and HMBC Spectra



70d_{minor}
NOESY correlations:

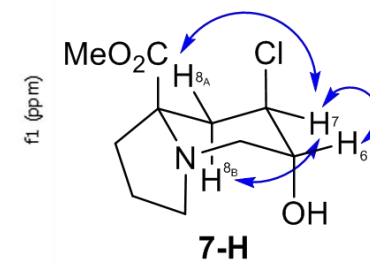


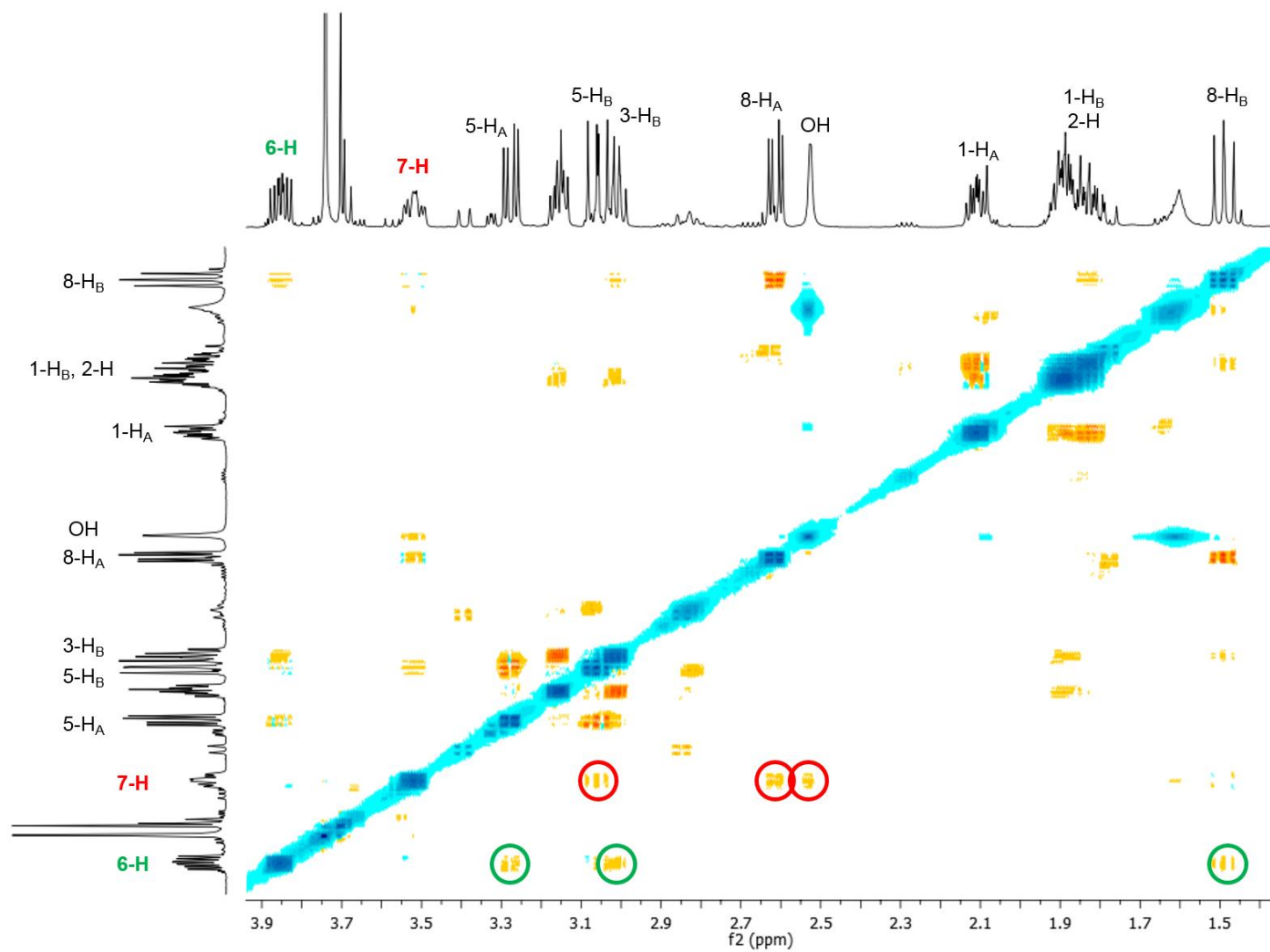
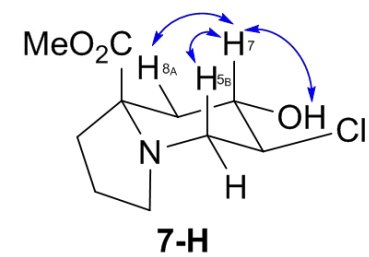
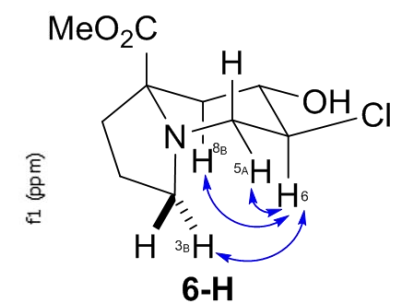


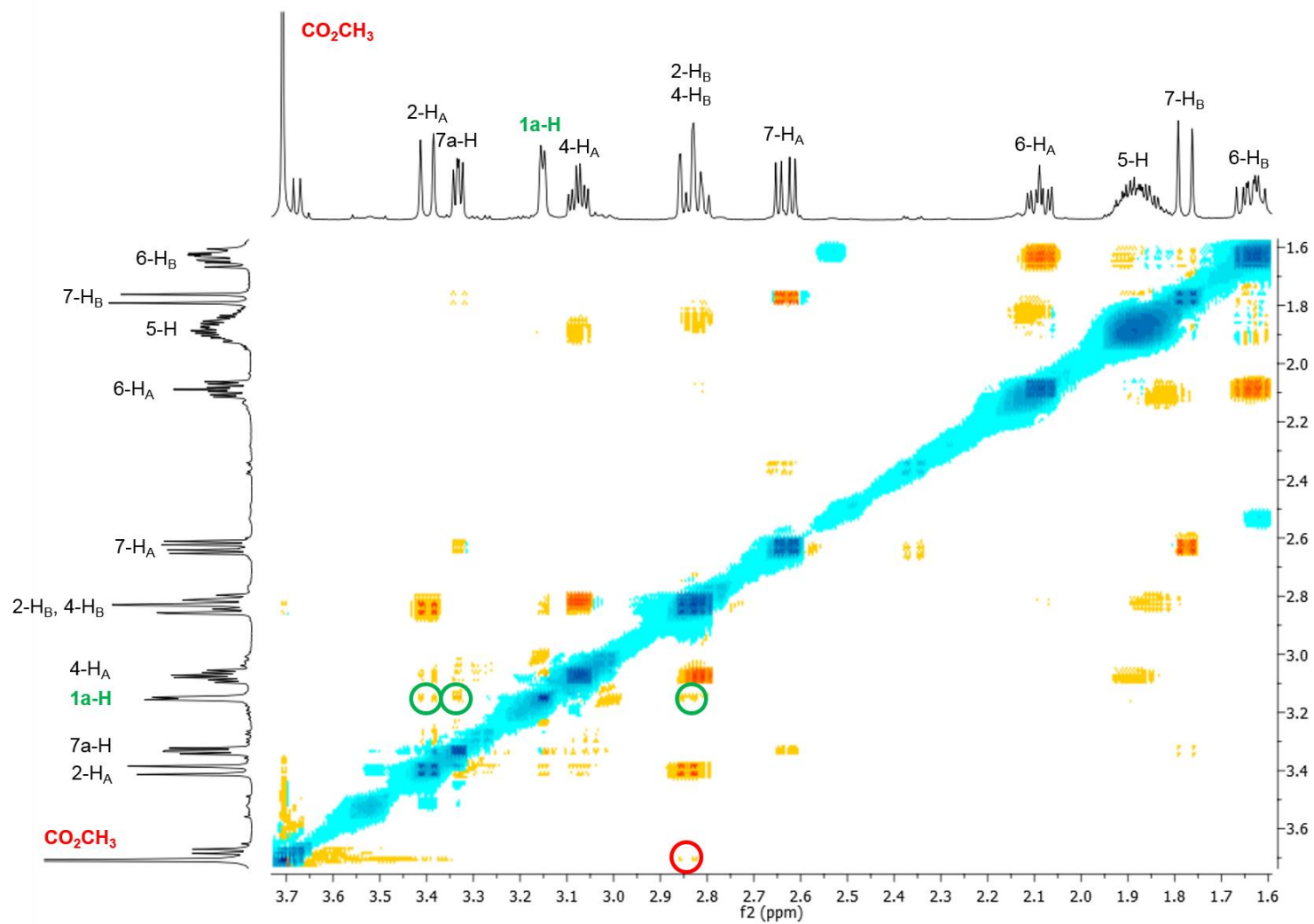
111 NOESY correlations:

6-H: 7-H

7-H: 6-H; 8-H_A; 8-H_B



**112 NOESY correlations:****5- H_B :** 5- H_A , 7- H **6- H :** 3- H_B ; 5- H_A ; 8- H_B **7- H :** OH, 5- H_B , 8- H_A **8- H_A :** 7- H , 8- H_B **8- H_B :** 3- H_B , 6- H , 8- H_A 



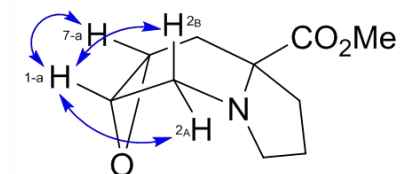
115 NOESY correlations:

1a-H: 2-H_A, 2-H_B and 7a-H

2-H_A: 1a-H, 2-H_B, 4-H_A

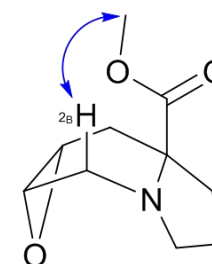
7a-H: 1a-H, 7-H_A

CO₂CH₃: 2-H_B

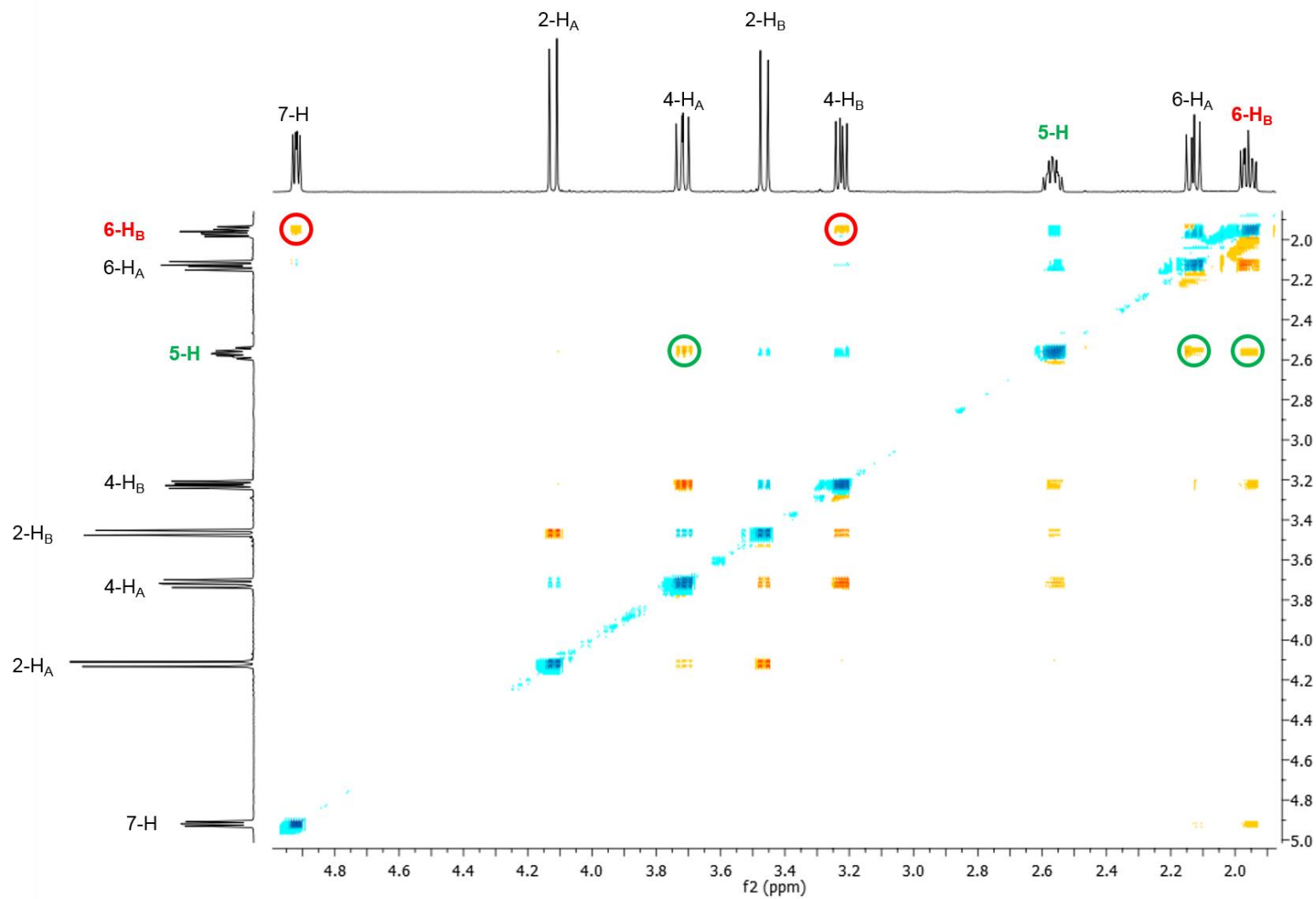


f1 (ppm)

1a-H



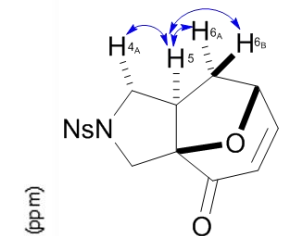
CO₂CH₃



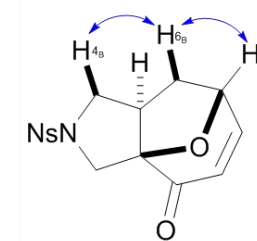
140a NOESY correlations:

5-H: 4-H_A; 6-H_A; 6-H_B

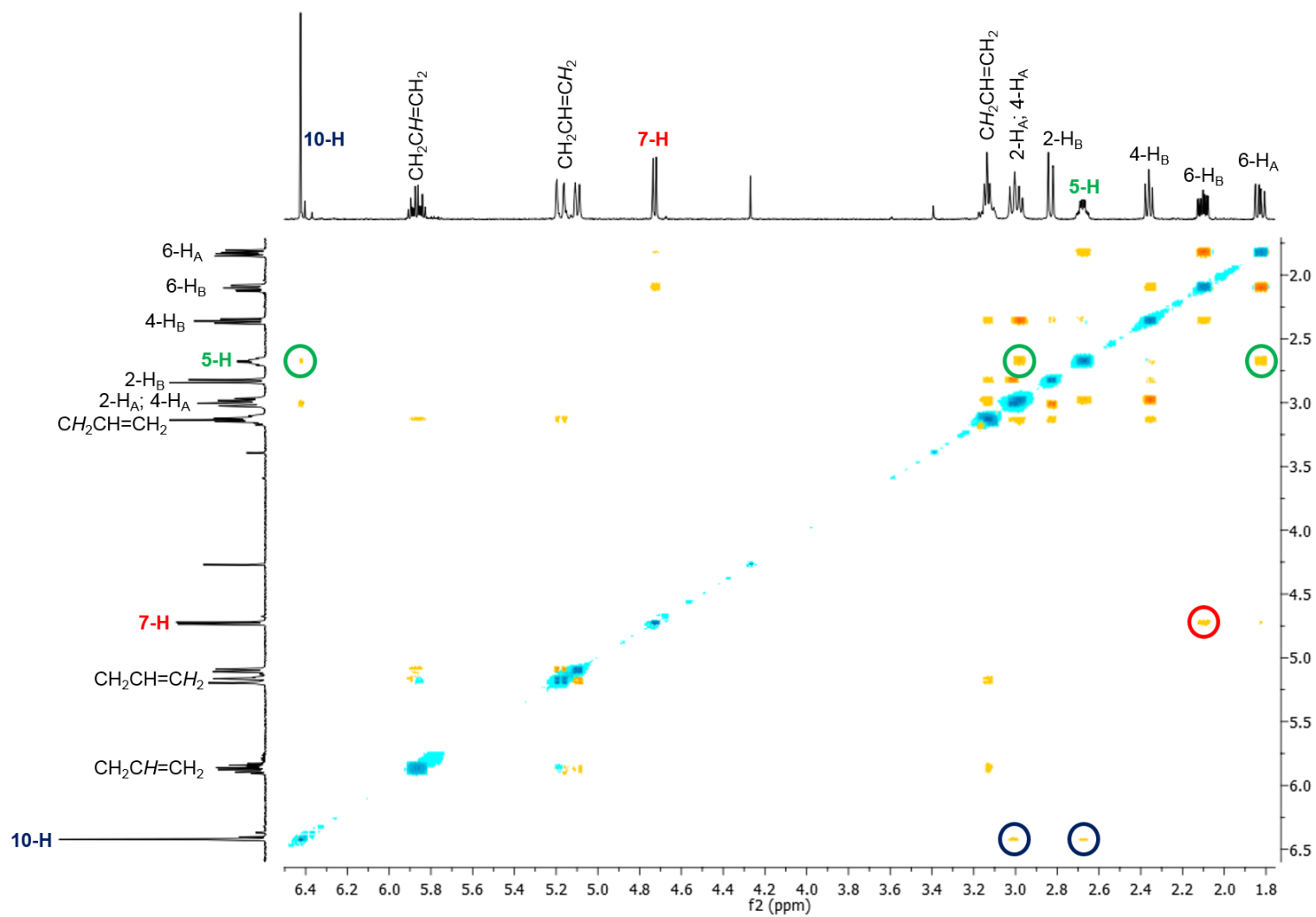
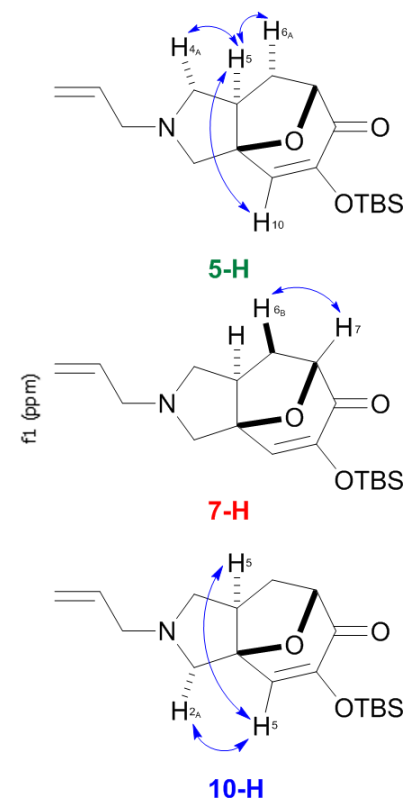
6-H_B: 4-H_B; 7-H

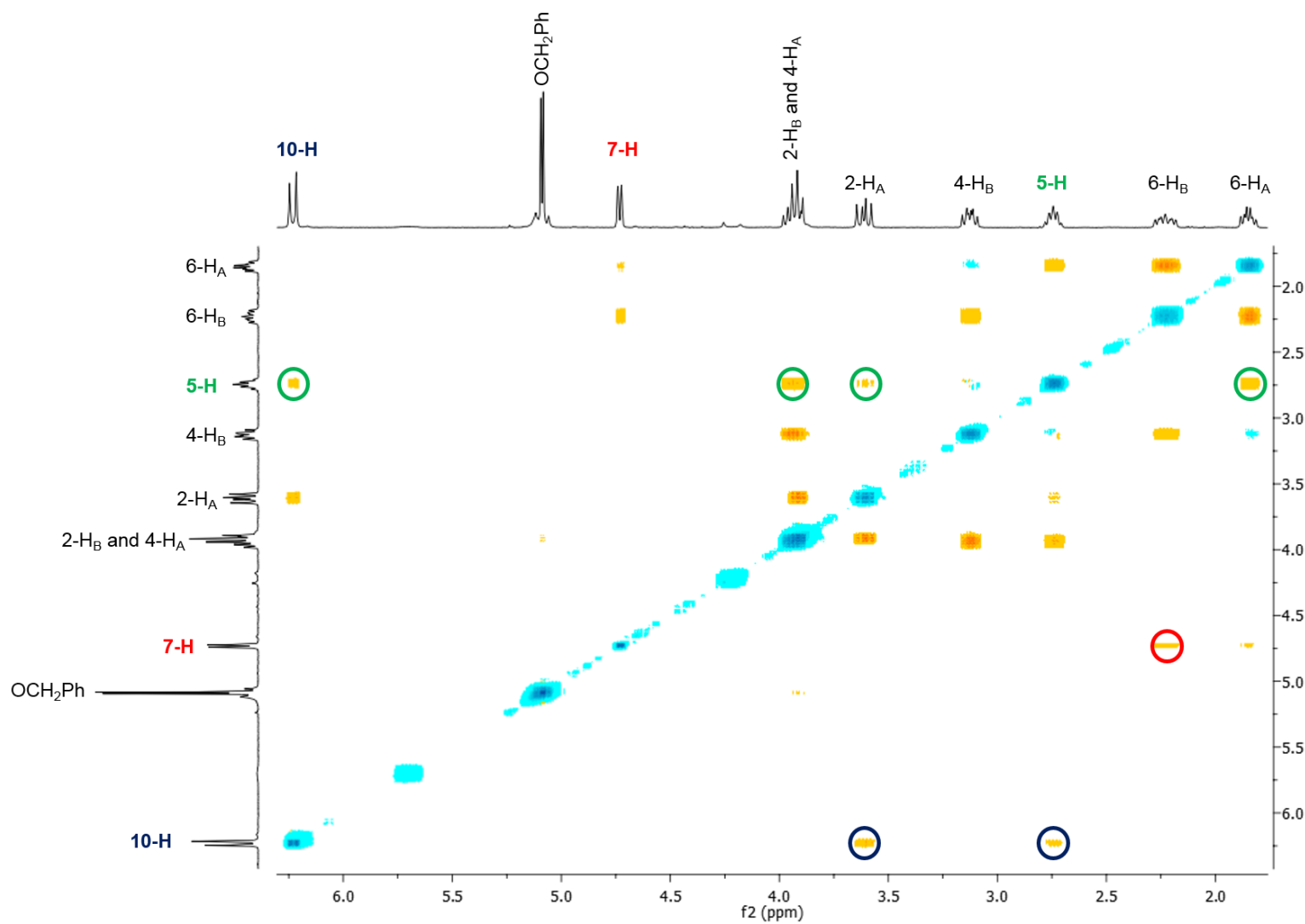
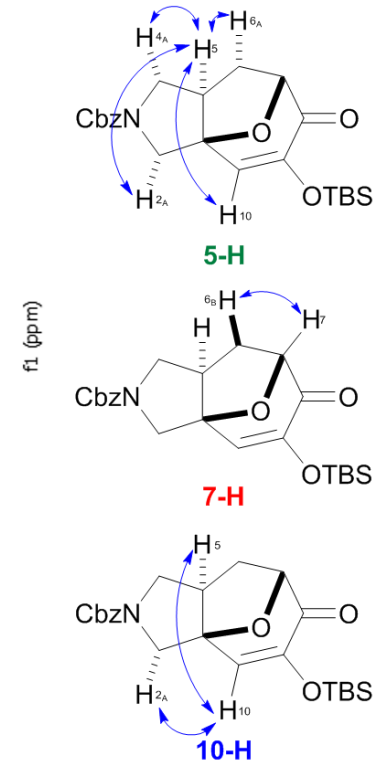


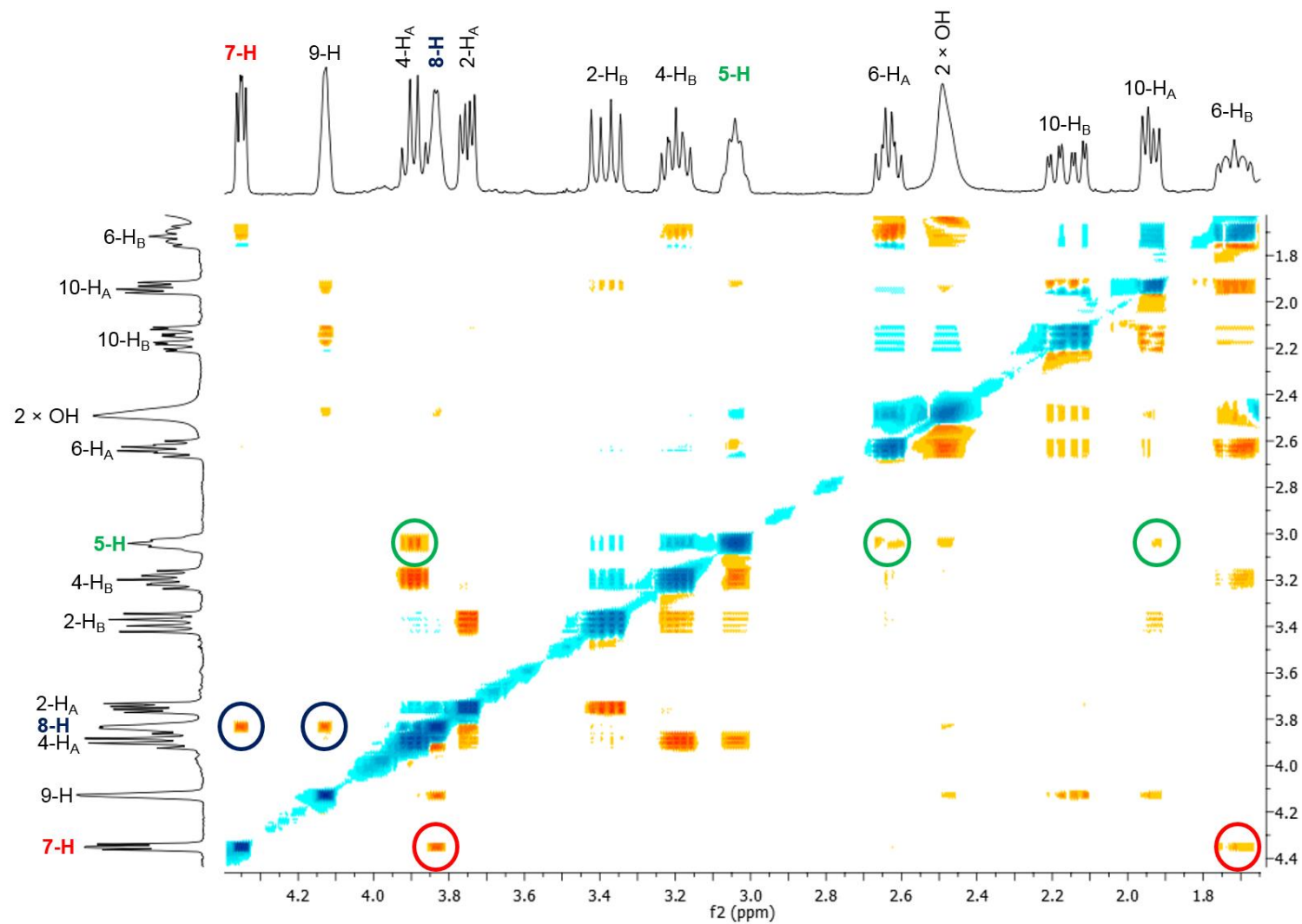
5-H



6-H_B

**181 NOESY correlations:****5-H:** 4- H_A ; 6- H_A ; 10-H**7-H:** 6- H_B **10-H:** 2- H_A ; 5-H

**183 NOESY correlations:****5-H:** 2-H_A; 4-H_A; 6-H_A; 10-H**7-H:** 6-H_B**10-H:** 2-H_A; 5-H

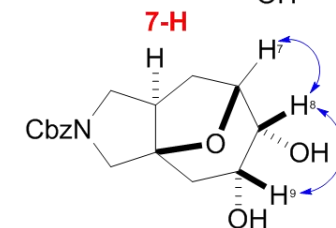
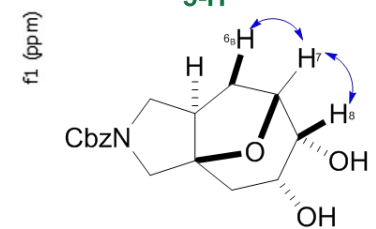
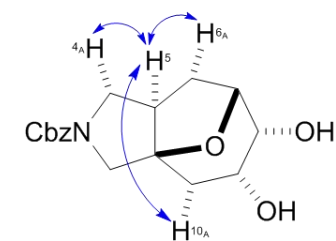


214 NOESY correlations:

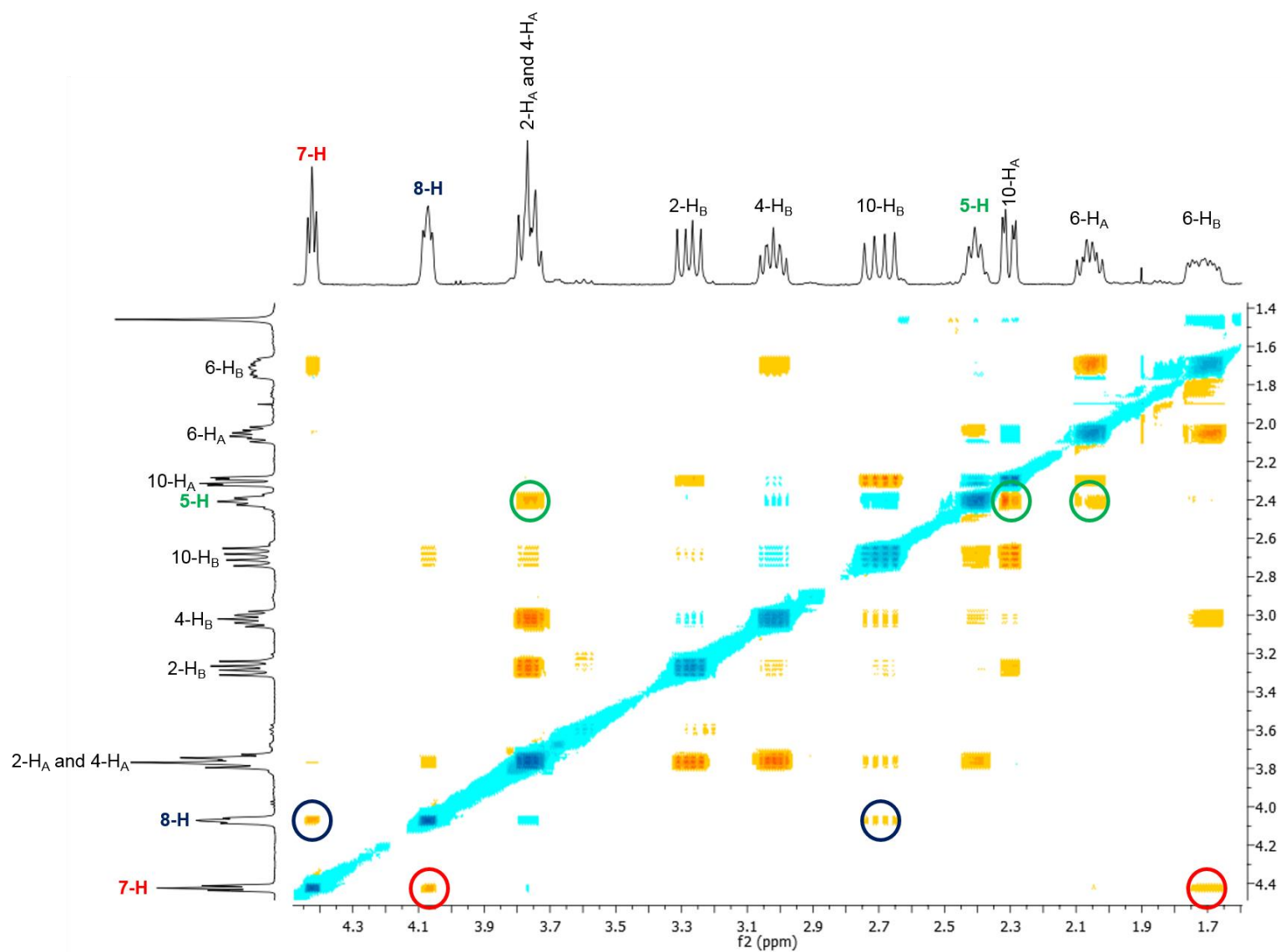
5-H: OH; 4-H_A; 6-H_A; 10-H_A

7-H: 6-H_B; 8-H

8-H: OH; 7-H; 9-H



8-H

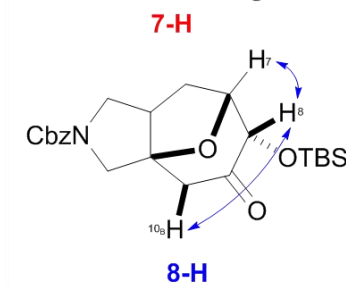
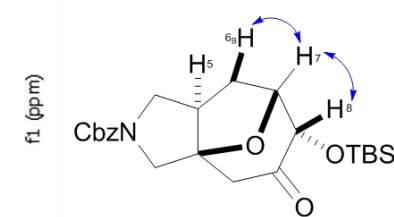
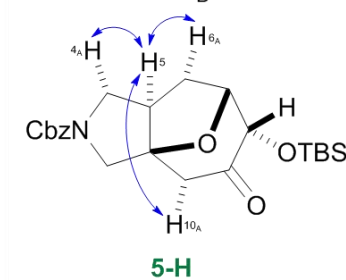


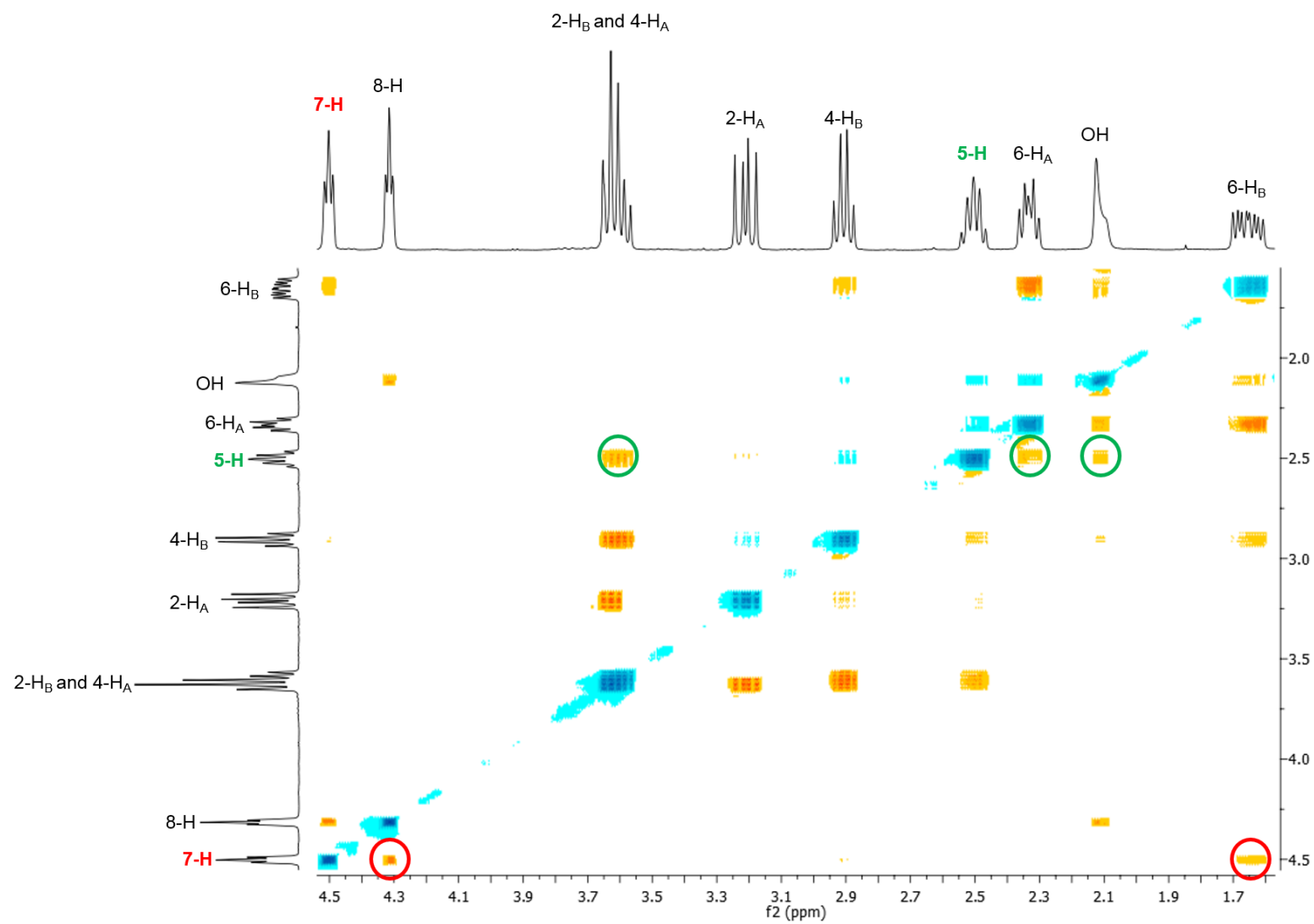
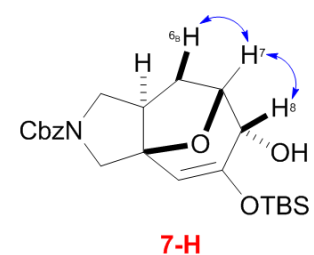
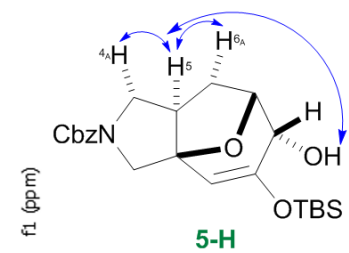
216 NOESY correlations:

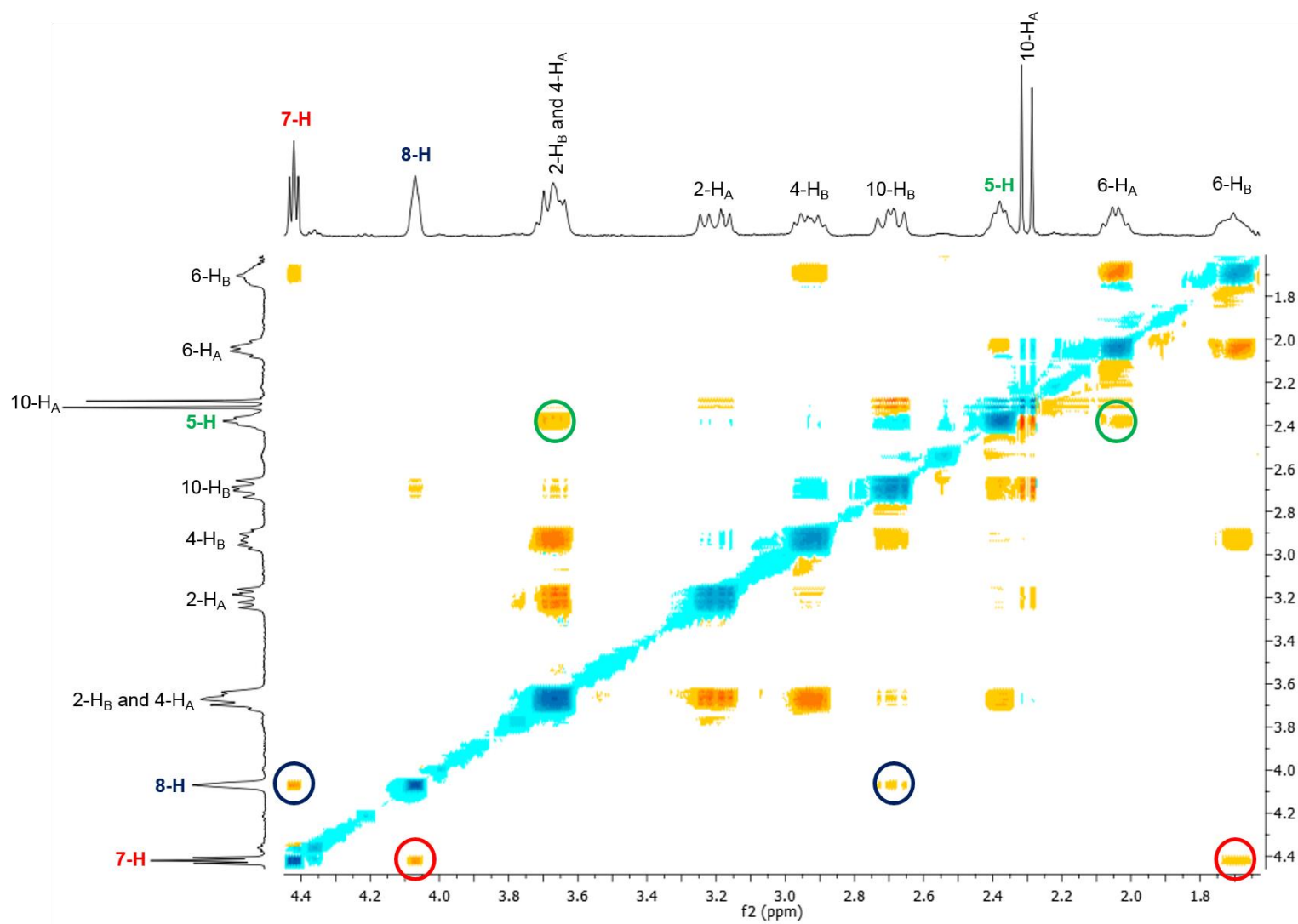
5-H: 4-H_A; 6-H_A; 10-H_A

7-H: 6-H_B; 8-H

8-H: 7-H; 10-H_B



**217 NOESY correlations:**5-H: OH, 4-H_A; 6-H_A7-H: 6-H_B; 8-H

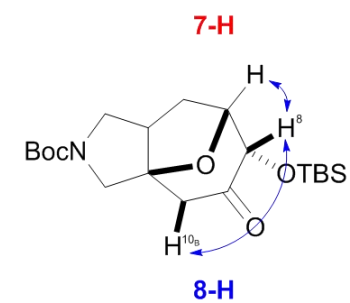
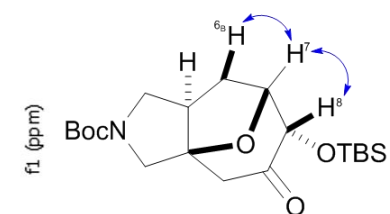
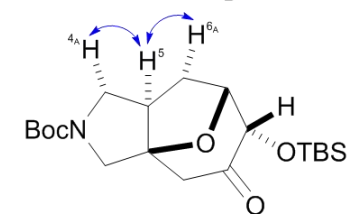


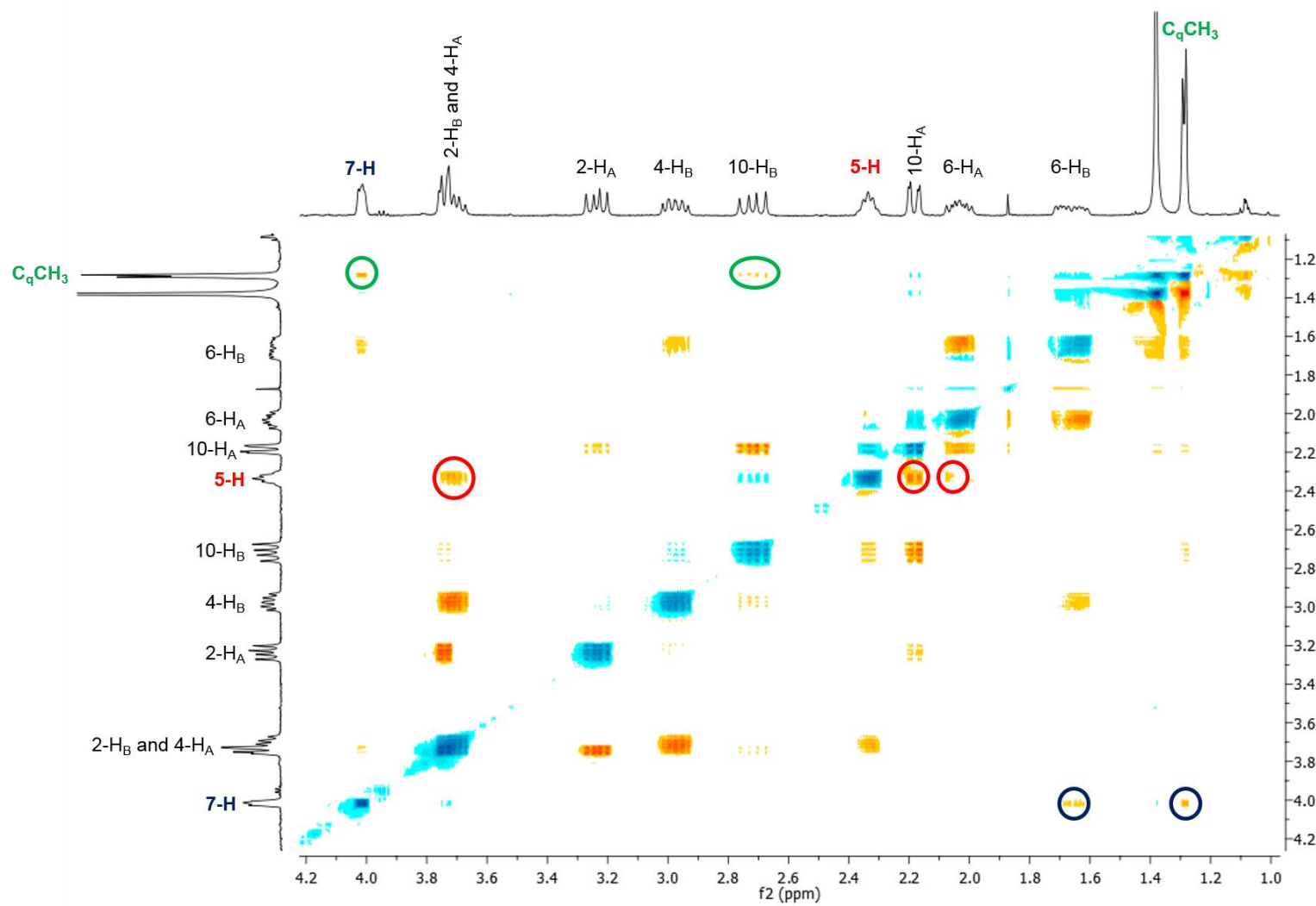
219 NOESY correlations:

5-H: 4-H_A; 6-H_A

7-H: 6-H_B; 8-H

8-H: 7-H; 10-H_B



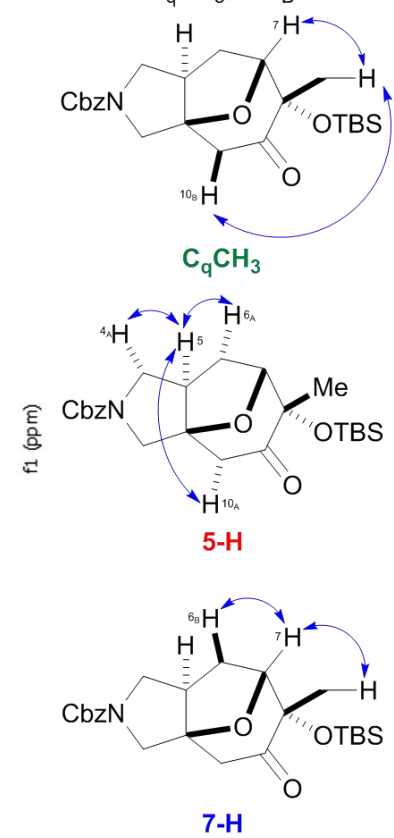


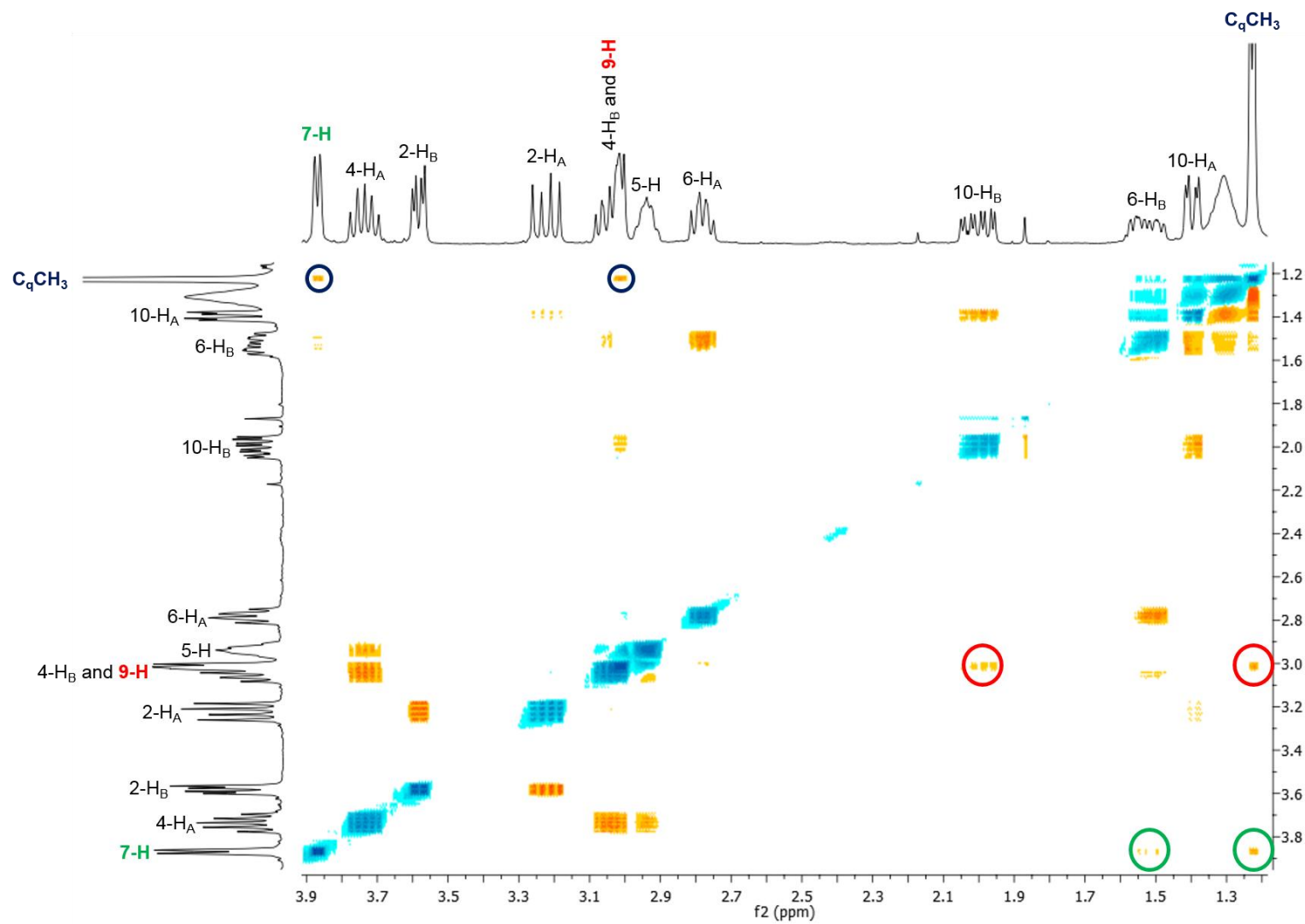
221 NOESY correlations:

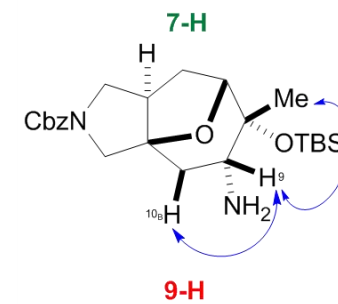
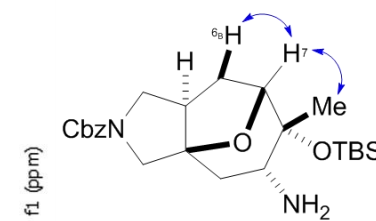
C_qCH₃: 7-H; 10-H_B

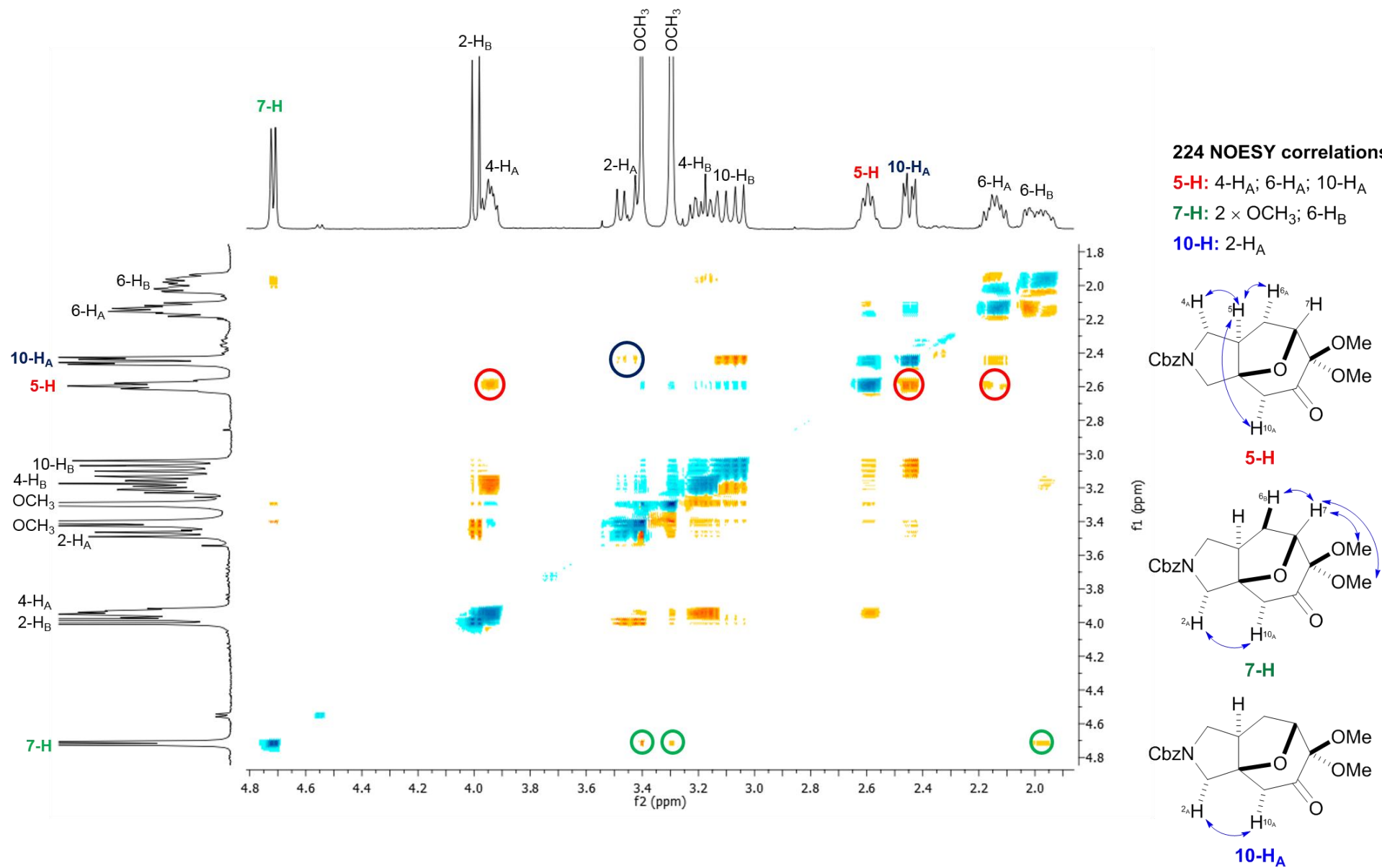
5-H: 4-H_A; 6-H_A; 10-H_A

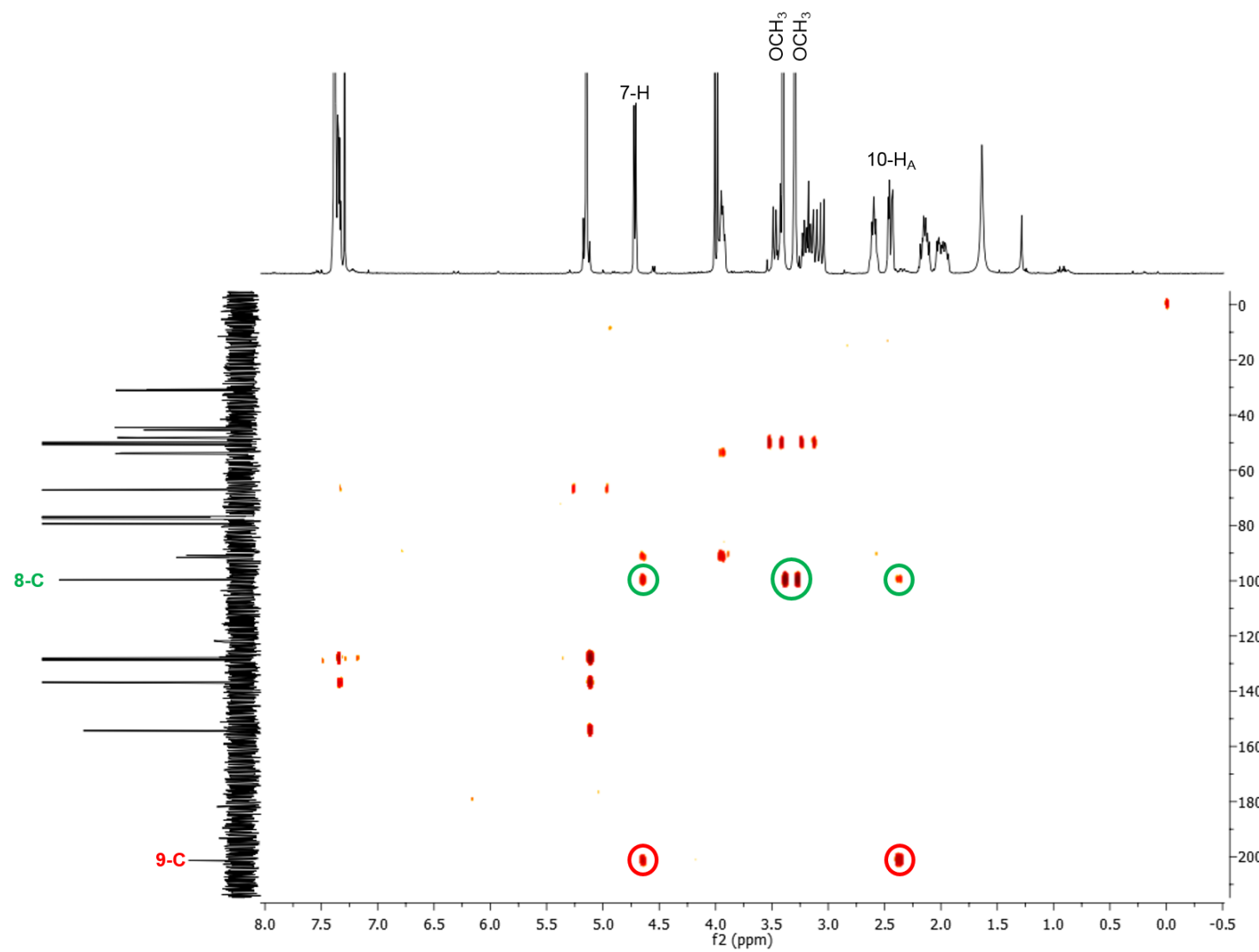
7-H: C_qCH₃; 6-H_B




222 NOESY correlations:
Me: 7-H; 9-H

7-H: Me; 6-H_B
9-H: Me; 10-H_B




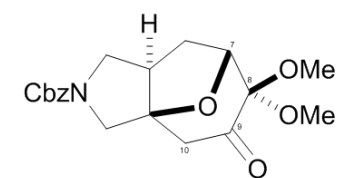
**224 HMBC correlations:**

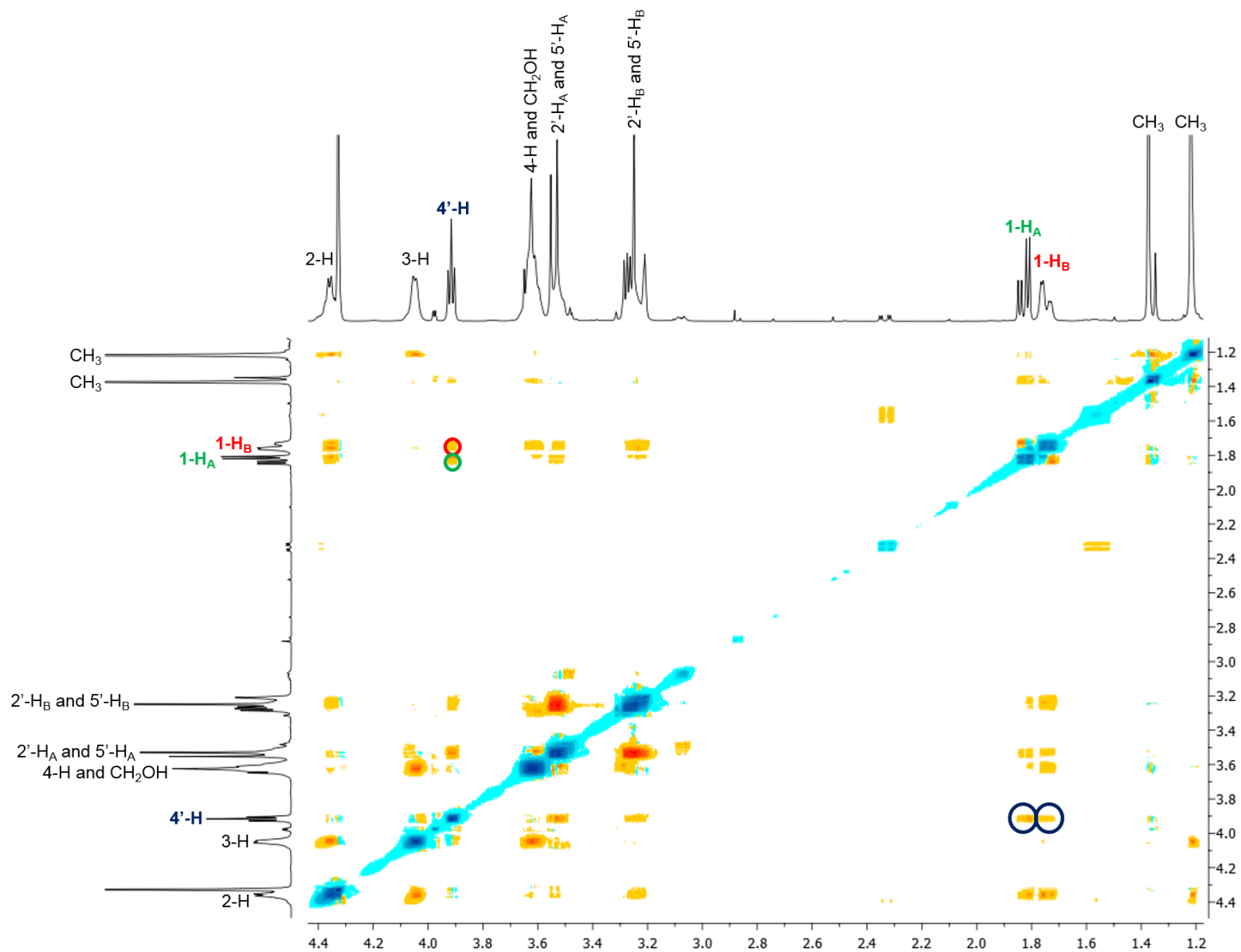
8-C: 2J with 7-H, $2 \times \text{OCH}_3$;

3J with 10-H_A

9-C: 2J with 10-H_A ;

3J with 7-H



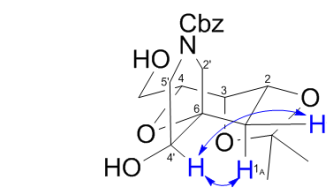
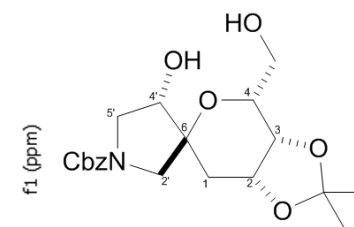


237 NOESY correlations:

1-H_A: 4'-H

1-H_B: 4'-H

4'-H: 1-H_A and 1-H_B



**key observed nOe
enhancements**

8.0 References

- (1) *The economic benefits of chemistry research to the UK*; Oxford Economics, 2010.
- (2) Khanna, I. *Drug Discov. Today* **2012**, 17 (19-20), 1088–1102.
- (3) Paul, S. M.; Mytelka, D. S.; Dunwiddie, C. T.; Persinger, C. C.; Munos, B. H.; Lindborg, S. R.; Schacht, A. L. *Nat. Rev. Drug Discov.* **2010**, 9 (3), 203–214.
- (4) Staton, T. Top 10 Drug Patent Losses of 2014 <http://www.fiercepharma.com/special-reports/top-10-drug-patent-losses-2014> (accessed Apr 6, 2015).
- (5) McKee, S. NHS spend on new drugs set to shrink http://www.pharmatimes.com/article/12-07-03/NHS_spend_on_new_drugs_set_to_shrink.aspx (accessed Apr 6, 2015).
- (6) Cohen, F. J. *Nat. Rev. Drug Discov.* **2005**, 4 (1), 78–84.
- (7) Schneider, C. K.; Schäffner-Dallmann, G. *Nat. Rev. Drug Discov.* **2008**, 7 (11), 893–899.
- (8) Wood, A. J. J. *New Engl. J. Med.* **2006**, 355 (6), 618–623.
- (9) Leeson, P. D.; Springthorpe, B. *Nat. Rev. Drug Discov.* **2007**, 6 (11), 881–890.
- (10) Nadin, A.; Hattotuwigama, C.; Churcher, I. *Angew. Chem. Int. Ed.* **2012**, 51 (5), 1114–1122.
- (11) MacLellan, P.; Nelson, A. *Chem. Commun.* **2013**, 49 (24), 2383–2393.
- (12) Doveston, R.; Marsden, S.; Nelson, A. *Drug Discov. Today* **2014**, 19 (7), 813–819.

- (13) Wild, H.; Heimbach, D.; Huwe, C. *Angew. Chem. Int. Ed.* **2011**, *50* (33), 7452–7453.
- (14) *Novel New Drugs 2014 Summary*; U.S. Food and Drug Administration Center for Drug Evaluation and Research, 2015.
- (15) Morrow, T.; Felcone, L. H. *Biotechnol. Healthc.* **2004**, *1* (4), 24–29.
- (16) Hughes, J. P.; Rees, S.; Kalindjian, S. B.; Philpott, K. L. *Br. J. Pharmacol.* **2011**, *162* (6), 1239–1249.
- (17) Macarron, R.; Banks, M. N.; Bojanic, D.; Burns, D. J.; Cirovic, D. A.; Garyantes, T.; Green, D. V. S.; Hertzberg, R. P.; Janzen, W. P.; Paslay, J. W.; Schopfer, U.; Sittampalam, G. S. *Nat. Rev. Drug Discov.* **2011**, *10* (3), 188–195.
- (18) Cooper, T. W. J.; Campbell, I. B.; Macdonald, S. J. F. *Angew. Chem. Int. Ed.* **2010**, *49* (44), 8082–8091.
- (19) Lovering, F.; Bikker, J.; Humblet, C. *J. Med. Chem.* **2009**, *52* (21), 6752–6756.
- (20) Tosatti, P.; Horn, J.; Campbell, A. J.; House, D.; Nelson, A.; Marsden, S. P. *Adv. Synth. Catal.* **2010**, *352* (18), 3153–3157.
- (21) Tosatti, P.; Campbell, A. J.; House, D.; Nelson, A.; Marsden, S. P. *J. Org. Chem.* **2011**, *76* (13), 5495–5501.
- (22) Roughley, S. D.; Jordan, A. M. *J. Med. Chem.* **2011**, *54* (10), 3451–3479.
- (23) Walters, W. P.; Green, J.; Weiss, J. R.; Murcko, M. A. *J. Med. Chem.* **2011**, *54* (19), 6405–6416.
- (24) Shelat, A. A.; Guy, R. K. *Nat. Chem. Biol.* **2007**, *3* (8), 442–446.
- (25) Krier, M.; Bret, G.; Rognan, D. *J. Chem. Inf. Model.* **2006**, *46* (2), 512–524.
- (26) Lipkus, A. H.; Yuan, Q.; Lucas, K. A.; Funk, S. A.; Bartelt, W. F.; Schenck, R. J.; Trippe, A. J. *J. Org. Chem.* **2008**, *73* (12), 4443–4451.

- (27) Collins, K. D.; Glorius, F. *Nat. Chem.* **2013**, *5* (7), 597–601.
- (28) Lipinski, C. A.; Lombardo, F.; Dominy, B. W.; Feeney, P. J. *Adv. Drug Deliv. Rev.* **1997**, *23* (1-3), 3–25.
- (29) Ajay, A.; Walters, W. P.; Murcko, M. A. *J. Med. Chem.* **1998**, *41* (18), 3314–3324.
- (30) Walters, W. P.; Murcko, A. A.; Murcko, M. A. *Curr. Opin. Chem. Biol.* **1999**, *3* (4), 384–387.
- (31) Lipinski, C. A. *J. Pharm. Toxicol. Methods* **2001**, *44* (1), 235–249.
- (32) Muegge, I.; Heald, S. L.; Brittelli, D. *J. Med. Chem.* **2001**, *44* (12), 1841–1846.
- (33) Walters, W. P.; Murcko, M. A. *Adv. Drug Deliv. Rev.* **2002**, *54* (3), 255–271.
- (34) Veber, D. F.; Johnson, S. R.; Cheng, H.-Y.; Smith, B. R.; Ward, K. W.; Kopple, K. D. *J. Med. Chem.* **2002**, *45* (12), 2615–2623.
- (35) Proudfoot, J. R. *Bioorg. Med. Chem. Lett.* **2002**, *12* (12), 1647–1650.
- (36) Muegge, I. *Med. Res. Rev.* **2003**, *23* (3), 302–321.
- (37) Lajiness, M. S.; Vieth, M.; Erickson, J. *Curr. Opin. Drug Discov. Devel.* **2004**, *7* (4), 470–477.
- (38) Hughes, J. D.; Blagg, J.; Price, D. A.; Bailey, S.; Decrescenzo, G. A.; Devraj, R. V.; Ellsworth, E.; Fobian, Y. M.; Gibbs, M. E.; Gilles, R. W.; Greene, N.; Huang, E.; Krieger-Burke, T.; Loesel, J.; Wager, T.; Whiteley, L.; Zhang, Y. *Bioorg. Med. Chem. Lett.* **2008**, *18* (17), 4872–4875.
- (39) Gleeson, M. P. *J. Med. Chem.* **2008**, *51* (4), 817–834.
- (40) Gleeson, P.; Bravi, G.; Modi, S.; Lowe, D. *Bioorg. Med. Chem.* **2009**, *17* (16), 5906–5919.

- (41) Sperandio, O.; Reynès, C. H.; Camproux, A.-C.; Villoutreix, B. O. *Drug Discov. Today* **2010**, *15* (5-6), 220–229.
- (42) Wager, T. T.; Chandrasekaran, R. Y.; Hou, X.; Troutman, M. D.; Verhoest, P. R.; Villalobos, A.; Will, Y. *ACS Chem. Neurosci.* **2010**, *1* (6), 420–434.
- (43) Waring, M. J.; Johnstone, C. *Bioorg. Med. Chem. Lett.* **2007**, *17* (6), 1759–1764.
- (44) Waring, M. J. *Bioorg. Med. Chem. Lett.* **2009**, *19* (10), 2844–2851.
- (45) Leeson, P. D.; Empfield, J. R. In *Annual Reports in Medicinal Chemistry*; Macor, J. E., Ed.; Academic Press, 2010; Vol. 45, pp 393–407.
- (46) Waring, M. J. *Expert Opin. Drug Discov.* **2010**, *5* (3), 235–248.
- (47) Wenlock, M. C.; Austin, R. P.; Barton, P.; Davis, A. M.; Leeson, P. D. *J. Med. Chem.* **2003**, *46* (7), 1250–1256.
- (48) Ritchie, T. J.; Macdonald, S. J. F. *Drug Discov. Today* **2009**, *14* (21-22), 1011–1020.
- (49) Oprea, T. I.; Davis, A. M.; Teague, S. J.; Leeson, P. D. *J. Chem. Inf. Model.* **2001**, *41* (5), 1308–1315.
- (50) Perola, E. *J. Med. Chem.* **2010**, *53* (7), 2986–2997.
- (51) Hann, M. M. *Med. Chem. Commun.* **2011**, *2* (5), 349–355.
- (52) Keserü, G. M.; Makara, G. M. *Nat. Rev. Drug Discov.* **2009**, *8* (3), 203–212.
- (53) Hann, M. M.; Oprea, T. I. *Curr. Opin. Chem. Biol.* **2004**, *8* (3), 255–263.
- (54) O’Connell, K. M. G.; Galloway, W. R. J. D.; Spring, D. R. In *Diversity-Oriented Synthesis: Basics and Application in Organic Synthesis, Drug Discovery and Chemical Biology*; Trabocchi, A., Ed.; Wiley: Hoboken, New Jersey, USA, 2013; pp 1–28.
- (55) Spring, D. R. *Org. Biomol. Chem.* **2003**, *1* (22), 3867–3870.

- (56) Kennedy, J. P.; Williams, L.; Bridges, T. M.; Daniels, R. N.; Weaver, D.; Lindsley, C. W. *J. Comb. Chem.* **2008**, *10* (3), 345–354.
- (57) Newman, D. J.; Cragg, G. M. *J. Nat. Prod.* **2007**, *70* (3), 461–477.
- (58) Ertl, P.; Roggo, S.; Schuffenhauer, A. *J. Chem. Inf. Model.* **2008**, *48* (1), 68–74.
- (59) Dow, M.; Fisher, M.; James, T.; Marchetti, F.; Nelson, A. *Org. Biomol. Chem.* **2011**, *10* (1), 17–28.
- (60) *Diversity-Oriented Synthesis: Basics and Application in Organic Synthesis, Drug Discovery and Chemical Biology*; Trabocchi, A., Ed.; Wiley: Hoboken, New Jersey, USA, 2013.
- (61) Schreiber, S. L. *Science* **2000**, *287* (5460), 1964–1969.
- (62) Spandl, R. J.; Díaz-Gavilán, M.; O'Connell, K. M. G.; Thomas, G. L.; Spring, D. R. *Chem. Rec.* **2008**, *8* (3), 129–142.
- (63) Spandl, R. J.; Bender, A.; Spring, D. R. *Org. Biomol. Chem.* **2008**, *6* (7), 1149–1158.
- (64) Nielsen, T. E.; Schreiber, S. L. *Angew. Chem. Int. Ed.* **2008**, *47* (1), 48–56.
- (65) Burke, M. D.; Berger, E. M.; Schreiber, S. L. *J. Am. Chem. Soc.* **2004**, *126* (43), 14095–14104.
- (66) Oguri, H.; Schreiber, S. L. *Org. Lett.* **2005**, *7* (1), 47–50.
- (67) Burke, M. D.; Berger, E. M.; Schreiber, S. L. *Science* **2003**, *302* (5645), 613–618.
- (68) Murrison, S.; Maurya, S. K.; Einzinger, C.; McKeever-Abbas, B.; Warriner, S.; Nelson, A. *European J. Org. Chem.* **2011**, *2011* (12), 2354–2359.
- (69) Oguri, H.; Hiruma, T.; Yamagishi, Y.; Oikawa, H.; Ishiyama, A.; Otoguro, K.; Yamada, H.; Ōmura, S. *J. Am. Chem. Soc.* **2011**, *133* (18), 7096–7105.

- (70) Wyatt, E. E.; Fergus, S.; Galloway, W. R. J. D.; Bender, A.; Fox, D. J.; Plowright, A. T.; Jessiman, A. S.; Welch, M.; Spring, D. R. *Chem. Commun.* **2006**, No. 31, 3296–3298.
- (71) Kumagai, N.; Muncipinto, G.; Schreiber, S. L. *Angew. Chem. Int. Ed. Engl.* **2006**, *45* (22), 3635–3638.
- (72) Robbins, D.; Newton, A. F.; Gignoux, C.; Legeay, J.-C.; Sinclair, A.; Rejzek, M.; Laxon, C. A.; Yalamanchili, S. K.; Lewis, W.; O'Connell, M. A.; Stockman, R. A. *Chem. Sci.* **2011**, *2* (11), 2232–2235.
- (73) Cui, J.; Hao, J.; Ulanovskaya, O. A.; Dundas, J.; Liang, J.; Kozmin, S. A. *Proc. Natl. Acad. Sci.* **2011**, *108* (17), 6763–6768.
- (74) Pizzirani, D.; Kaya, T.; Clemons, P. A.; Schreiber, S. L. *Org. Lett.* **2010**, *12* (12), 2822–2825.
- (75) Thomas, G. L.; Spandl, R. J.; Glansdorp, F. G.; Welch, M.; Bender, A.; Cockfield, J.; Lindsay, J. A.; Bryant, C.; Brown, D. F. J.; Loiseleur, O.; Rudyk, H.; Ladlow, M.; Spring, D. R. *Angew. Chemie Int. Ed.* **2008**, *47* (15), 2808–2812.
- (76) Moura-Letts, G.; Diblasi, C. M.; Bauer, R. A.; Tan, D. S. *Proc. Natl. Acad. Sci. U. S. A.* **2011**, *108* (17), 6745–6750.
- (77) Morton, D.; Leach, S.; Cordier, C.; Warriner, S.; Nelson, A. *Angew. Chem. Int. Ed.* **2009**, *48* (1), 104–109.
- (78) Isidro-Llobet, A.; Hadje Georgiou, K.; Galloway, W.; Giacomini, E.; Hansen, M. R.; Méndez-Abt, G.; Tan, Y. S.; Carro, L.; Sore, H.; Spring, D. *Org. Biomol. Chem.* **2015**, *13* (15), 4570–4580.
- (79) Beckmann, H. S. G.; Nie, F.; Hagerman, C. E.; Johansson, H.; Tan, Y. S.; Wilcke, D.; Spring, D. R. *Nat. Chem.* **2013**, *5* (10), 861–867.
- (80) O'Connell, K. M. G.; Beckmann, H. S. G.; Laraia, L.; Horsley, H. T.; Bender, A.; Venkitaraman, A. R.; Spring, D. R. *Org. Biomol. Chem.* **2012**, *10* (37), 7545–7551.

- (81) Lipinski, C.; Hopkins, A. *Nature* **2004**, *432* (7019), 855–861.
- (82) Doveston, R. G.; Tosatti, P.; Dow, M.; Foley, D. J.; Li, H. Y.; Campbell, A. J.; House, D.; Churcher, I.; Marsden, S. P.; Nelson, A. *Org. Biomol. Chem.* **2015**, *13* (3), 859–865.
- (83) Carr, R. A. E.; Congreve, M.; Murray, C. W.; Rees, D. C. *Drug Discov. Today* **2005**, *10* (14), 987–992.
- (84) Blaazer, A. R.; Orrling, K. M.; Shanmugham, A.; Jansen, C.; Maes, L.; Edink, E.; Sterk, G. J.; Siderius, M.; England, P.; Bailey, D.; de Esch, I. J. P.; Leurs, R. *J. Biomol. Screen.* **2015**, *20* (1), 131–140.
- (85) Murray, C. W.; Verdonk, M. L. In *Fragment-based approaches in Drug Discovery*; Wolfgang, J., Erlanson, D. A., Eds.; Wiley-VCH: Weinheim, Germany, 2006; pp 55–65.
- (86) Erlanson, D. A.; McDowell, R. S.; O'Brien, T. *J. Med. Chem.* **2004**, *47* (14), 3463–3482.
- (87) Hung, A. W.; Ramek, A.; Wang, Y.; Kaya, T.; Wilson, J. A.; Clemons, P. A.; Young, D. W. *Proc. Natl. Acad. Sci. U. S. A.* **2011**, *108* (17), 6799–6804.
- (88) Wetzel, S.; Bon, R. S.; Kumar, K.; Waldmann, H. *Angew. Chemie Int. Ed.* **2011**, *50* (46), 10800–10826.
- (89) Goldberg, F. W.; Kettle, J. G.; Kogej, T.; Perry, M. W. D.; Tomkinson, N. P. *Drug Discov. Today* **2015**, *20* (1), 11–17.
- (90) James, T.; Simpson, I.; Grant, J. A.; Sridharan, V.; Nelson, A. *Org. Lett.* **2013**, *15* (23), 6094–6097.
- (91) Craven, P.; Aimon, A.; Dow, M.; Fleury-Bregeot, N.; Guilleux, R.; Morgentin, R.; Roche, D.; Kalliokoski, T.; Foster, R.; Marsden, S. P.; Nelson, A. *Bioorg. Med. Chem.* **2014**, in press.

- (92) James, T.; Maclellan, P.; Burslem, G. M.; Simpson, I.; Grant, J. A.; Warriner, S.; Sridharan, V.; Nelson, A. *Org. Biomol. Chem.* **2014**, *12* (16), 2584–2591.
- (93) Colomer, I.; Adeniji, O.; Burslem, G. M.; Craven, P.; Rasmussen, M. O.; Willaume, A.; Kalliokoski, T.; Foster, R.; Marsden, S. P.; Nelson, A. *Bioorg. Med. Chem.* **2015**, in press.
- (94) Lüthy, M.; Wheldon, M. C.; Haji-Cheteh, C.; Atobe, M.; Bond, P. S.; O'Brien, P.; Hubbard, R. E.; Fairlamb, I. J. S. *Bioorg. Med. Chem.* **2015**, in press.
- (95) Doveston, R. G.; Marsden, S. P.; Nelson, A. *Unpubl. Work* **2015**.
- (96) Irwin, J. J.; Sterling, T.; Mysinger, M. M.; Bolstad, E. S.; Coleman, R. G. *J. Chem. Inf. Model.* **2012**, *52* (7), 1757–1768.
- (97) Bemis, G. W.; Murcko, M. A. *J. Med. Chem.* **1996**, *39* (15), 2887–2893.
- (98) Wang, Y. F.; Izawa, T.; Kobayashi, S.; Ohno, M. *J. Am. Chem. Soc.* **1982**, *104* (23), 6465–6466.
- (99) Davies, S. G.; Ichihara, O. *Tetrahedron Lett.* **1999**, *40* (52), 9313–9316.
- (100) Davies, S. G.; Kelly, R. J.; Price Mortimer, A. J. *Chem. Commun.* **2003**, No. 17, 2132–2133.
- (101) Davies, S. G.; Haggitt, J. R.; Ichihara, O.; Kelly, R. J.; Leech, M. A.; Price Mortimer, A. J.; Roberts, P. M.; Smith, A. D. *Org. Biomol. Chem.* **2004**, *2* (18), 2630–2649.
- (102) Pattarozzi, M.; Zonta, C.; Broxterman, Q. B.; Kaptein, B.; De Zorzi, R.; Randaccio, L.; Scrimin, P.; Licini, G. *Org. Lett.* **2007**, *9* (12), 2365–2368.
- (103) Takeda, Y.; Okumura, S.; Tone, S.; Sasaki, I.; Minakata, S. *Org. Lett.* **2012**, *14* (18), 4874–4877.
- (104) Knapp, J. M.; Kurth, M. J.; Shaw, J. T.; Younai, A. In *Diversity-Oriented Synthesis: Basics and Application in Organic Synthesis, Drug Discovery*

and Chemical Biology; Trabocchi, A., Ed.; Wiley: Hoboken, New Jersey, USA, 2013; pp 29–57.

- (105) Nishibayashi, Y.; Uemura, S. In *Comprehensive Organometallic Chemistry III, Volume 11*; Hiyama, T., Crabtree, R. H., Mingos, D. M. P., Eds.; Elsevier: Amsterdam, 2007; pp 75–116.
- (106) Lu, Z.; Ma, S. *Angew. Chem. Int. Ed.* **2008**, *47* (2), 258–297.
- (107) Trost, B. M.; Ariza, X. *Angew. Chem. Int. Ed.* **1997**, *36* (23), 2635–2637.
- (108) Trost, B. M.; Ariza, X. *J. Am. Chem. Soc.* **1999**, *121* (46), 10727–10737.
- (109) Melhado, A. D.; Luparia, M.; Toste, F. D. *J. Am. Chem. Soc.* **2007**, *129* (42), 12638–12639.
- (110) Macovei, C.; Vicennati, P.; Quinton, J.; Nevers, M.; Volland, H.; Créminon, C.; Taran, F. *Chem. Commun.* **2012**, *48* (37), 4411–4413.
- (111) Solà, J.; Fletcher, S. P.; Castellanos, A.; Clayden, J. *Angew. Chem. Int. Ed.* **2010**, *49* (38), 6836–6839.
- (112) Solà, J.; Helliwell, M.; Clayden, J. *J. Am. Chem. Soc.* **2010**, *132* (13), 4548–4549.
- (113) Boddaert, T.; Solà, J.; Helliwell, M.; Clayden, J. *Chem. Commun.* **2012**, *48*, 3397–3399.
- (114) Andersen, K. K.; Gloster, D. F.; Bray, D. D.; Shoja, M.; Kjær, A. *J. Heterocycl. Chem.* **1998**, *35* (2), 317–324.
- (115) Avenozaa, A.; Bustoa, J. H.; Cativielab, C.; Peregrinaa, J. M.; Rodrígueza, F. *Tetrahedron Lett.* **2002**, *43* (8), 1429–1432.
- (116) Liang, T.; Neumann, C. N.; Ritter, T. *Angew. Chem. Int. Ed.* **2013**, *52* (32), 8214–8264.
- (117) McGrath, N. A.; Brichacek, M.; Njardarson, J. T. *J. Chem. Educ.* **2010**, *87* (12), 1348–1349.

- (118) Vitaku, E.; Ilardi, E. A.; Njardarson, J. T. Top 200 Brand Name Drugs by US Retail Sales in 2012 <http://cbc.arizona.edu/njardarson/group/top-pharmaceuticals-poster> (accessed Jan 23, 2015).
- (119) Allendörfer, N.; Es-Sayed, M.; Nieger, M.; Bräse, S. *Tetrahedron Lett.* **2012**, 53 (4), 388–391.
- (120) Jones, J. H.; Witty, M. J. *J. Chem. Soc. Perkin Trans. 1* **1979**, 3203–3206.
- (121) Benoiton, N. L.; Chen, F. M. F. *Can. J. Chem.* **1981**, 59 (2), 384–389.
- (122) Benoiton, N. L.; Chen, F. M. F. *J. Chem. Soc. Chem. Commun.* **1981**, 1225–1227.
- (123) Paquet, A.; Chen, F. M. F.; Benoiton, N. L. *Can. J. Chem.* **1984**, 62 (7), 1335–1338.
- (124) Berkowitz, D. B.; McFadden, J. M.; Chisowa, E.; Semerad, C. L. *J. Am. Chem. Soc.* **2000**, 122 (44), 11031–11032 .
- (125) Greene, T. W.; Wuts, P. G. M. *Protective Groups in Organic Synthesis*; John Wiley & Sons: Chichester, U.K., 1991.
- (126) Ries, U.; Huel, N.; Priepke, H.; Nar, H.; Stassen, J. M.; Wienen, W. *US 6200976 B1* **2001**.
- (127) Breitholle, E. G.; Stammer, C. H. *J. Org. Chem.* **1976**, 41 (8), 1344–1349.
- (128) Hugener, M.; Heimgartner, H. *Helv. Chim. Acta* **1989**, 72 (1), 172–179.
- (129) Breman, A.; Smits, J.; de Gelder, R.; van Maarseveen, J.; Ingemann, S.; Hiemstra, H. *Synlett* **2012**, 23 (15), 2195–2200.
- (130) Hugener, M.; Heimgartner, H. *Helv. Chim. Acta* **1995**, 78 (7), 1863–1878.
- (131) Stirling, C. J. M. *J. Chem. Soc.* **1958**, 4531–4536.
- (132) Peter, H.; Brugger, M.; Schreiber, J.; Eschenmoser, A. *Helv. Chim. Acta* **1963**, 46 (2), 577–586.

- (133) Mandić, Z.; Herak, J. J.; Tomić, M.; Vranešić, B.; Kovačević, M.; Gašpert, B. *Croat. Chem. Acta* **1981**, *54*, 127–139.
- (134) Confalone, P. N.; Huie, E. M.; Ko, S. S.; Cole, G. M. *J. Org. Chem.* **1988**, *53* (3), 482–487.
- (135) Thaisrivongs, S.; Pals, D. T.; Turner, S. R.; Kroll, L. T. *J. Med. Chem.* **1988**, *31* (7), 1369–1376.
- (136) Donohoe, T. J.; Callens, C. K. A.; Flores, A.; Lacy, A. R.; Rathi, A. H. *Chem. Eur. J.* **2011**, *17* (1), 58–76.
- (137) Lucet, D.; Le Gall, T.; Mioskowski, C. *Angew. Chem. Int. Ed.* **1998**, *37* (19), 2580–2627.
- (138) Fujita, M.; Kitagawa, O.; Suzuki, T.; Taguchi, T. *J. Org. Chem.* **1997**, *62* (21), 7330–7335.
- (139) De Clercq, E. *Biochim. Biophys. Acta* **2002**, *1587* (2-3), 258–275.
- (140) Takai, H.; Obase, H.; Teranishi, M. *Chem. Pharm. Bull.* **1988**, 4659–4670.
- (141) Kusakabe, K.-I.; Yoshida, S.; Nakahara, K.; Hasegawa, T.; Tadano, G.; Fuchino, K. *WO2014065434 A1* **2014**.
- (142) Babij, N. R.; Wolfe, J. P. *Angew. Chem. Int. Ed.* **2013**, *52* (35), 9247–9250.
- (143) Malik, M.; Witkowski, G.; Ceborska, M.; Jarosz, S. *Org. Lett.* **2013**, *15* (24), 6214–6217.
- (144) *The Nobel Prize in Chemistry 2005 was awarded to Chauvin, Grubbs and Schrock for the development of transition metal-catalysed metathesis reactions.*
- (145) *The Nobel Prize in Chemistry 2010 was awarded to Heck, Negishi and Suzuki for the development of Pd-catalysed cross coupling reactions.*
- (146) Gibson, S. E.; Middleton, R. J. *Contemp. Org. Synth.* **1996**, *3* (6), 447–471.

- (147) Dounay, A. B.; Overman, L. E. *Chem. Rev.* **2003**, *103* (8), 2945–2964.
- (148) Barrows, S. E.; Eberlein, T. H. *J. Chem. Educ.* **2005**, *82* (9), 1334.
- (149) *Metathesis in Natural Product Synthesis*; Cossy, J., Arseniyadis, S., Meyer, C., Eds.; WILEY-VCH: Weinheim, Germany, 2010.
- (150) Gracias, V.; Gasiecki, A. F.; Moore, J. D.; Akritopoulou-Zanze, I.; Djuric, S. W. *Tetrahedron Lett.* **2006**, *47* (50), 8977–8980.
- (151) VanRheenen, V.; Kelly, R. C.; Cha, D. Y. *Tetrahedron Lett.* **1976**, *17* (23), 1973–1976.
- (152) Emmanuvel, L.; Shaikh, T. M. A.; Sudalai, A. *Org. Lett.* **2005**, *7* (22), 5071–5074.
- (153) Bonet, A.; Pubill-Ulldemolins, C.; Bo, C.; Gulyás, H.; Fernández, E. *Angew. Chem. Int. Ed.* **2011**, *50* (31), 7158–7161.
- (154) Csatayová, K.; Davies, S. G.; Ford, J. G.; Lee, J. A.; Roberts, P. M.; Thomson, J. E. *J. Org. Chem.* **2013**, *78* (24), 12397–12408.
- (155) Liu, D.; Chen, J.; Ai, L.; Zhang, H.; Liu, J. *Org. Lett.* **2013**, *15* (2), 410–413.
- (156) Young, I. S.; Ortiz, A.; Sawyer, J. R.; Conlon, D. A.; Buono, F. G.; Leung, S. W.; Burt, J. L.; Sortore, E. W. *Org. Process Res. Dev.* **2012**, *16* (9), 1558–1565.
- (157) Fürst, A.; Plattner, P. A. *Helv. Chim. Acta* **1949**, *32* (1), 275–283.
- (158) Kabalka, G. W.; Shoup, T. M.; Goudgaon, N. M. *J. Org. Chem.* **1989**, *54* (25), 5930–5933.
- (159) Duran-Lara, E. F.; Shankaraiah, N.; Geraldo, D.; Santos, L. S. *J. Braz. Chem. Soc.* **2009**, *20* (5), 813–819.
- (160) Schuffenhauer, A.; Ertl, P.; Roggo, S.; Wetzler, S.; Koch, M. A.; Waldmann, H. *J. Chem. Inf. Model.* **2006**, *47* (1), 47–58.

- (161) Böhm, H.-J.; Flohr, A.; Stahl, M. *Drug Discov. Today Technol.* **2004**, 1 (3), 217–224.
- (162) Sauer, W. H. B.; Schwarz, M. K. *J. Chem. Inf. Comput. Sci.* **2003**, 43 (3), 987–1003.
- (163) Ylijoki, K. E. O.; Stryker, J. M. *Chem. Rev.* **2013**, 113 (3), 2244–2266.
- (164) Kumar, N.; Kiuchi, M.; Tallarico, J. A.; Schreiber, S. L. *Org. Lett.* **2005**, 7 (13), 2535–2538.
- (165) Balthaser, B. R.; Maloney, M. C.; Beeler, A. B.; Porco, J. A.; Snyder, J. K. *Nat. Chem.* **2011**, 3 (12), 969–973.
- (166) Kopp, F.; Stratton, C. F.; Akella, L. B.; Tan, D. S. *Nat. Chem. Biol.* **2012**, 8 (4), 358–365.
- (167) Huigens, R. W.; Morrison, K. C.; Hicklin, R. W.; Flood, T. A.; Richter, M. F.; Hergenrother, P. J. *Nat. Chem.* **2013**, 5 (3), 195–202.
- (168) Rafferty, R. J.; Hicklin, R. W.; Maloof, K. A.; Hergenrother, P. J. *Angew. Chem. Int. Ed. Engl.* **2014**, 53 (1), 220–224.
- (169) Hicklin, R. W.; López Silva, T. L.; Hergenrother, P. J. *Angew. Chem. Int. Ed. Engl.* **2014**, 53 (37), 9880–9883.
- (170) José L. Mascareñas. In *Advances in cycloaddition, volume 6*; Jai Press Inc: Stamford, Connecticut, 1999; pp 1–54.
- (171) Procter, D. J.; Flowers, R. A.; Skrydstrup, T. *Organic Synthesis using Samarium Diodide: A Practical Guide*; The Royal Society of Chemistry: Cambridge, 2009.
- (172) Barraja, P.; Spanò, V.; Patrizia, D.; Carbone, A.; Cirrincione, G.; Vedaldi, D.; Salvador, A.; Viola, G.; Dall'acqua, F. *Bioorg. Med. Chem. Lett.* **2009**, 19 (6), 1711–1714.
- (173) Burns, N. Z.; Witten, M. R.; Jacobsen, E. N. *J. Am. Chem. Soc.* **2011**, 133 (37), 14578–14581.

- (174) Achmatowicz, O.; Bukowski, P.; Szechner, B.; Zwierzchowska, Z.; Zamojski, A. *Tetrahedron* **1971**, 27 (10), 1973–1996.
- (175) Haukaas, M. H.; O'Doherty, G. A. *Org. Lett.* **2001**, 3 (24), 3899–3902.
- (176) Caddick, S.; Judd, D. B.; Lewis, A. K.; Reich, M. T.; Williams, M. R. . *Tetrahedron* **2003**, 59 (29), 5417–5423.
- (177) Crawford, C.; Nelson, A.; Patel, I. *Org. Lett.* **2006**, 8 (19), 4231–4234.
- (178) Sammes, P. G.; Street, L. J.; Kirby, P. *J. Chem. Soc. Perkin Trans. 1* **1983**, 2729.
- (179) Woodall, E. L.; Simanis, J. A.; Hamaker, C. G.; Goodell, J. R.; Mitchell, T. A. *Org. Lett.* **2013**, 15 (13), 3270–3273.
- (180) Garst, M. E.; McBride, B. J.; Douglass, J. G. *Tetrahedron Lett.* **1983**, 24 (16), 1675–1678.
- (181) Wender, P. A.; McDonald, F. E. *J. Am. Chem. Soc.* **1990**, 112 (12), 4956–4958.
- (182) Rumbo, A.; Mouriño, A.; Castedo, L.; Mascareñas, J. L. *J. Org. Chem.* **1996**, 61 (18), 6114–6120.
- (183) Mascareñas, J. L.; Rumbo, A.; Castedo, L. *J. Org. Chem.* **1997**, 62 (25), 8620–8621.
- (184) Rumbo, A.; Castedo, L.; Mouriño, A.; Mascareñas, J. L. *J. Org. Chem.* **1993**, 58 (21), 5585.
- (185) Rumbo, A.; Castedo, L.; Mascareñas, J. L. *Tetrahedron Lett.* **1997**, 38 (33), 5885–5886.
- (186) Wender, P. A.; Mascarenas, J. L. *J. Org. Chem.* **1991**, 56 (22), 6267–6269.
- (187) López, F.; Castedo, L.; Mascareñas, J. L. *Org. Lett.* **2000**, 2 (7), 1005–1007.

- (188) López, F.; Castedo, L.; Mascareñas, J. L. *Chem. Eur. J.* **2002**, *8* (4), 884–899.
- (189) López, F.; Castedo, L.; Mascareñas, J. L. *J. Org. Chem.* **2003**, *68* (25), 9780–9786.
- (190) López, F.; Castedo, L.; Mascareñas, J. L. *Org. Lett.* **2001**, *3* (4), 623–625.
- (191) Miyazaki, S.; Katoh, S.; Adachi, K.; Isoshima, H.; Kobayashi, S.; Matsuzaki, Y.; Watanabe, W.; Yamataka, K.; Kiyonari, S.; Wamaki, S. *US 2005/54645 A1* **2005**.
- (192) Rodríguez, J. R.; Rumbo, A.; Castedo, L.; Mascareñas, J. L. *J. Org. Chem.* **1999**, *64* (3), 966–970.
- (193) Rodríguez, J. R.; Castedo, L.; Mascareñas, J. L. *J. Org. Chem.* **2000**, *65* (8), 2528–2531.
- (194) Rodríguez, J. R.; Rumbo, A.; Castedo, L.; Mascareñas, J. L. *J. Org. Chem.* **1999**, *64* (12), 4560–4563.
- (195) Rodríguez, J. R.; Castedo, L.; Mascareñas, J. L. *Synthesis* **2000**, No. 07, 980–984.
- (196) Miriyala, B.; Bhattacharyya, S.; Williamson, J. S. *Tetrahedron* **2004**, *60* (7), 1463–1471.
- (197) Heravi, M. M.; Bakhtiari, K.; Tehrani, M. H.; Javadi, N. M.; Oskooie, H. A. *Arkivoc* **2006**, No. 16, 16–22.
- (198) Fu, H.-J.; Zhou, Y.-R.; Bao, B.-H.; Jia, M.-X.; Zhao, Y.; Zhang, L.; Li, J.-X.; He, H.-L.; Zhou, X.-M. *J. Med. Chem.* **2014**, *57* (11), 4692–4709.
- (199) Quiliano, M.; Aldana, I. *Rev. Virtual Quim.* **2013**, *5* (6), 1120–1133.
- (200) Wolkenberg, S. E.; Wisnoski, D. D.; Leister, W. H.; Wang, Y.; Zhao, Z.; Lindsley, C. W. *Org. Lett.* **2004**, *6* (9), 1453–1456.

- (201) Stütz, A. E.; Wrodnigg, T. M. In *Carbohydrate Chemistry*; Rauter, A. P., Lindhorst, T., Eds.; Carbohydrate Chemistry; Royal Society of Chemistry: Cambridge, 2013; Vol. 39, pp 120–149.
- (202) Günay, M. E.; Richards, C. J. *Organometallics* **2009**, *28* (19), 5833–5836.
- (203) Sikdar, A. P.; Chetri, A. B.; Das, P. J. *Indian J. Chem., Sect B* **2003**, *42*, 2878–2882.
- (204) Schnyder, J.; Rottenberg, M. *Helv. Chim. Acta* **1975**, *58* (2), 521–523.
- (205) Padwa, A.; Hamilton, L. *J. Heterocycl. Chem.* **1967**, *4*, 118–123.
- (206) Berkessel, A.; Mukherjee, S.; Muller, T. N.; Cleemann, F.; Roland, K.; Brandenburg, M.; Neud J.-M.; Lex, J. *Org. Biomol. Chem.*, **2006**, *4*, 4319–4330.
- (207) Hugener, M.; Heimgartner, H. *Helv. Chim. Acta* **1989**, *72*, 172–179.
- (208) Barraclough, P.; Dieterich, P.; Spray, C. A.; Young, D. W. *Org. Biomol. Chem.* **2006**, *4* (8), 1483–1491.
- (209) Loughlin, W. A.; Schweiker, S. S.; Jenkins, I. D.; Henderson, L. C. *Tetrahedron* **2013**, *69* (5), 1576–1582.
- (210) Dolbeare, K.; Pontoriero, G. F.; Gupta, S. K.; Mishra, R. K.; Johnson, R. L. *J. Med. Chem.* **2003**, *46* (5), 727–733.
- (211) Fang, P.; Chaulagain, M. R.; Aron, Z. D. *Org. Lett.* **2012**, *14* (8), 2130–2133.
- (212) Kaneko, T.; Clark, R.; Ohi, N.; Ozaki, F.; Kawahara, T.; Kamada, A.; Okano, K.; Yokohama, H.; Muramoto, K.; Arai, T.; Ohkuro, M.; Takenaka, O.; Sonoda, J. *US 6518432 B1* **2003**.
- (213) Adderley, N. J.; Buchanan, D. J.; Dixon, D. J.; Lainé, D. I. *Angew. Chem. Int. Ed.* **2003**, *42* (35), 4241–4244.

- (214) Schrittwieser, J. H.; Coccia, F.; Kara, S.; Grischek, B.; Kroutil, W.; D'Alessandro, N.; Hollmann, F. *Green Chem.* **2013**, *15* (12), 3318–3331.
- (215) Bezanson, M.; Pottel, J.; Bilbeisi, R.; Toumieux, S.; Cueto, M.; Moitessier, N. *J. Org. Chem.* **2013**, *78* (3), 872–885.
- (216) Jadhav, A. H.; Kim, H. *Tetrahedron Lett.* **2012**, *53* (39), 5338–5342.
- (217) Hawkins, P. C. D.; Skillman, A. G.; Warren, G. L.; Ellingson, B. A.; Stahl, M. T. *J. Chem. Inf. Model.* **2010**, *50* (4), 572–584.